# Responding to different types of damaged telomeres

**Marta Aleksandra Markiewicz-Potoczny**

Thesis submitted for the degree of Doctor of Philosophy

Institute for Cell and Molecular Biosciences

Newcastle University

October 2016


## Abstract

Telomeres are bound by multiple 'capping' proteins, which protect chromosome ends from fusion and degradation. Mutations of telomeric proteins of *Saccharomyces cerevisiae*, *cdc13-1* and *yku70*Δ, induce a telomere uncapping, generation of ssDNA by nucleases, cell cycle arrest and the DNA Damage Response (DDR). In other context the Mec1 checkpoint kinase is activated by Ddc1, Dpb11 and Dna2 in response to DNA damage. I tested how Ddc1, Dpb11 and Dna2 affect *cdc13-1* and *yku70*Δ fitness. *DPB11* and *DNA2* are essential genes, therefore I analysed checkpoint defective alleles of *DPB11, DNA2* and *DDC1*. I showed that Dpb11 and Dna2 have no effect on *yku70*Δ fitness in contrast to Ddc1, which slightly affects *yku70*Δ fitness and might have a role in cell cycle arrest of *yku70*Δ mutants. I confirmed that Ddc1 strongly, whereas Dpb11 slightly, affects *cdc13-1* fitness. Dpb11 may contribute to the checkpoint function of Ddc1. I also found that the *cdc13-1* defect was suppressed by the *dna2-W128A,Y130A* allele when on a plasmid, but enhanced when integrated into the genome, and these effects might be due to variable *dna2-W128A,Y130A* copy number (in the genome versus on a plasmid).

Surprisingly, in the course of my experiments, I found that deletion of *DDC1* suppressed *dna2*Δ lethality. I confirmed that deletion of *RAD9* suppresses *dna2*Δ lethality, and I found that deletion of *RAD17*, *CHK1*, *MEC1* and *POL32* also allows *dna2*Δ viability. I observed that elimination of Tel1, Rad53, Exo1, Mre11 or Rad27 do not suppress *dna2*Δ lethality. Based on the observation that checkpoint gene deletions suppress *dna2*Δ, whereas they exacerbate defects in other core DNA replication proteins, I propose that the essential function of Dna2 is in the telomeric Okazaki fragment processing.

I also found that deletions of *HCM1*, *XBP1* and *ULS1*, genes selected from a genome-wide screen, suppress growth defect of *cdc13-1* and *yku70*Δ mutants, and *ULS1* suppresses *stn1-13* defect. Finally, I showed that thermo-sensitive *cdc13-1* and *cdc15-2* strains adapt to chronic low-dose stress. Adapted cells are fitter if more stress is applied, but are less fit in the absence of stress. I found the consequences of adaptation to be reversible.

# Dedication

This PhD is dedicated to my mother, Jolanta Markiewicz, who has always been an inspiration to me.

## Acknowledgements

I would like to thank my supervisor, David Lydall, for giving me the opportunity to work in his lab, and for his great support and scientific guidance. Thanks for allowing me to think independently and for arousing my scientific curiosity. David Lydall's lab would not exist without all great people working in (and around) it, therefore I would like to thank all lab members, past and present, for their advice, encouragement and friendship throughout my PhD. Listed alphabetically: Peter Banks, Adrian Blackburn, Marion Dubarry, Eva-Maria Holstein, Conor Lawless, Alan Leake, Laura Maringele, Siddharth Narayanan, Greg Ngo, Cameron Robertson, Joana Cristina Pedro-Rodrigues, Victoria Torrance, Ben Wetherall. I would like to thank Peter Burgers, Judith Campbell, Marco Muzi-Falconi and Yeon-Soo Seo, who provided me with plasmids carrying alleles of *DDC1*, *DPB11* and *DNA2*. These contributions are detailed in full in the Appendix B. Finally, I would like to thank the Marie Curie ITN CodeAge project for funding my PhD; I am very grateful and fortunate to receive their support. Last, but not least, I thank my father, brother and loving husband for great support and permanent encouragement. Thank you for believing in me.

# Table of contents

# List of Figures

**Figures in Chapter 6, numbered consecutively with the Figure numbering from a publication:**

# List of Tables



**Table in Chapter 6, numbered consecutively with the Table numbering from a publication:**

# Publications

MARKIEWICZ-POTOCZNY, M. & LYDALL, D. 2016. Costs, benefits and redundant mechanisms of adaption to chronic low-dose stress in yeast. Cell Cycle, 15, 2732-2741.

The above mentioned publication is presented in Chapter 6 of this thesis.

# Yeast and human nomenclature

Yeast nomenclature

| | |
|---|---|
| *YFG* | Denotes that this is a wild-type gene |
| *yfg*Δ | Denotes that this gene has been deleted |
| *yfg::XXX* | Denotes that the gene *yfg* has been disrupted by the integration of gene *XXX* |
| *yfg-1* | Denotes a conditional mutation of *YFG* gene |
| *yfg*Δ*C* | Denotes a C-terminal truncation allele |
| *yfg*Δ*N* | Denotes an N-terminal truncation allele |
| Yfg | Denotes that this is a protein |

Human nomenclature

| | |
|---|---|
| *YFG* | Denotes a human gene |
| YFG | Denotes a human protein |

# List of Abbreviations

| | |
|---|---|
| 5-FOA | 5-fluoroorotic acid |
| aa | Amino acid |
| ALT | Alternative Lengthening of Telomeres |
| ATM | Ataxia Telangiectasia Mutated |
| ATR | Ataxia Telangiectasia and Rad3-related protein |
| ATRIP | ATR-Iinteracting Protein in human |
| BLAST | Basic Local Alignment Search Tool |
| bp | Base pairs |
| BSA | Bovine Serum Albumin |
| Cdc | Cell division cycle replication protein |
| Chk1 | Checkpoint kinase 1 |
| CST | Cdc13-Stn1-Ten1 |
| DAmP | Decreased abundance by perturbation of mRNA |
| Ddc1 | DNA damage checkpoint protein 1 |
| DDR | DNA Damage Response |
| DDY | Diploid yeast strain from Lydall Lab collection |
| DLY | Haploid yeast strain from Lydall Lab collection |
| DNA | Deoxyribonucleic aid |
| Dna2 | DNA replication helicase 2-like |
| dNTP | Deoxyribonucleotide triphosphate |
| Dpb11 | DNA polymerase B 11 |
| DSB | DNA Double Strand Break |
| dsDNA | Double stranded DNA |
| DTT | Dithiothreitol |
| EDTA | Ethylenediaminetetraacetic acid |
| ESM | Enriched Sporulation Medium |
| Est1,2,3 | Ever shorter telomeres 1, 2, 3 |
| Exo1 | Exonuclease 1 |
| FIGA | Fluorescent In Gel Assay |
| g | Gramme |
| GINS | Go-Ichi-Nii-San (Sld5/Cdc105-Psf1/Cdc101-Psf2/Cdc102-Psf3) |
| GIS | Genetic Interaction Strength |
| G418 | Geneticin |

| | |
|---|---|
| HIS | Histidine |
| HR | Homologous Recombination |
| kb | Kilobases |
| Ku | Yku70/Yku80 complex |
| L | Litre |
| LB | Lysogeny Broth |
| LEU | Leucine |
| LiAc | Lithium Acetate |
| Lif1 | Ligase-interacting factor 1 |
| Lig4 | Lligase 4 |
| LYS | Lysine |
| M | Molar |
| µg | Microgrammes |
| µL | Microlitre |
| mg | Milligrammes |
| mL | Millilitre |
| MAT | Mating type locus |
| mtDNA | Mitochondrial DNA |
| MRN | Mre11/Rad50/Nbs1 complex |
| MRX | Mre11/Rad50/Xrs2 complex |
| NER | Nucleotide Excision Repair |
| ng | nanogrammes |
| NHEJ | Non-Homologous End Joining |
| PCNA | Proliferating Cell Nuclear Antigen |
| PCR | Polymerase Chain Reaction |
| PIKK | Phosphatidylinositol 3-kinase-related protein kinase |
| qPCR | Quantitative Polymerase Chain Reaction |
| Rad | Radiation sensitive |
| Rap1 | Repressor activator protein 1 |
| rDNA | Ribosomal DNA |
| RFC | Replication factor C |
| Rif1,2 | RAP1 interacting factor 1, 2 |
| RNA | Ribonucleic acid |
| RPA | Replication Protein A, Rfa1/Rfa2/Rfa3 |
| rpm | Revolution per minute |

| | |
|---|---|
| s | Seconds |
| SD | Synthetic Dropout medium |
| SDS | Sodium Dodecyl Sulphate |
| SGA | Synthetic Genetic Array |
| SGD | *Saccharomyces* genome database |
| SOC | Super Optimal broth with Catabolite repression |
| SSC | Saline Sodium Citrate |
| ssDNA | Single stranded DNA |
| Stn1 | Suppressor of cdc thirteen 1 |
| TBE | Tris/Boric Acid/EDTA |
| TE | Tris/EDTA |
| Ten1 | Telomeric pathways with Stn1 |
| Tlc1 | Telomerase component 1 |
| Tm | Melting temperature (of DNA) |
| TRP | Tryptophan |
| ts | Thermo-sensitive (e. g. mutation) |
| URA | Uracil |
| UV | Ultra Violet |
| WT | Wild Type |
| YCp | Yeast Centromeric plasmid |
| YEPD | Yeast Extract/Peptone/Dextrose |
| Δ | Indicates gene deletion |

# Chapter 1. Introduction

## 1.1 Yeast as a model organism

"For many biological problems, there is an animal on which it can be most conveniently studied (…)" the statement of the Nobel prize laureate in 1920, August Krogh, indicates the importance of conducting experiments on the research model of correct choice. The aim of using model organisms is to obtain information and knowledge about other species which are more complex to study, like humans (de Magalhaes, 2004). It is inconvenient and difficult to study the processes of e.g. ageing and age-related pathologies in humans *in vivo*, because the long life expectancy of humans and ethical issues (Leonelli and Ankeny, 2013). Thus human cell culture and animal models, such as yeast, nematode*,* fruit fly and laboratory mouse are widely applied in research (Buffenstein et al., 2008, Yeoman et al., 2012).

Using the single cellular eukaryote *Saccharomyces cerevisiae* as a model organism is advantageous due to the easiness of breeding, rapid growth and cost-effectiveness (Lander et al., 2001, Liti, 2015). The genomic information of haploid budding yeast genome (12 Mb) is already well known as it was sequenced in 1996 (Goffeau et al., 1996). The genome does not contain many repetitive sequences, also non-coding DNA is less common than in higher eukaryotes, which is favourable for genetic studies (Goffeau et al., 1996, Conconi et al., 2005).

Budding yeast provide useful insights into genetics, molecular and biochemical processes (Kaeberlein et al., 1999, Boiteux and Jinks-Robertson, 2013, Sarto-Jackson and Tomaska, 2016). Diverse cellular pathways have been investigated in yeast; those include the influence of DNA damage factors or cytotoxic compounds on yeast physiology (Conconi et al., 2005, Saka et al., 2013). I used yeast as a model to investigate the role of genes, e.g. *DDC1* or *DNA2,* which have human orthologues, *RAD9* or *DNA2*, respectively. Human and yeast share similarities in some pathways that control key aspects of cell biology, e.g. cell cycle arrest (Hartwell, 2002), programmed cell death (Munoz et al., 2012), metabolism (Petranovic et al., 2010) and many other pathways (Mohammadi et al., 2015). It was proposed that about 50% of human genes involved in heritable diseases show the homology with budding yeast genes (Hartwell, 2002). *S. cerevisiae* serves also as a tool to investigate the

basis of longevity, cancer and other mammalian diseases. Although yeast culture can be propagated continuously, individual yeast cells age and eventually die (Lippuner et al., 2014). Each cell produces a number of buds during their lifespan, which is defined as a replicative lifespan. The replicative lifespan can be measured by counting cell divisions, reflected by the number of new buds appearing and being subsequently removed by microdissection. Another approach to study yeast aging is to measure the time a cell spends in a non-dividing state, known as the chronological lifespan (Lippuner et al., 2014).

### 1.2 Aging and cancer

Most definitions describe ageing as a process that is progressive, deleterious, irreversible, and connected to changes that adult organisms accumulate in time, finally leading to death. Ageing is a complex process which arises from environmental and inherited stimuli (Phipps et al., 2007). Cells are constantly prone to DNA damage that occurs due to errors of DNA replication, recombination and exogenous agents, such as UV radiation (Kobayashi, 2011, McIsaac et al., 2016). Accumulation of DNA damage with age is regarded as one of possible explanations of ageing (Soares et al., 2014). DNA damage accumulation may cause irreversible physiological alterations in, among others, cellular component synthesis, cell cycle machinery and signalling pathways that control cell cycle arrest (Lombard et al., 2005). Such alterations affect genome stability and cause the homeostasis loss, which in turn may accelerate ageing (Soares et al., 2014).

Telomeres, the nucleoprotein structures localized at the end of eukaryotic linear chromosomes, get shorter with each cell division in the process known as telomere shortening or the end replication problem (Okazaki et al., 1968, de Lange, 2009). Due to telomere shortening during an organismal lifespan, telomere length became a lifespan determinant (Harley et al., 1990). Shortening of telomeres can trigger the checkpoint and DNA damage response (DDR), leading to genomic instability (d'Adda di Fagagna et al., 2003, Fumagalli et al., 2012).

In some cells telomerase, an enzyme responsible for telomere elongation, protects telomeres from shortening (Churikov et al., 2013, Lu et al., 2013). Embryonic stem cells, germ cells and cell lines obtained from tumours have the telomerase active and do not enter replicative senescence (Hayflick, 1998, de Magalhaes, 2004).

Telomerase activity was also found in yeast (Cohn and Blackburn, 1995). In higher eukaryotes telomerase activity is undetectable; in most of somatic human tissues telomerase is absent, and in e.g. mice telomerase has a very low activity (Kipling, 1997). Due to absence or decreased activity of telomerase, telomeres become shorter with each cell division, which is considered a main factor contributing to ageing (Harley et al., 1990, Allsopp et al., 1995, Carneiro et al., 2016).

Telomeres are one of the most influential barriers of cancer development (Kiyono et al., 1998, Artandi, 2003). Most of cancer cells (85-90%) exhibit increased activity of telomerase resulting in telomere lengthening (Cesare and Reddel, 2010, Lu et al., 2013). Human cancers are also characterised by genomic instability arisen from defective telomeres and fusions between them (Negrini et al., 2010). Therefore senescence, which is a hallmark of aging, is believed to serve as an anti-cancer mechanism and contribute to the cell and organism survival (Coppe et al., 2010, Yeoman et al., 2012, Bhatia-Dey et al., 2016).

### 1.3 Telomeres and telomerase - structure and function

Telomeres are comprised of multiple telomere binding proteins and repeated DNA sequences. Mammalian telomeres form tandem repeats (TTAGGG) and measure between 5 and 15 kb (Palm and de Lange, 2008, Samassekou et al., 2010). *S. cerevisiae* telomeres consist of heterogeneous $TG_{1-3}$ repeats, the length of which is maintained at about 250-400 bp (Ray and Runge, 1999). Telomeres contain of short G-rich 3' overhangs, which possibly provide the substrate for telomerase function (Wellinger et al., 1993). Yeast contain also sub-telomeric X and Y' repeats. A single sub-telomeric X repeat exists at all natural budding yeast telomeres and consists of a 473 bp core sequence (Pryde and Louis, 1997). Approximately half telomeres contain one to four copies of Y' repeat (Louis et al., 1994). Y' repeats might be of two predominant sizes, 5.2 and 6.7 kb (Lundblad and Blackburn, 1993).

Human telomeres shorten with each cell division, while yeast telomeres are maintained by a ribonucleoprotein enzyme telomerase, which synthesizes telomere repeat units (Greider and Blackburn, 1985). Telomerase consists of a protein catalytic subunit, one or more associated proteins and an integral RNA component which serves as a template for telomeric repeat synthesis (Nugent and Lundblad, 1998). In *S. cerevisiae* $Tlc1^{hTERC}$ is a noncoding, 1.2 kb RNA moiety of telomerase

which binds to catalytic subunit Est2$^{hTERT}$ and to accessory proteins (Greider and Blackburn, 1985, Singer and Gottschling, 1994, Dandjinou et al., 2004). Est2$^{hTERT}$ is a catalytic reverse transcriptase component of yeast telomerase, which uses a RNA subunit (Tlc1$^{hTERC}$) as a template for a *de novo* DNA synthesis (Lingner et al., 1997, Counter et al., 1997). The yeast telomerase associated proteins, Est1, Est3 and Cdc13/Est4, regulate access of telomerase to the telomere through direct and indirect associations between RNA and Est2 components (Chandra et al., 2001, Evans and Lundblad, 1999, Hughes et al., 2000).

Yeast cells lacking telomerase activity resemble mammalian somatic cells, which divide for a limited number of times before cell divisions are inhibited by short telomeres (Lundblad and Szostak, 1989). Such cells enter a senescence, a state of permanent growth arrest. Rarely, some “survivors” are generated; such cells can escape senescence by amplification of telomeric and sub-telomeric regions using recombination-dependent telomere elongation (Lundblad and Blackburn, 1993). Some immortalised human cells also use a recombination-dependent mechanism to maintain telomeres, known as alternative lengthening of telomeres (ALT) (Dunham et al., 2000, Varley et al., 2002). In buddying yeast amplification of Y’ repeats leads to generation of Type I survivors, whereas amplification of G-rich repeats leads to generation of Type II survivors (Lundblad and Blackburn, 1993, Teng and Zakian, 1999). Cells with telomere capping defects, caused by the absence of telomere protective genes *YKU70* and *MRE11* (*yku70*Δ *mre11*Δ mutants), senescence rapidly during the early growth of germinated spores and are example of type I survivors (Maringele and Lydall, 2002, Maringele and Lydall, 2004a). Telomerase-deficient strains, for example *est1*Δ*, est2*Δ or *tlc1*Δ, are able to escape replicative senescence using a homologous-recombination-based mechanism and are example of type II survivors (Lundblad and Blackburn, 1993, Maringele and Lydall, 2004a).

Genes important for recombination at double-strand breaks (DSBs) are also responsible for amplification of telomeres in the absence of telomerase (Chen et al., 2001b). Such genes can be divided into two groups: *RAD51, RAD54, RAD55, RAD57, RAD52*-dependent pathway is responsible for Y’ sub-telomeric region amplification, and *MRE11-RAD50-XRS2* (MRX complex, MRN in humans)*, RAD52, RAD59, SRS2, TID1*-dependent pathway is responsible for TG-telomeric repeats amplification (Chen et al., 2001b). In addition, *EXO1* 5’-3’ exonuclease, involved in

resection of DSBs, is important for generating recombination-dependent type I and II survivors (Maringele and Lydall, 2004b).

### 1.4 Telomere shortening – the end replication problem

Mammalian and yeast cells which are deprived of telomerase activity lose telomeric DNA with each cell division. Possible reason for DNA depletion is so called “end replication problem” (Watson, 1972, Olovnikov, 1973). DNA replication is performed by 5’ to 3’ polymerases from one RNA primer on the leading strand, and multiple primers discontinuously on the lagging strand (Fig. 1). A replication fork cannot replicate the 3′ end of a telomere because the last primer that is required for lagging strand synthesis cannot be removed, thus this region is not synthesized (Fig. 1C). As a result, a G-tail is formed, and an unreplicated 3’ tail is of the same length as before replication event, in the absence of nuclease activity. Possible role of single-stranded DNA (ssDNA) overhang is to provide a substrate for telomerase, as 3’ overhang is in demand for telomerase function (Lingner and Cech, 1996, Wang and Blackburn, 1997). Replication of leading strand causes blunt chromosome end (Fig. 1D) (Lydall, 2003, Vega et al., 2003).

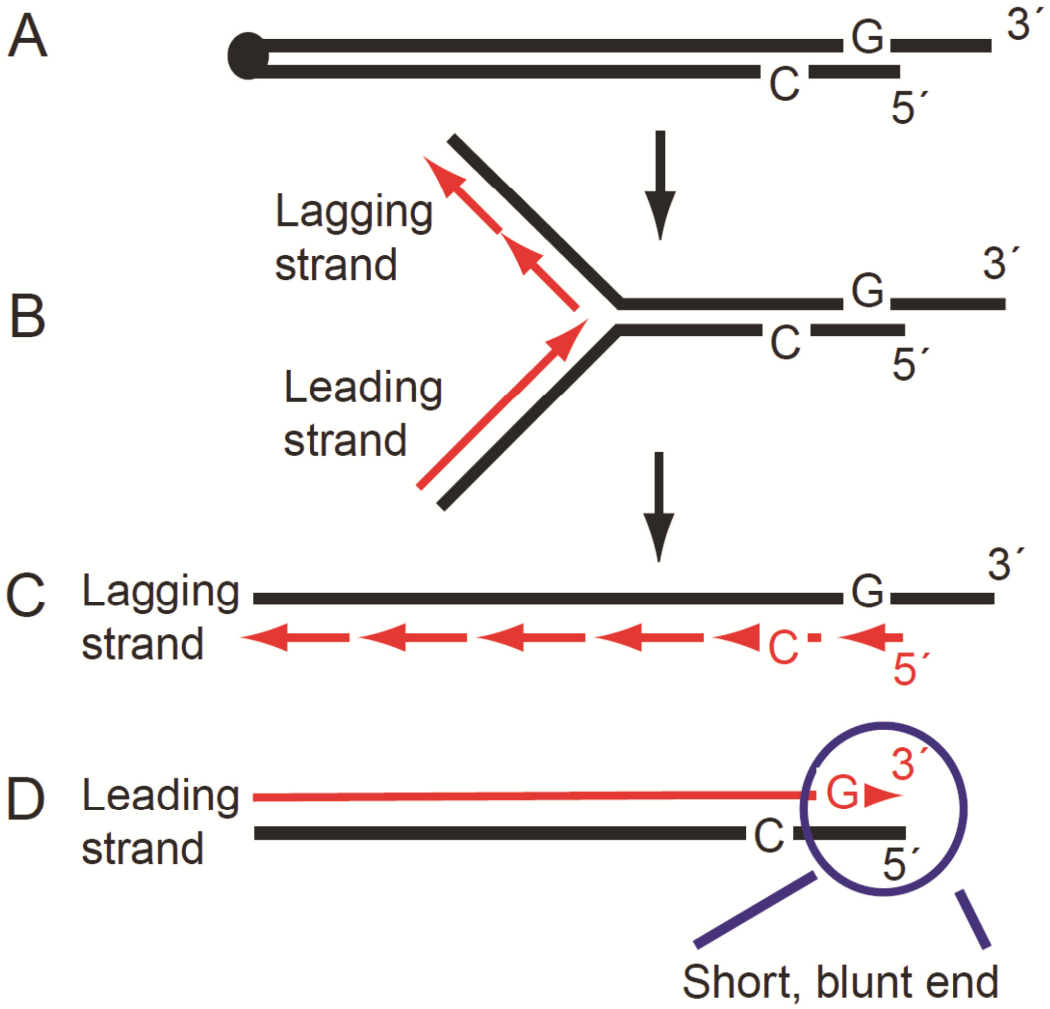


**Figure 1. Telomere replication**

Figure and text adapted from Figure 2 (Lydall, 2003).

(A) Telomeres in all organisms contain a short 3' overhang on the G rich strand.

(B) A replication fork moving towards the end of the chromosome.

(C) The newly replicated, lagging C strand, will generate a natural 3' overhang when the RNA primer is removed from the final Okazaki fragment, or if the lagging strand replication machinery cannot reach the end of the chromosome. In the absence of nuclease activity the unreplicated 3' strand will be the same length as it was prior to replication. (D) The newly replicated leading G strand will be the same length as the parental 5' C strand, and blunt ended if the replication fork reaches the end of the chromosome. Therefore the newly replicated 3' G strand will be shorter than the parental 3' strand and unable to act as a substrate for telomerase because it does not contain a 3' overhang. If the leading strand replication fork does not reach the end of the chromosome a 5' rather than 3' overhang would be generated, but this would not be a suitable substrate for telomerase.

## 1.5 Telomere binding proteins in budding yeast

Telomeres resemble DSBs and in order not to be recognised as such, are bound by multiple protein complexes (Eckert-Boulet and Lisby, 2010, Kobayashi, 2011). Telomere-binding proteins are required for telomere maintenance and inhibition of DNA-damage responses, such as checkpoint pathways, homologous recombination and non-homologous end joining (de Lange, 2009). Telomere structure is conserved in eukaryotes, and analogous protein complexes exist from budding yeast to humans (Fig. 2). Telomeric DNA in budding yeast is bound by the CST (Cdc13-Stn1-Ten1), Yku (Yku70-Yku80) and Rap1-Rif1-Rif2 complexes (Gilson et al., 1993, Boulton and Jackson, 1996, Porter et al., 1996, Pennock et al., 2001). Since my work concerns *cdc13-1* and *yku70*Δ strains, I will describe only the CST and Yku complexes.

### *1.5.1 CST complex*

Cdc13, together with Ten1 and Stn1, forms the heterotrimeric CST complex which exhibits telomere capping features (Fig. 3) (Pennock et al., 2001, Anbalagan et al., 2011, Churikov et al., 2013). In budding yeast the CST complex, like other telomeric complexes, protects telomeres from being processed as DSBs (Garvik et al., 1995, Surovtseva et al., 2009). Cdc13, Stn1 and Ten1 localize to chromosome ends by binding to the G-rich ssDNA (Nugent et al., 1996, Taggart et al., 2002). Yeast Stn1 and Ten1 contribute to the telomere capping role of Cdc13, and depletion of any subunit of the complex results in extensive C-strand degradation and cell cycle arrest (Weinert and Hartwell, 1993, Garvik et al., 1995, Grandin et al., 2001). Ten1 prevents accumulation of ssDNA at telomeres by limiting degradation of the 5' end by Exo1 (Xu et al., 2009). Stn1 interacts with Ten1 by its N-terminus (Puglisi et al., 2008), and competes with Est1 for binding to Cdc13, thus negatively regulates telomerase (Chandra et al., 2001, Puglisi et al., 2008). Cdc13, on the other hand, recruits telomerase to telomere ends (Chandra et al., 2001). Stn1 and Cdc13 have affinity to DNA polymerase α, allowing CST complex to mediate C-strand fill-in at the telomere end (Grandin et al., 1997, Puglisi et al., 2008).

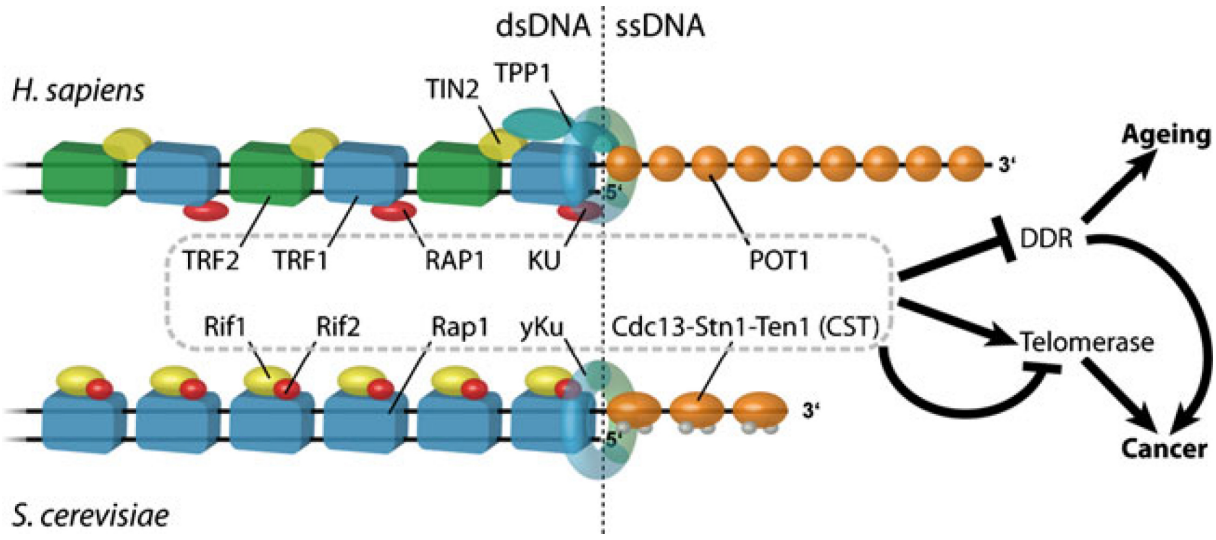


**Figure 2. The telomere cap is evolutionarily conserved**

Figure and text adapted from Figure 1 (Dewar and Lydall, 2012a).

Telomeres are nucleoprotein caps present at the ends of most eukaryotic chromosomes, consisting of dsDNA with a ssDNA overhang, bound by dsDNA- and ssDNA-binding proteins. Collectively, the telomere binding proteins “cap” the telomere and serve to regulate telomerase activity and inhibit the DDR. In budding yeast, the telomeric dsDNA is bound by Rap1, which recruits the accessory factors Rif1 and Rif2. In humans, the telomeric dsDNA is bound by TRF1 and TRF2 (held together by TIN2) and TRF2 recruits RAP1 to telomeres. In budding yeast, Cdc13 binds the telomeric ssDNA and recruits Stn1 and Ten1 to form the CST complex, while in humans, the telomeric ssDNA is bound by POT1. In human beings, POT1 and TRF1–TRF2–TIN2 are linked together by TPP1, which may permit the adoption of higher-order structures. In both budding yeast and humans, the Ku complex, a DDR component that binds to both telomeres and DSB, also binds and plays a protective role.

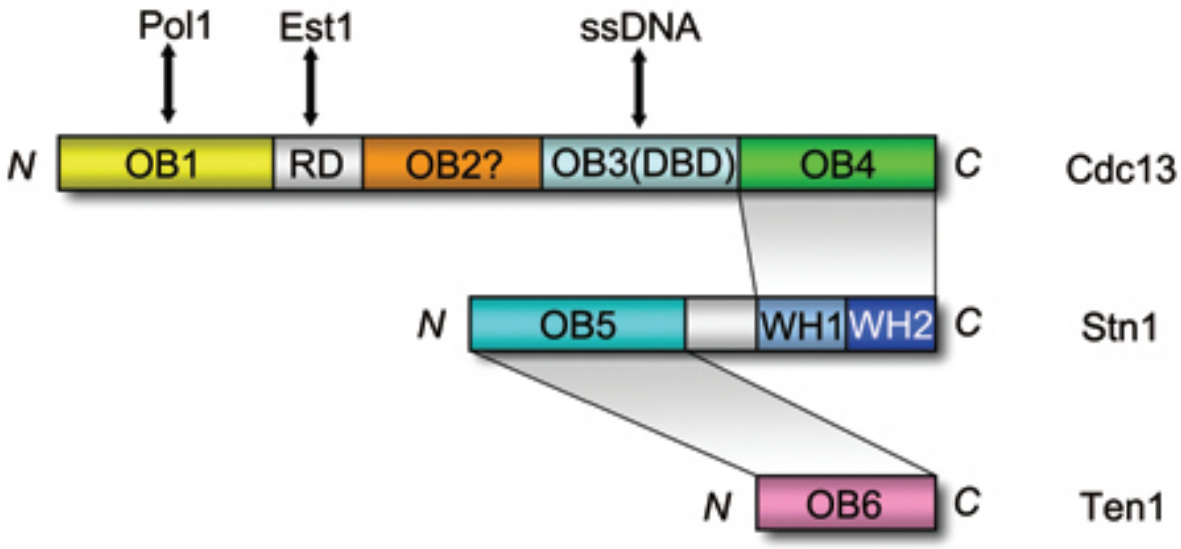


**Figure 3. Domain organization of the CST**

Figure and text adapted from Figure 1, upper panel (Sun et al., 2011b).

The CST complex. In Cdc13 the four OB folds from the N- to C-terminus, are colored in yellow, orange, light blue, and green, respectively. The RD domain between the first and second OB folds in Cdc13 is colored in gray. In Stn1 the OB folds are colored in cyan, the WH1 motif of Stn1 in marine, and the WH2 motif of Stn1 in blue. Ten1 is colored in pink. The shaded areas are used to indicate the interdomain interactions among the components within the complex. OB -oligonucleotide/ oligosaccharide binding; RD – telomerase recruitment domain; WH - winged helix–turn–helix motif.

The CST complex shows structural similarity to RPA, another heterotrimeric complex that binds ssDNA with high affinity (Wold, 1997), and is essential for chromosomal DNA replication, repair and recombination, as well as in DNA damage signaling in eukaryotic cells (Wold, 1997, Yuzhakov et al., 1999, Binz et al., 2004). In mammals the CST (CTC1, STN1 and TEN1) complex is important for telomere maintenance and replication, but not for telomere protection (Miyake et al., 2009). The shelterin capping complex, composed of TRF1, TRF2, POT1, RAP1, TIN2 and TPP1 proteins, is responsible for protecting telomeres in mammals

### *1.5.2 Ku heterodimer*

Yeast heterodimeric Yku complex consists of two protein subunits, Yku70 and Yku80, and plays a role in telomere protection (Cosgrove et al., 2002). Yku affects telomerase function at telomeres by recruiting Est1 and Est2 to telomeres during S-phase, which suggest its role in telomere length maintenance (Stellwagen et al., 2003, Bianchi and Shore, 2008, Hass and Zappulla, 2015). The heterodimer has a ring-like conformation, so it can easily wrap around DNA (Fig. 4) (Walker et al., 2001, Balestrini et al., 2013). Yku has the affinity to double-stranded DNA (dsDNA) and inhibits resection by Exo1 at DSBs and telomeres, as its depletion increases the ssDNA telomeric overhangs formation (Maillet et al., 2001, Maringele and Lydall, 2002, Sun et al., 2011a). The Yku complex is also an important component of Non Homologous End Joining (NHEJ) repair pathway; it stabilizes DNA ends for ligation and recruits crucial proteins to DSBs (Daley et al., 2005, Clerici et al., 2008). There is evidence for two pools of Yku complexes in a cell, one binding directly to telomeric DNA in a mode similar to NHEJ, and one being associated with telomeric chromatin via Yku80-Sir4 interaction (Martin et al., 1999, Roy et al., 2004).

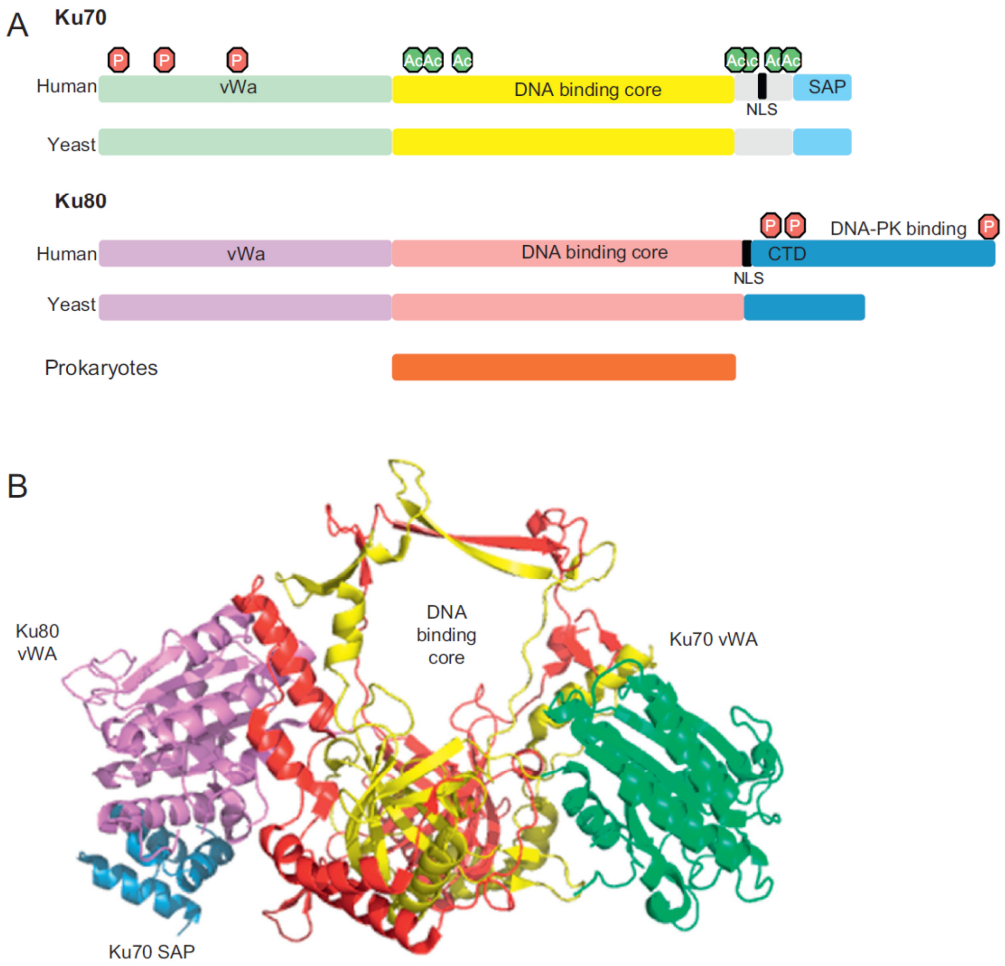


**Figure 4. Representation of yeast and human Ku structure**

Figure and text adapted from Figure 1 (Fell and Schild-Poulter, 2015).

(A) Schematic diagram of domain representation of the Ku70 and Ku80 subunits. The subunit domain structure of yeast and human Ku consists of the alpha helix, beta barrel N-terminal vWA domain, a central DNA binding core and a C-terminal helical domain (CTD). The eukaryotic Ku80 CTD contains the region required for binding DNA-PKCS, while the Ku70 CTD is shorter and contains a SAF-A/B, Acinus and PIAS domain (SAP). The location of the nuclear localization signals and post translation modifications (phosphorylation and acetylation) on the human Ku protein is indicated. Yeast Ku is comprised of a similar domain structure to human Ku, except for a truncated C-terminal domain in Ku80. Prokaryotes encode for a single Ku subunit that is homologous to the eukaryotic core DNA binding domain.

(B) The crystal structure of human Ku colored according to the domain structure. The dimer forms an asymmetrical basket structure with a positively charged ring large enough to accommodate two turns of the DNA. The Ku80 C-terminus is not included in this crystal structure.

### *1.5.3 Uncapped telomeres – cdc13-1 and yku70*Δ

Short 3' ssDNA overhangs can be found at sites of DNA damage as well as at telomeres. Although ssDNA generated as a result of DNA damage induces DNA repair pathways, at telomeres repair events are prevented. Telomeres are protected from being recognized and treated as DSBs by telomere binding proteins (de Magalhaes, 2004, Longhese et al., 2010). Telomere "uncapping", induced by inactivation of any subunit of telomere binding complexes, results in changes in telomere length, resection of telomeric DNA and chromosome fusions, consequently leading to cell cycle arrest, activation of DDR and senescence (Blasco, 2007, Lydall, 2009).

Budding yeast Cdc13, a member of the CST complex, is an essential protein. One of the most studied mutations of *CDC13* is the temperature sensitive *cdc13-1* allele. *cdc13-1* mutants are functional at 23°C (permissive temperature), but gradually lose growth ability above 26°C (Weinert and Hartwell, 1993). At higher temperatures *cdc13-1* strains have dysfunctional, uncapped telomeres and accumulate 3' ssDNA overhangs that become RPA bound on the 3' G-tail. The Mec1-dependent checkpoint pathway is activated through interaction with DNA-bound RPA, resulting in cell cycle arrest in G2 phase of the cell cycle (Fig. 5) (Garvik et al., 1995, Lydall and Weinert, 1995). Rad24, a member of a sliding clamp complex, loads the 9-1-1 checkpoint clamp to the site of DNA damage (Majka and Burgers, 2003). *RAD24, RAD17, MEC3* and *DDC1* are termed the *RAD24* group because deleting any or all of these genes results in similar checkpoint and DNA damage sensitivity phenotypes (Lydall and Weinert, 1995). Rad24 contributes to ssDNA generation in *cdc13-1* mutants through regulation of nuclease activities (Lydall and Weinert, 1995, Zubko and Lydall, 2006). Deletion of *RAD24* improves growth of *cdc13-1* strains at 27-28°C (Lydall and Weinert, 1995, Zubko et al., 2004). Exo1 is also responsible for ssDNA generation in *cdc13-1* mutants, and when deleted, levels of ssDNA are reduced and growth of *cdc13-1* at 27°C is improved (Tsubouchi and Ogawa, 2000, Zubko et al., 2004). Rad9, a checkpoint mediator protein in a Mec1-dependent pathway, inhibits production of ssDNA in *cdc13-1* mutants (Lydall and Weinert, 1995, Zubko and Lydall, 2006). Deletion of *RAD9* improves *cdc13-1* growth, presumably because cells cannot signal the presence of ssDNA at telomeres when checkpoint is defective (Weinert and Hartwell, 1993, Zubko et al., 2004).

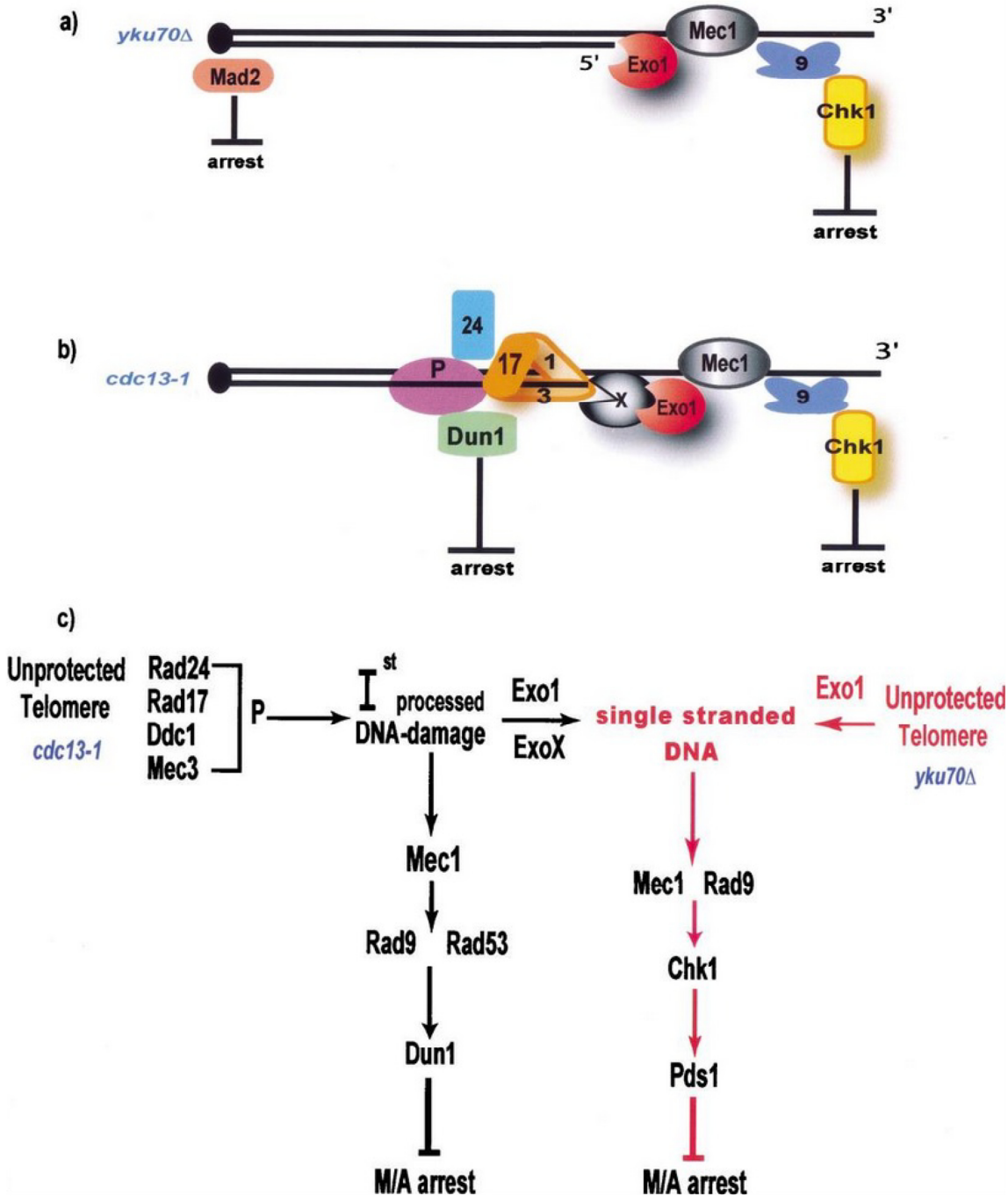
a)
yku70Δ
Mad2
arrest
5'
Exo1
Mec1
3'
9
Chk1
arrest
b)
cdc13-1
24
P
17
1
3
X
Exo1
Mec1
3'
9
Dun1
Chk1
arrest
arrest
c)
Unprotected
Telomere
cdc13-1
Rad24
Rad17
Ddc1
Mec3
P
1st
processed
DNA-damage
Exo1
ExoX
single stranded
DNA
Exo1
Unprotected
Telomere
yku70Δ
Mec1
Rad9
Rad53
Dun1
M/A arrest
Mec1
Rad9
Chk1
Pds1
M/A arrest

**Figure 5. A model for the roles of checkpoint proteins in responding to *cdc13-1* and *yku70*Δ-induced DNA damage**

Figure and text adapted from Figure 8; Figure description was taken from text on p1928 (Maringele and Lydall, 2002).

(*a*) A representation of the proteins that are responsible for the arrest of *yku70*Δ mutants. (*b*) A representation of proteins that are responsible for the arrest of *cdc13-1* mutants. (*c*) A schematic model of the DNA damage checkpoint pathways responsible for metaphase/anaphase arrest of *cdc13-1* and *yku70*Δ mutants. According to this model, in *cdc13-1* mutants, unprotected telomeres are perceived as DSB with a short 3' overhang. The Rad24p/Rfc2-5p clamp loader complex (Green et al., 2000) recognizes this structure and loads the Ddc1p, Mec3p, Rad17p sliding clamp (Venclovas and Thelen, 2000). The sliding clamp tethers an unknown protein, "P" (e.g., a helicase), which processes the telomeric termini to generate the "1$^{st}$ processed DNA damage". The "1$^{st}$ processed DNA damage" is the substrate that activates a Mec1p/Rad53p/Dun1p-dependent checkpoint pathway. Rad9p might also participate in Rad53p activation (Gilbert et al., 2001). Rad53p and Dun1p are known to be responsible for 50 % of the arrest observed in *cdc13-1* mutants (Gardner et al., 1999). We suggest that protein "P" is then replaced by Exo1p and by another 5 to 3 exonuclease ExoXp, which have affinity for the "1$^{st}$ processed DNA damage." The ssDNA generated by Exo1p and ExoXp activates a Rad9p/Mec1p/Chk1p- and Pds1p-dependent pathway. Chk1p/Pds1p are required for 50 % of the arrest observed in *cdc13-1* mutants. Thus, together Rad53p/Dun1p and Chk1p/Pds1p pathways are responsible for 100 % arrest of *cdc13-1* cells (Gardner et al., 1999, Sanchez et al., 1999). In *yku70*Δ mutants, unprotected telomeres are also perceived as DSB with a short 3' overhang. But in cells lacking Yku70p, Exo1p can be recruited independently of Rad24p and the Rad17p, Mec3p, Ddc1p sliding clamp. Exo1p generates ssDNA that activates the Rad9p/ Mec1p/Chk1p- and Pds1p-dependent checkpoint pathway. In *yku70*Δ mutants, this checkpoint pathway is responsible for the arrest of 75 % of cells, and together with a MAD2-dependent pathway, results in arrest of 95 % of cells.

Elimination of any subunit of Yku complex results in telomere shortening and temperature sensitive growth at high temperatures. *yku70*Δ mutants grow well at 30°C (permissive temperature), but are unable to form colonies at 37°C (Feldmann and Winnacker, 1993). Telomeres became uncapped and the resection occurs followed by ssDNA accumulation and cell cycle arrest (Maringele and Lydall, 2002, Zubko et al., 2004). Rad9 is required for efficient cell cycle arrest of *yku70*Δ mutants at non-permissive temperature (Maringele and Lydall, 2002). However in cells lacking Yku70, Exo1 can be recruited to damage telomeres independently of Rad24, Ddc1, Rad17 and Mec3, and generates ssDNA that activates Rad9/Mec1/Chk1-dependent checkpoint pathway (Maringele and Lydall, 2002).

### 1.6 DNA Damage Response (DDR)

For each cell it is essential to preserve genomic stability for proper cell functioning and transmission of genetic material to the progeny. However, DNA lesions occur frequently in chromosomal DNA as an effect of exogenous (e.g. ionizing radiation or genotoxic chemicals) and endogenous (e.g. replication errors or free radical species) DNA damaging factors (Eckert-Boulet and Lisby, 2010). Structural changes of DNA may affect the function of key genomic processes, such as transcription and replication, and play a major role in age-related diseases and cancer (Hoeijmakers, 2001, Hoeijmakers, 2009, Giglia-Mari et al., 2011). Therefore cells have evolved a sophisticated network of DDR systems, including DNA repair mechanisms, cell-cycle checkpoints and damage tolerance processes (Giglia-Mari et al., 2011). In response to genomic insults that are too severe, the cell cycle arrest might be activated, leading to senescence or apoptosis (Polo and Jackson, 2011, Finn et al., 2012).

Cellular DNA damage repair mechanisms include: Base Excision Repair (BER) pathway, which corrects small base lesions that do not significantly distort DNA structure (Wallace et al., 2012, Krokan and Bjoras, 2013), Nucleotide Excision Repair (NER) pathway, which removes single-strand lesions that cause local helix destabilization (Scharer, 2013, Marteijn et al., 2014) and DNA Double-Strand Break Repair (DSBR), which mediates the repair of the most deleterious form of DNA damage (Chapman et al., 2012). Since I studied yeast with uncapped telomeres which resemble a DSB, I will describe in details the mechanism of DSB repair.

### *1.6.1 Double Strand Break Repair – HR and NHEJ*

Two most prominent DSBs repair mechanisms are homologous recombination (HR) and NHEJ (Fig. 6). HR is considered high-efficient and more accurate, because genetic information is copied directly from a homologous DNA template (Fig. 6a) (Kadyk and Hartwell, 1992, Guirouilh-Barbat et al., 2014). In yeast HR can take place between sister chromatids, between alleles on homologous chromosomes in a diploid cell or between non-allelic homologous sequences (Ira et al., 2004, Barzel and Kupiec, 2008, Jasin and Rothstein, 2013). While hundreds of nucleotides are required for HR, a few tens of nucleotides are sufficient for microhomology mediated end joining (MMEJ), an alternative NHEJ pathway (Betermier et al., 2014). The cell cycle can also affect the DSBs repair pathway choice – while HR is active in S and G2 phases, NHEJ is active throughout the cell cycle (Guirouilh-Barbat et al., 2008). In haploid cells NHEJ is critical in G1 cells and stationary phase cells, due to the lack of the homologous chromosome template (Lieber, 2010).

The initial step of HR involves the 5’ to 3’ resection of the DSBs to produce a ssDNA 3’ overhang. The ssDNA overhang is important both for Mec1 checkpoint kinase association and for Rad51 recombination protein loading (Ira et al., 2004). The DSBs ends of sister chromatids are recognized by the MRX complex (Mre11-Rad50-Xrs2; in humans MRN, MRE11-RAD50-NBS1) (Pfeiffer et al., 2000, Zhou et al., 2014). Mre11 component of the MRX complex has a 3’ to 5’ exonuclease and DNA structure-specific endonuclease activities, and is involved in the formation of 3’ overhang at DSBs (Paull and Gellert, 1998, D'Amours and Jackson, 2002). The function of the MRX complex depends on the Sae2 protein in the initial resection of approximately 100 nt 5’ end DNA (Mimitou and Symington, 2008). Exo1, which possesses 5’ to 3’ dsDNA exonuclease and 5’ flap-endonuclease activities, participates in HR, and has also roles in DNA damage signalling and telomere maintenance (Tran et al., 2004). Exo1 is involved in more extensive resection of DSB ends that have been initially processed by MRX-Sae2 (Zhu et al., 2008). Dna2, a 5’ flap endonuclease and DNA helicase which forms a complex with Sgs1 helicase, acts redundantly with Exo1 in DSB ends resection (Mimitou and Symington, 2008, Symington and Gautier, 2011, Cannavo and Cejka, 2014).

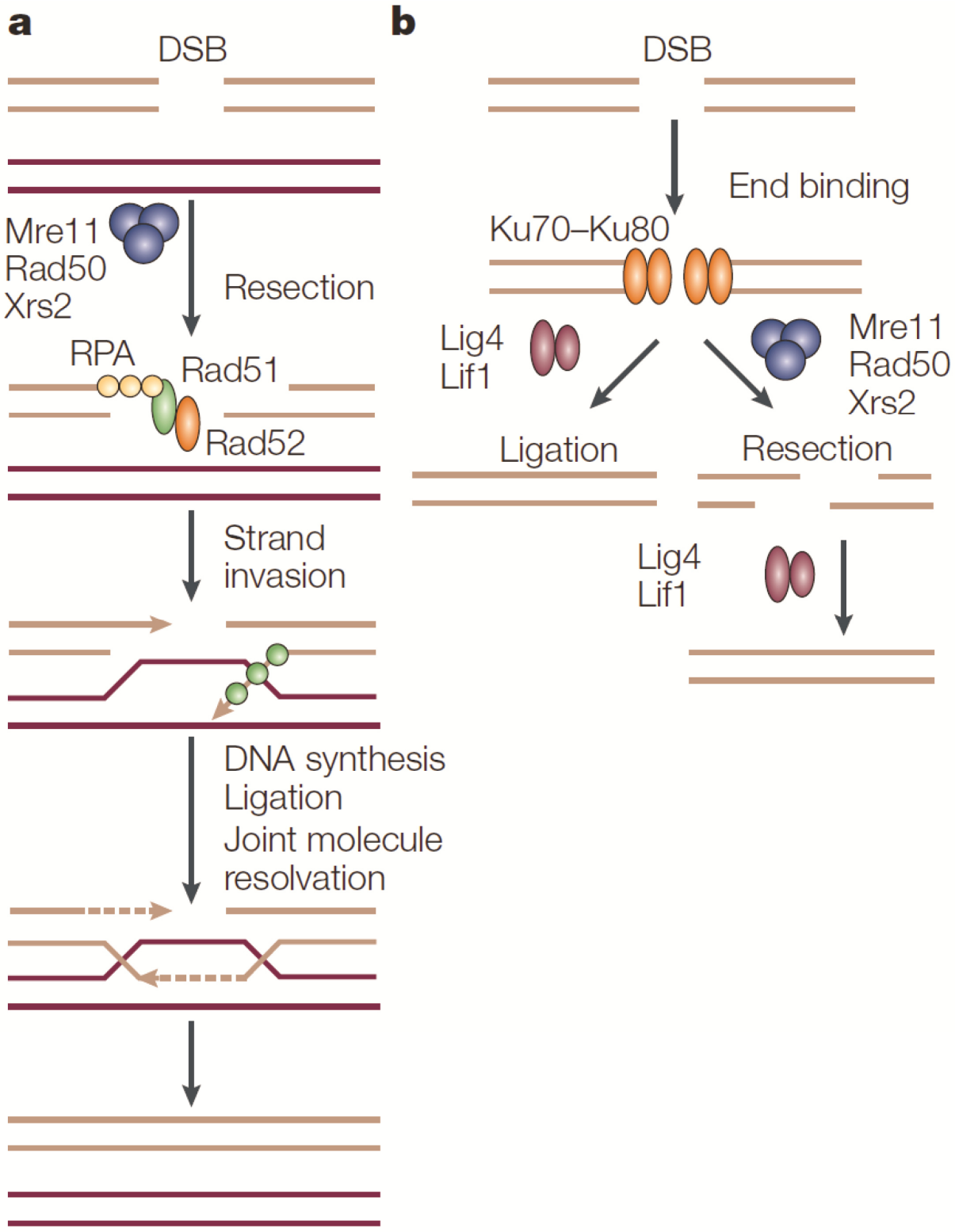
a
DSB
Mre11
Rad50
Xrs2
Resection
RPA
Rad51
Rad52
Strand
invasion
DNA synthesis
Ligation
Joint molecule
resolvation
b
DSB
End binding
Ku70–Ku80
Lig4
Lif1
Mre11
Rad50
Xrs2
Ligation
Resection
Lig4
Lif1

**Figure 6. Pathways for DNA double strand break repair**

Figure and text adapted from Box1, (van Attikum and Gasser, 2005).

A DNA double strand break (DSB) can be repaired by homologous recombination (HR, a) or nonhomologous end joining (NHEJ, b).

a) HR: When a DSB occurs in one of two sister chromatids, the ends of the DSB are recognized by the Mre11–Rad50–Xrs2 (MRX) complex (or Mre11–Rad50–Nbs1 (MRN) complex in mammals). Processing of the ends occurs by the MRX complex and results in the formation of 3′ single stranded (ss) DNA overhangs. The ssDNA-binding protein replication protein A (RPA) binds to the ssDNA overhangs, and Rad51 and Rad52 are recruited to the DSB. Both RPA and Rad52 help to load Rad51 onto ssDNA to form ssDNA–Rad51 nucleoprotein filaments. This nucleoprotein filament searches for the homologous duplex DNA in the undamaged sister chromatid. A successful search results in strand invasion, strand exchange and joint molecule formation. In yeast, these events are facilitated by one or more proteins from the Rad52 epistasis group, which, as well as Rad51, Rad52 and MRX, includes Rad54, Rad57 and Rad59. In mammals, these events involve the action of BRCA1, BRCA2 and the Rad51-like proteins XRCC2, XRCC3, RAD51B, RAD51C and RAD51D. DNA synthesis by DNA polymerases generates the genetic information that is required to seal the break. Ligation and the resolution of the two double helices joined by strand exchange complete this **“**error-free” repair event.

b) NHEJ: The ends of a DSB are detected and bound by KU, a heterodimer consisting of Ku70 and Ku80 proteins. In mammals, KU forms a complex, known as DNA-PK, with DNA-PK catalytic subunit (DNA-PKcs). It is thought that KU holds the two ends together and facilitates end-to-end ligation by the complex of ligase 4 (Lig4) and ligase-interacting factor 1 (Lif1) in yeast (or XRCC4 in mammals), which usually results in accurate repair of the DSB (left branch of pathway). Alternatively, binding of the ends by KU can be followed by resection of the free ends by the MRX (or MRN) complex. Processing by MRX, followed by Lig4–Lif1-mediated ligation (Lig4–XRCC4 in mammals) has been implicated in the joining of ssDNA overhangs at regions where microhomology exists. This pathway generally leads to “error-prone” repair of the DSB (right branch of pathway).

The ssDNA resulting from the nuclease activities at DSBs is coated by Rad51 and forms a filament structure which then invades a template DNA to initiate synthesis (Li and Heyer, 2008). Rad51, a DNA-dependent ATPase, catalyses the reaction of homology search and DNA strand invasion during HR. In the nucleus, ssDNA is bound by ssDNA-binding replication protein A (RPA), which has higher affinity and specificity for ssDNA than Rad51 (Sung and Klein, 2006). The formation of Rad51 filaments on RPA-coated ssDNA is facilitated by mediator proteins which displace RPA from DNA: Rad55-Rad57 complex and Rad52 (Sung, 1997, Shinohara et al., 1998, Sugawara et al., 2003). Rad52 interacts with Rad51 and RPA, and accelerates displacement of RPA from DNA by Rad51 (Sugiyama and Kowalczykowski, 2002). The Rad51-ssDNA filament can then pair with the undamaged homologous duplex, if such homologous donor sequence has been found (Heyer et al., 2010). A structure known as D-loop (displacement loop) is formed between the target DNA and Rad51 filament, and DNA synthesis is primed from the 3' end (Renkawitz et al., 2014). The repair event is completed by DNA polymerases and ligases (van Attikum and Gasser, 2005).

In the NHEJ pathway DSB ends are joined in a less accurate manner than HR (Fig. 6b) (Daley et al., 2005). After DSBs formation the MRX complex is recruited to DNA to promote tethering of broken DNA ends together (Chen et al., 2001a, Lewis et al., 2004). The joining reaction includes recognition of broken ends by the Ku complex, followed by re-ligation (Fig. 6b, left panel) (Daley et al., 2005). The Ku complex, a DNA binding heterodimer consisting of Yku80 and Yku70, forms a β-barrel ring structure which binds DNA by slipping the DSB end through the ring (Walker et al., 2001). DNA binding by Ku may serve as a site for binding of other NEHJ proteins, e.g. Yku80 utilises the contact with Dnl4, a component of DNA ligase IV (Palmbos et al., 2008). The Ku complex also promotes NHEJ by inhibiting DNA resection (Downs and Jackson, 2004, Eckert-Boulet and Lisby, 2010).

DNA ends may be altered prior to ligation by removal of damaged nucleotides, and addition or removal of undamaged nucleotides (van Attikum and Gasser, 2005). Such alternative end joining, referred to as a microhomology-mediated end joining (MMEJ, Fig. 6b, right panel), is initiated by DNA resection due to the MRX and Sae2 nuclease activities, and is followed by DNA ligation (Lee and Lee, 2007).

### 1.7 Mec1-dependent cell cycle checkpoint

The cell cycle consists of DNA synthesis (S) and mitosis (M) phases, separated by gap phases, G1 and G2. The cell cycle progression is driven by the cyclin-dependent serine/threonine protein kinases (CDKs) and their regulatory subunits (cyclin); budding yeast have only one essential cyclin-dependent kinase Cdk1. CDKs phosphorylate key substrates to regulate different cell cycle events: progression through G1 phase and commitment to S phase; initiation and completion of DNA replication, enter into mitosis and restrain re-entry into G1 phase (Barnum and O'Connell, 2014).

The cell cycle checkpoints are signalling pathways that ensure the successful completion of preceding phases of the cell cycle, by controlling e.g. the cell size, DNA damage response, DNA replication or mitotic spindle checkpoint activation (Rhind and Russell, 2012, Barnum and O'Connell, 2014). DNA damage, resulting from e.g. intermediates of metabolism or attrition of telomeres, activates a signalling network that arrests the cell cycle by inactivating CDKs (Zhou and Elledge, 2000). The cell cycle arrest allows time for repair in order to enter the next phase of the cell cycle (Barnum and O'Connell, 2014). However, if the damage is too severe and cannot be repaired, cells may initiate cellular senescence, a naturally irreversible cell-cycle arrest that is induced by DNA damage response signalling. Alternatively, cells undergo programmed cell death (apoptosis) (Harper and Elledge, 2007, d'Adda di Fagagna, 2008).

Activation of DNA damage checkpoints is controlled by apical protein kinases that are members of phosphatidylinositol 3-kinase-related kinases (PIKKs) family. Tel1 and Mec1 are part of the PIKK family in *S. cerevisiae*, and orthologues of Tel1 and Mec1 in mammals are ATM (Ataxia Telangiectasia Mutated) and ATR (ATM and Rad3-related), respectively (Ritchie et al., 1999, Falck et al., 2005, di Domenico et al., 2009, Navadgi-Patil and Burgers, 2009). Tel1 functions in response to DSBs through the MRX complex. Mec1 is activated by its recruitment to RPA-coated ssDNA followed by replication stress or resection at DSBs (Puddu et al., 2008, Zeman and Cimprich, 2013). In budding yeast Tel1 plays a major role in telomere maintenance, whereas Mec1 is the principle kinase responsible for checkpoint

activation in response to replication stress and DNA damage, but also may participate in short telomere protection (di Domenico et al., 2009).

In this thesis I focused on the Mec1-dependent checkpoint pathway. Mec1 is the principle kinase responsible for checkpoint activation in *S. cerevisiae*, and together with Ddc2 (ATRIP, ATR-Interacting Protein in humans) forms a heterodimeric complex (Paciotti et al., 2000). In the Mec1-Ddc2 complex, Mec1 is the catalytic subunit required for checkpoint activation, and Ddc2 is the regulatory subunit responsible for binding to DNA by interacting with RPA (Zou and Elledge, 2003). Independently the heterotrimeric checkpoint clamp 9-1-1 is loaded onto RPA-coated ssDNA by the clamp loader Rad24-RFC, and may recruit Dpb11 (human TopBP1) (Navadgi-Patil and Burgers, 2011). Activation of Mec1 induces Mec1-dependent phosphorylation of many downstream proteins, including effector kinases like Chk1 and Rad53 in *S. cerevisiae* (in humans CHK1 and CHK2, respectively). Initially activated Rad53 undergoes autophosphorylation and promotes activation of the mediator protein, Rad9 or Mrc1 (53BP1, BRCA1, MDC1 or Claspin in humans). Mediator proteins regulate effector kinases and mediate the phosphorylation of target proteins, contributing to activation of downstream pathways, including cell cycle arrest (Harper and Elledge, 2007, Navadgi-Patil and Burgers, 2009, Finn et al., 2012).

Loading of the Mec1-Ddc2 complex onto RPA-coated ssDNA is not sufficient for Mec1 activation. Three sensors, Ddc1, Dpb11 and Dna2 (RAD9, TopBP1, DNA2 in humans, respectively) transduce the DNA damage response signal to Mec1 stimulating its kinase activity. In budding yeast, all three checkpoint initiators interact with and likely activate Mec1, since each contains an AAD domain, the homologous motif of ATR activation domain in mammals, that interacts directly with the Mec1-Ddc2 complex (Kumar and Burgers, 2013, Zhou et al., 2013).

### *1.7.1 Ddc1 (DNA damage checkpoint protein)*

The 9-1-1 complex consists of Ddc1-Mec3-Rad17 and is required for Mec1 checkpoint activation (Davies et al., 2010). The complex shares homology of structure to proliferating-cell nuclear antigen (PCNA) which clamps onto DNA and confers processivity to DNA polymerases δ and ε (Venclovas and Thelen, 2000,

Hong and Roeder, 2002). In *S. cerevisiae*, the 9-1-1 checkpoint clamp functions in two pathways. First, Ddc1 directly activates the Mec1 kinase dependently on two conserved aromatic amino acids, tryptophans W352 and W544. Second, Ddc1 recruits Dpb11 to Mec1 through conserved Ddc1-T602 residue. Substitution of three residues into alanine, W352A, W544A and T602A, results in defective G2/M checkpoint, as Ddc1 is not able to stimulate Mec1 and recruit Dpb11 (Navadgi-Patil et al., 2011, Kumar and Burgers, 2013). The stimulatory activity of Ddc1 is located in the C-terminus, where localised are three residues that are target sites for cyclin-dependent kinase (Cdk) phosphorylation, and eight residues that are target sites for Mec1 phosphorylation (Puddu et al., 2008). Conversion of phosphorylatable residues into alanine in *ddc1-M8* mutant lacking Mec1 target sites, and in *ddc1-M11* mutant lacking Cdk and Mec1 target sites, results in loss of DNA damage-dependent phosphorylation of Ddc1 by Mec1 or Mec1 and Cdk1, respectively (Puddu et al., 2008).

### *1.7.2 Dpb11 (DNA polymerase B (II))*

Dpb11 is a DNA replication initiation protein which loads DNA pol ε onto pre-replication complexes at origins of replication. Dpb11 is also recruited to stalled replication forks by the 9-1-1 complex in order to activate Mec1 (Zegerman and Diffley, 2007). The interaction with Ddc1 involves the distal BRCT domain of Dpb11 and Ddc1-T602 residue (Puddu et al., 2008). Dpb11 plays an important role in three aspects of checkpoint signalling: cell-cycle regulation, mediator recruitment and the Mec1 kinase activation. Activation of Mec1 requires the T731 residue considered to be part of AAD (ATR activation domain) (Pfander and Diffley, 2011, Zhou et al., 2013). Human orthologue of Dpb11, TopBP1, was found to recruit topoisomerase TOP2A to anaphase bridges, which indicates the importance ofTopBP1 in maintaining the genome stability (Broderick et al., 2015).

### *1.7.3 Dna2 (DNA synthesis defective)*

Yeast *DNA2* encodes a conserved and essential helicase/nuclease which is involved in Okazaki fragment processing during DNA replication and DNA resection at DSBs (Mimitou and Symington, 2009, Hu et al., 2012). In mammalian cells DNA2 preferentially associates with telomeres during replication and has a role in

G-quadruplex DNA cleavage. Expression of *DNA2* is significantly increased in human cancers (Lin et al., 2013, Ronchi et al., 2013, Strauss et al., 2014).

Yeast Dna2 contains an unstructured N-terminal domain (NTD). The NTD of Dna2 is important for Mec1 kinase stimulation, and two residues present in this region, tryptophan W128 and tyrosine Y130, were suggested to significantly affect Mec1 stimulatory activity (Kumar and Burgers, 2013). It was shown that deletion of the N-terminal amino acids of Dna2 resulted in temperature-sensitive growth of mutant cells (Bae et al., 2001b). Moreover, Dna2 mutants lacking N-terminal domain are defective in S-phase checkpoint (Lee et al., 2013). Downstream of the nuclease active site, Dna2 contains four highly conserved cysteines which are likely part of a Fe-S cluster. Fe–S clusters have been identified as essential components of a wide variety of DNA and RNA processing enzymes (Pokharel and Campbell, 2012). Any disruptions of this cluster reduce nuclease and helicase activity of Dna2, indicating critical physiological role of the Fe-S cluster (Pokharel and Campbell, 2012). In yeast, *DNA2* deletion is lethal, but three mechanisms are known to suppress the lethality of *dna2*Δ: overexpression of *RAD27*, a nuclease involved in Okazaki fragment processing, deletion of *PIF1*, a helicase involved in long flap formation during DNA replication, or deletion of *RAD9*, a DNA damage checkpoint protein (Budd et al., 2006, Budd et al., 2011).

### 1.8 DNA replication

DNA replication is a biological process during which a genetic information of a cell is duplicated, so that one DNA copy can be passed to a new cell. DNA replication requires opening of DNA into two individual DNA strands to allow DNA polymerases access the DNA. DNA unwinding occurs at DNA replication origin sites and in eukaryotes requires the presence of the Origin Recognition Complex (ORC) that binds to DNA replication origins (Blow and Laskey, 1988) and two additional proteins, Cdc6 and Cdt1. The complex then allows recruitment of the replicative helicase, Mcm2-7. Six Mcm2-7 subunits form a complex with a central channel that encircles DNA; the helicase activity of Mcm2-7 complex is stimulated by association of Cdc45 and GINS proteins (Kanemaki and Labib, 2006, Ilves et al., 2010). The recruitment of GINS and subsequent formation of the replicative helicase complex (CMG; Cdc45-MCM-GINS) requires Sld2 and Sld3 (Tanaka et al., 2007, Zegerman and Diffley, 2007, Yeeles et al., 2015). CDK-phosphorylated proteins Sld2 and Sld3 bind to and

activate Dpb11. Activated Dpb11 provides the interaction between GINS and DNA polymerase, and allows the formation of the CMG complex (Fig. 7) (Yeeles et al., 2015).

DNA replication in yeast is carried out by three B family DNA polymerases: Pol α, Pol δ and Pol ε (Fig. 7) (reviewed in Burgers, 2009). Pol α contains a primase domain which initiates replication by generating short, 7-14 nt long RNA primers onto leading and lagging strands (Brooks and Dumas, 1989, Foiani et al., 1997). The RNA primers are extended in a 5′ to 3′ direction by Pol α. Pol α is displaced by RFC, which then loads the homotrimeric ring PCNA (Pol30 in budding yeast) around dsDNA at primer-template junctions and recruits Pol ε or Pol δ (Lovett, 2007, Burgers, 2009). Pol ε is required for GINS recruitment to origins and thus for CMG assembly. Pol ε then allows the incorporation of dNTPs continuously in the direction of DNA unwinding, which results in the leading strand synthesis (Miyabe et al., 2011, Pursell et al., 2007).

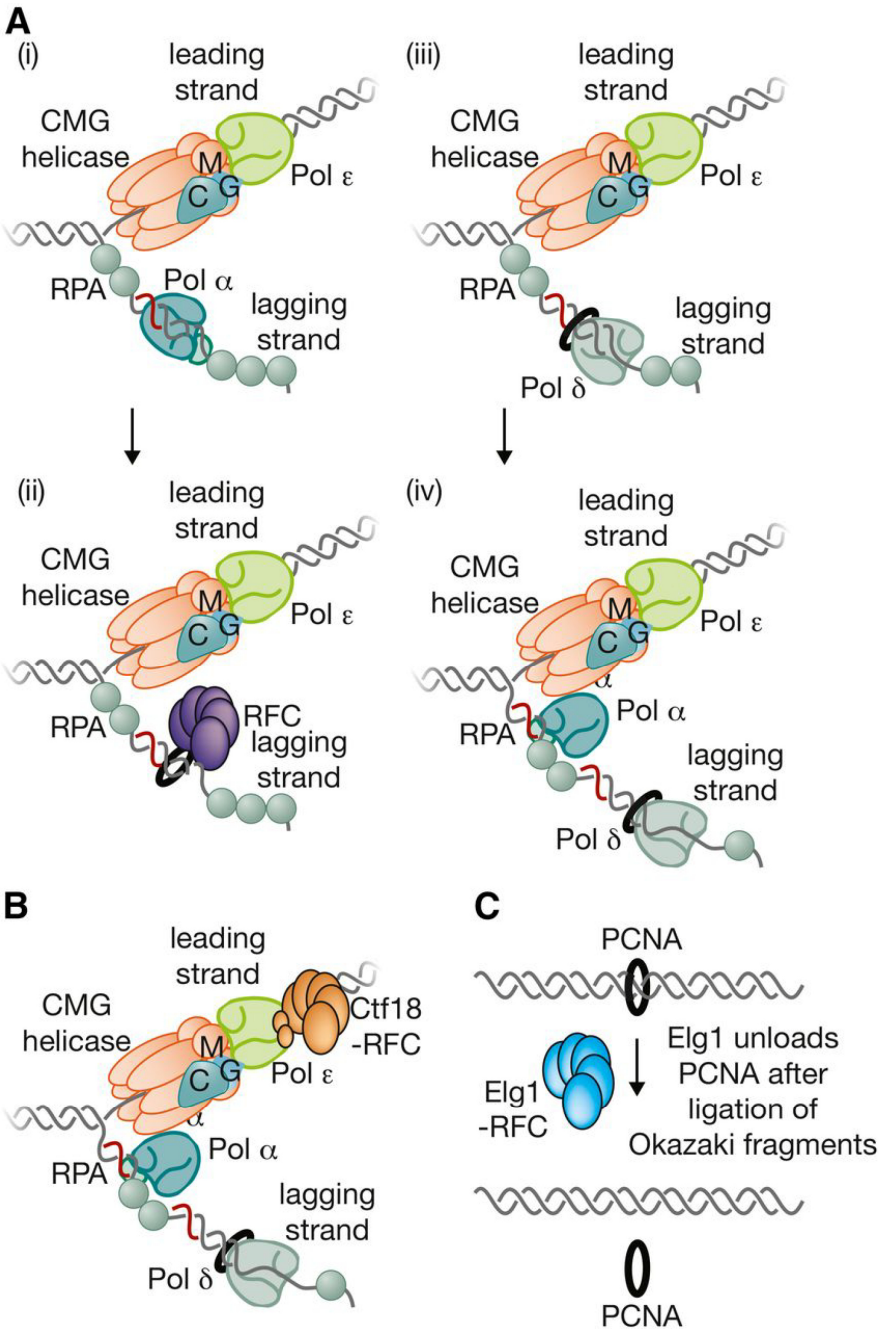


**Figure 7. Role of protein complexes at the yeast replication fork**

Figure and text adapted from Figure 8 (Bell and Labib, 2016).

(A) Pol α detaches from the template after synthesizing an RNA-DNA primer (i), and Rfc1-RFC is then very effective at competing for access to the 3′ end of the primer bound to template, leading to loading of PCNA around dsDNA (ii). This in turn leads to recruitment of Pol δ (iii), which then extends the new Okazaki fragment (iv). (B) Ctf18-RFC associates with Pol ε and might contribute to loading of PCNA onto the leading-strand side of the fork. (C) Elg1-RFC is recruited to PCNA (aided by sumoylation) after ligation of Okazaki fragments, leading to removal of PCNA from the replicated DNA.

On the lagging strand the Pol α/primase complex elongates RNA primers by addition of 10–20 dNTPs. Subsequently Pol α is displaced by Rfc1-RFC/PCNA, and Pol δ, recruited by PCNA, replicates the lagging strand in short, ~200 nt long segments called Okazaki fragments (Okazaki et al., 1968, Bambara et al., 1997, Maga et al., 2001, Burgers, 2009, Georgescu et al., 2014). Due to the repeated cycles of RNA priming by Pol α, lagging strand is coated with multiple PCNA rings, while this mechanism does not apply to the leading strand, where a single primer is extended from the origin continuously. The PCNA removal from nascent chromatin is critical to restore the pool of free PCNA for new replication forks or for DNA repair reactions. Elg1-RFC is recruited to PCNA after Okazaki fragments ligation, and removes PCNA from the replicated DNA (Fig. 7) (Kubota et al., 2013).

Rad27, flap endonuclease1 in yeast (FEN1 in mammals), removes RNA primers and short flaps arising in the replication of the lagging strand (Harrington and Lieber, 1995, Bambara et al., 1997, Shen et al., 2005). Exo1, a 5'-3' exonuclease, was proposed to take the role of flap processing in *rad27*Δ mutants (Lee and Wilson, 1999, Jin et al., 2003). The FEN1-dependent flap removal is conserved and deficiency of FEN1 causes severe developmental defects in mice (Zheng et al., 2007). Deletion of *RAD27* in yeast decreases the growth rate at 30°C and causes cell death at 37°C. *rad27*Δ cells display a mutator phenotype, likely due to the ligation of unremoved flaps downstream of the Okazaki fragments (Reagan et al., 1995, Tishkoff et al., 1997, Xie et al., 2001, Singh et al., 2007).

Pif1, a DNA helicase, promotes the generation of 30 nt long flaps which cannot be processed by Rad27 (Pike et al., 2009). ssDNA flaps attract RPA, which bind ssDNA and inhibit the activity of Rad27 (Bae et al., 2001a). DNA bounded RPA recruits Dna2, which contains nuclease, ATPase and helicase domains (Budd et al., 1995, Bae and Seo, 2000). Dna2 removes a portion of DNA within the long ssDNA flap, generating a shorter flap (Bae and Seo, 2000, Masuda-Sasa et al., 2006). The resulting short flap constitutes a substrate for Rad27 (Budd et al., 2011). Levikova and Cejka proposed however that Dna2, although incapable of cleaving solely short flaps, can be responsible for cleaving the RPA-bound long flaps entirely, which suggests a separate, Rad27 independent pathway of Okazaki fragment processing (Levikova and Cejka, 2015).

### 1.9 Hormesis and adaptation to low doses of stress

Humans' telomeres shorten with time, which leads to DNA damage accumulation and telomeric stress, resulting in cell cycle arrest and DNA damage response activation. Studies of the cellular responses to telomere damage or telomere shortening are important for understanding the basis of human aging, age-related diseases and cancer. Yeast studies presented in this thesis involve yeast strains with defective telomeres, like *cdc13-1*, and contribute to understanding of the responses to telomere stress.

In recent years multiple observations of positive effects of low dose stress (e.g. toxic compounds, temperature or caloric restriction) on organismal fitness were reported (Ermolaeva et al., 2013, Calabrese et al., 2015, Le Bourg, 2015). The phenomenon of positive role of small dose stress on organismal fitness, such as improved growth, longevity or fertility, is known today as "hormesis". The mechanisms of hormesis are not understood or well documented, but it is proposed that positive effects of low dose toxic treatment may be beneficial to cells and organisms (Calabrese and Baldwin, 2003, Calabrese, 2004, Ermolaeva et al., 2013, Calabrese et al., 2015). Beneficial effects of hormesis on human health involve e.g. small doses of UV radiation in protection against cancer formation or dietary restriction on expanded longevity (Calabrese, 2004, Calabrese et al., 2015). Small doses of stress protect cells and organisms from higher doses of the same or different stress in model organisms, such as yeast, worms, birds or mice. On the other hand, often the improvement of one biological feature, such as longevity, may have an adverse effect on another, e.g. fertility.

Adaptive responses involve the environmental or cellular stress responses which are activated by variety of stresses (Stranahan and Mattson, 2012, Perry et al., 2014, Singh et al., 2015). As a result cells/organisms better tolerate higher doses of the same or other stress in contrast to cells/organisms that were never exposed to stress. Hormesis resembles the adaptation to low-dose stress in a sense that low doses of stress may improve organismal fitness.

# Chapter 2. Materials and methods

## 2.1 Yeast strains

*S. cerevisiae* strains used in this study are given in the Appendix A. All strains are in the W303 genetic background (*ade2-1 can1-100 trp1-1 leu2-3,112 his3-11,15 ura3 GAL+ psi+ ssd1-d2 RAD5+)* apart from strains used for Synthetic Genetic Array screening (see below, 2.21), which are S288C.

## 2.2 Yeast media

For 1 L YEPD media 10 g/L yeast extract, 20 g/L bactopeptone, 2 % dextrose, 75 mg/L adenine were used. For 1 L YEPG media 10 g/L yeast extract, 20 g/L bactopeptone, 3 % glycerol, 75 mg/L adenine were used. Selective media were synthetic dropout (SD) media lacking tryptophan (-TRP), leucine (-LEU), histidine (-HIS) or uracil (-URA), or combination of those in 1.3 g/L amino acid powder, 1.7 g/L yeast nitrogen base, 5 g/L ammonium sulphate and 2 % dextrose. The amino acid powder contains: adenine 2.5 g, L-arginine (HCl) 1.2 g, L-aspartic acid 6.0 g, L-glutamic acid (monosodium salt) 6.0 g, L-histidine 1.2 g, L-leucine 3.6 g, L-lysine (HCl) 1.8 g, L-methionine 1.2 g, L-phenylalanine 3.0 g, L-serine 22.5 g, L-threonine 12.0 g, L-tryptophan 2.4 g, L-tyrosine 1.8 g, L-valine 9.0 g, uracil 1.2 g. Amino acid dropout powder was made by omitting the relevant amino acids from the dropout mix. Enriched sporulation media (ESM) was 1 g/L yeast extract, 0.05 % dextrose, 1 % potassium acetate, pH7.6.

Where specified, antibiotics were added to the media at the following concentrations: G418 - 200 mg/L, clonNAT - 100 mg/L, hygromycin B - 300 mg/L. Canavanine was added to the media at 50 mg/L. 5-fluoroorotic acid (5-FOA) medium was made with –URA dropout power (1.3 g/L), 6.7 g/L yeast nitrogen base, 50 mg/L uracil, 1 g/L 5-FOA and 2 % dextrose.

For solid media 20 g/L agar was added prior to autoclaving.

### 2.3 Yeast culture

Yeast strains were maintained at 23°C or 30°C. Strains routinely grown at 23°C were ts mutants, e.g. *cdc13-1*, *cdc15-2* or *dna2*∆.

### 2.4 Yeast passaging

5-10 colonies of each strain, or a single colony from germinated spore, were streaked onto YEPD plates for single colonies and incubated for 3 days at 23°C, unless stated otherwise, before photographing. Pooled colonies (5-10), and single colonies at times, were then re-streak on new YEPD plates and pictures were taken.

### 2.5 Growth assay – "spot test"

A few yeast colonies were pooled, inoculated into 2mL YEPD and grown to saturation on a wheel at 23°C or 30°C. From saturated cultures 40 µL were added to 160 µL sterile water and 5-fold dilutions were prepared, if not stated otherwise, using a 96-well plate and multichannel pipette. Yeast culture series were spotted onto agar round or rectangular plates (YEPD or selective media) with a pin tool. The plates were incubated at a range of temperatures for 3 days, unless stated otherwise, before photographing. Temperatures used in the experiments are included in the range of 20-37°C. Such a wide variety is due to semi- and non-permissive temperatures of telomere defective *cdc13-1* and *yku70*∆ mutants, as well as *dna2*∆ and *cdc15-2* thermo-sensitive (ts) strains.

### 2.6 Mating and diploid selection

*MAT a* and *MAT alpha* parental strains were mixed together on YEPD plate and incubated at 23°C or 30°C overnight to mate. Diploid selection was based on growth of diploids on selective media that would only permit the growth of diploid cells.

### 2.7 Sporulation

Usually, diploid colonies were inoculated into 2 mL of YEPD and grown overnight at 23°C or 30°C on the wheel. 0.5 mL of the culture was washed twice in 5 mL sterile water and re-suspended in 2 mL ESM media. Cultures were incubated at 23°C for 3-5 days and the presence of spores was examined by the phase contrast microscopy (40x).

Some strains, e. g. with deletions of *DNA2* or *DPB11*, contained the plasmids. Tetrad dissection and spore germination of such diploids revealed frequent plasmid lost and sometimes poor spore viability when standard protocol (described above ) was used. To avoid plasmid loss, strains containing the plasmids were grown in 2 mL media selective for plasmid (-LEU, -HIS, -TRP, -URA) prior to sporulation.

Diploids with deletion of *CDC13* did not sporulate at 23°, but formed tetrads at 20°. Therefore *cdc13Δ/CDC13* diploids were sporulated at 20° for 5 days, and dissected spores were subsequently germinated at 23° for 10 days.

**2.8 Tetrad dissection**

Sporulated cultures were washed twice in 1 mL sterile water and finally re-suspended in 1 mL sterile water, then stored at 4°C. 20 µL of cells were incubated with 1.8 µL glusulase enzyme (Perkin Elmer) at 30°C for digestion of the asci surrounding tetrads. After 15-20 min cells were resuspended in 1 mL sterile water on ice, and 50 µL of suspensions were spread on YEPD plates. Standard tetrad dissection technique was used, using a microscope with 10x and 20x lens and a microneedle to dissect spores onto YEPD plates. Spores were germinated at 20°C, 23°C or 30°C for 3-10 days before photographing, then patched onto YEPD plates and grown for 2-4 days at 23°C or 30°C. Strains grown on YEPD plates were then replica-plated onto selective plates to allow identification of tetrads' genotype. The mating types were determined by mating with DLY26 (MAT a) and DLY2440 (MAT α) on -4 (-HIS, -LEU, -TRP, -URA) selective plates. Thermo-sensitive mutations, like *cdc13-1* and *cdc15-2*, were determined by replica-plating onto YEPD plates followed by incubation at 36°C for 2 days. Ts strains fail to form colonies at 36°C.

**2.9 Random Spore Analysis**

Standard protocol for sporulation has been applied (2.7). Cells were washed twice with 1 mL sterile water and re-suspended in 0.5 mL Zymolyase-20T solution (1 mg/mL in sterile water) and 10 µL 2-β-mercaptoethanol (Sigma). Cells were incubated overnight in 15 mL screw-cap Falcon tubes at 30°C on the wheel to allow lysis of diploid cells. The next day 5 mL of 1.5 % NP-40 detergent was added, cells were vortexed and spun down 3000 rpm for 5 min. 4 mL of supernatant were poured off and spores were resuspended in remaining 1 mL of solution, transferred to 1.5 mL

Eppendorf tubes and incubated on ice for 15 min. Spores were then sonicated (Sanyo Soniprep) on ice for 30 seconds at 10 microns power for 2 times, with 2 min periods of incubation on ice between cycles. Spores were spun at 13000 rpm for 30 seconds, supernatant was removed and spores were resuspended in 1 mL of 1.5 % NP-40. Sonication process was repeated twice, spores were spun again and resuspended in 1 mL of water. Finally, samples were sonicated one more time and were checked under the microscope for spore separation efficiency. Series of dilutions were prepared in sterile water (1:10 – 1:10000) for each sample and 100 µL of 1:1000 and 1:10000 dilutions were plated onto YEPD. If diploid strains used for RSA contained the plasmid, spore dilutions were plated onto selective plates to maintain the plasmid in haploid progeny. Spores were germinated at 20ºC or 23ºC for 4-10 days, and then strains were patched onto YEPD or selective media if spores contained a plasmid. Strains were genotyped by replica-plating onto appropriate selective plates.

### 2.10 Yeast transformation

Yeast were transformed in order to replace a gene of interest with a marker gene, introduce a plasmid carrying a specific allele of interest, or introduce an empty vector.

#### *2.10.1 Lithium acetate (LiAc) transformation*

Single colonies were inoculated into 2mL YEPD and incubated overnight at 23°C or 30°C. The next morning 49 mL of YEPD was inoculated with 1 mL of overnight culture, incubated in a shaking water bath until cells reach the concentration 2 x $10^7$ cells/mL. The number of cells was defined by using the haemocytometer. Cultures were washed once in 25 mL sterile water, then in 1 mL 1X LiAc and finally resuspended in 400 µL1x LiAc. Such prepared cells were kept on ice until ready for transformation. 50µL aliquots were spinned down (13000 rpm 15 sec), the supernatant was removed and following reagents were added: 240 µL 50 % PEG, 36µL 10x LiAc, 50 µL salmon sperm DNA (2 mg/mL), 50 µL miniprep plasmid DNA in water (1:50) or 30 µL PCR product, or 30 µL digested plasmid. Water was used for a no-DNA control. The positive control contained a plasmid carrying appropriate marker gene that could be used for selection on selective media. Samples were vortexed and incubated at 23°C for 30min, then heat-shocked at 42°C for 20 min. The spun down cells (6000 rpm 15 sec) were resuspended in 200 µL sterile water

and plated onto appropriate selective plates. Transformants were grown at 23°C or 30°C until colonies appeared. If strains were transformed with an antibiotic-resistance marker (e.g. *KANMX*, *NATMX*, *HPHMX*), transformants were grown on YEPD plates overnight and then were replica-plated onto media containing appropriate antibiotic. Individual colonies were collected with a toothpick and streaked for single colonies on selective media. Transformants were then purified by plating single colonies on selective media. If the genomic insertion occurred, transformants were verified by colony PCR as described below (2.14.2).

### *2.10.2 One Step transformation*

In 1.5 mL Eppendorf tube the following reagents for One Step Buffer were mixed: 1 mL 10x LiAc, 3.5 mL 50 % PEG, 0.5 mL DTT (for 50 transformations). Fresh cells were scraped from an agar plate using a toothpick and resuspended in 100 µL of One Step Buffer. 5.3 µL of salmon sperm DNA 10 mg/mL and 1 µL of plasmid DNA miniprep were added, samples were vortexed and incubated at 45°C for 30 min. After adding 100 µL sterile water, cells were plated onto appropriate selective media. Transformants were streaked for single colonies and a single colony was picked for further experiments.

## 2.11 Bacteria strains, media and transformation

Bacteria used in this study were Top10 competent cells (Invitrogen) of *Escherichia coli*. Bacteria were grown on agar LB liquid media or agar plates (1 L contained: 10 g/L bactopeptone, 5 g/L yeast extract, 10 g/L NaCl, 20 g/L agar) or SOC liquid media (1 L contained: 20 g/L bactotryptone, 5 g/L yeast extract, 0.585 g NaCl/L, 0.166 g/L KCl, 10 mL 1M $MgCl_2$, 10 mL 1M $MgSO_4$, 3.6 g/L glucose). LB media were supplemented with Ampicillin (100 mg/L ) when bacteria were carrying a plasmid, e.g. after transformation. 50 µL of *E. coli* competent cells were transformed with 1 µL of plasmid DNA and incubated on ice for 30 min in 1.5 mL Eppendorf tubes. Water was used for a no-DNA control. The positive control contained a pUC18 plasmid (Agilent) containing an Ampicillin resistance gene. Cells were heat-shocked at 42°C for 45 seconds and then incubated on ice for 5 min. 0.9 mL pre-warmed SOC medium was added to cells, and the cultures were then incubated on the wheel at 36°C for 1 hour. Cells were then transferred to sterile 1.5 mL Eppendorf tubes and spun for 5 min at 5000 rpm. 700 µL of supernatant was removed and cells were resuspended by

gentle pipetting in the remaining supernatant. Cells were then spread onto LB + Ampicillin plates and incubated overnight at 36°C. The next day usually two single colonies per plate were inoculated into 5 mL LB + Ampicillin (100 mg/L) liquid medium and incubated overnight on the wheel at 36°C.

## 2.12 Plasmids

### *2.12.1 Plasmids used in this study*

Plasmids containing *DNA2*, *DPB11* and *DDC1* alleles and empty vectors were gifts from: Peter Burgers, Judith Campbell, Marco Muzi-Falconi and Yeon-Soo Seo (Appendix B). Received plasmids were amplified in bacteria as described above (2.11), purified using QIAprep Spin Miniprep Kit (Qiagen) and stored in the collection at -20°C. Afterwards, the plasmids were tested by restriction digests and sent for sequencing to GATC Biotech company to confirm presence of mutations (as in 2.12.4). Plasmids are listed in Appendix B.

### *2.12.2 Plasmid purification*

Overnight cultures of single bacteria colony were centrifuged and QIAprep Spin Miniprep Kit (Qiagen) was applied to extract plasmid DNA, following the manufacturer's protocol.

### *2.12.3 Restriction digest*

Restriction digest (RE) was used to distinguish the empty vectors from plasmids which carried genes. Usually two restriction enzymes were chosen based on ability to cut the corresponding plasmid once, if it was empty vector, or more times, if the plasmid carried wild type gene sequence or an allele. RE was also used for cloning experiments, described below (2.16). Restriction digestions were performed as follows: 1 µL plasmid DNA miniprep was cut with 10 units restriction enzyme (New England Biolabs, usually: *Spe*I, *Xho*I, *Sac*II, *EcoR*I, *EcoR*V, *Nde*I, *Xma*I), 1x restriction enzyme buffer (New England Biolabs), 1x bovine serum albumin (BSA) and sterile water. Digests were incubated at 37°C (or another temperature appropriate for chosen enzyme) for 1-2 hours. Samples were run on a 1 % agarose gel, as described in 2.15.

### *2.12.4 DNA sequencing and alignment*

In order to confirm the sites of mutations, plasmids and primers for amplification of DNA sequence were prepared according to recommendations from GATC Biotech company and sent for sequencing. Primers were designed to amplify about 1kb DNA, should the mutation be located at least 100 bp away from either forward or reverse primer in order to avoid any nucleotide variances scored during the process of sequencing. The sequencing capacity is to identify approximately 700 bp, and therefore in longer sequences the uncertainty of an accurate base is denoted by either the letter “t” or “N”. To analyse sequences and visualise results the Peak Scanner 2 software was applied for viewing and printing chromatograms from the PC. The NCBI BLAST (http://www.ncbi.nlm.nih.gov) was used to compare acquired sequences to those provided by SGD (http://www.yeastgenome.org/).

## 2.13 Gene deletion

All the genetic modifications were made according to Longtine *et al.* (Longtine et al., 1998b). Genes were deleted by replacing the gene of interest with an antibiotic resistance cassette from a specific vector (Longtine et al., 1998a). An antibiotic resistance cassette was amplified by PCR as described below (2.14.1). Primers designed for gene deletion were 60 bp long, and had 40 bp homology to the region upstream (forward primer) or downstream (reverse primer) of the start or stop codons, respectively. Remaining 20 bp of primers were homologous to the antibiotic resistance cassette from the plasmid. PCR amplified fragments were transformed into yeast using lithium acetate as described above (2.10.1). Transformant colonies were streaked for single colonies on selective media, and events of integration were confirmed by colony PCR (2.14.2).

## 2.14 PCR

PCR was performed on the plasmid DNA template (for gene amplification and replacement), or on a single yeast colony (for confirmation of gene deletion). Primers were designed using the *ApE – A plasmid Editor* software and are shown in Appendix C.

### *2.14.1 Genomic/plasmid DNA PCR*

Primers used for gene amplification from genomic or plasmid DNA were usually 20 bp long and were design to be complementary to the sequence app. 500 bp upstream and downstream of the target gene. The 20 µL PCR reactions consisted of 0.3 µM forward and reverse primers (Sigma Aldrich), 0.5 units ExTaq polymerase (TaKaRa Bio Inc.), 0.2 mM dNTPs, 1x ExTaq buffer, genomic or plasmid DNA and sterile water. The following conditions were usually applied: 5 min 95°C, 30 cycles of 30 s at 94°C, 20 s at 55°C and 1 min per 1 kb amplified DNA at 72°C, 5 min at 72°C. The lengths of amplified products were verified on 0.8 % agarose gel (2.15).

### *2.14.2 Colony PCR*

Colony PCR was used to confirm the antibiotic resistance cassette integration into the genome after lithium acetate transformation (2.10.1). PCR primers were designed to anneal to app. 500 bp upstream the insert location (forward primer) and to anneal within the inserted marker gene (reverse primer). The 10 µL PCR reactions consisted of 0.3 µM forward and reverse primers (Sigma Aldrich), 0.5 units GoTaq HotStart polymerase (Promega), 0.2 mM dNTPs, 1x green GoTaq buffer, 25 mM $MgCl_2$, 1 µL cell suspension (in sterile water) and sterile water. PCR conditions usually were: 5 min 95°C, 30 cycles of 1 min at 94°C, 1 min at 55°C, 1 min per 1 kb amplified DNA at 72°C, 10 min at 72°C. The lengths of amplified products were verified on 0.8 % agarose gel (2.15).

### *2.14.3 cdc13-1 PCR*

In *cdc13-1* strains residue P371 is mutated to a serine (S) and the sequence becomes recognizable by *EcoR*I restriction enzyme (Lin and Zakian, 1996). The PCR followed by restriction digest allows to verify whether *cdc13-1* restriction fragment length polymorphism (RFLP) is still present in e. g. temperature resistant strains. 358 bp sequence of *CDC13* was amplified by PCR using compatible primers (Appendix C). The PCR products were digested with *EcoR*I, and digests were run on 2 % agarose gel. Digestion of DNA isolated from *cdc13-1* strains results in 2 products on an agarose gel (product sizes 160 bp and 198 bp), while DNA isolated from *CDC13* strains results in one product on the gel – full length PCR product of 358 bp.

## 2.15 Agarose gel electrophoresis

Usually 0.8 % agarose gels were made in 0.5x TBE buffer. SYBR Safe DNA Gel Stain (1/10000 dilution; Invitrogen) was added to molten agarose. 6x loading buffer was added to DNA samples and loaded on the gel together with +1 kb DNA ladder (Invitrogen). Agarose gels were run at 80-100 V. Products were visualised using a Fuji LAS 4000 Imager.

## 2.16 Cloning

*In vitro* and *in vivo* cloning were performed in order to generate novel plasmids, e. g. integrative plasmids (Appendix B). These plasmids were then used to integrate an allele of interest into the genome, or to cover the deletion of a gene of interest by allele on a plasmid.

### *2.16.1 In vitro cloning*

7 µL of QIAprep Spin Miniprep DNA plasmid vector was cut with 15 units of appropriate restriction enzyme (*Spe*I*, Xho*I or *Sac*II, New England Biolabs) as in 2.12.3. The vector was initially pDL452 (Appendix B). The insert was obtained by PCR (2.14.1) using DNA from a wild-type strain (DLY3001), or by restriction digest of plasmid DNA. Digestion was confirmed by running cut and uncut vector on a 1 % agarose gel. Cut vector and insert were extracted from the gel using QIAquick Gel Extraction Kit (Qiagen) following the manufacturer's protocol. Then 1 µL 5x CIP phosphatase (New England Biolabs) was added, and samples were incubated for additional 30 min at 37°C. Vector and insert were ligated by adding 1 µL T4 DNA ligase to 2 µL purified vector and 6 µL purified insert in a 10 µL reaction containing 5x T4 DNA ligase buffer. Ligation took place at 16°C during overnight incubation. Digested vector-only and insert-only ligations served as negative controls. 10 µL of the ligated DNA was then transformed into 100 µL *E.coli* Top10 competent cells as in 2.11.

### *2.16.2 In vivo cloning*

3 µL of QIAprep Spin Miniprep DNA plasmid vector was cut once with 10 units of appropriate restriction enzyme (*Xma*I, New England Biolabs), as in 2.12.3. Digestion was confirmed by running cut and uncut vector on a 1 % agarose gel. The insert was obtained by PCR (2.14) of a gene (*DNA2*) from the plasmid (pDL1544).

The lithium acetate method of transformation was used with 10 µL PCR-purified product, 5 µL digested plasmid and 5 µL water. A no-DNA control contained water and no DNA. Vector and insert controls contained water and 5 µL or 10 µL insert or digested vector, respectively. Transformant selection and verification was conducted as described above. The plasmid DNA was then isolated from yeast using the QIAprep Spin Miniprep Kit (Qiagen).

### *2.16.3 One-step isothermal assembly method in vitro (Gibson Assembly)*

One-step assembly method was performed following the protocol described by Gibson *et al.* (Appendix D) (Gibson et al., 2009). Briefly, three DNA fragments were amplified by PCR as in 2.14.1, and primer sequences are in Appendix C. Two PCR fragments were adjacent sequences from the plasmid (pDL1672 and pDL1673), and one fragment was amplified from genomic DNA (DLY3001). The genomic DNA consisted of the promoter and the N-terminal sequence of *DNA2* gene. The three PCR fragments overlapped by 100 bp end fragments were reassembled into a circle DNA molecule. 5 µL (10-100 ng) of DNA fragments were added in equimolar amounts. The DNA fragments were assembled in 15 µL reactions consisting of the assembly master mixture: 5x isothermal reaction buffer (25 % PEG-800, 500 nM Tris-HCl pH 7.5, 50 mM $MgCl_2$, 50 mM DTT, 1 mM each of the four dNTPs and 5 mM NAD), T5 exonuclease (10 U/µL; Epicentre), *Taq* DNA ligase (40 U/µL; NEB), Phusion DNA polymerase (2 U/µL; NEB) and water. Samples were incubated at 50°C for 60 min. The assembled DNA was transformed into 100 µL *E.coli* as in 2.11, and then purified and tested by restriction digest and PCR (2.12.3, 2.14.1). PCR products were sent for sequencing, as in 2.12.4.

### *2.16.4 Quick Change in vitro method*

Gibson Assembly resulted in a point mutation (T→C ) within a *DNA2* sequence located close to PCR fragments overlap. In order to revert the nucleotide, the Quick Change *in vitro* method was used by applying combined protocols of Stratagene and BioTechniques. Primers contained the nucleotide to be changed in the middle of the sequence (Appendix C). Individual reactions, one for forward and one for reverse primer were prepared. 25 µL reactions were made of: 10x Pfu Buffer, dNTPs (2.5 mM), Pfu polymerase, forward or reverse primer (10 pm/µL), plasmid DNA (app. 100 ng) and water. Both reactions were run in a thermocycler separately at following

conditions: initial amplification for 1 min at 94°C, then 2 cycles of 30 sec at 94°C, 1 min at 55°C, 16 min at 68°C. Then the forward and reverse amplifications were combined and 1 µL of Pfu polymerase was added. The PCR settings were: 1 min at 94°C, and 18 cycles of 30 sec at 94°C, 1 min at 55°C, 16 min at 68°C. The plasmid DNA which remained unchanged was degraded by following restriction digest with *Dpn*I (10 U; New England Biolabs) at 37°C for 3 hours. The degradation of unaltered plasmid was check on 1 % agarose gel. 20 µL reactions were transformed into 100 µL *E.coli* as in 2.11, plasmids were purified and tested by restriction digest and sequencing.

### *2.16.5 Pop-in/Pop-out assay*

*URA3*-marked integrative plasmids pDL1731 and pDL1733 were cut with *Nde*I restriction enzyme, and transformed into haploid yeast by high efficiency LiAc transformation (2.10.1). Single colonies from the transformation plates were restruck onto -URA plates to ensure purity. Single colonies were then patched onto YEPD plates, grown overnight at 23°C, replica plated to –URA and FOA, and allowed to grow overnight once more. This procedure was repeated (re-patching onto YEPD and replica-plating onto –URA and FOA) until single colonies were growing on FOA, but not on –URA plates, which indicated that strains had lost the plasmid. Colony PCR was used to confirm the pop-in and pop-out events. Purified PCR products were sent for sequencing to confirm the presence of point mutations.

## 2.17 Genomic DNA preparation

For Southern Blotting, and PCR at times, genomic DNA was prepared using the Yale DNA isolation method. For In-gel assay, and PCR at times, genomic DNA was extracted using phenol method according to (Dewar and Lydall, 2012b).

### *2.17.1 Yale quick DNA isolation method*

2 mL saturated cultures were spun down and resuspended in 250 µL of 0.1M EDTA (pH7.5), 1:1000 beta-mercaptoethanol and 2.5 mg/mL zymolyase 20T (Sigma Aldrich). After one hour incubation at 37°C, 55 µL of 0.25M EDTA (pH 8.5), 0.5M Tris, 2.5 % SDS was added and samples were incubated at 65°C for 30 min. 68 µL of 5 M potassium acetate (KAc) was added and samples were incubated on ice for 30 min. Samples were then spun for 20 min at 13000 rpm and the supernatant was

transferred to a new 1.5 mL Eppendorf tube. Each tube was filled with 100 % ethanol. Samples were inverted and spun for 10 min at 13000 rpm. The supernatant was removed and pellets were briefly dried before being resuspended in 130 µL TE containing 1 mg/mL RNAse A. Samples were incubated at 37°C for 35 min. 150 µL isopropanol was added, samples were inverted and spun for 20 min at 13000 rpm. 100 µL of 70 % ethanol was used to wash samples by centrifuging for 5 min at 13000 rpm. The ethanol was removed and pellets were dried for 30 min under the hood. Pellets were incubated at 37°C for 30 min in 40 µL TE (10 mM Tris–HCl, pH 8.0, 1 mM EDTA pH 8.0).

### *2.17.2 Phenol-based DNA isolation method*

2 mL saturated cultures were washed twice in 1 mL sterile water and the cell pellets were stored at -80°C. Thawed pellets were resuspended in 400 µL of freshly made lysis buffer (2 % Triton X-100, 1 % SDS, 100 mM NaCl, 10 mM Tris–HCl, pH 8.0, 100 mM EDTA, pH 8.0) and app. 0.5 mL glass beads were added. 400 µL phenol:chlorofom:isoamyl alcohol (25:24:1, v/v/v) was added under the hood and cells were lysed using a Precellys 24 ribolyser (Bertin Technologies) on 5.5 power setting for 3 x 20 s, with a 2 min pause on ice between each 10 sec cycles. 400 µL TE buffer was added and samples were spun at 4°C for 5 min at 13000 rpm. At this time 2 mL light phase lock gel tubes (5-Prime) were centrifuged at 13000 rpm for 1 min. 750 uL of aqueous (upper) phase of each sample was transferred to the phase lock tube and 750 µL phenol:chlorofom:isoamyl alcohol (25:24:1, v/v/v) was added. Tubes were centrifuged at 13000 rpm for 5 min. The aqueous phase was transferred to the sterile 2 mL Eppendorf tubes and 100 % ethanol was added to fill the tubes. Tubes were left for 5 min at room temperature. Nucleic acid was harvested by centrifugation at 13000 rpm for 3 min. The pellet was air-dried for 5 min and then resuspended in 806 µL TE/RNAse solution (7.5 µg/mL RNAse) while samples were incubated at 37°C for 30 min. 50 µL of 3 M sodium acetate (pH5.2) was added along with 100 % ethanol (to fill the tube) to precipitate DNA for 15 min. Samples were centrifuged at 13000 rpm for 3 min and pellets were air dried. DNA was dissolved in 40 µL TE during incubation at 37 °C for 20 min. DNA yield and purity was determined using a Nanodrop 2000 (Thermo Scientific).

### 2.18 Southern blotting

Southern blot analysis was used to assess telomere length and performed as previously described (Dewar and Lydall, 2010a). The probe was acquired by digestion of 10 µL plasmid pDL987 using 10 units *BamH*I and 10 units *Xho*I in a 20 µL reaction with 2 µL 10x NEBuffer 4, 2 µL 10x BSA and 5 µL sterile water. pDL987 contains 120 bp of TG repeats and 752 bp of the upstream Y' element from telomere VIII-R. Plasmid was digested for 2-3 hours at 37°C and then was run on a 1 % agarose gel. Digestion product of 1 kb size (which contains the TG repeats and Y' element) was extracted from the gel using a Qiaprep Gel Extraction Kit (Qiagen) and served as the Southern blot probe. The probe was DIG labelled using the DIG High Prime Labelling and Detection Starter Kit II (Roche).

2.5 µL of DNA (isolated by Yale method) was run on a 1 % agarose gel and ImageJ software was used to equalize samples' concentrations for loading based on band intensity. 2.5 µL of DNA was then digested with 0.5 µL *Xho*I (20 units/µL), 2 µL 5x NEBuffer 4, 1 µL 10x BSA and 4 µL water for 3 hours at 37°C. Samples were run on a 1 % agarose gel at 19V for approximately 14 hours. The gel was photographed using a Fuji LAS 4000 imager and served as a loading control. Gel was then washed in 0.25M hydrochloric acid for 15 min, rinsed twice in sterile water and washed in 0.5M sodium hydroxide for 30 min. The gel was blotted to positively-charged nylon membrane (Roche) using a vacuum blotter (Model 785, BioRad) at 5 Hg in 10x SSC for 90 min. Afterwards DNA was cross-linked to the wet membrane using auto UV cross-linking (Stratalinker). The membrane was rinsed in sterile water and was allowed to air-dry. The labelled probe was hybridized to the DNA on the membrane and detected using the DIG High Prime Labelling and Detection Starter Kit II (Roche). The membrane was imaged using a Fuji LAS 4000 imager for chemiluminescence, for 20 min.

### 2.19 Fluorescent in-gel assay

In-gel assay was performed as previously described (Dewar and Lydall, 2010b). 10 µL of phenol prep DNA samples were cut with *Xho*I (1.5 µL *Xho*I (20 units/ µL), 2 µL NEB Buffer 4 (10x), 0.2 µL BSA (100x), 5.8 µL sterile water in a 37°C water bath overnight. The next morning samples were incubated at 65°C for 20 min to heat-inactivate *Xho*I. Then samples were incubated on ice, centrifuged briefly and 1 µL of

IRDye 800 AC probe (M3157 oligo, 500nM) was added to each tube. The tubes were flicked, incubated at 37°C for 10 min to anneal the probe to TG ssDNA and then incubated 30 min on ice. No-DNA sample and the ladder were prepared by adding 10 µL of TE (no-DNA) or 1 kb DNA ladder (Invitrogen) together with 1 µL IRDye 800 AC oligo to 10 µL solution of NEB buffer 4 (2x), BSA (2x) and water.

5 µL of Orange G Loading buffer (6x) was added to each tube and samples were run on a 1% agarose gel in 0.5x TBE (no SYBR Safe dye). Gel was run at 50 V for 180 min and signal was then detected on a LI-COR (Odyssey) imaging system. Gel was post-stained for 30 min using 1x SYBR Safe in 0.5x TBE buffer and total DNA was detected using a FUJI LAS-4000 imager. ssDNA of the IRDye 800 image was quantified using ImageJ software. Determined background signal was subtracted from quantified signal of ssDNA from each lane.

**2.20 Genomic quantitative PCR (qPCR)**

DNA for genomic qPCR was isolated using the Yale method. Primers were designed to amplify a 100bp region within the gene of interest, and the measurements were performed in triplicate for each sample. Quantitative PCR was performed in a 96-well reaction plate. 2 µL of DNA (2 ng/µL) were added to 5 µL 1x Platinum SYBR Green qPCR SuperMix-UDG with ROX (Invitrogen), 2.6 µL water, 0.2 µL forward primer (10 µM ) and 0.2 µL reverse primer (10 µM ). The no-DNA control contained water instead of DNA. A standard curve of DNA concentrations was generated from wild-type (DLY3001) genomic DNA. The standard curve was obtained by plotting the log (DNA concentration) versus CTs, and the efficiency of PCR was calculated as:

$$Efficiency = 10^{\left(-\frac{1}{slope}\right)-1} \text{ x } 100\ \%$$

All primers used in this study had efficiencies of app. 95 %, and are listed in Appendix C.

The qPCR programme was 50°C for 2 min, 95°C for 2 min, 40 cycles of 95°C for 15s and 60°C for 30s, then 40°C for 1 min followed by melting curve analysis, using an ABI Systems StepOnePlus thermal cycler. *BUD6* or *PAC2* genes were used as internal controls to normalize the DNA loaded. Fold changes were calculated using the formula: $2^{-(Sample\ CT - Reference\ CT)}$. Data was then exported as an Excel sheet and analysed relative to WT values (WT fold change equals 1).

### 2.21 Synthetic genetic array (SGA)

An unbiased genome-wide screen was used to understand the mechanisms allowing suppression of *dna2*Δ. *S. cerevisiae* yeast strains used for synthetic genetic array (SGA) high throughput screens were in the S288C or W303 genetic backgrounds. Single query strain *dna2*Δ pDL1758 (*pCAN1-URA3-DNA2*) was mated with a single gene deletion library of approximately 5,000 strains (S288C background). The SGA in W303 background included only 308 gene deletions from the library.

The query *dna2*Δ strain (*MAT*α, *dna2*::*NATMX,* containing *HPHMX* and *LEU2* marker genes, and the *MAT*a-specific *STE2* promoter cassette *can1*Δ*::STE2pr-Sp_his5* and *lyp1*Δ) carried the pDL1758 plasmid (*pCAN1-URA3-DNA2*), to assure successive *dna2*Δ *xyz*Δ strains viability during the process of further selection. The query strain was cultured in YEPD overnight at 23°C and spread onto YEPD + clonNAT plates. Plates were incubated for two days at 23°C until a lawn of culture was visible. All manipulations hereinafter described were conducted using a BM3 robot (S&P Robotics) and plates were photographed at each stage using a robotic plate imager (SPImager, S&P Robotics). The plates with the query strain were pinned to 18 fresh YEPD + clonNAT plates as 1536 individual strains per plate and were incubated for 2 days at 20°C. The *MAT*a library of approximately 5000 single deletion mutants was pinned to YEPD + G418 plates (384 individual strains per plate) and were incubated at 30°C for two days. The library was then pinned as 1536 colonies per plate (4 replicates of each strain from each 384-format plate) onto YEPD + G418 plates and were incubated for 2 days at 30°C.

The query strain was then mated with the library on YEPD and diploids were formed during 24-48 hours at 20°C. Diploids were then pinned to -URA + G418 and incubated for 1.5 days at 23°C before being pinned to sporulation media (ESM + G418), and were sporulated for 5 days at 23°C. Spores were pinned sequentially (and incubated for 2 days at 20°C) to:

- SD/MSG_rhlk_TNH (+hygromycin+thialysine+clonNAT)
- SD/MSG_rhlk_TGNH (+hygromycin+thialysine+clonNAT+G418)
- SD/MSG_rhlk_CTGNH (+hygromycin+thialysine+clonNAT+G418+canavanine; final selection media to remove the pDL1758 plasmid).

The selection process allowed for selection of *MAT*a haploid strains harbouring both the query (*dna2::NATMX)* and library *(yfg::KANMX*) mutations and *pCAN1-URA3-DNA2* plasmid. The final selection on plates containing canavanine was performed three times to remove *pCAN1-URA3-DNA2* plasmid from *dna2*Δ *xyz*Δ double mutants. The colony size of haploids from SGA, where *dna2*Δ *xyz*Δ strains lost the *pCAN1-URA3-DNA2* plasmid on CTGNH media, were compared to a control screen conducted on TGNH media.

Concentration of canavanine was 50 mg/L; thialysine was 50 mg/L; G418 was 200 mg/L; hygromycin was 300 mg/L and clonNAT was 100 mg/L. The robotic amino acid dropout recipe for robotic media was:
Adenine 3g
Inositol 2g
Para-aminobenzoic acid 0.2g
Alanine 2g
Arginine 2g
Asparagine 2g
Aspartic Acid 2g
Cysteine 2g
Glutamic acid 2g
Glutamine 2g
Glycine 2g
Histidine 2g
Isoleucine 2g
Leucine 10g
Lysine 2g
Methonine 2g
Phenylalanine 2g
Proline 2g
Serine 2g
Threonine 2g
Trytophan 2g
Tyrosine 2g
Valine 2g
Uracil 2g

### 2.22 Image Processing

All agar plate images were processed using Adobe Photoshop CS6 software. All agar plate images were adjusted identically within each Figure, there were slight differences across Figures. Images were adjusted as follows: in the Levels adjustment tool the low end of the intensity histogram was trimmed to between 80 - 120 and all other values left at default (1, 255). Using Photoshop's exposure tool, Exposure settings were adjusted to 0 - 0.8; Offset to 0.0 - -0.07; and Gamma Correction to 1 - 1.5. Colour was converted to greyscale after import into Adobe Illustrator. The drawings were created in Adobe Illustrator CS6 software, unless stated otherwise.

# Chapter 3. The roles of Ddc1, Dpb11 and Dna2 in telomere defective *cdc13-1* and *yku70*Δ mutants

Ddc1 was reported to play a role in Mec1 activation upon DNA damage (e.g. after UV or 4-NQO) (Puddu et al., 2008, Navadgi-Patil et al., 2011, Pfander and Diffley, 2011). DNA damage induced in telomere defective *yku70*Δ mutants activates a Mec1-dependent checkpoint pathway, but is independent of Ddc1 (Maringele and Lydall, 2002, Addinall et al., 2011). In another telomere defective mutant, *cdc13-1*, Addinall *et al.* identified deletion of *DDC1* as a strong suppressor of *cdc13-1* growth defect (Addinall et al., 2008). The different effect of *ddc1*Δ on *cdc13-1* and *yku70*Δ fitness is intriguing, because *cdc13-1* and *yku70*Δ employ similar DDR pathways, including Exo1, Rad9, Chk1 and Mec1-dependent checkpoint pathways (Maringele and Lydall, 2002, Zubko et al., 2004).

Ddc1, Dpb11 and Dna2 are direct Mec1 activators which function dependently of the phase of the cell cycle (Fig. 8). The hypothesis to be tested in this thesis is whether two DNA damage signal transducers, Dpb11 and/or Dna2, take the role of Ddc1 in Mec1-dependent checkpoint activation in *yku70*Δ mutants. In order to examine the impact of Ddc1, Dna2 and Dpb11 on fitness of *yku70*Δ strains, point mutations of *DDC1*, *DNA2* and *DPB11*, defective in Mec1 activation, have been chosen and analysed (Longhese et al., 1997, Bae et al., 2001, Puddu et al., 2008, Navadgi-Patil et al., 2011, Pfander and Diffley, 2011, Pokharel and Campbell, 2012, Kumar and Burgers, 2013). The same mutations were analysed in *cdc13-1* telomere defective strains.

For the purpose of this thesis, I adapted the word “fitness” which I used as a synonym of the word “growth”. Therefore, in the context of e.g. *cdc13-1* or *yku70*Δ decreased/increased fitness, I meant the ability of *cdc13-1* or *yku70*Δ mutants to grow in the range of temperatures.

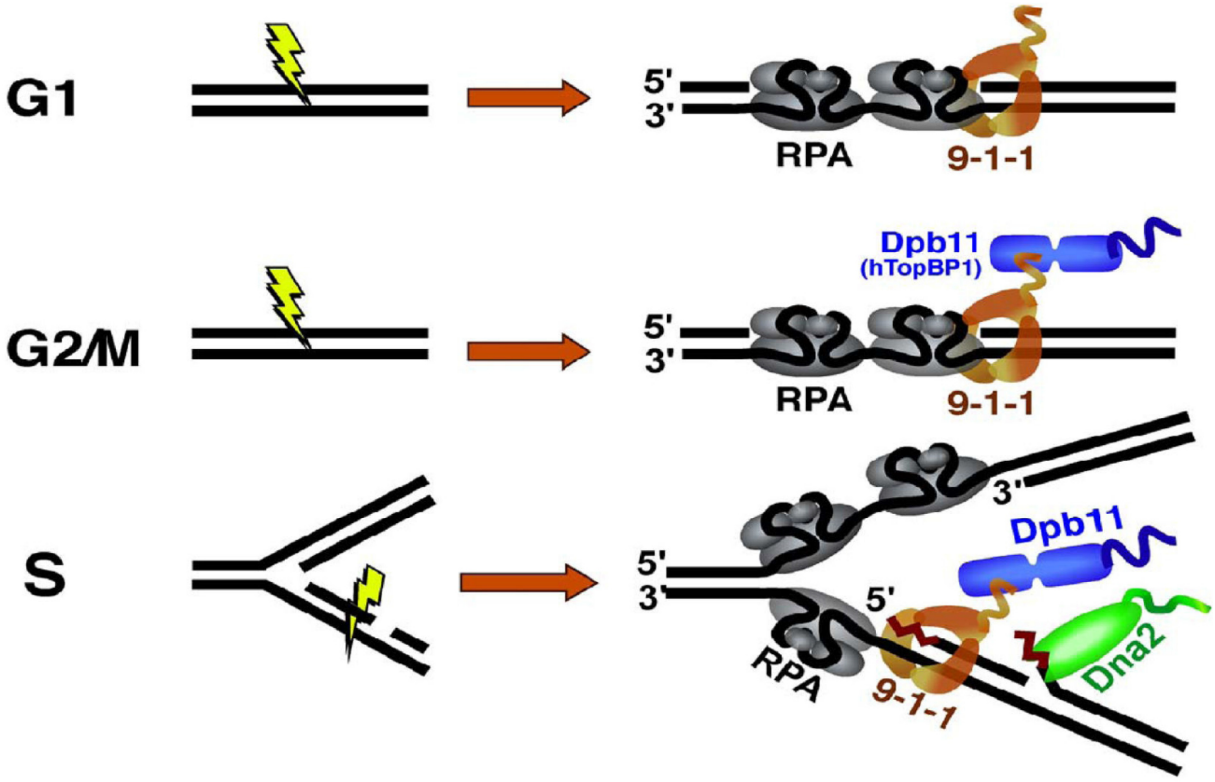


**Figure 8. Model for Mec1 activation during the cell cycle**

Figure and text adapted from Figure 2 (Wanrooij and Burgers, 2015).

Mec1$^{ATR}$ activation during different cell cycle phases in *S. cerevisiae*.

Top panel, 9–1–1 (orange; Ddc1, Rad17, Mec3 in yeast) is the sole activator of Mec1 in G1 phase.

Middle panel, In G2/M, Mec1 can be activated through two redundant pathways that are separable. The first involves direct activation by 9–1–1 and depends on two aromatic residues in the unstructured C-terminus of the Ddc1 subunit of 9–1–1. The second pathway relies on activation by Dpb11 (in blue), although 9–1–1 is still required for Dpb11 recruitment.

Bottom panel, Dna2 (green), 9–1–1 (orange) and Dpb11 (blue) act in a redundant fashion to stimulate Mec1 upon replication stalling induced by hydroxyurea. Dna2 is depicted as bound to long flaps, while 9–1–1 and thereby Dpb11 bind 5'-ssDNA-dsDNA junctions.

## 3.1 The role of Ddc1 in the fitness of *cdc13-1* and *yku70*Δ mutants

### *3.1.1 Confirmation of the known cdc13-1 ddc1*Δ *phenotype*

*DDC1* is not an essential gene, and the function of Ddc1 domains can be examined by introducing alleles of *DDC1* on plasmids into haploid *ddc1*Δ strains. First, it was confirmed that *ddc1*Δ suppresses temperature sensitivity of *cdc13-1* (Fig. 9) (Addinall et al., 2008). Strains were spot-tested on YEPD and incubated at a range of temperatures. Wild type, *ddc1*Δ and *exo1*Δ strains grew well at all temperatures in contrast to *cdc13-1*, which was unable to form colonies above 28°C (Fig. 9). *cdc13-1 ddc1*Δ mutants grew much better than *cdc13-1* and similarly to cdc13-1 *exo1*Δ mutants. It was shown that Rad24 or Mec3, which work with Ddc1, affect fitness of *cdc13-1* mutants (Zubko et al., 2004, Ngo and Lydall, 2010). *DDC1*, a member of the 9-1-1 complex, also seems to affect fitness of *cdc13-1* strains, and the effect is similar to that of *EXO1*.

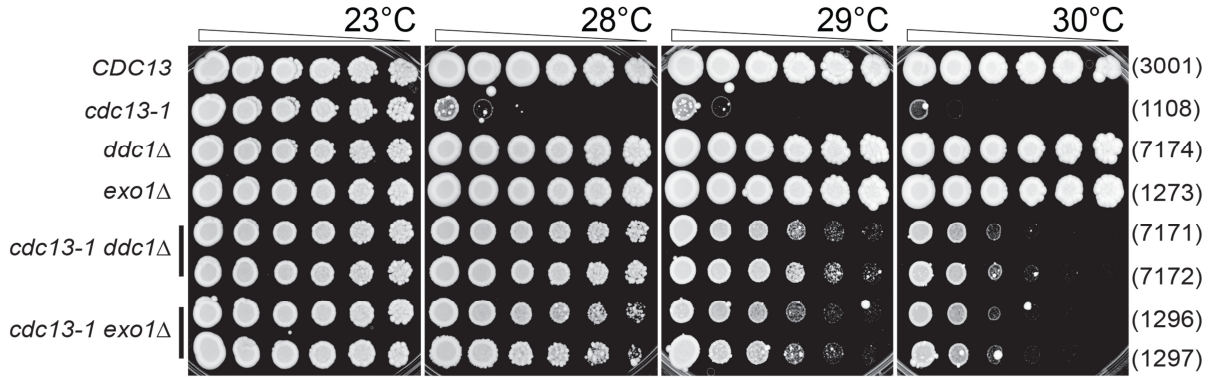


**Figure 9. Ddc1 and Exo1 similarly affect fitness of *cdc13-1* mutants.**
Pooled colonies were inoculated into 2 mL liquid YEPD and cultures were grown for 24 h at 23°C to saturation. Small aliquots were five-fold serially diluted in sterile water, spotted onto YEPD plates and incubated at shown temperatures for 3 days before being photographed. All 4 photographs had image features adjusted identically using Adobe Photoshop CS6. The relevant genotypes of the strains are indicated on the left, strain numbers on the right; strain details are in Appendix A.

### *3.1.2 Alleles of DDC1 chosen to study checkpoint function*

Specific alleles of *DDC1* had been reported to be Mec1-activation deficient upon DNA damage (Puddu et al., 2008, Pfander and Diffley, 2011, Kumar and Burgers, 2013). Some of these alleles, listed in Table 1, were chosen to test whether the effect on growth of *cdc13-1* strains may be observed. Figure 10 shows an alignment of the *DDC1* allele, *ddc1*-M11, with the wild type *DDC1* sequence. Other plasmids were analysed similarly and were used in further experiments.

| Plasmid (pDL) | *DDC1* alleles | Source | Mutation | Mutated sequence |
|---|---|---|---|---|
| **1543** | *pRS315-LEU2-DDC1* | P. Burgers | WT | N/A |
| **1470** | *YCplac111-LEU2-ddc1*-M3 | M. Muzi-Falconi | S413A<br>S436A<br>T444A | serine AGT into alanine GCT<br>serine AGT into alanine GCT<br>threonine ACC into alanine GCT |
| **1472** | *YCplac111-LEU2-ddc1*-M8 | M. Muzi-Falconi | T342A<br>S469A<br>S471A<br>S495A<br>T529A<br>S532A<br>S580A<br>T602A | threonine ACC into alanine GCT<br>serine AGC into alanine GCT<br>serine AGT into alanine GCT<br>serine AGT into alanine GCT<br>threonine ACC into alanine GCT<br>serine TCT into alanine GCT<br>serine TCC into alanine GCT<br>threonine ACA into alanine GCT |
| **1474** | *YCplac111-LEU2-ddc1*-M11 | M. Muzi-Falconi | T342A<br>S413A<br>S436A<br>T444A<br>S469A<br>S471A<br>S495A<br>T529A<br>S532A<br>S580A<br>T602A | threonine ACC into alanine GCT<br>serine AGT into alanine GCT<br>serine AGT into alanine GCT<br>threonine ACC into alanine GCT<br>serine AGC into alanine GCT<br>serine AGT into alanine GCT<br>serine AGT into alanine GCT<br>threonine ACC into alanine GCT<br>serine TCT into alanine GCT<br>serine TCC into alanine GCT<br>threonine ACA into alanine GCT |
| **1476** | *YCplac111-LEU2-ddc1-T602S* | M. Muzi-Falconi | T602S | threonine ACA into serine TCA |
| **1479** | *YCplac111-LEU2-ddc1-T602A* | M. Muzi-Falconi | T602A | threonine ACA into alanine GCT |
| **1546** | pRS315-*LEU2-ddc1-W352A* | P. Burgers | W352A | tryptophan TGG into alanine GCG |
| **1547** | pRS315-*LEU2-ddc1-W352A,W544A* | P. Burgers | W352A<br>W544A | tryptophan TGG into alanine GCG<br>tryptophan TGG into alanine GCG |
| **1548** | *pRS315-LEU2-ddc1 W352A, W544A, T602A* | P. Burgers | W352A<br>W544A<br>T602A | tryptophan TGG into alanine GCG<br>tryptophan TGG into alanine GCG<br>threonine ACA into alanine GCA |
| **1549** | *pRS315-LEU2-ddc1-(1-404), W352A* | P. Burgers | K404-STOP<br>W352A | lysine AAA into STOP codon TAA, aspartic acid GAC into STOP codon TAG<br>tryptophan TGG into alanine GCG |
| **1550** | *pRS315-LEU2-ddc1-T602A* | P. Burgers | T602A | threonine ACA into alanine GCA |

**Table 1. Mutations of *DDC1* used**. All mutations were confirmed by sequencing.

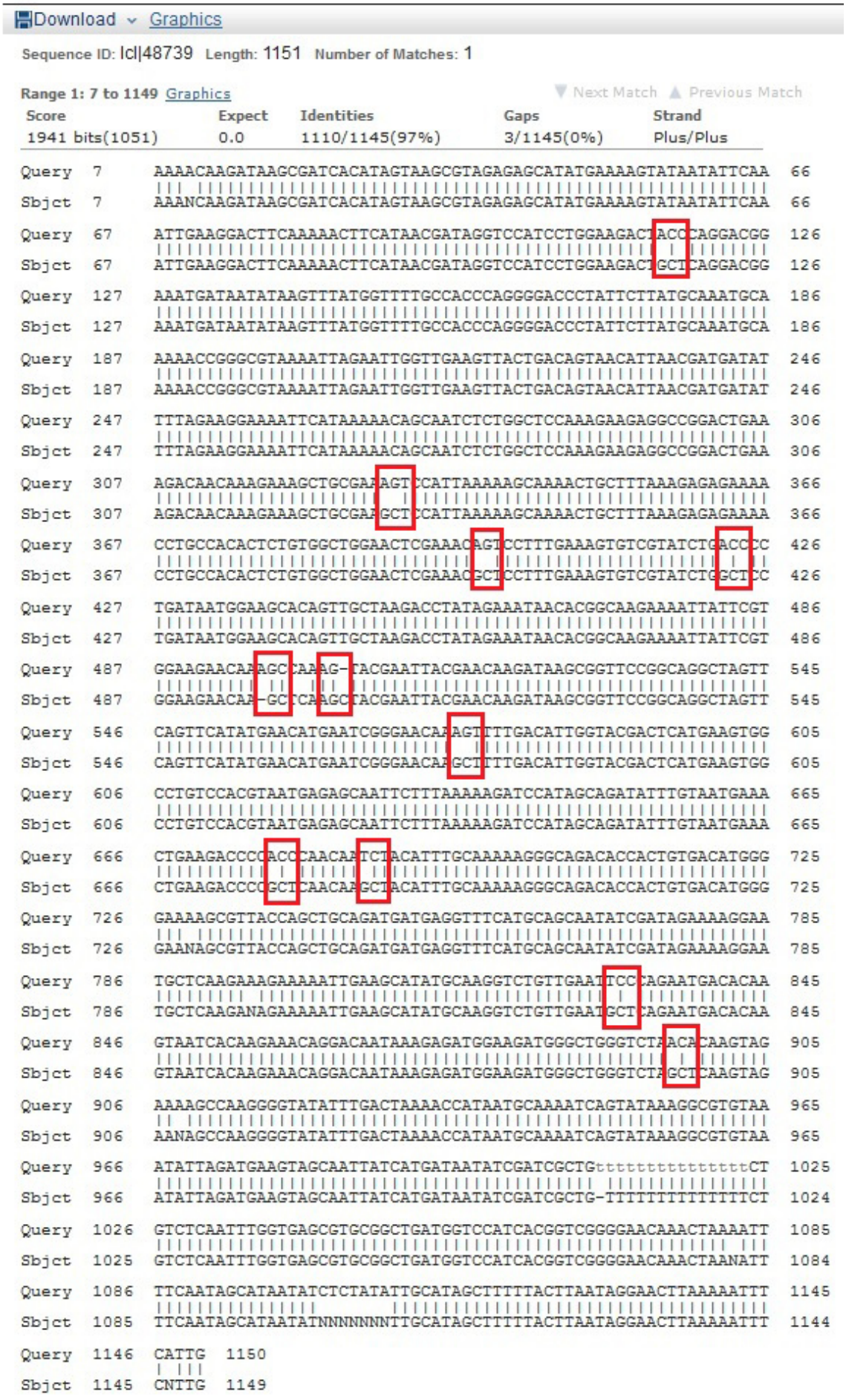
Download
Graphics
Sequence ID: lcl|48739 Length: 1151 Number of Matches: 1
Range 1: 7 to 1149 Graphics
Next Match
Previous Match
Score
Expect
Identities
Gaps
Strand
1941 bits(1051)
0.0
1110/1145(97%)
3/1145(0%)
Plus/Plus
Query 7 AAAACAAGATAAGCGATCACATAGTAAGCGTAGAGAGCATATGAAAAGTATAATATTCAA 66
Sbjct 7 AAANCAAGATAAGCGATCACATAGTAAGCGTAGAGAGCATATGAAAAGTATAATATTCAA 66
Query 67 ATTGAAGGACTTCAAAAACTTCATAACGATAGGTCCATCCTGGAAGACTACCCAGGACGG 126
Sbjct 67 ATTGAAGGACTTCAAAAACTTCATAACGATAGGTCCATCCTGGAAGACTGCTCAGGACGG 126
Query 127 AAATGATAATATAAGTTTATGGTTTTGCCACCCAGGGGACCCTATTCTTATGCAAATGCA 186
Sbjct 127 AAATGATAATATAAGTTTATGGTTTTGCCACCCAGGGGACCCTATTCTTATGCAAATGCA 186
Query 187 AAAACCGGGCGTAAAATTAGAATTGGTTGAAGTTACTGACAGTAACATTAACGATGATAT 246
Sbjct 187 AAAACCGGGCGTAAAATTAGAATTGGTTGAAGTTACTGACAGTAACATTAACGATGATAT 246
Query 247 TTTAGAAGGAAAATTCATAAAAACAGCAATCTCTGGCTCCAAAGAAGAGGCCGGACTGAA 306
Sbjct 247 TTTAGAAGGAAAATTCATAAAAACAGCAATCTCTGGCTCCAAAGAAGAGGCCGGACTGAA 306
Query 307 AGACAACAAAGAAAGCTGCGAAAGTCCATTAAAAAGCAAAACTGCTTTAAAGAGAGAAAA 366
Sbjct 307 AGACAACAAAGAAAGCTGCGAAGCTCCATTAAAAAGCAAAACTGCTTTAAAGAGAGAAAA 366
Query 367 CCTGCCACACTCTGTGGCTGGAACTCGAAACAGTCCTTTGAAAGTGTCGTATCTGACCCC 426
Sbjct 367 CCTGCCACACTCTGTGGCTGGAACTCGAAACGCTCCTTTGAAAGTGTCGTATCTGGCTCC 426
Query 427 TGATAATGGAAGCACAGTTGCTAAGACCTATAGAAATAACACGGCAAGAAAATTATTCGT 486
Sbjct 427 TGATAATGGAAGCACAGTTGCTAAGACCTATAGAAATAACACGGCAAGAAAATTATTCGT 486
Query 487 GGAAGAACAAAGCCAAAG-TACGAATTACGAACAAGATAAGCGGTTCCGGCAGGCTAGTT 545
Sbjct 487 GGAAGAACAA-GCCAAGCTACGAATTACGAACAAGATAAGCGGTTCCGGCAGGCTAGTT 545
Query 546 CAGTTCATATGAACATGAATCGGGAACAAAGTTTTGACATTGGTACGACTCATGAAGTGG 605
Sbjct 546 CAGTTCATATGAACATGAATCGGGAACAAGCTTTTGACATTGGTACGACTCATGAAGTGG 605
Query 606 CCTGTCCACGTAATGAGAGCAATTCTTTAAAAAGATCCATAGCAGATATTTGTAATGAAA 665
Sbjct 606 CCTGTCCACGTAATGAGAGCAATTCTTTAAAAAGATCCATAGCAGATATTTGTAATGAAA 665
Query 666 CTGAAGACCCCACCCAACAATCTACATTTGCAAAAAGGGCAGACACCACTGTGACATGGG 725
Sbjct 666 CTGAAGACCCCGCTCAACAAGCTACATTTGCAAAAAGGGCAGACACCACTGTGACATGGG 725
Query 726 GAAAAGCGTTACCAGCTGCAGATGATGAGGTTTCATGCAGCAATATCGATAGAAAAGGAA 785
Sbjct 726 GAANAGCGTTACCAGCTGCAGATGATGAGGTTTCATGCAGCAATATCGATAGAAAAGGAA 785
Query 786 TGCTCAAGAAAGAAAAATTGAAGCATATGCAAGGTCTGTTGAATTCCCAGAATGACACAA 845
Sbjct 786 TGCTCAAGANAGAAAAATTGAAGCATATGCAAGGTCTGTTGAATGCTCAGAATGACACAA 845
Query 846 GTAATCACAAGAAACAGGACAATAAAGAGATGGAAGATGGGCTGGGTCTAACACAAGTAG 905
Sbjct 846 GTAATCACAAGAAACAGGACAATAAAGAGATGGAAGATGGGCTGGGTCTAGCTCAAGTAG 905
Query 906 AAAAGCCAAGGGGTATATTTGACTAAAACCATAATGCAAAATCAGTATAAAGGCGTGTAA 965
Sbjct 906 AANAGCCAAGGGGTATATTTGACTAAAACCATAATGCAAAATCAGTATAAAGGCGTGTAA 965
Query 966 ATATTAGATGAAGTAGCAATTATCATGATAATATCGATCGCTGtttttttttttttttCT 1025
Sbjct 966 ATATTAGATGAAGTAGCAATTATCATGATAATATCGATCGCTG-TTTTTTTTTTTTTTCT 1024
Query 1026 GTCTCAATTTGGTGAGCGTGCGGCTGATGGTCCATCACGGTCGGGGAACAAACTAAAATT 1085
Sbjct 1025 GTCTCAATTTGGTGAGCGTGCGGCTGATGGTCCATCACGGTCGGGGAACAAACTAANATT 1084
Query 1086 TTCAATAGCATAATATCTCTATATTGCATAGCTTTTTACTTAATAGGAACTTAAAAATTT 1145
Sbjct 1085 TTCAATAGCATAATATNNNNNNNTTGCATAGCTTTTTACTTAATAGGAACTTAAAAATTT 1144
Query 1146 CATTG 1150
Sbjct 1145 CNTTG 1149

**Figure 10. Alignment of *DDC1* and *ddc1*-M11 allele on plasmids**

*Query* – WT *DDC1* sequence on pDL1543 plasmid; *Subject* – *ddc1*-M11 sequence on pDL1474 plasmid. *Query* and *Subject* sequences were sequenced by GATC Biotech company. Red boxes indicate the sites of mutations. Plasmid details are in Table 1 and Appendix B. WT *DDC1* sequence from pDL1543 was also aligned to the WT sequence obtained from SGD (not shown).

### *3.1.3 Some DDC1 alleles strongly affect cdc13-1 fitness*

It had been reported that Ddc1 can interact with Mec1 through two distinct pathways: i) directly, by two conserved aromatic amino acids, tryptophan W352 and W544, ii) indirectly, by recruitment of Dpb11 through threonine T602 (Navadgi-Patil and Burgers, 2009). When W352, W544 and T602 residues were changed into alanine, such *ddc1* mutants showed reduced phosphorylation of Rad53, a Mec1 downstream effector kinase, in response to DNA damage induced by 4-NQO or UV (Navadgi-Patil and Burgers, 2009, Navadgi-Patil et al., 2011, Kumar and Burgers, 2013). Three Cdk1 and eight Mec1 putative target sites of Ddc1 were also identified (Puddu et al., 2008). *DDC1* alleles in which three (M3 – CDK1 target sites), eight (M8 - Mec1 target sites) or eleven (M11 – CDK1 and Mec1 target sites) residues are changed into alanine, are denoted as *ddc1*-M3, *ddc1*-M8 and *ddc1*-M11 (Table 1).

To test whether different *DDC1* alleles affect fitness of *cdc13-1* mutants*, cdc13-1 ddc1*Δ strains were transformed with plasmids shown in Table 1 (Table 1, Fig. 11a). *cdc13-1 ddc1*Δ mutants grew at 30°C, and *cdc13-1* mutants did not grow above 27°C (Fig. 11b D-E, F-H). All *DDC1* alleles suppressed *cdc13-1* ts at 27-28°C, apart from *ddc1*-M3 and *ddc1-T602S* alleles (Fig. 11b I-S). The strongest suppressors of *cdc13-1* ts at 28°C were: *ddc1-W352A, W544A, T602A*, *ddc1-(1-404),W352, ddc1*-M11 and *ddc1*-M8 alleles (Fig. 13b K-L and P-R, compare to F-H). However none of the alleles suppressed *cdc13-1* ts as *ddc1*Δ mutation at 30°C. The evaluation of suppression effects by *ddc1* mutations on *cdc13-1* is shown in Fig 11, bottom.

The *T602A* mutation was present in all *DDC1* alleles which strongly suppressed *cdc13-1* defect. The threonine T602 of Ddc1 is a site of Dpb11 recruitment in response to DNA damage in G2/M and S-phase of the cell cycle (Navadgi-Patil and Burgers, 2009, Navadgi-Patil and Burgers, 2011, Navadgi-Patil et al., 2011). T602 residue was also identified as one of Mec1 target sites in Ddc1 (Puddu et al., 2008). Apparently the recruitment of Dpb11 or interaction between Ddc1 and Mec1 in response to telomere damage might be important for Ddc1 checkpoint function. *T602S* mutation, which did not affect *cdc13-1* growth, probably still permits Dpb11 recruitment or Ddc1-Mec1 interaction.

*ddc1*-M8 and *ddc1*-M11 alleles with mutated sites for Mec1 or Cdk1 and Mec1 phosphorylation, respectively, strongly suppressed *cdc13-1* defect at higher temperatures. In contrast, *ddc1*-M3 mutation, which was shown to be defective in the phosphorylation by CDK(Puddu et al., 2008), had no effect on *cdc13-1* fitness. The suppression of *cdc13-1* by *ddc1*-M8 and *ddc1*-M11 alleles suggests that the phosphorylation of Ddc1 by Mec1 might play an important role in response to damaged telomeres. Accordingly, lack of *cdc13-1* suppression by *ddc1*-M3 suggests that Ddc1 phosphorylation by Cdk1 does not play an important role in response to damaged telomeres. It was shown that *ddc1-M3* mutants maintained the checkpoint function after UV treatment (Puddu et al., 2008). It seems that in response to UV-generated damage and telomere defects, the checkpoint pathway remains functional in *ddc1*-M3 mutants. However, the phosphorylation of Ddc1 by Mec1 or Cdk1 was not tested in this thesis. I drew the conclusions about the checkpoint role of Ddc1 and the role of Ddc1 phosphorylation by Mec1 and Cdk1 based on the observed phenotypes of published *ddc1* alleles.

a)

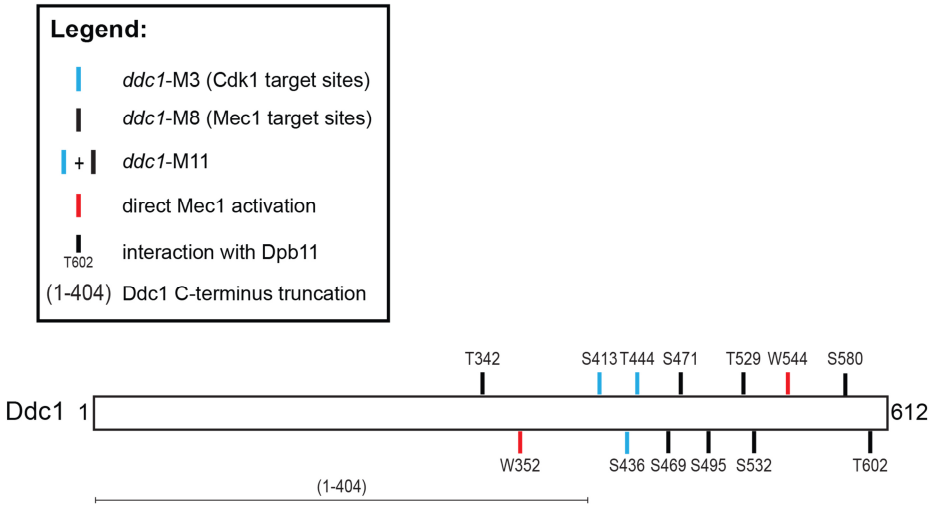


b)

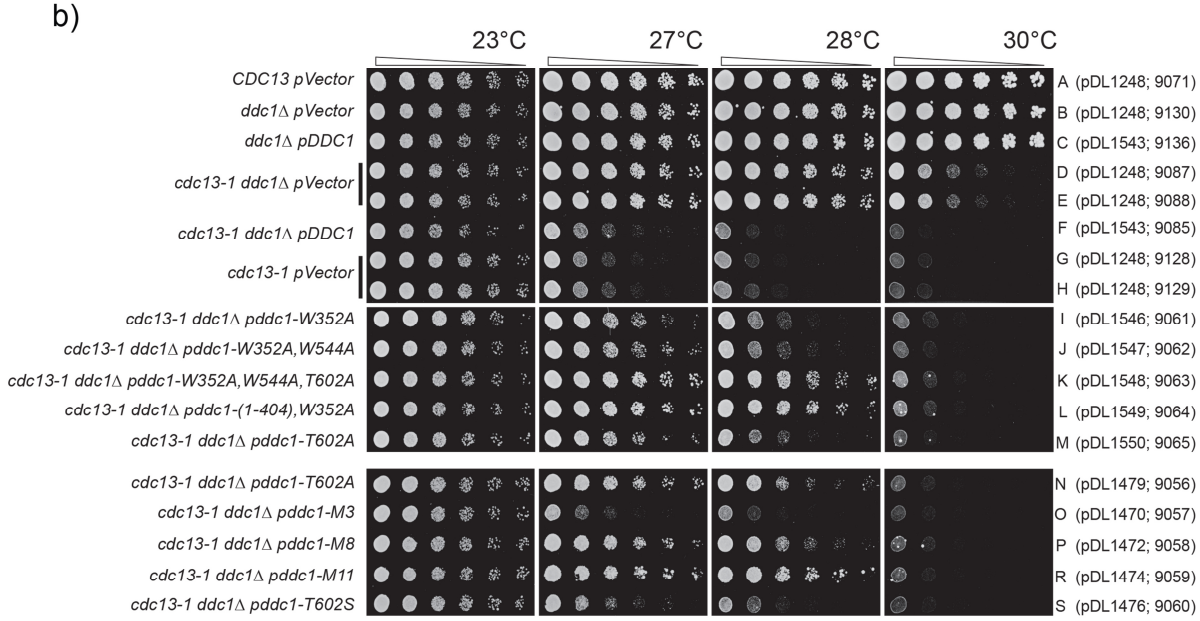


**Suppressors of *cdc13-1***:

*ddc1Δ* > *ddc1-M11* > *ddc1-(1-404),W352A* / *ddc1-W352A,W544A,T602A* > *ddc1-M8* > *ddc1-T602A* > *ddc1-W352A* / *ddc1-W352A,W544A*

**Figure 11. *DDC1* alleles affect growth of cdc13-1 mutants**

a) Point mutations used (adapted from (Puddu et al., 2008)).

b) Spot test done as in Figure 9. Yeast strains were spotted onto –LEU plates to select for plasmids. Strains A-M were grown on one rectangular plate. Strains N-S were grown on a different rectangular plate, which is indicated by wider space between bottom and top part of the picture. These strains were grown on the same batch of –LEU media, but on different days. The results acquired in this spot test are consistent with 2-3 other experiments prepared on the same batch of the media (not shown). *pVector* - pRS315. The relevant genotypes of the strains are indicated on the left, plasmid and strain numbers on the right; strain details are in Appendix A. Letters A-S on the right of the figure are assigned to relevant genotypes from the left. Beneath is shown the evaluation of suppression effects on *cdc13-1* strains by tested *ddc1* mutations.

### *3.1.4 The 9-1-1 complex mutations and rad24Δ slightly affect yku70Δ fitness*

It was shown that *yku70Δ* does not require Ddc1 checkpoint function in Mec1-dependent cell cycle arrest (Maringele and Lydall, 2002). I wanted to confirm previous data and therefore I generated and spot tested some new *yku70Δ ddc1Δ* strains (Fig. 12). Figure 12a from Maringele and Lydall shows that Ddc1, Mec3 and Rad17 components of the 9-1-1 complex, do not affect the growth of *yku70Δ* mutants (Maringele and Lydall, 2002). Figure 12b shows somewhat different growth patterns. Wild type, *ddc1Δ* and *exo1Δ* strains grew well at all temperatures, *yku70Δ* mutants did not grow above 36°C. Interestingly, the deletion of *DDC1* mildly affected the fitness of *yku70Δ* strains above 36°C, which is different to published results (Maringele and Lydall, 2002). Consistent with previous results, *exo1Δ* had much stronger effect on fitness of *yku70Δ* mutants than *ddc1Δ*.

In order to test whether other members of the 9-1-1 complex also affect *yku70Δ* fitness, more growth assays involving *mec3Δ, rad17Δ*, as well as *rad24Δ* and *chk1Δ,* were carried out. One example is shown in Figure 13. Wild type strain and *ddc1Δ, mec3Δ, rad17Δ* strains grew well at all temperatures, *yku70Δ* mutants did not grow above 36°C (Fig. 13). Although there is a heterogeneity between strains of the same genotype, mutations of the 9-1-1 complex and *rad24Δ* slightly suppress *yku70Δ* ts. *chk1Δ* has the strongest effect on *yku70Δ* growth at higher temperatures, consistently with published data (Fig. 12a).

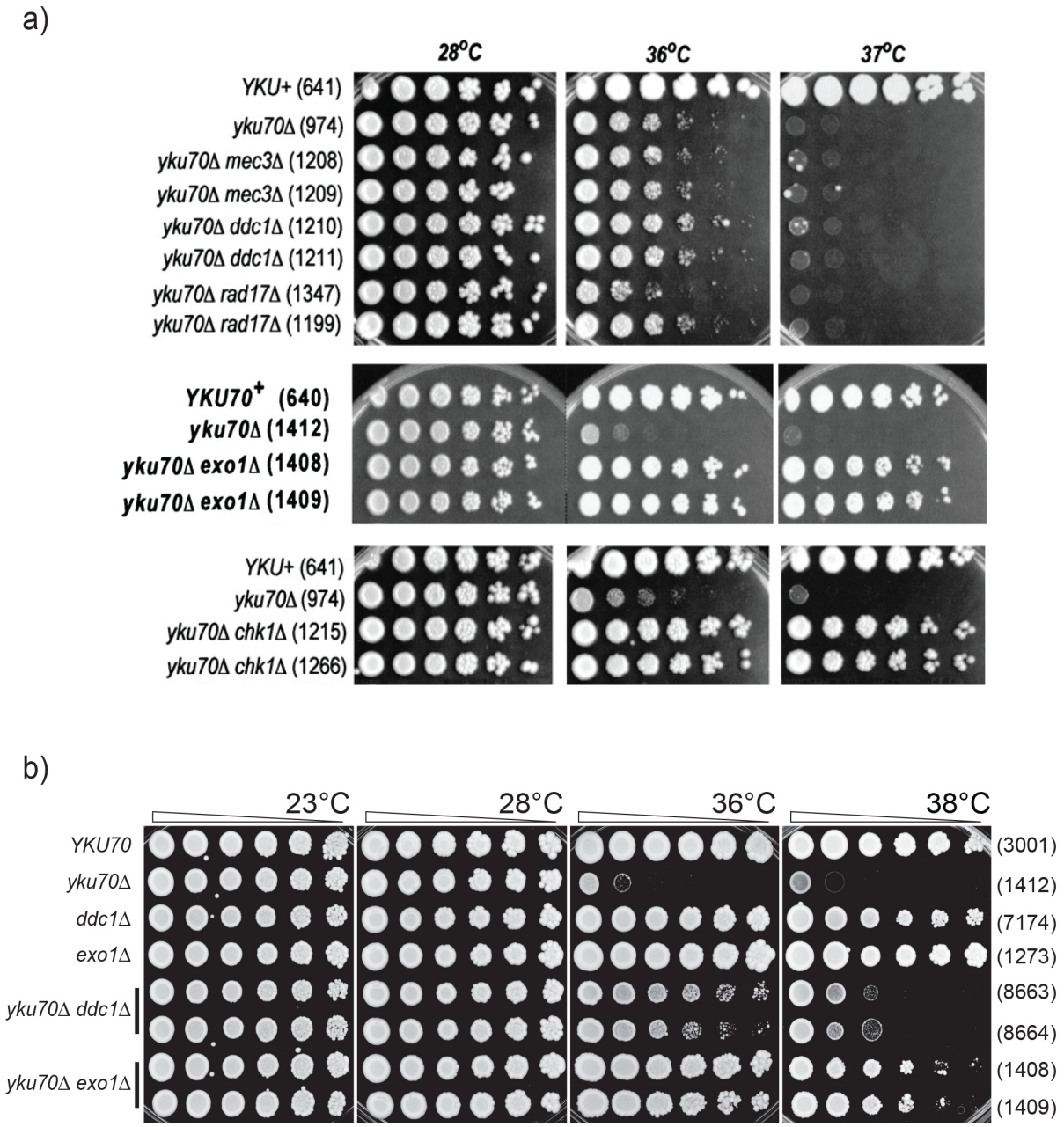


**Figure 12. Effect of Ddc1 on *yku70*Δ fitness**

a) Figures and text adapted from (Maringele and Lydall, 2002), Fig.1a-c, Fig.6a, Fig.1g-i. Small aliquots of five-fold dilution series of several yeast strains were transferred to plates and incubated at the temperatures indicated for 2 days before being photographed. The relevant genotypes of the strains are indicated on the *left,* and the strain numbers shown in parentheses.

b) Yeast strains were pre-grown at 30°C, spot test done as in Figure 9. The relevant genotypes of the strains are indicated on the left, strain numbers on the right; strain details are in Appendix A.

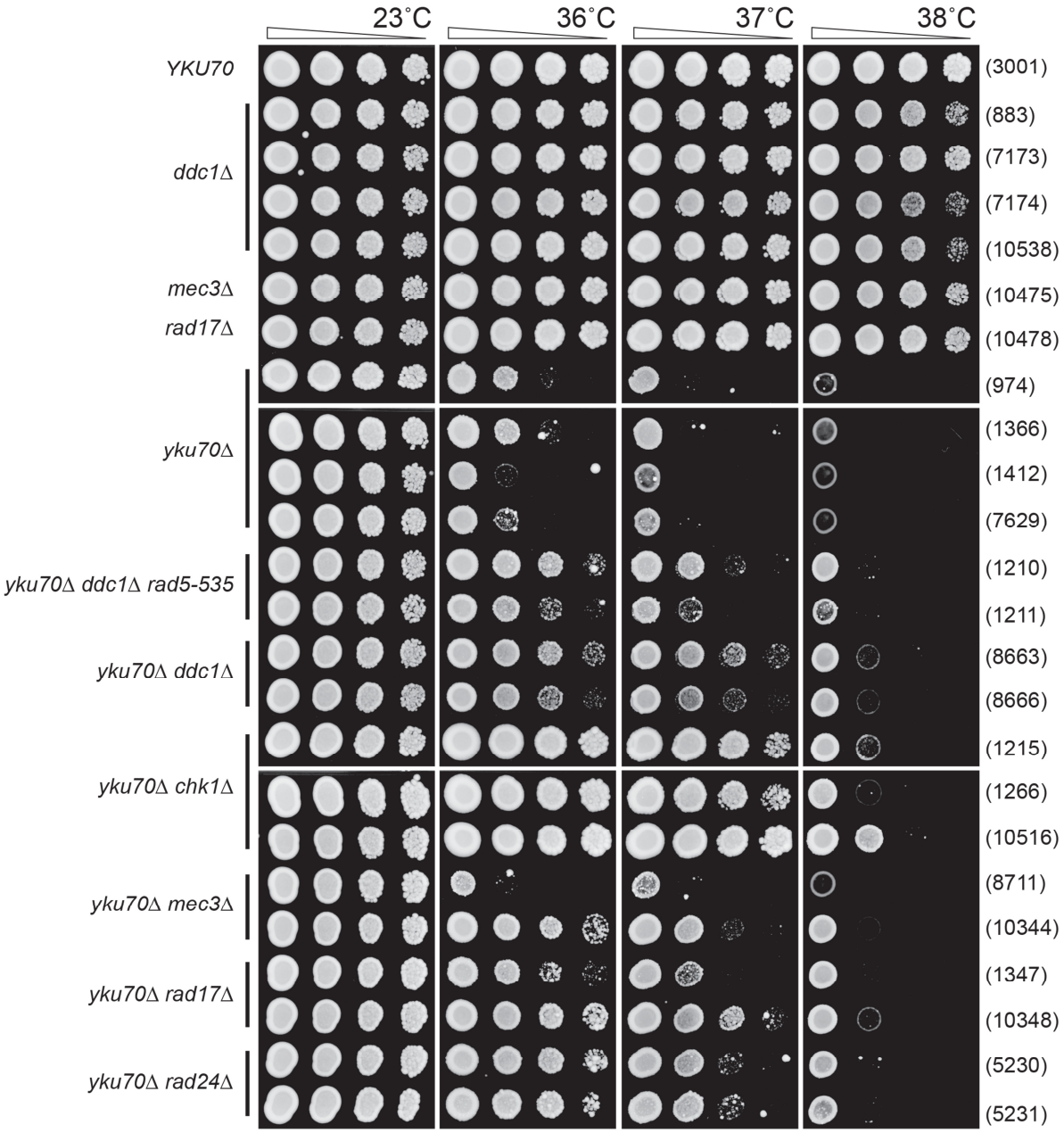


**Figure 13. Checkpoint proteins affect *yku70*Δ fitness**

Yeast strains were pre-grown at 30°C, spot test done as in Figure 9. The relevant genotypes of the strains are indicated on the left, strain numbers on the right; strain details are in Appendix A.

The 9-1-1 complex, Rad24 and Exo1 regulate ssDNA generation at telomeres (Maringele and Lydall, 2002, Ngo et al., 2014). Exo1 generates high levels of ssDNA in *yku70*Δ mutants, and contributes to ssDNA in *cdc13-1* strains (Maringele and Lydall, 2002, Zubko et al., 2004). Rad24, Rad17 and Mec3 belong to one phenotypic group based on their checkpoint function and effects on DNA degradation (Lydall and Weinert, 1995). Rad24 and the 9-1-1 complex members belong to one functional group, and *rad24*Δ decreases ssDNA accumulation in *cdc13-1* mutants. (Lydall and Weinert, 1995, Zubko et al., 2004). It was shown that *yku70*Δ *rad24*Δ mutants accumulated comparable amounts of ssDNA to *yku70*Δ strains (Maringele and Lydall, 2002). Due to the fact that I observed that the 9-1-1 complex and Rad24 affect *yku70*Δ fitness in contrast to published data (Maringele and Lydall, 2002), I hypothesised that the 9-1-1 complex might be required for ssDNA generation in *yku70*Δ cells.

To test this hypothesis the fluorescent in-gel assay was used to measure the ssDNA accumulation (Fig. 14a and b). As expected, *yku70*Δ strains accumulated more ssDNA than control strains. *yku70*Δ mutants with deletions of members of the 9-1-1 complex, *CHK1* and *RAD24* accumulated ssDNA amounts comparable to *yku70*Δ cells (Fig. 14b). These results are consistent with published data (Maringele and Lydall, 2002). Cells, from which DNA was isolated and used (Fig. 14a-b), were in different phases of the cell cycle. Maybe the differences in ssDNA accumulation would be visible if DNA was isolated from synchronous cultures. The application of the Quantitative Amplification of Single-Stranded DNA (QAOS) method, which uses qPCR to measure ssDNA accumulation (Holstein and Lydall, 2012), might be more accurate to observe ssDNA accumulation than in-gel assay.

*yku70*Δ strains with deletions of *DDC1, MEC3, RAD17* and *RAD24* were slightly fitter than *yku70*Δ mutants, which raised the possibility that double mutants' growth resulted from different telomere structures. To address this, telomere length was examined by Southern blot (Fig. 14c). Wild type, *ddc1*Δ*, mec3*Δ and *rad17*Δ strains have similar telomere lengths (Fig. 14c lines 3-9, 27). *yku70*Δ mutants have short telomeres and deletions of *DDC1, MEC3* or *RAD17* did not affect telomere structure of *yku70*Δ strains (Fig. 14c lines 10-13, compare to line 14-26). I conclude that the 9-1-1 complex and Rad24 do not affect the telomere length of *yku70*Δ strains, and so the role of the 9-1-1 complex in this context remains unclear.

a)

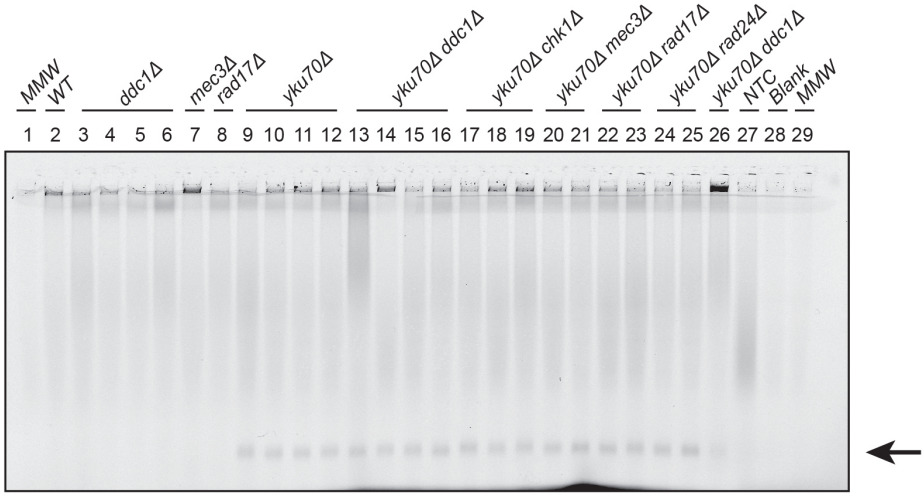
MMW
WT
ddc1Δ
mec3Δ
rad17Δ
yku70Δ
yku70Δ ddc1Δ
yku70Δ chk1Δ
yku70Δ mec3Δ
yku70Δ rad17Δ
yku70Δ rad24Δ
yku70Δ ddc1Δ
NTC
Blank
MMW
1 2 3 4 5 6 7 8 9 10 11 12 13 14 15 16 17 18 19 20 21 22 23 24 25 26 27 28 29

b)

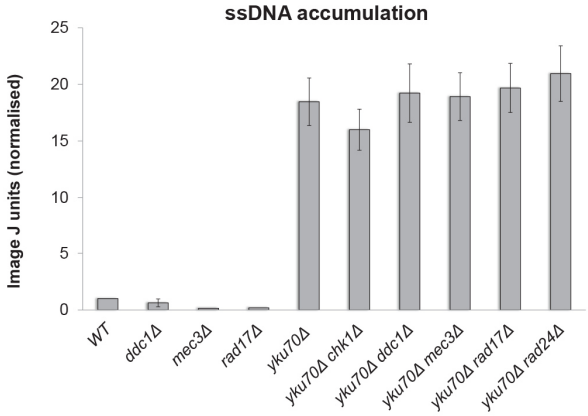
ssDNA accumulation
Image J units (normalised)
25
20
15
10
5
0
WT
ddc1Δ
mec3Δ
rad17Δ
yku70Δ
yku70Δ chk1Δ
yku70Δ ddc1Δ
yku70Δ mec3Δ
yku70Δ rad17Δ
yku70Δ rad24Δ

c)

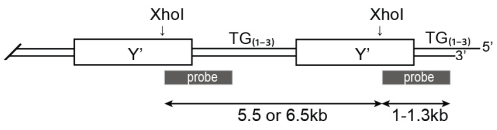
XhoI
XhoI
TG(1–3)
TG(1–3)
Y'
Y'
3'
5'
probe
probe
5.5 or 6.5kb
1-1.3kb

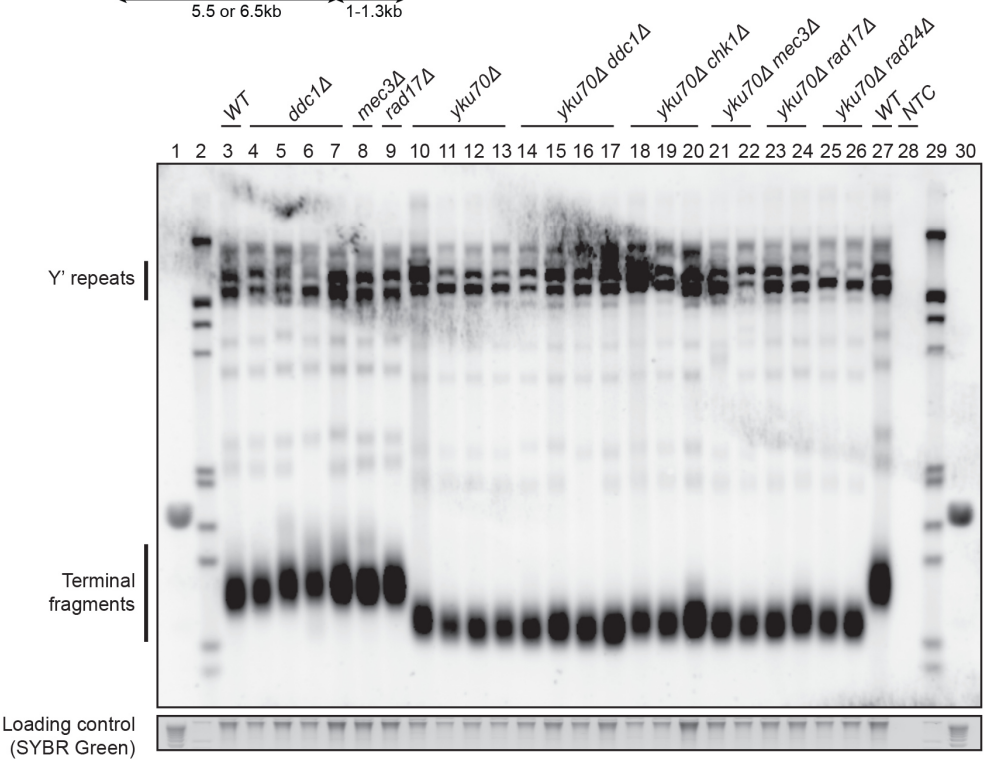
WT
ddc1Δ
mec3Δ
rad17Δ
yku70Δ
yku70Δ ddc1Δ
yku70Δ chk1Δ
yku70Δ mec3Δ
yku70Δ rad17Δ
yku70Δ rad24Δ
WT
NTC
1 2 3 4 5 6 7 8 9 10 11 12 13 14 15 16 17 18 19 20 21 22 23 24 25 26 27 28 29 30
Y' repeats
Terminal fragments
Loading control (SYBR Green)

**Figure 14. Unaltered ssDNA accumulation and telomere structure of *yku70*Δ mutants with checkpoint gene deletions**

a) 3 mL liquid cultures of indicated strains were incubated overnight at 30°C prior to phenol DNA isolation and In-gel assay. Image was adjusted in ImageJ. The black arrow indicates the position of ssDNA.

b) Quantification of a). Wild type (WT) strain was given the value of 1; all other genotypes were expressed relative to the wild type strain. WT, *mec1*Δ and *rad17*Δ were single strains. For *ddc1*Δ*, yku70*Δ*, yku70*Δ *chk1*Δ and *yku70*Δ *ddc1*Δ the mean of three-four independent strain is shown, and error bars indicate the SD. For *yku70*Δ *mec3*Δ*, yku70*Δ *rad17*Δ *and yku70*Δ *rad24*Δ the mean of two independent strains is shown and error bars indicate the individual values of each strain.

c) Genomic DNA was isolated from the same yeast strains as in a) by Yale method after overnight incubation at 30°C. Telomeres were analysed by Southern blot. The probe (Y' and TG) used for Southern blot is shown. SYBR Safe was used as a loading control. Lines 1-2 & 29-30 – molecular ladders. Strains were: *YKU70* (DLY3001), *ddc1*Δ *rad5-535* (DLY883), *ddc1*Δ (DLY7173), *ddc1*Δ (DLY7174), *ddc1*Δ (DLY10538), *mec3*Δ (DLY10475), *rad17*Δ (DLY10478), *yku70*Δ (DLY974), *yku70*Δ (DLY1366), *yku70*Δ (DLY1412), *yku70*Δ (DLY7629), *yku70*Δ *ddc1*Δ *rad5-535* (DLY1210), *yku70*Δ *ddc1*Δ *rad5-535* (DLY1211), *yku70*Δ *ddc1*Δ (DLY8663), *yku70*Δ *ddc1*Δ (DLY8666), *yku70*Δ *chk1*Δ (DLY1215), *yku70*Δ *chk1*Δ (DLY10516), *yku70*Δ *mec3*Δ (DLY8711), *yku70*Δ *mec3*Δ (DLY8711), *yku70*Δ *mec3*Δ (DLY10344), *yku70*Δ *rad17*Δ (DLY1347), *yku70*Δ *rad1117*Δ (DLY10348), *yku70*Δ *rad24*Δ (DLY5230), *yku70*Δ *rad24*Δ (DLY5231), *yku70*Δ *ddc1*Δ *rad5-535* (DLY1210). Strain details are in Appendix A.

### *3.1.5 Yeast culture conditions affect the effect of the 9-1-1 complex and Rad24 on yku70∆ fitness*

Results in this chapter so far show that the 9-1-1 complex affects the growth of *yku70∆* mutants at higher temperature in contrast to previously published results (Maringele and Lydall, 2002). One possible explanation was different culture condition. In order to test whether the culture conditions influenced spot test assays, two methods of yeast culture were compared (Fig. 15). In a first method yeast strains were collected in the exponential phase as described before (Fig. 15a) (Maringele and Lydall, 2002). In a second method the same strains were grown till saturation and spot tested as earlier (Fig. 15b).

Strains grown till saturation prior to spotting exhibited stronger growth at all temperatures tested when compared to strains collected at exponential growth phase (Fig. 15b and a). The experiment is however not definite, because *yku70∆* mutants exhibited heterogeneous growth independently of the method used (Fig. 15a and b, B-D). I will compare *yku70∆* DLY1412 mutant (Fig. 15a and b B) with other strains, because it exhibits an average phenotype. Mutations of the 9-1-1 complex and *RAD24* only slightly affected *yku70∆* growth when cells from exponential growth phase were spotted (Fig. 15a E-J). It was easier to observe the suppression effect when strains were grown to saturation prior to spotting (Fig. 15b E-J). Consistent with the previous results *chk1∆, rad9∆* and *exo1∆* are much stronger suppressors of *yku70∆* ts independently of method used (Fig. 15a and b, K-P) (Maringele and Lydall, 2002).

The yeast culture conditions had impact on *yku70∆* strain growth. For reasons that are unclear, *yku70∆* mutants are fitter at higher temperature when cells were first grown till saturation, being able to grow at 38°C. Cells from saturated culture might somehow escape telomere damage and cell cycle arrest, which resulted in improved fitness. The role of the 9-1-1 complex and Rad24 in *yku70∆* cells, and the difference between saturated and the exponentially cultured cells should be clarified. One explanation for different growth might be the stress response (Gasch, 2007). Strains grown till saturation at permissive temperature started possibly experiencing nutrient depletion and the stress response was activated. In response to starvation cells may not resume growth but enter a quiescent state until nutrients become available. In

response to stress the environmental stress response (ESR) program is triggered and leads to gene expression changes which persist until starvation is alleviated (Gasch et al., 2000, Gasch and Werner-Washburne, 2002). The ESR is a general response observed regardless of the type of stress involved (Gasch et al., 2000). The budding yeast ESR genes are involved in oxidation processes, stress signalling, the Msn2/Msn4 network, as well as essential processes assuring optimal cell growth, e.g. ribosome biogenesis (Brion et al., 2016). It is therefore possible that when starved *yku70*Δ cells were spotted onto fresh YEPD at higher temperature the stress response could be activated. Such response before the first cell division would protect cells and facilitate their further growth.

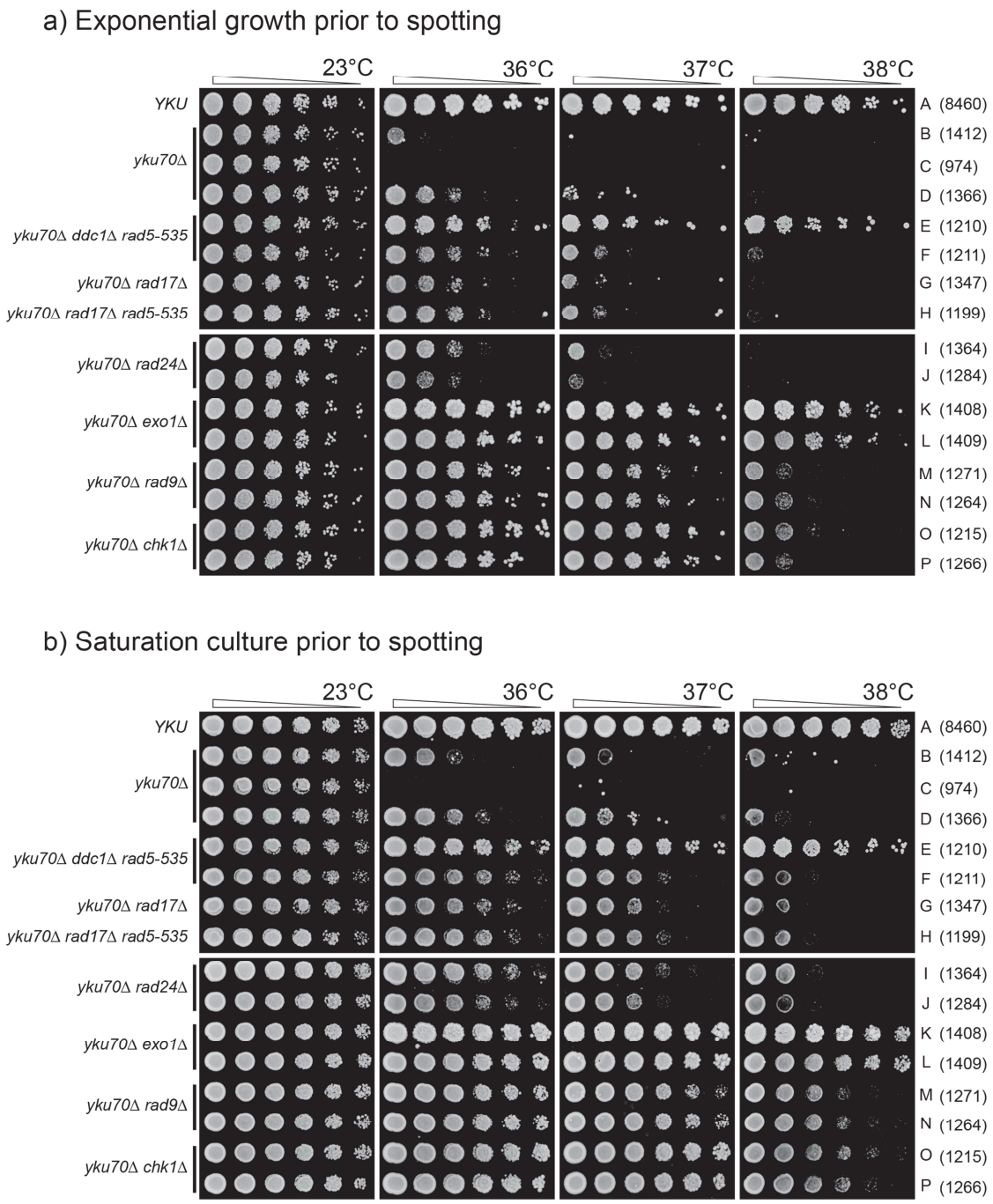


**Figure 15. Culture conditions affect the apparent fitness of *yku70*Δ mutants with deletions of checkpoint genes**

a) Exponential growth method. Experiment performed as described previously (Maringele and Lydall, 2002).

b) Saturation growth method. Yeast strains were pre-grown at 23°C, spot test done as in Figure 9. Plates were incubated at shown temperatures for 2 days before being photographed. The relevant genotypes of the strains are indicated on the left, strain numbers on the right; strain details are in Appendix A. Letters A-P on the right of the figure are assigned to relevant genotypes from the left. Strains used in this study, apart from *YKU70*, are the same as published before (Maringele and Lydall, 2002).

### *3.1.6 Discussion/Conclusions*

I confirmed that deletion of *DDC1* drastically suppresses the temperature sensitivity of *cdc13-1* strains and that growth of *cdc13-1 ddc1*Δ is similar to *cdc13-1 exo1*Δ mutants (Zubko et al., 2004, Addinall et al., 2008). I showed for the first time that mutations previously shown to be critical for Ddc1 checkpoint function upon DNA damage (e.g. induced by UV or 4-NQO) play similar role in response to defective telomeres of *cdc13-1* mutants (Table 2). However, none of tested alleles showed the same effect on *cdc13-1* fitness as *DDC1* deletion. All *DDC1* alleles which strongly suppressed *cdc13-1* fitness contained the *T602A* mutation. It seems that T602 residue, which facilitates Dpb11 recruitment and subsequent Mec1 activation (Navadgi-Patil and Burgers, 2009) is important for Ddc1 checkpoint function. Ddc1 protein with multiple mutated residues (e.g. in *ddc1*-M8, *ddc1*-M11 or *ddc1-W352A, W544A, T602A*) might not fold properly to acquire biologically functional conformation, which could result in checkpoint function loss by *DDC1* alleles.

I observed that *yku70*Δ strains with mutations of checkpoint genes were fitter at higher temperatures than *yku70*Δ mutants. The 9-1-1 complex and Rad24 had no effect on ssDNA accumulation or on telomere length of *yku70*Δ strains. I also showed that the method of cell culture affected subsequent yeast growth. I reproduced the published experiment where cells were in exponential growth phase (Maringele and Lydall, 2002). However, when cells were grown till saturation it was easier to observe the suppression effect of the 9-1-1 complex and *RAD24* mutations on *yku70*Δ growth. There are some possible explanations for difference in growth between saturated cells and exponentially grown culture: i) cells growing until saturation prior to spotting onto fresh YEPD may enter a quiescent state until nutrients become available or become arrested in G1 phase of the cell cycle. Subsequent growth at higher temperature might activate stress response, which protect cells from high temperature stress and facilitate growth; ii) perhaps *yku70*Δ cells, if arrested in G1 phase of the cell cycle, accumulated DNA damage due to defects in NHEJ repair pathway. This hypothesis would explain why mutations of checkpoint gene deletions slightly suppressed growth of *yku70*Δ cells at higher temperature; iii) first cell cycles after prolonged culture of *yku70*Δ cells might be longer, and therefore slower growing cells would be observed as “fitter” at higher temperatures; iv) problems at telomeres somehow might be not recognised by cells grown until saturation. None of these

explanations were tested in the thesis, and it might be interesting to see if any addresses the question. The effects of *DDC1* alleles on *yku70*Δ fitness were not tested and it would be interesting to see if mutation of T602 residue of Ddc1 affects the growth of *yku70*Δ mutants.

| Source | *DDC1* alleles | Growth of *cdc13-1* at restrictive temp. § | UV-induced Ddc1 phospho-rylation | UV-induced Rad53 phospho-rylation * | 4-NQO-induced Rad53 phospho-rylation | UV sensitivity (60-70 J/m$^2$) | CPT sensitivity (10 µg/mL) |
|---|---|---|---|---|---|---|---|
| M. Muzi-Falconi | *ddc1-M3* | — | +++ | +++ | N/A | N/A | N/A |
| | *ddc1-M8* | ++ | — | — | N/A | N/A | N/A |
| | *ddc1-M11* | ++ | — | — | N/A | N/A | N/A |
| | *ddc1-T602A* | + | N/A | — | N/A | N/A | N/A |
| | *ddc1-T602S* | — | N/A | +++ | N/A | N/A | N/A |
| | *DDC1* | — | +++ | +++ | N/A | N/A | N/A |
| P. Burgers | *DDC1* | — | N/A | N/A | +++ | + | — |
| | *ddc1*Δ | +++ | N/A | N/A | — | +++ | +++ |
| | *ddc1-W352A* | + | N/A | N/A | ++ | + | + |
| | *ddc1-W352A,W544A* | + | N/A | N/A | + | + | + |
| | *ddc1-W352A,W544A,T602A* | ++ | N/A | N/A | — | ++ | ++ |
| | *ddc1-(1-404),W352A* | ++ | N/A | N/A | — | ++ | N/A |
| | *ddc1-T602A* | + | N/A | N/A | + | + | — |

**Table 2. Response of *DDC1* alleles to DNA damage**

§ - analysed in this thesis; * - *dot1*Δ background. Response of tested alleles to DNA damage is indicated by: — - no response, + - weak response, ++ - moderate response, +++ - strong response; N/A – not tested. Based on (Puddu et al., 2008, Navadgi-Patil and Burgers, 2009).

## 3.2 The role of Dpb11 in the fitness of *cdc13-1* and *yku70*Δ mutants

### *3.2.1 Alleles of DPB11 chosen to study checkpoint function*

Dpb11 is a candidate to take over the checkpoint role of Ddc1 in *yku70*Δ mutants. In order to examine the effect of *DPB11* on *yku70*Δ fitness the *DPB11* endogenous gene was knocked out. *DPB11* is an essential gene and therefore was deleted in diploids: *cdc13-1/CDC13* and *yku70*Δ*/YKU70* (DDY606 and DDY611, Appendix A). Point mutations of *DPB11* shown previously to be crucial for Mec1 activation were introduced on plasmids (Table 3) (Navadgi-Patil et al., 2011).

| Plasmid (pDL) | *DPB11* alleles | Source | Mutation | Mutated sequence |
|---|---|---|---|---|
| **1545** | *pRS313-HIS3-DPB11* | P. Burgers | WT | N/A |
| **1552** | *pRS313-HIS3-dpb11-(1-601)* | P. Burgers | Y601-STOP | tyrosine TAC into STOP codon TAG |
| **1553** | *pRS313-HIS3-dpb11-W700A* | P. Burgers | W700A | tryptophan TGG into alanine GCG |
| **1554** | *pRS313-HIS3-dpb11-Y735A* | P. Burgers | Y735A | tyrosine TAT into alanine GCT |
| **1555** | *pRS313-HIS3-dpb11-W700A,Y735A* | P. Burgers | W700A | tryptophan TGG into alanine GCG |
| | | | Y735A | tyrosine TAT into alanine GCT |
| **1556** | *pRS313-HIS3-dpb11-W700A,T731A,Y735A* | P. Burgers | W700A | tryptophan TGG into alanine GCG |
| | | | T731A | threonine ACT into alanine GCT |
| | | | Y735A | tyrosine TAT into alanine GCT |

**Table 3. Mutations of *DPB11* used**. All mutations were confirmed by sequencing.

### *3.2.2 Plasmids carrying DPB11 alleles are unable to rescue dpb11*Δ *at high rate*

The plasmids carrying mutations of *DPB11* were introduced into diploid strains in order to rescue *dpb11*Δ, then diploids were sporulated, spores were dissected and germinated. Haploid strains were used in further experiments. I observed higher than expected spore inviability of strains, in which *DPB11* was deleted and covered by a plasmid (Fig. 16a). If the plasmids fully rescued *DPB11* deletion and plasmids were transmitted at 100 % efficiency, 100 % of *dpb11*Δ spores should germinate into colonies. However, as presented in Figure 16a, on average 45 % of colonies contained the plasmid, and on average 27 % of colonies with the plasmid had the *DPB11* gene deleted ($G418^r$). I never observed *dpb11*Δ strain without the plasmid carrying *DPB11* or alleles. Due to poor spore viability and frequent plasmid loss

I wondered whether the spore lethality was caused by *DPB11* deletion in diploid strains. I tested the spore viability of "parental" diploid strains: prior to *DPB11* deletion and after *DPB11* deletion in *cdc13-1* and *yku70*Δ backgrounds (Fig. 16b). Germination of spores of *cdc13-1/CDC13* strain was less efficient than expected – spore viability was 75 % (Fig. 16b). 100 % spore viability was expected because there is no reason for spore lethality of *cdc13-1* cells. When *DPB11* was deleted the spore viability was 39 %. Spore viability of *cdc13-1/CDC13 dpb11*Δ*/DPB11 pDPB11* diploid was 53 % and plasmid *pDPB11* (pDL1545) was transmitted to *dpb11*Δ cells at 29 % efficiency (Fig. 16a and b). Spore viability of *yku70*Δ*/YKU70* diploids was 94 %. When *DPB11* was deleted, the spore viability was 50 % as expected for deletion of essential gene (Fig. 16c). In *yku70*Δ*/YKU70 dpb11*Δ*/DPB11 pDPB11* diploid the spore viability was 73 %, and plasmid *pDPB11* (pDL1545) was transmitted to *dpb11*Δ cells at 23 % efficiency (Fig. 16a and c).

The spore germination efficiency, shown in Figure 16b and c, indicates that meiotic problems in *cdc13-1/CDC13* strain might occur, as the spore viability was only 75%. The spore viability of *cdc13-1/CDC13 dpb11*Δ*/DPB11* was also low and might be due to haploinsufficiency, when a single functional copy of the gene does not fulfil a gene's function in a diploid. *CDC13* and *DPB11* are essential genes; therefore mutations of both genes in one diploid might result in combined haploinsufficiency and/or other, unknown defects. Another problem observed was frequent plasmid loss. The alleles of *DPB11* were carried by centromeric plasmids and cells have the tendency to lose the plasmid during division.

a)

| DDY | Plasmid (pDL) | No. of tetrads | No. of spores | No. of visible colonies from germinated spores (%) | No. of colonies with plasmid (%) | No. of G418$^r$ colonies with plasmid (%) |
|---|---|---|---|---|---|---|
| ***cdc13-1/CDC13 dpb11Δ/DPB11*** **(DDY606)** | p*DPB11* | 40 | 160 | 85 (53) | 41 (48) | 25 (29) |
| | p*DPB11* alleles | 219 | 876 | 458 (52) | 219 (48) | 117 (25) |
| ***yku70Δ/YKU70 dpb11Δ/DPB11*** **(DDY611)** | p*DPB11* | 16 | 64 | 47 (73) | 18 (38) | 11 (23) |
| | p*DPB11* alleles | 162 | 636 | 379 (59) | 178 (47) | 114 (30) |
| | | | | **On average:** | **45 %** | **27 %** |

b)

*cdc13-1/CDC13* (75 %)

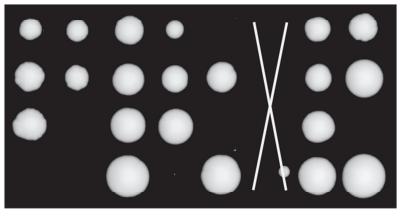

*cdc13-1/CDC13 dpb11Δ/DPB11* (DDY606) (39 %)

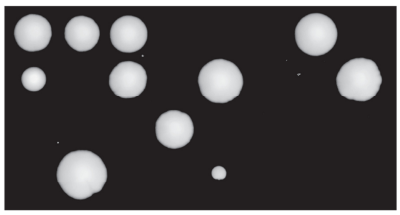

*cdc13-1/CDC13 dpb11Δ/DPB11 pDPB11* (DDY606/pDL1545) (53 %)

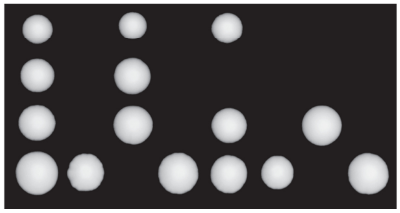

c)

*yku70Δ/YKU70* (94 %)

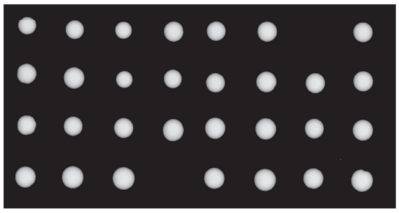

*yku70Δ/YKU70 dpb11Δ/DPB11* (DDY611) (50 %)

*yku70Δ/YKU70 dpb11Δ/DPB11 pDPB11* (DDY611/pDL1545) (73 %)

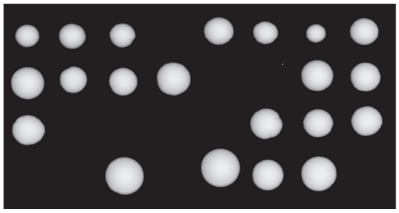

**Figure 16. Spore viability prior to *DPB11* deletion and plasmid transformation**

a) Spore viability of *dpb11Δ/DPB11* strains and plasmid transmission efficiency. *G418$^r$* – G418 resistant *dpb11::KANMX* cells, *pDPB11* – pDL1545.

b) Examples of germinated spores of *cdc13-1/CDC13* diploids.

c) Examples of germinated spores of *yku70Δ/YKU70* diploids.

Top panels – spores germinated of yeast strains before *DPB11* was deleted. Spore viabilities calculated for one plate of each genotype are shown.

Medium panels - spores germinated of yeast strains after *DPB11* deletion. Spore viabilities calculated for two plates of each genotype are shown.

Bottom panels – spores germinated of yeast strains after *DPB11* deletion and pDL1545 transformation. Spore viabilities calculated for four plates (a) and two plates (b) of each genotype are shown. *White cross* – no tetrad was dissected at this location. Strains were first grown in YEPD, or –HIS liquid if contained the plasmid. Then strains were sporulated in ESM, tetrads were dissected and germinated on YEPD plates. Pictures of colonies were taken after 5 days at 23°C for *cdc13-1* background (b), and after 2-3 days at 30°C for *yku70Δ* background (c). Strains were: *yku70Δ/YKU70* (DLY6885xDLY3001), *cdc13-1/CDC13 (*DLY1108xDLY3001), *cdc13-1/CDC13 dpb11Δ/DPB11* (DDY606), *yku70Δ/YKU70 dpb11Δ/DPB11* (DDY611), *cdc13-1/CDC13 dpb11Δ/DPB11* pDL1545 (DDY606/pDL1545), *yku70Δ/YKU70 dpb11Δ/DPB11* pDL1545 (DLY611/pDL1545). Strain details are in Appendix A.

### *3.2.3 DPB11 alleles affect cdc13-1 fitness much less than DDC1 alleles*

It was reported that three conserved aromatic amino acids of *DPB11,* W700, T731 and Y735, are critical for Mec1 activation by Dpb11 (Fig. 17a) (Pfander and Diffley, 2011, Navadgi-Patil et al., 2011). In order to test whether different *DPB11* alleles respond to telomere damage, *cdc13-1 dpb11*Δ haploid strains carrying *DPB11* alleles were generated. Figure 17 illustrates how alleles of *DPB11* affect the growth of *cdc13-1* cells.

All tested *DPB11* alleles slightly suppressed *cdc13-1* ts at 27-28°C, but not at 30°C (Fig. 17b G-P, compare to C-F). Due to a small effect of *DPB11* alleles on *cdc13-1* growth and the fact, that Dpb11 was shown to be recruited to the site of damage by Ddc1 (Navadgi-Patil and Burgers, 2009), I decided to combine *ddc1*Δ with *dpb11*Δ p*dpb11-W700A,T731A,Y735A* mutations in *cdc13-1* background. I observed, that when *DDC1* was also deleted, the triple mutants, *cdc13-1 ddc1*Δ *dpb11*Δ p*dpb11-W700A,T731A,Y735A* were fitter than double mutants at all temperatures (Fig. 17c W-X, compare to T) and grew similarly to *cdc13-1 ddc1*Δ strains (Fig. 17c W-X, compare to U).

Residues W700, T731 and Y735 of Dpb11 were reported as important for Mec1 activation to some extent, and therefore point mutants show partial defects in the G2 checkpoint upon 4-NQO treatment, as measured by Rad53 phosphorylation (Navadgi-Patil et al., 2011, Pfander and Diffley, 2011). I observed that all *DPB11* alleles indicated in Table 3 had the same small effect on *cdc13-1* growth, and the effect was much smaller than of *ddc1*Δ. *cdc13-1* strains with mutations of *DPB11* and *DDC1* grew like *cdc13-1 ddc1*Δ mutants. Dpb11 might contribute a little to Ddc1 checkpoint function. However, the role of Ddc1 is more important than of Dpb11.

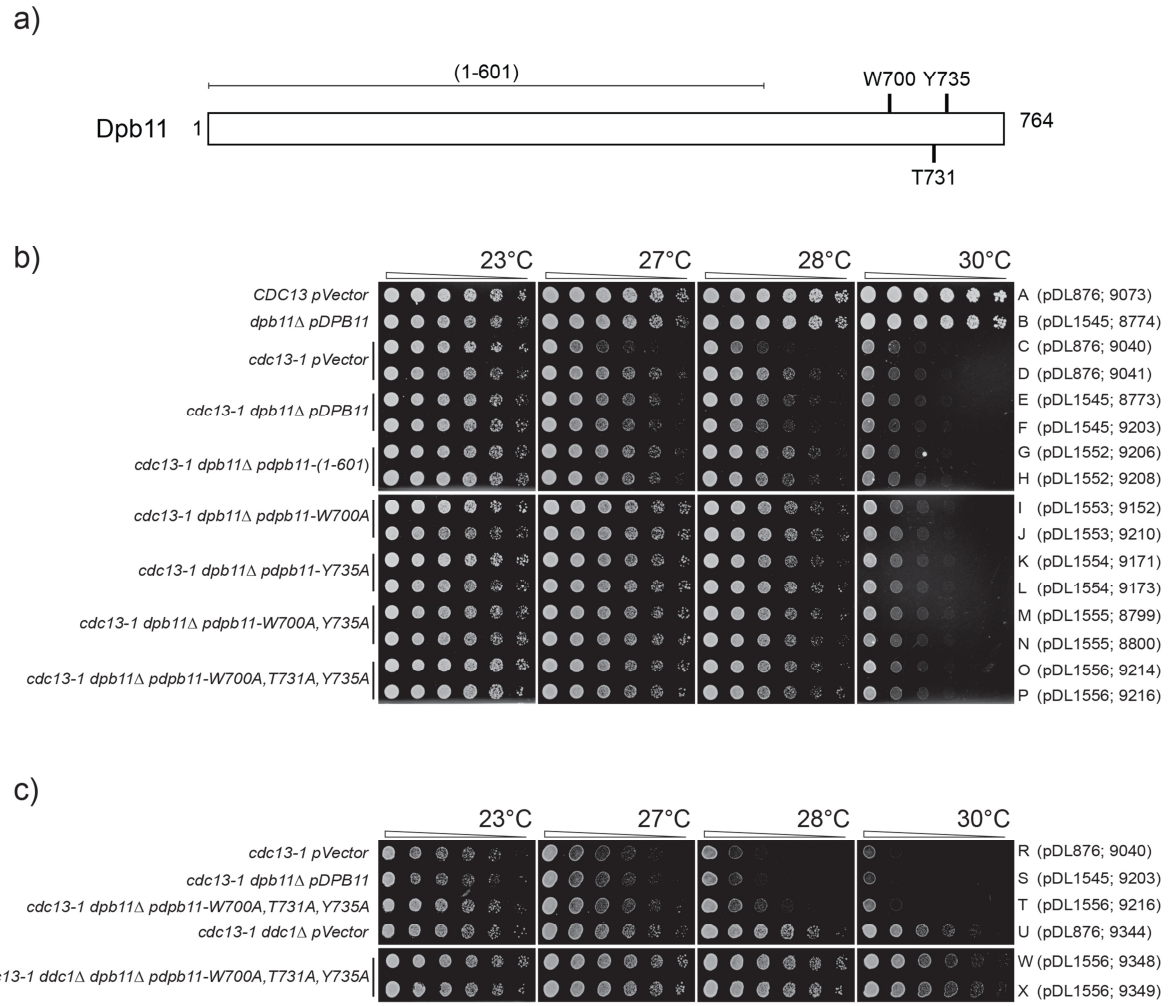


**Figure 17. *DPB11* alleles slightly affect growth of *cdc13-1* mutants**

a) Mutations used (adapted from (Navadgi-Patil et al., 2011)). (1-601) – Dpb11 C-terminal truncation.

b-c) Spot test done as in Figure 9. Yeast strains were spotted onto –HIS plates to select for plasmids. Strains A-P were grown on one rectangular plate. Strains R-X were grown on a different rectangular plate. *pVector* - pRS314. The relevant genotypes of the strains are indicated on the left, plasmid and strain numbers on the right; strain details are in Appendix A. Letters A-X on the right of the figure are assigned to relevant genotypes from the left.

### *3.2.4 DPB11 alleles do not affect yku70∆ fitness*

In order to test how *DPB11* alleles affect *yku70∆* fitness the spot test was performed (Fig. 18). One *yku70∆ dpb11∆ pDPB11* strain grew better at 35 - 36°C than the other strain (Fig. 18 D-E). The better growth of one strain might be caused e. g. by plasmid copy number, if cells contain more than one copy of *pDPB11* plasmid. This however was not tested. I will compare *yku70∆ dpb11∆ pDPB11* DLY8784 mutant with other strains.

All strains, apart from wild type, looked like *yku70∆* and were less fit above 35°C (Fig. 18 F-N, compare to A-E). None of tested *DPB11* alleles affected *yku70∆* growth. Deletion of *DDC1* in *yku70∆ dpb11∆ pdpb11 W700A, T731A,Y735A* mutants slightly improved strains fitness (Fig. 18 O-P, compare to M-N). The suppression of *yku70∆* by *ddc1∆* is hardly detectable, possibly because cells grow slower in selective media (-HIS) and might have been collected for spot testing at exponential growth phase. In sections 3.1.4 and 3.1.5 I showed that *ddc1∆* slightly suppressed *yku70∆* ts dependent on the culture conditions. The effect of culture condition remains to be tested by growing cells till saturation prior spotting. Also, the *yku70∆ ddc1∆ pVector* control strain was not included in this spot test, which makes comparisons hard to make.

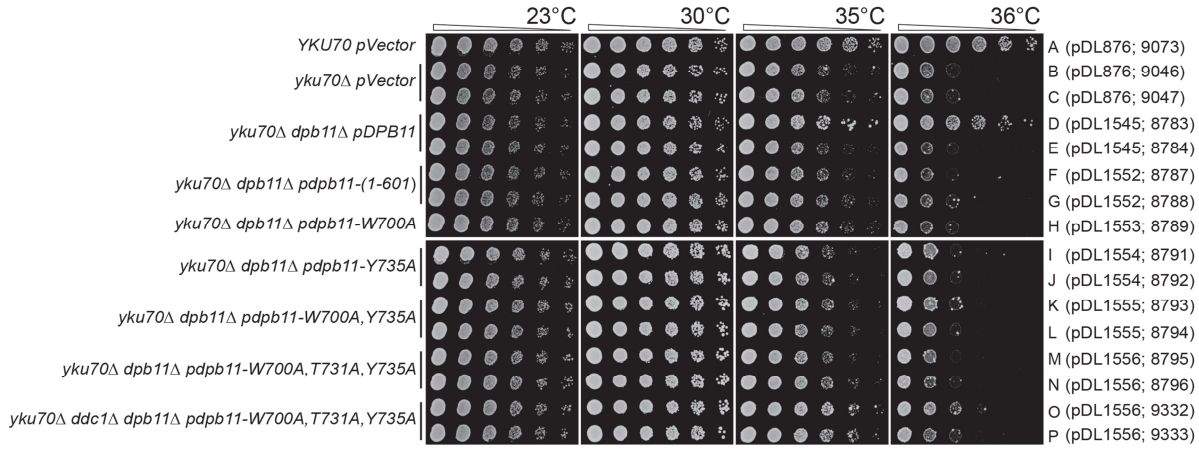


**Figure 18. *DPB11* alleles do not affect growth of *yku70*Δ mutants**

Spot test done as in Figure 9. Yeast strains were spotted onto –HIS plates to select for plasmids. Strains A-P were grown on one rectangular plate. *pVector* – pRS413. The relevant genotypes of the strains are indicated on the left, plasmid and strain numbers on the right; strain details are in Appendix A. Letters A-P on the right of the figure are assigned to relevant genotypes from the left.

### *3.2.5 Discussion/Conclusions*

Low spore viability was observed when *DPB11* was deleted in *cdc13-1/CDC13* strain. Cdc13 and Dpb11 are important for chromosomal and telomere replication, respectively (Boos et al., 2011, Tanaka et al., 2013, Chen and Lingner, 2013). It might be therefore possible that poor spore viability was caused by severe defects in replication process in a heterozygous *cdc13-1/CDC13 dpb11Δ/DPB11* diploid. Also, low spore viability might be the result of haploinsufficiency due to presence of only one functional copy of a gene in a diploid. I also observed that plasmids carrying *DPB11* and its alleles are not efficiently transmitted to daughter cellsbecause on average only 45 % of viable spores contained the plasmid, and on average 27% of viable spores contained the plasmid and were G418 resistant (*dpb11Δ*). Cells have the tendency to lose centromeric plasmids. If *DPB11* alleles were integrated into the genome, it would probably facilitate addressing the question regarding the role of Dpb11 at uncapped telomeres.

All alleles of *DPB11* slightly suppressed the *cdc13-1* defect at higher temperatures. However, it was shown that only *dpb11-(1-601)* and *dpb11-W700A,T731A,Y735A* mutants lost Rad53 phosphorylation after 4-NQO treatment (Table 4) (Navadgi-Patil et al., 2011). It was also shown that Dpb11 cooperate with Ddc1 in Mec1 activation, and also that Ddc1 recruits Dpb11 in response to DNA damage (Puddu et al., 2011, Navadgi-Patil and Burgers, 2011, Pfander and Diffley, 2011). *cdc13-1 ddc1Δ dpb11Δ dpb11-W700A,T731A,Y735A* mutants did not differ from a *cdc13-1 ddc1Δ* strain. This suggests that Ddc1 and Dpb11 function in the same pathway, but Ddc1 has much stronger phenotype and is more important in response to *cdc13-1* defective telomeres.

None of tested *DPB11* alleles affected growth of *yku70Δ* strains, and *yku70Δ ddc1Δ dpb11Δ dpb11-W700A,T731A,Y735A* mutants did not grow much better than *yku70Δ dpb11Δ dpb11-W700A,T731A,Y735A* strains. In section 3.1.5 I observed that *ddc1Δ* slightly suppressed *yku70Δ* ts, and the suppression was easier to observe when cells were grown until saturation prior spotting. In this experiment however, cells were grown in liquid–HIS medium in order to select for the plasmids at all times. It might be possible that cells carrying plasmids, although grown for approximately 24h in liquid –HIS, did not reach the saturation. This might explain why the effect of *ddc1Δ* on

*yku70*Δ *dpb11*Δ *dpb11-W700A,T731A,Y735A* cells is relatively weak. It might be interesting to test whether saturated cultures of *yku70*Δ *ddc1*Δ mutants with *DPB11* alleles would affects strains' growth more.

| Source | *DPB11* alleles | Growth at restrictive temp. § | | Mec1 activity stimulation | 4-NQO-induced Rad53 phosphorylation | |
|---|---|---|---|---|---|---|
| | | *cdc13-1* | *yku70*Δ | | | * |
| P. Burgers | *DPB11* | — | — | +++ | +++ | +++ |
| | *dpb11-(1-601)* | + | — | — | +++ | + |
| | *dpb11-W700A* | + | — | + | N/A | +++ |
| | *dpb11-Y735A* | + | — | + | N/A | +++ |
| | *dpb11-W700A,Y735A* | + | — | — | +++ | ++ |
| | *dpb11-W700A,T731A,Y735A* | + | — | N/A | N/A | + |
| | *ddc1*Δ *dpb11-W700A,T731A,Y735A* | +++ | + | N/A | N/A | + |

**Table 4. Response of *DPB11* alleles to DNA damage**

§ - analysed in this thesis; * - *ddc1-W352A,W544A* background. Response of tested alleles to DNA damage is indicated by: — - no response, + - weak response, ++ - moderate response, +++ - strong response; N/A – not tested. Based on (Navadgi-Patil et al., 2011).

## 3.3 The role of Dna2 in cell cycle arrest of *cdc13-1* and *yku70*Δ mutants

### *3.3.1 Alleles of DNA2 chosen to study checkpoint function*

Dna2 is a conserved nuclease/helicase involved in DNA replication and telomere resection (Pokharel and Campbell, 2012, Ngo et al., 2014). In yeast, Dna2 shows partial redundancy with the 9-1-1 complex and Dpb11 in the replication checkpoint and Mec1 activation (Kumar and Burgers, 2013). Therefore Dna2 is another candidate to replace the checkpoint role of Ddc1 in *yku70*Δ mutants. In order to examine the effect of Dna2 on *yku70*Δ fitness, the *DNA2* endogenous gene was knocked out. *DNA2* is an essential gene and therefore was deleted in diploids: *cdc13-1/CDC13* and *yku70*Δ*/YKU70* (DDY607 and DDY609, Appendix A). Point mutations of *DNA2* shown previously to be important for Mec1 activation were introduced on plasmids (Table 5). Two alleles of *DNA2*, *dna2*Δ*500* and *dna2*Δ*450,* turned out to be inviable and for this reason their effects in telomere defective strains could not be tested.

| Plasmid (pDL) | *DPB11* alleles | Source | Mutation | Mutated sequence |
|---|---|---|---|---|
| **1544** | *pRS314-TRP1-DNA2* | P. Burgers | WT | N/A |
| **1561** | *pRS314-TRP1-dna2-W128A,Y130A* | P. Burgers | W128A<br>Y130A | tryptophan TGG into alanine GCC<br>tyrosine TAT into alanine GCT |
| **1560** | *pRS314-TRP1-DNA2* | Y. Seo | WT | N/A |
| **1558** | *pRS314-TRP1-dna2*Δ*500* | Y. Seo | N-terminal Deletion | DNA sequence starts after phenylalanine TTT (F500) |
| **1557** | *pRS314-TRP1-dna2*Δ*450* | Y. Seo | N-terminal Deletion | DNA sequence starts after lysine AAG (K450) |
| **1568** | *pRS314-TRP1-dna2-C519A* | J. Campbell | C519A | cysteine TGT into alanine GCT |
| **1569** | *pRS314-TRP1-dna2-C768A* | J. Campbell | C768A | cysteine TGT into alanine GCT |
| **1570** | *pRS314-TRP1-dna2-C771A* | J. Campbell | C771A | cysteine TGT into alanine GCT |
| **1571** | *pRS314-TRP1-dna2-C777A* | J. Campbell | C777A | cysteine TGC into alanine GCC |

**Table 5. Mutations of *DNA2* used**. All mutations were confirmed by sequencing.

### *3.3.2 Plasmids carrying DNA2 alleles are unable to rescue dna2∆ at high rate*

The plasmids carrying mutations of *DNA2* were introduced into diploid strains in order to rescue *dna2∆*, as described for *dpb11∆* (3.2.2). Plasmids with *DNA2* alleles tend to be lost at higher rate than observed for *DPB11* alleles (Fig.19 and Fig.16). On average only 29 % of viable colonies contained the plasmid carrying *DNA2* or its alleles, and on average 12 % of colonies with the plasmid had the *DNA2* gene deleted ($G418^r$) (Figure 19a).
I analysed the spore viability of "parental" diploid strains: prior to *DNA2* deletion and after *DNA2* deletion in *cdc13-1* and *yku70∆* backgrounds (Fig. 19 b and c), similarly as described for *DPB11*. Spore viability of *cdc13-1/CDC13-1* was 75 % and spore viability of *cdc13-1/CDC13-1 dna2∆/DNA2* was 41 % (Fig. 19b). In *cdc13-1/CDC13 dna2∆/DNA2 pDNA2* diploid the spore viability was 42 %, and the plasmid *pDNA2* was transmitted to *dna2∆* cells at 4 % efficiency (Fig. 19a and b). Spore viability of *yku70∆/YKU70* was 100 % and only 22 % when *DNA2* was deleted (Fig. 19c). The spore viability of *yku70∆/YKU70 dna2∆/DNA2 pDNA2* (pDL1544) was 30 %, and plasmid pDL1544 was transmitted to *dna2∆* cells at 17 % efficiency (Fig. 19a and c).

Poor spore viability of tested diploids might be a result of deficiency of one *DNA2* and one *YKU70* copy, leading to meiotic defects or haploinsufficiency. Cells also tend to lose the plasmid at a very high rate, since on average only 29 % viable colonies have the plasmid, and only 12 % of colonies with the plasmid are G418 resistant (*dna2∆*).

a)

| DDY | Plasmid (pDL) | No. of tetrads | No. of spores | No. of visible colonies from germinated spores (%) | No. of colonies with plasmid (%) | No. of G418$^r$ colonies with plasmid (%) |
|---|---|---|---|---|---|---|
| ***cdc13-1/CDC13 dna2Δ/DNA2* (DDY607)** | p*DNA2* | 89 | 356 | 149 (42) | 19 (13) | 6 (4) |
| | p*DNA2* alleles | 189 | 756 | 308 (41) | 51 (17) | 18 (6) |
| ***yku70Δ/YKU70 dna2Δ/DNA2* (DDY609)** | p*DNA2* | 135 | 540 | 160 (30) | 45 (49) | 28 (17) |
| | p*DNA2* alleles | 299 | 1196 | 391 (33) | 147 (38) | 71 (18) |
| | | | | **On average:** | **29 %** | **12 %** |

b)

*cdc13-1/CDC13* (75 %)

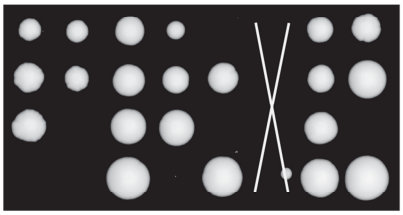

*cdc13-1/CDC13 dna2Δ/DNA2* (DDY607) (41 %)

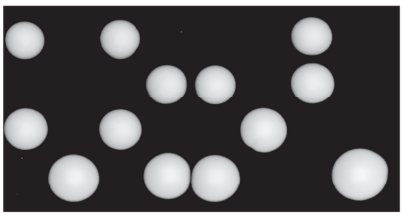

*cdc13-1/CDC13 dna2Δ/DNA2 pDNA2* (DDY607/pDL1544) (42 %)

c)

*yku70Δ/YKU70* (100 %)

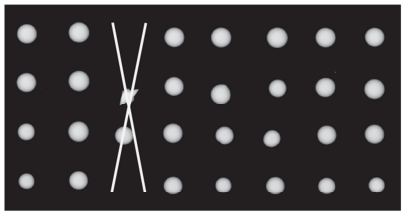

*yku70Δ/YKU70 dna2Δ/DNA2* (DDY609) (22 %)

*yku70Δ/YKU70 dna2Δ/DNA2 pDNA2* (DDY609/pDL1544) (30 %)

**Figure 19. Spore viability prior to *DNA2* deletion and plasmid transformation**

a) Spore viability of *dna2Δ/DNA2* strains and plasmid transmission efficiency. *G418$^r$* – G418 resistant *dna2::KANMX* cells, *pDNA2* – pDL1544.

b) Examples of germinated spores of *cdc13-1/CDC13* diploids.

c) Examples of germinated spores of *yku70Δ/YKU70* diploids.

Top panels – spores germinated of yeast strains before *DNA2* was deleted. Spore viabilities calculated for one plate of each genotype are shown. *cdc13-1/CDC13* was a starting strain for *DPB11* and *DNA2* deletions, therefore the dissection of tetrads was performed once and the picture of *cdc13-1/CDC13* is also shown in Figure 16.

Medium panels - spores germinated of yeast strains after *DNA2* deletion. Spore viabilities calculated for two plates of each genotype are shown.

Bottom panels – spores germinated of yeast strains after *DNA2* deletion and pDL1544 transformation. Spore viabilities calculated for six plates (a) and seven plates (b) of each genotype are shown.

*White cross* – no spores were scored at this location. Strains were first grown in YEPD, or –TRP liquid if contained the plasmid. Then strains were sporulated in ESM, tetrads were dissected and germinated on YEPD plates. Pictures of colonies were taken after 3-5 days at 23°C for *cdc13-1* background (b), and after 2-3 days at 30°C for *yku70Δ* background (c). Strains were: *yku70Δ/YKU70* (DLY1412xDLY3001), *cdc13-1/CDC13 (*DLY1108xDLY3001), *cdc13-1*/*CDC13 dna2Δ/DNA2* (DDY607), *yku70Δ*/*YKU70 dna2Δ*/*DNA2* (DDY609), *cdc13-1*/*CDC13 dna2Δ/DNA2* pDL1544 (DDY607/pDL1544), *yku70Δ*/*YKU70 dna2Δ*/*DNA2* pDL1545 (DLY609/pDL1544). Strain details are in Appendix A.

### *3.3.3 Some DNA2 alleles strongly affect cdc13-1 fitness*

Kumar and Burgers reported that a double point mutation, *dna2-W128A,Y130A,* abrogated the checkpoint function of Dna2 (Kumar and Burgers, 2013). Pokharel and Campbell found that four mutations in nuclease domain, *C519A, C768A, C771A, C777A*, caused defects in DNA replication and repair (Pokharel and Campbell, 2012) (Fig. 20a). In order to test whether *DNA2* alleles respond to telomere damage, the *cdc13-1 dna2*Δ haploid strains carrying *DNA2* alleles were generated and spot tested.

Figure 20b illustrates that otherwise WT cells with *DNA2* alleles grew well, apart from *dna2-C771A* which was thermos-sensitve at 36°C (Fig. 20b A-E). Perhaps due to spore lethality and too few tetrads dissected no *cdc13-1 dna2*Δ *pdna2-C777A* strains were generated, and the effect of *pdna2-C777A* on *cdc13-1* was not tested. *cdc13-1* mutants with *pVector* were able to form colonies at 28°C. The heterogeneity between strains with *pVector* and *pDNA2* might be caused by *DNA2* copy number, if fitter cells carried more copies of *pDNA2* plasmid (Fig. 20b F-H). None of tested cysteine to alanine substitutions of *DNA2* suppressed *cdc13-1* defect (Fig. 20b I-M, compare to F-H). One *cdc13-1 dna2*Δ *pdna2-C771A* strain was extraordinary and grew up to 36°C, and I assume it was a single *dna2-C771A* mutant rather than *cdc13-1 dna2*Δ *pdna2-C771A* double mutant (Fig. 20b M, compare to E); I did not confirm my assumption. The double point mutation *dna2-W128A,Y130A* strongly suppressed *cdc13-1* defect so that double mutants grew at 30°C (Fig. 20b N-P, compare to F-H).

Mutation of two residues of Dna2, W128 and Y130, significantly affected the growth of *cdc13-1* strains. Such strong suppression might be due to defective Mec1 activation and cell cycle arrest, or defective nuclease function of Dna2. If Dna2 contributes to the checkpoint activation, than *ddc1*Δ and *dna2-W128A,Y130A* allele should have similar effect on *cdc13-1* fitness. To test this hypothesis the effect of *ddc1*Δ and *dna2-W128A,Y130A* mutations on *cdc13-1* was verified (Fig. 20c). *cdc13-1 dna2*Δ *pdna2-W128A,Y130A* double mutants grew up to 30°C, but were slightly less fit than *cdc13-1 ddc1*Δ strains (Fig. 20c G-H, compare to F and I-L). Surprisingly, *cdc13-1 ddc1*Δ *dna2*Δ *pdna2-W128A,Y130A* triple mutants grew at 36°C (Fig. 20c M-P, compare to I-L). It was reported that simultaneous mutations of *ddc1, dpb11* and *dna2,* which eliminate the checkpoint functions of all three genes, abrogate the

Mec1-dependent checkpoint (Kumar and Burgers, 2013). It might be possible thatin *cdc13-1 ddc1*Δ *dna2*Δ *pdna2-W128A,Y130A* triple mutants the Mec1-dependent checkpoint is defective due to lack of functional Ddc1, Dpb11 (which is recruited by Ddc1) and Dna2 checkpoint proteins. However, the Mec1 activation was not tested in this thesis, and at least another spot test involving *cdc13-1* and *mec1*Δ mutation should be performed to compare to the phenotype of *cdc13-1 ddc1*Δ *dna2*Δ *pdna2-W128A,Y130A* mutants.

Alternative explanation for better growth of *cdc13-1 dna2*Δ *pdna2-W128A,Y130A* and *cdc13-1 ddc1*Δ *dna2*Δ *pdna2-W128A,Y130A* mutants at higher temperatures might be less DNA damage in those strains. *cdc13-1 dna2*Δ *pdna2-W128A,Y130A* and *cdc13-1 ddc1*Δ *dna2*Δ *pdna2-W128A,Y130A* mutants grow at 30°C and 36°C, respectively, and both contain a *dna2-W128A,Y130A* allele. It might be therefore possible that the *dna2-W128A,Y130A* allele counteracts the *cdc13-1* defect. This could be the case if e.g. *dna2-W128A,Y130A* was defective in nuclease function of Dna2, or in nuclease recruitment to damaged telomeres. In turn, uncapped telomeres of *cdc13-1* cells would not be resected and the accumulation of ssDNA would be abrogated. Such telomeres would not be detected as DNA damage by checkpoints and *cdc13-1* cells, although uncapped, would be able to grow at higher temperatures. This is however a hypothesis which remains to be tested.

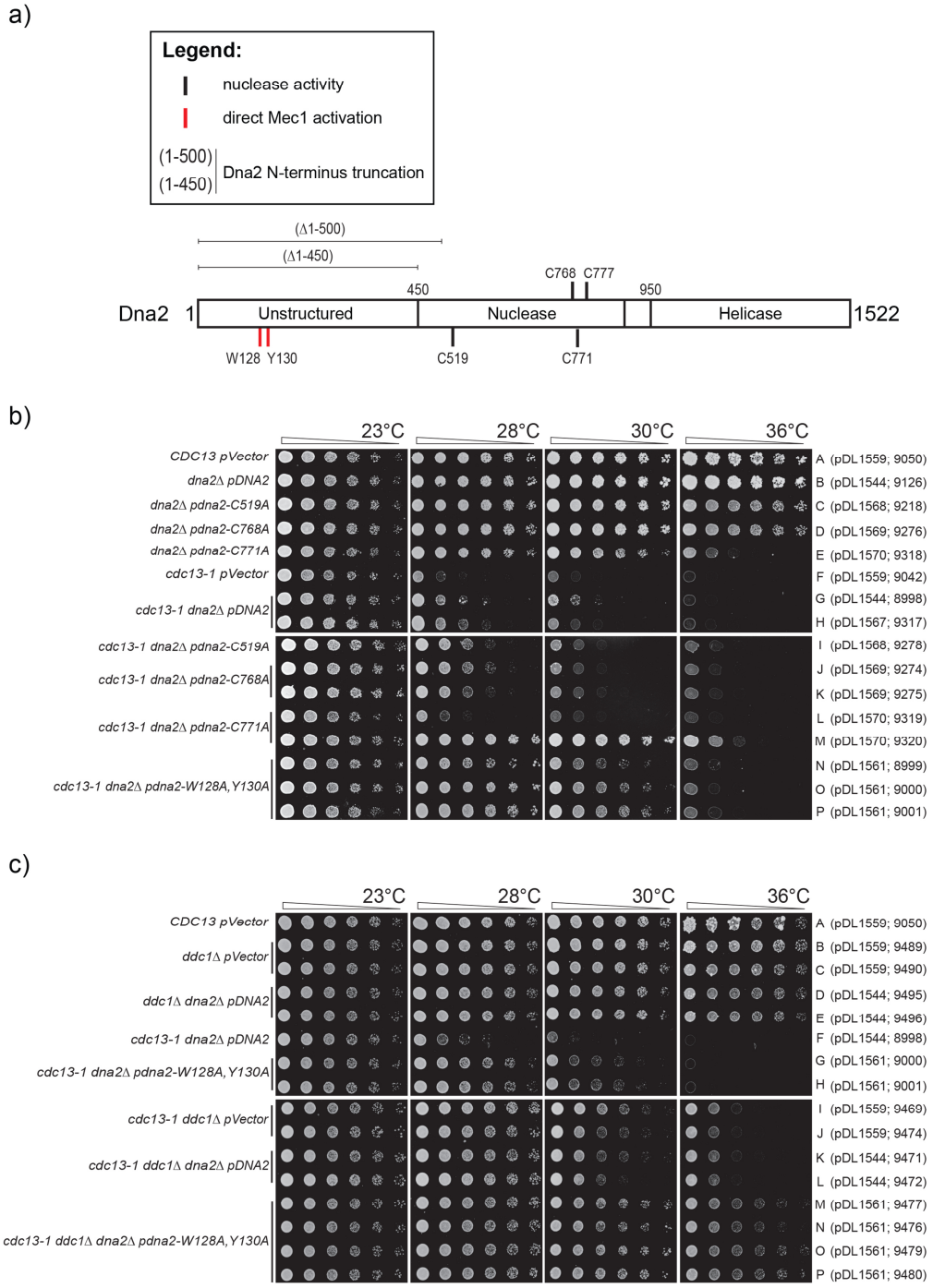


**Figure 20. *DNA2* alleles affect growth of *cdc13-1* mutants**

a) Mutations used (adapted from (Pokharel and Campbell, 2012, Kumar and Burgers, 2013)). (Δ1-450), (Δ1-500) – Dna2 N-terminal truncations.

b-c) Spot test done as in Figure 9. Yeast strains were spotted onto –TRP plates to select for plasmids. Strains A-P in b) and c) were grown on individual rectangular plates. Spot tests in b) and c) were performed on different days. *pVector* - pRS314. The relevant genotypes of the strains are indicated on the left, plasmid and strain numbers on the right; strain details are in Appendix A. Letters A-P on the right of the figure are assigned to relevant genotypes from the left.

### *3.3.4 cdc13-1 dna2Δ pdna2-W128A,Y130A and cdc13-1 ddc1Δ dna2Δ pdna2-W128A,Y130A mutants rearrange telomeres*

The ability of *cdc13-1 ddc1Δ dna2Δ pdna2-W128A,Y130* strains to grow at 36°C was surprising because such improved fitness is not commonly seen for *cdc13-1* mutants. It was possible that *cdc13-1* mutation reverted into the WT *CDC13,* thereby allowing strains to grow at higher temperatures. Another explanation of extraordinary growth at 36°C would be that *cdc13-1 ddc1Δ dna2Δ pdna2-W128A,Y130A* mutants have rearranged telomeres. Telomere rearrangements were reported to suppress *cdc13-1* defects (Larrivee and Wellinger, 2006), which strongly supports this hypothesis. On the other hand Holstein *et al.* showed that *cdc13Δ* lethality can be bypassed by defects in nonsense-mediated decay (NMD) pathway (Holstein et al., 2014). Therefore one more possibility is that *ddc1Δ dna2Δ pdna2-W128A,Y130A* mutations cause similar effect on *cdc13-1* as e. g. *nmd2Δ,* permitting cells growth at 36°C.

To test whether *cdc13-1* mutation reverted into *CDC13,* I performed a PCR (as in 2.14.3) to distinguish a *cdc13-1* allele from *CDC13* in double and triple mutants (Fig. 21a). A *cdc13-1* allele has an *Eco*RI site which is not present in *CDC13* and allows for quick sequence distinction (Lin and Zakian, 1996). I confirmed that *cdc13-1* restriction fragment length polymorphism (RFLP) is still present in temperature resistant strains (Fig.21a). This indicates that *cdc13-1 ddc1Δ dna2Δ pdna2-W128A,Y130A* strains did not revert *cdc13-1* mutation into WT *CDC13* sequence.

To test the hypothesis about telomere rearrangements I determined the telomere structure of *cdc13-1 ddc1Δ dna2Δ pdna2-W128A,Y130A* and control strains by Southern blot (Fig. 21b). Interestingly, *cdc13-1 dna2Δ pdna2-W128A,Y130A* and *cdc13-1 ddc1Δ dna2Δ pdna2-W128A,Y130A* mutants indeed had rearranged telomeres (Fig. 21b, lines 10, 15-16, compare to 18-19). Some survivors maintain telomere length and recover at a low frequency by recombination and amplification of Y' or $TG_{1-3}$ repeats (Lundblad and Szostak, 1989, Lundblad and Blackburn, 1993, Lydall, 2003). The telomere structures of *cdc13-1 dna2Δ pdna2-W128A,Y130A* and *cdc13-1 ddc1Δ dna2Δ pdna2-W128A,Y130A* mutants were similar to telomeres of *tlc1Δ* mutant. Such similarity indicates that strains carrying the *dna2-W128A,Y130A* allele formed Type II survivors, which amplified $TG_{1-3}$ repeats. Interestingly, colonies from germinated spores of a diploid carrying *pdna2-W128A,Y130A* plasmid were

heterogeneous in size and viability (Fig. 22), although survivors initially form small colonies and grow slowly. The formation of survivors in the presence of *dna2-W128A,Y130A* allele suggests, that *dna2-W128A,Y130A* allele is important for the telomerase function at uncapped telomeres of *cdc13-1* mutants, the mechanism of which is unclear to me. Based on the spot tests presented in Figure 20, and Southern blot shown in Figure 21, I conclude that the increased fitness of *cdc13-1* strains correlates with telomere rearrangements.

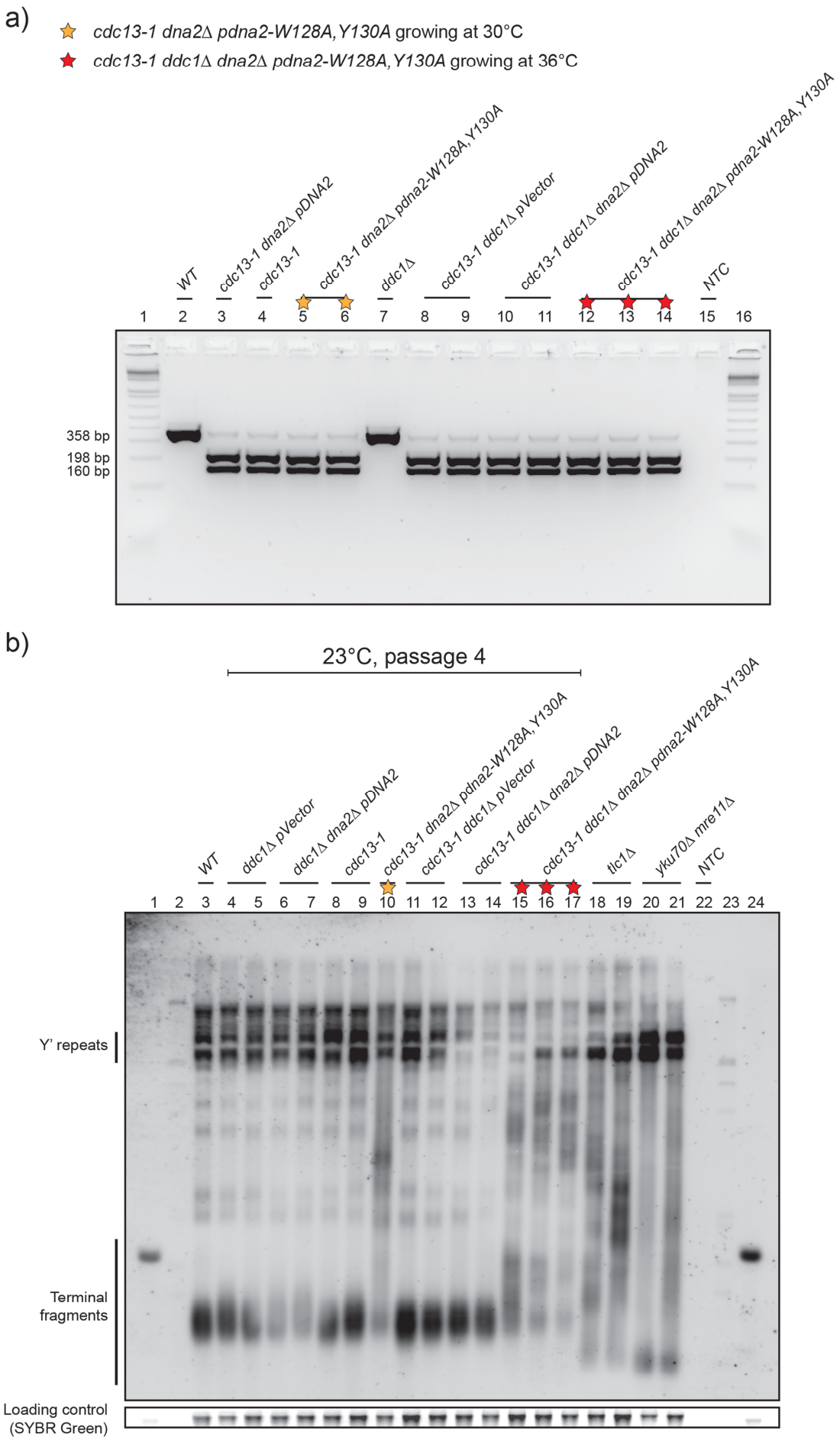
a)
cdc13-1 dna2Δ pdna2-W128A,Y130A growing at 30°C
cdc13-1 ddc1Δ dna2Δ pdna2-W128A,Y130A growing at 36°C
WT
cdc13-1 dna2Δ pDNA2
cdc13-1
cdc13-1 dna2Δ pdna2-W128A,Y130A
ddc1Δ
cdc13-1 ddc1Δ pVector
cdc13-1 ddc1Δ dna2Δ pDNA2
cdc13-1 ddc1Δ dna2Δ pdna2-W128A,Y130A
NTC
1 2 3 4 5 6 7 8 9 10 11 12 13 14 15 16
358 bp
198 bp
160 bp
b)
23°C, passage 4
WT
ddc1Δ pVector
ddc1Δ dna2Δ pDNA2
cdc13-1
cdc13-1 dna2Δ pdna2-W128A,Y130A
cdc13-1 ddc1Δ pVector
cdc13-1 ddc1Δ dna2Δ pDNA2
cdc13-1 ddc1Δ dna2Δ pdna2-W128A,Y130A
tlc1Δ
yku70Δ mre11Δ
NTC
1 2 3 4 5 6 7 8 9 10 11 12 13 14 15 16 17 18 19 20 21 22 23 24
Y' repeats
Terminal fragments
Loading control (SYBR Green)

**Figure 21. *cdc13-1* and *cdc13-1 ddc1*Δ mutants have telomeres rearranged in the presence of *dna2-W128A,Y130A***

a) The presence of mutation at P371S, which confers *Eco*RI restriction enzyme site (Lin and Zakian, 1996), was confirmed by PCR. Primers were M550 and M551, primer details are in Appendix C. DNA was isolated from strains grown overnight in liquid YEPD at 23°C using Yale method. Restriction digest of DNA was performed following PCR, and run on 2 % agarose gel. Orange stars – *cdc13-1 dna2*Δ *pdna2-W128A,Y130A* strains which grew at 30°C; red stars - *cdc13-1 ddc1*Δ *dna2*Δ *pdna2-W128A,Y130A* strains which grew at 36°C. Strain genotypes are indicated above gel lines. Lines 1 & 16 - +1kb molecular ladder. Lines 3-14 – DNA isolated from strains of passage 4. Strains were: 2 – *CDC13 Vector* (DLY9050), 3 – *cdc13-1 dna2*Δ *pDNA2* (DLY8998), 4 – *cdc13-1* (DLY1108), 5 – *cdc13-1 dna2*Δ *pdna2-W128A,Y130A* (DLY9000), 6 – *cdc13-1 dna2*Δ *pdna2-W128A,Y130A* (DLY9001),
7 – *ddc1*Δ *Vector* (DLY9490), 8 – *cdc13-1 ddc1*Δ *Vector* (DLY9469), 9 – *cdc13-1 ddc1*Δ *Vector* (DLY9474), 10 – *cdc13-1 ddc1*Δ *dna2*Δ *pDNA2* (DLY9471),
11 – *cdc13-1 ddc1*Δ *dna2*Δ *pDNA2* (DLY9472), 12 – *cdc13-1 ddc1*Δ *dna2*Δ *pdna2-W128A,Y130A* (DLY9476), 13 – *cdc13-1 ddc1*Δ *dna2*Δ *pdna2-W128A,Y130A* (DLY9479), 14 – *cdc13-1 ddc1*Δ *dna2*Δ *pdna2-W128A,Y130A* (DLY9480), 15 – NTC - $H_2O$.

b) Genomic DNA from a) was used. Telomeres were analysed by Southern blot. SYBR Safe was used as a loading control. *tlc1*Δ and *yku70*Δ *mre11*Δ strains were used as controls for type II and I survivors, respectively (Maringele and Lydall, 2004). Lines 1-2 & 23-24 – molecular ladders. Lines 4-17 – DNA isolated from strains of passage 4. Strains were: 3 – *CDC13 Vector* (DLY9050), 4 – *ddc1*Δ *Vector* (DLY9489), 5 – *ddc1*Δ *Vector* (DLY9490), 6 – *ddc1*Δ *dna2*Δ *pDNA2* (DLY9495), 7 – *ddc1*Δ *dna2*Δ *pDNA2* (DLY9496), 8 – *cdc13-1 dna2*Δ *pDNA2* (DLY8998), 9 – *cdc13-1* (DLY1108),
10 – *cdc13-1 dna2*Δ *pdna2-W128A,Y130A* (DLY9001), 11 – *cdc13-1 ddc1*Δ *Vector* (DLY9469), 12 – *cdc13-1 ddc1*Δ *Vector* (DLY9474), 13 – *cdc13-1 ddc1*Δ *dna2*Δ *pDNA2* (DLY9471), 14 – *cdc13-1 ddc1*Δ *dna2*Δ *pDNA2* (DLY9472), 15 – *cdc13-1 ddc1*Δ *dna2*Δ *pdna2-W128A,Y130A* (DLY9476), 16 – *cdc13-1 ddc1*Δ *dna2*Δ *pdna2-W128A,Y130A* (DLY9479), 17 – *cdc13-1 ddc1*Δ *dna2*Δ *pdna2-W128A,Y130A* (DLY9480), 18 – *tlc1*Δ (DLY1845), 19 – *tlc1*Δ (DLY1846), 16 – NTC-$H_2O$. Strain details are in Appendix A.

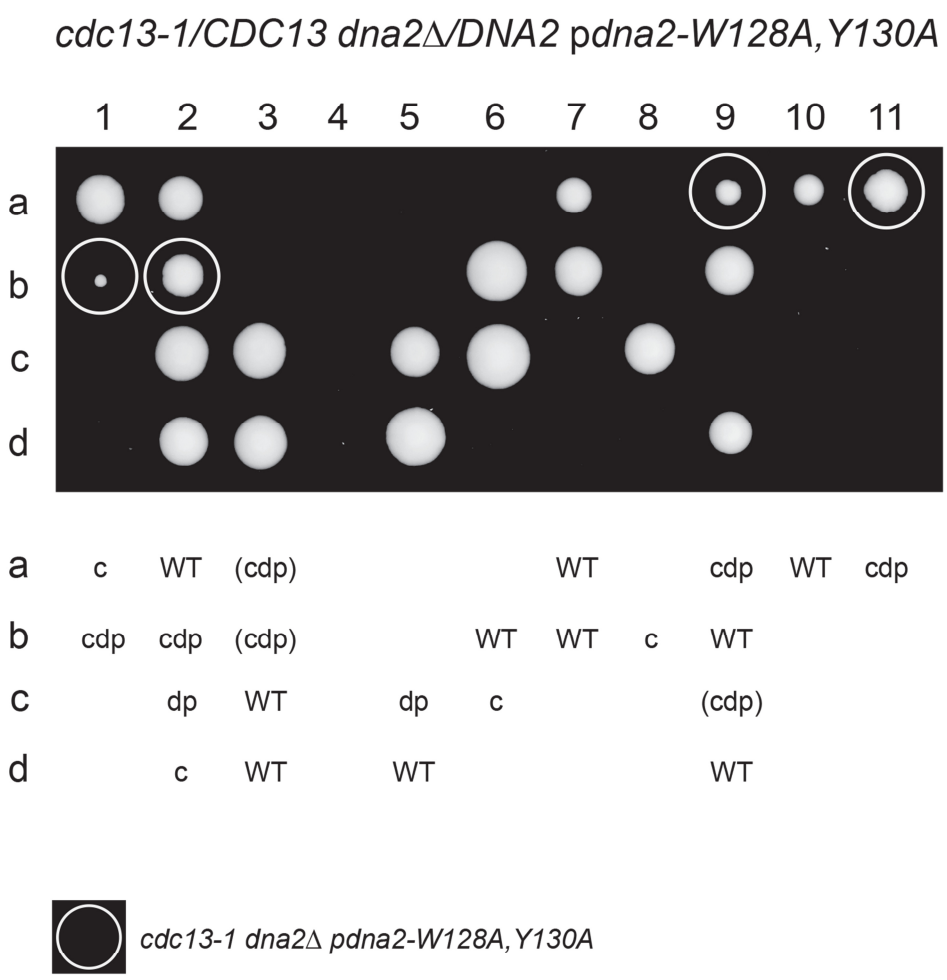


**Figure 22. *cdc13-1 dna2Δ pdna2-W128A,Y130A* colonies have heterogeneous size**

Example of tetrad dissection (in total 69 tetrads were dissected) from a sporulated diploid (DDY607/pDL1561). Spores were germinated for 5 days at 23°C before photographing. Viable *cdc13-1 dna2Δ pdna2-W128A,Y130A* strains are encircled.

### *3.3.5 cdc13Δ lethality is not bypassed by ddc1Δ dna2-W128A,Y130A mutations*

One of the hypotheses concerning the growth of *cdc13-1 ddc1Δ dna2Δ dna2-W128A,Y130A* strains at 36°C was that *ddc1Δ dna2Δ dna2-W128A,Y130A* mutations may bypass *cdc13Δ* lethality, like defects of NMD do (Holstein et al., 2014). To test the hypothesis, *cdc13Δ/CDC13 ddc1Δ/DDC1 dna2Δ/DNA2 pdna2-W128A,Y130A* and other diploids were generated, sporulated and dissected (Fig. 23). Interestingly, none of the strains with deletion of *CDC13* sporulated at 23°C, while those with *cdc13-1* mutation did. Differently to the standard protocol of sporulation, all strains sporulated at 20°C within 5 days, then spores were dissected and germinated at 23°C.

The massive spore lethality is noticeable for all diploids (Fig. 23 a-j). Spore viability of *cdc13Δ/CDC13 ddc1Δ/DDC1 dna2Δ/DNA2 pdna2-W128A,Y130A* strain was only 1.6 %, and spore viability of other strains varied between 11.1-32.4 % (Fig. 23 a-b, compare to c-j). More spores were viable when diploid *cdc13Δ/CDC13 ddc1Δ/DDC1 dna2Δ/DNA2* carried *pDNA2* plasmid (11.1 %) or an empty *pVector* (29.5 %) (Fig. 23 c-d and e-f). More spores were also viable when diploids contained a *cdc13-1* mutation instead of *CDC13* deletion and carried a *pdna2-W128A,Y130A* (12.9 %) or *pDNA2* plasmid (32.4 %). *CDC13* gene could not be deleted in *ddc1Δ dna2Δ* p*dna2-W128A,Y130A* nor *ddc1Δ dna2Δ* p*DNA2* backgrounds, and therefore the hypothesis of *cdc13Δ* bypass by *ddc1Δ dna2Δ pdna2W128A,Y130A* was discounted.

Spore viability of *cdc13Δ ddc1Δ dna2Δ pdna2-W128A,Y130A* heterozygous diploid was extremely poor. I hardly observed any colonies germinated at 23°C (7 colonies out of 432 dissected spores (Fig. 23 a-b). Maybe if spores were germinated at 20°C and not at 23°C, more spores would form colonies. I conclude that simultaneous heterozygous deletions of *CDC13, DDC1* and *DNA2* cause severe defects in meiosis, resulting in generation of spores that are inviable. It is to be further tested whether such defects are related to genomic DNA replication and S-phase checkpoint or spindle checkpoint perturbations. I observed that p*Vector* and p*DNA2* allowed slightly higher spore viability (29.5 % and 11.1 %, respectively) than p*dna2-W128A,Y130A* (1.6 %). One explanation could be a dominant effect of the *dna2-W128A,Y130A* allele, which may cause e.g. an increased activity of a gene product, or a loss of gene function. However, this hypothesis was not tested.

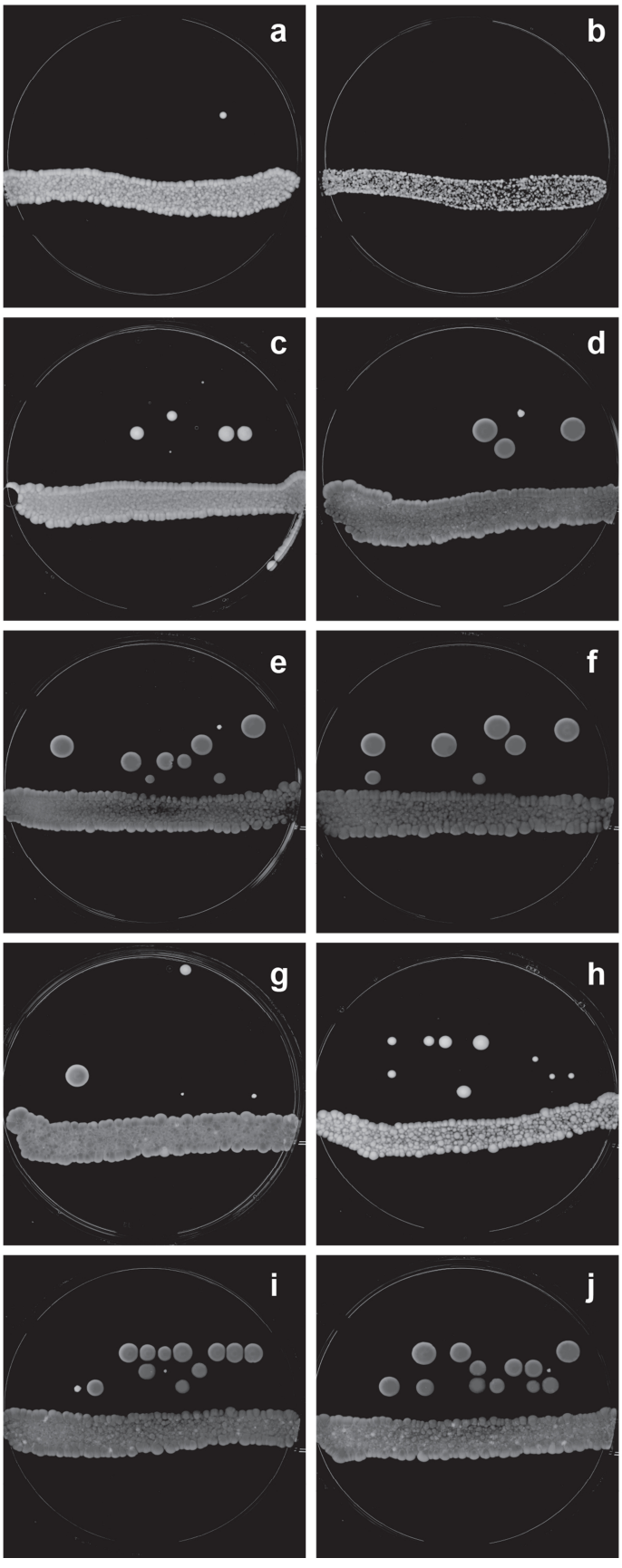


*cdc13Δ/CDC13*
*dna2Δ/DNA2*
*ddc1Δ/DDC1*
*pdna2-W128A,Y130A*
(pDL1561; DDY696)

1.6 %
spore viability
(7/432 spores)

*cdc13Δ/CDC13*
*dna2Δ/DNA2*
*ddc1Δ/DDC1*
*pDNA2*
(pDL1544; DDY723)

11.1 %
spore viability
(8/72 spores)

*cdc13Δ/CDC13*
*dna2Δ/DNA2*
*ddc1Δ/DDC1*
*pVector*
(pDL1559; DDY725)

29.5 %
spore viability
(26/88 spores)

*cdc13-1/CDC13*
*dna2Δ/DNA2*
*ddc1Δ/DDC1*
*pdna2-W128A,Y130A*
(pDL1561; DDY700)

12.9 %
spore viability
(16/124 spores)

*cdc13-1/CDC13*
*dna2Δ/DNA2*
*ddc1Δ/DDC1*
*pDNA2*
(pDL1544; DDY698)

32.4 %
spore viability
(61/188 spores)

**Figure 23. *ddc1*Δ *dna2*Δ *pdna2-W128A,Y130A* and *ddc1*Δ *dna2*Δ *pDNA2* mutations do not suppress the lethality of *cdc13*Δ**

Examples of tetrad dissection from DDY696, DDY723, DDY725, DDY700 and DDY698 diploids. Strains were grown in -TRP liquid at 23°C, then were sporulated in ESM at 20°C for 5 days, tetrads were dissected and germinated on YEPD plates. Spores were germinated for 10 days at 23°C before photographing. The relevant genotypes of the strains are indicated on the left, spore viability (percentage of the number of viable colonies/number of total dissected spores) on the right; strain details are in Appendix A.

### *3.3.6 Aneuploidy or more copies of pdna2-W128A,Y130A plasmid improve cdc13-1 fitness*

Aneuploidy is the condition of presence of an abnormal number (gain or loss) of chromosomes in a cell. Aneuploidy is associated with diseases and developmental disorders, and is observed in approximately 90 % of tumors (Weaver and Cleveland, 2006). Haploid yeast strains usually become aneuploid when they gain an extra chromosome which arises through chromosome missegregation, or as a result of endoreduplication (Schwerer et al., 2003, Bennett et al., 2014). Poor spore viability of diploids with deletion of *DNA2* in *cdc13-1* background, regardless of the presence of *dna2-W128A,Y130A* or *DNA2* on the plasmid, was a cause for concern. One explanation of spore lethality might be aneuploidy. Moreover, it has been reported that deficiency of *DNA2* in mice led to aneuploidy and development of aneuploidy-associated cancers (Lin et al., 2013). Therefore I examined whether there was a variety in the copy number of *DNA2* and its adjacent genes, *SOL3* and *PRP8,* in haploid *cdc13-1 ddc1*Δ *dna2*Δ *pdna2-W128A,Y130A* and control strains (Fig. 24).

As expected, analysis of genomic DNA revealed that *cdc13-1* and *cdc13-1 ddc1*Δ strains have the same copy number of *DNA2, SOL3* and *PRP8* genes as WT strain (Fig. 24b). Interestingly, strains carrying the plasmid p*dna2-W120A,Y130A*, but not p*DNA2,* showed a 2-fold increase of *DNA2* level. These strains however did not have more copies of *SOL3* or *PRP8* genes. Sequencing revealed that *cdc13-1 ddc1*Δ *dna2-W128A,Y130A* strains contained only *dna2-W128A,Y130A* but not WT *DNA2* sequence (not shown). The change in DNA level might be possibly due to additional copies of the plasmid carrying *dna2-W128A,Y130A* allele in these strains. One possible explanation is that *DNA2* allele on the plasmid does not fully fulfil the function(s) of Dna2*,* and therefore cells carrying more copies of the plasmid might be selected by the process of natural selection.

a)

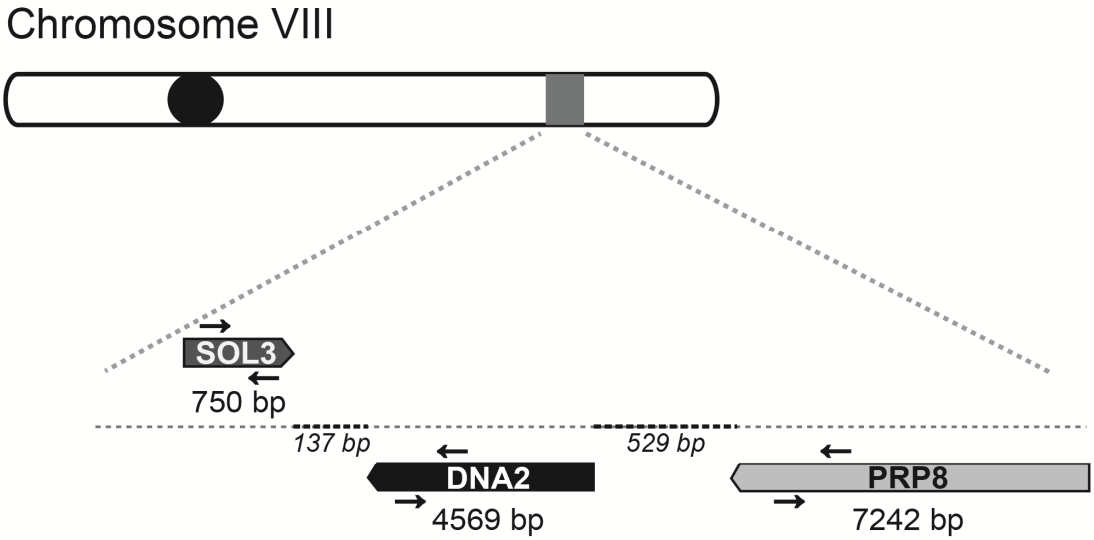
Chromosome VIII
SOL3
750 bp
137 bp
529 bp
DNA2
4569 bp
PRP8
7242 bp

b)

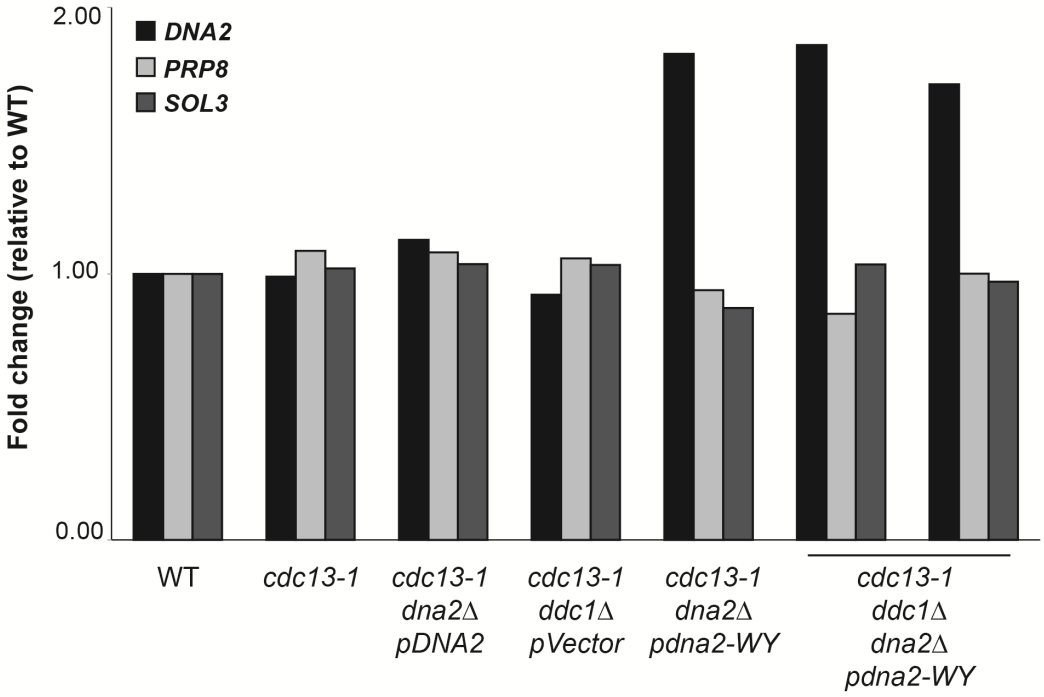
2.00
1.00
0.00
Fold change (relative to WT)
DNA2
PRP8
SOL3
WT
cdc13-1
cdc13-1 dna2Δ pDNA2
cdc13-1 ddc1Δ pVector
cdc13-1 dna2Δ pdna2-WY
cdc13-1 ddc1Δ dna2Δ pdna2-WY

**Figure 24. *dna2*∆ *dna2-W128A,Y130A* strains have more copies of p*dna2-W128A,Y130A* plasmid**

a) Map showing the localization of *DNA2* on chromosome VIII (adapted from SGD http://www.yeastgenome.org/). *SOL3* and *PRP8* are located in close proximity to *DNA2*, 137 bp and 529 bp away, respectively. The length of *DNA2, SOL3* and *PRP8* genes is shown, and primers designed to check the level of genomic DNA are marked as black arrows. Primers were: M3275, M3276, M3772, M3773, M3778, M3779, M3780, M3781. Black circle – centromere; dark square – location of *DNA2*, *SOL3* and *PRP8* on the chromosome VIII. *DNA2* and *PRP8* are encoded on Crick strand, *SOL3* is encoded on Watson strand, indicated by the direction of arrows.
b) qPCR analysis of *DNA2*, *SOL3* and *PRP8* DNA level in strains with p*dna2-W128A,Y130A* plasmid and control strains. DNA was as in Figure 21. The level of DNA from single independent strains were measured, each value was normalised to the level of *BUD6* genomic DNA. *pVector* – pRS314. Strains were: *CDC13* (DLY3001), *cdc13-1* (DLY1108), *cdc13-1 dna2*∆ *pDNA2* (pDL1554; DLY8998), *cdc13-1 ddc1*∆ *pVector* (pDL1559; DLY9469), *cdc13-1 dna2*∆ *pdna2-W128A,Y130A* (pDL1561; DLY9000), *cdc13-1 ddc1*∆ *dna2*∆ *pdna2-W128A,Y130A* (pDL1561; DLY9479), *cdc13-1 ddc1*∆ *dna2*∆ *pdna2-W128A,Y130A* (pDL1561; DLY9480).

### *3.3.7 Integrated dna2-W128A,Y130A allele does not suppress cdc13-1 defect*

To overcome problems such as observed poor spore viability and presence of more than one copy of the plasmid carrying *dna2-W128A,Y130A* allele, I decided to introduce *dna2-W128A,Y130A* allele into the genome of *cdc13-1* and WT strains. As a control, I also integrated the *DNA2* sequence into the genome. To integrate *dna2-W128A,Y130A* allele at its genomic locus, the pop-in/pop-out method was used (as in 2.16.5). I used a truncated version of *DNA2* (1599 bp instead of 4569 bp) (Fig. 25a). Thus the integrated plasmid should be flanked by a non-functional, truncated version of *DNA2* and the whole-length copy of *dna2-W128A,Y130A* allele (Fig. 25b-f).

*DNA2* and *dna2-W128A,Y130A* sequences from pDL1544 and pDL1561 plasmids were used to generate integrative plasmids (Fig. 25a). However, sequencing of these plasmids revealed the presence of additional 4 base pairs (ATCC) next to the START codon of *DNA2* and *dna2-W128A,Y130A* sequences. These 4 base pairs might significantly affect the initiation of the translation process (Kozak, 1989). To remove the additional 4 bp, the Gibson Assembly (as in 2.16.3 and Appendix D) and Quick Change (as in 2.16.4) methods were used. The Gibson Assembly method is an isothermal, single-reaction method which allows for assembling of multiple overlapping DNA molecules (Gibson et al., 2009). The assembly method was used to integrate the promoter sequence from genomic WT *DNA2* into the integrative plasmid (Appendix D). The Quick Change site-directed mutagenesis was then used to change a single point mutation T→C within the *DNA2* sequence which arose during Gibson Assembly.

The integration of the plasmids carrying *dna2-W128A,Y130A* and *DNA2* genes were confirmed by PCR and sequencing (not shown). Pop-out of the plasmid revealed that out of 20 sequenced colonies (10 *cdc13-1* and 10 WT) only one *cdc13-1* and two WT colonies had *dna2-W128A,Y130A* allele integrated (not shown). Remaining 17 colonies contained only *DNA2* sequence which might be due to reversion of *dna2-W128A,Y130A* mutation into WT *DNA2,* or integration of *DNA2* allele into a random locus.

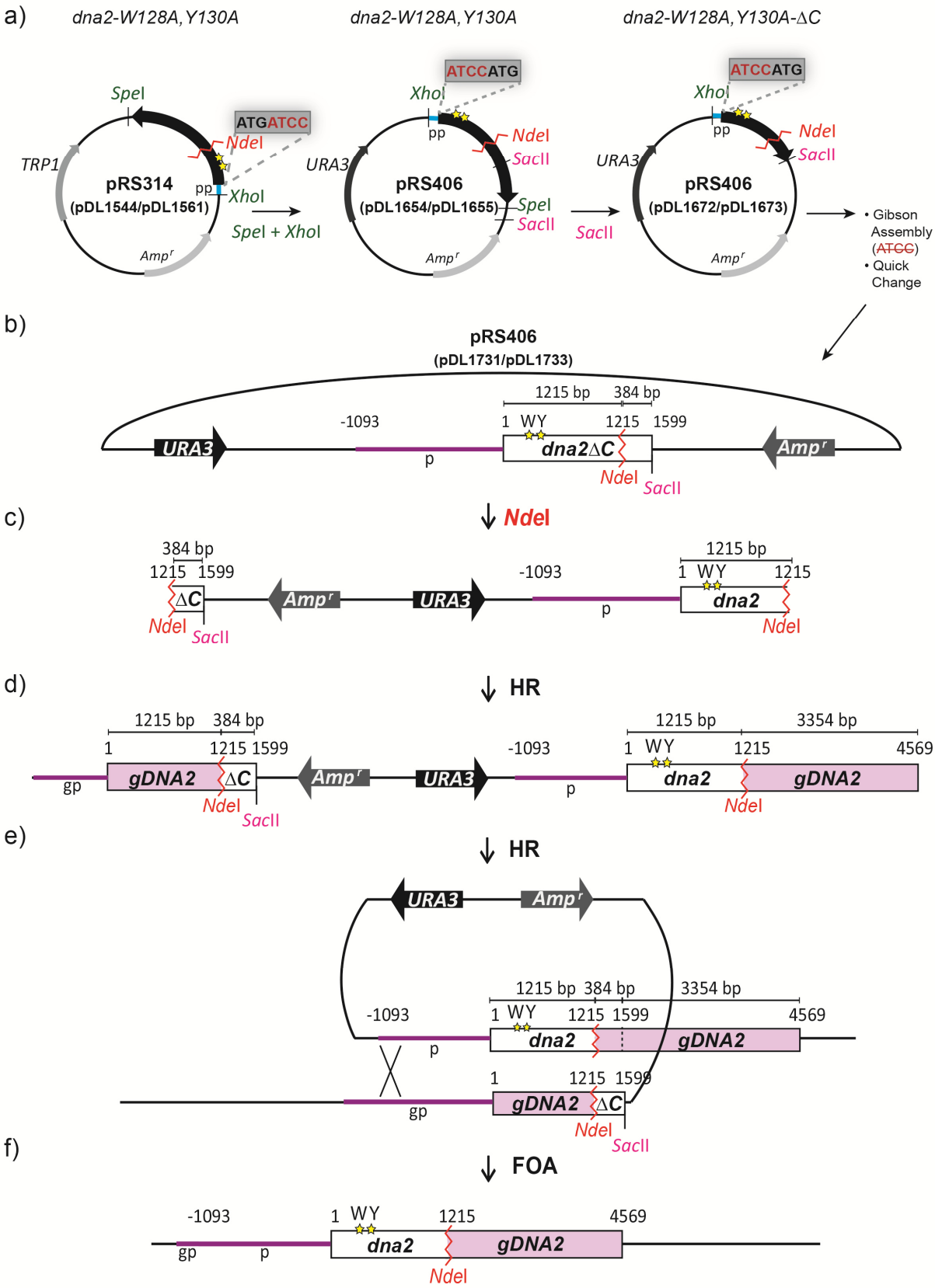
a)
dna2-W128A,Y130A
dna2-W128A,Y130A
dna2-W128A,Y130A-ΔC
SpeI
ATGATCC
NdeI
TRP1
pRS314
(pDL1544/pDL1561)
pp
XhoI
Ampr
SpeI + XhoI
ATCCATG
XhoI
NdeI
SacII
URA3
pRS406
(pDL1654/pDL1655)
SpeI
SacII
SacII
pRS406
(pDL1672/pDL1673)
• Gibson Assembly (ATCC)
• Quick Change
b)
pRS406
(pDL1731/pDL1733)
1215 bp
384 bp
-1093
1 WY
1215
1599
URA3
p
dna2ΔC
Ampr
NdeI
SacII
c)
NdeI
384 bp
1215 1599
ΔC
Ampr
URA3
-1093
1215 bp
1 WY
1215
dna2
NdeI
SacII
NdeI
d)
HR
1215 bp
384 bp
1
1215 1599
gp
gDNA2
ΔC
Ampr
URA3
-1093
1215 bp
3354 bp
1 WY
1215
4569
p
dna2
gDNA2
NdeI
SacII
NdeI
e)
HR
URA3
Ampr
1215 bp
384 bp
3354 bp
-1093
1 WY
1215
1599
4569
p
dna2
gDNA2
1
1215
1599
gp
gDNA2
ΔC
NdeI
SacII
f)
FOA
-1093
1 WY
1215
4569
gp
p
dna2
gDNA2
NdeI

**Figure 25. Pop-in/pop-out of *dna2-W128A,Y130A* allele into the genome**

a) *dna2-W128A,Y130A* (or *DNA2* as a control) was cut out from a centromeric plasmid pRS314 (pDL1544/pDL1561) with *Spe*I and *Xho*I restriction enzymes and cloned into an integrative plasmid pRS406 carrying *URA3* marker gene (pDL1654-5). Reverse orientation of *DNA2* allele is due to the plasmid sequence; plasmids pRS406 contain polylinker oriented conversely compared with pRS314. From pDL1654-5 plasmids the C-terminal part of *DNA2* or *dna2-W128A,Y130A* was cut out using *Sac*II enzyme following plasmid re-ligation (pDL1672-3). Gibson Assembly was then used to get rid of the 4 bp (ATCC) upstream ATG codon, as described in Appendix D and in 2.16.3. During assembly, a single point mutation arose in the *DNA2* sequence (T→C), and was reverted back into WT sequence using Quick Change method; as a result pDL1731/pDL1733 plasmids were generated. *TRP1, URA3* – marker genes allowing for selection on –TRP or -URA media; *Amp*$^r$ – bacterial selective marker from the plasmid; *Spe*I, *Xho*I, *Sac*II – restriction enzyme sites; *Nde*I – unique site for *Nde*I restriction enzyme within *DNA2* sequence. The *Nde*I site of *URA3* gene from pRS406 was previously destroyed in pDL452 plasmid. pDL452 served then as a backbone; stars - point mutations (affected amino acids are tryptophan W128 and tyrosine Y130); *pp* – promoter sequence from the plasmid; *p* - promoter sequence amplified from genomic DNA using Gibson Assembly method.

b) Truncated *dna2-W128A,Y130A* allele (1599 bp) contained 1093 bp endogenous promoter sequence and a unique *Nde*I restriction enzyme site. ∆*C* –C-terminal truncation of *DNA2* (2970 bp was cut out).

c) After restriction digestion with *Nde*I, linearized plasmid was transformed into yeast. The enzyme cut the plasmid in such a way that an N-terminal part (1215 bp) of *DNA2* allele was on one side of the linearized plasmid, and remaining shorter part of *DNA2* (384 bp) was on the other side.

d) The event of HR resulted in the presence of two copies of *DNA2* flanking the plasmid sequence on the chromosome. One copy contained endogenous promoter followed by 1215 bp of WT *DNA2* sequence and small part from the plasmid (384 bp). The other copy consisted of 1215 bp *dna2-W128A,Y130A* allele from the plasmid and 3354 bp of genomic *DNA2*. *gp* – genomic promotor sequence; *HR* – homologous recombination event; *gDNA2* – endogenous *DNA2* sequence.

e) FOA selection would result in a pop-out event.

f) *dna2-W128A,Y130A* allele driven by native promoter should remain on chromosome VIII. *FOA* – 5-fluoroorotic acid.

The effect of *dna2-W128A,Y130A-int* mutation, integrated within *DNA2* locus, on *cdc13-1* fitness was tested (Fig. 26a). WT and *dna2-W128A,Y130A-int* strains grew well at all temperatures, and *cdc13-1* cells did not grow at 30°C (Fig. 26a D-E, compare to A-C). *cdc13-1 dna2*∆ *pdna2-W128A,Y130A* grew at 30°C, as shown previously (Fig. 26a, F-G, compare to D-E and Fig. 20b and c). However the *cdc13-1* strain in which *dna2-W128A,Y130A* allele was integrated in the genome grew much worse than strains with the same allele on the plasmid (Fig. 26a H, compare to F-G). Moreover, this strain was less fit than *cdc13-1* mutants at 26°C (Fig. 26a H, compare to D-E).

In section 3.3.6 I described that *cdc13-1 dna2*∆ *pdna2-W128A,Y130A* strains contained more *pdna2-W128A,Y130A* copies, therefore I considered that extra copies of *dna2-W128A,Y130A* mutation might improve *cdc13-1* fitness. To test this hypothesis, *cdc13-1 dna2-W128A,Y130A-int* strains were transformed with plasmids carrying *DNA2* or *dna2-128A,Y130A* allele. *cdc13-1 dna2-W128A,Y130A-int* mutants grew worse than *cdc13-1* strains (Fig. 26b I-J, compare to C-D). Opposite to what was expected, more copies of *dna2-W128A,Y130A* allele from the plasmid slightly enhanced the ts of *cdc13-1 dna2-W128A,Y130A-int* mutants (Fig. 26b K-M, compare to I-J and C-D). On the other hand more copies of *DNA2* from the plasmid slightly improved *cdc13-1 dna2-W128A,Y130A-int* fitness (Fig. 26b N-P, compare to K-M and C-D).

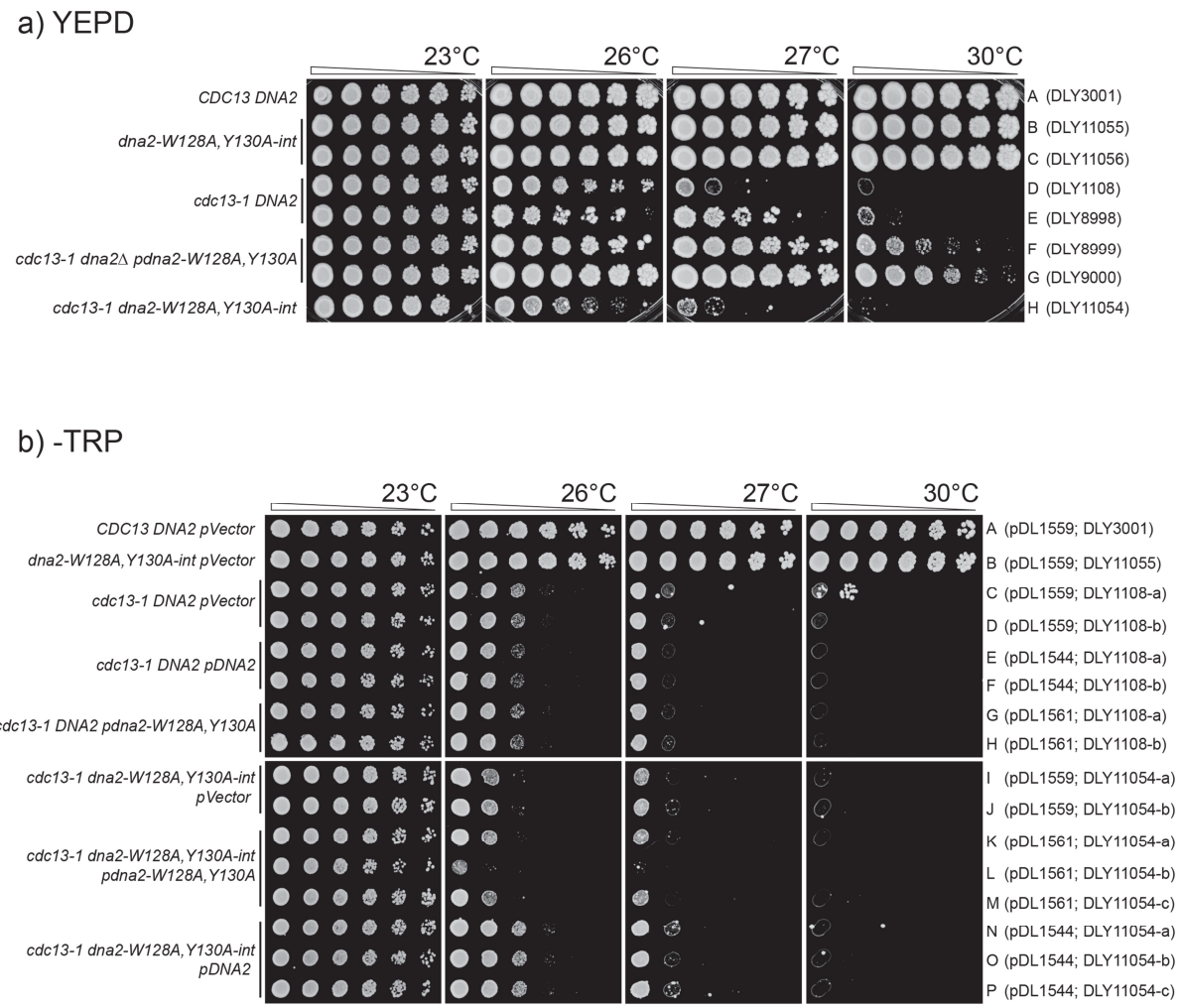


**Figure 26. The effect of *dna2-W128A,Y130A* integrated into the genome and from the plasmid on *cdc13-1* fitness is divergent**

a) Spot tests done as in Figure 9. Strains A-H were grown on one round YEPD plate. b) Spot tests done as in Figure 9. Yeast strains were spotted onto –TRP plates to select for plasmids. Strains carrying *dna2-W128A,Y130A-int* allele and control strains were transformed with *pDNA2, pdna2-W128A,Y130A* or *pVector* and passaged several times on –TRP media. Spot test was performed from passage 5. Strains A-P were grown on one rectangular –TRP plate. Strains transformed with plasmids were not frozen down and therefore do not have the collection number. Individual transformants are assigned by colony name “a-c”. *pVector* - pRS314. The relevant genotypes of the strains are indicated on the left, plasmid and strain numbers on the right; strain details are in Appendix A. Letters A-H in a) and A-P in b) on the right of the figure are assigned to relevant genotypes from the left.

I conclude that multiple problems arose during the process of strains mating and spores germination of *cdc13-1/CDC13 dna2∆/DNA2 pdna2-W128A,Y130A* strains. Telomere capping and DNA replication/resection might be affected in *cdc13-1/CDC13 dna2∆/DNA2* diploids if haploinsuffiency occurs. The altered *DNA2* promoter region from the plasmid (additional ATCC base pairs prior to START codon) might lead to protein deficiency in a cell, and in turn affect the *cdc13-1 dna2∆ pdna2-W128A,Y130A* fitness. Decreased levels of Dna2 might affect the checkpoint or nuclease functions of Dna2. The checkpoint or nuclease deficiency might lead to induction of alternative repair pathways, like HR, which favour cell growth despite the telomere damage. This however is only speculation and the deficiency of Dna2 function(s) was not tested.

Once integrated into the genome, *dna2-W128A,Y130A* allele should be transcribed and translated as endogenous gene. I observed that *dna2-W128A,Y130A-int* slightly enhanced *cdc13-1* ts. However, I cannot conclude whether *dna2-W128A,Y130A-int* mutants had defects in replication, nuclease function or checkpoint, and how these defect(s) influenced the growth of *cdc13-1* strains.

I noted in section 3.3.6 that *cdc13-1 dna2∆ pdna2-W128A,Y130A* and *cdc13-1 dna2∆ ddc1∆ pdna2-W128A,Y130A* strains had more copies of the plasmid carrying *dna2-W128A,Y130A*. More copies of *pdna2-W128A,Y130A* might be a result of plasmid instability due to segregational instability. Segregational instability occurs as a result of uneven partitioning of plasmid during cell division. Some daughter cells may receive two copies of a plasmid rather than one, and some may get no plasmid at all (Zhang et al., 1996). Sometimes, more copies of a plasmid might cause sickness and death due to plasmid centromeres interfering with natural chromosome segregation event (Stearns et al., 1990). Segregational instability might be due to the fact that *dna2-W128A,Y130A* allele is not fully functional, and cells compensate the partially loss of function of *dna2-W128A,Y130A* by selecting for more copies of the plasmid or gene. To sum up, I conclude that W128 and Y130 residues of Dna2 affect *cdc13-1* fitness, however the mechanism(s) are not fully understood.

### *3.3.8 DNA2 alleles do not affect yku70Δ fitness*

In order to test whether *DNA2* alleles affect *yku70Δ* fitness, spot tests were performed. Figure 27 illustrates that WT and *ddc1Δ* strains grew at all temperatures and *yku70Δ* grew less well at high temperature (Fig. 27a F-G, compare to A-E). *dna2Δ pdna2-W128A,Y130A*, *ddc1Δ* and *ddc1Δ dna2Δ pdna2-W128A,Y130A* mutations did not affect growth of *yku70Δ* strains (Fig. 27a H-P, compare to F-G). The effects of *dna2-C771A* and *dna2-C777A* alleles on *yku70Δ* fitness were not tested. *yku70Δ dna2Δ* strains carrying *pdna2-C771A* or *pdna2-C777A* were not generated, possibly due to spore lethality and too few tetrads dissected. *dna2-C519A* and *dna2-C768A* mutations did not affect *yku70Δ* fitness (Fig. 27b E and G-H, compare to B). I conclude that Dna2 does not affect *yku70Δ* fitness, and therefore Dna2 might not be important in cell cycle arrest in *yku70Δ* strains.

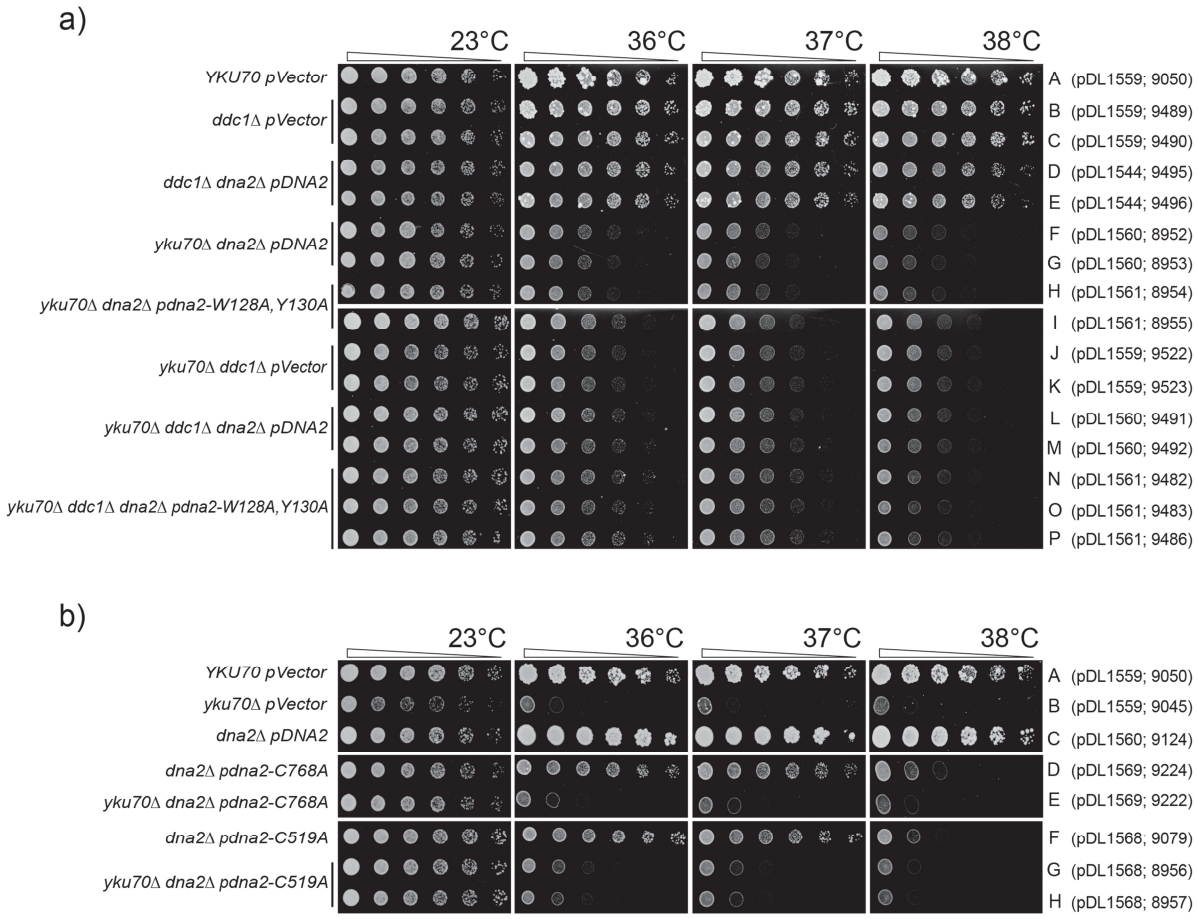


**Figure 27. *dna2* mutations do not affect the fitness of *yku70*Δ mutants**

Spot tests done as in Figure 9. Yeast strains were spotted onto –TRP plates to select for plasmids.

a) Strains A-P were grown on one rectangular plate.

b) Strains A-H were grown on one rectangular plate. Pictures were cut and reorganised using Adobe Illustrator to make comparisons easier. *pVector* - pRS314. The relevant genotypes of the strains are indicated on the left, plasmid and strain numbers on the right; strain details are in Appendix A. Letters A-P in a) and A-H in b) on the right of the figure are assigned to relevant genotypes from the left.

### *3.3.9 Potential mitochondrial defects caused by DNA2 and PIF1 mutations affect yku70Δ fitness*

One of known suppressors of *dna2*Δ lethality is *pif1*Δ (Budd et al., 2006). Both Pif1 and Dna2 function in Okazaki fragment processing (OFP) and play important roles in maintaining the mitochondrial DNA stability in yeast and humans (Foury and Lahaye, 1987, Van Dyck et al., 1992, Budd et al., 2006, Cheng et al., 2007, Pokharel and Campbell, 2012). It was observed previously that *pif1*Δ suppresses *yku70*Δ growth defect at higher temperatures (J. Dewar PhD thesis), consistent with published data that Pif1 inhibits the growth of *yku70*Δ mutants (Vega et al., 2007, Smith et al., 2008). Pif1 and Dna2 have similar function in OFP and mitochondria, and deletion of *PIF1* suppresses *yku70*Δ and *dna2*Δ. I hypothesised that Dna2 may affect *yku70*Δ fitness similarly to Pif1. Therefore I decided to test how simultaneous mutations of *PIF1* and *DNA2* affect *yku70*Δ growth.

Spot tests of *yku70*Δ strains with mutations of *PIF1* and *DNA2* were performed on YEPG and YEPD plates (Fig. 28). Glycerol is a non-fermentable carbon and energy source that forces yeast to grow aerobically, therefore only cells which maintain mitochondrial function can grow on YEPG media. The YEPG media served as an indirect method to test the mitochondrial function (Fig. 28a). *dna2*Δ *pDNA2* and *dna2*Δ *pdna2-W128A,Y130A* strains did not grow well 23°C (Fig. 28a B-E, compare to A). As expected *pif1*Δ mutants were ts at 38°C (Fig. 28a F-H). One *pif1*Δ *dna2*Δ *pDNA2* strain grew better at 38°C than another strain of the same genotype (Fig. 28a G and H). The fitter strain might carry more copies of the *pDNA2* plasmid which could improve growth, but the plasmid copy number was not tested. *pif1*Δ suppressed the growth defect of *dna2*Δ mutants at all temperatures, and only slightly suppressed the growth defect of *dna2*Δ *pdna2-W128A,Y130A* mutants (Fig. 28a I-L). This might indicate that *dna2-W128A,Y130A* mutants have more severe defects in mitochondria maintenance than *dna2*Δ. *yku70*Δ mutants were ts at 38°C (Fig. 28a M-P). Strikingly, *yku70*Δ *dna2*Δ *pdna2-W128A,Y130A* mutants looked like *yku70*Δ *pif1*Δ *dna2*Δ *pDNA2* and *pif1*Δ *dna2*Δ *pdna2-W128A,Y130A* mutants and grew at 23°C, but not above 37°C (Fig. 28a R-U and I-J). Triple mutants *yku70*Δ *pif1*Δ *dna2*Δ *dna2-W128A,Y130A* and *yku70*Δ *pif1*Δ *dna2*Δ looked alike and did not grow well at 23°C (Fig. 28a V-X).

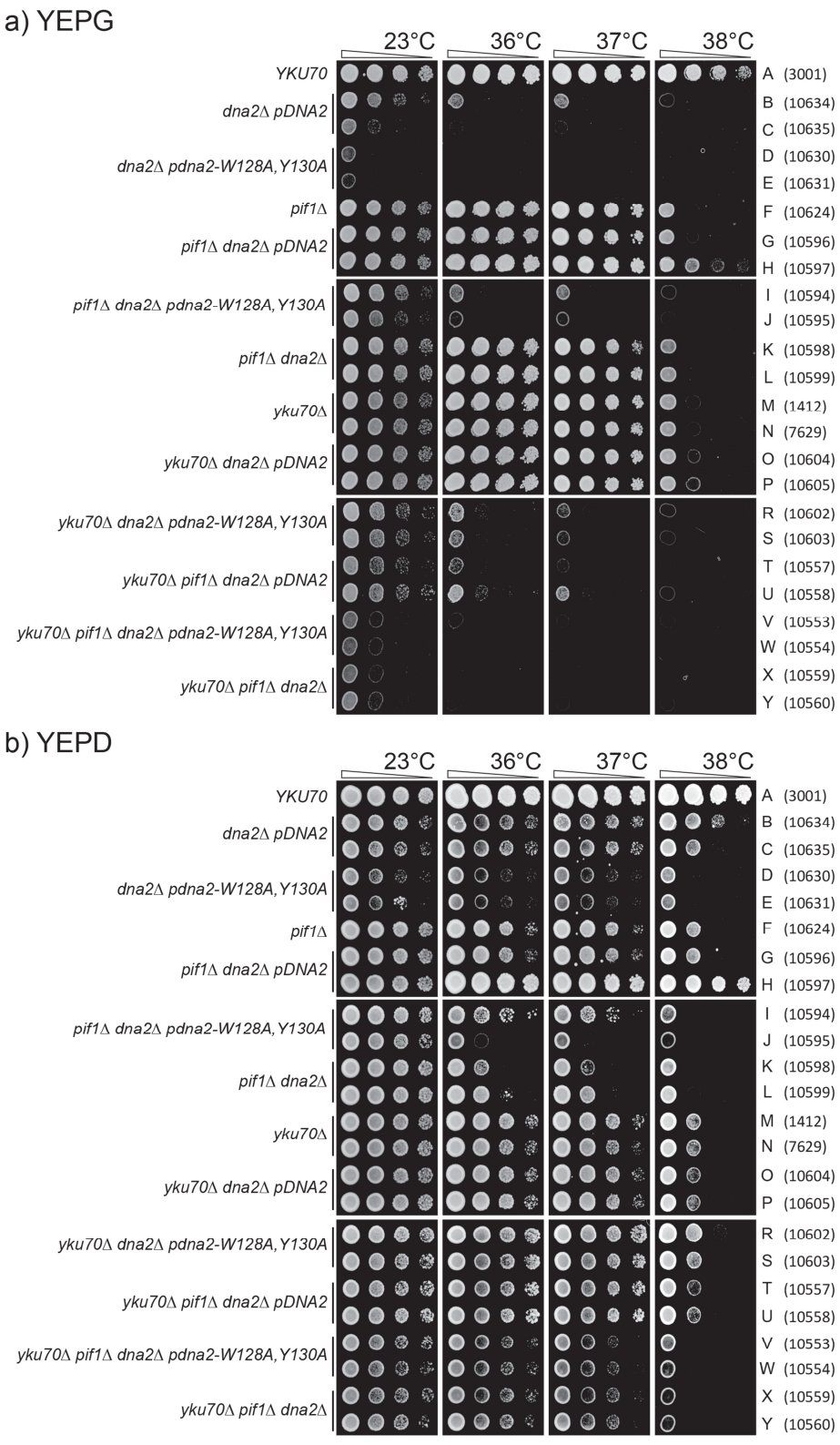


**Figure 28. Mitochondrial function affects *yku70*Δ fitness**

a)-b) Spot tests done as in Figure 9. The relevant genotypes of the strains are indicated on the left, strain numbers on the right; strain details are in Appendix A. Letters A-Y on the right of the figure are assigned to relevant genotypes from the left.

a) Strains were grown on one rectangular YEPG plate.

b) Strains from A were also spotted onto YEPD and grown on one rectangular plate.

A somewhat different growth pattern was observed on YEPD plates (Fig. 28b). Strikingly, *yku70*Δ mutants grew well at 37°C, and *yku70*Δ *dna2*Δ *pdna2-W128A,Y130A* strains were much less fit at 36°C (Fig. 28b M-P, compare to D-E). In contrast, previously I observed no effect of *pdna2-W128A,Y130A* on *yku70*Δ fitness (Fig.27). Possible differences in strains growth might be due to different media used (-TRP vs. YEPD), or different culture conditions, if strains from YEPD were grown till saturation prior spotting. However, these hypotheses were not tested.

*dna2*Δ strains carrying *pdna2-W128A,Y130A* plasmid are unable to grow well on YEPG. For reasons I do not understand *pif1*Δ *dna2*Δ mutants are fitter than *pif1*Δ *dna2*Δ *pdna2-W128A,Y130A* mutants. Double point mutation of W128 and Y130 residues is more severe for cells than deletion of *DNA2* in *pif1*Δ background. It might be possible that W128 and Y130 residues of *DNA2* are important for the mitochondrial DNA maintenance function of Dna2. For example, the interaction between Dna2 and unknown protein “A” through W128 and Y130 residues might be lost, but interaction(s) between Dna2 and protein “B” (which might be Dna2 inhibitor) could be maintained in *pif1*Δ *dna2*Δ *pdna2-W128A,Y130A* mutants. This is only a speculation which remains to be tested.

It was observed previously that *pif1*Δ *yku70*Δ strains grew better than *yku70*Δ mutants on YEPD plates (J. Dewar PhD thesis). I observed that *yku70*Δ *pif1*Δ *dna2*Δ *pDNA2* mutants grew worse than *yku70*Δ mutants on YEPG plates (Fig. 28a and b T-U, compare to M-P). However the same *yku70*Δ *pif1*Δ *dna2*Δ *pDNA2* strains resembled *yku70*Δ mutants on YEPD plates. I never observed that *pif1*Δ *dna2*Δ *pDNA2* mutations suppressed *yku70*Δ growth defect. However, I did not use *yku70*Δ *pif1*Δ strains and for that reason it is not accurate to conclude the inconsistency with Dewar’s observations. Another spot test should be performed on YEPG and YEPD plates, involving strains used by Dewar to clarify the effect of *pif1*Δ on *yku70*Δ fitness. It was shown that loss of Ku complex affects the rate of spontaneous mitochondrial deletions and repair of mitochondrial DSBs (Kalifa et al., 2012). I propose that Yku70 might be important in mitochondrial DNA maintenance since it probably interacts with Pif1 and Dna2 (Fig. 28a).

### *3.3.10 Discussion/Conclusions*

None of tested mutations in nuclease domain of Dna2, *dna2-C519A, dna2-C768A, dna2-C771A,* affected growth of *cdc13-1* or *yku70*Δ strains, although all were shown previously as sensitive to MMS (Table 6) (Pokharel and Campbell, 2012). Two residues, W128 and Y130, which responded to 4-NQO and HU treatments, strongly affected growth of *cdc13-1* mutants (Kumar and Burgers, 2013).

| Source | *DNA2* alleles | Growth at restrictive temp. § | | 4-NQO-induced Rad53 phospho-rylation | HU-induced Rad53 phospho-rylation * | UV sensitivity (70 J/m$^2$) | MMS sensitivity (0.01 %) |
|---|---|---|---|---|---|---|---|
| | | *cdc13-1* | *yku70*Δ | | | | |
| J. Campbell | *dna2-C519A* | — | — | N/A | N/A | N/A | ++ |
| | *dna2-C768A* | — | — | N/A | N/A | N/A | +++ |
| | *dna2-C771A* | — | N/A | N/A | N/A | N/A | +++ |
| | *dna2-C777A* | N/A | N/A | N/A | N/A | N/A | +++ |
| | *DNA2* | — | — | N/A | N/A | N/A | + |
| P. Burgers | *DNA2* | — | — | +++ | +++ | + | N/A |
| | *dna2-W128A,Y130A* | ++ | — | +++ | ++ | N/A | N/A |
| | *dna2-W128A,Y130A ddc1*Δ | +++ | — | N/A | + | N/A | N/A |
| | *dna2-W128A,Y130A ddc1-(1-404),W352A* | N/A | N/A | — | N/A | ++ | N/A |

**Table 6. Response of *DNA2* alleles to DNA damage**

§ - analysed in this thesis; * - *tel1*Δ background. Response of tested alleles to DNA damage is indicated by: — - no response, + - weak response, ++ - moderate response, +++ - strong response; N/A – not tested. Based on (Pokharel and Campbell, 2012, Kumar and Burgers, 2013)

I showed that *dna2-W128A,Y130A* improved *cdc13-1* growth when on a plasmid, but slightly reduced *cdc13-1* fitness when integrated into the genome. *cdc13-1 dna2*Δ strains carrying *pdna2-W128A,Y130A* were able to grow at 30°C, and the growth was improved by deletion of *DDC1.* The checkpoint of *cdc13-1 ddc1*Δ *dna2*Δ *pdna2-W128A,Y130A* strains might be defective and thus permit strains growth at 36°C. Fit

strains carried more copies of *dna2-W128A,Y130A*, most likely due to additional copies of the plasmid, and had the telomeres rearranged. Possibly, *dna2-W128A,Y130A* allele is not fully functional and cells with Dna2 function deficiency select for more copies of the plasmid in favour of maintaining Dna2 functionality. It seems that more copies of *pdna2-W128A,W130A* led to telomere amplification and this caused a *cdc13-1* cell growth improvement. *dna2-W128A,Y130A* allele may be defective in an "unknown" function of Dna2, which could be: DNA resection, replication, checkpoint and DNA damage signalling, telomere maintenance or mitochondrial DNA maintenance, however none of these were examined in the context of *dna2-W128A,Y130A* allele.

*dna2-W128A,Y130A* slightly enhanced the growth of *yku70*Δ strains when on YEPD media, and strongly enhanced *yku70*Δ growth when on YEPG media. Deletion of *PIF1* also enhanced growth defect of *yku70*Δ mutants, and mutations of *DNA2* enhanced *yku70*Δ *pif1*Δ growth defect more. This indicates that Pif1 and Dna2 function in parallel pathways in mitochondrial DNA maintenance since deletion of both genes in *yku70*Δ mutants have an additive effect. Yku70, Dna2 and Pif1 might interact to provide mitochondrial DNA stability, although the mechanisms are not yet understood.

### 3.4 Discussion

I hypothesised that Dpb11 and/or Dna2 take the role of Ddc1 in cell cycle arrest of *yku70*Δ mutants, based on structural and functional similarities of Dpb1 and Dna2 to Ddc1. I expected to see that some alleles of *DPB11* or *DNA2* suppress the temperature sensitivity of *yku70*Δ cells at higher temperatures. This would indicate the potential role of tested alleles in cell cycle arrest.

I found that *DNA2* alleles did not suppress the *yku70*Δ ts at higher temperatures. None of tested *DPB11* alleles affected *yku70*Δ fitness, either. Surprisingly, I found that *DDC1* deletion slightly suppressed the growth of *yku70*Δ strains, and the effect was stronger when yeast from saturated cultures were analysed. I conclude therefore that there is no evidence for Dpb11 or Dna2 to have a potential role in cell cycle arrest of *yku70*Δ mutants. Alternatively, Ddc1 seems to be the only one known Mec1 activator with likely function in cell cycle arrest of *yku70*Δ strains. It is still possible that there is another protein(s) which may take part in cell cycle arrest of *yku70*Δ mutants.

I found that two residues of Dna2, W128 and Y130, might be important for mitochondrial respiration, which has not been described before. It was shown that many mitochondrial genes are upregulated in telomerase-deficient strains and the interaction between mitochondria and telomeres appear to be evolutionary conserved (Nautiyal et al., 2002, Passos et al., 2007, Addinall et al., 2008). It was reported that Dna2 has a role in mitochondrial DNA maintenance (Budd et al., 2006, Duxin et al., 2009). *dna2-W128A,Y130A* allele might be upregulated in telomerase-deficient strains, but no experiments were done to confirm this hypothesis so far.

# Chapter 4. What is the essential function of Dna2?

## 4.1 Deletion of some checkpoint and replication-related genes suppress *dna2*Δ lethality

*DNA2* encodes a conserved and essential helicase/nuclease which is involved in DNA replication, Okazaki fragment maturation and DNA resection during DSB repair. In yeast, *DNA2* deletion is lethal, but three mechanisms are known to date to suppress the lethality of *dna2*Δ: overexpression of *RAD27*, a nuclease involved in Okazaki fragment processing, deletion of *PIF1*, a helicase involved in long flap formation during DNA replication, and deletion of *RAD9*, a DNA damage checkpoint protein (Budd and Campbell, 2000, Budd et al., 2006, Budd et al., 2011). One plausible reason for *rad9*Δ suppressing *dna2*Δ was defective checkpoint in response to replication errors. In the absence of Dna2 the Okazaki fragments remain unprocessed, are RPA-bound and activate Mec1 (Fig. 29). Mec1 phosphorylates Rad9 and Rad53, which induces cell cycle arrest. When *RAD9* is deleted, Mec1 is not activated and cell cycle is not arrested (Budd et al., 2011).

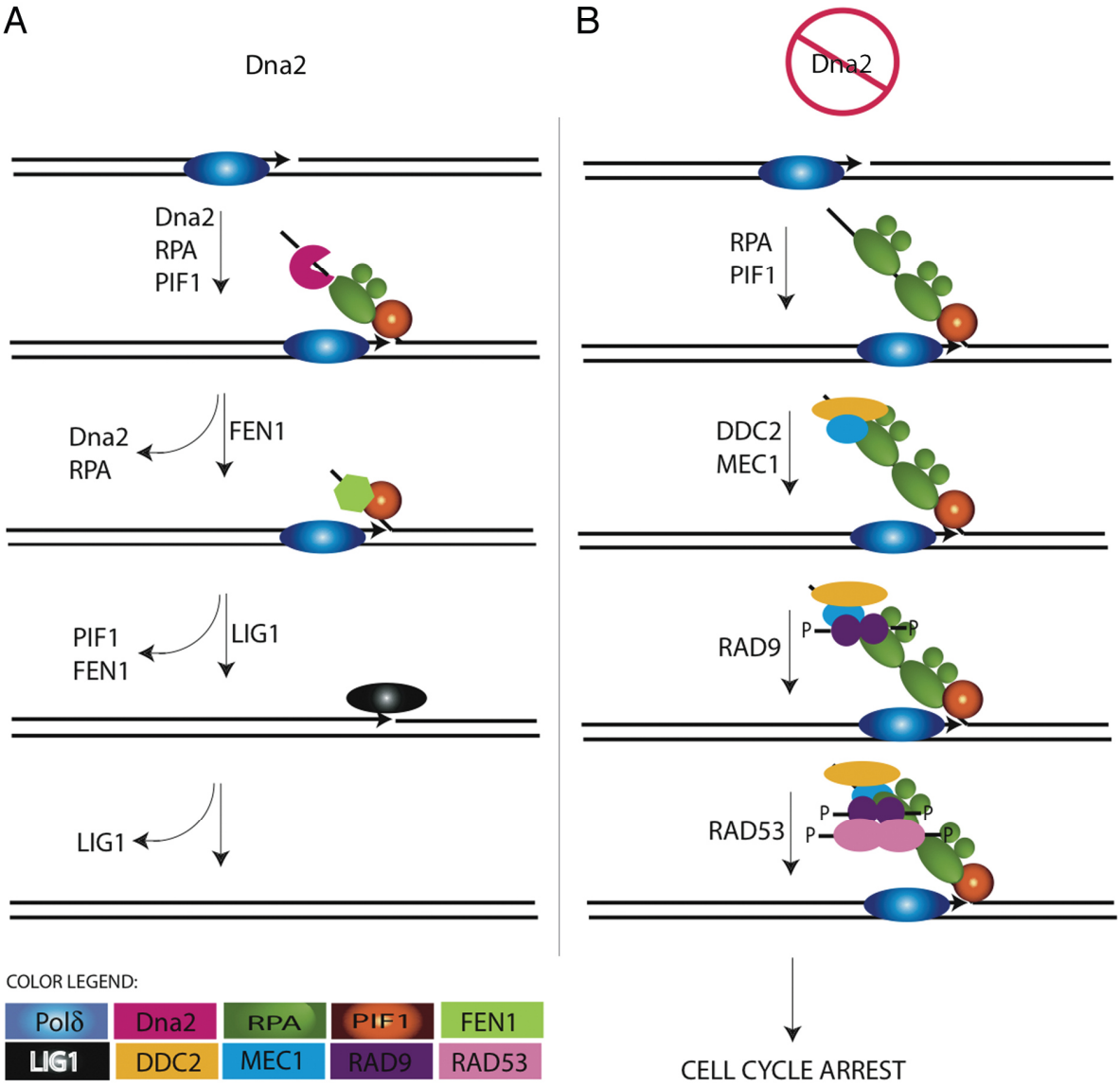
A
Dna2
Dna2
RPA
PIF1
Dna2
RPA
FEN1
PIF1
FEN1
LIG1
LIG1
COLOR LEGEND:
Polδ
Dna2
RPA
PIF1
FEN1
LIG1
DDC2
MEC1
RAD9
RAD53
B
Dna2
RPA
PIF1
DDC2
MEC1
RAD9
P
P
RAD53
P
P
P
P
CELL CYCLE ARREST

**Figure 29. Checkpoint activation due to replication errors in the absence of Dna2**

Figure and text taken from (Budd et al., 2011), Figure 5.

In vitro, DNA strand displacement synthesis by pol Δ in the presence of Rad27$^{scFEN1}$ protein on a primer adjacent to an upstream fragment results in the appearance of cleaved flaps. Although most of the cleaved flaps are short, 8–12 nt, a small subset are about 30 nt (Ayyagari et al., 2003, Rossi and Bambara, 2006). Pol Δ strand displacement is stimulated by Pif1, and a significant increase in the 30 bp cleaved product is observed in the presence of Pif1, although the 30 nt cleaved product is still only 1–2% of the total cleaved products (Rossi et al., 2008, Pike et al., 2009). The 30 nt flap synthesized by PolΔ/Pif1 becomes refractory to cleavage by Rad27$^{scFEN1}$ in the presence of RPA, which may result in even further lengthening of the flap (Rossi et al., 2008, Pike et al., 2009). As shown in (A), in normal cells containing Dna2, the RPA bound flap is bound by Dna2, which cleaves the long flap, releasing RPA and allowing Rad27$^{scFEN1}$ to further cleave the flap, resulting in a ligatable nick (Bae et al., 2001, Ayyagari et al., 2003, Bae et al., 2003, Stewart et al., 2008, Pike et al., 2009). In the absence of Dna2, (B), the RPA-bound flap, however, persists and can bind Mec1/Ddc2 kinase. The 5′ flap-bound Mec1/Ddc2 then recruits and phosphorylates Rad9, which binds methylated histone H3-K79 with its Tudor domain. Mec1/Ddc2 may also phosphorylate histone H2A, providing an additional site for Rad9 binding to chromatin. Chromatin bound Rad9 then recruits Rad53, resulting in dimerization, autophosphorylation and Rad53 kinase activation, allowing Rad53 to activate the DNA damage response and cell cycle arrest. (Similarly, the MCM helicase and pol *ε* may target Mrc1 to Mec1-bound 5′ flaps). After checkpoint activation, cells normally repair the DNA damage, deactivate the checkpoint and resume cell division. *dna2*Δ strains would be unable to repair the unprocessed Okazaki fragments during the $G_2$ division delay; thus the Rad9/Mrc1-dependent $G_2$ division delay contributes to cell death rather than recovery.

### *4.1.1 Rare ddc1Δ dna2Δ clones indicate a novel pathway for dna2Δ bypass*

As a result of dissection described in section 3.3.5 (Figure 23i), I used to find some *dna2Δ ddc1Δ* colonies occasionally emerging (Fig. 30). The viability of *ddc1Δ dna2Δ* clones was not expected because lack of suppression of *dna2Δ* lethality by *ddc1Δ, ddc1Δ tel1Δ sml1Δ* or *ddc1Δ mec1Δ sml1Δ* was previously reported (Kumar and Burgers, 2013). Kumar and Burgers concluded that suppression of *dna2Δ* lethality was *RAD9*-specific and other checkpoint genes, like *DDC1, TEL1* or *MEC1,* only indirectly function in *DNA2* pathway (Kumar and Burgers, 2013). Dna2 processes Okazaki fragments, while the 9-1-1 complex is loaded onto dsDNA-ssDNA junctions and is important for checkpoint activation in response to e. g. replication stress (Ellison and Stillman, 2003, Majka et al., 2006, Navadgi-Patil and Burgers, 2009). Budd *et al.* discovered the role of *rad9Δ* in *dna2Δ* suppression, but they did not verify whether other checkpoint proteins, apart from Rad9 and Mrc1, are also important for *dna2Δ* viability.

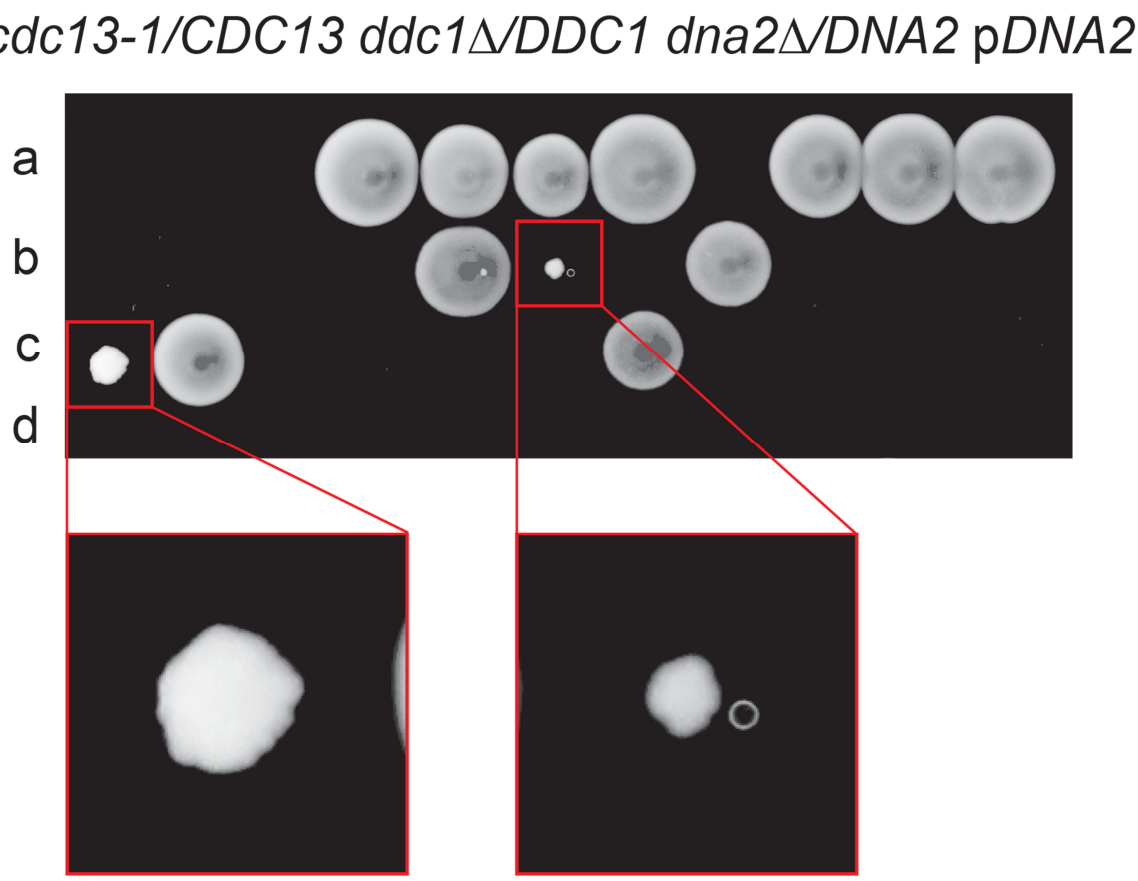


**Figure 30. Unexpected *dna2*Δ *ddc1*Δ clones**

Magnification of Figure 23i. Example of tetrad dissection from a sporulated diploid (DDY698). Two colonies of *dna2*Δ *ddc1*Δ genotypes are shown in red squares. Strains were grown in -TRP liquid at 23°C, then were sporulated in ESM at 20°C for 5 days, tetrads were dissected and germinated on YEPD plates. Spores were germinated for 10 days at 23°C before photographing. Five *dna2*Δ *ddc1*Δ colonies out of 188 dissected spores were found from this particular cross.

### *4.1.2 Some gene deletions affect dna2Δ viability at lower temperatures*

To test whether Ddc1, and perhaps other checkpoint proteins, affect *dna2*Δ viability I created diploids: *rad9Δ/RAD9 dna2Δ/DNA2*, a positive control for *dna2*Δ suppression, *ddc1Δ/DDC1 dna2Δ/DNA2, rad17Δ/RAD17 dna2Δ/DNA2* and *chk1Δ/CHK1 dna2Δ/DNA2*. Spores of these diploids were dissected and germinated (Fig. 31). Usually spores are allowed to germinate at 23°C for a ts mutation and at 30°C for WT strains. Spores may be germinated at 20°C if mutants are sick or slow growing. Interestingly, when spores of all genotypes were germinated at 20°C some tiny colonies emerged (Fig. 31a). Small colonies appeared also, though less frequently, when incubated at 23°C(Fig. 31b), and were smaller than those that emerged at 20°C. Spore viability of spores germinated at 30°C was 50 %, as expected for deletion of essential *DNA2* gene, and no small colonies were observed (Fig. 31c).

The small clones were verified as *dna2*Δ mutants with deletions of *RAD9, DDC1, RAD17* or *CHK1*. Figure 31d summarizes that *rad9Δ, ddc1*Δ and *chk1*Δ efficiently suppressed approximately 50 % of *dna2*Δ strains at 20°C, while *rad17*Δ suppressed 87 % of *dna2*Δ mutants. I conclude that double mutants with deletions of checkpoint genes and *DNA2* are often viable but sick and grow slowly. Importantly, *ddc1Δ, rad17*Δ and *chk1*Δ were similar to *rad9*Δ in the effect on *dna2*Δ mutants. Double mutants were viable only at lower temperature, indicating that *dna2*Δ mutants may be ts. Possibly at lower temperature cells have more time to repair the damage caused by deletion of *DNA2*, or have time to adapt to the damage. It is intriguing that *dna2*Δ was never suppressed at 20°C at 100 % by any of tested mutations. At lower temperature, e.g. 15°C, more spores might be viable, but this has to be tested.

I deduce that Kumar and Burgers never observed *dna2*Δ *ddc1*Δ mutants (Kumar and Burgers, 2013) if spores were germinated at higher temperatures, such as 30°C. Budd *et al.* presumably germinated spores at lower temperature, such as 23°C, because they worked with *dna2-2* and *dna2-1* ts mutants before (Budd et al., 2011). Deletions of *DDC1, RAD17, CHK1* and *RAD9* equally permit *dna2*Δ viability and I observed no differences between the effect of *rad9*Δ and *ddc1*Δ mutations on *dna2*Δ viability. I conclude that functional checkpoint is critical for *dna2*Δ lethality. My data is consistent with Budd *et al.* and Kumar and Burgers at what I presume are the temperatures of spore germination.

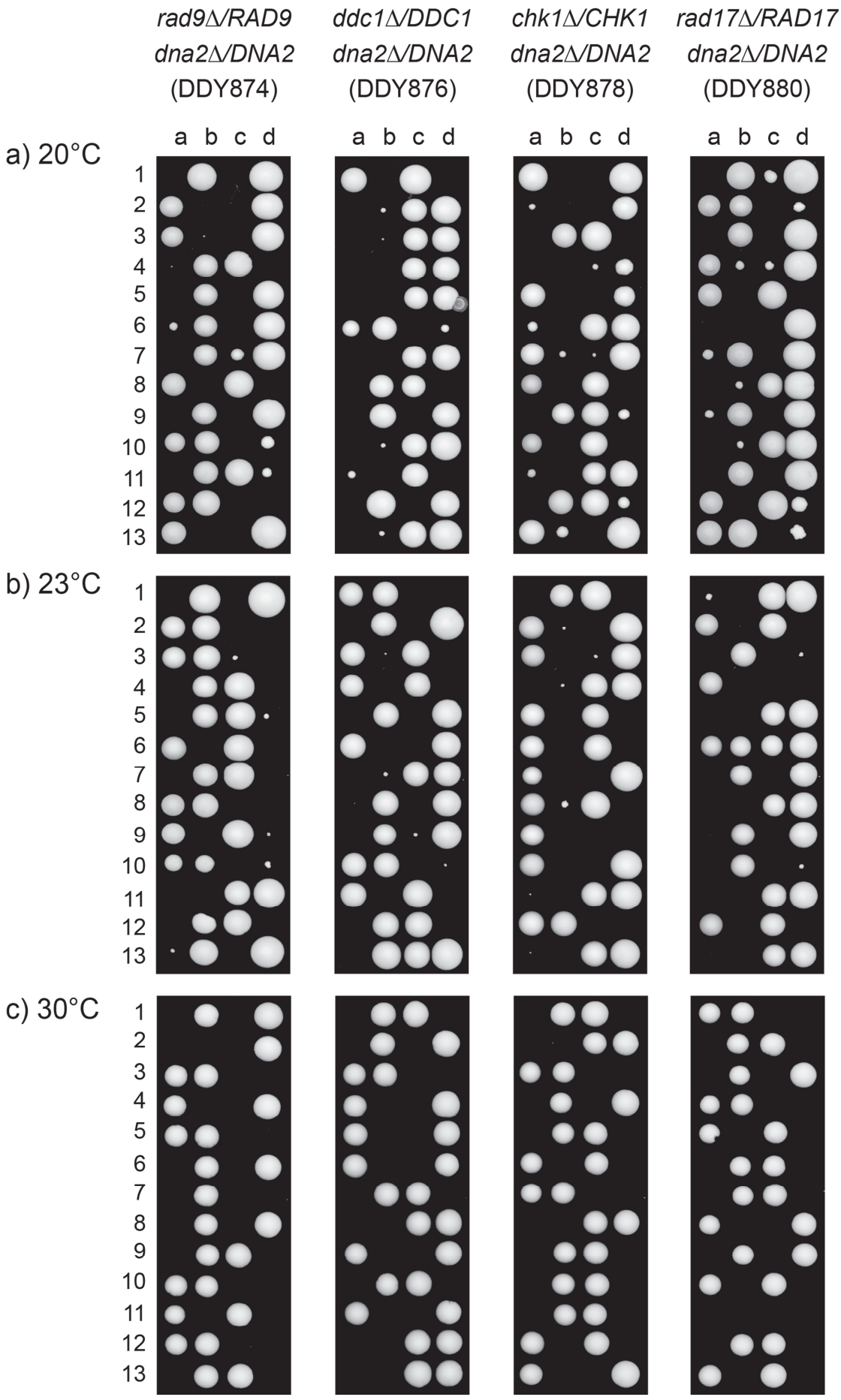
rad9Δ/RAD9 dna2Δ/DNA2 (DDY874)
ddc1Δ/DDC1 dna2Δ/DNA2 (DDY876)
chk1Δ/CHK1 dna2Δ/DNA2 (DDY878)
rad17Δ/RAD17 dna2Δ/DNA2 (DDY880)
a) 20°C
b) 23°C
c) 30°C
a b c d
1 2 3 4 5 6 7 8 9 10 11 12 13

d)

| Temp. | Genotype | No. of visible colonies | No. of *yfg*Δ | No. of *yfg*Δ *dna2*Δ | Suppression efficiency [%] |
|---|---|---|---|---|---|
| 20°C | *rad9*Δ *dna2*Δ (DDY874) | 65 (n=104) | 26 | 14 | 53.8 |
| | *ddc1*Δ *dna2*Δ (DDY876) | 64 (n=104) | 25 | 13 | 50.0 |
| | *chk1*Δ *dna2*Δ (DDY878) | 65 (n=104) | 26 | 14 | 53.8 |
| | *rad17*Δ *dna2*Δ (DDY880) | 63 (n=92) | 23 | 20 | 87.0 |
| 23°C | *rad9*Δ *dna2*Δ (DDY874) | 58 (n=104) | 28 | 7 | 26.9 |
| | *ddc1*Δ *dna2*Δ (DDY876) | 63 (n=104) | 27 | 11 | 42.3 |
| | *chk1*Δ *dna2*Δ (DDY878) | 55 (n=100) | 22 | 7 | 26.9 |
| | *rad17*Δ *dna2*Δ (DDY880) | 61 (n=104) | 23 | 12 | 46.1 |
| 30°C | *rad9*Δ *dna2*Δ (DDY874) | 47 (n=100) | 23 | 0 | 0.0 |
| | *ddc1*Δ *dna2*Δ (DDY876) | 51 (n=104) | 25 | 0 | 0.0 |
| | *chk1*Δ *dna2*Δ (DDY878) | 50 (n=104) | 31 | 0 | 0.0 |
| | *rad17*Δ *dna2*Δ (DDY880) | 47 (n=100) | 22 | 0 | 0.0 |

**Figure 31. *ddc1*Δ, *rad17*Δ and *chk1*Δ suppress *dna2*Δ similarly to *rad9*Δ**

*dna2*Δ *pDNA2* strain was mated with checkpoint gene deletion strains. Diploids lost the plasmid by passaging on YEPD for approximately 5 times. Next strains were grown in YEPD liquid, sporulated in ESM, tetrads were dissected and germinated on YEPD plates. Spores were dissected on 2 plates for each diploid at each temperature; one plate for each diploid is shown.

a) Spores germinated at 20°C for 10 days before photographing.

b) Spores germinated at 23°C for 7 days before photographing.

c) Spores germinated at 30°C for 4 days before photographing.

d) Calculations of visible colonies (single and double mutants) grown at 20°C, 23°C and 30°C.

Suppression efficiency was calculated as follows:

Number of dissected spores (104, 100 or 92) was divided by 4 – the number of possible haploid genotypes (WT, *yfg*Δ, *dna2*Δ, *yfg*Δ *dna2*Δ). Calculated number (26, 25 or 23) serves as 100 % and indicates the amount of colonies of each genotype. Scored number of *yfg*Δ *dna2*Δ double mutants was converted into %. The result is shown as % suppression efficiency.

To test if other checkpoint genes have similar suppressive role on *dna2*Δ lethality more diploids were generated, sporulated and spores were dissected; numbers of viable colonies are in Figure 32. *MEC1*, *TEL1* and *RAD53* are checkpoint genes and therefore it might be possible that, when deleted, suppress *dna2*Δ similarly to *rad9*Δ, *ddc1*Δ, *rad17*Δ and *chk1*Δ. Mec1 and Rad53 remove the inhibitory effect of Sml1 on dNTP synthesis during DNA replication, and *sml1*Δ allows for bypass of *RAD53* and *MEC1* deletions (Zhao et al., 1998). *SML1* serves here as a control for *MEC1* and *RAD53* deletions. *EXO1* encodes an exonuclease which resects DNA in response to DNA damage (Zhu et al., 2008, Ngo and Lydall, 2010). Dna2 functions redundantly to Exo1 in DNA resection (Zhu et al., 2008, Ngo et al., 2014) so it might be possible that *exo1*Δ suppresses *dna2*Δ lethality. Rif1 acts synergistically with Rif2 in telomere length control; Rif1 is involved in DNA replication, and Rif1/Rif2 contribute to DNA resection at DSBs and elongated telomeres are present in null mutants (Wotton and Shore, 1997, Teixeira et al., 2004, Shi et al., 2013, Hiraga et al., 2014, Martina et al., 2014). It was hypothesised that long telomeres of *rif1*Δ and *rif2*Δ strains might suppress *dna2*Δ lethality. This assumption was based on the fact that *pif1*Δ mutants also have long telomeres and allow for *dna2*Δ bypass. Pol32 is a subunit of DNA polymerase delta and is involved in chromosomal DNA replication (Johansson et al., 2004). It was hypothesised that at lower temperature the deletion of *POL32* may suppress *dna2*Δ lethality similarly to *pif1*Δ. *pol32*Δ was previously shown to improve the growth of *dna2-1* and *dna2-2* mutants, but not to suppress the lethality of *dna2*Δ mutants (Budd et al., 2005, Budd et al., 2006).

While *pol32*Δ and *mec1*Δ suppressed *dna2*Δ lethality similarly to *rad9*Δ, no suppression was noted when *TEL1, RAD53, SML1, EXO1, MRE11, RAD27, RIF1* or *RIF2* were deleted (Fig. 32). Long telomeres of *rif1*Δ and *rif2*Δ mutants did not bypass *dna2*Δ viability. This indicates that only a subset of proteins that are important in e.g. telomere biology (Ddc1, Rad9, Chk1, Mec1 and Pol32) influence the *dna2*Δ viability, while other proteins (Tel1, Exo1, Rad53, Sml1, Rif1, Rif2, Mre11, Rad27) do not affect *dna2*Δ viability. It is therefore interesting to examine whether the viability of *dna2*Δ is due to defects in DNA replication, or maybe is specific to telomere DNA replication. Although important, this question has not been addressed yet.

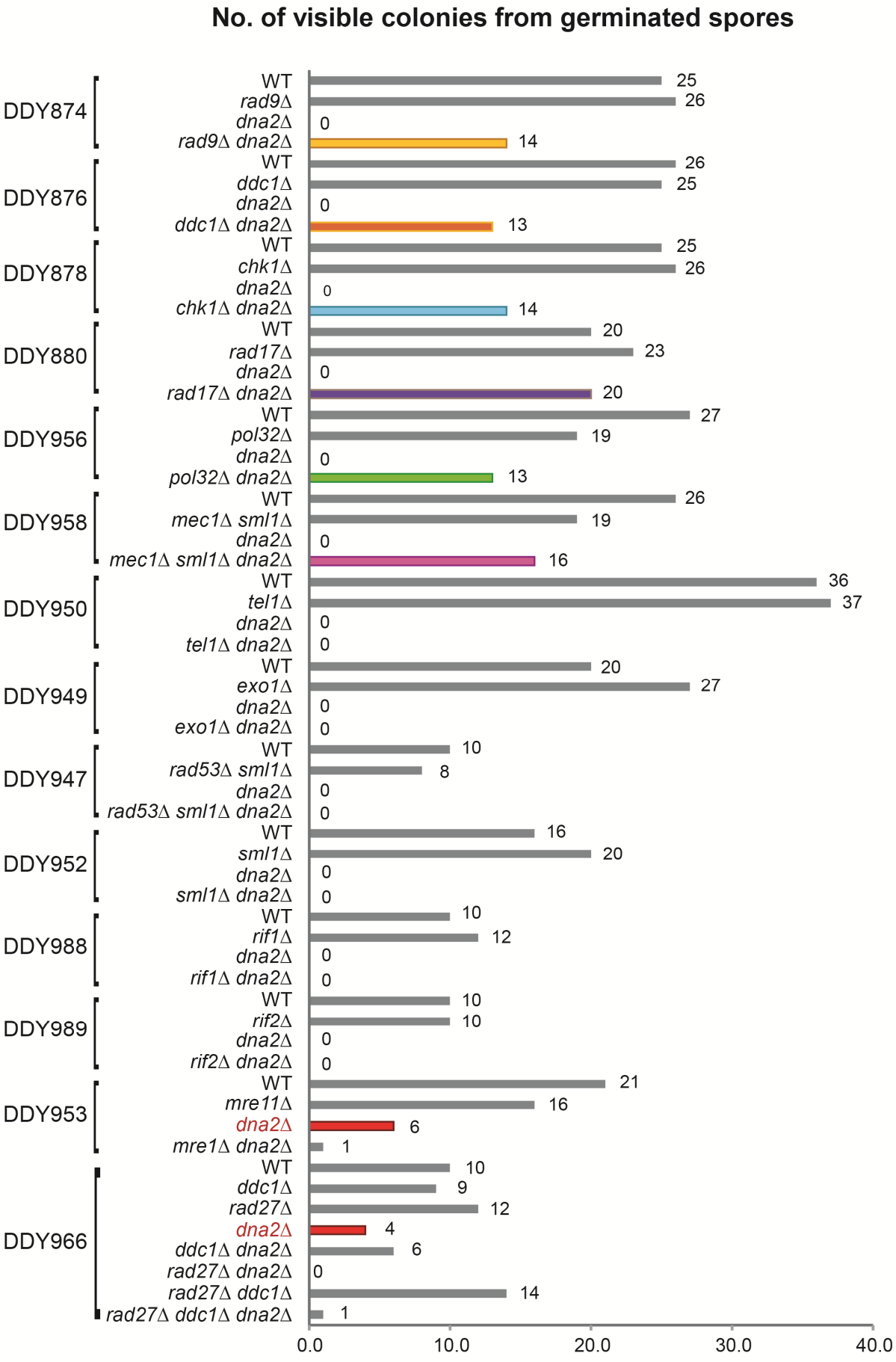
No. of visible colonies from germinated spores
DDY874
WT
rad9Δ
dna2Δ
rad9Δ dna2Δ
25
26
0
14
DDY876
WT
ddc1Δ
dna2Δ
ddc1Δ dna2Δ
26
25
0
13
DDY878
WT
chk1Δ
dna2Δ
chk1Δ dna2Δ
25
26
0
14
DDY880
WT
rad17Δ
dna2Δ
rad17Δ dna2Δ
20
23
0
20
DDY956
WT
pol32Δ
dna2Δ
pol32Δ dna2Δ
27
19
0
13
DDY958
WT
mec1Δ sml1Δ
dna2Δ
mec1Δ sml1Δ dna2Δ
26
19
0
16
DDY950
WT
tel1Δ
dna2Δ
tel1Δ dna2Δ
36
37
0
0
DDY949
WT
exo1Δ
dna2Δ
exo1Δ dna2Δ
20
27
0
0
DDY947
WT
rad53Δ sml1Δ
dna2Δ
rad53Δ sml1Δ dna2Δ
10
8
0
0
DDY952
WT
sml1Δ
dna2Δ
sml1Δ dna2Δ
16
20
0
0
DDY988
WT
rif1Δ
dna2Δ
rif1Δ dna2Δ
10
12
0
0
DDY989
WT
rif2Δ
dna2Δ
rif2Δ dna2Δ
10
10
0
0
DDY953
WT
mre11Δ
dna2Δ
mre1Δ dna2Δ
21
16
6
1
DDY966
WT
ddc1Δ
rad27Δ
dna2Δ
ddc1Δ dna2Δ
rad27Δ dna2Δ
rad27Δ ddc1Δ
rad27Δ ddc1Δ dna2Δ
10
9
12
4
6
0
14
1
0.0
10.0
20.0
30.0
40.0

**Figure 32. Quantification of suppressors and no-suppressors of *dna2*Δ lethality**
Spores (among others from Figure 31, DDY874, DDY876, DDY878, DDY880) were scored and plotted. Bars present numbers of viable colonies WT, *yfg*Δ and *dna2*Δ *yfg*Δ and (usually inviable) *dna2*Δ spores. **Grey bars** – WT or *yfg*Δ; **coloured bars** - viable *dna2*Δ *yfg*Δ*;* **red bars** – viable *dna2*Δ*;* '0' and no bar – inviable *dna2*Δ or *dna2*Δ *yfg*Δ.
Strains were: DDY874 *(rad9Δ/RAD9 dna2Δ/DNA2),* DDY876 *(ddc1Δ/DDC1 dna2Δ/DNA2),* DDY878 *(chk1Δ/CHK1 dna2Δ/DNA2),* DDY880 *(rad17Δ/RAD17 dna2Δ/DNA2),* DDY956 *(pol32Δ/POL32 dna2Δ/DNA2),* DDY958 *(mec1Δ/MEC1 sml1Δ/SML1 dna2Δ/DNA2),* DDY950 *(tel1Δ/TEL1 dna2Δ/DNA2),* DDY949 *(exo1Δ/EXO1 dna2Δ/DNA2),* DDY947 *(rad53Δ/RAD53 sml1Δ/SML1 dna2Δ/DNA2),* DLY6854xDLY10635 *(sml1Δ/SML1 dna2Δ/DNA2),* DDY988 *(rif1Δ/RIF1 dna2Δ/DNA2),* DDY989 *(rif2Δ/RIF2 dna2Δ/DNA2),* DDY953 *(mre11Δ/MRE11 dna2Δ/DNA2),* DDY966 *(rad27Δ/RAD27 ddc1Δ/DDC1 dna2Δ/DNA2).* Strain details are in Appendix A.

*rad27*Δ and *mre11*Δ did not suppress *dna2*Δ lethality (Fig. 32). Strangely, some *dna2*Δ single mutants emerged when *RAD27* or *MRE11* were deleted in *dna2*Δ heterozygous background. The unexpected growth of *dna2*Δ colonies indicates that deletions of *MRE11* and *RAD27* along with *DNA2* might cause severe genomic instability, aneuploidy and/or spontaneous mutations which promote the growth of *dna2*Δ cells. None of these events were tested nor confirmed. Whole genome sequencing would confirm additional mutations and aneuploidy. Simpler experiments involving qPCR would clarify the copy number of *DNA2* gene if chromosome VIII carrying *DNA2* underwent amplification in those diploids.

Mre11, a subunit of the MRX complex, functions in repair of DSBs and replication of telomeric DNA (D'Amours and Jackson, 2002, Lewis et al., 2004, Ghosal and Muniyappa, 2005). The MRX complex is regulated by the Tel1-dependent DSB signal (Usui et al., 2001) which suggests function of the MRX complex and Tel in the same pathway. However, dissection of diploid with heterozygous deletions of *TEL1* and *DNA2* did not promote the growth of single *dna2*Δ mutants, while diploid with deletions of *MRE11* and *DNA2* gave rise to *dna2*Δ cells (Fig. 32). It is possible that Mre11 and Tel1 have different effects on *dna2*Δ strains, and deletion of *MRE11* cause severe genomic problems. Diploid with deletions of *RAD27* and *DNA2* also gave rise to *dna2*Δ cells. However, overexpression of *RAD27* suppresses *dna2*Δ lethality (Budd and Campbell, 2000). It might be possible that overexpression of *MRE11* affects *dna2*Δ growth, as was observed for overexpression of *RAD27*. To check the effect of *MRE11* overexpression, high copy number plasmids (e.g. 2μ plasmid) carrying *MRE11* might be introduced into *dna2*Δ mutants and growth assays performed. However, Mre11 is a member of the MRX complex which is involved in many different cellular functions e.g. in DSB end resection, DNA repair and telomere maintenance. Therefore it might be difficult to interpret any phenotypes associated with *MRE11* overexpression.

### *4.1.3 Viability of dna2Δ is not caused by extra DNA2 copies*

Deficiency of *DNA2* might lead to aneuploidy as observed in mice (Lin et al., 2013). It might be therefore possible that in diploids with heterozygous deletions of *DDC1, RAD17, CHK1, RAD9, POL32* and *MEC1 SML1* in *dna2Δ/DNA2* background the aneuploidy resulted in more copies of *DNA2*. If so, additional *DNA2* copies might be inherited by haploid progeny. Such cells would be scored as *dna2Δ* due to the presence of selective marker gene used for deletion (*KANMX*), but the viability of strains would be a result of *DNA2* on the extra, unmarked chromosome.
In order to test the hypothesis that *dna2Δ* mutants with deletions of checkpoint genes contain an extra *DNA2* sequence, the PCR was performed (Fig. 33). First, I looked whether viable *dna2Δ* strains with deletion of *DDC1, RAD17 or CHK1* contained the *KANMX* cassette, or if they contained *DNA2* sequence at the *DNA2* locus (Fig. 33a and b). The PCR of WT and *dna2Δ pDNA2* control strains resulted in appropriate *DNA2* sequence sizes (Fig. 33b, two top gels). As expected none of tested double mutants contained *DNA2* sequence, yet all contained the *KANMX* cassette at *DNA2* locus (Fig. 33b, compare bottom with top gels).

Second, I performed qPCR to compare the amount of *DNA2* and two adjacent genes, *PRP8* and *SOL3*, in the genome of some rare *dna2Δ ddc1Δ* clones (Fig. 33c). Strains used for qPCR were of the same genotype as strains from Figure 33b, but were generated in a different cross, and were not used for further study. qPCR analysis revealed that *dna2Δ ddc1Δ* strains had similar copy number of *PRP8* and *SOL3* genes as WT strains, but did not contain the *DNA2* sequence at all (Fig. 33c).

I confirmed that genomic *DNA2* was replaced with *KANMX* cassette in *ddc1Δ dna2Δ*, *rad17Δ dna2Δ* and *chk1Δ dna2Δ* double mutants, and that no extra *DNA2* sequence was present in the three *ddc1Δ dna2Δ* strains. To sum up the results of both PCRs indicate that the viability of *dna2Δ* depends on deletion of *DDC1, RAD17* or *CHK1* and not on aneuploidy.

a)

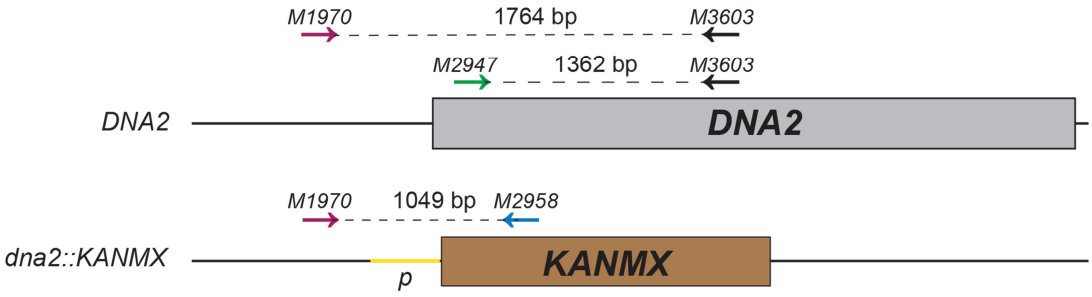
M1970
1764 bp
M3603
M2947
1362 bp
M3603
DNA2
DNA2
M1970
1049 bp
M2958
dna2::KANMX
p
KANMX

b)

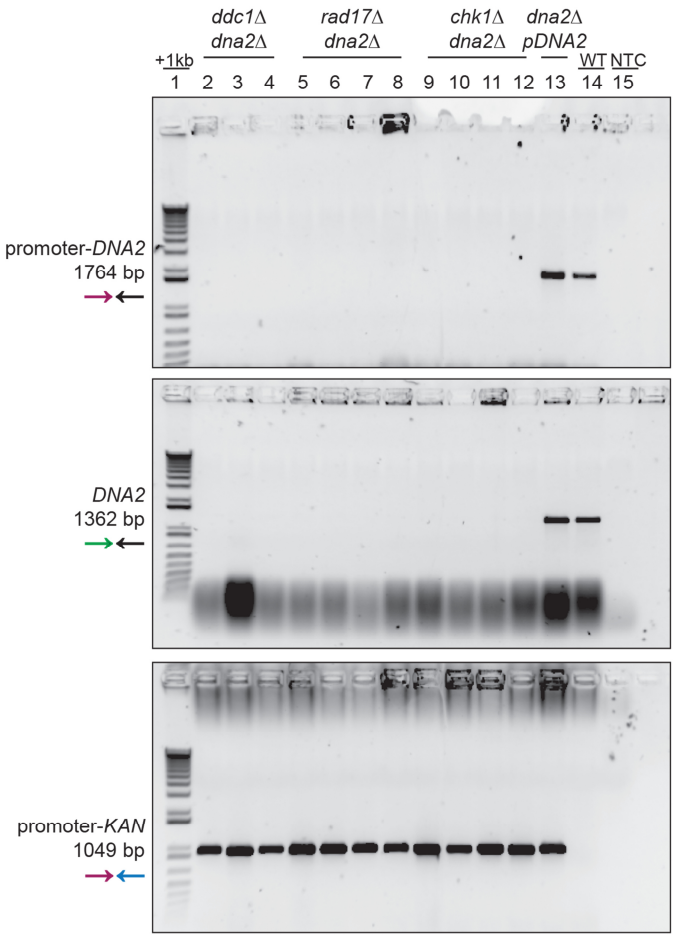
ddc1Δ dna2Δ
rad17Δ dna2Δ
chk1Δ dna2Δ
dna2Δ pDNA2
+1kb
1 2 3 4 5 6 7 8 9 10 11 12 13 14 15
WT
NTC
promoter-DNA2
1764 bp
DNA2
1362 bp
promoter-KAN
1049 bp

c)

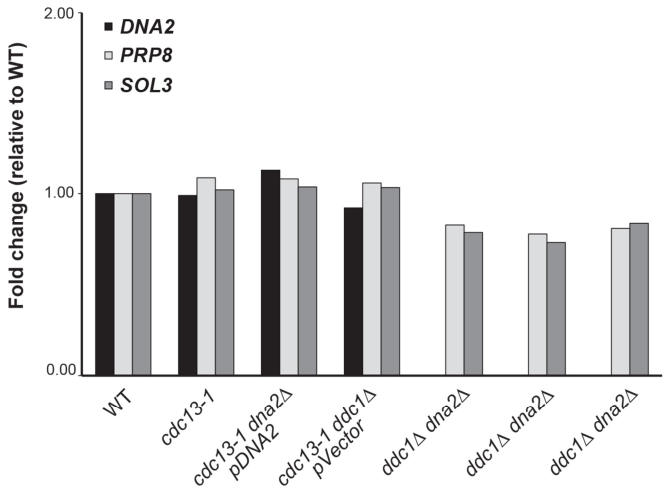
2.00
1.00
0.00
Fold change (relative to WT)
DNA2
PRP8
SOL3
WT
cdc13-1
cdc13-1 dna2Δ pDNA2
cdc13-1 ddc1Δ pVector
ddc1Δ dna2Δ
ddc1Δ dna2Δ
ddc1Δ dna2Δ

**Figure 33. Viability of *dna2*Δ mutants is not due to extra *DNA2* copies**

a) The presence of *KANMX* cassette and absence of *DNA2* was confirmed by PCR. Arrows – primers used. Each primer has colour assigned: **red** – M1970, **black** – M3603, **green** – M2947, **blue** – M2958; ***p*** – *KANMX* promoter from plasmid pDL1575.

b) DNA was isolated from strains growing in YEPD liquid medium at 23°C for 24 h using Yale method. Strain genotypes are indicated above gel lines. Line 1 - +1kb molecular ladder. Strains were: 2 –*ddc1*Δ *dna2*Δ (DLY10971), 3 – *ddc1*Δ *dna2*Δ (DLY10972), 4 – *ddc1*Δ *dna2*Δ (DLY10974), 5 – *rad17*Δ *dna2*Δ (DLY10979), 6 – *rad17*Δ *dna2*Δ (DLY10980), 7 – *rad17*Δ *dna2*Δ (DLY10981), 8 – *rad17*Δ *dna2*Δ (DLY10982), 9 – *chk1*Δ *dna2*Δ (DLY10975), 10 – *chk1*Δ *dna2*Δ (DLY10976), 11 – *chk1*Δ *dna2*Δ (DLY10977), 12 – *chk1*Δ *dna2*Δ (DLY10978),13 – *dna2*Δ *pDNA2* (DLY10635), 14 – WT (DLY3001), 15 – NTC-$H_2O$.

c) qRT-PCR analysis performed as in Figure 24. The level of DNA from single independent strains were measured, each value was normalised to the level of *BUD6* genomic DNA. Strains were: WT (DLY3001), *cdc13-1* (DLY1108), *cdc13-1 dna2*Δ *pDNA2* (DLY8998), *cdc13-1 ddc1*Δ *pVector* (DLY9469), *ddc1*Δ *dna2*Δ (DLY10616), *ddc1*Δ *dna2*Δ (DLY10617), *ddc1*Δ *dna2*Δ (DLY10618).

## 4.2 Viable *dna2*Δ strains recover fitness with time, but remain thermo-sensitive

### *4.2.1 dna2*Δ *mutants form colonies of heterogeneous size*

As shown in section 4.1.2 spores of *dna2*Δ mutants germinated at 20°C into heterogeneous and slowly growing colonies. To test whether *dna2*Δ mutants with deletions of *RAD9, DDC1, RAD17,CHK1* and *MEC1 SML1* recover with time, strains were passaged six times on YEPD plates (Fig. 34). Double mutants become fitter during passaging, but they never look like WT strains, the colonies are always smaller than those of WT (Fig. 34). Strains of the same genotype often show heterogeneity in growth. I did not notice much difference in colony size or growth between *rad9*Δ *dna2*Δ*, ddc1*Δ *dna2*Δ*, rad17*Δ *dna2*Δ or *chk1*Δ *dna2*Δ strains. Therefore I conclude that deletions of *RAD9, DDC1, RAD17,CHK1* and *MEC1 SML1* suppress *dna2*Δ lethality alike. The inability of strains to recover completely and resemble WT strain indicates that *dna2*Δ mutants are sick and cannot recover because of reasons that remain to be defined.

a) *rad9Δ/RAD9 dna2Δ/DNA2* (DDY874)

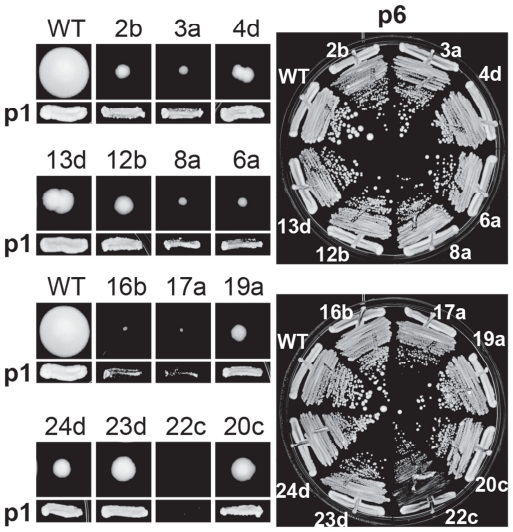


b) *ddc1Δ/DDC1 dna2Δ/DNA2* (DDY876)

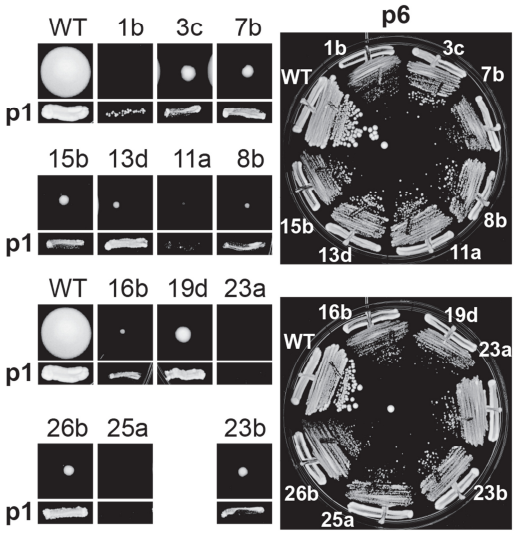


c) *chk1Δ/CHK1 dna2Δ/DNA2* (DDY878)

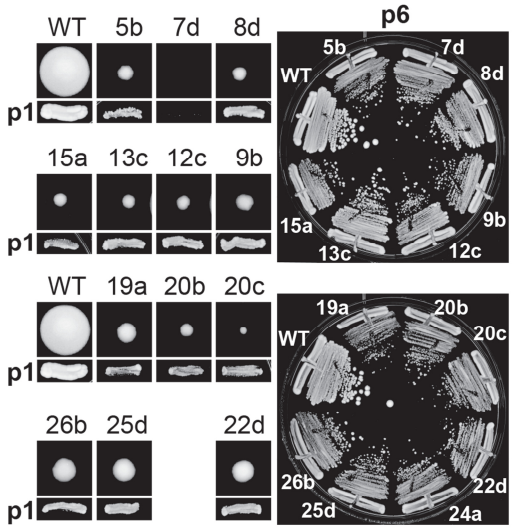


d) *rad17Δ/RAD17 dna2Δ/DNA2* (DDY880)

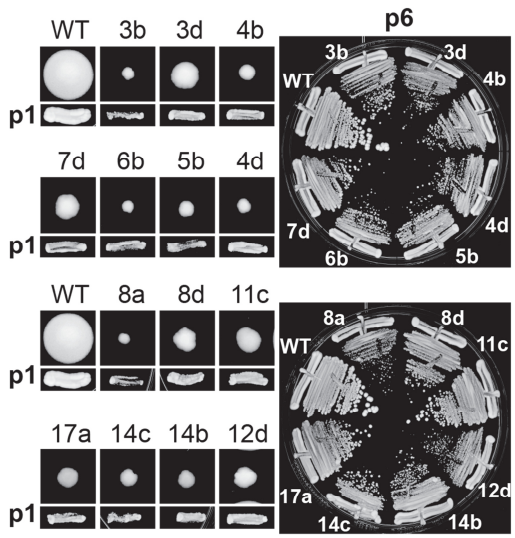


e) *mec1Δ/MEC1 sml1Δ/SML1 dna2Δ/DNA2* (DDY958)

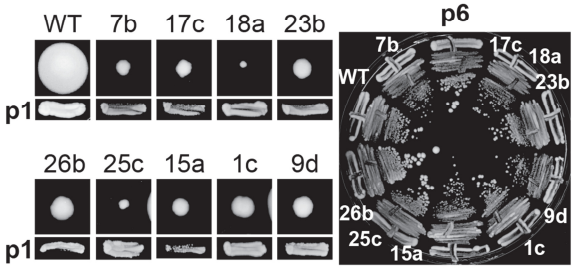

**Figure 34. *dna2*∆ mutants form heterogeneous colonies and slightly recover fitness with time**

Representation of colony sizes from spores and passages 1 and 6 of double mutants. A single WT colony represents the colony size of WT strain and a single picture is used for comparison. Double mutants formed very small colonies which were then patched on YEPD and incubated for 4 days at 23°C before photographing. A small amount of each patch was then streaked for single colonies on YEPD plates and incubated for 4 days at 23°C. Then 5-10 colonies were pooled and streaked onto YEPD plates for 5 more passages. *p1, p6* – passage 1 and 6, respectively.

a) Germinated spores of *rad9∆/RAD9 dna2∆/DNA2* diploid (DDY874);

b) Germinated spores of *ddc1∆/DDC1 dna2∆/DNA2* diploid (DDY876);

c) Germinated spores of *chk1∆/CHK1 dna2∆/DNA2* diploid (DDY878);

d) Germinated spores of *rad17∆/RAD17 dna2∆/DNA2* diploid (DDY880);

e) Germinated spores of *mec1∆/MEC1 sml1∆/SML1 dna2∆/DNA2* diploid (DDY958).

WT colony and double mutant colonies (apart from e) were cut from Figure 31a using Photoshop CS6 and organised using Adobe Illustrator.

### *4.2.2 dna2Δ mutants are thermo-sensitive*

*dna2Δ ddc1Δ* spores germinate more efficiently at 20°C than at 23°C. To see if the strains remain ts, the growth assays were performed for *dna2Δ* mutants with deletions of *RAD9, DDC1, RAD17* and *CHK1*. Figure 35 shows that double mutants, perhaps apart from *rad9Δ dna2Δ,* slightly recover fitness with time, so that strains from passage 6 grow better at higher temperatures than strains from passage 1 or 2 (Fig. 35a). However, all *dna2Δ* strains remain thermo-sensitive and rarely grow above 36°C, and strains of the same genotype often show heterogeneity in growth.

Growth assays were also performed for deletions of *MEC1 SML1* and *POL32* in *dna2Δ* background (Fig. 35b). *mec1Δ sml1Δ dna2Δ* strains show heterogeneity in growth and remain thermo-sensitive (Fig.35b, top panel). Interestingly, *pol32Δ dna2Δ* strains seem to be more homogenous than other tested double mutants (Fig.35b, bottom panel). *pol32Δ dna2Δ* strains do not recover with time and look similar when spot tested from passage 1 and 6. These strains remain thermo-sensitive and do not grow above 30°C.

I conclude that *dna2Δ* strains are very sick and this correlates with thermo-sensitivity. I do not exclude that further passaging would suppress the *dna2Δ* growth defect more. It was proposed by Budd *et al*. that Pol32, Dna2 and Rad9 function in Okazaki fragment processing and therefore might be in one functional group (Budd et al., 2011). However, based on the spot tests from Figure 35 I observe that *pol32Δ dna2Δ* mutants from passage 6 resemble strains from passage 1, and growth of individual strains of the same genotype is homogenous. This might indicate that the function of *POL32* in *dna2Δ* lethality might be somewhat different from *RAD9, DDC1, RAD17, CHK1, MEC1 SML1.* It would be interesting to investigate this difference in growth, by e.g. analysing the cell cycle arrest of checkpoint defective mutants versus polymerase defective mutants with *dna2Δ* mutation.

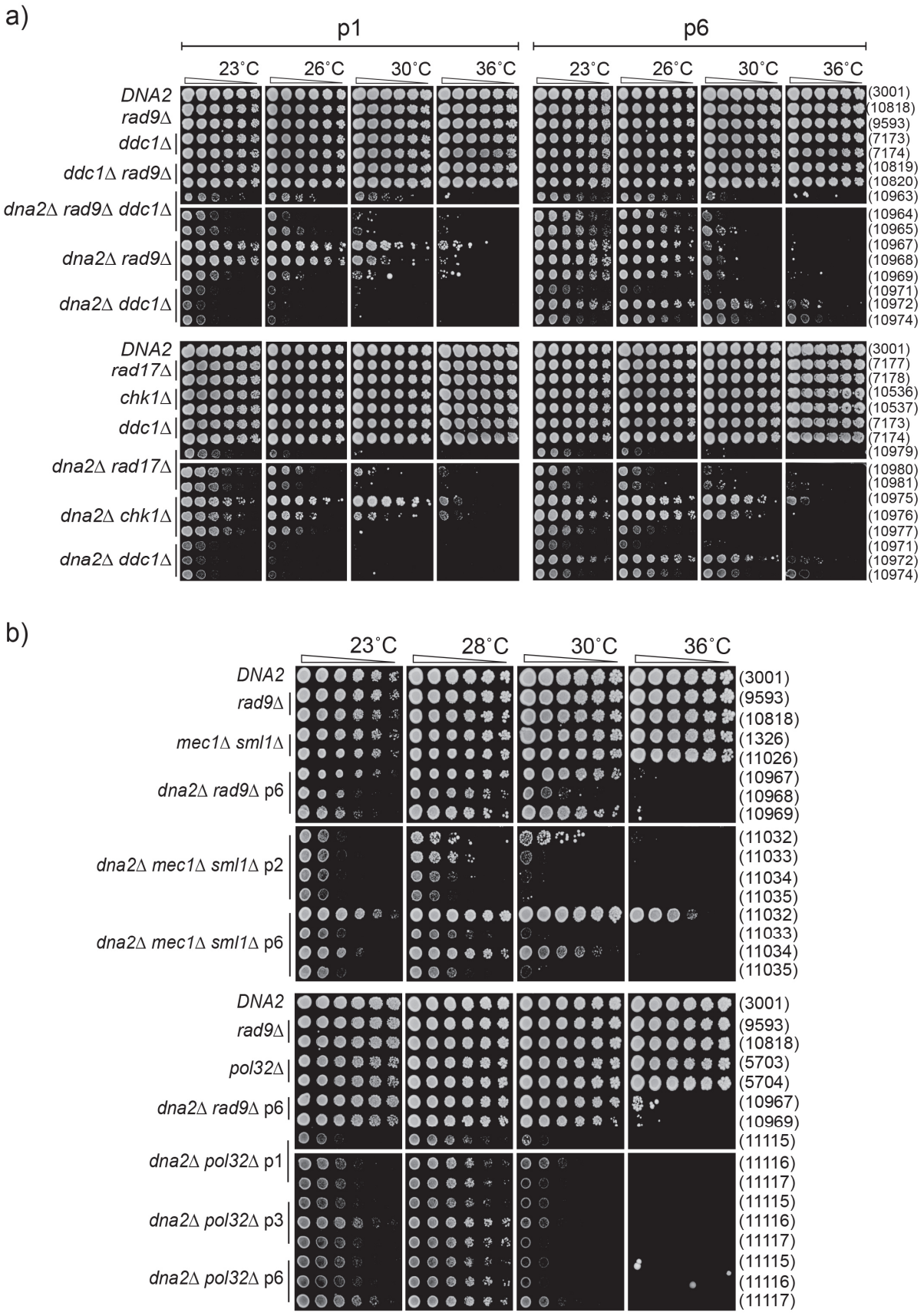
a)
p1
p6
23˚C
26˚C
30˚C
36˚C
DNA2 (3001)
rad9Δ (10818)
(9593)
ddc1Δ (7173)
(7174)
ddc1Δ rad9Δ (10819)
(10820)
dna2Δ rad9Δ ddc1Δ (10963)
(10964)
(10965)
dna2Δ rad9Δ (10967)
(10968)
(10969)
dna2Δ ddc1Δ (10971)
(10972)
(10974)
DNA2 (3001)
rad17Δ (7177)
(7178)
chk1Δ (10536)
(10537)
ddc1Δ (7173)
(7174)
(10979)
dna2Δ rad17Δ (10980)
(10981)
dna2Δ chk1Δ (10975)
(10976)
(10977)
dna2Δ ddc1Δ (10971)
(10972)
(10974)
b)
23˚C
28˚C
30˚C
36˚C
DNA2 (3001)
rad9Δ (9593)
(10818)
mec1Δ sml1Δ (1326)
(11026)
dna2Δ rad9Δ p6 (10967)
(10968)
(10969)
dna2Δ mec1Δ sml1Δ p2 (11032)
(11033)
(11034)
(11035)
dna2Δ mec1Δ sml1Δ p6 (11032)
(11033)
(11034)
(11035)
DNA2 (3001)
rad9Δ (9593)
(10818)
pol32Δ (5703)
(5704)
dna2Δ rad9Δ p6 (10967)
(10969)
(11115)
dna2Δ pol32Δ p1 (11116)
(11117)
(11115)
dna2Δ pol32Δ p3 (11116)
(11117)
dna2Δ pol32Δ p6 (11115)
(11116)
(11117)

**Figure 35. *dna2*Δ mutants remain thermo-sensitive**

a) Spot test done as in Figure 9. Strains within passage 1 were grown on two rectangular plates, indicated by wider white space between photographs, and were spot tested and incubated at the same time. Strains within passage 6 were grown on two rectangular plates, indicated by wider white space between photographs, and were spot tested and incubated at the same time.

b) Spot test done as in Figure 9. Strains from the top and bottom panels were grown on two rectangular plates and on different days, indicated by wider white space between photographs. The relevant genotypes of the strains are indicated on the left, strain numbers on the right. Strain details are in Appendix A.

### *4.2.3 Viability of dna2Δ mutants is not an effect of additional mutation*

In most cases checkpoint gene deletions suppressed *dna2*Δ lethality for approximately 50 %; half of double mutants were viable, while half were dead (Fig. 32). Such composition (50 %) of spore viability suggests that there might be another mutation, denoted '*xyz-1'*, which suppresses *dna2*Δ lethality. To test whether mutation was present in cells with deletions of checkpoint genes and *DNA2*, first a *ddc1*Δ *dna2*Δ strain was backcrossed to the WT strain. The diploid was then sporulated, and spores were dissected (Fig. 36a). *ddc1*Δ suppressed only 46 % of *dna2*Δ mutants (Fig. 36c). It might be therefore possible that a mutation *xyz-1* inherited by *ddc1*Δ *dna2*Δ strains was passed to their progeny.

To better test for an *xyz-1* mutation in *dna2*Δ strains, a diploid homozygous for checkpoint gene deletion was to be generated and dissected. This experiment however could not be performed in *ddc1*Δ*/ddc1*Δ diploid due to likely low meiotic spore viability, as was observed for strains with defects of other members of the 9-1-1 complex and Rad24 (Lydall et al., 1996). Therefore another diploid, *rad9*Δ*/rad9*Δ *dna2*Δ*/DNA2*, was generated, sporulated and spores were dissected (Fig. 36b). If *rad9*Δ *dna2*Δ contained *xyz-1* mutation, than *dna2*Δ strains would be viable only in the presence of *xyz-1* mutation. Spore viability of *rad9*Δ*/rad9*Δ *dna2*Δ*/DNA2* diploid should be 50 % if *xyz-1* mutation suppresses *dna2*Δ lethality. Spore viability of 100 % would suggest there is no *xyz-1* mutation suppressing *dna2*Δ.

98 % spore viability and 96 % of suppression efficiency indicates there is no *xyz-1* mutation (Fig. 36b and c). I conclude that there is no evidence for *xyz-1* mutation suppressing the lethality of *dna2*Δ mutants. Rather, *rad9*Δ*, ddc1*Δ*, rad17*Δ*, chk1*Δ*, mec1*Δ and *pol32*Δ*,* suppress *dna2*Δ without a requirement of an additional mutation(s). However, only *rad9*Δ *dna2*Δ strain was tested for containing an additional mutation(s), and other strains, e.g. *ddc1*Δ *dna2*Δ or *chk1*Δ *dna2*Δ should be tested as well.

a)

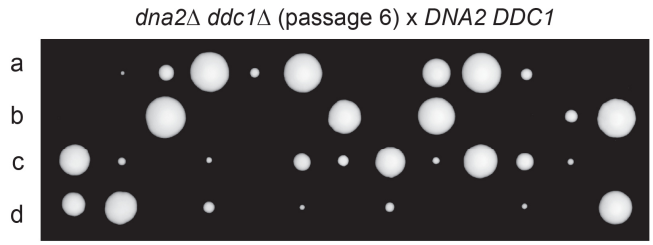


b)

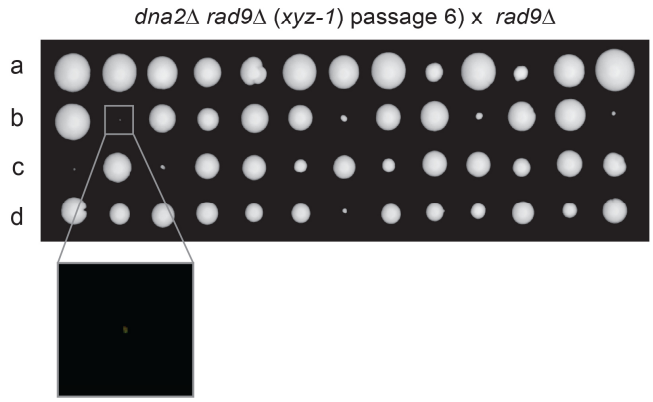


c)

| DDY | No. of tetrads | No. of spores | No. of visible colonies from germinated spores (%) | No. of G418$^r$ and HIS3 colonies (%) | Suppression efficiency (observed/ expected) (%) |
|---|---|---|---|---|---|
| *dna2Δ/DNA2 ddc1Δ/DDC1* | 39 | 156 | 81 (52) | 18 (22) | 18/39 (46) |
| *dna2Δ/DNA2 rad9Δrad9Δ* | 52 | 208 | 203 (98) | 100 (49) | 100/104 (96) |

**Figure 36. Suppression of *dna2*Δ lethality is independent of "unknown" mutations**

Strains were grown in YEPD liquid, sporulated in ESM, tetrads were dissected and germinated on YEPD plates. Pictures of colonies were taken after 10 days at 20°C.

a) Tetrad dissection from a sporulated diploid *dna2Δ/DNA2 ddc1Δ/DDC1* (diploid strain was not frozen and was originated from the cross: DLY10974 x DLY8460). Three plates were dissected; one is shown. Suppression efficiency was 46 % (18 viable *dna2*Δ *ddc1*Δ colonies out of 39 *dna2*Δ *ddc1*Δ expected strains).

b) Tetrad dissection from a sporulated diploid *dna2Δ/DNA2 rad9Δ/ rad9*Δ (DDY1042). Four plates were dissected, one is shown. One colony of *dna2*Δ *rad9*Δ genotype is in magnification (grey square).

c) Spore viability of *dna2Δ/DNA2* strains and plasmid transmission efficiency. *G418$^r$* – G418 resistant *dna2::KANMX* cells, *HIS3* – *ddc1::HIS3* or *rad9::HIS3*. Spore viabilities were calculated for three plates of *dna2Δ/DNA2 ddc1Δ/DDC1* genotype and for four plates of *dna2Δ/DNA2 rad9Δ/ rad9*Δ genotype.

### 4.3 Telomeres of *dna2*Δ mutants are long and diffuse

Dna2 has a role in telomeric DNA maintenance and was proposed to be involved in telomere replication (Choe et al., 2002, Chai et al., 2013, Lin et al., 2013). Thus it was possible that telomeres of *dna2*Δ strains might change structure and length. To test this hypothesis a Southern blot was performed to check if loss of *DNA2* leads to altered telomere structure.

Figure 37 shows that telomeres of *dna2*Δ mutants with deletions of *RAD17, DDC1* and *POL32* are longer and more diffuse than WT telomeres. This is visible as early as passage 1, and remains so in passage 6 (Fig. 37 lines 20-25). Although telomeres were also slightly longer when *RAD9, CHK1* and *MEC1 SML1* were deleted, the difference was less noticeable (Fig. 37 lines16-19 and 26-27). For reasons that are unclear, one *rad17*Δ and one *ddc1*Δ strain have slightly longer telomeres when compared to other strains of the same genotypes or to WT. Longer telomeres might be inherited during meiosis of a diploid, if diploid strain had long telomeres, too (Petreaca et al., 2007). However, this hypothesis was not tested. Also observed longer telomeres might be a side effect of culture conditions (e.g. prolong culture with mutations accumulation), or an artefact arisen during DNA isolation. It is also possible that the longer telomeres of *rad17*Δ strain could affect the viability of spores shown in Figure 31a (87 % *dna2*Δ suppression). I would suggest repeating the experiment by mating a *rad17*Δ mutant which has WT telomere length with *dna2*Δ *pDNA2* strain. Overall, I conclude that longer telomeres might assist *dna2*Δ double mutants' viability.

In summary, I observed at least two classes of genes which suppressed *dna2*Δ, based on: i) the heterogeneous growth of strains of the same genotype and ability to recover with time (deletions of *RAD9, DDC1, RAD17, CHK1, MEC1 SML1* versus deletion of *POL32* in *dna2*Δ mutants); ii) telomere length (deletions of *RAD9, CHK1* and *MEC1 SML1* versus deletions of *DDC1, RAD17* and *POL32* in *dna2*Δ mutants). I do not understand where the differences in *dna2*Δ suppression came from, and to test it unbiased robotic screens were used.

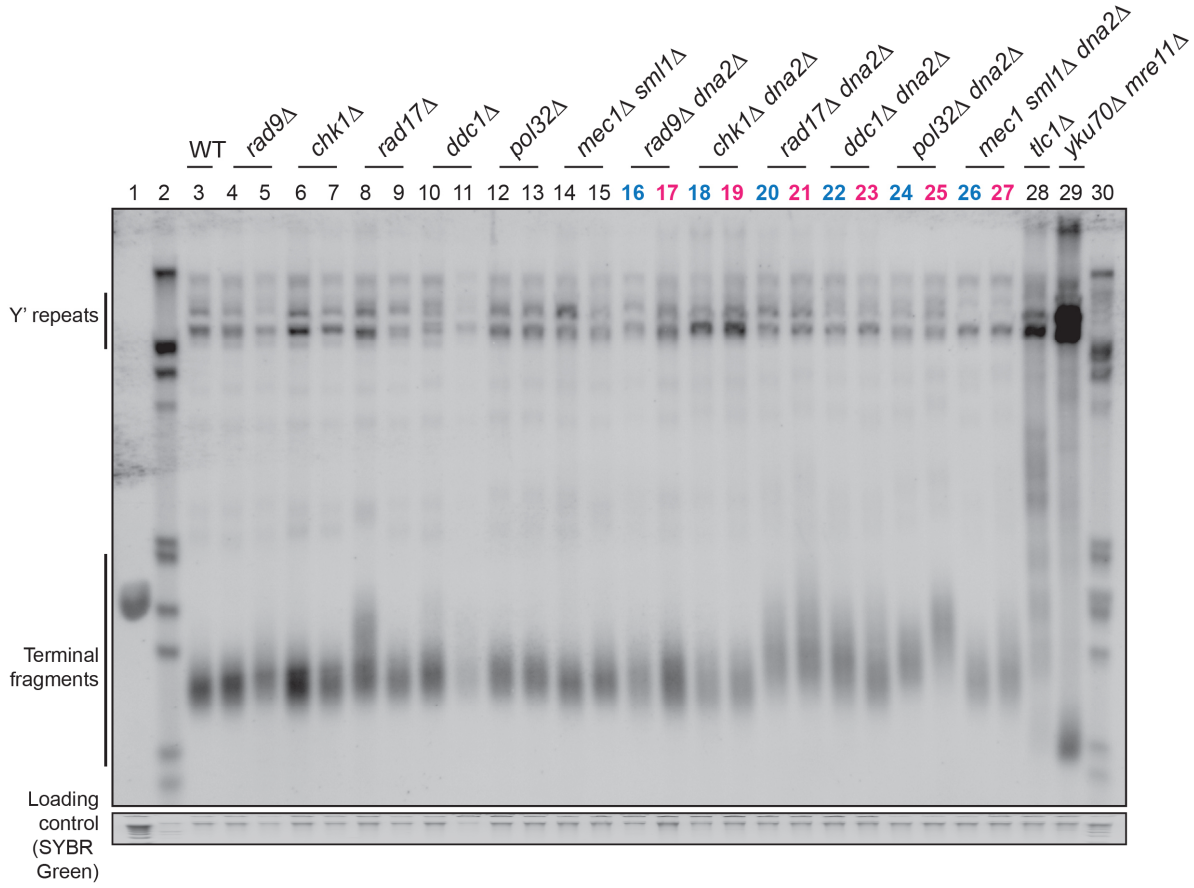


**Figure 37. Telomeres of *dna2*Δ mutants are long and diffuse**

Genomic DNA was isolated from yeast strains indicated using Yale method after 24 h incubation at 23°C. Telomeres were analysed by Southern blot. SYBR Safe was used as a loading control. Lines 1-2 & 30 – molecular ladders. *tlc1*Δ and *yku70*Δ *mre11*Δ strains were used as controls for type II and I survivors (Maringele and Lydall, 2004). **Passage 1** – lines: 16, 18, 20, 22, 24, 26; **Passage 6** – lines: 17, 19, 21, 23, 25, 27. Strains were: 3 – WT (DLY3001), 4 – *rad9*Δ (DLY9593), 5 – *rad9*Δ (DLY10818), 6 – *chk1*Δ (DLY10536), 7 – *chk1*Δ (DLY10537), 8 – *rad17*Δ (DLY7177), 9 – *rad17*Δ (DLY10478), 10 – *ddc1*Δ (DLY7173), 11 – *ddc1*Δ (DLY7174), 12 – *pol32*Δ (DLY5703), 13 – *pol32*Δ (DLY5704), 14 – *mec1*Δ *sml1*Δ (DLY1326), 15 – *mec1*Δ *sml1*Δ (DLY11026), 16 – *rad9*Δ *dna2*Δ passage 1 (DLY10968), 17 – *rad9*Δ *dna2*Δ passage 6 (DLY10968), 18 – *chk1*Δ *dna2*Δ passage 1 (DLY10976), 19 – *chk1*Δ *dna2*Δ passage 6 (DLY10976), 20 – *rad17*Δ *dna2*Δ passage 1 (DLY10982), 21 – *rad17*Δ *dna2*Δ passage 6 (DLY10982), 22 – *ddc1*Δ *dna2*Δ passage 1 (DLY10972), 23 – *ddc1*Δ *dna2*Δ passage 6 (DLY10972), 24 – *pol32*Δ *dna2*Δ passage 1 (DLY11116), 25 – *pol32*Δ *dna2*Δ passage 6 (DLY11116), 26 – *mec1*Δ *sml1*Δ *dna2*Δ passage 1 (DLY11033), 27 – *mec1*Δ *sml1*Δ *dna2*Δ passage 6 (DLY11033), 28 – *tlc1*Δ (DLY2147), 29 – *yku70*Δ *mre11*Δ (DLY1845). Strain details are in Appendix A.

## 4.4. Synthetic Genetic Arrays (SGA) to understand mechanisms of *dna2*Δ suppression

### *4.4.1 Genome-wide screens using dna2*Δ *pCAN1-URA3-DNA2 query strain*

An unbiased genome-wide screen was used to understand the mechanisms allowing suppression of *dna2*Δ. Synthetic genetic array (SGA) was performed using a query strain, to see if it is possible to identify genes that suppress and/or enhance *dna2*Δ lethality. Due to the fact that haploid *dna2*Δ mutants are inviable, the plasmid (p*CAN1-URA3-DNA2*; pDL1758) had to be maintained at all time to assure *dna2*Δ strain viability. Therefore so called 'plasmid SGA' was designed as a variation of standard protocol (Fig. 38).

Single query strain *dna2*Δ *pCAN1-URA3-DNA2* (Fig. 38 left panel) was mated with a single gene deletion library of approximately 5000 gene deletions, *xyz*Δ (Fig. 38 right panel). Diploids were sporulated and double mutants carrying plasmids were selected (Fig. 38 middle part). The plasmids had to be lost at the final stage of the SGA process to allow *xyz*Δ mutants to reveal the effect on *dna2*Δ viability. Plasmid loss was achieved by yeast growth on canavanine media (CAN) (Fig. 38, CTGNH media).

*CAN1* gene from the plasmid encodes a membrane arginine permease which is involved in transmembrane transport of amino acid (Ahmad and Bussey, 1986). Canavanine is a toxic analogue of arginine and therefore can enter cell via an arginine transporter Can1 (Whelan et al., 1979). Mutation of *CAN1* gene confers resistance to the toxic canavanine, which cannot be up-taken into the cell. Therefore *dna2*Δ *xyz*Δ cells with *can1* mutation should lose the *pCAN1-URA3-DNA2* plasmid on canavanine media and proceed the growth if *xyz*Δ is a *dna2*Δ suppressor, or die if *xyz*Δ is not a suppressor.

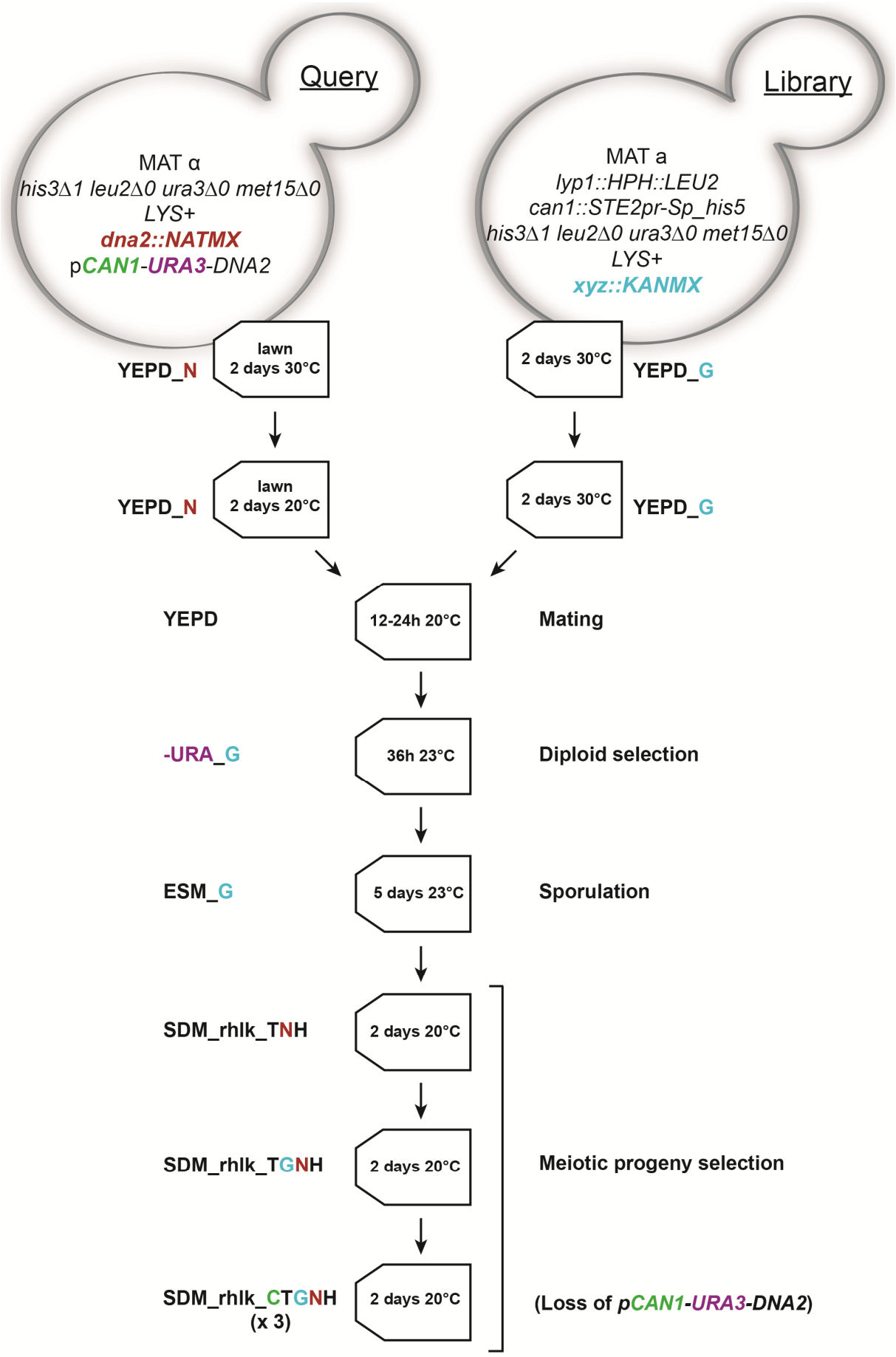
Query
MAT α
his3Δ1 leu2Δ0 ura3Δ0 met15Δ0
LYS+
dna2::NATMX
pCAN1-URA3-DNA2
Library
MAT a
lyp1::HPH::LEU2
can1::STE2pr-Sp_his5
his3Δ1 leu2Δ0 ura3Δ0 met15Δ0
LYS+
xyz::KANMX
YEPD_N
lawn
2 days 30°C
2 days 30°C
YEPD_G
YEPD_N
lawn
2 days 20°C
2 days 30°C
YEPD_G
YEPD
12-24h 20°C
Mating
-URA_G
36h 23°C
Diploid selection
ESM_G
5 days 23°C
Sporulation
SDM_rhlk_TNH
2 days 20°C
SDM_rhlk_TGNH
2 days 20°C
Meiotic progeny selection
SDM_rhlk_CTGNH
(x 3)
2 days 20°C
(Loss of pCAN1-URA3-DNA2)

**Figure 38. SGA plasmid method for *dna2*Δ *pCAN1-URA3-DNA2* strain**

SGA protocol for crossing a *dna2*Δ *pCAN1-URA3-DNA2* query strain with single gene deletion library (~5000 genes), sporulating diploids and obtaining *dna2*Δ *xyz*Δ haploids. Once haploid double mutants were selected, the colony sizes were measured. *lyp1::HPH::LEU2* – *lyp1* confers resistance to thialysine, *HPH* is a marker gene; *can1::STE2pr-Sp_his5* – *can1* confers resistance to canavanine, and *STE2pr_Sp_his5* is a MAT locus specific promoter which allows for selection on –HIS media only when strain is MAT a; *his3*Δ *leu2*Δ*0 ura3*Δ*0 met15*Δ*0* – mutations in the genome which allow to use marker genes; *LYS+* –- strains can grow on –Lys media; *dna2*Δ*::NATMX* – *NATMX* confers resistance to clonNat (N); *pCAN1-URA3-DNA2* – pDL1758, allows yeast to grow on –URA media, and should be lost on canavanine; *xyz::KANMX* – gene deletion from the library, *KANMX* confers G418 resistance (G). N – clonNat; G – G418; H – hygromycine; T – thialysine, C – canavanine.

-

### *4.4.2 SGA reveals novel suppressors and enhancers of dna2*Δ

It was important to first check whether it was at all possible to obtain reliable and consistent results from SGA of *dna2*Δ *pCAN1-URA3-DNA2* mutants. Therefore a pilot SGA was performed for *dna2*Δ *pDNA2* query strain with plate 15 of the lab collection (Fig. 39). Plate 15 was chosen because it contains several copies of several checkpoint gene deletions which I showed earlier to suppress *dna2*Δ*,* like *ddc1*Δ or *chk1*Δ*,* and positive control *rad9*Δ*.*

The final selection on CTGNH was performed three times, which allowed us to empirically choose the passage which gives the most reliable and informative results (Fig. 39a). Passage 1 revealed some synthetic lethal interactions of *dna2*Δ *xyz*Δ mutants, but it was not possible to distinguish fitter colonies – feasible suppressors of *dna2*Δ lethality. Passage 2 gave the most reliable information about likely suppressors of *dna2*Δ; usually all four colonies within a genotype were bigger than other colonies from the plate. Passage 3 on the other hand was a mosaic of big and small colonies. It was difficult to distinguish suppressors of *dna2*Δ on this plate, because often colony sizes were not consistent within genotypes, e. g. one colony was very big, two were of average size and one was small, like for *TSA1* (Fig. 39a and b, Column 16 Row 11).

The most informative was passage 2 and analysis of a raw plate allowed to conclude that some gene deletions suppressed *dna2*Δ lethality, like expected *rad9*Δ*, chk1*Δ etc., while many other gene deletions did not suppress *dna2*Δ*.* I deduce that the pilot SGA of plate 15 was successful and consistent with my earlier observations that *RAD9, RAD17, DDC1* and *CHK1* suppress *dna2*Δ lethality.

a) Plate 15, CTGNH, 20°C, S288C pilot SGA

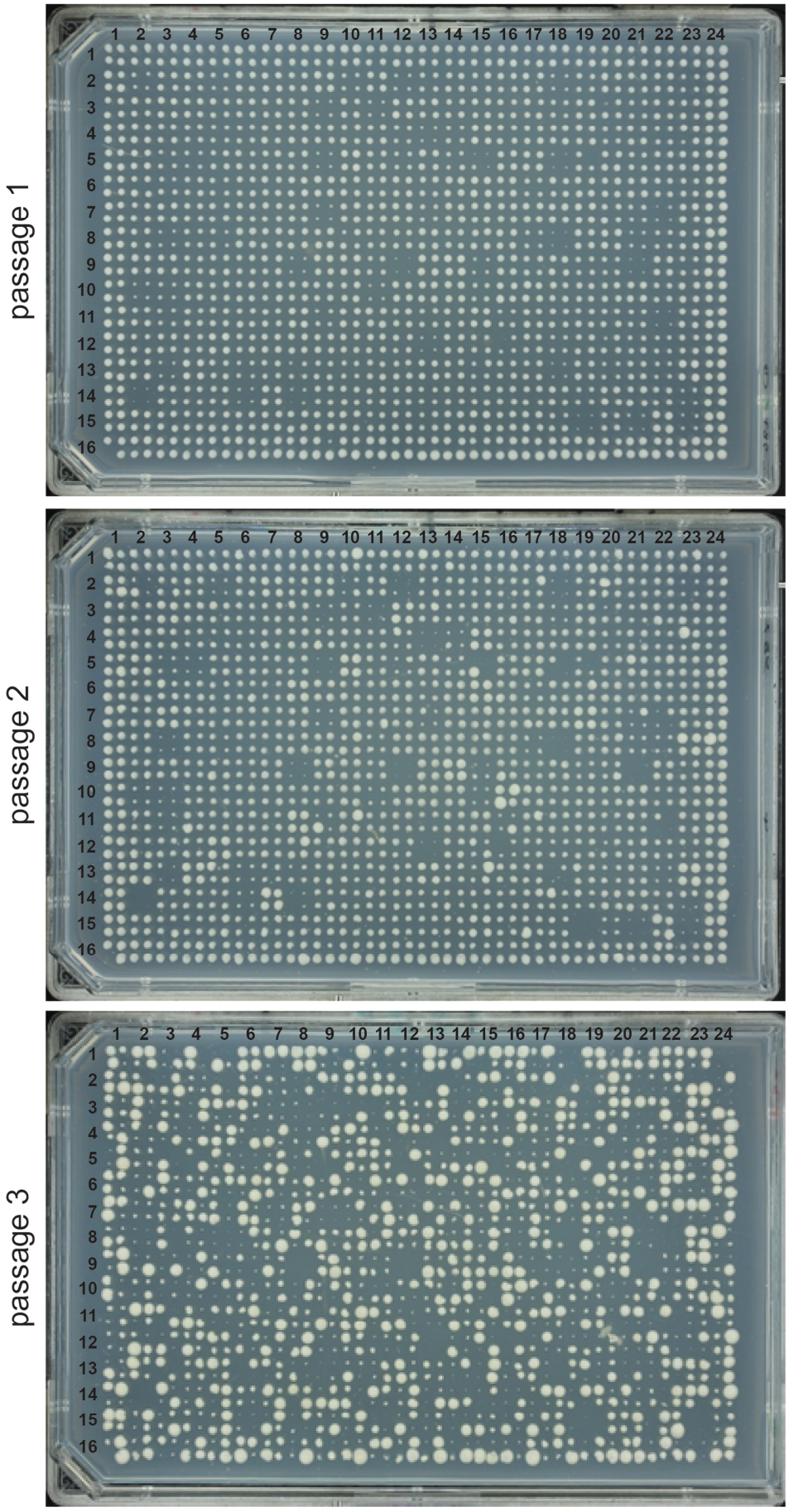

b)

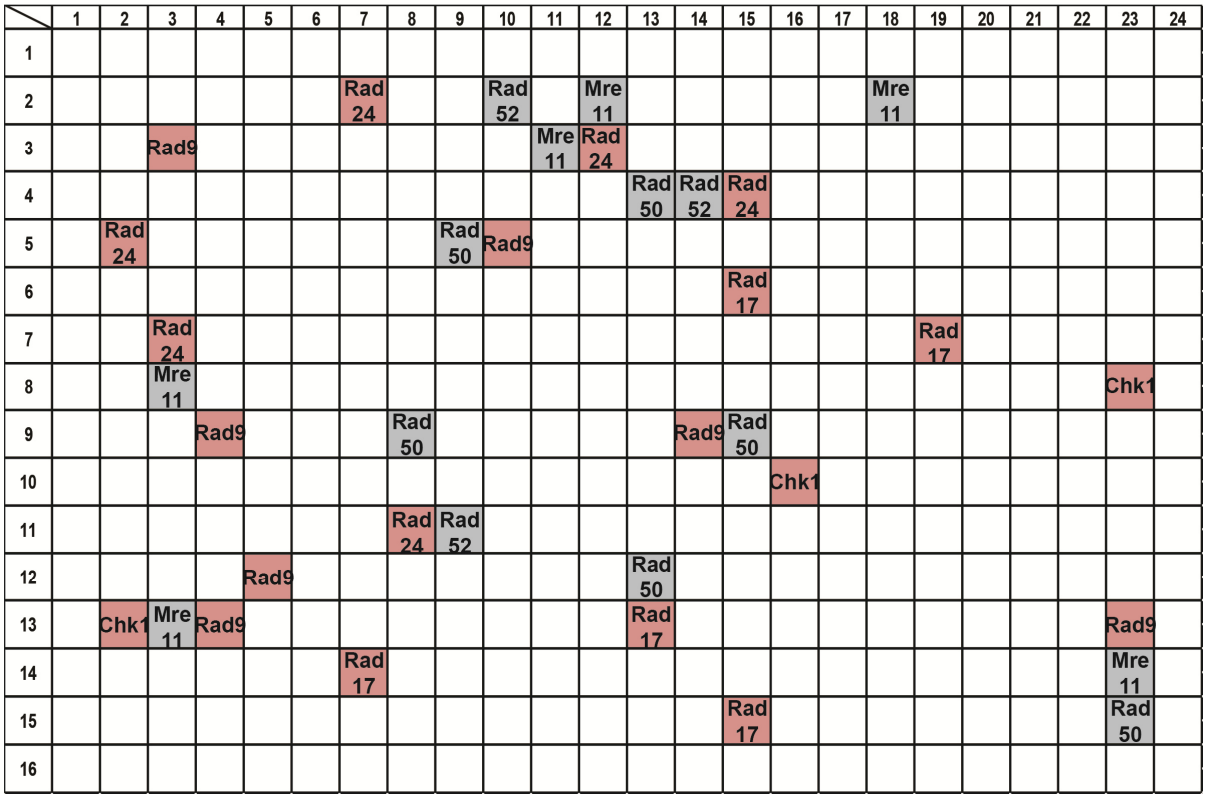


**Figure 39. S288C pilot SGA of plate 15 containing checkpoint gene deletions**

a) Pictures of final selection plates CTGNH, passage 1, 2 and 3 at 20°C. Double mutants were pinned in quadruples.

b) Template of plate 15. Horizontal numbers – numbers of columns; vertical numbers – numbers of rows. The positions of several highlighted genes are assigned to their position on plates in a). Pink – position of a gene whose deletion suppresses *dna2*Δ strains; grey – position of a gene whose deletion enhances *dna2*Δ strains. The complete template of plate 15 is in Appendix E.

The SGA of *dna2*Δ *pCAN1-URA3-DNA2* and the whole library of approximately 5000 gene deletions was performed and data acquired from passage 2 on CTGNH media were analysed. Figure 40 shows the colony sizes from the *dna2*Δ *xyz*Δ ( CTGNH) and *dna2*Δ *xyz*Δ *pCAN1-URA3-DNA2* (TGNH) SGAs plotted against each other. Highlighted on the plot are:

- Suppressors of *dna2*Δ lethality which I tested in sections 4.1 and 4.2, like *RAD9, DDC1, RAD17, CHK1, POL32* (red dots);
- No-suppressors of *dna2*Δ lethality which I tested in section 4.1.2, like *MRE11, RAD27, EXO1, RIF1, RIF2, TEL1, SML1* (blue dots);
- Genes which deletions might suppress *dna2*Δ lethality based on their localization on the plot (yellow rectangle, above the regression line), like *RAD24, BUB3, CTF3, MPH1, LSM1, RTT109, CDC15, DBP7* (purple dots);
- Genes that may not affect *dna2*Δ viability, based on their localization on the plot (beneath the regression line) like *SGS1, TOP3, BUB2* (purple dots).

I conclude that the SGA plasmid method was efficient. The suppressors of *dna2*Δ lethality which I identified by tetrad dissection were shown on the plot as gene deletions which suppressed *dna2*Δ growth defect, and were localised above the regression line (Fig. 40). No-suppressors (enhancers) of *dna2*Δ lethality were localized beneath the regression line, indicating that these gene deletions did not affect *dna2*Δ fitness. Based on the SGA screens I was able to select some novel suppressors of *dna2*Δ for further study, like *mph1*Δ or *rtt109*Δ.

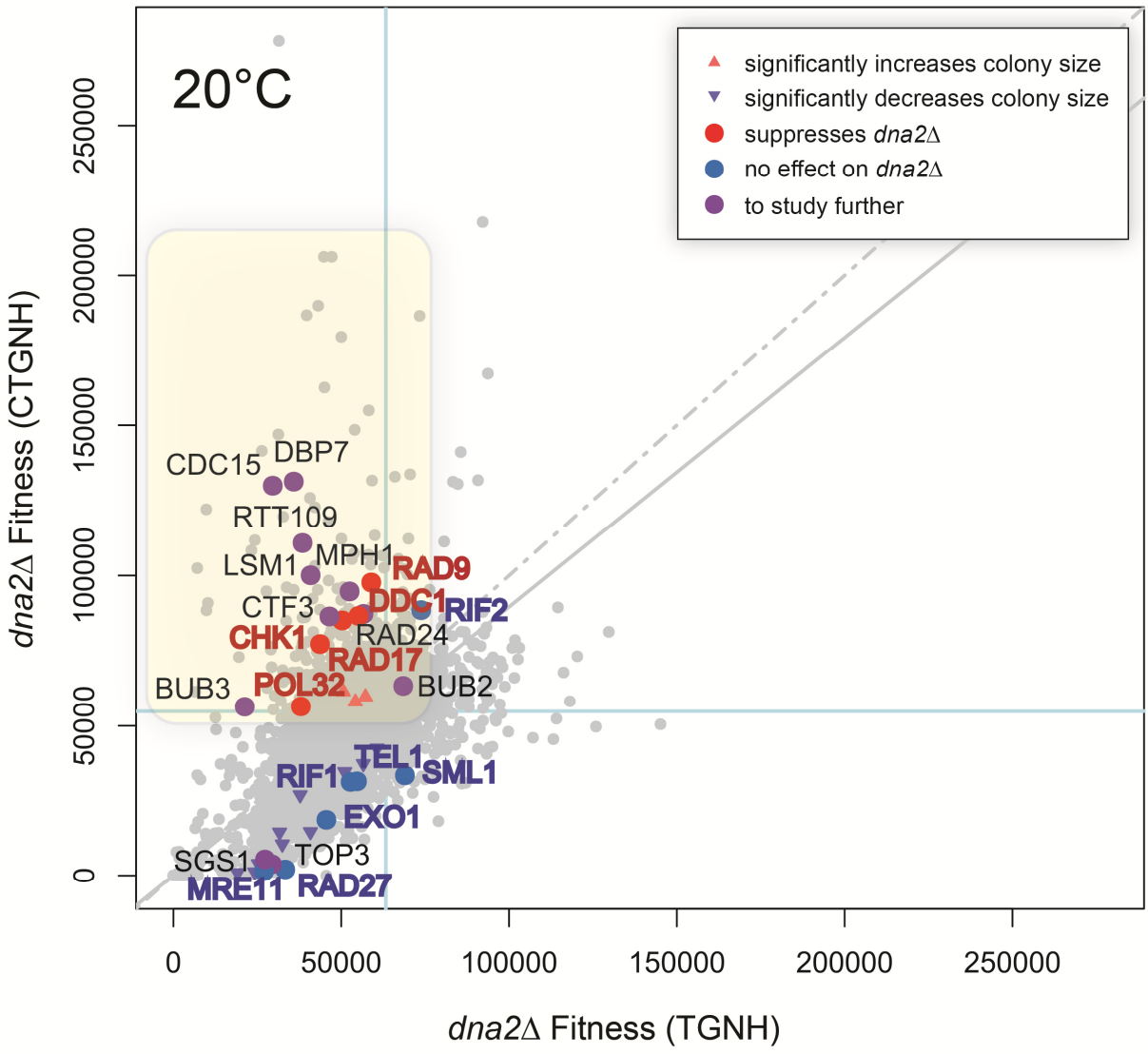


**Figure 40. Single gene deletions affecting *dna2*Δ fitness**

Median colony sizes from the two SGA screens indicated (from CTGNH media and TGNH media) were plotted against each other. The solid line - a regression line indicating population model of expected fitness. The dashed line - the line of equal growth. Fitness – colony size. **Red upwards arrows** - a single gene deletion that significantly increases *dna2*Δ colony size. **Purple downwards arrows** - a single gene deletion that significantly decreases *dna2*Δ colony size. **Red dots** - positions of gene deletions which suppress *dna2*Δ lethality (confirmed manually). **Blue dots** - positions of gene deletions which do not suppress *dna2*Δ lethality (confirmed manually). **Purple dots** - positions of gene deletions which suppress or enhance *dna2*Δ lethality and are to be studied. **Grey dots** – all remaining gene deletions (~5000). **Yellow rectangle** – indicates the area of interest in the sense that *dna2*Δ lethality may be suppressed by genes localized in this area.

### *4.4.3 mph1Δ suppresses dna2Δ, while rtt109Δ and dgr2Δ do not affect dna2Δ fitness*

The SGA of *dna2Δ pCAN1-URA3-DNA2* strain gave insights into novel mechanisms that might be required for Dna2 viability. 702 genes were selected based on a q value ($q \leq 0.05$). This set of genes was then ordered by GIS (genetic interaction strength) which resulted in identification of 130 suppressors and 572 no-suppressors (enhancers) of *dna2Δ* defect (Appendix F).

*MPH1*, *RTT109* and *DGR2* were selected for further study in W303, because all three genes were in a group of 130 potential suppressors of *dna2Δ* lethality. *MPH1* and *RTT109* were chosen due to their roles in DNA replication, the process in which Dna2 functions, too. Dgr2 was a randomly selected gene. It was hypothesised that Mph1 and Rtt109 may interact with Dna2 based on e. g. shared common function in DNA replication. Mph1, a helicase acting in Okazaki fragment processing, was shown to stimulate Rad27 and Dna2 activities (Kang et al., 2009). Similarly to human FANCM protein, Mph1 is involved in stabilizing and remodelling of blocked replication forks (Yan et al., 2010). Rtt109, a histone acetyltransferase, is critical for cell survival in presence of DNA damage during
S-phase (Han et al., 2007, Ide et al., 2013). Dgr2 is a protein of so far unknown function (Ralser et al., 2008).

*dna2Δ/DNA2* diploid strains of W303 background with heterozygous deletions of *MPH1, RTT109* or *DGR2* were generated, sporulated and tetrads were dissected. Only *mph1Δ* suppressed the lethality of *dna2Δ* (Fig. 41), while no *rtt109Δ dna2Δ* or *dgr2Δ dna2Δ* double mutants were observed (not shown). Surprisingly, six *dna2Δ* single mutants emerged when *MPH1* was deleted in heterozygous *dna2Δ* background, similarly to what was observed for *RAD27* and *MRE11* deletions (Fig. 32). The role of *mph1Δ* on *dna2Δ* is different from *rad27Δ,* because deletion of *RAD27* did not suppress *dna2Δ* lethality, while deletion of *MPH1* did suppress *dna2Δ* (Fig. 41 and Fig. 32). *mph1Δ* is also similar to *rad27Δ* in a sense that gave rise to *dna2Δ* single mutants. *dna2Δ* strains from germinated spores were struck on YEPD plates and incubated at 23°C, but none of the colonies proceed growth (not shown). *dna2Δ* mutants might continue to grow at lower temperature, e. g. 20°C or 18°C, but this was not tested.

I conclude that Mph1 regulates Dna2 activity and/or is involved in the same process (like Okazaki fragment processing) based on the fact that *mph1*Δ suppresses *dna2*Δ. However, the mechanism of Mph1 regulation remains unknown, and should be studied in the future. Also, the similarities and differences in the roles of Mph1 and Rad27 on *dna2*Δ viability should be clarified. The growth of *dna2*Δ cells indicates that deletions of *MPH1* along with *DNA2* results in genomic instability or aneuploidy. Whole genome sequencing would confirm genomic instability. I did not observe the suppression of *dna2*Δ by *rad27*Δ*,* it might be worth checking whether deletion of *MPH1* suppresses *dna2*Δ *rad27*Δ lethality.

Deletions of *RTT109* and *DGR2* did not suppress *dna2*Δ lethality and therefore did not prove to be real hits in the SGA. It seems that *rtt109*Δ *dna2*Δ and *dgr2*Δ *dna2*Δ mutants formed fitter or bigger colonies, and thus were recognised and scored in the SGA as suppressors of *dna2*Δ*.* One explanation for *dna2*Δ cells to form big colonies, apart from being suppressed, would be the maintenance of the p*DNA2* plasmid. It might be possible that the selection pressure against the plasmid on canavanine media, the last stage of the SGA selection, was not strong enough for some cells to lose the plasmid. Such cells maintained the plasmid and grew well on canavanine, which could result in a false score as a *dna2*Δ suppression. Maybe another selection method would clarify the SGA hits. The p*DNA2* plasmid carries CAN1 and URA3 genes, therefore the selection against the plasmid could be performed on 5-FOA media. The hypothesis concerning selection difficulties in the SGA remains to be tested.

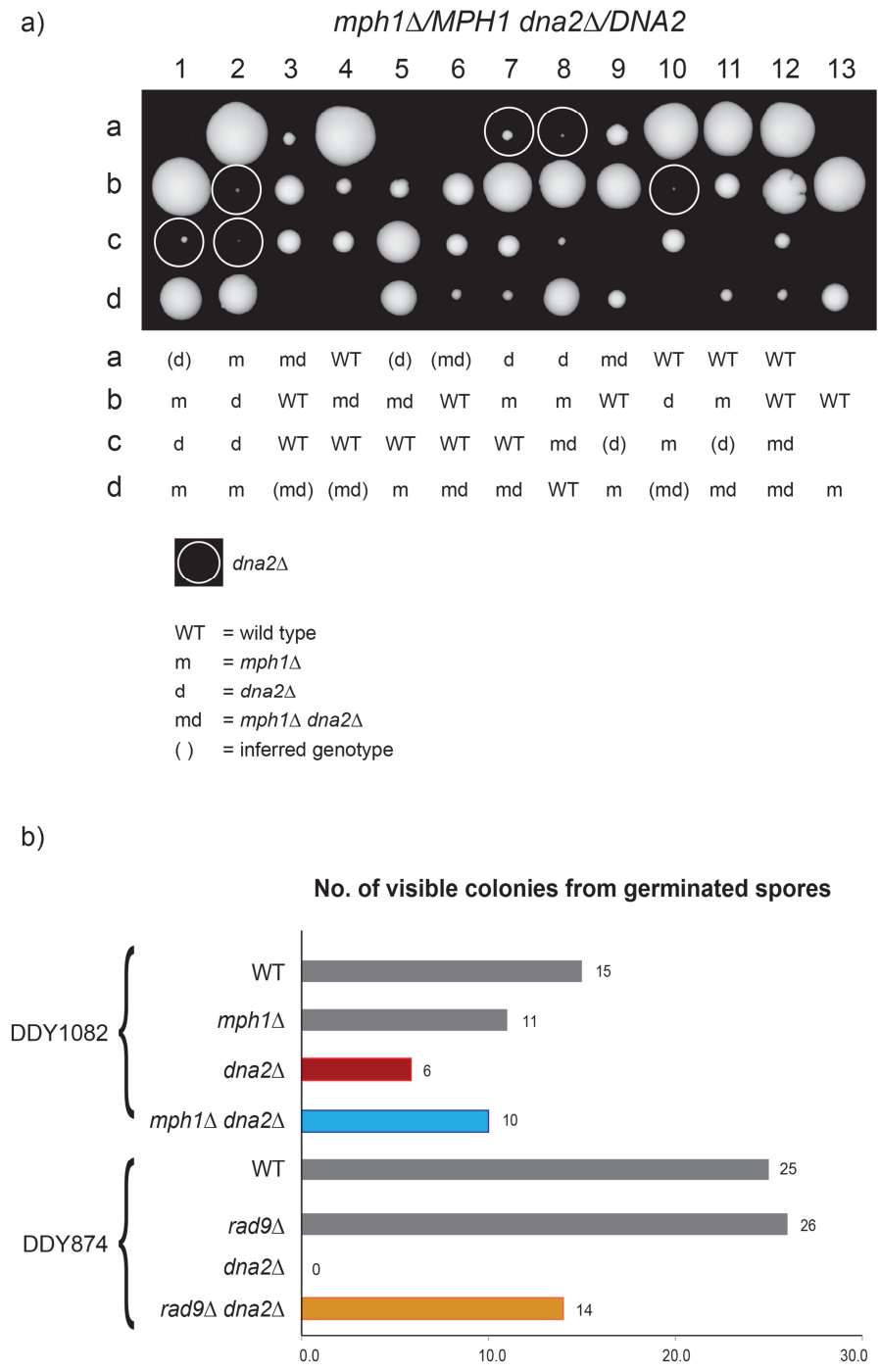


**Figure 41. *mph1*Δ suppresses *dna2*Δ similarly to *rad9*Δ**

a) Example of germinated spores of *mph1*Δ*/MPH1 dna2*Δ*/DNA2* diploid (DDY1082). Spores were germinated at 20°C for 10 days before being photographed. *dna2*Δ *pDNA2* strain was mated with *mph1*Δ strain, and diploid was treated as in Figure 31. b) Spores from a) were scored and plotted for comparisons with quantifications for *rad9*Δ (DDY874) from Figure 32. Bars present numbers of viable colonies WT, *yfg*Δ and *dna2*Δ *yfg*Δ and (mostly) inviable *dna2*Δ spores: **Grey bars** – WT or *yfg*Δ; **coloured bars** - viable *dna2*Δ *yfg*Δ*;* **red bars** – viable *dna2*Δ*;* '0' and no bar – inviable *dna2*Δ.

### *4.4.4 Inability to lose pCAN1-URA3-DNA2 on canavanine impedes verification of dna2Δ suppressors in W303*

Twenty one hits which appeared on the S288C SGA plot as strong suppressors or no-suppressors (enhancers) of *dna2*Δ lethality, were randomly selected for further studies in W303 background and are indicated below. Diploid strains heterozygous for deletions of no-suppressors of *dna2*Δ (*RAD51, XRS2, SGS1, EXO1, TOP3, BUB2*) and likely suppressors of *dna2*Δ (*RAD9, RAD17, RAD24, DDC1, CHK1, MPH1, BUB3, POL32, MEC1 SML1, CTF3, DGR2, LSM1, RPS4A, RTT109* and *cdc15-2* mutation) in *dna2*Δ*/DNA2 pCAN1-URA3-DNA2* background were generated and random spore analysis was performed. Spores were germinated on –URA plates to select for the plasmid at all time. So called "manual SGA" was applied involving culture conditions which mimic the conditions of robotic SGA (Fig. 42a). Yeast strains *dna2*Δ *xyz*Δ *pCAN1-URA3-DNA2* (*xyz*Δ indicates any of twenty one gene deletions tested) were cultured in liquid YEPD followed by growth for three passages in canavanine media to enhance the ability of strains to lose the *pCAN1-URA3-DNA2* plasmid. Finally the ability to lose the plasmid was assessed by spotting strains onto canavanine, FOA, YEPD and –URA plates (Fig. 42b and c). Yeast growth was assessed after 3 and 5 days incubation at 23°C. Such "manual SGA" was considered to be a more efficient and informative method, and at the same time less time consuming than tetrad dissection.

*dna2*Δ *xyz*Δ *pCAN1-URA3-DNA2* double mutants and control strains carrying *pCAN1-URA3-DNA2* plasmid were used. The plate template with assigned position of each strain on a plate, strain genotypes and numbers, is shown in Figure 42d. Some strains contained wild type *CAN1* gene and served as a control for canavanine media (Fig. 42d 11-12B, 3-4C). Some control strains contained *URA3* gene and served as a control for FOA media (Fig. 42d 1-2C). Finally, some strains did not contain the plasmid but were shown earlier to grow well despite *dna2*Δ mutation and served as positive control for *dna2*Δ suppression (Fig.42d 3-12H).

Most of yeast strains carrying *pCAN1-URA3-DNA2* plasmid were still able to grow on –URA, canavanine and FOA plates, which indicates that the plasmid was not efficiently lost. Moreover, yeast grew better on canavanine plate than on FOA, which suggests that FOA serves as a better media for plasmid counter-selection. The most

informative growth of yeast was observed on FOA plates after 5 days incubation at 23°C (Fig. 42c). WT and single gene deletion control mutants grew well on FOA plate, but did not completely lose the *pCAN2-URA3-DNA2* plasmid (Fig. 42c, compare to b, -URA). The control strains carrying *CAN1* gene on a chromosome were still able to from colonies on FOA plate, although the ability to growth should be lost during passaging in canavanine liquid media (Fig. 42c 11-12B, 3-4C). One strain carrying *URA3* gene on a chromosome formed colonies on FOA but should be inviable (Fig. 42c 1-2C).

Due to the fact that strains which served as controls for plate selection grew, the conclusions about the growth of *dna2*Δ *xyz*Δ double mutants are difficult to make. Moreover, *dna2*Δ *xyz*Δ strains exhibit very heterogeneous growth patterns, e. g. *dna2*Δ *chk1*Δ (Fig. 42c and d, 10-12D) or *dna2*Δ *rtt109*Δ (Fig. 42c and d, 1-2H).

I conclude that the experimental set up was not perfect and did not yield valuable and reliable information. It seems that prolong incubation in canavanine medium does not impose the plasmid loss, which is reflected by subsequent yeast growth on all types of selective media used. The difference in growth between control *dna2*Δ *pCAN1-URA3-DNA2* strains and *dna2*Δ *xyz*Δ double mutants is not obvious on selective canavanine plate, and is slightly better to notice on FOA plates. The possible explanation might be too low concentration on canavanine to force plasmid loss. Also, FOA may confer a more severe defect than canavanine. SGA may yield more reliable results if final selection step was performed on FOA, and not on canavanine media. Also, if strains were diluted in water before inoculation into canavanine media (and not in YEPD, Fig. 42a), cells might be more sensitive to canavanine.

a) “Manual SGA” Procedure

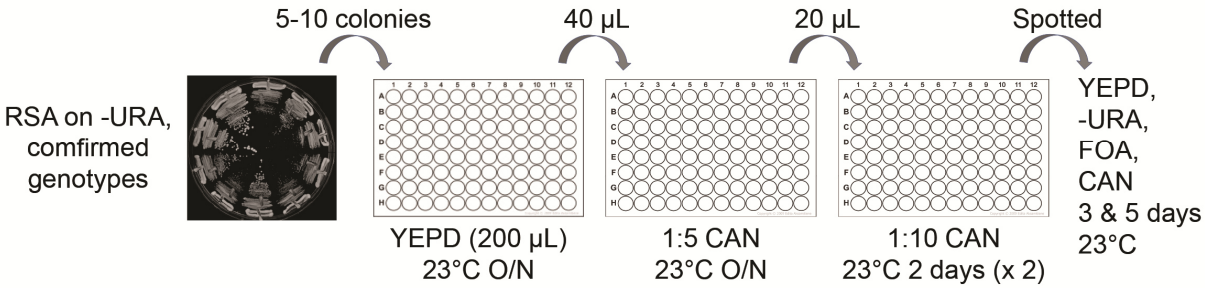


b) 3 days at 23°C

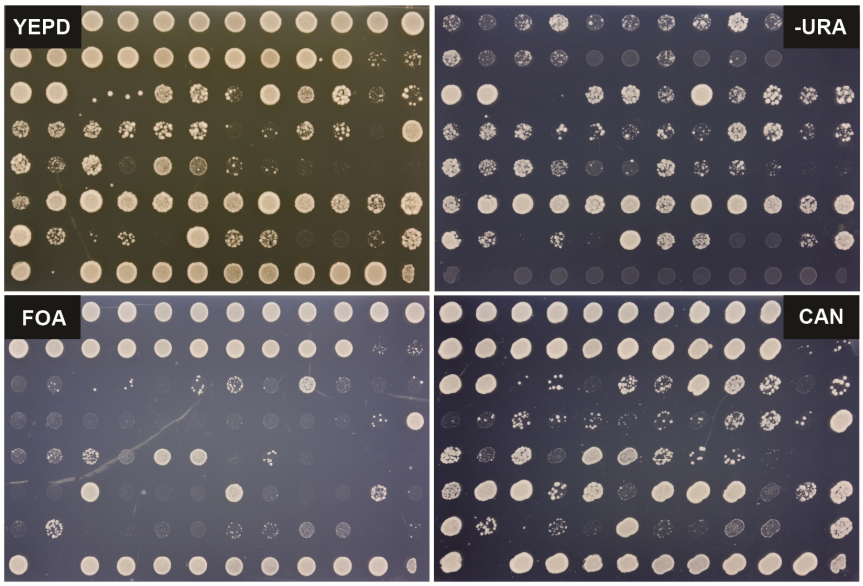


c) FOA, 5 days at 23°C

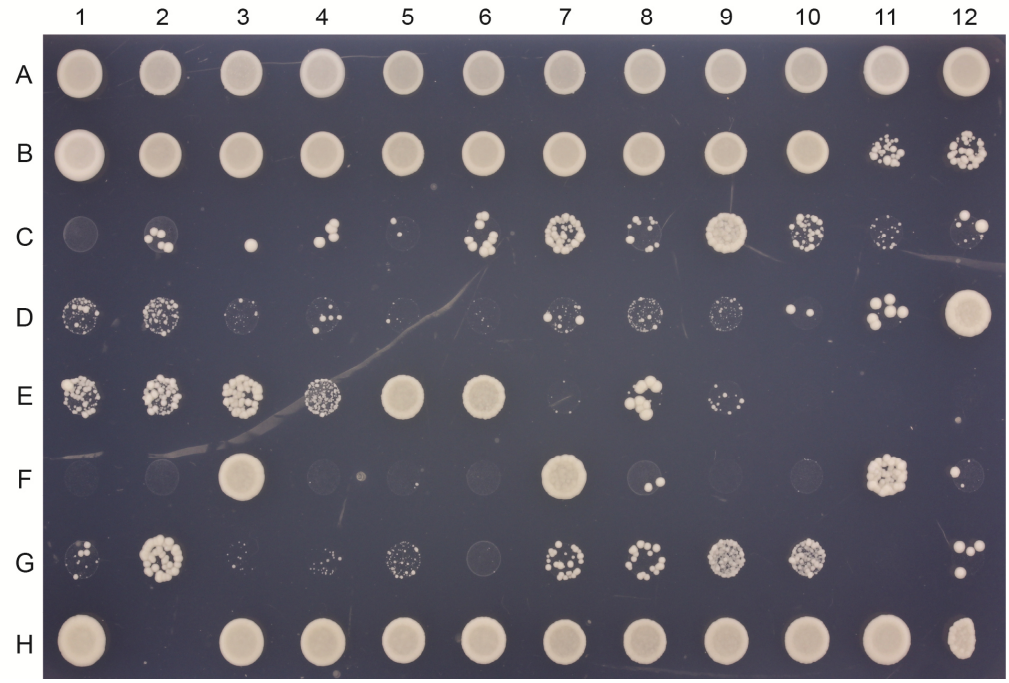

d)

| | 1 | 2 | 3 | 4 | 5 | 6 | 7 | 8 | 9 | 10 | 11 | 12 |
|---|---|---|---|---|---|---|---|---|---|---|---|---|
| A | WT p | *rad51::KAN* p | *rad9::HIS3* p | *rad17::LEU2* p | *rad24::TRP1* p | *ddc1::HIS3* p | *chk1::HIS3* p | *mph1::KAN* p | *pol32::KAN* p | *mec1::HIS3 sml1::KAN* p | *xrs2::LEU2* p | *sgs1::KAN* p |
| | DLY11958 | DLY11419 | DLY11479 | DLY11411 | DLY11425 | DLY11469 | DLY11431 | DLY11441 | DLY11463 | DLY11443 | DLY11417 | DLY11455 |
| B | *exo1::LEU2* p | *top3::HPH* p | *cdc15-2* p | *bub2::HPH* p | *bub3::HPH* p | *ctf3::HPH* p | *dgr2::HPH* p | *lsm1::HPH* p | *rps4a::HPH* p | *rtt109::HPH* p | WT (*CAN1*) p | |
| | DLY11393 | DLY11392 | DLY11383 | DLY11508 | DLY11512 | DLY11516 | DLY11520 | DLY11524 | DLY11528 | DLY11532 | DLY5626 | DLY5536 |
| C | *rad50::URA* | | *dna2::NAT* (*CAN1*) p | | *dna2::NAT* p | | *rad51::KAN dna::NAT* p | | | *rad9::HIS3 dna::NAT* p | | |
| | DLY10876 | DLY10877 | DLY11534 | DLY11535 | DLY11190 | DLY11274 | DLY11421 | DLY11422 | DLY11423 | DLY11475 | DLY11476 | DLY11477 |
| D | *rad17::LEU2 dna::NAT* p | | | *rad24::TRP1 dna::NAT* p | | | *ddc1::HIS3 dna::NAT* p | | | *chk1::HIS3 dna::NAT* p | | |
| | DLY11407 | DLY11408 | DLY11409 | DLY11427 | DLY11428 | DLY11429 | DLY11471 | DLY11472 | DLY11473 | DLY11434 | DLY11345 | DLY11436 |
| E | *mph1::KAN dna::NAT* | | | *pol32::KAN dna::NAT* | | | *mec1::HIS3 sml1::KAN dna::NAT* | | | *xrs2::LEU2 dna::NAT* p | | |
| | DLY11481 | DLY11482 | DLY11485 | DLY11465 | DLY11466 | DLY11467 | DLY11447 | DLY11448 | DLY11449 | DLY11413 | DLY11414 | DLY11415 |
| F | *sgs1::KAN dna::NAT* | | | *exo1::LEU2 dna::NAT* p | | | *top3::HPH dna::NAT* p | | | *cdc15-2 dna::NAT* p | | |
| | DLY11451 | DLY11452 | DLY11453 | DLY11394 | DLY11395 | DLY11396 | DLY11388 | DLY11389 | DLY11390 | DLY11384 | DLY11385 | DLY11386 |
| G | *bub2::HPH dna::NAT* p | | *bub3::HPH dna::NAT* p | | *ctf3::HPH dna::NAT* p | | *dgr2::HPH dna::NAT* p | | *lsm1::HPH dna::NAT* p | | *rps4a::HPH dna::NAT* p | |
| | DLY11506 | DLY11507 | DLY11510 | DLY11511 | DLY11514 | DLY11515 | DLY11518 | DLY11519 | DLY11522 | DLY11523 | DLY11526 | DLY11527 |
| H | *rtt109::HPH dna::NAT* p | | *rad9::HIS3 dna2::KAN* (*p6*) | | *rad17::LEU2 dna2::KAN* (*p6*) | | *ddc1::HIS3 dna2::KAN* (*p6*) | | *chk1::HIS3 dna2::KAN* (*p6*) | | *mec1::HIS3 sml1::KAN dna2::NAT* (*p6*) | |
| | DLY11530 | DLY11531 | DLY11195 | DLY11196 | DLY11199 | DLY11200 | DLY11201 | DLY11202 | DLY11197 | DLY11207 | DLY11205 | DLY11206 |

**Figure 42. *pCAN1-URA3-DNA2* plasmid is not efficiently lost**

a) “Manual SGA” procedure.

Strains of appropriate genotypes obtained from RSA were grown at 23°C on –URA plates to select for *pCAN1-URA3-DNA2* plasmid. Then 5-10 colonies of each strain were inoculated with a pipette tip into 200 µL YEPD in 96-well plate and grown O/N at 23°C; 23°C temperature was maintained throughout the whole experiment. The next day cultures were diluted 1:5 in canavanine (CAN) media (40 µL O/N culture + 160 µL CAN) and grown O/N. The next morning cultures were diluted 1:10 in CAN (20 µL O/N culture + 180 µL CAN) and grown for 2 days (this step was repeated twice). Finally, cultures were spotted onto YEPD, -URA, CAN, FOA plates and grown for 3 and 5 days before photographing.

b) YEPD, -URA, CAN, FOA plates after 3 days incubation at 23°C.

c) Magnification of an FOA plate from a), after 5 days incubation at 23°C.

d) Template of a plate set up. The position of each gene is assigned to their position on plates in b) and c). p – *pCAN1-URA3-DNA2* (pDL1758). Strain details are in Appendix A.

### *4.4.5 W303 SGA results are different from the S288C SGA results*

Another way to confirm results acquired from 2S88C SGA in an unbiased and shorter manner was an SGA in W303 background. This time however only 308 out of ~5000 genes were tested (list of these genes is in the Appendix G). Figure 43a shows three passages of W303 strains on CTGNH media (containing canavanine). Colonies were rather homogeneous in size at passage 1, but became very heterogeneous at passage 3 (Fig. 43a). In contrast to passage 2 of S288C SGA (Fig. 39a), passage 2 of W303 SGA was much less informative in a sense that 4 replicates were usually heterogeneous and very few fit strains were noted (Fig. 43a). Moreover, none of previously shown gene deletions, like *rad9*Δ or *chk1*Δ, effected the growth of *dna2*Δ in W303 SGA (Fig. 43a and b, Column 13 Row 15, Column 13 Row 4). *mph1*Δ*,* which was selected in S288C SGA as a suppressor of *dna2*Δ lethality, and later confirmed by tetrad dissection, was synthetically lethal with *dna2*Δ in W303 SGA (Fig. 43a and b, Column 14 Row 2).

Due to enormous heterogeneity in fitness of strains of the same genotype, it is problematic to conclude the efficiency of W303 SGA and to select hits likely affecting *dna2*Δ viability. It might be that selection pressure against *pCAN1-URA3-DNA2* was too weak for individual strains, either because canavanine concentration was low, or strains with the plasmid somehow adapted to the canavanine-caused stress and remained viable. It might be worth testing whether final growth on FOA would bring more uniform and reliable information.

Another explanation for a difference in growth between S288C and W303 backgrounds might be the background specificity. The genome of S288C was sequenced and the deletion and ORF libraries are available (Goffeau et al., 1996, Winzeler et al., 1999, Ghaemmaghami et al., 2003). Although other strains, e.g. W303, are used for studying particular aspects of biology, only their relevant genotypes, but not the complete background, is known (Young and Court, 2008). The S288C background is widely used for robotic screens and the phenotypes of certain gene deletions are known, in contrast to W303 background. W303 yeast may not tolerate the robotic conditions (e. g. incubation time and selection processes) as well and efficiently as S288C cells. Additionally, the W303 library had never been tested and the knowledge about it is not as comprehensive as of S288C library.

a) CTGNH, 20°C, W303 SGA

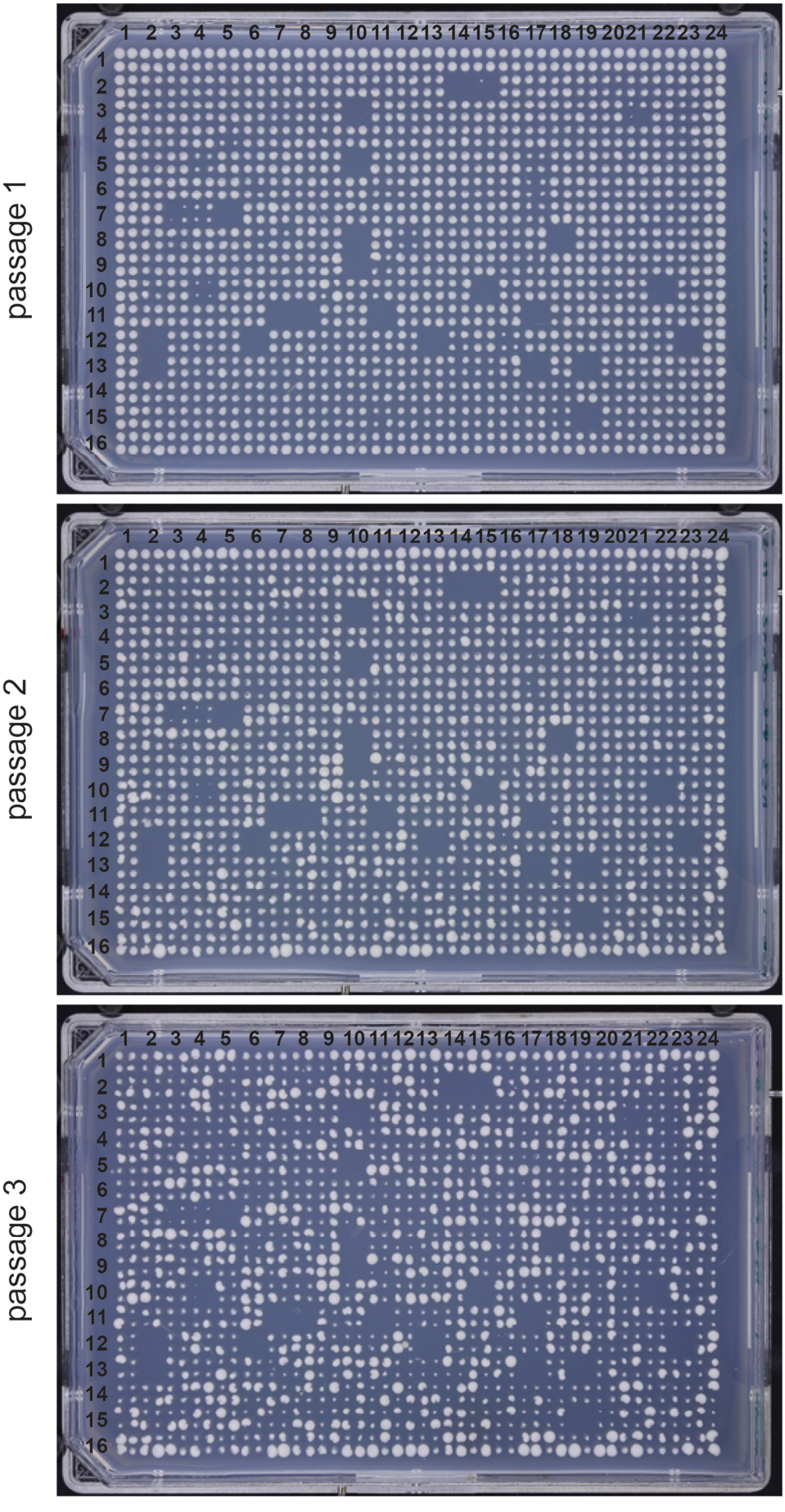

b)

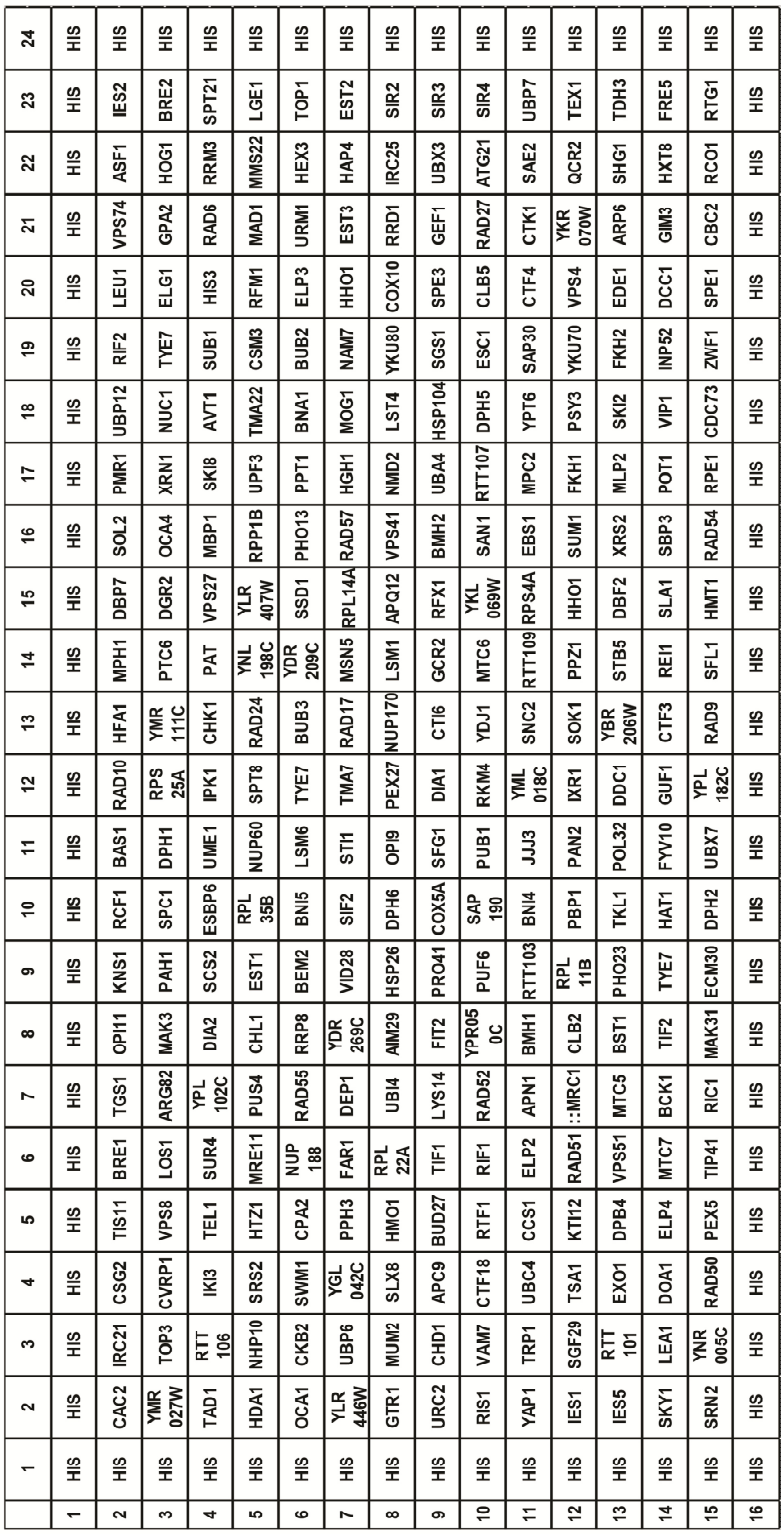

| | 1 | 2 | 3 | 4 | 5 | 6 | 7 | 8 | 9 | 10 | 11 | 12 | 13 | 14 | 15 | 16 | 17 | 18 | 19 | 20 | 21 | 22 | 23 | 24 |
|---|---|---|---|---|---|---|---|---|---|---|---|---|---|---|---|---|---|---|---|---|---|---|---|---|
| 1 | HIS | HIS | HIS | HIS | HIS | HIS | HIS | HIS | HIS | HIS | HIS | HIS | HIS | HIS | HIS | HIS | HIS | HIS | HIS | HIS | HIS | HIS | HIS | HIS |
| 2 | HIS | CAC2 | IRC21 | CSG2 | TIS11 | BRE1 | TGS1 | OPI11 | KNS1 | RCF1 | BAS1 | RAD10 | HFA1 | MPH1 | DBP7 | SOL2 | PMR1 | UBP12 | RIF2 | LEU1 | VPS74 | ASF1 | IES2 | HIS |
| 3 | HIS | YMR 027W | TOP3 | CVRP1 | VPS8 | LOS1 | ARG82 | MAK3 | PAH1 | SPC1 | DPH1 | RPS 25A | YMR 111C | PTC6 | DGR2 | OCA4 | XRN1 | NUC1 | TYE7 | ELG1 | GPA2 | HOG1 | BRE2 | HIS |
| 4 | HIS | TAD1 | RTT 106 | IKI3 | TEL1 | SUR4 | YPL 102C | DIA2 | SCS2 | ESBP6 | UME1 | IPK1 | CHK1 | PAT | VPS27 | MBP1 | SKI8 | AVT1 | SUB1 | HIS3 | RAD6 | RRM3 | SPT21 | HIS |
| 5 | HIS | HDA1 | NHP10 | SRS2 | HTZ1 | MRE11 | PUS4 | CHL1 | EST1 | RPL 35B | NUP60 | SPT8 | RAD24 | YNL 198C | YLR 407W | RPP1B | UPF3 | TMA22 | CSM3 | RFM1 | MAD1 | MMS22 | LGE1 | HIS |
| 6 | HIS | OCA1 | CKB2 | SWM1 | CPA2 | NUP 188 | RAD55 | RRP8 | BEM2 | BNI5 | LSM6 | TYE7 | BUB3 | YDR 209C | SSD1 | PHO13 | PPT1 | BNA1 | BUB2 | ELP3 | URM1 | HEX3 | TOP1 | HIS |
| 7 | HIS | YLR 446W | UBP6 | YGL 042C | PPH3 | FAR1 | DEP1 | YDR 269C | VID28 | SIF2 | STI1 | TMA7 | RAD17 | MSN5 | RPL14A | RAD57 | HGH1 | MOG1 | NAM7 | HHO1 | EST3 | HAP4 | EST2 | HIS |
| 8 | HIS | GTR1 | MUM2 | SLX8 | HMO1 | RPL 22A | UBI4 | AIM29 | HSP26 | DPH6 | OPI9 | PEX27 | NUP170 | LSM1 | APQ12 | VPS41 | NMD2 | LST4 | YKU80 | COX10 | RRD1 | IRC25 | SIR2 | HIS |
| 9 | HIS | URC2 | CHD1 | APC9 | BUD27 | TIF1 | LYS14 | FIT2 | PRO41 | COX5A | SFG1 | DIA1 | CTI6 | GCR2 | RFX1 | BMH2 | UBA4 | HSP104 | SGS1 | SPE3 | GEF1 | UBX3 | SIR3 | HIS |
| 10 | HIS | RIS1 | VAM7 | CTF18 | RTF1 | RIF1 | RAD52 | YPR050C | PUF6 | SAP 190 | PUB1 | RKM4 | YDJ1 | MTC6 | YKL 069W | SAN1 | RTT107 | DPH5 | ESC1 | CLB5 | RAD27 | ATG21 | SIR4 | HIS |
| 11 | HIS | YAP1 | TRP1 | UBC4 | CCS1 | ELP2 | APN1 | BMH1 | RTT103 | BNI4 | JJJ3 | YML 018C | SNC2 | RTT109 | RPS4A | EBS1 | MPC2 | YPT6 | SAP30 | CTF4 | CTK1 | SAE2 | UBP7 | HIS |
| 12 | HIS | IES1 | SGF29 | TSA1 | KTI12 | RAD51 | ::MRC1 | CLB2 | RPL 11B | PBP1 | PAN2 | IXR1 | SOK1 | PPZ1 | HHO1 | SUM1 | FKH1 | PSY3 | YKU70 | VPS4 | YKR 070W | QCR2 | TEX1 | HIS |
| 13 | HIS | IES5 | RTT 101 | EXO1 | DPB4 | VPS51 | MTC5 | BST1 | PHO23 | TKL1 | POL32 | DDC1 | YBR 206W | STB5 | DBF2 | XRS2 | MLP2 | SKI2 | FKH2 | EDE1 | ARP6 | SHG1 | TDH3 | HIS |
| 14 | HIS | SKY1 | LEA1 | DOA1 | ELP4 | MTC7 | BCK1 | TIF2 | TYE7 | HAT1 | FYV10 | GUF1 | CTF3 | REI1 | SLA1 | SBP3 | POT1 | VIP1 | INP52 | DCC1 | GIM3 | HXT8 | FRE5 | HIS |
| 15 | HIS | SRN2 | YNR 005C | RAD50 | PEX5 | TIP41 | RIC1 | MAK31 | ECM30 | DPH2 | UBX7 | YPL 182C | RAD9 | SFL1 | HMT1 | RAD54 | RPE1 | CDC73 | ZWF1 | SPE1 | CBC2 | RCO1 | RTG1 | HIS |
| 16 | HIS | HIS | HIS | HIS | HIS | HIS | HIS | HIS | HIS | HIS | HIS | HIS | HIS | HIS | HIS | HIS | HIS | HIS | HIS | HIS | HIS | HIS | HIS | HIS |

**Figure 43. W303 SGA of 308 genes**

a) Pictures of final selection plates CTGNH, passage 1, 2 and 3 at 20°C. Double mutants were pinned in quadruples.

b) Template of a plate set up. Horizontal numbers – numbers of columns; vertical numbers – numbers of rows. The position of each gene is assigned to their position on plates in a).

### 4.5 Discussion/Conclusions

I observed at least two classes of genes which suppressed *dna2*Δ, based on the growth pattern of strains of the same genotype and ability to recover with time; one group is *RAD17, DDC1, MEC1 SML1, RAD9* and *CHK1*, and the other one is *POL32*. Genes can be divided in different groups when telomere length is considered; *RAD9, CHK1* and *MEC1 SML1* null mutants with *dna2*Δ have longer telomeres than single mutants, but the difference in telomere length is less obvious than in *DDC1, RAD17* and *POL32* null mutants with *dna2*Δ. I do not understand where the differences between groups may come from. Maybe cell cycle arrest analysis of *dna2*Δ with deletions of *RAD9, DDC1, RAD17, CHK1 MEC1 SML1* and *POL32* strains would help to clarify the mechanisms of *dna2*Δ suppression.

Dna2 was shown to function at telomeres (Choe et al., 2002, Budd et al., 2006), and its essential role was proposed inOkazaki fragment processing and lagging strand synthesis (Budd et al., 2011). It is however possible that the essential function of Dna2 is in telomere replication, specifically in the synthesis/processing of the terminal telomeric Okazaki fragment, (Figure 44). This hypothesis of the essential role in telomeric DNA replication is based on several observations; first, most checkpoint gene deletions suppress *dna2*Δ, whereas they exacerbate defects in other core DNA replication proteins (Dubarry et al., 2015). *dna2*Δ defect, like *cdc13-1* defect, is suppressed by checkpoint mutations, which suggests that Dna2 is similar to telomere capping protein Cdc13, rather than DNA polymerases. Second, *dna2*Δ strains recover with time, which is characteristic for survivors with telomere rearrangements. Third,telomeres are long when *DNA2* is deleted, which indicates the role of Dna2 at telomeres and, perhaps, interactions with telomerase.

The hypothesis that the essential role of Dna2 is in telomere replication fits published data, which show that DNA2 binds telomeres in yeast and mammalian cells, and is specifically required for maturation of telomeric DNA replication intermediates in yeast (Choe et al., 2002, Budd et al., 2005, Budd and Campbell, 2013, Lin et al., 2013). In addition, suppressors of *dna2*Δ lethality , *RAD9, DDC1, RAD17, CHK1 MEC1 SML1* and *POL32,* are important in telomere biology. Null mutations of other suppressors, *PIF1* and *RAD27,* increase telomere length (Parenteau and Wellinger, 1999, Gatbonton et al., 2006). Dna2 might be therefore a telomere-focused DNA

replication protein, similar to the CST complex. The mechanisms, by which Dna2 might perform its critical function in Okazaki fragment processing during telomere replication, remain to be tested.

S288C SGA brought some information regarding Dna2 regulation. It is difficult to distinguish mechanisms of *dna2*Δ suppression due the heterogeneity in strains growth. The heterogeneity might be a result of strains maintaining the plasmid (*pCAN2-URA2-DNA2*) despite the selection on canavanine against the plasmid, as was shown in “manual SGA experiment”. Some cells might adapt to harmful conditions in the presence of canavanine and continue to grow. Another explanation is that the deletion of essential *DNA2* gene resulted in genomic instability and aneuploidy. Aneuploid strains would exhibit heterogeneous growth pattern between cells of the same genotype. Also, if cells carried more copies of *pCAN1-URA3-DNA2* plasmid, they could have more copies of *DNA2* gene, which in turn might affect cells growth and viability. It was shown that upregulation of *DNA2* in mice led to cancer formation (Lin et al., 2013) and it might be possible that upregulation of *DNA2* in yeast cells causes genomic instability, too.

Despite problems in losing the plasmid, it was possible to select several novel suppressors of *dna2*Δ lethality in S288C SGA. Deletion of *MPH1,* a helicase which regulates Dna2 and Rad27 in Okazaki fragment processing, suppressed *dna2*Δ lethality. However, due to possible genome instability, single *dna2*Δ mutants emerged. Deletion of *RTT109* gene, encoding acetyltransferase which acetylates histone H3 in response to DNA replication stress, did not suppress *dna2*Δ lethality. It has to be verified which gene highlighted in SGA as suppressors of *dna2*Δ affect *dna2*Δ fitness, to understand and indicate the mechanism(s) of *dna2*Δ suppression.

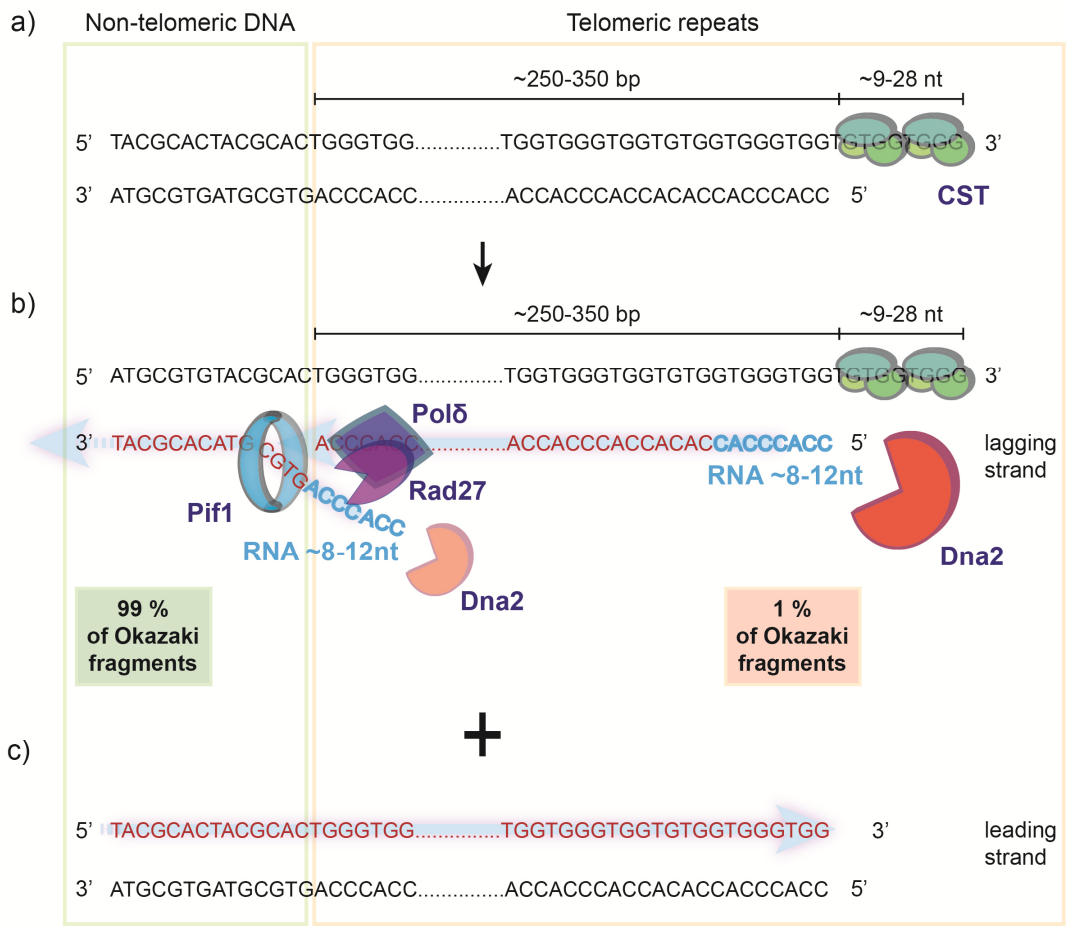


**Figure 44. The model for Dna2 essential function at the terminal telomeric Okazaki fragment**

a) Budding yeast telomeres consist of 250-350 bp of repetitive sequences ($TG_{1-3}/C_{1-3}A$) and terminate in short 3' overhangs. The ssDNA binding CST complex, is shown.

b) The lagging strand is synthesised by DNA Pol δ in short, ~200 bp long Okazaki fragments. Pol δ and Pif1 helicase displace the previously synthesised Okazaki fragment and a short flap is formed. The short flap is removed by $Rad27^{FEN1}$ flap endonuclease. Randomly appearing long flaps are removed by Dna2 nuclease. In a haploid budding yeast cell 99 % of Okazaki fragments resemble the one from the non-telomeric DNA (green box), while 1 % forms terminal telomeric Okazaki fragments, TTOF (orange box). The 5' end of the TTOF is probably not displaced due to the lack of Pol δ/Pif1 activities at this site. The essential role of Dna2 might be in: i) separation the RNA from DNA to facilitate RNA primer degradation; ii) resection of 5' RNA fragment; iii) assembling the complex with Pol δ for TTOF synthesis and RNA degradation. RNA primers are indicated by blue font. Arrowheads indicate the direction of DNA synthesis.

c) The leading strand is synthesised in a continuous manner by DNA pol ε.

# Chapter 5. Novel genes with potential functions at telomeres

## 5.1 Selection and overview of genes with potential functions at telomeres

Genes that may play roles in telomere-defective strains have been identified in genome wide suppressor and enhancer screens, performed previously in the lab, using the R tool (Fig. 45) (Addinall et al., 2011). In the literature I searched for genes that were suggested to be involved in processes such as DNA damage repair or DNA replication, cancer development or aging. Some of these genes were proposed to function at telomeres in genome-wide screens, but their role in telomere biology was not well established. Among these genes I selected *HCM1, XBP1, ULS1, IRC5* and *RAD1* that are particularly interesting due to their potential role in ageing or cancer. Below is a short overview of these genes:

***HCM1 (High-Copy suppressor of calmodulin)***

Hcm1*,* a forkhead transcription factor, was identified in a genome-wide screen of genes whose deletions affect telomere length; *hcm1*Δ increases telomere length (Askree et al., 2004). Deletion of *HCM1* suppresses *cdc13-1* and *yku70*Δ mutants (Fig.44a and c). Hcm1 controls life span independently of calorie restriction, and deletion of *HCM1* results in decreased replicative lifespan (Maoz et al., 2015). The *Caenorabditis elegans* ortholog of *HCM1*, *PHA-4*, also regulates lifespan (Panowski et al., 2007, Sheaffer et al., 2008, Zhong et al., 2010). Hcm1 drives S-phase activation of genes involved in e. g. chromosome segregation, and activates genes involved in respiration or oxidative stress resistance (Pramila et al., 2006, Rodriguez-Colman et al., 2013).

***XBP1 (XhoI site-Binding Protein)***

Xbp1 is a transcription factor induced by various stresses and nutrient limitations; null mutants have shortened lifespan (Mai and Breeden, 1997, Choi et al., 2013, Miles et al., 2013). Xbp1 is important for maintaining G1 arrest, which is initiated before the diauxic shift (when the glucose from the media is used) (Miles et al., 2013). Xbp1 is upregulated in response to DNA damage in a Mec1-Rad9-Rad53 checkpoint pathway-dependent manner (Tao et al., 2011).

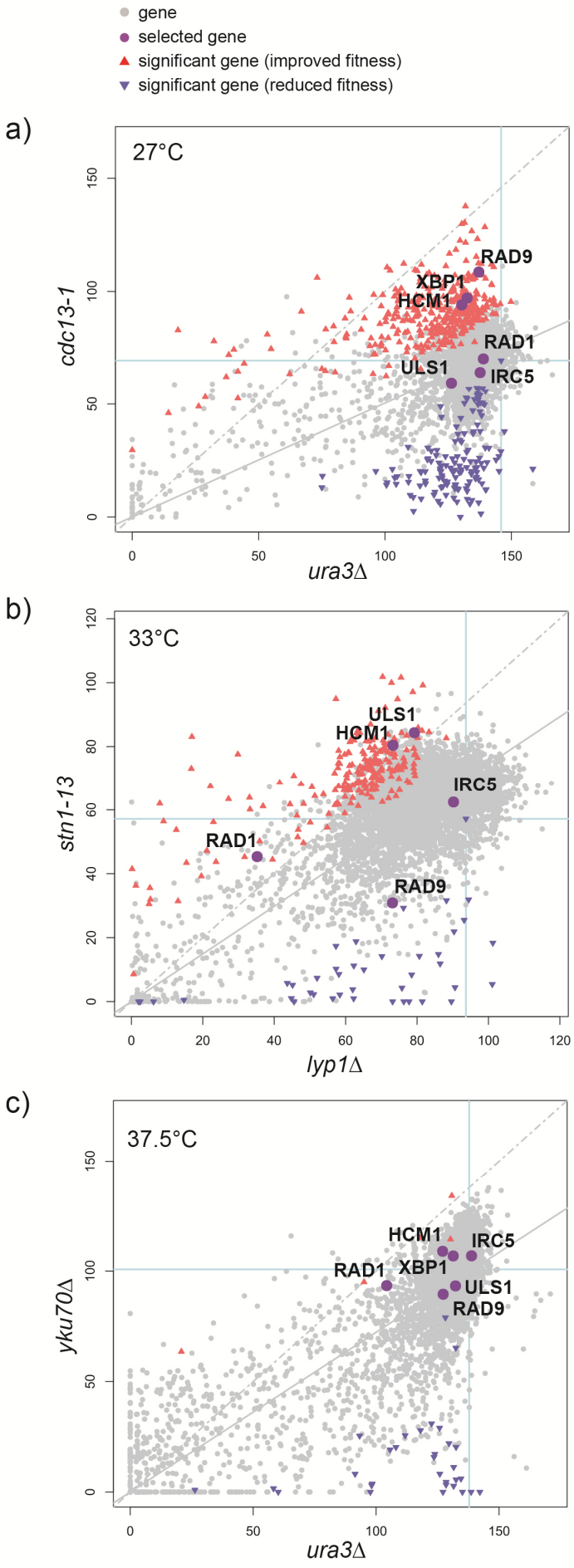
gene
selected gene
significant gene (improved fitness)
significant gene (reduced fitness)
a)
27°C
RAD9
XBP1
HCM1
RAD1
ULS1
IRC5
cdc13-1
ura3Δ
b)
33°C
ULS1
HCM1
IRC5
RAD1
RAD9
stn1-13
lyp1Δ
c)
37.5°C
HCM1
IRC5
RAD1
XBP1
ULS1
RAD9
yku70Δ
ura3Δ

**Figure 45. Genes with potential function at telomeres**

Fitness plots comparing mean fitnesses for each *xyz*Δ in a query and control screen. **Red upward triangle** indicates a single gene deletion that significantly improves fitness of *cdc13-1, stn1-13* or *yku70*Δ. **Purple downward triangle** indicates a single gene deletion that significantly decreases fitness of *cdc13-1, stn1-13* or *yku70*Δ fitness. **Purple dots** indicate selected gene deletions. **Grey dots** indicate gene deletions. Data in a) and c) are from (Addinall et al., 2011), data in b) are from M. Greetham (PhD thesis).

a) Fitness plots of *cdc13-1* query screen at 27°C.

b) Fitness plots of *stn1-13* query screen at 33°C.

c) Fitness plots of *yku70*Δ query screen at 37.5°C.

***ULS1 (Ubiquitin Ligase for SUMO conjugates)***

Uls1 is a SUMO-Targeted Ubiquitin Ligase (STUbL) with a translocase activity (Uzunova et al., 2007). Uls1 is required for maintenance of NHEJ inhibition at telomeres by its role in translocation and ubiquitinylation of poly-sumoylated Rap1 for proteosomal degradation (Pardo and Marcand, 2005, Lescasse et al., 2013, Kramarz et al., 2014). Additionally, Uls1 is involved in repair of replication-associated DNA damage and facilitates Sgs1-dependent remodelling of stalled replication forks (Cal-Bakowska et al., 2011, Kramarz et al., 2014).

***IRC5 (Increased Recombination Centers)***

Irc5 is an ATPase and a putative DNA helicase belonging to Snf2 family with homology to the mammalian LSH/HELLS (Lymphoid-Specific Helicase) (Shiratori et al., 1999, McCarroll et al., 2004). Genetic interactions of the *irc5*Δ mutant correlate strongly with replicative proteins (e. g. *rad27*Δ*, elg1*Δ*, pol30–79*), suggesting that Irc5 may be involved in DNA replication (Alvaro et al., 2007). Deletion of *IRC5* in yeast increases HR between homologous chromosomes (Zhou et al., 2008), and overexpression of *HELLS* was found in several human tumours (von Eyss et al., 2012).

***RAD1 (RADiation sensitive)***

Rad1 forms a complex with Rad10 which functions as ssDNA endonuclease and cleaves single-stranded DNA during nucleotide excision repair (NER) and DSB repair (Tomkinson et al., 1993, Ivanov and Haber, 1995). In addition to their requirement in NER, the *RAD1* and *RAD10* genes function in mitotic recombination (Schiestl and Prakash, 1990, Kirkpatrick and Petes, 1997). Inactivation of the human homolog, *XPF/ERCC4*, leads to the *Xeroderma Pigmentosum* (XP), a disorder in which the ability to repair damage caused by UV light is deficient (Sijbers et al., 1996). Importantly, *XPF/ERCC4* was found to process 3’ overhang from uncapped telomeres in humans (Zhu et al., 2003)

The roles of selected genes in DNA damage repair, DNA replication, cancer formation or in telomere processing raise the possibility that those genes have some important roles at uncapped telomeres. In order to test this hypothesis I checked whether gene deletions affected the fitness of *cdc13-1, yku70*Δ*,* and if *uls1*Δ affects *stn1-13*.

To test whether deletion of each gene, denoted '*YFG'*, affects the growth of *cdc13-1* or *yku70*Δ mutants, diploids *yfg*Δ*/YFG cdc13-1/CDC13 yku70*Δ*/YKU70 rad9*Δ*/RAD9* were generated, their haploid progeny was isolated and spot tested. Such diploid background served as a good starter strain for all tested gene deletions, because strains with *cdc13-1* and *yku70*Δ mutations could be generated simultaneously. Moreover, *rad9*Δ is a known suppressor of *cdc13-1* (Weinert and Hartwell, 1993, Zubko et al., 2004). At higher temperatures *cdc13-1* strains have dysfunctional telomeres and activate Rad9-dependent checkpoint pathway which induces cell cycle arrest (Garvik et al., 1995). Deletion of *RAD9* improves *cdc13-1* fitness, presumably because cells cannot signal the presence of ssDNA at telomeres when checkpoint is defective (Weinert and Hartwell, 1993, Zubko et al., 2004). Although *rad9*Δ does not seem to affect *yku70*Δ growth in the genome-wide screen (Fig. 45c), it was in fact shown that *rad9*Δ suppresses *yku70*Δ fitness (chapter 3.1.5) (Maringele and Lydall, 2002). Thus *rad9*Δ served as a relevant control in this experiment.

### 5.2 Hcm1 slightly affects the growth of *cdc13-1* and *yku70*Δ mutants

Haploid strains with deletion of *HCM1* in *cdc13-1* and *yku70*Δ backgrounds were spot tested; in parallel, the effect of *rad9*Δ was compared (Fig. 46). The *hcm1*Δ mutation slightly suppressed *cdc13-1* ts at 26-27°C, and this effect was much weaker than of *rad9*Δ on *cdc13-1* mutation (Fig. 46a). *rad9*Δ suppressed *cdc13-1 hcm1*Δ strains so that triple mutants were able to grow slightly better than *cdc13-1 rad9*Δ mutants at 27-28°C.

*hcm1*Δ mutation slightly suppressed *yku70*Δ ts at 36-37°C, and this effect was much weaker than of *rad9*Δ on *yku70*Δ mutants (Fig. 46b). Similarly to what was observed in *cdc13-1* strains, *rad9*Δ slightly suppressed *yku70*Δ *hcm1*Δ growth.

Hcm1 in yeast, its orthologue in *C. elegans* PHA-4 and other forkhead proteins, regulate organismal lifespan (Maoz et al., 2015). *hcm1*Δ mutants have increased telomere length (Askree et al., 2004). I observe that deletion of *HCM1* resulted in improved growth of *cdc13-1* and *yku70*Δ strains, which suggests that Hcm1 has a role at uncapped telomeres. It might be interesting to test the telomere length of *cdc13-1 hcm1*Δ and *yku70*Δ *hcm1*Δ strains versus *hcm1*Δ mutants.

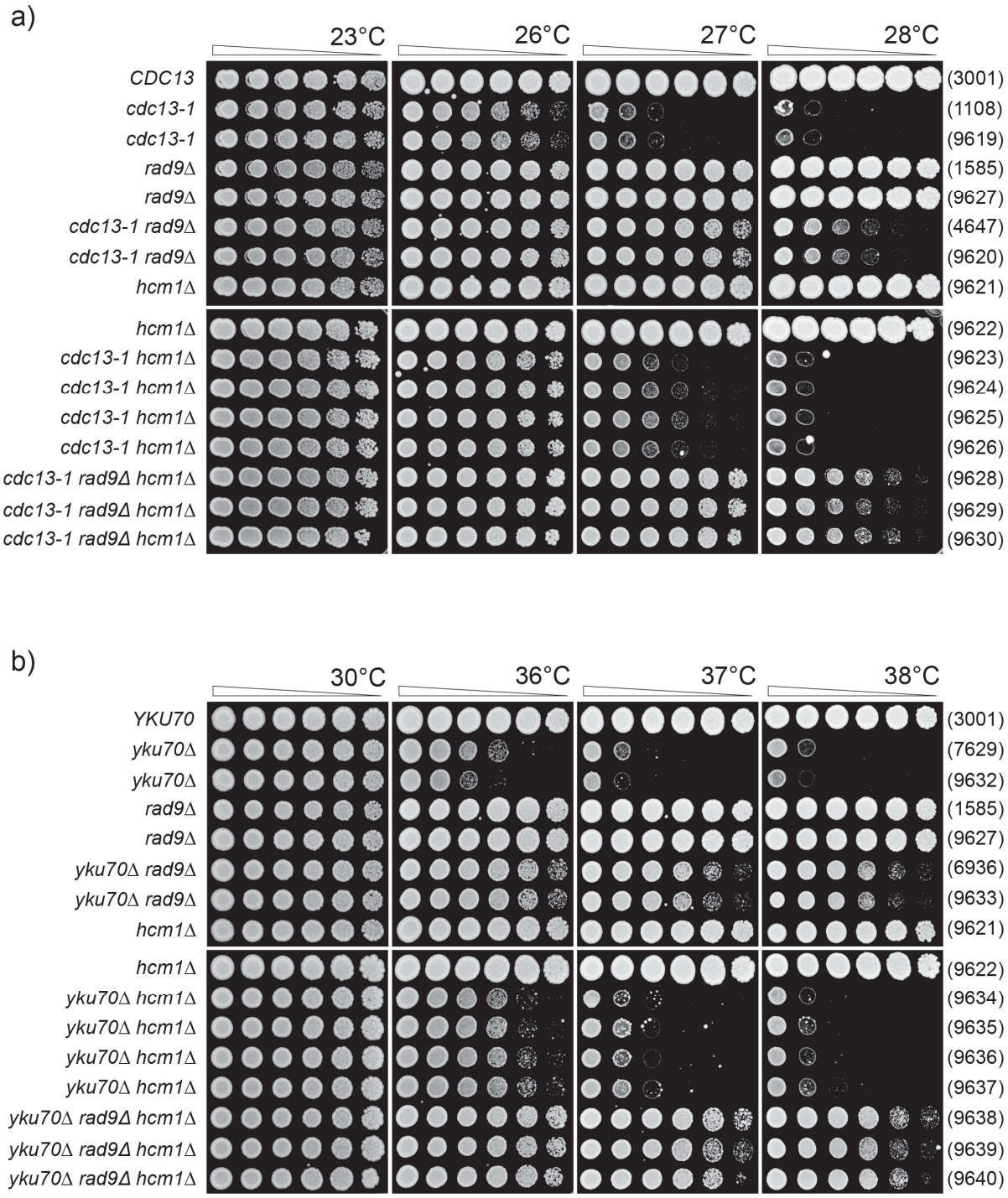


**Figure 46. Hcm1 slightly affects fitness of *cdc13-1* and *yku70*Δ mutants**

a-b) Spot tests done as in Figure 9. Strains in a) were grown on one rectangular plate. Strains in b) were grown on one rectangular plate. Spot tests in a) and b) were performed on different days. The relevant genotypes of the strains are indicated on the left, strain numbers on the right; strain details are in Appendix A.

a) The effect of *hcm1*Δ on *cdc13-1* and *cdc13-1 rad9*Δ mutants.

b) The effect of *hcm1*Δ on *yku70*Δ and *yku70*Δ *rad9*Δ mutants.

### 5.3 Xbp1 slightly affects the growth of *cdc13-1* and *yku70*∆ mutants

Haploid strains with deletions of *XBP1* in *cdc13-1* and *yku70*∆ backgrounds were spot tested and the effect of *rad9*∆ was compared (Fig. 47). Deletion of *XBP1* suppressed *cdc13-1* mutants at 26-28°C (Fig. 47a). The effect of *rad9*∆ on *cdc13-1* was much stronger than the effect of *xbp1*∆ mutation. Triple mutants grew slightly better than *cdc13-1 rad9*∆ strains at 28°C.

Similarly, deletion of *XBP1* suppressed *yku70*∆ mutants at 36-38°C (Fig. 47b). Iobserve that Xbp1 slightly affects *yku70*∆ fitness. Deletion of *RAD9* slightly suppressed *yku70*∆ fitness at 38°C.

Xbp1 is a transcription factor and is activated by various stresses and nutrient limitations; deletion of *XBP1* reduces yeast lifespan (Mai and Breeden, 1997, Choi et al., 2013, Miles et al., 2013). Null *XBP1* mutation affects *cdc13-1* and *yku70*∆ growth and therefore Xbp1 might have a role in telomere biology. The mechanisms of Xbp1 function are not understood. It might be possible that transcription factor regulates transcription of DDR or checkpoint genes in response to telomere stress.

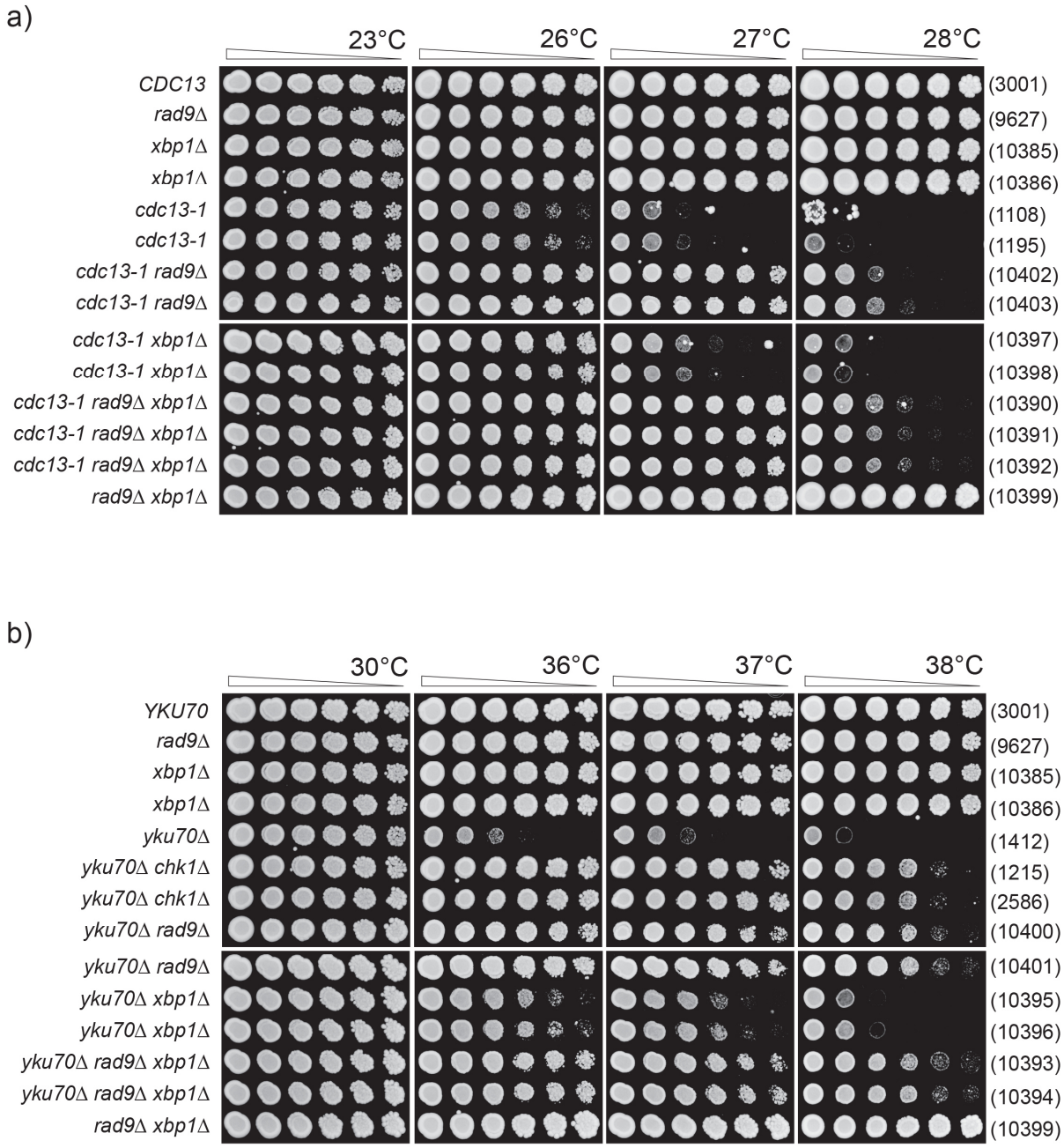


**Figure 47. Xbp1 slightly affects fitness of *cdc13-1* and *yku70*Δ mutants**

a-b) Spot tests done as in Figure 9. Strains in a) were grown on one rectangular plate. Strains in b) were grown on one rectangular plate. Spot tests in a) and b) were performed on different days. The relevant genotypes of the strains are indicated on the left, strain numbers on the right; strain details are in Appendix A.

a) The effect of *xbp1*Δ on *cdc13-1* and *cdc13-1 rad9*Δ mutants.

b) The effect of *xbp1*Δ on *yku70*Δ and *yku70*Δ *rad9*Δ mutants.

### 5.4 Uls1 similarly affects fitness of *stn1-13, cdc13-1* and *yku70*Δ mutants

It was suggested that in fission yeast SUMOylation of Tpz1 (TPP1 orthologue) inhibits telomerase and restricts telomere elongation through stimulation of Stn1-Ten1 association with telomeres (Garg et al., 2014). Stn1, together with Cdc13 and Ten1, forms the CST complex which binds telomeric ssDNA (Grandin et al., 1997, Grandin et al., 2001). Stn1, apart from a telomere capping function, was shown to interact with Pol12, a subunit of DNA Pol α, in telomere length regulation (Grossi et al., 2004). I analyzed the effect of defective SUMOylation on *stn1-13* fitness in budding yeast by deleting *uls1*Δ in *stn1-13* background. *STN1* is an essential gene (Grandin et al., 1997) therefore a ts allele, *stn1-13*, defective in telomere capping, was used. The effects of *uls1*Δ on *stn-13,* as well as on *cdc13-1* and *yku70*Δ growth were analyzed by spot tests (Fig. 48).

Two *stn1-13* mutants were significantly different from each other; one strain was able to grow at 38°C, while the other one did not grow at 37°C (Fig. 48a). All strains used in Figure 47 have *RAD5* gene, apart from the fitter *stn1-13* strain which contains *rad5-535* mutation. *stn1-13 rad5-535* strain was used as a second control strains of *stn1-13* mutation. It was not my intention to test the effect of *rad5-535* mutation on *stn1-13* because I assumed *rad5-535* has no effect on *stn1-13* growth, as it did not significantly affect the growth of *yku70*Δ mutants in Figure 15 (section 3.1.5). Apparently, *rad5-535* mutation strongly affects the growth of *stn1-13* and it would be interesting to investigate the mechanisms for *stn1-13* suppression by *rad5-535.* However, in this section I describe the effect of *uls1*Δ on *stn13-1,* and therefore I will compare *stn1-13* mutant (DLY9898), and not *stn1-13 rad5-535* double mutant (DLY8993), with other strains.

Deletion of *ULS1* suppressed the *stn1-13* growth defect at 36-37°C (Fig. 48a). In contrary, *rad9*Δ decreased the fitness of *stn1-13* and *stn1-13 uls1*Δ at higher temperatures. I conclude that Uls1 and Rad9 have different roles in *stn1-13* strains; Uls1 has an inhibitory role on growth of *stn1-13* mutants, while Rad9 facilitates *stn1-13* viability. *uls1*Δ slightly suppressed *cdc13-1* ts at 27-28°C, but the suppression was much weaker than of *rad9*Δ mutation (Fig. 48b). *uls1*Δ did not affect the fitness of *cdc13-1 rad9*Δ double mutants. I conclude that Uls1 and Rad9 may function in the

same pathway in *cdc13-1* strains. Uls1 may also contribute to Rad9-dependent checkpoint pathway, but this hypothesis was not tested.

a) *uls1Δ stn1-13*

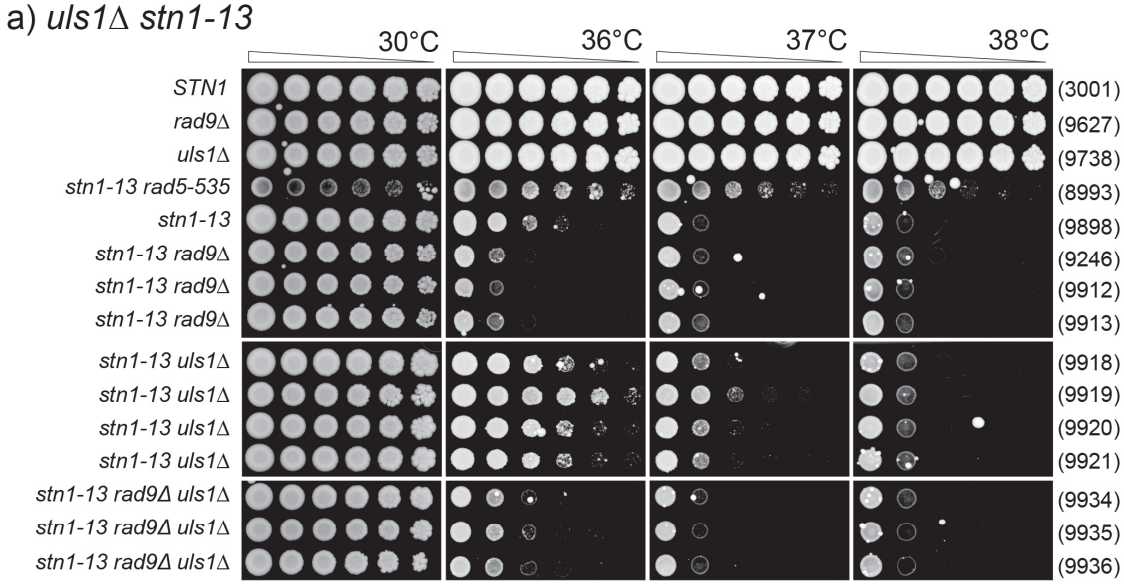


b) *uls1Δ cdc13-1*

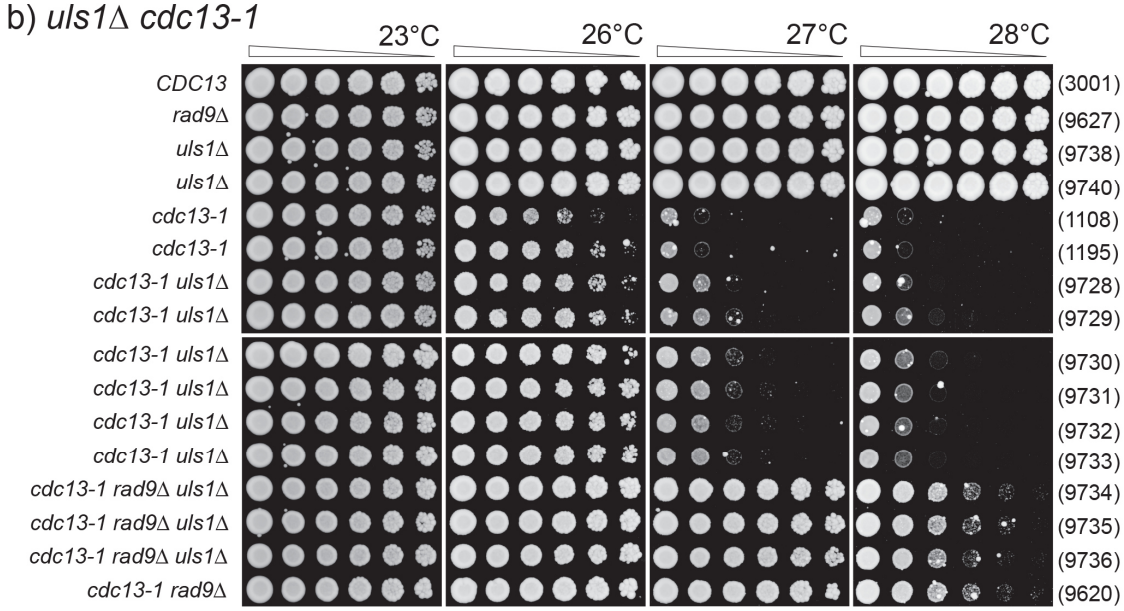


c) *uls1Δ yku70Δ*

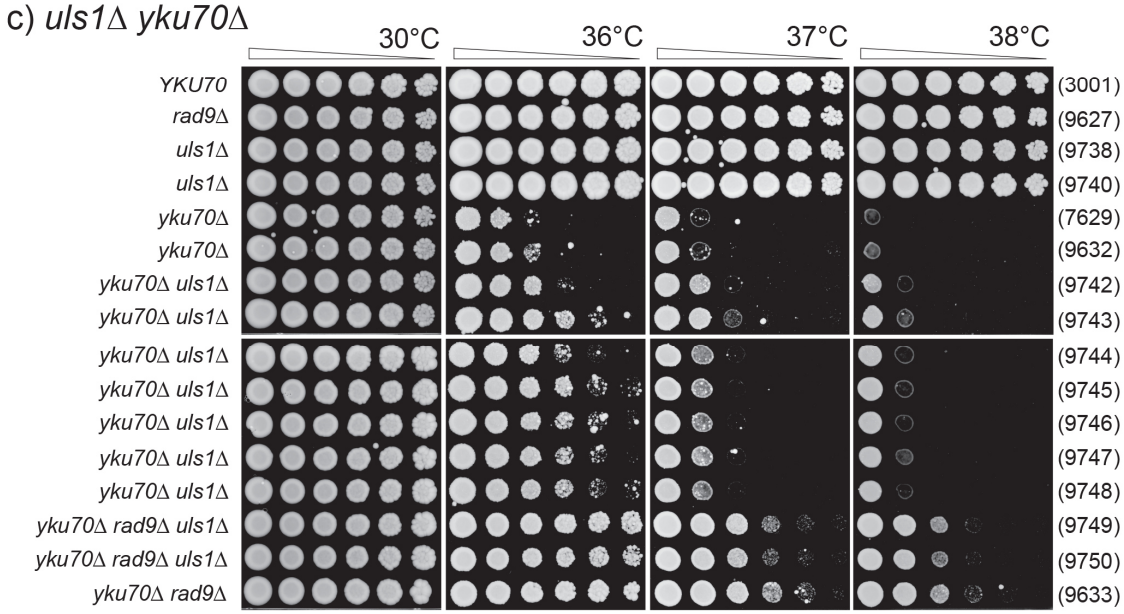

**Figure 48. Uls1 affects fitness of *stn1-13, cdc13-1* and *yku70*△ mutants**

a-c) Spot tests done as in Figure 9. Strains in a)-c) were grown on single rectangular plates. Spot tests in a), b) and c) were performed on different days. All strains are *RAD5* unless otherwise indicated. The relevant genotypes of the strains are indicated on the left, strain numbers on the right; strain details are in Appendix A.

a) The effect of *uls1*△ on *stn1-13* and *stn1-13 rad9*△ mutants.

b) The effect of *uls1*△ on *cdc13-1* and *cdc13-1 rad9*△ mutants.

c) The effect of *uls1*△ on *yku70*△ and *yku70*△ *rad9*△ mutants.

*uls1*Δ slightly suppressed *yku70*Δ defect at 36-38°C, but the suppression was much weaker than of *rad9*Δ mutation (Fig. 48c). *uls1*Δ did not affect the fitness of *yku70*Δ *rad9*Δ double mutants. The same conclusions could be drawn as described for *cdc13-1;* Uls1 and Rad9 may function in the same pathway, or Uls1 can contribute to the function of Rad9.

I confirmed the genome-wide results that *uls1*Δ suppressed the fitness of *stn1-13* (Fig. 45b). In contrast to genome-wide screen (Fig. 45a and c) I observed that *uls1*Δ also slightly suppressed the fitness of *cdc13-1* and *yku70*Δ mutants. I also observed that *RAD9* deletion enhances growth defect of *stn1-13* strains. My observations are consistent with previous observations (M. Greetham, PhD thesis). It was suggested that the different effect of Rad9 on Stn1 and Cdc13 is due to the fact that Stn1 employs a separate capping mechanism (Petreaca et al., 2007).

Ubiquitin ligases, e. g. Uls1, bind polysumoylated chains attached to proteins and mediate polyubiquitination of those proteins and their subsequent targeting to the proteasome for degradation (Fig. 49) (Sriramachandran and Dohmen, 2014). Rfp1 and Rfp2, which share functional similarity with Uls1, function in DNA repair in fission yeast (Kosoy et al., 2007, Galanty et al., 2012). Uls1 also functions in DNA repair in budding yeast; the ligase can partially substitute Rdh54 and Rad54, the two DNA recombination proteins, in the removal of toxic, damage-associated Rad51-DNA complexes (Shah et al., 2010, Chi et al., 2011).

Uncapped telomeres of *cdc13-1, stn1-13* and *yku70*Δ mutants resemble DSBs, which triggers DNA damage responses and repair. Perhaps in the absence of ubiquitin ligase Uls1, defective protein-DNA complexes (e.g. mutated Cdc13-1 protein bound to telomeric ssDNA) are not polyubiquitinylated and targeted for the proteasomal degradation. As a consequence, mutated proteins, like Cdc13-1, may still be attached to DNA and exhibit the remnant function, thus permitting cells' growth at elevated temperature.

It was proposed that Uls1 functions in removing non-functional poly-SUMOylated Rap1 proteins from telomeres to ensure NHEJ inhibition (Lescasse et al., 2013). Sine Yku70 is a key player in NHEJ repair pathway, it might be possible that there is an

interaction between Uls1 and Yku70 in inhibiting the NHEJ at telomeres, or elsewhere in the genome, which remains to be tested.

Rad5 is a DNA helicase/ubiquitin ligase which is involved in postreplication repair and promotes synthesis of polyubiquitin chains (Fig. 50) (Torres-Ramos et al., 2002, Blastyak et al., 2007, Carlile et al., 2009, Chang and Cimprich, 2009). Strikingly, a *stn1-13 rad5-535* strain has similar phenotype to *stn1-13 uls1*Δ (Fig. 48a), which reveals that different ubiquitin ligases might affect *stn1-13* similarly (Fig. 49). This hypothesis was not tested, and more *stn1-13 rad5-535* should be spotted to confirm the ability of double mutants to grow at higher temperatures..

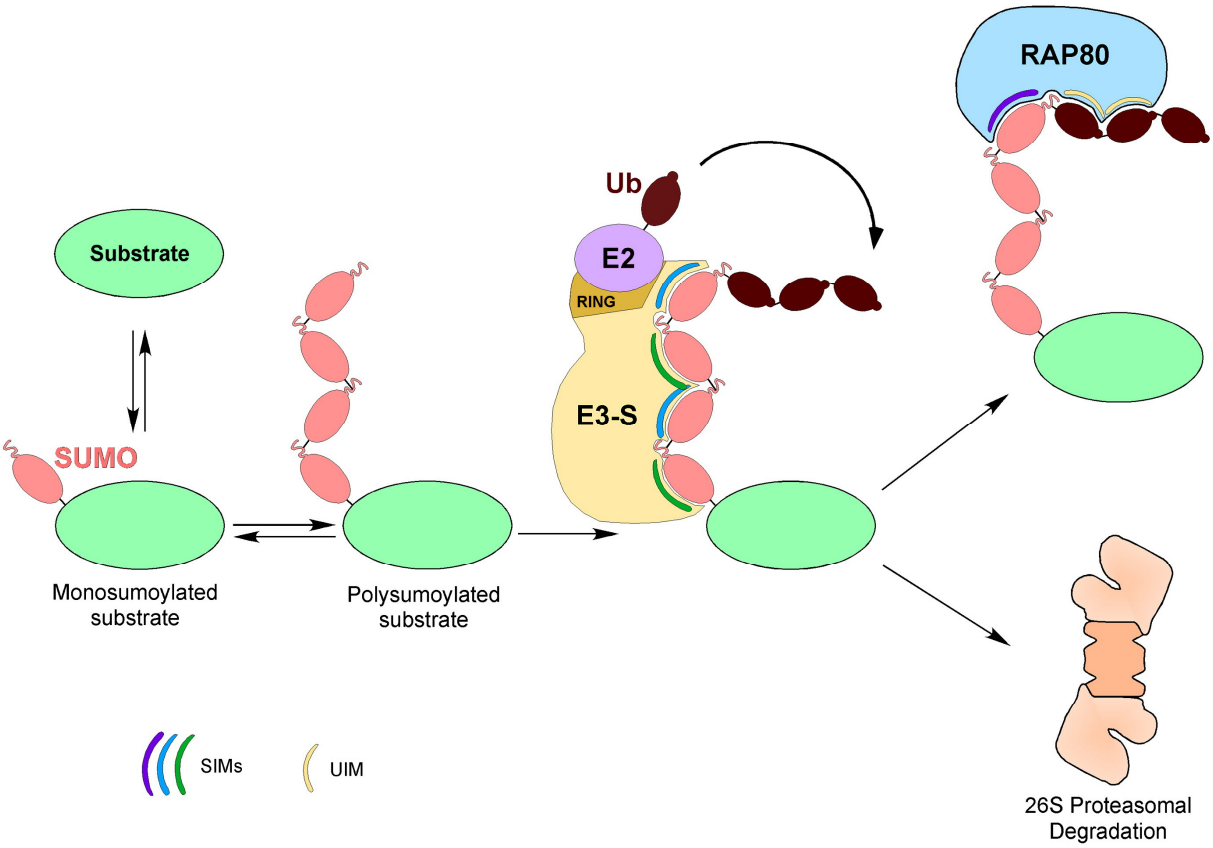


**Figure 49. Role of SUMO-ubiquitin hybrid conjugates in protein targeting.** Figure and text adapted from (Sriramachandran and Dohmen, 2014), Figure 2. Depicted is a model illustrating targeting of sumoylated forms of a substrate mediated by ubiquitin ligases (E3) for sumoylated proteins (ULSs or E3-S). A mono-sumoylated form of a substrate can either be desumoylated by an ULP/SENP enzyme or be polysumoylated. The substrate-attached SUMO chain is recognized by multiple SUMO interaction motifs (SIMs) of the ULS enzyme, a RING finger protein that, in conjunction with a ubiquitin-conjugating enzyme (E2) attaches additional ubiquitin (Ub) moieties to the already SUMO modified substrate. The ubiquitin modification may finally result in targeting of the substrate to the proteasome (lower part). As an alternative (upper part), a substrate carrying a hybrid SUMO-ubiquitin chain is recognized by a protein such as Rap80 (a subunit of the Brca1 complex) bearing a SIM as well as ubiquitin interaction motifs (UIMs). This mechanism was shown to mediate recruitment of the Brca1-A complex to the sites of DNA damage, where such hybrid conjugates are generated as the result of the activity of the ULS Rnf4. ULP, SENP or SUSP - SUMO isopeptidases.

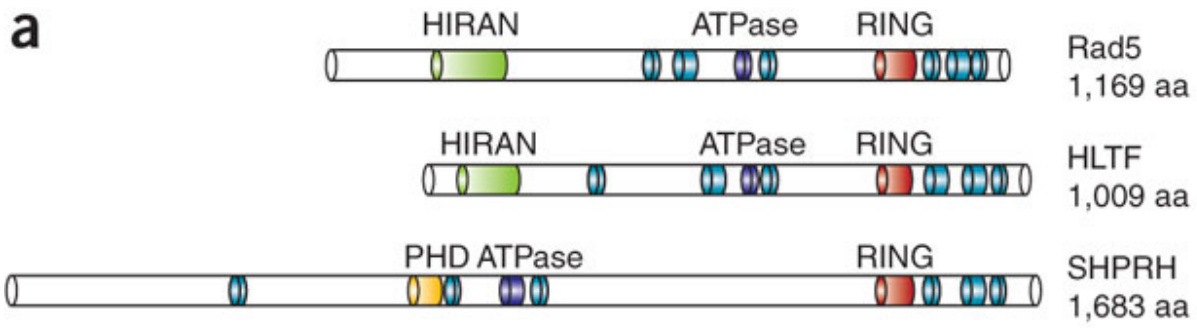


**Figure 50. Domain architecture of the E3 ubiquitin ligase Rad5 and its putative orthologs SHPRH and HLTF.**

Figure and text adapted from (Chang and Cimprich, 2009), Figure 4a.

a) Structural comparisons between *S. cerevisiae* Rad5 and its putative human orthologs, HLTF and SHPRH. Blue and purple modules represent the seven helicase motifs characteristic of the SWI/SNF2 family of ATP-driven motor proteins. Although these motifs are spread over the length of the protein, they are collectively referred to as a helicase domain. Other domain names and descriptions are as listed through the US National Center for Biotechnology Information conserved domain database and are described in the text. *HIRAN* - a hypothetical domain found in a group of known chromatin/DNA binding proteins, which suggests that it could be important for recognition of damaged DNA or stalled replication forks; *RING* - domain necessary for ubiquitination.

### 5.5 Irc5 and Rad1 do not affect the growth of *cdc13-1* and *yku70*Δ mutants

Although *IRC5 and RAD1* did not appear as suppressors or enhancers in the high-throughput screen, they were shown to function in DNA damage repair or DNA replication, cancer development and aging (Tomkinson et al., 1993, Zhu et al., 2003, Alvaro et al., 2007, von Eyss et al., 2012). The role in caner and aging was an indication for potential function of *IRC5* and *RAD1* in telomere biology, therefore I decided to test the roles of *IRC5 and RAD1* in telomere defective strains. Haploid strains with deletions of *IRC5* and *RAD1* in *cdc13-1* and *yku70*Δ backgrounds were spot tested and the effect of *rad9*Δ was compared (not shown). Deletion of *IRC5* and *RAD1* did not affect the fitness of *cdc13-1* or *yku70*Δ mutants, and triple mutants grew like *cdc13-1 rad9*Δ and *yku70*Δ *rad9*Δ strains. Therefore
I observe that Irc5 and Rad1 do not affect fitness of telomere defective strains, which is consistent with the genome-wide results presented in Figure 44 (Addinall et al., 2011). I propose that Irc5 and Rad1 are not important in telomere biology in the context of *cdc13-1* and *yku70*Δ mutants.

### 5.6 Discussion/Conclusions

The effects of deletions of genes with potential roles in telomere biology were tested in *cdc13-1* and *yku70*Δ mutants and are presented in Table 7. Hcm1 and Xbp1 affect fitness of *cdc13-1* and *yku70*Δ mutants, and this effect is much weaker than of *rad9*Δ. Hcm1 and Xbp1 are transcription factors and may regulate the transcription and gene expression of genes involved in response to defective telomeres of *cdc13-1* or *yku70*Δ strains, e .g. checkpoint genes and DDR genes (Mai and Breeden, 1997, Pramila et al., 2006, Miles et al., 2013, Rodriguez-Colman et al., 2013, Negishi et al., 2016). However, mechanisms of the transcriptional roles of Hcm1 or Xbp1 were not studied in this thesis.

| Gene name | Name description | Ortholog(s) | QFA results | Function (SGD) | Effect on *cdc13-1* | Effect on *yku70*Δ |
|---|---|---|---|---|---|---|
| ***HCM1*** | High-Copy suppressor of calmodulin | *PHA-4* (*C. elegans*) | No effect on *yku70*Δ, suppressor of *cdc13-1* | Forkhead transcription factor, telomere maintenance role | Weak suppressor | Weak suppressor |
| ***XBP1*** | XhoI site-Binding Protein | N/A | No effect on *yku70*Δ, suppressor of *cdc13-1* | Transcriptional repressor | Weak suppressor | Weak suppressor |
| ***ULS1*** | Ubiquitin Ligase for SUMO conjugates | *RFP1/2* (*S. pombe*) | No effect on *yku70*Δ and *cdc13-1* | SUMO-Targeted Ubiquitin Ligase (STUbL) | Weak suppressor § | Weak suppressor |
| ***IRC5*** | Increased Recombination Centers | *LSH, HELLS, PASG, SMARCA6* | No effect on *yku70*Δ and *cdc13-1* | Putative ATPase containing the DEAD/H helicase-related sequence motif | No effect | No effect |
| ***RAD1*** | RADiation sensitive | *XPF, ERCC4* | No effect on *yku70*Δ and *cdc13-1* | Single-stranded DNA endonuclease (with Rad10p); involved in NER and DSBs repair | No effect | No effect |

**Table 7. The effect of each gene deletion on *cdc13-1* and *yku70*Δ mutants**
§ - the same effect on *stn1-13* strain.

A SUMO-targeted ubiquitin ligase Uls1 has a role in DNA repair (Shah et al., 2010, Chi et al., 2011). Since *uls1*Δ slightly suppresses *stn1-13, cdc13-1* and *yku70*Δ mutants I conclude that Uls1 functions at telomeres. Defective telomeres resemble DSB damage, hence the role of Uls1 in *cdc13-1, stn1-13* and *yku70*Δ mutants might affect the DNA repair machinery e.g. by inhibiting NHEJ at telomeres (Lescasse et al., 2013). Interestingly, it was found that SUMOylation of Cdc13 promotes the association of Cdc13-1 with Stn1 to inhibit telomerase function (Hang et al., 2011). SUMOylation-mediated accumulation of Stn1-Ten1 to telomeres could also serve as a regulatory mechanism for controlling telomerase activity in yeast (Miyagawa et al., 2014, Garg et al., 2014). Fission yeast Tpz1, an orthologue of TPP1, along with Rap1 and Poz1, facilitates the connection between Taz1 and Pot1 through protein–protein interactions (Miyoshi et al., 2008). Tpz1 SUMOylation prevents telomerase accumulation at telomeres by promoting recruitment of Stn1-Ten1 to telomeres (Miyagawa et al., 2014). It might be therefore possible that an interaction between Uls1 and Stn1, Cdc13 and Yku70 is important for telomere length homeostasis in

yeast. Strikingly, *stn1-13 rad5-535* strain exhibit similar growth pattern to *stn1-13 uls1*Δ*,* which suggests that a role of ubiquitin ligases might be conserved in the context of *stn1-13* mutant.

Rad1 and Irc5 did not affect fitness of *cdc13-1* and *yku70*Δ mutants. Rad1 is an endonuclease, which is involved in NER and DNA repair, and was shown to process ssDNA overhangs at uncapped human telomeres (Tomkinson et al., 1993, Ivanov and Haber, 1995, Zhu et al., 2003). Irc5 is a putative DNA helicase involved in HR (Shiratori et al., 1999, McCarroll et al., 2004). I conclude however that Irc5 and Rad1 have no role in telomere biology in the context of *cdc13-1* and *yku70*Δ strains.

# Chapter 6. Hormesis and adaptation to low-doses of stress

In recent years multiple observations of positive effects of low dose stress (e. g. UV radiation or toxic compounds) on organismal fitness were reported (Ermolaeva et al., 2013, Calabrese et al., 2015, Le Bourg, 2015). Small doses of stress seem to have a protective role when pre-treated cells and organisms are exposed to higher doses of the same or different stress, in contrast to cells/organisms that were never exposed to stress. In this thesis yeast with defects in cell division cycle, *cdc13-1* and *cdc15-2*, were used to test the effect of low-dose telomeric and mitotic kinase activity stresses, respectively.

The data obtained from studies on yeast adaptation to low-dose stress were published (Markiewicz-Potoczny and Lydall, 2016), and are presented in section 6.1 of this thesis. Figures are numbered consecutively with the Figure numbering from the publication (Figures 1 - 6, Supplementary Table 1 and Supplementary Figures 1 - 6).

## 6.1 Costs, benefits and redundant mechanisms of adaption to chronic low-dose stress in yeast

**Keywords:** Adaptation, low-dose, stress, fitness, yeast

**List of abbreviations**

cdc – cell division cycle
ESR – environmental stress response
CSR **–** cellular stress response
DDR – DNA damage response
NMD – nonsense mediated RNA decay

### *6.1.1 Abstract*

All organisms live in changeable, stressful environments. It has been reported that exposure to low-dose stresses or poisons can improve fitness. However, examining the effects of chronic low-dose chemical exposure is challenging. To address this issue we used temperature sensitive mutations affecting the yeast cell division cycle

to induce low-dose stress for 40 generation times, or more. We examined *cdc13-1* mutants, defective in telomere function, and *cdc15-2* mutants, defective in mitotic kinase activity. We found that each stress induced similar adaptive responses. Stress-exposed cells became resistant to higher levels of stress but less fit, in comparison with unstressed cells, in conditions of low stress. The costs and benefits of adaptation to chronic stress were reversible. In the *cdc13-1* context we tested the effects of Rad9, a central player in the response to telomere defects, Exo1, a nuclease that degrades defective telomeres, and Msn2 and Msn4, two transcription factors that contribute to the environmental stress response. We also observed, as expected, that Rad9 and Exo1 modulated the response of cells to stress. In addition we observed that adaptation to stress could still occur in these contexts, with associated costs and benefits. We conclude that functionally redundant cellular networks control the adaptive responses to low dose chronic stress. Our data suggests that if organisms adapt to low dose stress it is helpful if stress continues or increases but harmful should stress levels reduce.

### *6.1.2 Introduction*

All organisms, from single celled bacteria and yeasts to complex mammals, experience a variety of environmental conditions, many of which are stressful. Organisms have evolved to adapt to different stresses and to thrive in varying conditions (Kirkwood, 2005). Experiments in bacteria, yeast, worms, fish and mammals have revealed that different types of stress each induce common responses, termed the environmental stress response (ESR) or the cellular stress response (CSR) (Gasch et al., 2000, Kultz, 2005, Lopez-Maury et al., 2008, Schulte, 2014, Young et al., 2013, de Nadal et al., 2011, Tauffenberger and Parker, 2014). Responses induced by the ESR/CSR affect oxidative stress responses, protein folding, protein degradation, carbohydrate and fatty acid metabolism, DNA damage responses and intracellular signalling (Gasch, 2002, Kultz, 2005, Hahn et al., 2013, Fulda et al., 2010). Organisms exposed to stress often become resistant to higher levels of the same stress and cross-resistant to other stresses (Lewis et al., 1995, Gasch, 2007, Milisav et al., 2012, Long et al., 2015, Tauffenberger and Parker, 2014). The evidence is that a complex network of interactions regulates general as well as more specific responses to stress (Berry et al., 2011, Guan et al., 2012, Chasman et al., 2014).

There is evidence that low-level stress can improve aspects of organismal fitness. In 1888 it was reported that yeast cells grew better when exposed to low-doses of poisons, such as arsenic trioxide, than in the absence of poison (Schulz, 1888). This type of dose-response relationship, in which exposure to low-doses of a “poison” (e.g. environmental factor or chemical agent) improves some aspect of the fitness of an organism, is known today as hormesis. Hormesis has been reported in a variety of different systems from bacteria to yeast to vertebrates (Calabrese and Baldwin, 2003, Calabrese, 2004, Calabrese et al., 2007, Mattson, 2008, Costantini et al., 2010, Ermolaeva et al., 2013, Cope et al., 2014, Calabrese et al., 2015). A hormesis type response can often be observed in human cells growing in culture. Figure 1, adapted from Cope *et al*. (Cope et al., 2014), shows an example where growth of two human cancer cell lines, as measured by tritiated thymidine incorporation, is increased by low-doses of a Tor kinase inhibitor (Fig. 1) (Cope et al., 2014). Numerous other studies with different biological end points, such as the effects of gamma radiation on mouse tumour formation or of DNA damage on worm longevity, support the idea that low-dose stresses can have a positive effect on organism fitness (Calabrese and Baldwin, 2003, Calabrese, 2004, Ermolaeva et al., 2013, Calabrese et al., 2015).

It is suggested that the biochemical mechanisms that explain hormesis are adaptive stress responses (Stranahan and Mattson, 2012, Perry et al., 2014, Singh et al., 2015). Any amount of extrinsic stress will cause harm, for example by damaging DNA or other cellular components. However, it is thought up-regulation of maintenance and repair systems, in response to low-dose stress, protects not only from the extrinsic stress but also from intrinsic stresses that affect carcinogenesis, ageing or other aspects of organismal fitness (Haendeler et al., 2004, Watson et al., 2004, Christmann and Kaina, 2013). If so, then perhaps it is mild induction of the ESR/CSR that explains the hormesis response (Douglas, 2008, Milisav et al., 2012). However, up-regulation of maintenance and repair systems must come at some type of metabolic cost, otherwise organisms would never reduce maintenance and repair levels (Kirkwood, 2005). These arguments suggest that hormesis is unlikely to occur very frequently.

When measuring the positive or negative effects of low-dose stress it is important to carefully consider what end point is measured. For example, mutations that extend

lifespan in worms, and are considered positive by this criterion, also dramatically reduce the ability of worms to produce offspring in the laboratory environment and therefore have clear negative effects too (Walker et al., 2000, Jenkins et al., 2004). Moreover, the biochemical mechanisms underlying any positive responses to low dose stresses are poorly understood (Schumacher, 2009, Vaiserman, 2010, Wiegant et al., 2012). The lack of good biochemical understanding of the response to chronic low-dose stresses or poisons stems, in part, because the effects induced are small and difficult to measure (Calabrese, 2004, Peake et al., 2015). Another difficulty, particularly for studies on the effects of chemicals, is that low-dose impurities, or chemical break down products, might confound interpretation. For example, at low concentrations the poison methotrexate improves viability of breast cancer cell lines (Kelly and Owusu-Apenten, 2015). If methotrexate were contaminated with the chemically similar growth promoter, folate, then this might make interpretation of any positive effects of methotrexate difficult to distinguish from the effects of lower concentrations of the contaminant folate.

In this paper we carefully examined the responses of budding yeast, *Saccharomyces cerevisiae*, to chronic low-dose stress. Budding yeast is perhaps the best-studied model organism and much is known about its responses to stress (Botstein and Fink, 2011). Although growth of yeast in the laboratory is artificial, for example with unlimited food supply or constant temperature, laboratory growth conditions mimic part of the natural yeast life cycle. It is thought that when yeast cells arrive on fruit, after being carried there by wasps, they divide rapidly from single cells (Liti, 2015). For this reason the rapid growth of yeast cultures in the laboratory is a biologically relevant measure of fitness.

To study the effects of chronic stress in yeast we used genetic mutations, rather than chemicals, to poison different aspects of the cell cycle. Temperature sensitive *cdc* (**c**ell **d**ivision **c**ycle) mutations affecting different aspects of cell cycle progression were used (Hartwell et al., 1973, Weinert and Hartwell, 1993). We considered *cdc* mutations particularly attractive tools for this purpose because the dose of stress can be simply adjusted by controlling the culture temperature. The higher the temperature the more "poisoned" cell cycle events become. Furthermore, since each cell in the population carries the same mutation we can be sure that each cell in the environment is stressed to a similar extent. *cdc13-1* mutants are defective in

telomere related functions. At high temperatures telomeres of *cdc13-1* cells induce a DNA damage response, akin to the response to DNA double strand breaks elsewhere in the genome (Garvik et al., 1995, Lydall, 2009). In this sense, the effect of *cdc13-1* mutation mimics that of genotoxic agents. Temperature sensitive *cdc15-2* mutants are defective in a kinase required for exit from mitosis and arrest cell division in late anaphase at high temperatures (Schweitzer and Philippsen, 1991). Using these yeast genetic tools we asked: Does adaptation to chronic low-dose stress have a positive effect, a negative effect, neither, or both? We also addressed whether adaptation to stress is reversible and dependent on specific pathways.

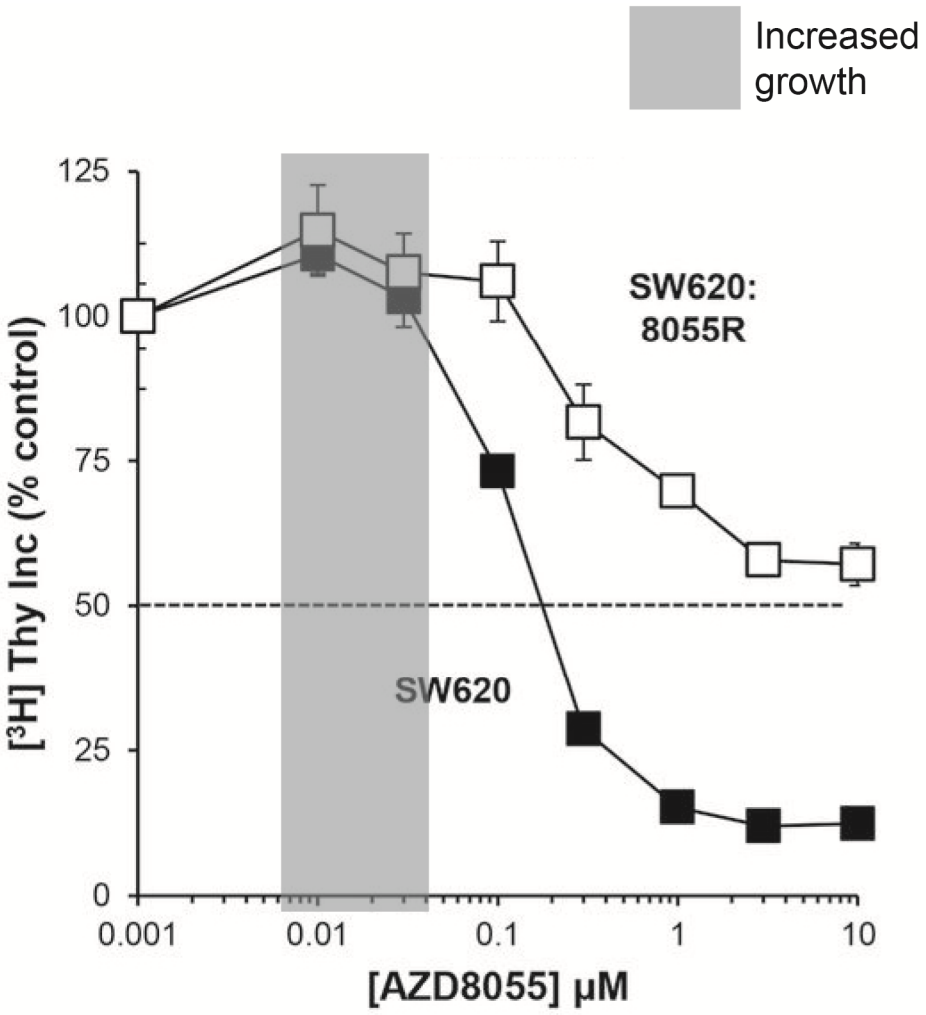


**Figure 1. Hormetic response to mild stress in human cell lines**

Human SW620 and SW620:8055R cell lines, the parental sensitive and a derived resistance line, were exposed to increasing concentrations of TOR kinase inhibitor, AZD8055, for 24 hours. Proliferation was assayed by [$^3$H]thymidine incorporation. This figure is based on Figure 2A of Cope *et al.* (Cope et al., 2014). We added a grey box to highlight the area of increased fitness.

### *6.1.3 Results*

#### *cdc13-1* mutants adapt to chronic telomeric stress

To examine the response of yeast cells to chronic low-dose of telomere stress we used strains containing the *cdc13-1* allele, affecting the essential telomere capping protein Cdc13. *cdc13-1,* a point mutation, causes a P371S amino acid change and this induces temperature dependent Cdc13-1 protein degradation (Hughes et al., 2000, Gardner et al., 2005). In our lab *cdc13-1* strains are routinely cultured at 23°C (a permissive temperature). However, *cdc13-1* shows synthetic genetic interactions with mutations affecting the KU or MRX complexes at this temperature and thus we know that Cdc13-1 is not fully functional at 23°C (Polotnianka et al., 1998, Foster et al., 2006). Therefore we also sometimes culture *cdc13-1* strains at 20°C, where Cdc13-1 is more functional. At higher temperatures *cdc13-1* mutants have dysfunctional telomeres, generate long telomeric 3' ssDNA G-tails and activate Rad9-dependent cell cycle arrest (Garvik et al., 1995, Lydall and Weinert, 1995). We have previously reported that *cdc13-1* mutants cultured at 30°C, a normal temperature for growing yeast, induce the ESR (Greenall et al., 2008).

It is know that many recessive, loss of function mutations, for example affecting DNA damage response (DDR) or nonsense mediated RNA decay (NMD) pathways, improve the fitness of *cdc13-1* strains grown at >26°C (Weinert et al., 1994, Addinall et al., 2011). Therefore we performed all experiments in diploid cells to reduce the chance that recessive loss of function mutations affecting DDR, NMD or other genes were selected during our experiments. We passaged *cdc13-1* cells at 23°C, as usual, or at 25°C, a slightly higher temperature, to induce chronic low-dose telomere stress. 25°C slightly reduced the fitness (colony size) of *cdc13-1* mutants grown on agar plates, and therefore 25°C was considered the maximum permissive temperature (Garvik et al., 1995) (Supplementary Fig. 1A). Interestingly, there was heterogeneity in colony size after the first passage at 25°C, but this disappeared by the second passage (Fig. 2B). This suggests that all cells in the population have adapted to the increased stress by the second passage. The heterogeneity in colony size was never been observed when cells were passaged at 23°C (Fig. 2C).

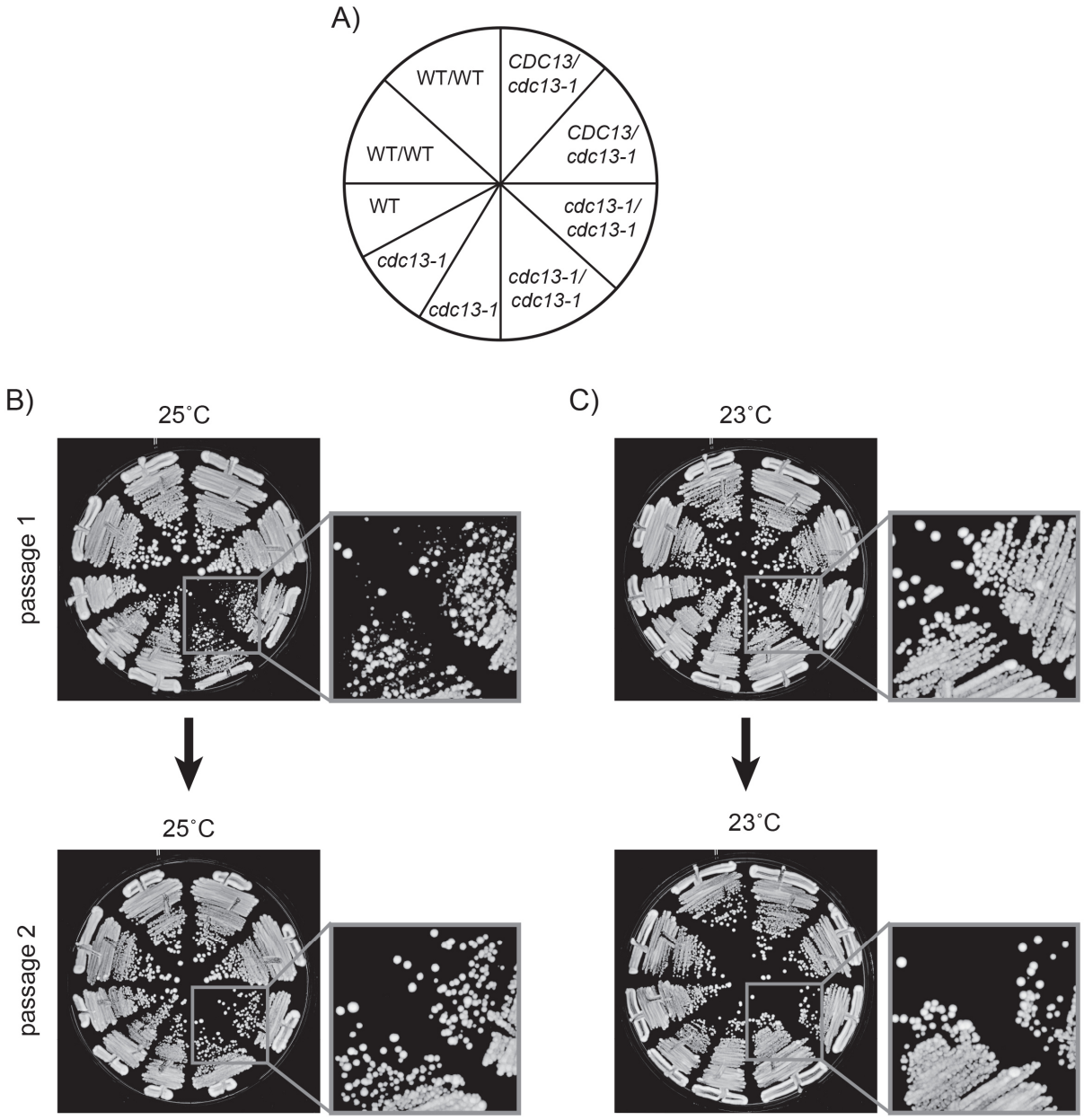


**Figure 2. Passaging procedure**

Freshly unfrozen strains were patched on YEPD agar plates and incubated at 23°C for 3 days, then passaged at 23°C or 25°C on YEPD agar plates as shown. 5 - 10 colonies from each genotype were pooled at each passage. Strains were: DDY81, 739, 738, 737, 736, 735, DLY1108, 1195, 3001. A) Genotypes of strains streaked on agar plates. B) Cells passaged for two passages at 25°C. C) Cells passaged for two passages at 23°C. DDY strains are diploids. DLY strains are haploids.

Importantly, we never observed, at any temperature or time, that *cdc13-1* cells grew better than *CDC13* cells grown on the same plate (Fig. 3). By this criterion we see no evidence for a hormetic effect in this experimental system. In other words we see no evidence that exposure to chronic low-dose telomere stress improved fitness. However, we did observe that *cdc13-1* strains previously passaged at 25°C grew better at 26°C or 27°C than genetically identical strains passaged at 23°C (Fig. 3). We conclude that, as expected, adaptation to chronic mild telomere stress improves the fitness of strains exposed to even higher levels of telomere stress.

Interestingly, we observed that *cdc13-1* strains, previously passaged at 25°C, grew less well at 20°C than genetically identical strains previously passaged at 23°C. This phenomenon is telomere stress related, rather than temperature stress related, since equivalent *CDC13* cells, previously passaged at 23°C, were fully fit at 20°C. The simplest interpretation of these data is that the adaptation to telomere stress caused by growth at 25°C comes at a cost (trade off) affecting growth rate when telomere stress is reduced. Thus, in this context, adaptation to chronic telomere stress reduces fitness and is, in a sense, the opposite of hormetic.

Finally we tested whether the positive and negative effects of passaging *cdc13-1* cells at 25°C were reversible. Cells grown for 7 passages at 25°C were grown for a further three passages at 23°C before fitness was assessed. At 26°C such cells exhibited an intermediate growth phenotype, somewhere between the fitness of strains previously grown at 23°C or 25°C. Thus adaptation to telomere stress seems to be at least partially reversible. As predicted, the haploid *cdc13-1* strain cultured at 25°C and then at 23°C did not reverse its ability to grow well at 26°C and above. Presumably this strain accumulated genetic mutations during growth at 25°C that suppressed *cdc13-1* defects. Interestingly, the cost of adaptation to growth at 25°C, seen at 20°C, seems to be fully reversed by growth for 3 passages at 23°C. Again, therefore, adaptation seems to be reversible and is, by this criterion, epigenetic rather than genetic.

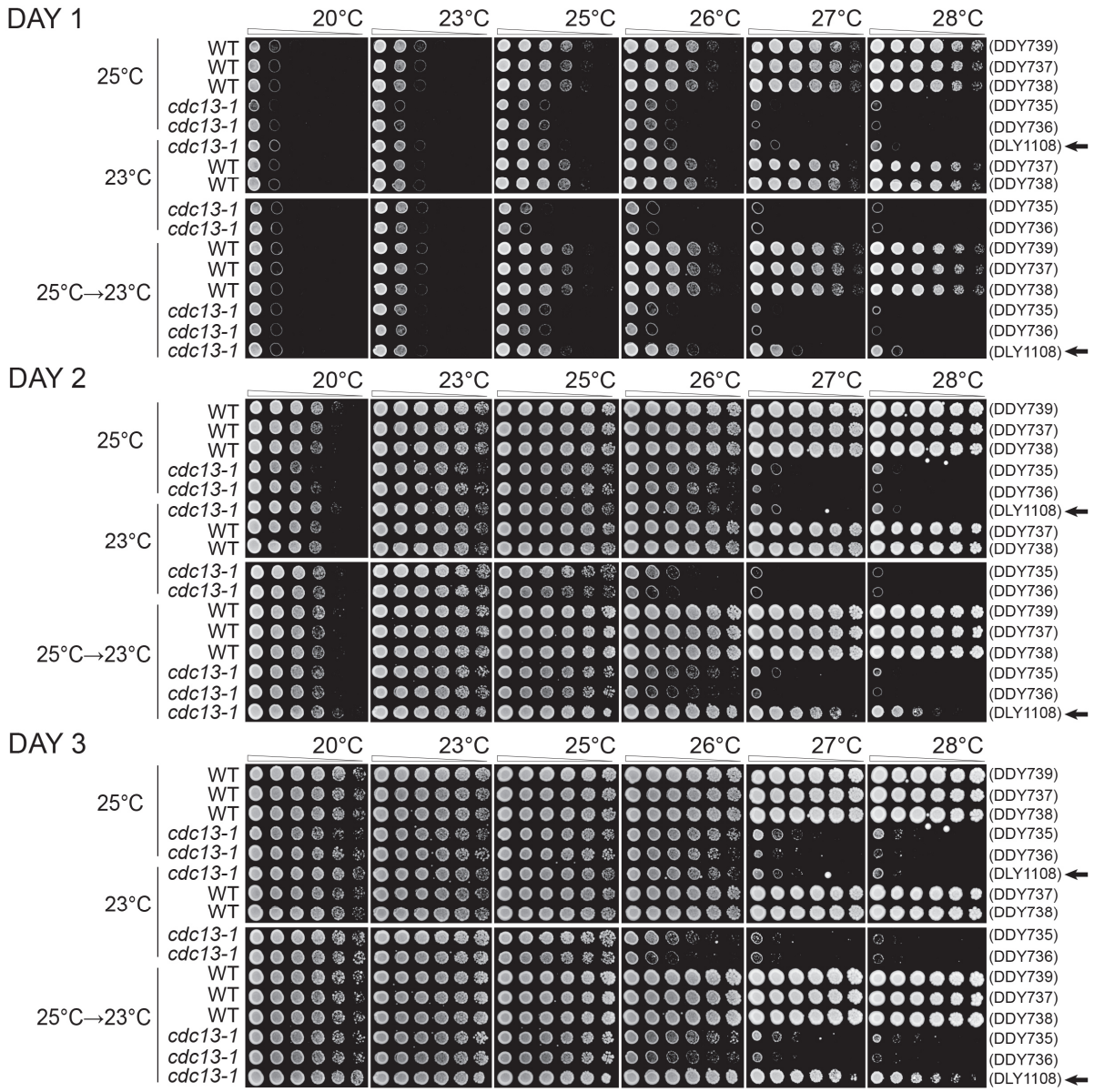


**Figure 3. The effects of adaptation to low-level of telomere stress in *cdc13-1* mutants**

Diploid strains with the genotypes indicated were grown on solid agar plates for 10 passages at 23°C, 10 passages at 25°C, or for 7 passages at 25°C followed by 3 passages at 23°C as indicated on the left of the Figure. Strains (DDY735, 736, 737, 738, 739 and DLY1108) were then inoculated into liquid and grown overnight at 23°C or 25°C. Fivefold dilution series of strains were set up in 96 well plates transferred to several independent solid YEPD agar plates using a pin tool. Individual plates were incubated at different temperatures, indicated across the top of the Figure, and photographs taken after 24, 48 and 72 hours of incubation. Arrows on the right indicate haploid cultures.

**Adaptation to low-level of chronic telomeric stress is a robust response**

Budding yeast responses to *cdc13-1* induced telomere defects are complex and have been well studied (Weinert and Hartwell, 1993, Garvik et al., 1995, Greenall et al., 2008, Addinall et al., 2011, Holstein et al., 2014). We tested whether removal of Rad9, a central player in the response to *cdc13-1* induced telomere defects, affected adaptation. Rad9 was the first DNA damage checkpoint protein to be classified and plays at least three critically important roles in *cdc13-1* mutants. Rad9 is essential for cell cycle arrest of *cdc13-1* cells in metaphase, to inhibit ssDNA production near uncapped telomeres, and to maintain cell viability (Weinert and Hartwell, 1988, Lydall and Weinert, 1995, Zubko et al., 2004, Ngo et al., 2014). Using temperature sensitive *cdc13-1 rad9*Δ mutants we performed analogous experiments to those performed on *cdc13-1* mutants. The maximum permissive temperature of *cdc13-1 rad9*Δ mutants is about 26°C, higher than *cdc13-1* mutants, presumably because low-levels of telomere damage induced at 26°C are sufficient to activate Rad9-dependent checkpoint pathways (inducing metaphase arrest), but insufficient to cause much cell death (as judged by colony size on plates) (Supplementary Fig. 1A).

Interestingly, we observed that *cdc13-1 rad9*Δ strains adapted after two passages at 26°C, similarly to *cdc13-1* strains at 25°C (Fig. 4A-B, Supplementary Fig. 2). That is, *cdc13-1 rad9*Δ strains previously grown at 26°C grew better at higher temperatures, 28°C or 29°C, than genetically identical cells grown at 23°C (Fig. 4B). However, such cells exhibited poorer growth at lower temperatures, 20°C and 23°C. If *cdc13-1 rad9*Δ mutants were moved back from 26°C to 23°C, then the effects of adaptation were partially reversed. We conclude that *cdc13-1 rad9*Δ strains, like *cdc13-1* strains, can adapt to telomere damage and that the adaptation is reversible and comes with costs and benefits.

We also tested adaptation in the absence of Exo1, an exonuclease that degrades defective telomeres in *cdc13-1* strains (Ngo and Lydall, 2010). The maximum permissive temperature of *cdc13-1 exo1*Δ mutants is also about 26°C (Supplementary Fig. 1B). Similarly to what was observed in *cdc13-1 rad9*Δ strains, we observed that *cdc13-1 exo1*Δ strains adapted after two passages at 26°C and grew better at 27°C and 28°C but exhibited poorer growth at lower temperatures, 20°C and 23°C (Fig. 4C, Supplementary Fig. 3). When moved back from 26°C to

23°C, the effects of cells' adaptation were partially reversed. We conclude that *cdc13-1 exo1*Δ strains, like *cdc13-1* or *cdc13-1 rad9*Δ strains, can adapt to telomere damage and that the adaptation is reversible and comes with costs and benefits.

Finally we tested adaptation in the absence of Msn2/Msn4, two transcriptional activators that underlie the transcriptional response to numerous stresses (Elfving et al., 2014, Gasch et al., 2000, Martinez-Pastor et al., 1996, Sadeh et al., 2011, Berry and Gasch, 2008). The maximum permissive temperature of *cdc13-1 msn2*Δ *msn4*Δ mutants is about 25°C (Supplementary Fig. 1C). *cdc13-1 msn2*Δ *msn4*Δ strains adapted to 25°C after two passages, and grew better at 26°C, but exhibited poorer growth at lower temperatures, 20°C and 23°C (Fig. 4D, Supplementary Fig. 4). As before, the effects of adaptation were partially reversed when cells were returned from 25°C to 23°C (Fig. 4D).

In summary Figure 4 clearly shows that loss of critically important components of the DNA damage or stress induction networks, active in *cdc13-1* strains, still permits *cdc13-1* strains to adapt to stress. Thus we conclude that adaptation to chronic telomere-induced stress involves a robust network of responses.

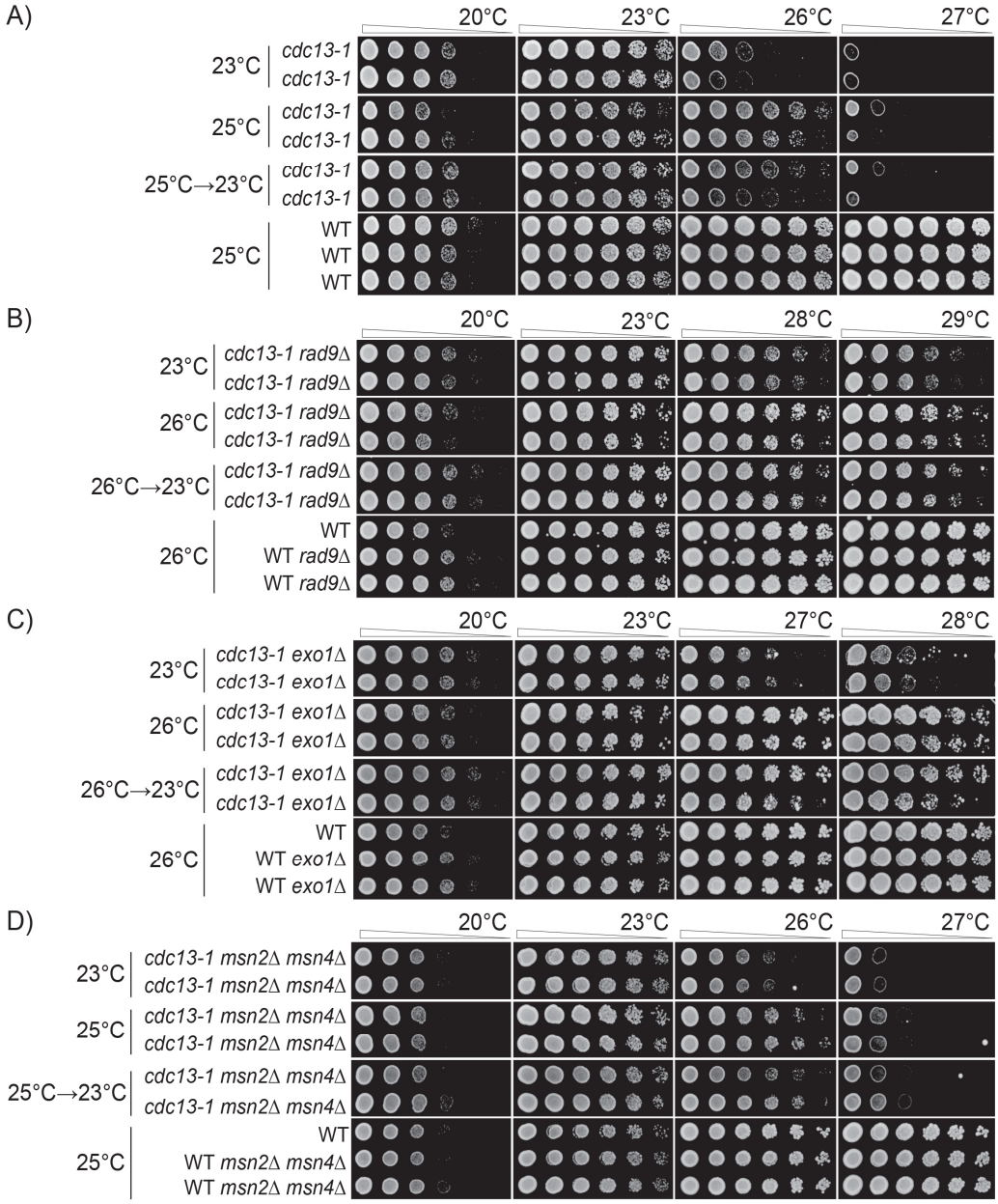


**Figure 4. Adaptation to telomere stress in the absence of key stress response proteins**

Diploid strains of different genotypes were analysed as in Figure 3 except that strains were passaged twice at high temperature (25°C or 26°C), or once at high temperature followed by a single passage at low temperature, before being spotted onto agar plates. A) Strains as in Figure 3. Strains were DDY735, 736, 737, 738 and 739. B) Strains were DDY739; 868, 869, 860 and 861. C) Strains were DDY739, 992, 993, 994 and 995. D) Strains were DDY739, 974, 975, 972, 973. All strains shown in each subsection, at each temperature, were grown on single agar plates but images have been cut and pasted to make comparisons easier. Images were taken at 48 hours of incubation. Images taken after 24, 48 and 72 hours incubation are shown in Supplementary Figures: 2, 3 and 4, respectively.

**Adaptation to mitotic kinase inhibition**

Mammalian cells exposed to low-doses of Tor kinase inhibitor grow better than cells not exposed to the inhibitor (Fig. 1) (Cope et al., 2014). We therefore extended our genetic studies to examine responses to low-level inhibition of kinase activity. We chose to examine mutations affecting the Cdc15 kinase, not a member of the Tor kinase family, but which is an essential component of the Mitotic Exit Network and is critical for the completion of mitosis (Jaspersen and Morgan, 2000, Bardin et al., 2003). Using temperature sensitive *cdc15-2* mutants we performed analogous experiments to those performed in telomere defective *cdc13-1* mutants. Since the maximum permissive temperature of *cdc15-2* mutants is about 31°C, the temperature used to cause mild stress was 30°C (Supplementary Fig. 1A, D). We determined that we could observe adaptation to growth at 30°C after as little as three passages (Fig. 5A, Supplementary Fig. 5).

We could draw very similar conclusions about how cells adapt to *cdc15-2* induced kinase defects as we had drawn earlier for *cdc13-1* mutants. We never observed, at any temperature or time, that *cdc15-2* cells grew better than *CDC15* cells grown on the same plate (Fig. 5A, Supplementary Fig. 5). By this criterion we see no evidence for a hormetic effect in *cdc15-2* strains. Analysis of *cdc15-2* mutants showed clear evidence for adaptation to kinase inhibition, a clear cost of adaption to kinase inhibition and strong evidence that adaptation was reversible (Fig. 5A). In fact, adaptation to *cdc15-2* stress seemed nearly fully reversible after two passages at 23$^{o}$C (Fig. 5A).

We also examined the effects of Msn2/Msn4 in the context of Cdc15 defects. *cdc15-2 msn2*Δ *msn4*Δ mutants adapted after two passages to 30°C, to exhibit better growth at 31°C and 32°C but poorer growth at lower temperatures, 20°C and 23°C (Fig. 5B, Supplementary Fig. 6). The effects of adaptation were partially reversed when moved from 30°C to 23°C (Fig. 5B).

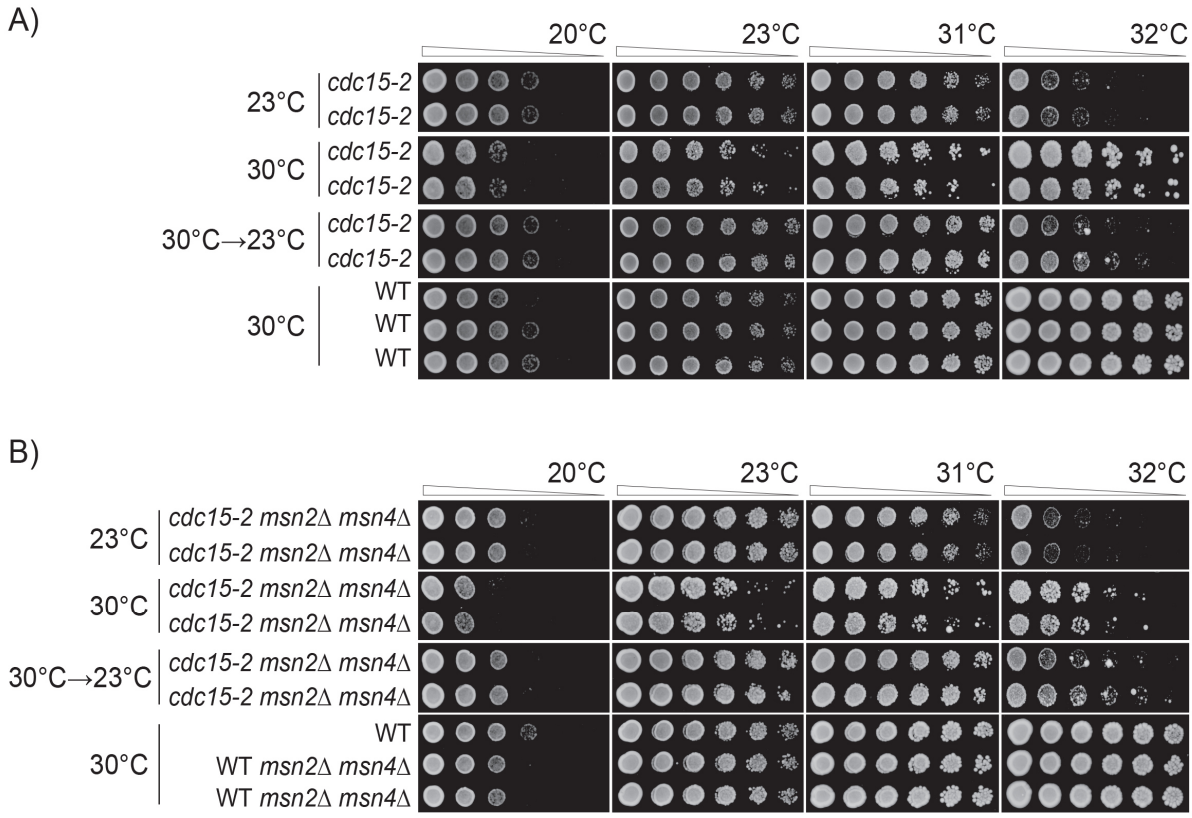


**Figure 5. Adaptation to low-level kinase inhibition in *cdc15-2* mutants**

Diploid strains of different genotypes were analysed as in Figure 3. Strains were grown for 3 passages at 23°C or 30°C on agar plates, or for 1 passage at 30°C and two at 23°C. A) Strains were DDY739; 839, 840, 841, 842. B) Strains were DDY739; 1036, 1037 1038, 1039. All strains shown in each subsection, at each temperature, were grown on single agar plates. Images taken after 24, 48 and 72 hours incubation are shown in Supplementary Figures: 5 and 6, respectively.

### *6.1.4 Discussion*

We analysed yeast mutants defective in the cell division cycle to measure the costs and benefits of adapting to chronic low-level stress. We were particularly interested to determine if we could find evidence for hormesis, which has been defined as "a low-dose stimulation or beneficial effect and a high dose inhibitory or toxic effect" (Mattson, 2008), in this simple model system. Figure 6 summarizes our observations and shows the positive and negative effects of adapting to different types of low-dose stress. We observe that previous exposure to low-dose stress improves the ability of yeast to survive higher doses of the same stress (Fig. 6, position B). However, the trade-off for adapting to low-dose stress is that cells are less fit, in comparison with unstressed cells, when grown in low stress conditions (Fig. 6, position A). We see no evidence for hormesis in this experimental system, that is that yeast cells exposed to low-dose stresses are fitter than cells not exposed to stress (Fig. 6, the predicted hormesis response curve, above the black dashed line). We cannot, of course, exclude that hormesis occurs in response to other types of stress, or could be observed if other biological end points were measured. For example, if we measured genetic stability rather than growth rate we might observe that cells with a slight induction of the DNA damage response were more stable than cells that had not induced the response.

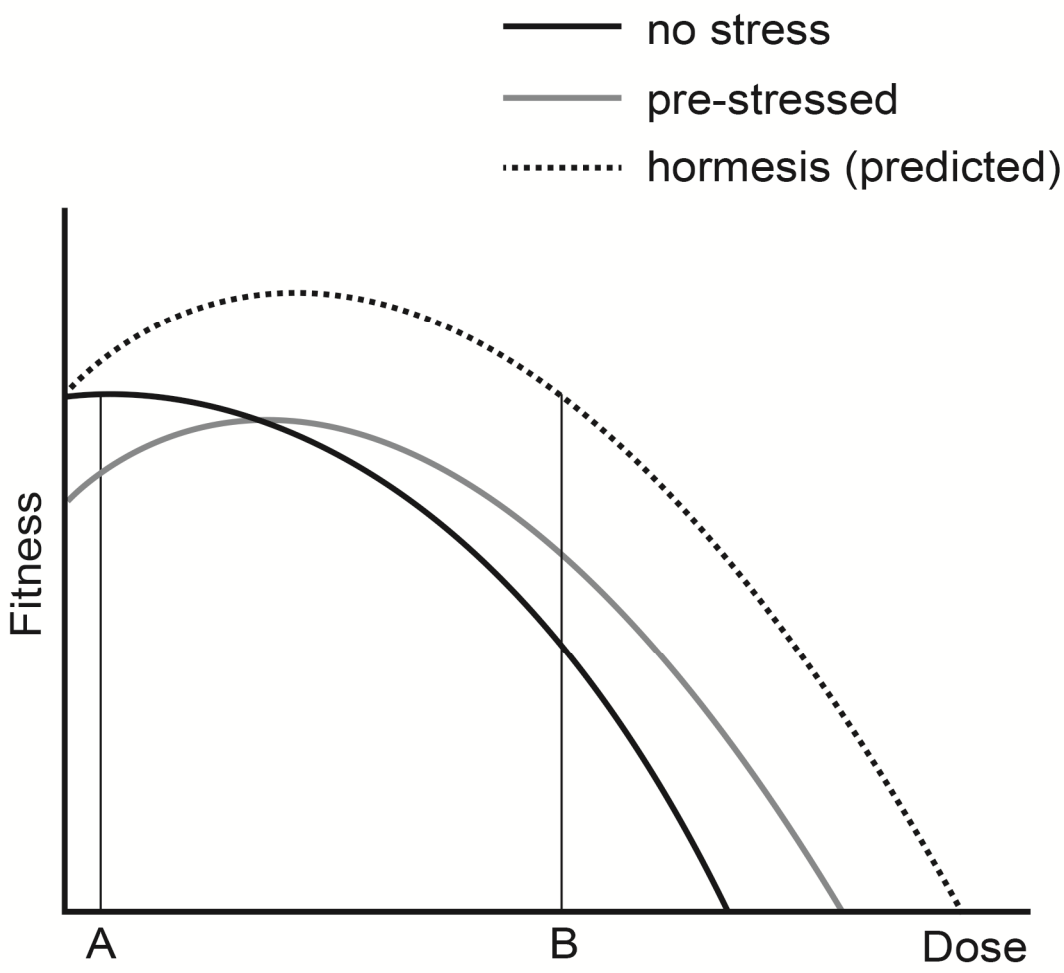


**Figure 6. The effects of adaptation to mild stress**

Three curves are used to represent the fitness of yeast cells that were previously not stressed (black line), pre-stressed (gray line) or show a hormetic response (dashed line). A and B indicate low and high doses of stress.

What mechanisms might explain the different effects of the adaptive response to low-dose stress? *cdc13-1* and *cdc15-2* affect different aspects of cell cycle progression, but we imagine the types of adaptive response are somewhat similar. Defective telomeres in *cdc13-1* mutants induce a DNA damage checkpoint kinase dependent network, involving at least five kinases, Mec1, Tel1, Chk1, Rad53 and Dun1 to affect cell cycle arrest and DNA repair. Therefore effects on phosphorylation-dependent biochemical processes such as signalling, transcription and proteolysis must underlie the adaptive responses. Rad9, for example, is essential for cell cycle arrest of *cdc13-1* strains, for activating downstream kinase activities and for inhibiting the accumulation of single stranded DNA near telomeres (Weinert and Hartwell, 1988, Lydall and Weinert, 1995, Gilbert et al., 2001, Usui et al., 2001, Jia et al., 2004, Sweeney et al., 2005, Lazzaro et al., 2008, Lydall, 2009, Ngo and Lydall, 2015). Furthermore rearrangements in telomere DNA structure can also reduce cellular dependence on Cdc13 (Larrivee and Wellinger, 2006).

Since adaptation can occur in *cdc13-1 rad9*Δ, *cdc13-1 exo1*Δ and *cdc13-1 msn2*Δ *msn4*Δ strains, we conclude that much redundancy exists in the responses to telomere defects and that a strong network structure must underlie the adaptive responses. Consistent with this Berry *et al*. (Berry et al., 2011) have shown acquired stress resistance is complex and context dependent. The fact that adaptation can occur in the absence of Rad9, which plays so many different and important roles in telomere defective strains, shows how robust (and presumably important) this adaptive response is. The complex network structure that underlies adaption may explain that numerous mechanisms have been proposed to account for hormetic mechanisms (Schumacher, 2009, Vaiserman, 2010, Stranahan and Mattson, 2012, Wiegant et al., 2012, Perry et al., 2014, Singh et al., 2015). We have not examined the mechanisms that control adaptation to *cdc15-2* defects but we imagine that these mechanisms are equally as robust since Cdc15 is part of the mitotic exit network. We found that cells adapting to *cdc13-1* or *cdc15-2* induced stress incurred a detectable cost to fitness when the stress was reduced. Furthermore, cells seemed to reverse adaptation to *cdc15-2* stress more rapidly that they reversed adaptation to *cdc13-1* stress. This comparison suggests that the each type of stress can induce quite different adaptive mechanisms.

All organisms live in stressful, variable environments, encountering harmful physical and chemical stressors such as sunlight, radiation and oxygen. All of these poisons are unavoidably dangerous and cells have evolved powerful mechanisms to overcome most, but not all, of their harmful effects. It is likely that complex networks of biochemical interactions help cells tolerate and thrive in the context of these different stresses. Presumably, therefore, *cdc* mutants growing at slightly elevated temperatures up-regulated responses that counteract the negative cues caused by *cdc* defects. This up regulation, or adaptation, is positive because it prepares cells for exposure to even more stress. On the other hand adaptation is harmful when the stress is removed. In a sense *cdc* adapted cells have become "addicted" to stress, presumably because the energetic cost of maintaining a stress response when stress is no longer present reduces fitness. In animals too there seems to be both a benefit and a cost of adapting to stress. Zebra finches exposed to heat stress in early life are more tolerant of heat later in life, but have shorter lifespans than unstressed birds if no further stress is received (Costantini et al., 2014).

*cdc13-1*, which essentially damages chromosomes, can be considered as a model for environmental stresses that cannot be avoided, such as radiation and oxygen exposure. We routinely grow *cdc13-1* cells at 23°C, although we know that telomeres of *cdc13-1* mutants at 23°C are imperfect, because synthetic lethal interactions are seen in combination with *yku70*Δ*, yku80*Δ*, mre11*Δ*, rad50*Δ and *xrs2*Δ mutations at this temperature (Polotnianka et al., 1998, Foster et al., 2006). Presumably, therefore, the *cdc13-1* strains growing at 23°C have adapted to growth with defective telomeres. Along similar lines, most mammalian cells are grown in the laboratory in 20% oxygen, yet when cells have adapted to grow in lower oxygen concentrations and are switched back to 20% oxygen, then a strong stress response is observed (Rupec and Baeuerle, 1995, Laderoute and Webster, 1997, Seko et al., 1997). Similarly, all organisms are exposed to low-levels of radiation, but exposure can be increased environmentally. Interestingly, the most recent studies show that comparatively small radiation exposure in radiation workers leads to increased risk of death from leukaemia (Abbott, 2015, Leuraud et al., 2015). Our experiments measured growth rate, as a measure of fitness, but of course there are many other relevant measures of organism fitness. For example, it is likely that if we were to measure genetic stability of *cdc13-1* or *cdc15-2* cells grown at high temperature then stability would be reduced.

Experiments on mammalian cells in culture clearly show hormetic type responses to stress (Cope et al., 2014), so why do we not see evidence for hormesis in yeast? We favour the explanation that culture of transformed cancer cells in the laboratory does not reflect the carefully regulated cell growth that occurs in an organism. In tissue culture, perhaps, slightly inhibiting growth promoting signal transduction pathways (e.g. TOR) actually improves the fidelity of cell division and increases fitness. We suggest that the yeast experimental system is a better model for real organism growth. We cannot exclude, of course, that with a different experimental set up we might see hormesis in yeast, as was apparently seen in 1888 (Calabrese, 2010).

If organisms could be truly fitter after exposure to a toxin/poison/stress, then natural selection would surely select for organisms that generated or mimicked their own toxin/poison/stress. Environments change rapidly and it is not possible to predict what stresses are in store for the future. Our data suggests the idea that responses to chronic low-dose stress are not universally positive. The good news is that organisms can, if necessary, adapt to stress and this helps them survive increased stress. The bad news is that there is a price to be paid if the stress reduces. It has been suggested that positive responses to low-doses poisons will protect humans against cancer and/or ageing (Calabrese, 2004, Calabrese et al., 2015). We caution against this view.

In summary our analyses of yeast cells exposed to chronic low-level telomere stress or mitotic kinase inhibition show clear evidence for adaption to stress. Adaptation improves cell fitness if cells are exposed to more of the same stress, but reduces fitness when stress levels are reduced. We found that adaptation to stress is reversible and that functionally redundant, robust networks of biochemical interactions must be responsible for the adaptive responses. Our results suggest that adaptation to low-level stress is favourable should stress remain or increase, but harmful when stress levels reduce.

### *6.1.5 Materials and Methods*

**Yeast strains used in this study**

All *S. cerevisiae* strains used in this study are in the W303 genetic background: *ade2-1 can1-100 trp1-1 leu2-3,112 his3-11,15 ura3 GAL+ psi+ ssd1-d2 RAD5+* and are shown in Supplementary Table 1.

**Media**

Strains contain an *ade2-1* mutation and therefore the liquid or solid medium was supplemented with adenine (1L YEPD: 10g yeast extract, 20g bactopeptone, 50ml 40% dextrose, 15ml 0.5% adenine, 935ml $H_20$).

**Cell passage**

Yeast strains were passaged on YEPD agar plates by streaking by toothpick at the indicated temperatures. Between 5 to 10 colonies from each genotype were pooled at each passage. We counted the cells in representative colonies and estimate that for each passage, for a single cell to form a colony represents approximately 21 cell generations.

**Spot test assays**

Pooled colonies from cell passage plates were inoculated into 2ml liquid YEPD and grown on a wheel for 12-18 hours to reach saturation. Saturated liquid cultures were 5-fold serially diluted in sterile water in 96-well plates, and small aliquots were spotted onto YEPD plates with a sterile, metal pin-tool. Plates were incubated at the temperatures indicated and photographed at 24, 48 and 72 hours.

**Image Processing**

All agar plate images were processed using Adobe Photoshop CS6 software. In each Figure, all images were adjusted identically; there were slight differences across Figures. Images were adjusted as follows: in the Levels adjustment tool the low end of the intensity histogram was trimmed to between 100 - 130 and all other values left at default (1, 255). Using Photoshop's exposure tool, Exposure settings were adjusted to 0.3 - 0.8; Offset to -0.02 - -0.05; and Gamma Correction to 1.2 - 1.5. Colour was converted to greyscale after import into Adobe Illustrator.

**Acknowledgements**

We thank all our lab members and Phil Aldridge, Simon Cook, Audrey Gasch, Niall Kenneth, Tom Kirkwood, Ed Louis, Neil Perkins, Janet Quinn and Daryl Shanley for input. This work was funded by EU Marie Curie ITN network CodeAge and the BBSRC.

### *6.1.6 Supplementary material*

| Diploid strain no. (DDY) | Genotype | Origin (DLY x DLY) |
|---|---|---|
| **81** | *CDC13/CDC13* | 640 x 641 |
| **735** | *cdc13-1/cdc13-1* | 1108 x 1195 |
| **736** | *cdc13-1/cdc13-1* | 1108 x 1195 |
| **737** | *cdc13-1/CDC13* | 1108 x 3001 |
| **738** | *cdc13-1/CDC13* | 1108 x 3001 |
| **739** | *CDC13/CDC13* | 3001 x 8460 |
| **837** | *yku70::HIS3/YKU70 exo1::LEU2/EXO1* | 1273 x 1412 |
| **838** | *yku70::HIS3/YKU70 exo1::LEU2/EXO1* | 1273 x 1412 |
| **839** | *cdc15-2/CDC15 yku70::HIS3/YKU70 exo1::LEU2/EXO1* | 1273 x 10725 |
| **840** | *cdc15-2/CDC15 yku70::HIS3/YKU70 exo1::LEU2/EXO1* | 1273 x 10725 |
| **841** | *cdc15-2/cdc15-2 yku70::HIS3/YKU70 exo1::LEU2/EXO1* | 10724 x 10726 |
| **842** | *cdc15-2/cdc15-2 yku70::HIS3/YKU70 exo1::LEU2/EXO1* | 10724 x 10726 |
| **860** | *cdc13-1/cdc13-1 rad9::HIS3/rad9::HIS3 rad24::TRP1/RAD24 exo1::LEU2/EXO1* | 1260 x 1692 |
| **861** | *cdc13-1/cdc13-1 rad9::HIS3/rad9::HIS3 rad24::TRP1/RAD24 exo1::LEU2/EXO1* | 1260 x 1692 |
| **868** | *cdc13-1/CDC13 rad9::HIS3/rad9::HIS3 rad24::TRP1/RAD24 exo1::LEU2/EXO1* | 1693 x 6931 |
| **869** | *cdc13-1/CDC13 rad9::HIS3/rad9::HIS3 rad24::TRP1/RAD24 exo1::LEU2/EXO1* | 1693 x 6931 |
| **972** | *cdc13-1/cdc13-1 msn2::URA3/msn2::HIS3 msn4::KAN/msn4::URA3* | 4149 x 4153 |
| **973** | *cdc13-1/cdc13-1 msn2::URA3/msn2::HIS3 msn4::KAN/msn4::URA3* | 4149 x 4153 |
| **974** | *cdc13-1/CDC13 msn2::URA3/msn2::HIS3 msn4::KAN/msn4::URA3* | 4148 x 4153 |
| **975** | *cdc13-1/CDC13 msn2::URA3/msn2::HIS3 msn4::KAN/msn4::URA3* | 4148 x 4153 |
| **976** | *msn2::URA3/msn2::HIS3 msn4::KAN/msn4::URA3* | 4148 x 4154 |
| **977** | *msn2::URA3/msn2::HIS3 msn4::KAN/msn4::URA3* | 4148 x 4154 |
| **992** | *cdc13-1/CDC13 exo1::LEU2/exo1::LEU2 yku70::HIS3/YKU70 rad24::TRP1/RAD24* | 1408 x 1696 |
| **993** | *cdc13-1/CDC13 exo1::LEU2/exo1::LEU2 yku70::HIS3/YKU70 rad24::TRP1/RAD24* | 1408 x 1696 |
| **994** | *cdc13-1/cdc13-1 exo1::LEU2/exo1::LEU2 yku70::HIS3/YKU70 rad24::TRP1/RAD24* | 5097 x 6793 |
| **995** | *cdc13-1/cdc13-1 exo1::LEU2/exo1::LEU2 yku70::HIS3/YKU70 rad24::TRP1/RAD24* | 5097 x 6793 |
| **996** | *exo1::LEU2/exo1::LEU2 yku70::HIS3/YKU70 rad24::TRP1/RAD24* | 1408 x 1701 |
| **997** | *exo1::LEU2/exo1::LEU2 yku70::HIS3/YKU70 rad24::TRP1/RAD24* | 1408 x 1701 |
| **1034** | *msn2::URA3/msn2::HIS3 msn4::KAN/msn4::URA3* | 11082 x 11097 |
| **1035** | *msn2::URA3/msn2::HIS3 msn4::KAN/msn4::URA3* | 11082 x 11097 |
| **1036** | *cdc15-2/CDC15 msn2::URA3/msn2::HIS3 msn4::KAN/msn4::URA3* | 11083 x 11086 |
| **1037** | *cdc15-2/CDC15 msn2::URA3/msn2::HIS3 msn4::KAN/msn4::URA3* | 11063 x 11097 |
| **1038** | *cdc15-2/cdc15-2 msn2::URA3/msn2::HIS3 msn4::KAN/msn4::URA3* | 11065 x 11086 |
| **1039** | *cdc15-2/cdc15-2 msn2::URA3/msn2::HIS3 msn4::KAN/msn4::URA3* | 11063 x 11085 |
| **DLY1108** | *cdc13-1* | |
| **DLY1195** | *cdc13-1* | |
| **DLY3001** | *CDC13* | |

**Table S1 Strains used in this study**

All *S. cerevisiae* strains are in the W303 genetic background (*ade2-1 can1-100 trp1-1 leu2-3,112 his3-11,15 ura3 GAL+ psi+ ssd1-d2 RAD5*).

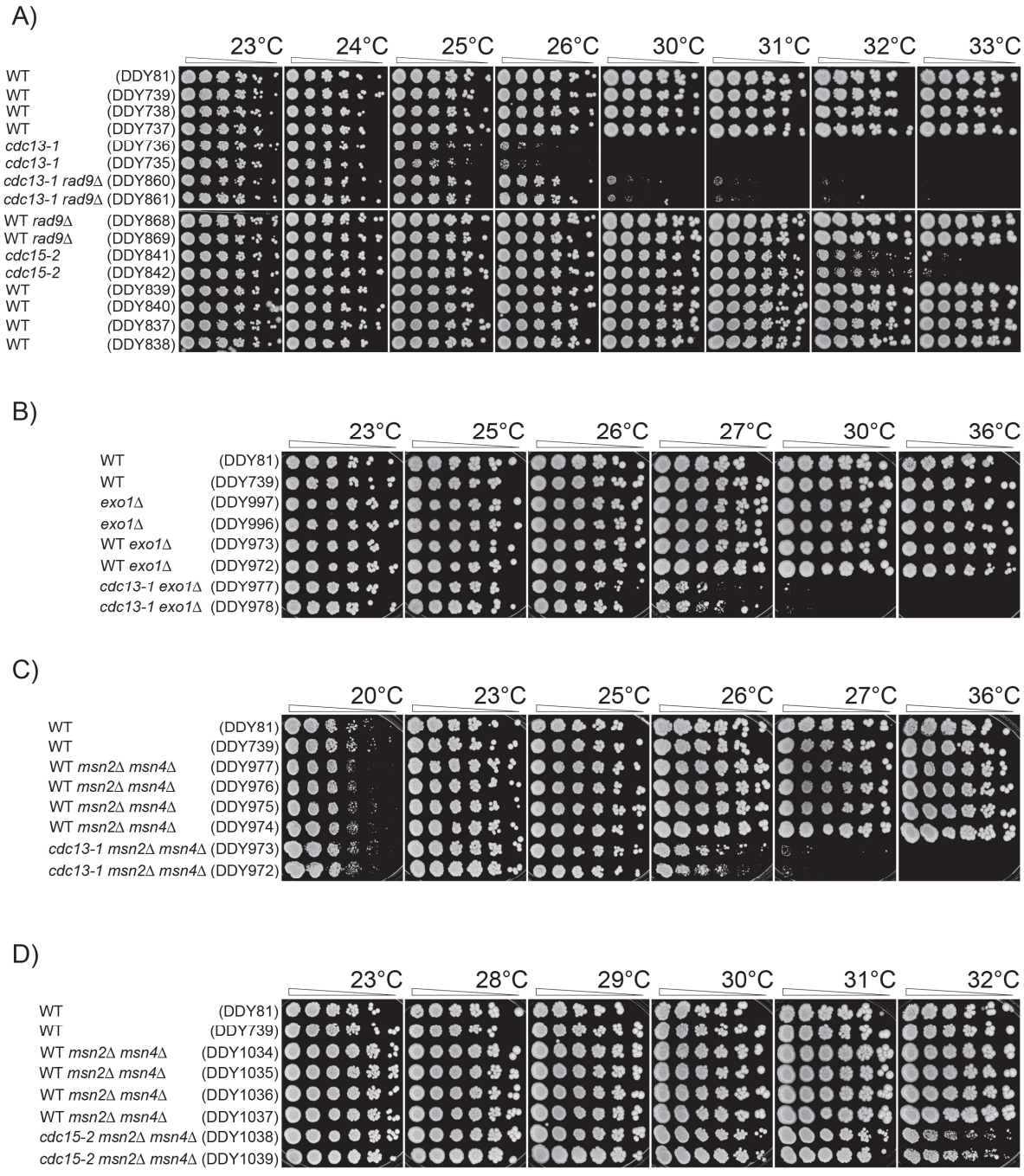


**Figure S1. The fitness of *cdc13-1* and *cdc15-2* mutants at a range of temperatures**

Diploid strains with different genotypes were grown for one passage at 23°C on YEPD plates. Spot tests were performed as described in Figure 3. Photographs were taken after 72 hours. All strains shown at each temperature were grown on a single agar plate within A). Strains' details are shown in Supplementary Table 1.

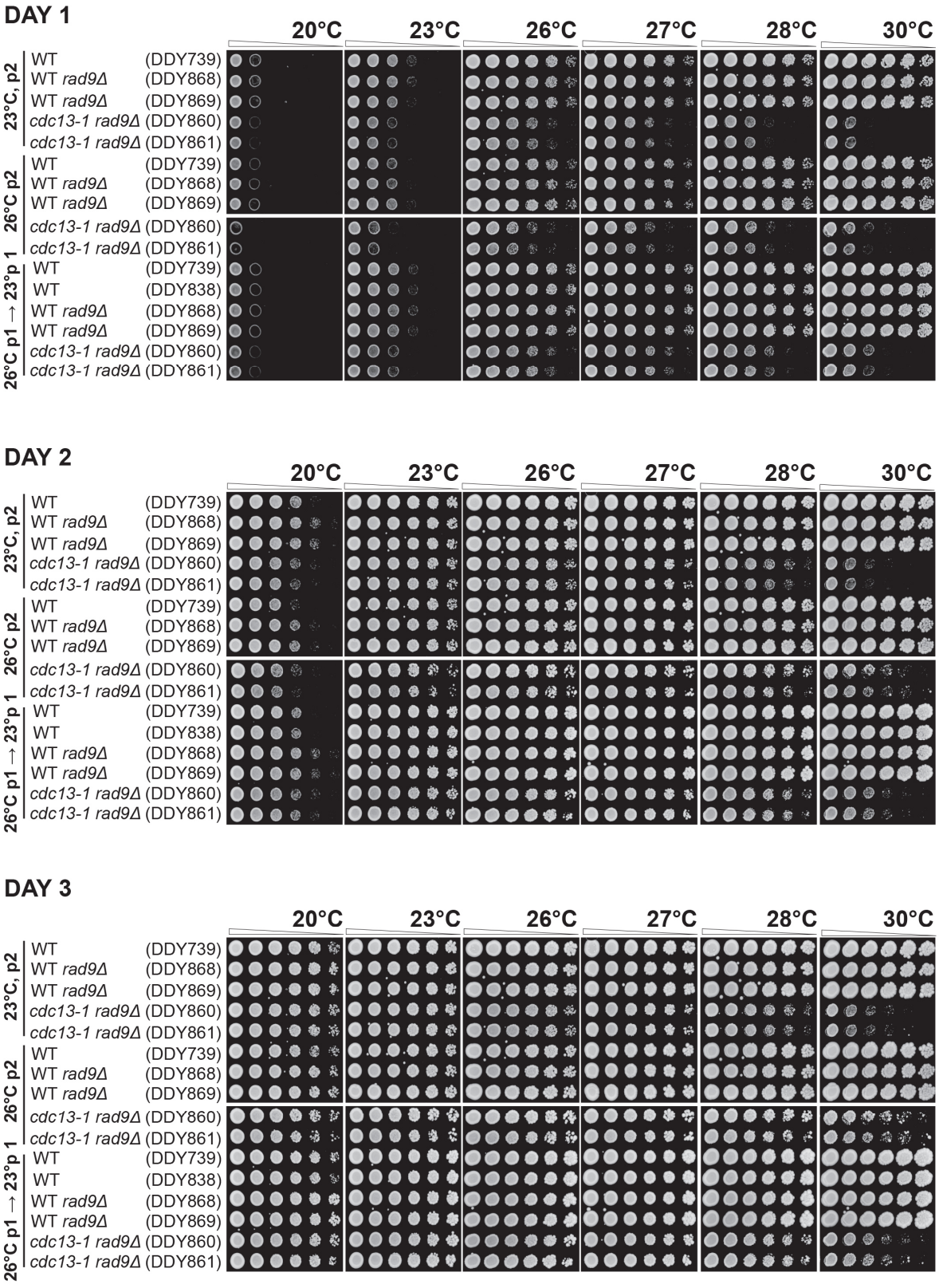


**Figure S2. The effects of adaptation to telomere stress in *cdc13-1 rad9*Δ mutants**

Pictures were taken periodically after 24, 48 and 72 hours of incubation.

Experimental design described in Figure 4.

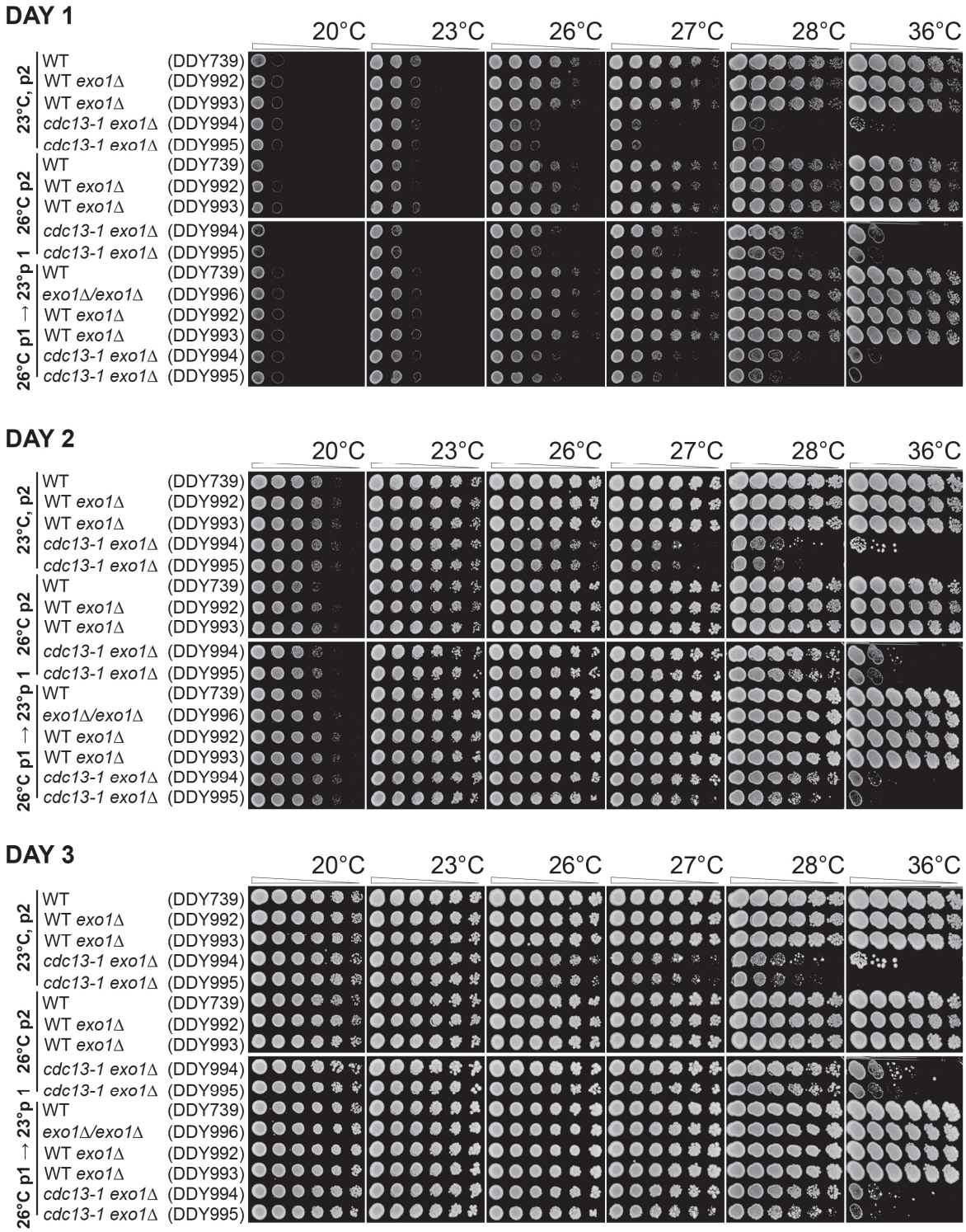


**Figure S3. The effects of adaptation to telomere stress in *cdc13-1 exo1*Δ mutants**

Pictures were taken periodically after 24, 48 and 72 hours of incubation.

Experimental design described in Figure 4.

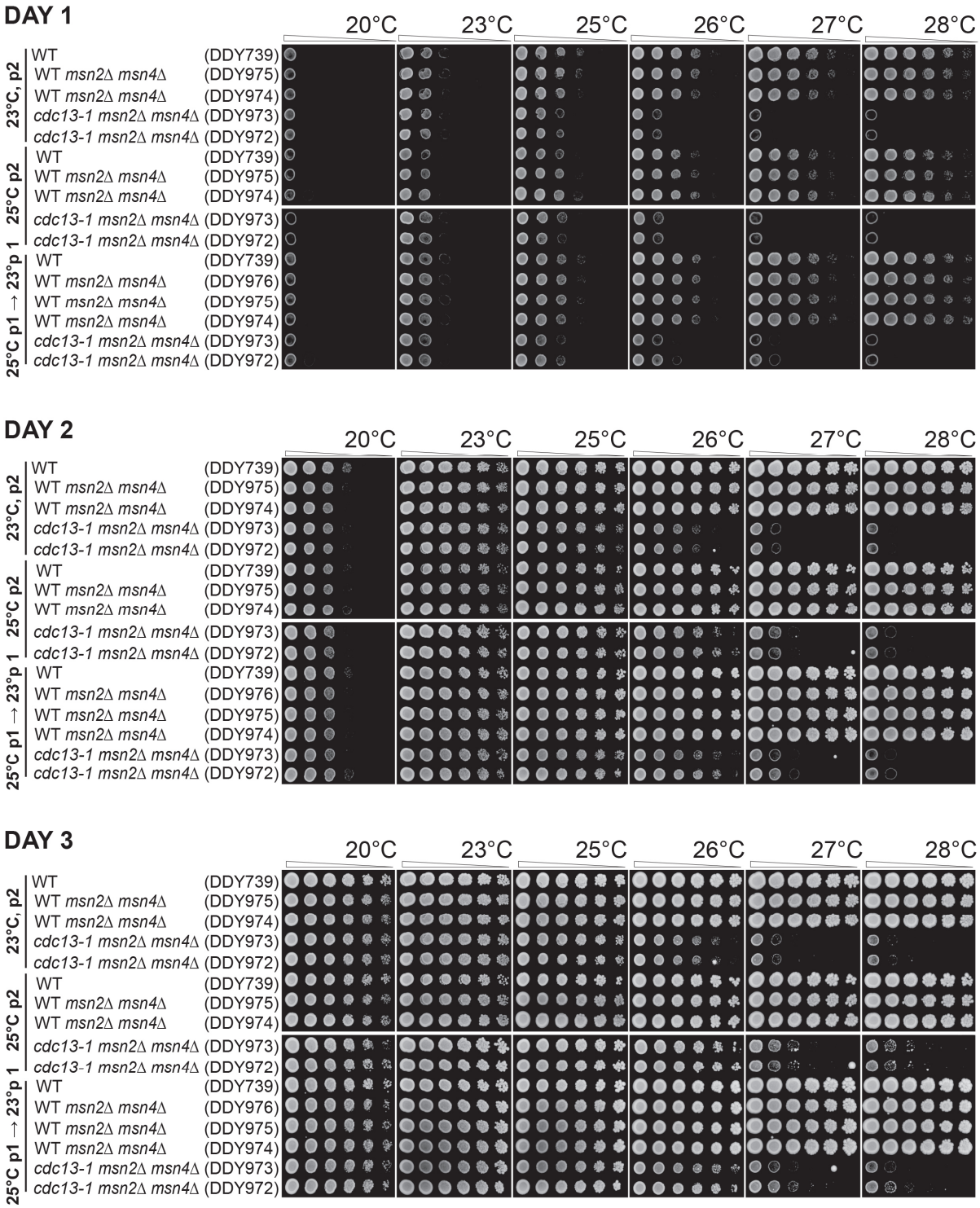


**Figure S4. The effects of adaptation to telomere stress in *cdc13-1 msn2*Δ *msn4*Δ mutants**

Pictures were taken periodically after 24, 48 and 72 hours of incubation.

Experimental design described in Figure 4.

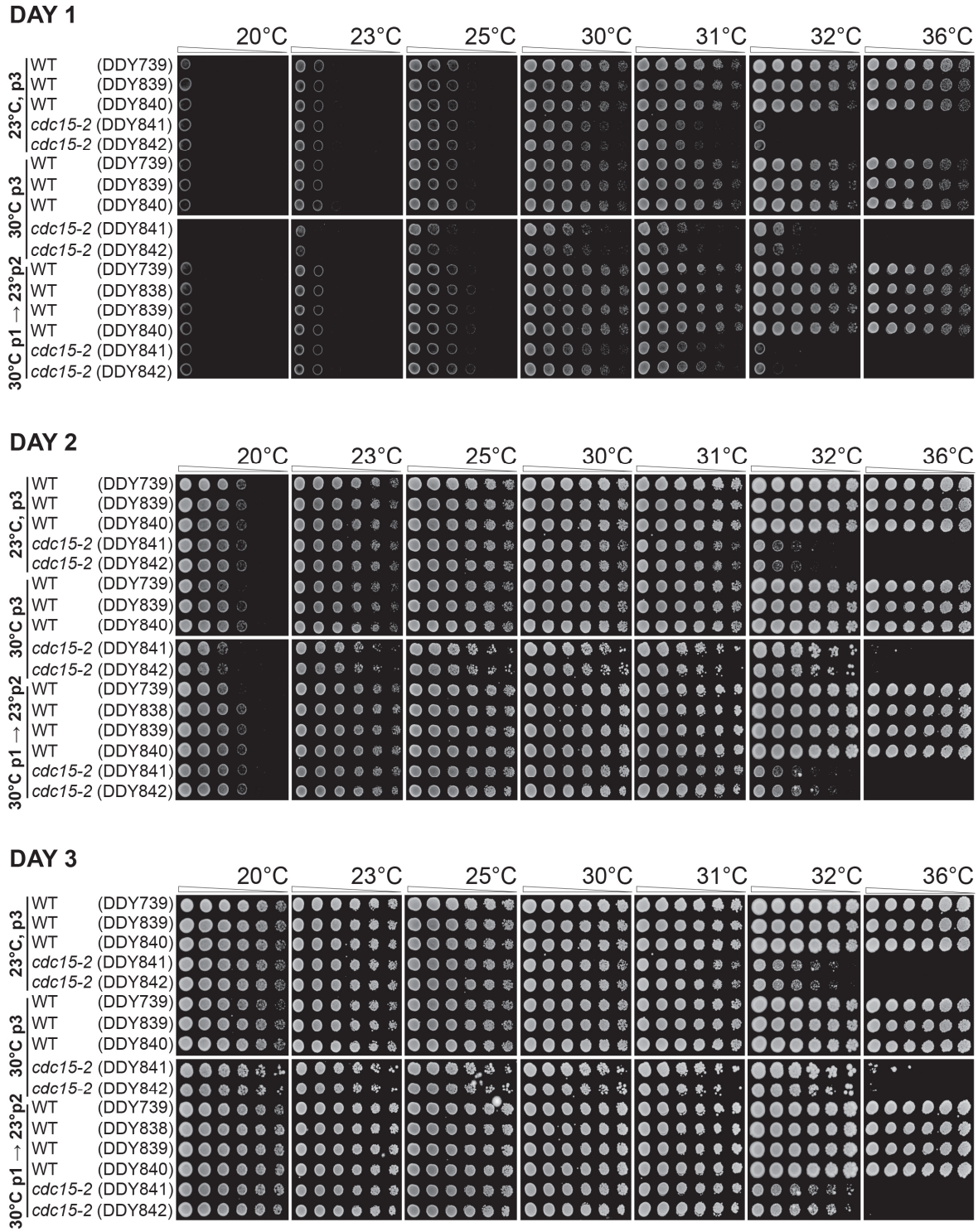


**Figure S5. The effects of adaptation to low level kinase inhibition in *cdc15-2* mutants**

Pictures were taken periodically after 24, 48 and 72 hours of incubation.

Experimental design described in Figure 5.

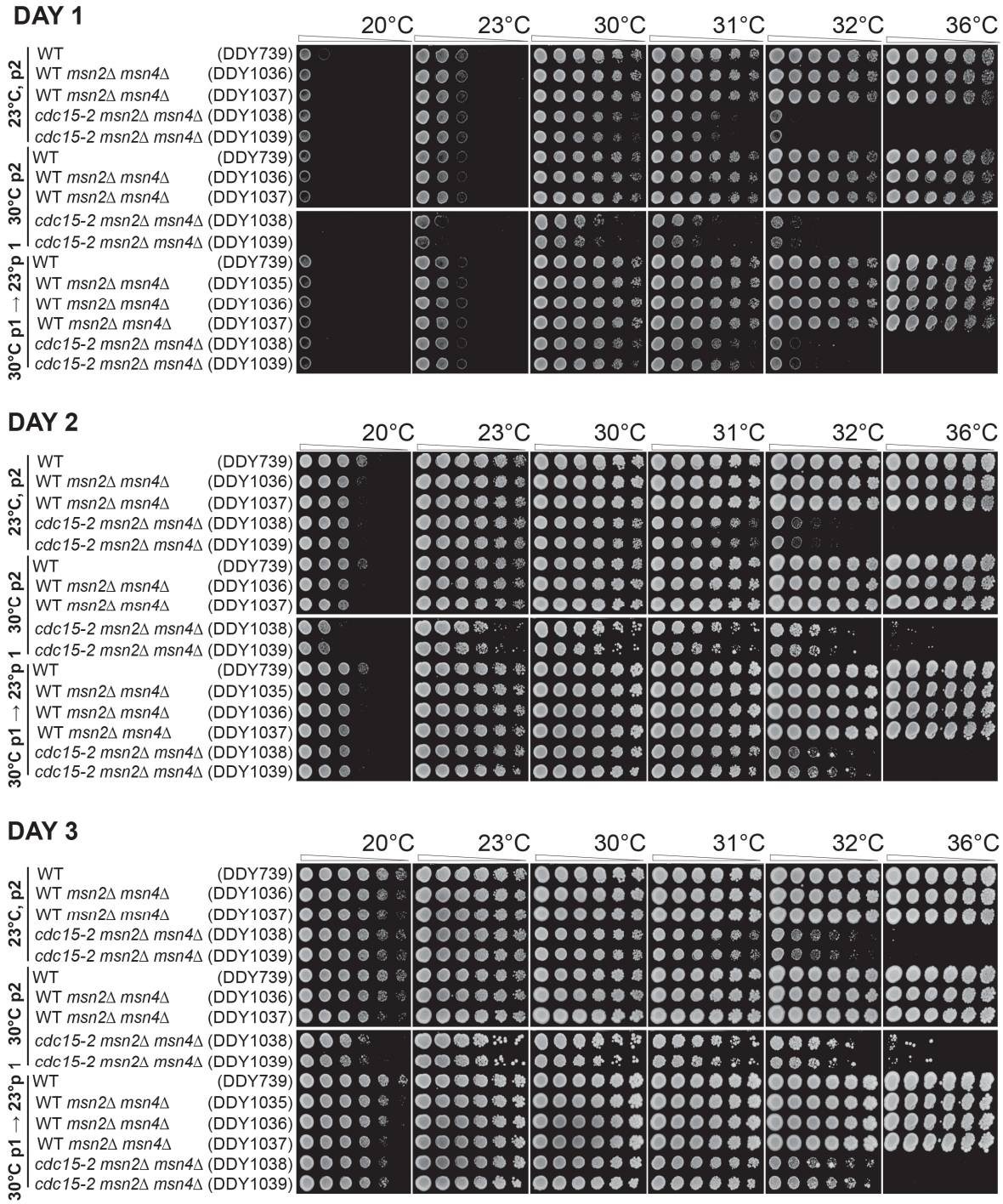


**Figure S6. The effects of adaptation to low level kinase inhibition in *cdc15-2 msn2*Δ *msn4*Δ mutants**

Pictures were taken periodically after 24, 48 and 72 hours of incubation.

Experimental design described in Figure 5.

# Chapter 7. Discussion

I will start my discussion with the results I acquired for Dna2 because I find the section about Dna2 the most interesting. Later, I will discuss the effects of Ddc1, Dpb11 and Dna2 on fitness of *cdc13-1* and *yku70*Δ strains. Finally, I will mention the possible roles of Hcm1, Xbp1 and Uls1 at telomeres, and the consequences of yeast adaptation to low-dose stress.

## 7.1 Role of Dna2 in telomere biology

It was proposed that the essential function of Dna2 is in long flap processing during Okazaki fragment maturation (Fig. 32) (Budd and Campbell, 2000, Budd et al., 2006, Budd et al., 2011). However, my hypothesis is that Dna2 has the most critical role at telomeres, presumably in Okazaki fragment processing during telomere replication. *DNA2* is an essential gene, but its lethality is bypassed by overexpression of *RAD27* and deletions of *PIF1* and *RAD9.* I now report that *dna2*Δ cells are also viable when *DDC1, CHK1, RAD17, MEC1 (SML1)* or *POL32* genes are deleted, and in these other cases resemble *dna2*Δ *rad9*Δ mutants. Consistent with some of this data, it was previously shown that deletion of *POL32* suppresses thermo-sensitivity of *dna2-1* and *dna2-2* mutants but not the lethality of *dna2*Δ (Budd et al., 2005, Budd et al., 2006). I also found that deletions of *TEL1, RAD53, EXO1, RIF1, RIF2, MRE11* and *RAD27* do not suppress *dna2*Δ lethality.

*DDC1*, *RAD17*, *CHK1* and *RAD9* checkpoint gene deletions suppress *dna2*Δ lethality. Interestingly, the same gene deletions suppress the *cdc13-1* fitness defect (Addinall et al., 2008), which indicates possible similarities between Cdc13 telomere capping protein and Dna2. On the other hand, DNA damage checkpoint mutations reduced fitness of DNA polymerase mutants (Weinert, 1992, Dubarry et al., 2015). In this respect Dna2 is different from a group of DNA polymerases and, possibly, general DNA replication enzymes. Choe *et al.* showed that in *S. cerevisiae* Dna2 localizes to telomeres in a cell cycle regulated manner (in late S-phase), and might have a role in telomere replication and capping (Choe et al., 2002). Similarly to Cdc13, Dna2 might regulate telomerase activity, or replication of telomeres. It would be interesting to confirm my hypotheses that Dna2, a proposed telomere capping protein, has its essential function in Okazaki fragment processing at telomeres, and to find the mechanisms for its function.

An unbiased genome-wide screen (yeast of S288C background) confirmed suppressors and enhancers of *dna2*Δ*,* found earlier by tetrad analysis (e. g. *rad9*Δ or *ddc1*Δ). The SGA screen also allowed for the identification of novel genes whose deletions suppress *dna2*Δ lethality. One of the *dna2*Δ suppressors is *mph1*Δ, affecting a DNA helicase which stimulates activities of Rad27 and Dna2 (Kang et al., 2009). I found that in another genetic background (W303) *mph1*Δ also suppresses *dna2*Δ lethality, similarly to *rad9*Δ*.* However, after tetrad dissection of *dna2*Δ*/DNA2 mph1*Δ*/MPH1* diploid, some single *dna2*Δ mutants emerged. Viability of such *dna2*Δ cells might be a result of genome instability and/or aneuploidy events. Interestingly, although *dna2*Δ spores germinated into very small colonies, they ceased to grow after passaging onto fresh YEPD media, which implied that i) likely no other mutations suppress *dna2*Δ lethality in such cells, ii) presumably DNA damage in the *dna2*Δ cells is too severe to permit growth. Since Dna2, Pif1, Pol32, Mph1 and Rad27 function in Okazaki fragment processing, it might be interesting to test why deletions of *PIF1, POL32* and *MPH1,* but *RAD27* overexpression, suppress *dna2*Δ lethality.

### 7.2 Ddc1, Dpb11 and Dna2 checkpoint control in *yku70*Δ and *cdc13-1* mutants

It has been reported that DNA damage induced in telomere defective *yku70*Δ mutants activates a Mec1-dependent checkpoint pathway, but is independent of the Ddc1 checkpoint protein (Maringele and Lydall, 2002, Addinall et al., 2011). On the other hand *ddc1*Δ is a strong suppressor of another telomere defective mutant, *cdc13-1* (Addinall et al., 2008). Ddc1, Dpb11 and Dna2 directly activate Mec1 in response to DNA damage (Puddu et al., 2008, Navadgi-Patil et al., 2011, Kumar and Burgers, 2013). In order to examine the impact of Ddc1, Dna2 and Dpb11 on fitness of *yku70*Δ and *cdc13-1* strains, I analysed point mutations of *DDC1*, *DNA2* and *DPB11*, defective in Mec1 activation.

I confirmed that *ddc1*Δstrongly suppresses *cdc13-1* defect. Dpb11 may contribute to the checkpoint function of Ddc1 in *cdc13-1* and *yku70*Δ strains, but its role is less important on fitness. Surprisingly, I found that out of the three, Ddc1 was the only protein that most clearly affects *yku70*Δ fitness and therefore might play a minor role in checkpoint of *yku70*Δ strains. The observations that *ddc1*Δ affected *yku70*Δ fitness were inconsistent with published data (Maringele and Lydall, 2002). I showed that yeast culture conditions affect the effect of *ddc1*Δ on *yku70*Δ fitness. Yeast cells

grown till saturation prior spotting were fitter at higher temperatures than strains spotted form the exponential culture.

There are differences in the growth of cells spotted from saturated and exponential cultures, and one possible explanation might be that first cell cycles of *yku70*∆ cells grown till saturation prior spotting might be longer. Longer cell cycle of such cells would result in slower growing, “fitter” cells at higher temperatures. Also, cells grown till saturation prior spotting onto fresh YEPD media might activate stress responses, which protect cells from high temperature stress. Another idea would be that telomere defects of *yku70*∆ mutants are somehow not recognised by checkpoint/ DNA damage machinery when cells were first grown till saturation. It might be interesting to test whether any of these explanations addresses the question regarding the role of culture conditions on yeast strains’ growth.

The checkpoint function of Dna2 is affected by the *dna2-W128A,Y130A* allele (Kumar and Burgers, 2013). I observed that the *dna2-W128A,Y130A* mutation on a plasmid strongly suppressed *cdc13-1* fitness. Such cells carried more copies of a plasmid and had telomeres rearranged. These cells might have selected for more copies of the plasmid with the *dna2-W128A,Y130A* allele. However, the same allele integrated into the genome slightly enhanced the growth defects of *cdc13-1* strains. Interestingly, mutations of other telomere binding proteins (e. g. *yku70*∆) also enhance *cdc13-1* fitness (Polotnianka et al., 1998, Addinall et al., 2008). It might be possible that the residues W128 and Y130 are important for the telomere protection role of Dna2.

Another role of Dna2 which seems to be affected in *dna2-W128A,Y130A* mutants is mitochondrial DNA maintenance. I observed that on glycerol *dna2-W128A,Y130A* mutants were sick, and deletion of *PIF1* slightly improved their fitness. Pif1 and Dna2 have roles in mitochondria (Duxin et al., 2009, Pokharel and Campbell, 2012), and I observed that strains carrying the *dna2-W128A,Y130A* allele were prone to forming petite colonies, an indication of mitochondrial problems. Based on my observations I propose that *dna2-W128A,Y130* allele is defective in the mitochondrial DNA maintenance. Protein stability, and therefore Dna2 enzyme function(s) might be reduced in *dna2-W128A,Y130A* cells.

Overall, Dna2 most likely does not take the role of Ddc1 in checkpoint arrest of *yku70*Δ and *cdc13-1* mutants, while Dpb11 may contribute to the checkpoint function of Ddc1 in *yku70*Δ and *cdc13-1* mutants. Ddc1 itself plays a major checkpoint role in *cdc13-1* mutants, and may play a minor checkpoint role in *yku70*Δ strains.

### 7.3 Hcm1, Xbp1 and Uls1 function at telomeres

I tested whether Hcm1, Xbp1 and Uls1 have roles at uncapped telomeres. I found that Hcm1 and Xbp1 transcription factors affect telomeres, which might involve the regulation of transcription of genes important for the cell cycle arrest in telomere defective strains. Uls1, SUMO-targeted ubiquitin ligase, also plays a role in telomere biology. SUMOlyation and ubiquitynation are involved in regulatory mechanism for controlling telomerase function, e. g. it was shown that SUMOylation of Cdc13 promotes the association of Cdc13 with Stn1 to inhibit telomerase function (Hang *et al.,* 2011). I confirmed the results of genome wide screen in the context of *stn1-13, cdc13-1* and *yku70*Δ in W303 (Addinall et al., 2011). However, mechanisms by which Hcm1, Xbp1 and Uls1 perform roles at telomeres remain to be tested.

### 7.4 Consequences of low-dose stress adaptation

I include published results regarding the consequences of yeast adaptation to chronic low-dose stress (Markiewicz-Potoczny and Lydall, 2016). We observed that yeast cells adapt to chronic low-dose stress, and grow better when higher doses of the stress are applied, in contrast to cells that were not pre-treated with stress; these effects are reversible. Adapted yeast cells are less fit in the stress-free environment; these effects are also reversible. Due to the fact that adaptation to low-dose stress reduces fitness in the absence of stress, precautions should be taken before putting the proverb “What doesn't kill you makes you stronger” into practice.

# Appendix A: Yeast strains

*S. cerevisiae* strains used are in the W303 genetic background (*ade2-1 can1-100 trp1-1 leu2-3,112 his3-11,15 ura3 GAL+ psi+ ssd1-d2 RAD5+*) unless otherwise stated. Haploid strain numbers are prefixed DLY unless otherwise stated (DDY in diploid strains). *pDL* – plasmid. RSA – random spore analysis. Yeast strain are ordered by strain number.

| Strain no. | MAT | Genotype | Origin (If in this work) | pDL |
|---|---|---|---|---|
| 640 | a | WT W303 | | |
| 641 | α | WT W303 | | |
| 883 | a | *ddc1::KAN rad5-535* | | |
| 974 | a | *yku70::HIS3 rDNA::ADE2* | | |
| 1108 | a | *cdc13-1* | | |
| 1195 | α | *cdc13-1* | | |
| 1199 | a | *yku70::HIS3 rad17::LEU2 rad5-535* | | |
| 1208 | α | *yku70::LEU2 mec3::TRP1 rad5-535* | | |
| 1209 | a | *yku70::LEU2 mec3::TRP1 rad5-535* | | |
| 1210 | a | *ddc1::KAN yku70::LEU2 rad5-535* | | |
| 1211 | α | *ddc1::KAN yku70::LEU2 rad5-535* | | |
| 1215 | a | *yku70::LEU2 chk1::HIS3* | | |
| 1264 | α | *yku70::LEU2 rad9::HIS3* | | |
| 1266 | a | *yku70::LEU2 chk1::HIS3* | | |
| 1271 | a | *yku70::LEU2 rad9::HIS3* | | |
| 1273 | α | *exo1::LEU2* | | |
| 1284 | a | *rad24::TRP1 yku70::HIS3* | | |
| 1296 | a | *cdc13-1 exo1::LEU2* | | |
| 1297 | α | *cdc13-1 exo1::LEU2* | | |
| 1326 | α | *mec1::HIS3 sml1::KAN* | | |
| 1347 | α | *yku70::HIS3 rad17::LEU2* | | |
| 1364 | a | *yku70::HIS3 rad24::TRP1* | | |
| 1366 | α | *yku70::HIS3* | | |
| 1408 | a | *yku70::HIS3 exo1::LEU2* | | |
| 1409 | α | *yku70::HIS3 exo1::LEU2* | | |
| 1412 | a | *yku70::HIS3* | | |
| 1585 | α | *rad9::KAN mfa::MFA1 pr-HIS3 can1 ura3 leu2 his3 lys2 (S288C)* | | |
| 1845 | a | *yku70::HIS3 mre11::hisG::URA3* | | |
| 1846 | α | *yku70::HIS3 mre11::hisG::URA3* | | |

| | | | | |
|---|---|---|---|---|
| 2147 | α | *tlc1::HIS3* | | |
| 2586 | α | *yku70::LEU2 chk1::HIS3* | | |
| 3001 | α | WT W303 | | |
| 4647 | a | *cdc13-1 rad9::HIS3* | | |
| 5230 | a | *yku70::HIS rad24::TRP* | | |
| 5231 | a | *yku70::HIS rad24::TRP* | | |
| 5536 | a | *ade2-1 trp1-1 CAN1 leu2-3,112 his3-11,15 ura3 GAL+ psi+ ssd1-d2 RAD5 (W303 wild type)* | | |
| 5626 | a | *ade2-1 trp1-1 CAN1 leu2-3,112 his3-11,15 ura3 GAL+ psi+ ssd1-d2 RAD5 (W303 wild type)* | | |
| 5703 | a | *pol32::KAN* | | |
| 5704 | α | *pol32::KAN* | | |
| 6854 | a | *sml1::URA3* | | |
| 6936 | a | *yku70::LEU2 rad9::HIS3* | | |
| 6885 | a | *yku70::LEU2* | | |
| 7171 | a | *cdc13-1 ddc1::KAN* | | |
| 7172 | α | *cdc13-1 ddc1::KAN* | | |
| 7173 | a | *ddc1::KAN* | | |
| 7174 | α | *ddc1::KAN* | | |
| 7177 | a | *rad17::LEU2* | | |
| 7629 | α | *yku70::LEU2* | | |
| 8460 | a | *WT W303* | | |
| 8663 | a | *yku70::HIS3 ddc1::KAN* | 1412 x 7174 | |
| 8664 | a | *yku70::HIS3 ddc1::KAN* | 1412 x 7174 | |
| 8666 | α | *yku70::HIS3 ddc1::KAN* | 1412 x 7174 | |
| 8711 | α | *yku70::LEU2 mec3::TRP1* | 6885 x 7182 | |
| 8773 | a | *cdc13-1 dpb11::KAN* | 1108 x 3001 | 1545 |
| 8774 | α | *cdc13-1 dpb11::KAN* | 1108 x 3001 | 1545 |
| 8783 | α | *yku70::LEU2 dpb11::KAN* | 6885 x 3001 | 1545 |
| 8784 | a | *yku70::LEU2 dpb11::KAN* | 6885 x 3001 | 1545 |
| 8787 | a | *yku70::LEU2 dpb11::KAN* | 6885 x 3001 | 1552 |
| 8788 | α | *yku70::LEU2 dpb11::KAN* | 6885 x 3001 | 1552 |
| 8789 | a | *yku70::LEU2 dpb11::KAN* | 6885 x 3001 | 1553 |
| 8791 | α | *yku70::LEU2 dpb11::KAN* | 6885 x 3001 | 1554 |
| 8792 | a | *yku70::LEU2 dpb11::KAN* | 6885 x 3001 | 1554 |
| 8793 | a | *yku70::LEU2 dpb11::KAN* | 6885 x 3001 | 1555 |
| 8794 | α | *yku70::LEU2 dpb11::KAN* | 6885 x 3001 | 1555 |
| 8795 | a | *yku70::LEU2 dpb11::KAN* | 6885 x 3001 | 1556 |
| 8796 | α | *yku70::LEU2 dpb11::KAN* | 6885 x 3001 | 1556 |
| 8799 | α | *cdc13-1 dpb11::KAN* | 1108 x 3001 | 1555 |
| 8800 | a | *cdc13-1 dpb11::KAN* | 1108 x 3001 | 1555 |
| 8952 | a | *yku70::HIS3 dna2::KAN* | 1412 x 3001 | 1560 |
| 8953 | α | *yku70::HIS3 dna2::KAN* | 1412 x 3001 | 1560 |
| 8954 | α | *yku70::HIS3 dna2::KAN* | 1412 x 3001 | 1561 |
| 8955 | a | *yku70::HIS3 dna2::KAN* | 1412 x 3001 | 1561 |
| 8956 | α | *yku70::HIS3 dna2::KAN* | 1412 x 3001 | 1468 |

| | | | | |
|---|---|---|---|---|
| 8957 | α | *yku70::HIS3 dna2::KAN* | 1412 x 3001 | 1568 |
| 8993 | a | *stn1-13 rad5-535* | | |
| 8998 | α | *cdc13-1 dna2::KAN* | 1108 x 3001 | 1544 |
| 8999 | a | *cdc13-1 dna2::KAN* | 1108 x 3001 | 1561 |
| 9000 | a | *cdc13-1 dna2::KAN* | 1108 x 3001 | 1561 |
| 9001 | α | *cdc13-1 dna2::KAN* | 1108 x 3001 | 1561 |
| 9040 | a | *cdc13-1* | 1108 | 876 |
| 9041 | a | *cdc13-1* | 1108 | 876 |
| 9042 | a | *cdc13-1* | 1108 | 1559 |
| 9045 | a | *yku70::HIS3* | 1412 | 1559 |
| 9046 | a | *yku70::LEU2* | 6885 | 876 |
| 9047 | a | *yku70::LEU2* | 6885 | 876 |
| 9050 | a | *WT W303* | 1412 x 3001 | 1559 |
| 9056 | α | *cdc13-1 ddc1::KAN* | 7172 | 1479 |
| 9057 | α | *cdc13-1 ddc1::KAN* | 7172 | 1470 |
| 9058 | α | *cdc13-1 ddc1::KAN* | 7172 | 1472 |
| 9059 | α | *cdc13-1 ddc1::KAN* | 7172 | 1474 |
| 9060 | α | *cdc13-1 ddc1::KAN* | 7172 | 1476 |
| 9061 | α | *cdc13-1 ddc1::KAN* | 7172 | 1546 |
| 9062 | α | *cdc13-1 ddc1::KAN* | 7172 | 1547 |
| 9063 | α | *cdc13-1 ddc1::KAN* | 7172 | 1548 |
| 9064 | α | *cdc13-1 ddc1::KAN* | 7172 | 1549 |
| 9065 | α | *cdc13-1 ddc1::KAN* | 7172 | 1550 |
| 9071 | a | *WT W303* | 8460 | 1248 |
| 9073 | α | *WT W303* | 3001 | 876 |
| 9079 | a | *dna2::KAN* | 1412 x 3001 | 1568 |
| 9085 | α | *cdc13-1 ddc1::KAN* | 7172 | 1543 |
| 9087 | α | *cdc13-1 ddc1::KAN* | 7172 | 1248 |
| 9088 | α | *cdc13-1 ddc1::KAN* | 7172 | 1248 |
| 9124 | α | *dna2::KAN* | 1412 x 3001 | 1560 |
| 9126 | a | *dna2::KAN* | 1412 x 3001 | 1544 |
| 9128 | a | *cdc13-1* | 1108 | 1248 |
| 9129 | a | *cdc13-1* | 1108 | 1248 |
| 9130 | a | *ddc1::KAN* | 7173 | 1248 |
| 9136 | a | *ddc1::KAN* | 7173 | 1543 |
| 9152 | α | *cdc13-1 dpb11::KAN* | 1108 x 3001 | 1553 |
| 9171 | a | *cdc13-1 dpb11::KAN* | 1108 x 3001 | 1554 |
| 9173 | α | *cdc13-1 dpb11::KAN* | 1108 x 3001 | 1554 |
| 9203 | α | *cdc13-1 dpb11::KAN* | 1108 x 3001 | 1545 |
| 9206 | α | *cdc13-1 dpb11::KAN* | 1108 x 3001 | 1552 |
| 9208 | a | *cdc13-1 dpb11::KAN* | 1108 x 3001 | 1552 |
| 9210 | α | *cdc13-1 dpb11::KAN* | 1108 x 3001 | 1553 |
| 9214 | α | *cdc13-1 dpb11::KAN* | 1108 x 3001 | 1556 |
| 9216 | α | *cdc13-1 dpb11::KAN* | 1108 x 3001 | 1556 |
| 9218 | a | *dna2::KAN* | 1412 x 3001 | 1568 |
| 9222 | a | *yku70::HIS3 dna2::KAN* | 1412 x 3001 | 1569 |

| | | | | |
|---|---|---|---|---|
| 9224 | α | *dna2::KAN* | 1412 x 3001 | 1569 |
| 9246 | a | *stn1-13 rad9::HIS3* | | |
| 9274 | α | *cdc13-1 dna2::KAN* | 1108 x 3001 | 1569 |
| 9275 | a | *cdc13-1 dna2::KAN* | 1108 x 3001 | 1569 |
| 9276 | α | *dna2::KAN* | 1108 x 3001 | 1569 |
| 9278 | α | *cdc13-1 dna2::KAN* | 1108 x 3001 | 1568 |
| 9317 | a | *cdc13-1 dna2::KAN* | 1108 x 3001 | 1567 |
| 9318 | a | *dna2::KAN* | 1108 x 3001 | 1570 |
| 9319 | a | *cdc13-1 dna2::KAN* | 1108 x 3001 | 1570 |
| 9320 | α | *cdc13-1 dna2::KAN* | 1108 x 3001 | 1570 |
| 9332 | α | *yku70::LEU2 dpb11::KAN ddc1::HPHNMX* | 8796 | 1556 |
| 9333 | α | *yku70::LEU2 dpb11::KAN ddc1::HPHNMX* | 8796 | 1556 |
| 9344 | a | *cdc13-1 ddc1::HPHNMX* | 9040 | 876 |
| 9348 | a | *cdc13-1 dpb11::KAN ddc1::HPHNMX* | 9216 | 1556 |
| 9349 | a | *cdc13-1 dpb11::KAN ddc1::HPHNMX* | 9216 | 1556 |
| 9469 | a | *cdc13-1 ddc1::HPH* | 9042 | 1559 |
| 9471 | α | *cdc13-1 dna2::KAN ddc1::HPH* | 8998 *ddc1*Δ | 1544 |
| 9472 | α | *cdc13-1 dna2::KAN ddc1::HPH* | 8998 *ddc1*Δ | 1544 |
| 9474 | a | *cdc13-1 ddc1::HPH* | 9043 *ddc1*Δ | 1559 |
| 9476 | a | *cdc13-1 dna2::KAN ddc1::HPH* | 9000 *ddc1*Δ | 1561 |
| 9477 | a | *cdc13-1 dna2::KAN ddc1::HPH* | 9000 *ddc1*Δ | 1561 |
| 9479 | α | *cdc13-1 dna2::KAN ddc1::HPH* | 9001 *ddc1*Δ | 1561 |
| 9480 | α | *cdc13-1 dna2::KAN ddc1::HPH* | 9001 *ddc1*Δ | 1561 |
| 9482 | α | *yku70::HIS3 dna2::KAN ddc1::HPH* | 8954 *ddc1*Δ | 1561 |
| 9483 | α | *yku70::HIS3 dna2::KAN ddc1::HPH* | 8954 *ddc1*Δ | 1561 |
| 9486 | a | *yku70::HIS3 dna2::KAN ddc1::HPH* | 8955 *ddc1*Δ | 1561 |
| 9489 | a | *ddc1::HPH* | 9050 *ddc1*Δ | 1559 |
| 9490 | a | *ddc1::HPH* | 9050 *ddc1*Δ | 1559 |
| 9491 | α | *yku70::HIS3 dna2::KAN ddc1::HPH* | 8953 *ddc1*Δ | 1560 |
| 9492 | α | *yku70::HIS3 dna2::KAN ddc1::HPH* | 8953 *ddc1*Δ | 1560 |
| 9495 | a | *dna2::KAN ddc1::HPH* | 9126 *ddc1*Δ | 1544 |
| 9496 | a | *dna2::KAN ddc1::HPH* | 9126 *ddc1*Δ | 1544 |
| 9522 | a | *yku70::HIS3 ddc1::HPH* | 9044 *ddc1*Δ | 1559 |
| 9523 | a | *yku70::HIS3 ddc1::HPH* | 9044 *ddc1*Δ | 1559 |
| 9593 | a | *rad9::HIS3* | 4647 x 7629 *irc5*Δ | |
| 9619 | α | *cdc13-1* | 4647 x 7629 *hcm1*Δ | |
| 9620 | α | *cdc13-1 rad9::HIS3* | 4647 x 7629 *hcm1*Δ | |
| 9621 | α | *hcm1::HPH* | 4647 x 7629 *hcm1*Δ | |
| 9622 | a | *hcm1::HPH* | 4647 x 7629 *hcm1*Δ | |
| 9623 | a | *cdc13-1 hcm1::HPH* | 4647 x 7629 *hcm1*Δ | |
| 9624 | a | *cdc13-1 hcm1::HPH* | 4647 x 7629 *hcm1*Δ | |
| 9625 | a | *cdc13-1 hcm1::HPH* | 4647 x 7629 *hcm1*Δ | |
| 9626 | α | *cdc13-1 hcm1::HPH* | 4647 x 7629 *hcm1*Δ | |
| 9627 | a | *rad9::HIS3* | 4647 x 7629 *hcm1*Δ | |
| 9628 | α | *cdc13-1 rad9::HIS3 hcm1::HPH* | 4647 x 7629 *hcm1*Δ | |
| 9629 | a | *cdc13-1 rad9::HIS3 hcm1::HPH* | 4647 x 7629 *hcm1*Δ | |

| | | | |
|---|---|---|---|
| 9630 | a | *cdc13-1 rad9::HIS3 hcm1::HPH* | 4647 x 7629 *hcm1*Δ |
| 9632 | a | *yku70::LEU2* | 4647 x 7629 *hcm1*Δ |
| 9633 | α | *yku70::LEU2 rad9::HIS3* | 4647 x 7629 *hcm1*Δ |
| 9634 | a | *yku70::LEU2 hcm1::HPH* | 4647 x 7629 *hcm1*Δ |
| 9635 | a | *yku70::LEU2 hcm1::HPH* | 4647 x 7629 *hcm1*Δ |
| 9636 | a | *yku70::LEU2 hcm1::HPH* | 4647 x 7629 *hcm1*Δ |
| 9637 | a | *yku70::LEU2 hcm1::HPH* | 4647 x 7629 *hcm1*Δ |
| 9638 | a | *yku70::LEU2 rad9::HIS3 hcm1::HPH* | 4647 x 7629 *hcm1*Δ |
| 9639 | α | *yku70::LEU2 rad9::HIS3 hcm1::HPH* | 4647 x 7629 *hcm1*Δ |
| 9640 | a | *yku70::LEU2 rad9::HIS3 hcm1::HPH* | 4647 x 7629 *hcm1*Δ |
| 9728 | α | *cdc13-1 uls1::HPH* | 4647 x 7629 *uls1*Δ |
| 9729 | a | *cdc13-1 uls1::HPH* | 4647 x 7629 *uls1*Δ |
| 9730 | α | *cdc13-1 uls1::HPH* | 4647 x 7629 *uls1*Δ |
| 9731 | α | *cdc13-1 uls1::HPH* | 4647 x 7629 *uls1*Δ |
| 9732 | a | *cdc13-1 uls1::HPH* | 4647 x 7629 *uls1*Δ |
| 9733 | a | *cdc13-1 uls1::HPH* | 4647 x 7629 *uls1*Δ |
| 9734 | α | *cdc13-1 rad9::HIS3 uls1::HPH* | 4647 x 7629 *uls1*Δ |
| 9735 | a | *cdc13-1 rad9::HIS3 uls1::HPH* | 4647 x 7629 *uls1*Δ |
| 9736 | a | *cdc13-1 rad9::HIS3 uls1::HPH* | 4647 x 7629 *uls1*Δ |
| 9738 | α | *uls1::HPH* | 4647 x 7629 *uls1*Δ |
| 9740 | α | *uls1::HPH* | 4647 x 7629 *uls1*Δ |
| 9742 | α | *yku70::LEU2 uls1::HPH* | 4647 x 7629 *uls1*Δ |
| 9743 | α | *yku70::LEU2 uls1::HPH* | 4647 x 7629 *uls1*Δ |
| 9744 | α | *yku70::LEU2 uls1::HPH* | 4647 x 7629 *uls1*Δ |
| 9745 | a | *yku70::LEU2 uls1::HPH* | 4647 x 7629 *uls1*Δ |
| 9746 | α | *yku70::LEU2 uls1::HPH* | 4647 x 7629 *uls1*Δ |
| 9747 | α | *yku70::LEU2 uls1::HPH* | 4647 x 7629 *uls1*Δ |
| 9748 | a | *yku70::LEU2 uls1::HPH* | 4647 x 7629 *uls1*Δ |
| 9749 | α | *yku70::LEU2 rad9::HIS3 uls1::HPH* | 4647 x 7629 *uls1*Δ |
| 9750 | α | *yku70::LEU2 rad9::HIS3 uls1::HPH* | 4647 x 7629 *uls1*Δ |
| 9898 | α | *stn1-13* | 9246 x 9746 *uls1*Δ |
| 9912 | a | *rad9::HIS3 stn1-13* | 9246 x 9746 *uls1*Δ |
| 9913 | α | *rad9::HIS3 stn1-13* | 9246 x 9746 *uls1*Δ |
| 9918 | α | *uls1::HPH stn1-13* | 9246 x 9746 *uls1*Δ |
| 9919 | a | *uls1::HPH stn1-13* | 9246 x 9746 *uls1*Δ |
| 9920 | a | *uls1::HPH stn1-13* | 9246 x 9746 *uls1*Δ |
| 9921 | a | *uls1::HPH stn1-13* | 9246 x 9746 *uls1*Δ |
| 9934 | a | *rad9::HIS3 uls1::HPH stn1-13* | 9246 x 9746 *uls1*Δ |
| 9935 | a | *rad9::HIS3 uls1::HPH stn1-13* | 9246 x 9746 *uls1*Δ |
| 9936 | α | *rad9::HIS3 uls1::HPH stn1-13* | 9246 x 9746 *uls1*Δ |
| 10344 | α | *yku70::HIS3 mec3::TRP1* | 8663 x 8714 |
| 10348 | a | *yku70::HIS3 rad17::LEU2* | 8663 x 8714 |
| 10385 | a | *xbp1::HPH* | 4647 x 7629 *xbp1*Δ |
| 10386 | α | *xbp1::HPH* | 4647 x 7629 *xbp1*Δ |
| 10390 | α | *cdc13-1 rad9::HIS3 xbp1::HPH* | 4647 x 7629 *xbp1*Δ |
| 10391 | a | *cdc13-1 rad9::HIS3 xbp1::HPH* | 4647 x 7629 *xbp1*Δ |

| | | | | |
|---|---|---|---|---|
| 10392 | a | *cdc13-1 rad9::HIS3 xbp1::HPH* | 4647 x 7629 *xbp1*Δ | |
| 10393 | α | *yku70::LEU2 rad9::HIS3 xbp1::HPH* | 4647 x 7629 *xbp1*Δ | |
| 10394 | α | *yku70::LEU2 rad9::HIS3 xbp1::HPH* | 4647 x 7629 *xbp1*Δ | |
| 10395 | α | *yku70::LEU2 xbp1::HPH* | 4647 x 7629 *xbp1*Δ | |
| 10396 | a | *yku70::LEU2 xbp1::HPH* | 4647 x 7629 *xbp1*Δ | |
| 10397 | a | *cdc13-1 xbp1::HPH* | 4647 x 7629 *xbp1*Δ | |
| 10398 | a | *cdc13-1 xbp1::HPH* | 4647 x 7629 *xbp1*Δ | |
| 10399 | a | *rad9::HIS3 xbp1::HPH* | 4647 x 7629 *xbp1*Δ | |
| 10400 | a | *yku70::LEU2 rad9::HIS3* | 4647 x 7629 *xbp1*Δ | |
| 10401 | a | *yku70::LEU2 rad9::HIS3* | 4647 x 7629 *xbp1*Δ | |
| 10402 | α | *cdc13-1 rad9::HIS3* | 4647 x 7629 *xbp1*Δ | |
| 10403 | a | *cdc13-1 rad9::HIS3* | 4647 x 7629 *xbp1*Δ | |
| 10475 | α | *mec3::TRP1* | 7110 x 8714 | |
| 10478 | α | *rad17::LEU2* | 7110 x 8714 | |
| 10516 | a | *yku70::LEU2 chk1::HIS3* | 1215 x 7198 | |
| 10536 | α | *chk1::HIS3* | 1215 x 7198 | |
| 10537 | a | *chk1::HIS3* | 1215 x 7198 | |
| 10538 | a | *ddc1::KAN* | 1215 x 7198 | |
| 10553 | α | *pif1::NAT yku70::HIS3 dna2::KAN* | 4872 x 9483 | 1561 |
| 10554 | a | *pif1::NAT yku70::HIS3 dna2::KAN* | 4872 x 9483 | 1561 |
| 10557 | a | *pif1::NAT yku70::HIS3 dna2::KAN* | 9495 x 5509 | 1544 |
| 10558 | α | *pif1::NAT yku70::HIS3 dna2::KAN* | 9495 x 5509 | 1544 |
| 10559 | α | *pif1::NAT yku70::HIS3 dna2::KAN* | 4872 x 9483 | |
| 10560 | a | *pif1::NAT yku70::HIS3 dna2::KAN* | 4872 x 9483 | |
| 10594 | a | *pif1::NAT dna2::KAN* | 4872 x 9483 | 1561 |
| 10595 | a | *pif1::NAT dna2::KAN* | 4872 x 9483 | 1561 |
| 10596 | α | *pif1::NAT dna2::KAN* | 9495 x 5509 | 1544 |
| 10597 | α | *pif1::NAT dna2::KAN* | 9495 x 5509 | 1544 |
| 10598 | α | *pif1::NAT dna2::KAN* | 4872 x 9483 | |
| 10599 | a | *pif1::NAT dna2::KAN* | 4872 x 9483 | |
| 10602 | a | *yku70::HIS3 dna2::KAN* | 4872 x 9483 | 1561 |
| 10603 | α | *yku70::HIS3 dna2::KAN* | 4872 x 9483 | 1561 |
| 10604 | α | *yku70::HIS3 dna2::KAN* | 9495 x 5509 | 1544 |
| 10605 | α | *yku70::HIS3 dna2::KAN* | 9495 x 5509 | 1544 |
| 10616 | a | *ddc1::HPH dna2::KANMX* | 4872 x 9483 | |
| 10617 | a | *ddc1::HPH dna2::KANMX* | 4872 x 9483 | |
| 10618 | a | *ddc1::HPH dna2::KANMX* | 4872 x 9483 | |
| 10624 | α | *pif1::NAT* | 4872 x 9483 | |
| 10630 | α | *dna2::KAN* | 4872 x 9483 | 1561 |
| 10631 | a | *dna2::KAN* | 4872 x 9483 | 1561 |
| 10634 | a | *dna2::KAN* | 9495 x 5509 | 1544 |
| 10635 | α | *dna2::KAN* | 9495 x 5509 | 1544 |
| 10818 | a | *rad9::HIS3* | 10539 x 9593 | |
| 10819 | α | *ddc1::KAN rad9::HIS3* | 10539 x 9593 | |
| 10820 | a | *ddc1::KAN rad9::HIS3* | 10539 x 9593 | |
| 10876 | a | *rad50::URA3* | | |

| | | | | |
|---|---|---|---|---|
| 10877 | a | *rad50::URA3* | | |
| 10963 | a | *dna2::KAN ddc1::HPH rad9::HIS3* | 10615 x 9593 | |
| 10964 | α | *dna2::KAN ddc1::HPH rad9::HIS3* | 10615 x 9593 | |
| 10965 | a | *dna2::KAN ddc1::HPH rad9::HIS3* | 10615 x 9593 | |
| 10967 | α | *dna2::KAN rad9::HIS3* | 10635 x 9593 | |
| 10968 | a | *dna2::KAN rad9::HIS3* | 10635 x 9593 | |
| 10969 | α | *dna2::KAN rad9::HIS3* | 10635 x 9593 | |
| 10971 | α | *dna2::KAN ddc1::HIS3* | 10635 x 8530 | |
| 10972 | α | *dna2::KAN ddc1::HIS3* | 10635 x 8530 | |
| 10974 | a | *dna2::KAN ddc1::HIS3* | 10635 x 8530 | |
| 10975 | a | *dna2::KAN chk1::HIS3* | 10635 x 10537 | |
| 10976 | a | *dna2::KAN chk1::HIS3* | 10635 x 10537 | |
| 10977 | a | *dna2::KAN chk1::HIS3* | 10635 x 10537 | |
| 10978 | α | *dna2::KAN chk1::HIS3* | 10635 x 10537 | |
| 10979 | α | *dna2::KAN rad9::LEU2* | 10635 x 7177 | |
| 10980 | α | *dna2::KAN rad9::LEU2* | 10635 x 7177 | |
| 10981 | a | *dna2::KAN rad9::LEU2* | 10635 x 7177 | |
| 10982 | a | *dna2::KAN rad9::LEU2* | 10635 x 7177 | |
| 11026 | a | *mec1::HIS3 sml1::KAN* | 1326 x 9788 | |
| 11032 | a | *mec1::HIS3 sml1::KAN dna2::NAT* | 1326 x 9788 | |
| 11033 | α | *mec1::HIS3 sml1::KAN dna2::NAT* | 1326 x 9788 | |
| 11034 | a | *mec1::HIS3 sml1::KAN dna2::NAT* | 1326 x 9788 | |
| 11035 | a | *mec1::HIS3 sml1::KAN dna2::NAT* | 1326 x 9788 | |
| 11054 | a | *cdc13-1-int dna2-W128A,Y130A-int* | 1108 colony 6R | |
| 11055 | α | *dna2-W128A,Y130A-int* | 3001 colony 5G-2 | |
| 11056 | α | *dna2-W128A,Y130A-int* | 3001 colony 5G-5 | |
| 11115 | α | *pol32::KAN dna2::NAT* | 5703 x 9789 | |
| 11116 | a | *pol32::KAN dna2::NAT* | 5703 x 9789 | |
| 11117 | α | *pol32::KAN dna2::NAT* | 5703 x 9789 | |
| 11190 | a | *dna2::NAT* | 9788 | 1758 |
| 11195 | α | *dna2::KAN rad9::HIS3* | 10967 passage 5 | |
| 11196 | a | *dna2::KAN rad9::HIS3* | 10968 passage 5 | |
| 11197 | a | *dna2::KAN chk1::HIS3* | 10975 passage 5 | |
| 11199 | α | *dna2::KAN rad17::LEU2* | 10979 passage 5 | |
| 11200 | α | *dna2::KAN rad17::LEU2* | 10980 passage 5 | |
| 11201 | α | *dna2::KAN ddc1::HIS3* | 10973 passage 5 | |
| 11202 | a | *dna2::KAN ddc1::HIS3* | 10974 passage 5 | |
| 11205 | a | *dna2::NAT mec1::HIS3 sml1::KAN* | 11032 passage 5 | |
| 11206 | α | *dna2::NAT mec1::HIS3 sml1::KAN* | 11033 passage 5 | |
| 11207 | a | *dna2::KAN chk1::HIS3* | 10976 passage 5 | |
| 11274 | α | *dna2::NAT* | DDY1070 RSA | 1758 |
| 11383 | a | *cdc15-2* | DDY1096 RSA | 1758 |
| 11384 | α | *cdc15-2 dna2::NAT* | DDY1096 RSA | 1758 |
| 11385 | a | *cdc15-2 dna2::NAT* | DDY1096 RSA | 1758 |
| 11386 | α | *cdc15-2 dna2::NAT* | DDY1096 RSA | 1758 |
| 11388 | a | *top3::HPH dna2::NAT* | DDY1098 RSA | 1758 |

| | | | | |
|---|---|---|---|---|
| 11389 | α | *top3::HPH dna2::NAT* | DDY1098 RSA | 1758 |
| 11390 | α | *top3::HPH dna2::NAT* | DDY1098 RSA | 1758 |
| 11392 | α | *top3::HPH* | DDY1098 RSA | 1758 |
| 11393 | α | *exo1::LEU2* | DDY1100 RSA | 1758 |
| 11394 | α | *exo1::LEU2 dna2::NAT* | DDY1100 RSA | 1758 |
| 11395 | a | *exo1::LEU2 dna2::NAT* | DDY1100 RSA | 1758 |
| 11396 | α | *exo1::LEU2 dna2::NAT* | DDY1100 RSA | 1758 |
| 11407 | α | *rad17::LEU2 dna2::NAT* | DDY1103 RSA | 1758 |
| 11408 | a | *rad17::LEU2 dna2::NAT* | DDY1103 RSA | 1758 |
| 11409 | α | *rad17::LEU2 dna2::NAT* | DDY1103 RSA | 1758 |
| 11411 | a | *rad17::LEU2* | DDY1103 RSA | 1758 |
| 11413 | α | *xrs2::LEU2 dna2::NAT* | DDY1107 RSA | 1758 |
| 11414 | a | *xrs2::LEU2 dna2::NAT* | DDY1107 RSA | 1758 |
| 11415 | a | *xrs2::LEU2 dna2::NAT* | DDY1107 RSA | 1758 |
| 11417 | a | *xrs2::LEU2* | DDY1107 RSA | 1758 |
| 11419 | α | *rad51::KAN* | DDY1111 RSA | 1758 |
| 11421 | a | *rad51::KAN dna2::NAT* | DDY1111 RSA | 1758 |
| 11422 | a | *rad51::KAN dna2::NAT* | DDY1111 RSA | 1758 |
| 11423 | a | *rad51::KAN dna2::NAT* | DDY1111 RSA | 1758 |
| 11425 | α | *rad24::TRP1* | DDY1115 RSA | 1758 |
| 11427 | α | *rad24::TRP1 dna2::NAT* | DDY1115 RSA | 1758 |
| 11428 | a | *rad24::TRP1 dna2::NAT* | DDY1115 RSA | 1758 |
| 11429 | a | *rad24::TRP1 dna2::NAT* | DDY1115 RSA | 1758 |
| 11431 | α | *chk1::HIS3* | DDY1119 RSA | 1758 |
| 11434 | a | *chk1::HIS3 dna2::NAT* | DDY1119 RSA | 1758 |
| 11435 | α | *chk1::HIS3 dna2::NAT* | DDY1119 RSA | 1758 |
| 11436 | α | *chk1::HIS3 dna2::NAT* | DDY1119 RSA | 1758 |
| 11441 | α | *mph1::KAN* | DDY1123 RSA | 1758 |
| 11443 | a | *mec1::HIS3 sml1::KAN* | DDY1127 RSA | 1758 |
| 11447 | a | *mec1::HIS3 sml1::KAN dna2::NAT* | DDY1127 RSA | 1758 |
| 11448 | α | *mec1::HIS3 sml1::KAN dna2::NAT* | DDY1127 RSA | 1758 |
| 11449 | a | *mec1::HIS3 sml1::KAN dna2::NAT* | DDY1127 RSA | 1758 |
| 11451 | a | *sgs1::KAN dna2::NAT* | DDY1129 RSA | 1758 |
| 11452 | α | *sgs1::KAN dna2::NAT* | DDY1129 RSA | 1758 |
| 11453 | a | *sgs1::KAN dna2::NAT* | DDY1129 RSA | 1758 |
| 11455 | α | *sgs1::KAN* | DDY1129 RSA | 1758 |
| 11463 | α | *pol32::KAN* | DDY1135 RSA | 1758 |
| 11465 | a | *pol32::KAN dna2::NAT* | DDY1135 RSA | 1758 |
| 11466 | a | *pol32::KAN dna2::NAT* | DDY1135 RSA | 1758 |
| 11467 | a | *pol32::KAN dna2::NAT* | DDY1135 RSA | 1758 |
| 11469 | α | *ddc1::HIS3* | DDY1139 RSA | 1758 |
| 11471 | a | *ddc1::HIS3* | DDY1139 RSA | 1758 |
| 11472 | α | *ddc1::HIS3 dna2::NAT* | DDY1139 RSA | 1758 |
| 11473 | a | *ddc1::HIS3 dna2::NAT* | DDY1139 RSA | 1758 |
| 11475 | α | *rad9::HIS3 dna2::NAT* | DDY1141 RSA | 1758 |
| 11476 | α | *rad9::HIS3 dna2::NAT* | DDY1141 RSA | 1758 |

| | | | | |
|---|---|---|---|---|
| 11477 | α | *rad9::HIS3 dna2::NAT* | DDY1141 RSA | 1758 |
| 11479 | α | *rad9::HIS3* | DDY1141 RSA | 1758 |
| 11481 | a | *mph1::KAN dna2::NAT* | DDY1143 RSA | 1758 |
| 11482 | α | *mph1::KAN dna2::NAT* | DDY1143 RSA | 1758 |
| 11485 | α | *mph1::KAN dna2::NAT* | DDY1143 RSA | 1758 |
| 11506 | a | *bub2::HPH dna2::NAT* | DDY1147 RSA | 1758 |
| 11507 | α | *bub2::HPH dna2::NAT* | DDY1147 RSA | 1758 |
| 11508 | a | *bub2::HPH* | DDY1147 RSA | 1758 |
| 11510 | a | *bub3::HPH dna2::NAT* | DDY1149 RSA | 1758 |
| 11511 | a | *bub3::HPH dna2::NAT* | DDY1149 RSA | 1758 |
| 11512 | a | *bub3::HPH* | DDY1149 RSA | 1758 |
| 11514 | α | *ctf3::HPH dna2::NAT* | DDY1151 RSA | 1758 |
| 11515 | a | *ctf3::HPH dna2::NAT* | DDY1151 RSA | 1758 |
| 11516 | α | *ctf3::HPH* | DDY1151 RSA | 1758 |
| 11518 | α | *dgr2::HPH dna2::NAT* | DDY1154 RSA | 1758 |
| 11519 | a | *dgr2::HPH dna2::NAT* | DDY1154 RSA | 1758 |
| 11520 | a | *dgr2::HPH* | DDY1154 RSA | 1758 |
| 11522 | α | *lsm1::HPH dna2::NAT* | DDY1156 RSA | 1758 |
| 11523 | a | *lsm1::HPH dna2::NAT* | DDY1156 RSA | 1758 |
| 11524 | α | *lsm1::HPH* | DDY1156 RSA | 1758 |
| 11526 | a | *rps4a::HPH dna2::NAT* | DDY1158 RSA | 1758 |
| 11527 | α | *rps4a::HPH dna2::NAT* | DDY1158 RSA | 1758 |
| 11528 | α | *rps4a::HPH* | DDY1158 RSA | 1758 |
| 11530 | a | *rtt109::HPH dna2::NAT* | DDY1160 RSA | 1758 |
| 11531 | α | *rtt109::HPH dna2::NAT* | DDY1160 RSA | 1758 |
| 11532 | a | *rtt109::HPH* | DDY1160 RSA | 1758 |
| 11534 | α | *dna2::NAT CAN1* | DDY1175 RSA | 1758 |
| 11535 | α | *dna2::NAT CAN1* | DDY1175 RSA | 1758 |
| 11958 | α | *W303 WT* | DDY1107 RSA | 1758 |
| DDY606 | | *cdc13-1/CDC13 dbp11::KAN/DPB11* | 1108/pDL1467 x 3001 | |
| DDY607 | | *cdc13-1/CDC13 dna2::KAN/DNA2* | 1108/pDL1467 x 3001 | |
| DDY609 | | *yku70::HIS3/YKU70 dna2::KAN/DNA2* | 1412 x 3001/pDL1467 | |
| DDY611 | | *yku70::LEU2/YKU70 dpb11::KAN/DPB11* | 6885 x 3001/pDL1467 | |
| DDY650 | | *cdc13-1/CDC13 rad9::HIS3/RAD9 yku70::LEU2/YKU70* | 4647 x 7529 | |
| DDY696 | | *cdc13::HPH/CDC13 dna2::KAN/DNA2 ddc1::NAT/DDC1* | 1108 x 3001 *ddc1*Δ *cdc13*Δ | 1561 |
| DDY698 | | *cdc13-1/CDC13 dna2::KAN/DNA2 ddc1::NAT/DDC1* | 1108 x 3001 *ddc1*Δ | 1544 |
| DDY700 | | *cdc13-1/CDC13 dna2::KAN/DNA2 ddc1::NAT/DDC1* | 1108 x 3001 *ddc1*Δ | 1561 |
| DDY723 | | *cdc13::HPH/CDC13 dna2::KAN/DNA2 ddc1::NAT/DDC1* | 1108 x 3001 *ddc1*Δ *cdc13*Δ | 1544 |
| DDY725 | | *cdc13::HPH/CDC13 dna2::KAN/DNA2 ddc1::NAT/DDC1* | 1108 x 3001 *ddc1*Δ *cdc13*Δ | 1559 |
| DDY874 | | *dna2::KAN/DNA2 rad9::HIS3/RAD9* | 10615 x 9593 | |

| | | | |
|---|---|---|---|
| DDY876 | *dna2::KAN/DNA2 ddc1::HIS3/DDC1* | 10635 x 8530 | |
| DDY878 | *dna2::KAN/DNA2 chk1::HIS3/CHK1* | 10635 x 10537 | |
| DDY880 | *dna2::KAN/DNA2 rad17::LEU2/RAD17* | 10635 x 7177 | |
| DDY947 | *rad53::HIS3/RAD53 sml1::URA3/SML1 dna2::KAN/DNA2* | 6662 x 10635 | |
| DDY949 | *exo1::LEU2/EXO1 dna2::KAN/DNA2* | 5927 x 10635 | |
| DDY950 | *tel1::NAT/TEL1 dna2::KAN/DNA2* | 6340 x 10635 | |
| DDY953 | *mre11::URA3/MRE11 dna2::NAT/DNA2* | 4457 x 9788 | |
| DDY956 | *pol32::KAN/POL32 dna2::NAT/DNA2* | 5703 x 9789 | |
| DDY958 | *mec1::HIS3/MEC1 sml1::KAN/SML1 dna2::NAT/DNA2* | 1326 x 9788 | |
| DDY966 | *dna2::KAN/DNA2 rif1::NAT/RIF1 rif2::HIS3/RIF2* | 10635 x 10954 | |
| DDY988 | *rif1::NAT/RIF1 dna2::KAN/DNA2* | 10310 x 10635 | |
| DDY989 | *rif2::HIS3/RIF2 dna2::NAT/DNA2* | 8931 x 9788 | |
| DDY1042 | *dna2::KAN/DNA2 rad9::HIS3/rad9::HIS3* | 10967 x 9593 | |
| DDY1070 | *pol32::KAN/POL32 dna2::NAT/DNA2* | 5704 x 11190 | 1758 |
| DDY1082 | *mph1::KAN/MPH1 dna2::NAT/DNA2* | 4282 x 9789 | 1758 |
| DDY1096 | *cdc15-2/CDC15 dna2::NAT/DNA2* | 10733 x 11274 | 1758 |
| DDY1098 | *top3::HPH dna2::NAT* | 6118 x 11274 | 1758 |
| DDY1100 | *exo1::LEU2/EXO1 dna2::KAN/DNA2* | 5939 x 11274 | 1758 |
| DDY1103 | *rad17::LEU2 dna2::NAT* | 10478 x 11190 | 1758 |
| DDY1107 | *xrs2::LEU2/XRS2 dna2::NAT/DNA2* | 1093 x 11274 | 1758 |
| DDY1111 | *rad51::KAN/RAD51 dna2::NAT/DNA2* | 3485 x 11274 | 1758 |
| DDY1115 | *rad24::TRP1/RAD24 dna2::NAT/DNA2* | 10534 x 11190 | 1758 |
| DDY1119 | *chk1::HIS3/CHK1 dna2::NAT/DNA2* | 10536 x 11190 | 1758 |
| DDY1123 | *mph1::KAN/MPH1 dna2::NAT/DNA2* | 4282 x 11274 | 1758 |
| DDY1127 | *mec1::HIS3/MEC1 sml1::KAN/SML1 dna2::NAT/DNA2* | 1326 x 11190 | 1758 |
| DDY1129 | *sgs1::KAN/SGS1 dna2::NAT/DNA2* | 4721 x 11274 | 1758 |
| DDY1135 | *pol32::KAN/POL32 dna2::NAT/DNA2* | 5704 x 11190 | 1758 |
| DDY1139 | *ddc1::HIS3/DDC1 dna2::NAT/DNA2* | 8530 x 11274 | 1758 |
| DDY1141 | *rad9::HIS3/RAD9 dna2::NAT/DNA2* | 9594 x 11190 | 1758 |
| DDY1143 | *mph1::KAN/MPH1 dna2::NAT/DNA2* | 11274 x 11275 | 1758 |
| DDY1147 | *bub2::HPH/BUB2 dna2::NAT/DNA2* | 11305 x 11190 | 1758 |
| DDY1149 | *bub3::HPH/BUB3 dna2::NAT/DNA2* | 11307 x 11190 | 1758 |
| DDY1151 | *ctf3::HPH/CTF3 dna2::NAT/DNA2* | 11309 x 11190 | 1758 |
| DDY1154 | *dgr2::HPH/DGR2 dna2::NAT/DNA2* | 11312 x 11190 | 1758 |
| DDY1156 | *lsm1::HPH/LSM1 dna2::NAT/DNA2* | 11314 x 11190 | 1758 |
| DDY1158 | *rps4a::HPH/RPS4A dna2::NAT/DNA2* | 11316 x 11190 | 1758 |
| DDY1160 | *rtt109::HPH/RTT109 dna2::NAT/DNA2* | 11318 x 11190 | 1758 |
| DDY1175 | *dna2::NAT/DNA2 can1-100/CAN1* | 5626 x 11274 | 1758 |

# Appendix B: Plasmids

Plasmids ordered by plasmid number (pDL).

***ddc1*-M3**: S413A, S436A, T444A; ****ddc1*-M8**: T342A, S469A, S471A, S495A, T529A, S532A, S580A, T602A; ***** ***ddc1*-M11**: T342A, S413A, S436A, S444A, S469A, S471A, S495A, T529A, S532A, S580A, T602A.

| pDL | Construction | Related Figure/Notes | Reference |
|---|---|---|---|
| 452 | pRS406-delNdeI | Backbone for cloning | Lab collection |
| 876 | pRS413-HIS3 | Vector control | Lab collection |
| 987 | pYTel based on pBluescriptII SK2 | For detecing Y' and telomere repeat sequences at telomers | Tsubouchi and Ogawa (2000) |
| 1042 | pFA6a-*KANMX6* | For gene deletions | Longtine *et al.* (1998) |
| 1239 | pFA6a-*KANMX6* | For gene deletions | Longtine *et al.* (1998) |
| 1248 | pRS315-*LEU2* | Vector control | Lab collection |
| 1467 | pRS316-CAN1-URA3 | Backbone for cloning | Lab collection |
| 1469 | YCplac111-*LEU2-DDC1* | Figure 14, Figure 15 | M. Muzi-Falconi |
| 1470 | YCplac111-*LEU2-ddc1-M3** | Figure 14, Figure 15 | M. Muzi-Falconi |
| 1472 | YCplac111-*LEU2-ddc1-M8*** | Figure 14, Figure 15 | M. Muzi-Falconi |
| 1474 | YCplac111-*LEU2-ddc1-M11**** | Figure 14, Figure 15 | M. Muzi-Falconi |
| 1476 | YCplac111-*LEU2-ddc1-T602S* | Figure 14, Figure 15 | M. Muzi-Falconi |
| 1479 | YCplac111-*LEU2-ddc1-T602A* | Figure 14, Figure 15 | M. Muzi-Falconi |
| 1543 | pRS315-*LEU2-DDC1* | Figure 14, Figure 15 | P. Burgers |
| 1544 | pRS314-*TRP1-DNA2* | Figure 23, Figure 30 | P. Burgers |
| 1545 | pRS313-*HIS3-DPB11* | Figure 20, Figure 21 | P. Burgers |
| 1546 | pRS315-*LEU2-ddc1-W352A* | Figure 14, Figure 15 | P. Burgers |
| 1547 | pRS315-*LEU2-ddc1-W352A,W544A* | Figure 14, Figure 15 | P. Burgers |
| 1548 | pRS315-*LEU2-ddc1-W352A,W544A,T602A* | Figure 14, Figure 15 | P. Burgers |
| 1549 | pRS315-*LEU2-ddc1-(1-404),W352A* | Figure 14, Figure 15 | P. Burgers |
| 1550 | pRS315-*LEU2-ddc1-T602A* | Figure 14, Figure 15 | P. Burgers |
| 1552 | pRS313-*HIS3-dpb11-601* | Figure 20, Figure 21 | P. Burgers |
| 1553 | pRS313-*HIS3-dpb11-W700A* | Figure 20, Figure 21 | P. Burgers |
| 1554 | pRS313-*HIS3-dpb11-Y735A* | Figure 20, Figure 21 | P. Burgers |
| 1555 | pRS313-*HIS3-dpb11-W700A,Y735A* | Figure 20, Figure 21 | P. Burgers |
| 1556 | pRS313-*HIS3-dpb11-W700A,T731A,Y735A* | Figure 20, Figure 21 | P. Burgers |
| 1557 | pRS314-*TRP1-dna2∆500N* | N/A | Y. S. Seo |
| 1558 | pRS314-*TRP1-dna2∆450N* | N/A | Y. S. Seo |
| 1559 | pRS314-*TRP1* | Figure 23, Figure 30 | Y. S. Seo |

| | | | |
|---|---|---|---|
| 1560 | pRS314-*TRP1-DNA2* | Figure 23, Figure 30 | Y. S. Seo |
| 1561 | pRS314-*TRP1-dna2-W128A,W130A* | Figure 23, Figure 30 | P. Burgers |
| 1566 | pRS314-*TRP1* | Figure 23, Figure 30 | J. Campbell |
| 1567 | pRS314-*TRP1-DNA2* | Figure 23, Figure 30 | J. Campbell |
| 1568 | pRS314-*TRP1-dna2-C519A* | Figure 23, Figure 30 | J. Campbell |
| 1569 | pRS314-*TRP1-dna2-C768A* | Figure 23, Figure 30 | J. Campbell |
| 1570 | pRS314-*TRP1-dna2-C771A* | Figure 23 | J. Campbell |
| 1571 | pRS314-*TRP1-dna2-C777A* | N/A | J. Campbell |
| 1575 | pFA6a-KANMX6 | For gene deletions | Longtine et al. (1998) |
| 1583 | pFA6a-HPHNT1 | For gene deletions | Yeast (2004) 21, 947-962 |
| 1599 | pAG25-NATMX4 | For gene deletions | Goldstein and McCusker, 1999 |
| 1654 | pRS406-URA3del*Nde*I-*DNA2* | Cloning; pDL452 cut with *Spe*I-*Xho*I and ligated with *DNA2* (cut with the same enzymes) from pDL1544 | This work |
| 1655 | pRS406-URA3del*Nde*I-*dna2-W128A,Y130A* | Cloning; pDL452 cut with *Spe*I-*Xho*I and ligated with *dna2-W128A,Y130A* (cut with the same enzymes) from pDL1561 | This work |
| 1672 | pRS406-URA3del*Nde*I-*DNA2*ΔC | Cloning; from pDL1654 C-terminal part of *DNA2* cut out with *Sca*II and religated | This work |
| 1673 | pRS406-URA3del*Nde*I-*dna2-W128A,Y130A*Δ*C* | Cloning; from pDL1655 C-terminal part of *dna2-W128A,Y130A*cut out with *Sca*II and religated | This work |
| 1727 | pRS316-CAN1-URA3 | Re-amplification of pDL1467 | |
| 1731 | pRS406-URA3del*Nde*I-*DNA2*ΔC-Gibson Assemby | Gibson Assembly; 2 PCR fragments from pDL1672 and *DNA2* promoter region from genomic DNA assembled | This work |
| 1732 | pRS406-URA3del*Nde*I-*dna2-W128A,Y130A*ΔC-Gibson Assemby-point mutation | Gibson Assembly; 2 PCR fragments from pDL1673 and *DNA2* promoter region from genomic DNA assembled | This work |
| 1733 | pRS406-URA3del*Nde*I-*dna2-W128A,Y130A*ΔC-Gibson Assemby | Point mutation from pDL1732 removed by QuickChange method | This work |
| 1758 | *pRS316-CAN1-URA3-DNA2* | Cloning; pDL1727 cut with *Xma*I and ligated with *DNA2* from pDL1544 | This work |

# Appendix C: Primers

Ordered by oligonucleotide number (M).

| No. (M) | Oligonucleotide Sequence | Target/Notes | Related Figure |
|---|---|---|---|
| 550 | ATTGGCACGATGATGATTCC | *CDC13,* to check the presence of *cdc13-1* mutation | Figure 21 |
| 551 | TTCGATCAGGCTTTTCCAGT | *CDC13,* to check the presence of *cdc13-1* mutation | Figure 21 |
| 1970 | ATCGTTCGGACAGAAAATGG | *DNA2*, used to confirm gene deletion | Figure 33 |
| 2947 | AAGAACAAGAGGTCTGCGAG | *DNA2*, used to confirm gene deletion | Figure 33 |
| 2958 | TGCTTGATGGTCGGAAGAGG | *KANMX*, used to confirm gene deletion | Figure 33 |
| 3157 | CCCACCACACACACCCACACCC | Conjugated probe for in gel hybridisation that binds to ssDNA-TG repeats | Figure 14 |
| 3275 | GACCGGGCACATTTAATCAG | *BUD6,* used for genomic qPCR | Figure 24 |
| 3276 | TCAGCCTTGTCAATAGCTTCG | *BUD6,* used for genomic qPCR | Figure 24 |
| 3603 | TACCCAAGGATGTCGAACG | *DNA2,* used for amplification | Figure 33 |
| 3772 | AAAGTGGAGCCCAGGAAAGT | *DNA2* used for genomic qPCR | Figure 24 |
| 3773 | TTGCCTGTTTTGGCTTGATT | *DNA2* used for genomic qPCR | Figure 24 |
| 3778 | AGGTGGCGGCCTTTATTTAT | *PRP8*, used for genomic qPCR | Figure 24 |
| 3779 | GATCCTACGTGGCCTAATTGA | *PRP8*, used for genomic qPCR | Figure 24 |
| 3780 | ATTTGGTACTGTTGGGCTGTG | *SOL3*, used for genomic qPCR | Figure 24 |
| 3781 | GCAACTCTTTTGGTTGTTTCG | *SOL3*, used for genomic qPCR | Figure 24 |
| 3939 | TCAATTAGGCCACGTAGGATCC GTTCAGATAAGCAACATC | *DNA2*, used to amplify genomic *DNA2* for Gibson Assembly | Appendix D |
| 3940 | AATTAGACATTTCCCGTTTCGGT TTAACTTGTGAATTTGG | *DNA2*, used to amplify genomic *DNA2* for Gibson Assembly | Appendix D |
| 3941 | CGAAATACATCAAGAACAAAAGA TATAAACAAAGCAGTTA | pDL1672-1673, used to amplify plasmid region for Gibson Assembly | Appendix D |
| 3942 | GACGAAAGGGCCTCGTGATACG CCTATTTTTATAGGTTAA | pDL1672-1673, used to amplify plasmid region for Gibson Assembly | Appendix D |
| 3943 | CCGCGCACATTTCCCCGAAAAG TGCCACCTGACGTCTAAG | pDL1672-1673, used to amplify plasmid region for Gibson Assembly | Appendix D |
| 3944 | GGTATGGATCCAACCGAGTAGT TCAAGGCCTTCAGTATCC | pDL1672-1673, used to amplify plasmid region for Gibson Assembly | Appendix D |
| **3595** | GTGTCCTAAAGTCAATAGCCGTT TCACAAGTACG | *DNA2*, used to revert point mutation by QuickChange | Figure 25 |
| **3960** | CGTACTTGTGAAACGGCTATTG ACTTTAGGACAC | *DNA2*, used to revert point mutation by QuickChange | Figure 25 |

# Appendix D. Gibson Assembly

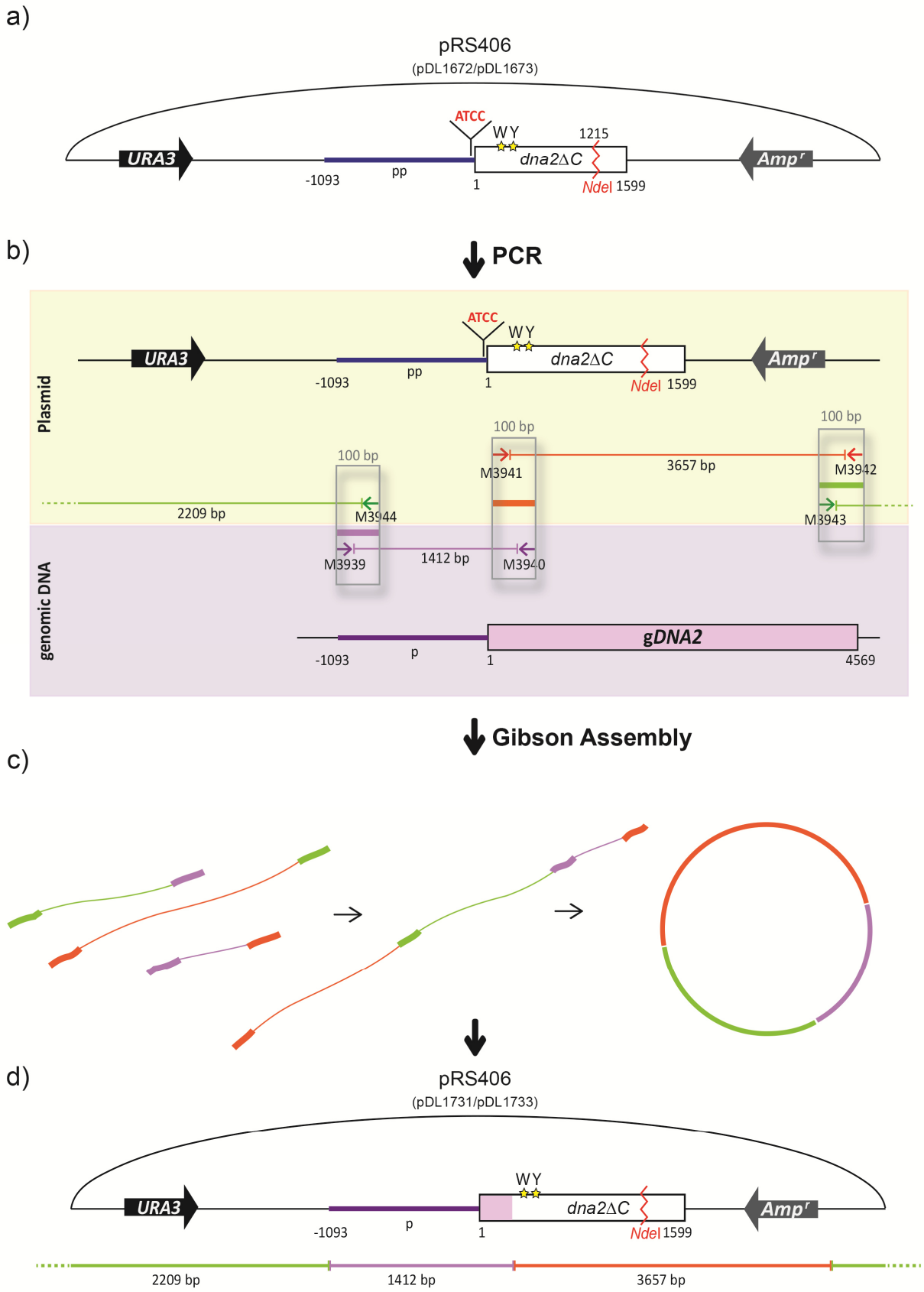

**Gibson Assembly method**

a) Plasmids pDL1672/pDL1673 contained additional, unwanted 4 bp (ATCC) upstream ATG codon.

b) Three DNA sequences were amplified by PCR: two fragments were from plasmids pDL1672/pDL1673 and primers were: **M3941 – M3942** and **M3943 – M3944**. One fragment was a promoter region of *DNA2* gene from genomic DNA of WT strain (DLY3001), primers were: **M3939 – M3940**. Grey boxes and thick coloured lines (purple, orange and green) indicate 100 bp-long overlapping sequences of PCR products.*URA3* – marker gene allowing selection on -URA media; *Amp*$^r$ – bacterial selective marker from the plasmid; *Nde*I – unique site for *Nde*I restriction enzyme. The *Nde*I site of *URA3* gene from pRS406 was previously destroyed in pDL452 plasmid. pDL452 served as a backbone; stars - point mutations (affected amino acids are tryptophan W128 and tyrosine Y130); *pp* – promoter sequence from the plasmid; *p* - promoter sequence amplified from genomic DNA.

c) Three PCR products were assembled in a One-step isothermal assembly reaction. DNA fragments share 100 bp terminal sequence overlaps which allow for recognition of complementary sequences. PCR products are incubated for 1 h at 50°C in the assembly mix, which consists of T5 exonuclease (removes nucleotides from the 5’ ends of double stranded DNA molecules), Phusion DNA polymerase (fills the gaps) and Taq DNA ligase (seals the nicks).

d) Newly assembled plasmids do not contain additional 4 bp upstream ATG codon of *DNA2* gene.

# Appendix E. Template of plate 15

Horizontal numbers – numbers of columns; vertical numbers – numbers of rows.

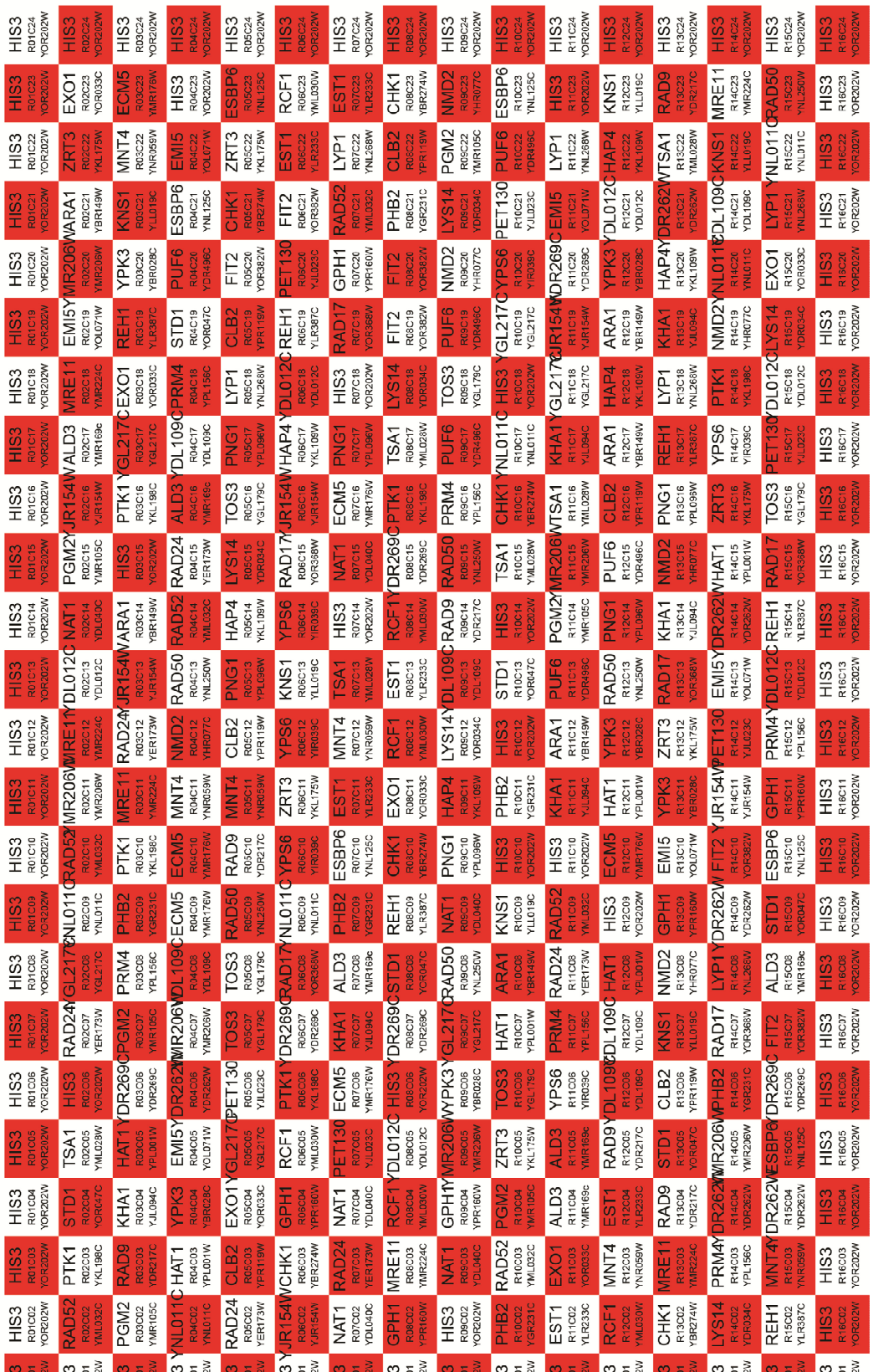

# Appendix F. 702 genes from S288C SGA

**R package version: 0.0-39**
**Summary type: mean**
**Test type: t-test**

x-axis treatment: 20°C
x-axis medium: SDM_rhlk_TGNH
x-axis screen ID: SGA0188
x-axis screen name: dna2_PI_PI
x-axis libraries: SDLV4_1536
x-axis client: MMA
x-axis user: AAB
x-axis date: 2016/01/06
x-axis PI: DAL
x-axis condition: SDM_rhlk_TGNH
x-axis inoculation type: PIN
x-axis fitness definition: Trimmed

y-axis treatment: 20°C
y-axis medium: SDM_rhlk_CTGNH
y-axis screen ID: SGA0189
y-axis screen name: dna2_PI_PI
y-axis libraries: SDLV4_1536
y-axis client: MMA
y-axis user: AAB
y-axis date: 2016/02/06
y-axis PI: DAL
y-axis condition: SDM_rhlk_CTGNH
y-axis inoculation type: PIN
y-axis fitness definition: Trimmed

Light grey cells – genes identified in S288C SGA as "enhancers" of *dna2*Δ*.*
Dark grey cells – genes identified in S288C SGA as "suppressors" of *dna2*Δ*.*
Out of app. 5000 genes, 702 had q ≤ 0.05 (False Discovery Rate (FDR) corrected p-value). These genes were ordered by GIS value and are presented in a table below (572 "enhancers" and 130 "suppressors" of *dna2*Δ lethality):

| No. | ORF | Gene | P | Q | GIS | Query Count | Type |
|---|---|---|---|---|---|---|---|
| 1 | YML102W | **CAC2** | 0,0005 | 0,0105 | -56141,5 | 4 | E |
| 2 | YMR034C | **YMR034C** | 0,0010 | 0,0159 | -55344,2 | 4 | E |
| 3 | YDR398W | **UTP5** | 0,0001 | 0,0039 | -49154 | 4 | E |
| 4 | YOL102C | **TPT1** | 0,0010 | 0,0162 | -48853,9 | 4 | E |
| 5 | YMR027W | **YMR027W** | 0,0032 | 0,0316 | -47690,7 | 4 | E |
| 6 | YOR353C | **SOG2** | 0,0025 | 0,0274 | -45724,6 | 4 | E |
| 7 | YGL243W | **TAD1** | 0,0066 | 0,0489 | -44766,4 | 4 | E |
| 8 | YOR139C | **YOR139C** | 0,0001 | 0,0047 | -42361,1 | 4 | E |
| 9 | YOR140W | **SFL1** | 0,0029 | 0,0301 | -41251,1 | 4 | E |
| 10 | YNL021W | **HDA1** | 0,0022 | 0,0255 | -41191,4 | 4 | E |
| 11 | YNL099C | **OCA1** | 0,0000 | 0,0013 | -38535,6 | 4 | E |
| 12 | YNR006W | **VPS27** | 0,0000 | 0,0010 | -37864,2 | 4 | E |
| 13 | YLR446W | **YLR446W** | 0,0011 | 0,0169 | -37286,5 | 4 | E |

| | | | | | | | |
|---|---|---|---|---|---|---|---|
| 14 | YML117W-A | **YML117W-A** | 0,0000 | 0,0010 | -35961,7 | 4 | E |
| 15 | YML121W | **GTR1** | 0,0030 | 0,0304 | -33846,4 | 4 | E |
| 16 | YPL266W | **DIM1** | 0,0023 | 0,0255 | -33170,9 | 4 | E |
| 17 | YBR088C | **POL30** | 0,0003 | 0,0076 | -33144,6 | 4 | E |
| 18 | YOR191W | **RIS1** | 0,0002 | 0,0052 | -33140,2 | 4 | E |
| 19 | YDR293C | **SSD1** | 0,0024 | 0,0264 | -33081,1 | 4 | E |
| 20 | YML007W | **YAP1** | 0,0005 | 0,0103 | -32945 | 4 | E |
| 21 | YDL162C | **YDL162C** | 0,0004 | 0,0090 | -32784,5 | 4 | E |
| 22 | YDR331W | **GPI8** | 0,0010 | 0,0162 | -32695,2 | 4 | E |
| 23 | YLR386W | **VAC14** | 0,0000 | 0,0018 | -32462 | 4 | E |
| 24 | YFL013C | **IES1** | 0,0000 | 0,0018 | -32349,4 | 4 | E |
| 25 | YER092W | **IES5** | 0,0003 | 0,0084 | -32030,4 | 4 | E |
| 26 | YMR216C | **SKY1** | 0,0004 | 0,0095 | -31762,1 | 4 | E |
| 27 | YMR103C | **YMR103C** | 0,0034 | 0,0327 | -31570,6 | 4 | E |
| 28 | YLR176C | **RFX1** | 0,0001 | 0,0041 | -31384 | 4 | E |
| 29 | YLR119W | **SRN2** | 0,0038 | 0,0352 | -31020,4 | 4 | E |
| 30 | YCL054W | **SPB1** | 0,0000 | 0,0016 | -30796,6 | 4 | E |
| 31 | YDR363W | **ESC2** | 0,0001 | 0,0035 | -30765,6 | 4 | E |
| 32 | YOL097C | **WRS1** | 0,0023 | 0,0255 | -30418,5 | 4 | E |
| 33 | YDL193W | **NUS1** | 0,0025 | 0,0268 | -29881 | 4 | E |
| 34 | YMR073C | **IRC21** | 0,0012 | 0,0176 | -29878,9 | 4 | E |
| 35 | YLR234W | **TOP3** | 0,0000 | 0,0001 | -29562,3 | 4 | E |
| 36 | YLR200W | **YKE2** | 0,0019 | 0,0224 | -29355,7 | 4 | E |
| 37 | YMR277W | **FCP1** | 0,0004 | 0,0094 | -29044,7 | 8 | E |
| 38 | YMR029C | **FAR8** | 0,0047 | 0,0404 | -28979,3 | 4 | E |
| 39 | YDR455C | **:::GUK1** | 0,0001 | 0,0036 | -28890,5 | 4 | E |
| 40 | YDR274C | **YDR274C** | 0,0000 | 0,0020 | -28629,2 | 4 | E |
| 41 | YNL206C | **RTT106** | 0,0002 | 0,0068 | -28591,8 | 4 | E |
| 42 | YDL002C | **NHP10** | 0,0004 | 0,0095 | -28400,6 | 4 | E |
| 43 | YDR279W | **RNH202** | 0,0001 | 0,0048 | -28221,5 | 4 | E |
| 44 | YOR039W | **CKB2** | 0,0000 | 0,0009 | -28185,7 | 4 | E |
| 45 | YFR010W | **UBP6** | 0,0000 | 0,0003 | -28150,4 | 4 | E |
| 46 | YOR038C | **HIR2** | 0,0068 | 0,0495 | -27885,7 | 4 | E |
| 47 | YBR057C | **MUM2** | 0,0000 | 0,0002 | -27803,4 | 4 | E |
| 48 | YER164W | **CHD1** | 0,0018 | 0,0220 | -27582,8 | 4 | E |
| 49 | YPR179C | **HDA3** | 0,0063 | 0,0476 | -27390,3 | 4 | E |
| 50 | YDL235C | **YPD1** | 0,0055 | 0,0439 | -27339,9 | 4 | E |
| 51 | YMR234W | **RNH1** | 0,0001 | 0,0027 | -27326,9 | 4 | E |
| 52 | YLR095C | **IOC2** | 0,0001 | 0,0033 | -27297,9 | 4 | E |
| 53 | YNL091W | **NST1** | 0,0001 | 0,0029 | -27268,5 | 4 | E |
| 54 | YGL212W | **VAM7** | 0,0000 | 0,0012 | -27252,8 | 4 | E |
| 55 | YLR374C | **YLR374C** | 0,0001 | 0,0052 | -26920,2 | 4 | E |
| 56 | YML027W | **YOX1** | 0,0008 | 0,0146 | -26882,7 | 4 | E |
| 57 | YML020W | **YML020W** | 0,0003 | 0,0073 | -26751,4 | 4 | E |
| 58 | YDR007W | **TRP1** | 0,0001 | 0,0048 | -26584,4 | 4 | E |
| 59 | YLR441C | **RPS1A** | 0,0036 | 0,0338 | -26570,3 | 4 | E |

| | | | | | | | |
|---|---|---|---|---|---|---|---|
| 60 | YCL010C | **SGF29** | 0,0002 | 0,0052 | -26420,5 | 4 | E |
| 61 | YJL047C | **RTT101** | 0,0010 | 0,0160 | -26385,5 | 4 | E |
| 62 | YGL142C | **GPI10** | 0,0028 | 0,0292 | -26330,3 | 4 | E |
| 63 | YDR123C | **INO2** | 0,0001 | 0,0043 | -26257,2 | 4 | E |
| 64 | YPL213W | **LEA1** | 0,0000 | 0,0003 | -26100,2 | 4 | E |
| 65 | YDL013W | **HEX3** | 0,0000 | 0,0024 | -26088,5 | 4 | E |
| 66 | YNR005C | **YNR005C** | 0,0000 | 0,0003 | -26070,8 | 4 | E |
| 67 | YOL058W | **ARG1** | 0,0007 | 0,0129 | -25861,3 | 4 | E |
| 68 | YPR070W | **MED1** | 0,0011 | 0,0165 | -25790,9 | 4 | E |
| 69 | YPL152W | **RRD2** | 0,0000 | 0,0020 | -25758 | 4 | E |
| 70 | YER041W | **YEN1** | 0,0001 | 0,0036 | -25731,9 | 4 | E |
| 71 | YBR036C | **CSG2** | 0,0000 | 0,0003 | -25722,6 | 4 | E |
| 72 | YLR337C | **VRP1** | 0,0058 | 0,0456 | -25381,5 | 4 | E |
| 73 | YNL284C | **MRPL10** | 0,0031 | 0,0309 | -25341,5 | 4 | E |
| 74 | YGR206W | **MVB12** | 0,0004 | 0,0091 | -25325,3 | 4 | E |
| 75 | YOR303W | **CPA1** | 0,0007 | 0,0129 | -25241,1 | 4 | E |
| 76 | YBL008W | **HIR1** | 0,0001 | 0,0051 | -25194,5 | 4 | E |
| 77 | YLR342W | **FKS1** | 0,0001 | 0,0051 | -25131,5 | 4 | E |
| 78 | YLR384C | **IKI3** | 0,0001 | 0,0035 | -24907,7 | 4 | E |
| 79 | YOR184W | **SER1** | 0,0001 | 0,0044 | -24860,5 | 4 | E |
| 80 | YML013C-A | **YML013C-A** | 0,0052 | 0,0424 | -24849,5 | 4 | E |
| 81 | YBR076W | **ECM8** | 0,0000 | 0,0002 | -24790,5 | 4 | E |
| 82 | YML057W | **CMP2** | 0,0001 | 0,0038 | -24729,1 | 4 | E |
| 83 | YGL168W | **HUR1** | 0,0000 | 0,0014 | -24720,1 | 4 | E |
| 84 | YJL092W | **SRS2** | 0,0000 | 0,0026 | -24540,2 | 4 | E |
| 85 | YDR260C | **SWM1** | 0,0000 | 0,0002 | -24459,4 | 4 | E |
| 86 | YPL187W | **MF(ALPHA)1** | 0,0000 | 0,0005 | -24450,9 | 4 | E |
| 87 | YMR063W | **RIM9** | 0,0006 | 0,0120 | -24360,1 | 4 | E |
| 88 | YGL042C | **YGL042C** | 0,0010 | 0,0162 | -24178,8 | 4 | E |
| 89 | YER069W | **ARG5** | 0,0001 | 0,0029 | -24140,8 | 4 | E |
| 90 | YML001W | **YPT7** | 0,0006 | 0,0121 | -24085 | 4 | E |
| 91 | YNL299W | **TRF5** | 0,0002 | 0,0068 | -23829,7 | 4 | E |
| 92 | YER116C | **SLX8** | 0,0000 | 0,0007 | -23723,8 | 4 | E |
| 93 | YGR055W | **MUP1** | 0,0017 | 0,0210 | -23723,1 | 4 | E |
| 94 | YLR102C | **APC9** | 0,0043 | 0,0378 | -23658,6 | 4 | E |
| 95 | YMR078C | **CTF18** | 0,0000 | 0,0011 | -23658,3 | 4 | E |
| 96 | YBR082C | **UBC4** | 0,0024 | 0,0264 | -23628 | 8 | E |
| 97 | YPR024W | **YME1** | 0,0001 | 0,0031 | -23615,9 | 4 | E |
| 98 | YBR143C | **SUP45** | 0,0017 | 0,0215 | -23550,4 | 4 | E |
| 99 | YGR022C | **YGR022C** | 0,0051 | 0,0420 | -23536,3 | 4 | E |
| 100 | YLR434C | **YLR434C** | 0,0010 | 0,0162 | -23534,9 | 4 | E |
| 101 | YOR106W | **VAM3** | 0,0002 | 0,0056 | -23396,3 | 4 | E |
| 102 | YML028W | **TSA1** | 0,0000 | 0,0000 | -23194,8 | 28 | E |
| 103 | YHR012W | **VPS29** | 0,0020 | 0,0232 | -23184,9 | 4 | E |
| 104 | YDR234W | **LYS4** | 0,0004 | 0,0089 | -23109,8 | 4 | E |
| 105 | YJL088W | **ARG3** | 0,0001 | 0,0033 | -23077,9 | 4 | E |

| | | | | | | | |
|---|---|---|---|---|---|---|---|
| 106 | YGR089W | **NNF2** | 0,0007 | 0,0131 | -22794,5 | 4 | E |
| 107 | YOR033C | **EXO1** | 0,0000 | 0,0002 | -22746,6 | 28 | E |
| 108 | YDR463W | **STP1** | 0,0001 | 0,0033 | -22706,4 | 4 | E |
| 109 | YPR180W | **AOS1** | 0,0037 | 0,0347 | -22623,3 | 4 | E |
| 110 | YMR155W | **YMR155W** | 0,0048 | 0,0407 | -22572 | 4 | E |
| 111 | YKL213C | **DOA1** | 0,0049 | 0,0412 | -22478,9 | 4 | E |
| 112 | YLR134W | **PDC5** | 0,0005 | 0,0108 | -22375,2 | 4 | E |
| 113 | YBR014C | **GRX7** | 0,0012 | 0,0176 | -22332,1 | 4 | E |
| 114 | YLR190W | **MMR1** | 0,0000 | 0,0022 | -22308,4 | 4 | E |
| 115 | YLR087C | **CSF1** | 0,0003 | 0,0076 | -22257,1 | 4 | E |
| 116 | YBR100W | **YBR100W** | 0,0003 | 0,0087 | -22252,6 | 4 | E |
| 117 | YBR248C | **HIS7** | 0,0000 | 0,0026 | -22250,5 | 4 | E |
| 118 | YFL013W-A | **YFL013W-A** | 0,0007 | 0,0129 | -22248,3 | 4 | E |
| 119 | YMR116C | **ASC1** | 0,0005 | 0,0109 | -22215 | 4 | E |
| 120 | YLR242C | **ARV1** | 0,0000 | 0,0014 | -22166,7 | 4 | E |
| 121 | YFL010C | **WWM1** | 0,0000 | 0,0010 | -22141,1 | 4 | E |
| 122 | YPL259C | **APM1** | 0,0068 | 0,0499 | -22120 | 4 | E |
| 123 | YMR166C | **YMR166C** | 0,0004 | 0,0091 | -22085,9 | 4 | E |
| 124 | YMR307W | **GAS1** | 0,0068 | 0,0495 | -21961,5 | 4 | E |
| 125 | YNL250W | **RAD50** | 0,0000 | 0,0000 | -21863,8 | 24 | E |
| 126 | YCR063W | **BUD31** | 0,0000 | 0,0000 | -21713,8 | 4 | E |
| 127 | YNL159C | **ASI2** | 0,0011 | 0,0168 | -21485 | 4 | E |
| 128 | YBR265W | **TSC10** | 0,0024 | 0,0265 | -21459,4 | 4 | E |
| 129 | YCR008W | **SAT4** | 0,0000 | 0,0001 | -21443,9 | 4 | E |
| 130 | YJR087W | **YJR087W** | 0,0001 | 0,0036 | -21374,9 | 4 | E |
| 131 | YKR072C | **SIS2** | 0,0007 | 0,0132 | -21360,5 | 4 | E |
| 132 | YJL071W | **ARG2** | 0,0000 | 0,0026 | -21340,5 | 4 | E |
| 133 | YOR156C | **NFI1** | 0,0037 | 0,0347 | -21293,4 | 4 | E |
| 134 | YPL067C | **YPL067C** | 0,0000 | 0,0012 | -21146,2 | 4 | E |
| 135 | YPL094C | **SEC62** | 0,0031 | 0,0309 | -21141,8 | 4 | E |
| 136 | YPR176C | **BET2** | 0,0048 | 0,0404 | -20942,1 | 4 | E |
| 137 | YDR510W | **SMT3** | 0,0001 | 0,0029 | -20732,8 | 4 | E |
| 138 | YHR101C | **BIG1** | 0,0000 | 0,0003 | -20715,5 | 4 | E |
| 139 | YAL002W | **VPS8** | 0,0000 | 0,0006 | -20712,5 | 4 | E |
| 140 | YHL006C | **SHU1** | 0,0002 | 0,0064 | -20703,9 | 4 | E |
| 141 | YER159C | **BUR6** | 0,0053 | 0,0432 | -20690,5 | 4 | E |
| 142 | YBL088C | **TEL1** | 0,0001 | 0,0039 | -20600,6 | 4 | E |
| 143 | YML048W-A | **YML048W-A** | 0,0018 | 0,0219 | -20564,9 | 4 | E |
| 144 | YBR252W | **DUT1** | 0,0000 | 0,0014 | -20400,2 | 4 | E |
| 145 | YOL012C | **HTZ1** | 0,0001 | 0,0050 | -20398 | 4 | E |
| 146 | YJR109C | **CPA2** | 0,0000 | 0,0010 | -20336,6 | 8 | E |
| 147 | YGR105W | **VMA21** | 0,0000 | 0,0003 | -20326 | 4 | E |
| 148 | YDR075W | **PPH3** | 0,0015 | 0,0198 | -20295,2 | 4 | E |
| 149 | YBL024W | **NCL1** | 0,0013 | 0,0183 | -20265,7 | 4 | E |
| 150 | YKL028W | **TFA1** | 0,0055 | 0,0439 | -20248,3 | 4 | E |
| 151 | YDR174W | **HMO1** | 0,0016 | 0,0208 | -20238,8 | 4 | E |

| | | | | | | | |
|---|---|---|---|---|---|---|---|
| 152 | YFL023W | **BUD27** | 0,0002 | 0,0068 | -20178,9 | 4 | E |
| 153 | YNL244C | **SUI1** | 0,0006 | 0,0123 | -20132,3 | 4 | E |
| 154 | YGL244W | **RTF1** | 0,0000 | 0,0016 | -20054,8 | 4 | E |
| 155 | YLR370C | **ARC18** | 0,0009 | 0,0156 | -20046,7 | 4 | E |
| 156 | YMR038C | **CCS1** | 0,0000 | 0,0001 | -19982,9 | 4 | E |
| 157 | YJR033C | **RAV1** | 0,0015 | 0,0198 | -19950,2 | 4 | E |
| 158 | YGR122W | **YGR122W** | 0,0011 | 0,0165 | -19905,6 | 4 | E |
| 159 | YDL194W | **SNF3** | 0,0015 | 0,0198 | -19848,1 | 4 | E |
| 160 | YKL110C | **KTI12** | 0,0001 | 0,0031 | -19830,7 | 4 | E |
| 161 | YDR388W | **RVS167** | 0,0000 | 0,0026 | -19778,7 | 4 | E |
| 162 | YJL154C | **VPS35** | 0,0002 | 0,0068 | -19736 | 4 | E |
| 163 | YEL007W | **MIT1** | 0,0010 | 0,0160 | -19679,2 | 4 | E |
| 164 | YPR045C | **THP3** | 0,0018 | 0,0218 | -19666,6 | 4 | E |
| 165 | YGR042W | **YGR042W** | 0,0006 | 0,0120 | -19635,9 | 4 | E |
| 166 | YLR431C | **ATG23** | 0,0066 | 0,0487 | -19591,5 | 4 | E |
| 167 | YOR302W | **YOR302W** | 0,0000 | 0,0020 | -19488,9 | 4 | E |
| 168 | YDR265W | **PEX10** | 0,0012 | 0,0171 | -19433,8 | 4 | E |
| 169 | YGR100W | **MDR1** | 0,0010 | 0,0162 | -19365,8 | 4 | E |
| 170 | YGR260W | **TNA1** | 0,0026 | 0,0278 | -19360,4 | 4 | E |
| 171 | YBR131W | **CCZ1** | 0,0007 | 0,0132 | -19341,6 | 4 | E |
| 172 | YBR255W | **MTC4** | 0,0000 | 0,0010 | -19341,3 | 4 | E |
| 173 | YBR170C | **NPL4** | 0,0000 | 0,0000 | -19293,1 | 4 | E |
| 174 | YMR139W | **RIM11** | 0,0040 | 0,0362 | -19265 | 4 | E |
| 175 | YKL048C | **ELM1** | 0,0000 | 0,0018 | -19237,5 | 4 | E |
| 176 | YOR078W | **BUD21** | 0,0001 | 0,0039 | -19237,5 | 4 | E |
| 177 | YDR121W | **DPB4** | 0,0001 | 0,0048 | -19208,2 | 4 | E |
| 178 | YER161C | **SPT2** | 0,0000 | 0,0018 | -19192,6 | 4 | E |
| 179 | YMR015C | **ERG5** | 0,0025 | 0,0271 | -19186 | 4 | E |
| 180 | YPL101W | **ELP4** | 0,0000 | 0,0003 | -19126,8 | 4 | E |
| 181 | YMR137C | **PSO2** | 0,0000 | 0,0026 | -19095,5 | 4 | E |
| 182 | YMR163C | **INP2** | 0,0028 | 0,0291 | -19082,5 | 4 | E |
| 183 | YDR244W | **PEX5** | 0,0010 | 0,0160 | -19042,1 | 4 | E |
| 184 | YBR247C | **ENP1** | 0,0003 | 0,0087 | -18953,8 | 4 | E |
| 185 | YOR304W | **ISW2** | 0,0062 | 0,0471 | -18942,5 | 4 | E |
| 186 | YDR245W | **MNN10** | 0,0001 | 0,0037 | -18921,1 | 4 | E |
| 187 | YPL105C | **SYH1** | 0,0001 | 0,0029 | -18912,6 | 4 | E |
| 188 | YDL074C | **BRE1** | 0,0000 | 0,0000 | -18897,7 | 8 | E |
| 189 | YPR108W | **RPN7** | 0,0046 | 0,0400 | -18873,6 | 8 | E |
| 190 | YCL030C | **HIS4** | 0,0000 | 0,0010 | -18797,7 | 4 | E |
| 191 | YLR372W | **SUR4** | 0,0001 | 0,0041 | -18793,6 | 4 | E |
| 192 | YMR224C | **MRE11** | 0,0000 | 0,0000 | -18753,8 | 28 | E |
| 193 | YOR381W | **FRE3** | 0,0047 | 0,0404 | -18688,4 | 4 | E |
| 194 | YPL226W | **NEW1** | 0,0002 | 0,0056 | -18664,2 | 4 | E |
| 195 | YGL022W | **STT3** | 0,0024 | 0,0262 | -18653,8 | 4 | E |
| 196 | YBR055C | **PRP6** | 0,0022 | 0,0248 | -18649,9 | 4 | E |
| 197 | YNR050C | **LYS9** | 0,0001 | 0,0033 | -18526,4 | 4 | E |

| | | | | | | | |
|---|---|---|---|---|---|---|---|
| 198 | YGL162W | **SUT1** | 0,0015 | 0,0201 | -18525,3 | 4 | E |
| 199 | YML103C | **NUP188** | 0,0027 | 0,0287 | -18491 | 4 | E |
| 200 | YLR193C | **UPS1** | 0,0001 | 0,0036 | -18458,9 | 4 | E |
| 201 | YOL133W | **HRT1** | 0,0004 | 0,0091 | -18444,4 | 8 | E |
| 202 | YLR317W | **YLR317W** | 0,0001 | 0,0051 | -18405,8 | 4 | E |
| 203 | YLR061W | **RPL22A** | 0,0002 | 0,0072 | -18331 | 4 | E |
| 204 | YOR014W | **RTS1** | 0,0010 | 0,0161 | -18292,3 | 4 | E |
| 205 | YKR007W | **MEH1** | 0,0000 | 0,0000 | -18207,2 | 4 | E |
| 206 | YKR059W | **TIF1** | 0,0065 | 0,0485 | -18149,7 | 4 | E |
| 207 | YBR094W | **PBY1** | 0,0020 | 0,0235 | -18119,9 | 4 | E |
| 208 | YDR330W | **UBX5** | 0,0040 | 0,0362 | -18105,2 | 4 | E |
| 209 | YLR089C | **ALT1** | 0,0005 | 0,0104 | -18009,1 | 4 | E |
| 210 | YML006C | **GIS4** | 0,0008 | 0,0133 | -17993,2 | 4 | E |
| 211 | YLR393W | **ATP10** | 0,0000 | 0,0007 | -17983,1 | 4 | E |
| 212 | YDR276C | **PMP3** | 0,0000 | 0,0020 | -17948,6 | 4 | E |
| 213 | YJR139C | **HOM6** | 0,0024 | 0,0262 | -17847,3 | 4 | E |
| 214 | YJR128W | **YJR128W** | 0,0001 | 0,0032 | -17830,9 | 4 | E |
| 215 | YOL139C | **CDC33** | 0,0016 | 0,0201 | -17824,1 | 4 | E |
| 216 | YIR023W | **DAL81** | 0,0031 | 0,0308 | -17644,3 | 4 | E |
| 217 | YBR275C | **RIF1** | 0,0020 | 0,0231 | -17579,5 | 4 | E |
| 218 | YGR200C | **ELP2** | 0,0018 | 0,0218 | -17530,6 | 4 | E |
| 219 | YOL001W | **PHO80** | 0,0057 | 0,0450 | -17496,1 | 4 | E |
| 220 | YMR053C | **STB2** | 0,0037 | 0,0347 | -17460 | 4 | E |
| 221 | YOR008C | **SLG1** | 0,0000 | 0,0000 | -17405,2 | 4 | E |
| 222 | YER095W | **RAD51** | 0,0003 | 0,0084 | -17379,2 | 4 | E |
| 223 | YCL006C | **YCL006C** | 0,0002 | 0,0052 | -17368,6 | 4 | E |
| 224 | YKR020W | **VPS51** | 0,0035 | 0,0330 | -17364,8 | 4 | E |
| 225 | YEL033W | **MTC7** | 0,0002 | 0,0061 | -17336,9 | 4 | E |
| 226 | YBL089W | **AVT5** | 0,0012 | 0,0171 | -17296,7 | 4 | E |
| 227 | YLR078C | **BOS1** | 0,0007 | 0,0127 | -17247,8 | 4 | E |
| 228 | YCL001W | **RER1** | 0,0006 | 0,0123 | -17238,5 | 4 | E |
| 229 | YJL165C | **HAL5** | 0,0004 | 0,0092 | -17212,7 | 4 | E |
| 230 | YPR040W | **TIP41** | 0,0005 | 0,0102 | -17205,1 | 4 | E |
| 231 | YLL040C | **VPS13** | 0,0017 | 0,0210 | -17165,3 | 4 | E |
| 232 | YPR155C | **NCA2** | 0,0007 | 0,0129 | -17159,8 | 4 | E |
| 233 | YPL157W | **TGS1** | 0,0000 | 0,0027 | -17003,7 | 4 | E |
| 234 | YDR173C | **ARG82** | 0,0000 | 0,0001 | -16937,6 | 4 | E |
| 235 | YPL102C | **YPL102C** | 0,0025 | 0,0268 | -16914,4 | 4 | E |
| 236 | YOR252W | **TMA16** | 0,0011 | 0,0164 | -16845,8 | 4 | E |
| 237 | YER131W | **RPS26B** | 0,0032 | 0,0316 | -16821,2 | 4 | E |
| 238 | YDR074W | **TPS2** | 0,0001 | 0,0050 | -16797,2 | 4 | E |
| 239 | YDL163W | **YDL163W** | 0,0039 | 0,0352 | -16756,4 | 8 | E |
| 240 | YGR058W | **PEF1** | 0,0028 | 0,0293 | -16690,8 | 4 | E |
| 241 | YGL041C | **YGL041C** | 0,0027 | 0,0289 | -16668,9 | 4 | E |
| 242 | YEL003W | **GIM4** | 0,0027 | 0,0283 | -16621,1 | 4 | E |
| 243 | YDR273W | **DON1** | 0,0001 | 0,0047 | -16590,1 | 4 | E |

| | | | | | | | |
|---|---|---|---|---|---|---|---|
| 244 | YPL177C | **CUP9** | 0,0015 | 0,0198 | -16554,9 | 4 | E |
| 245 | YKL211C | **TRP3** | 0,0052 | 0,0424 | -16554,7 | 4 | E |
| 246 | YBL017C | **PEP1** | 0,0008 | 0,0145 | -16549 | 4 | E |
| 247 | YOR357C | **SNX3** | 0,0053 | 0,0428 | -16491,2 | 4 | E |
| 248 | YDR076W | **RAD55** | 0,0020 | 0,0232 | -16489,2 | 4 | E |
| 249 | YAL013W | **DEP1** | 0,0004 | 0,0094 | -16449,3 | 4 | E |
| 250 | YLL039C | **UBI4** | 0,0005 | 0,0102 | -16424,4 | 4 | E |
| 251 | YKL220C | **FRE2** | 0,0003 | 0,0085 | -16410,3 | 4 | E |
| 252 | YOR050C | **YOR050C** | 0,0065 | 0,0484 | -16407,2 | 4 | E |
| 253 | YNR042W | **YNR042W** | 0,0004 | 0,0095 | -16402,7 | 4 | E |
| 254 | YDR034C | **LYS14** | 0,0000 | 0,0000 | -16392,2 | 28 | E |
| 255 | YBL037W | **APL3** | 0,0029 | 0,0299 | -16368,1 | 4 | E |
| 256 | YOR082C | **YOR082C** | 0,0003 | 0,0089 | -16360 | 4 | E |
| 257 | YER006W | **NUG1** | 0,0003 | 0,0074 | -16343,8 | 4 | E |
| 258 | YCL025C | **AGP1** | 0,0031 | 0,0308 | -16296,4 | 4 | E |
| 259 | YKL081W | **TEF4** | 0,0001 | 0,0032 | -16266,8 | 4 | E |
| 260 | YDL020C | **RPN4** | 0,0016 | 0,0207 | -16247,4 | 4 | E |
| 261 | YIL154C | **IMP2'** | 0,0000 | 0,0018 | -16235,2 | 4 | E |
| 262 | YCL011C | **GBP2** | 0,0000 | 0,0015 | -16154,8 | 4 | E |
| 263 | YML032C | **RAD52** | 0,0003 | 0,0078 | -16085,1 | 28 | E |
| 264 | YER083C | **GET2** | 0,0005 | 0,0104 | -16073,4 | 4 | E |
| 265 | YJR077C | **MIR1** | 0,0006 | 0,0115 | -16068 | 4 | E |
| 266 | YLR032W | **RAD5** | 0,0012 | 0,0171 | -16058,1 | 4 | E |
| 267 | YOL086C | **ADH1** | 0,0042 | 0,0375 | -15996,3 | 4 | E |
| 268 | YGL050W | **TYW3** | 0,0005 | 0,0104 | -15957 | 4 | E |
| 269 | YBL081W | **YBL081W** | 0,0000 | 0,0004 | -15949,5 | 4 | E |
| 270 | YNL227C | **JJJ1** | 0,0014 | 0,0187 | -15946,2 | 4 | E |
| 271 | YPL219W | **PCL8** | 0,0002 | 0,0068 | -15928,9 | 4 | E |
| 272 | YNL194C | **YNL194C** | 0,0055 | 0,0439 | -15918,9 | 4 | E |
| 273 | YKL114C | **APN1** | 0,0046 | 0,0399 | -15916,3 | 4 | E |
| 274 | YLR019W | **PSR2** | 0,0033 | 0,0319 | -15911,4 | 4 | E |
| 275 | YLR212C | **TUB4** | 0,0009 | 0,0159 | -15873,5 | 4 | E |
| 276 | YHR108W | **GGA2** | 0,0005 | 0,0104 | -15854,2 | 4 | E |
| 277 | YDL189W | **RBS1** | 0,0000 | 0,0016 | -15823,2 | 4 | E |
| 278 | YBL060W | **YBL060W** | 0,0007 | 0,0123 | -15811,4 | 4 | E |
| 279 | YLR220W | **CCC1** | 0,0013 | 0,0181 | -15769,5 | 4 | E |
| 280 | YKL010C | **UFD4** | 0,0007 | 0,0129 | -15699,3 | 4 | E |
| 281 | YCL060C | **:::MRC1** | 0,0000 | 0,0005 | -15602,2 | 4 | E |
| 282 | YGR032W | **GSC2** | 0,0013 | 0,0183 | -15533,6 | 4 | E |
| 283 | YDL133C-A | **RPL41B** | 0,0001 | 0,0042 | -15491 | 4 | E |
| 284 | YPR183W | **DPM1** | 0,0051 | 0,0420 | -15434,8 | 4 | E |
| 285 | YPL180W | **TCO89** | 0,0007 | 0,0129 | -15434,4 | 4 | E |
| 286 | YPR060C | **ARO7** | 0,0051 | 0,0420 | -15422,9 | 4 | E |
| 287 | YDR128W | **MTC5** | 0,0008 | 0,0145 | -15379,3 | 4 | E |
| 288 | YJL095W | **BCK1** | 0,0002 | 0,0066 | -15356,3 | 4 | E |
| 289 | YKR052C | **MRS4** | 0,0027 | 0,0289 | -15355,4 | 4 | E |

| | | | | | | | |
|---|---|---|---|---|---|---|---|
| 290 | YDR512C | **EMI1** | 0,0001 | 0,0042 | -15279,4 | 4 | E |
| 291 | YLR039C | **RIC1** | 0,0002 | 0,0068 | -15264,8 | 4 | E |
| 292 | YMR290C | **HAS1** | 0,0018 | 0,0216 | -15223 | 4 | E |
| 293 | YLR001C | **YLR001C** | 0,0011 | 0,0163 | -15195,9 | 4 | E |
| 294 | YPR044C | **OPI11** | 0,0006 | 0,0115 | -15109,4 | 4 | E |
| 295 | YOR273C | **TPO4** | 0,0005 | 0,0102 | -15093,1 | 4 | E |
| 296 | YMR202W | **ERG2** | 0,0028 | 0,0291 | -15056,6 | 4 | E |
| 297 | YJL204C | **RCY1** | 0,0003 | 0,0080 | -15041,1 | 4 | E |
| 298 | YNL297C | **MON2** | 0,0034 | 0,0329 | -14982,2 | 4 | E |
| 299 | YJR088C | **EMC2** | 0,0003 | 0,0072 | -14881,2 | 4 | E |
| 300 | YGL071W | **AFT1** | 0,0006 | 0,0116 | -14876,4 | 4 | E |
| 301 | YKL091C | **YKL091C** | 0,0005 | 0,0113 | -14840,7 | 4 | E |
| 302 | YLL013C | **PUF3** | 0,0025 | 0,0268 | -14810 | 4 | E |
| 303 | YPR051W | **MAK3** | 0,0012 | 0,0175 | -14800,4 | 4 | E |
| 304 | YNR061C | **YNR061C** | 0,0025 | 0,0268 | -14753,7 | 4 | E |
| 305 | YER113C | **TMN3** | 0,0042 | 0,0371 | -14701,1 | 4 | E |
| 306 | YOR112W | **CEX1** | 0,0013 | 0,0181 | -14695,2 | 4 | E |
| 307 | YDR435C | **PPM1** | 0,0049 | 0,0412 | -14653,7 | 4 | E |
| 308 | YOL013W-A | **YOL013W-A** | 0,0020 | 0,0231 | -14623,2 | 4 | E |
| 309 | YOR080W | **DIA2** | 0,0036 | 0,0338 | -14546,6 | 4 | E |
| 310 | YDR241W | **BUD26** | 0,0002 | 0,0067 | -14542,9 | 4 | E |
| 311 | YNL067W | **RPL9B** | 0,0013 | 0,0183 | -14488,1 | 4 | E |
| 312 | YDL188C | **PPH22** | 0,0039 | 0,0352 | -14454,5 | 4 | E |
| 313 | YBR098W | **MMS4** | 0,0028 | 0,0293 | -14451,1 | 4 | E |
| 314 | YOL134C | **YOL134C** | 0,0004 | 0,0093 | -14438,8 | 4 | E |
| 315 | YDR332W | **IRC3** | 0,0014 | 0,0184 | -14432,5 | 4 | E |
| 316 | YJL029C | **VPS53** | 0,0010 | 0,0162 | -14367,5 | 4 | E |
| 317 | YMR001C | **CDC5** | 0,0038 | 0,0352 | -14280,9 | 4 | E |
| 318 | YHR184W | **SSP1** | 0,0019 | 0,0229 | -14250,9 | 4 | E |
| 319 | YKL097C | **YKL097C** | 0,0043 | 0,0378 | -14241,4 | 4 | E |
| 320 | YER134C | **YER134C** | 0,0017 | 0,0214 | -14229,1 | 4 | E |
| 321 | YDR203W | **YDR203W** | 0,0016 | 0,0205 | -14155,4 | 4 | E |
| 322 | YIL027C | **EMC5** | 0,0010 | 0,0162 | -14099 | 4 | E |
| 323 | YPR057W | **BRR1** | 0,0018 | 0,0220 | -14049 | 4 | E |
| 324 | YPL232W | **SSO1** | 0,0011 | 0,0165 | -14025,3 | 4 | E |
| 325 | YCL064C | **CHA1** | 0,0010 | 0,0160 | -13986,7 | 4 | E |
| 326 | YPL008W | **CHL1** | 0,0028 | 0,0291 | -13977,7 | 4 | E |
| 327 | YHR114W | **BZZ1** | 0,0013 | 0,0183 | -13973,4 | 4 | E |
| 328 | YKL053C-A | **MDM35** | 0,0001 | 0,0035 | -13872,2 | 4 | E |
| 329 | YCR037C | **PHO87** | 0,0038 | 0,0349 | -13870,3 | 4 | E |
| 330 | YJR095W | **SFC1** | 0,0018 | 0,0219 | -13778,4 | 4 | E |
| 331 | YLR390W-A | **CCW14** | 0,0053 | 0,0432 | -13737,6 | 4 | E |
| 332 | YPL054W | **LEE1** | 0,0022 | 0,0254 | -13701,5 | 4 | E |
| 333 | YNL077W | **APJ1** | 0,0036 | 0,0343 | -13658,3 | 4 | E |
| 334 | YJL128C | **PBS2** | 0,0064 | 0,0481 | -13639,1 | 4 | E |
| 335 | YJL014W | **CCT3** | 0,0063 | 0,0477 | -13628,3 | 4 | E |

| | | | | | | | |
|---|---|---|---|---|---|---|---|
| 336 | YNL155W | **CUZ1** | 0,0010 | 0,0162 | -13574,6 | 4 | E |
| 337 | YKL160W | **ELF1** | 0,0010 | 0,0160 | -13573,3 | 4 | E |
| 338 | YDL179W | **PCL9** | 0,0001 | 0,0036 | -13531,4 | 4 | E |
| 339 | YNR014W | **YNR014W** | 0,0047 | 0,0404 | -13481 | 4 | E |
| 340 | YBR047W | **FMP23** | 0,0018 | 0,0218 | -13477,5 | 4 | E |
| 341 | YMR054W | **STV1** | 0,0068 | 0,0495 | -13435,5 | 4 | E |
| 342 | YER056C | **FCY2** | 0,0041 | 0,0363 | -13426,1 | 4 | E |
| 343 | YNR002C | **ATO2** | 0,0035 | 0,0333 | -13369,4 | 4 | E |
| 344 | YHL027W | **RIM101** | 0,0059 | 0,0458 | -13358,8 | 4 | E |
| 345 | YDL226C | **GCS1** | 0,0000 | 0,0027 | -13349,9 | 4 | E |
| 346 | YDR083W | **RRP8** | 0,0055 | 0,0438 | -13336,6 | 4 | E |
| 347 | YJL192C | **SOP4** | 0,0053 | 0,0432 | -13298,2 | 4 | E |
| 348 | YNL183C | **NPR1** | 0,0010 | 0,0162 | -13283,3 | 4 | E |
| 349 | YDR210W | **YDR210W** | 0,0034 | 0,0329 | -13245,7 | 4 | E |
| 350 | YLR062C | **BUD28** | 0,0019 | 0,0231 | -13231,2 | 4 | E |
| 351 | YHL044W | **YHL044W** | 0,0049 | 0,0412 | -13210,7 | 4 | E |
| 352 | YDL134C | **PPH21** | 0,0063 | 0,0476 | -13179,7 | 4 | E |
| 353 | YDR458C | **HEH2** | 0,0062 | 0,0471 | -13160,7 | 4 | E |
| 354 | YDR085C | **AFR1** | 0,0006 | 0,0114 | -13129,8 | 4 | E |
| 355 | YKR015C | **YKR015C** | 0,0026 | 0,0279 | -13128,8 | 4 | E |
| 356 | YKL074C | **MUD2** | 0,0011 | 0,0168 | -13115,5 | 4 | E |
| 357 | YJR034W | **PET191** | 0,0042 | 0,0375 | -13113,5 | 4 | E |
| 358 | YDR269C | **YDR269C** | 0,0000 | 0,0000 | -13112,5 | 28 | E |
| 359 | YJL147C | **YJL147C** | 0,0025 | 0,0272 | -13081,9 | 4 | E |
| 360 | YLR238W | **FAR10** | 0,0045 | 0,0394 | -13076,9 | 4 | E |
| 361 | YJR118C | **ILM1** | 0,0005 | 0,0102 | -13036,4 | 4 | E |
| 362 | YBR007C | **DSF2** | 0,0019 | 0,0224 | -13033,7 | 4 | E |
| 363 | YGL154C | **LYS5** | 0,0037 | 0,0347 | -13031 | 4 | E |
| 364 | YER090W | **TRP2** | 0,0064 | 0,0482 | -12991,9 | 4 | E |
| 365 | YPR073C | **LTP1** | 0,0002 | 0,0064 | -12988,5 | 4 | E |
| 366 | YDL006W | **PTC1** | 0,0017 | 0,0211 | -12987,6 | 4 | E |
| 367 | YIL052C | **RPL34B** | 0,0016 | 0,0205 | -12947,3 | 4 | E |
| 368 | YCR048W | **ARE1** | 0,0004 | 0,0092 | -12919,7 | 4 | E |
| 369 | YOL053C-A | **YOL053C-A** | 0,0010 | 0,0160 | -12897,1 | 4 | E |
| 370 | YKL093W | **MBR1** | 0,0012 | 0,0171 | -12862,4 | 4 | E |
| 371 | YKR074W | **AIM29** | 0,0048 | 0,0407 | -12748,7 | 4 | E |
| 372 | YOL091W | **SPO21** | 0,0058 | 0,0454 | -12729,7 | 4 | E |
| 373 | YPR038W | **IRC16** | 0,0029 | 0,0302 | -12666,6 | 4 | E |
| 374 | YJL064W | **YJL064W** | 0,0014 | 0,0191 | -12617,4 | 4 | E |
| 375 | YOR382W | **FIT2** | 0,0000 | 0,0004 | -12598 | 28 | E |
| 376 | YER007W | **PAC2** | 0,0061 | 0,0470 | -12576,9 | 4 | E |
| 377 | YGR229C | **SMI1** | 0,0045 | 0,0393 | -12525 | 4 | E |
| 378 | YGL009C | **LEU1** | 0,0012 | 0,0175 | -12496,8 | 4 | E |
| 379 | YDL214C | **PRR2** | 0,0014 | 0,0184 | -12489,9 | 4 | E |
| 380 | YDL112W | **TRM3** | 0,0007 | 0,0131 | -12428,9 | 4 | E |
| 381 | YGR238C | **KEL2** | 0,0056 | 0,0444 | -12415,8 | 4 | E |

| | | | | | | | |
|---|---|---|---|---|---|---|---|
| 382 | YOL054W | **PSH1** | 0,0022 | 0,0251 | -12335,7 | 4 | E |
| 383 | YDR092W | **UBC13** | 0,0002 | 0,0068 | -12314,6 | 4 | E |
| 384 | YBR043C | **QDR3** | 0,0013 | 0,0181 | -12211,3 | 4 | E |
| 385 | YGL001C | **ERG26** | 0,0005 | 0,0104 | -12188,1 | 4 | E |
| 386 | YKL142W | **MRP8** | 0,0031 | 0,0309 | -12168,3 | 4 | E |
| 387 | YBR016W | **YBR016W** | 0,0029 | 0,0301 | -12146,6 | 4 | E |
| 388 | YCR032W | **BPH1** | 0,0016 | 0,0205 | -12132,4 | 4 | E |
| 389 | YOL152W | **FRE7** | 0,0034 | 0,0329 | -12097,3 | 4 | E |
| 390 | YDR532C | **YDR532C** | 0,0002 | 0,0060 | -12057,4 | 4 | E |
| 391 | YPR050C | **YPR050C** | 0,0005 | 0,0103 | -12053,8 | 4 | E |
| 392 | YAL031C | **GIP4** | 0,0006 | 0,0123 | -12028,7 | 4 | E |
| 393 | YDL100C | **GET3** | 0,0013 | 0,0181 | -12021,3 | 4 | E |
| 394 | YDL155W | **CLB3** | 0,0048 | 0,0404 | -12009,2 | 4 | E |
| 395 | YCL075W | **YCL075W** | 0,0025 | 0,0268 | -11972,2 | 4 | E |
| 396 | YMR195W | **ICY1** | 0,0014 | 0,0187 | -11909,5 | 4 | E |
| 397 | YBL069W | **AST1** | 0,0054 | 0,0434 | -11906,3 | 4 | E |
| 398 | YER168C | **CCA1** | 0,0005 | 0,0102 | -11849,1 | 4 | E |
| 399 | YER177W | **BMH1** | 0,0001 | 0,0051 | -11798,4 | 4 | E |
| 400 | YOR343C | **YOR343C** | 0,0006 | 0,0123 | -11775,6 | 4 | E |
| 401 | YJL053W | **PEP8** | 0,0011 | 0,0165 | -11767,4 | 4 | E |
| 402 | YFL014W | **HSP12** | 0,0049 | 0,0412 | -11754,7 | 4 | E |
| 403 | YDR101C | **ARX1** | 0,0047 | 0,0404 | -11752,7 | 4 | E |
| 404 | YDL122W | **UBP1** | 0,0000 | 0,0013 | -11731,2 | 4 | E |
| 405 | YAL040C | **CLN3** | 0,0035 | 0,0335 | -11723,2 | 4 | E |
| 406 | YJL149W | **DAS1** | 0,0055 | 0,0439 | -11676,9 | 4 | E |
| 407 | YDR067C | **OCA6** | 0,0018 | 0,0219 | -11665,6 | 4 | E |
| 408 | YBR214W | **SDS24** | 0,0001 | 0,0039 | -11658,9 | 4 | E |
| 409 | YPR170C | **YPR170C** | 0,0039 | 0,0357 | -11641,7 | 4 | E |
| 410 | YPR114W | **YPR114W** | 0,0022 | 0,0255 | -11580,6 | 4 | E |
| 411 | YBL051C | **PIN4** | 0,0013 | 0,0180 | -11527,3 | 4 | E |
| 412 | YBR010W | **HHT1** | 0,0006 | 0,0117 | -11482,8 | 4 | E |
| 413 | YDR108W | **TRS85** | 0,0034 | 0,0329 | -11454,2 | 4 | E |
| 414 | YGR164W | **YGR164W** | 0,0010 | 0,0159 | -11431,1 | 4 | E |
| 415 | YDL190C | **UFD2** | 0,0014 | 0,0191 | -11424,6 | 4 | E |
| 416 | YEL015W | **EDC3** | 0,0013 | 0,0180 | -11359,3 | 4 | E |
| 417 | YNL170W | **YNL170W** | 0,0014 | 0,0191 | -11354,5 | 4 | E |
| 418 | YKL103C | **APE1** | 0,0011 | 0,0163 | -11341 | 4 | E |
| 419 | YNR074C | **AIF1** | 0,0000 | 0,0026 | -11294,4 | 4 | E |
| 420 | YEL043W | **YEL043W** | 0,0002 | 0,0066 | -11238,3 | 4 | E |
| 421 | YBL075C | **SSA3** | 0,0009 | 0,0154 | -11231,2 | 4 | E |
| 422 | YIL005W | **EPS1** | 0,0004 | 0,0101 | -11223,2 | 4 | E |
| 423 | YJR062C | **NTA1** | 0,0013 | 0,0181 | -11155,6 | 4 | E |
| 424 | YOL088C | **MPD2** | 0,0023 | 0,0259 | -11125,1 | 4 | E |
| 425 | YPR119W | **CLB2** | 0,0062 | 0,0473 | -11121,1 | 28 | E |
| 426 | YKR036C | **CAF4** | 0,0010 | 0,0160 | -11112,2 | 4 | E |
| 427 | YER167W | **BCK2** | 0,0037 | 0,0347 | -11079,5 | 4 | E |

| | | | | | | | |
|---|---|---|---|---|---|---|---|
| 428 | YLR093C | **NYV1** | 0,0054 | 0,0435 | -10966,1 | 4 | E |
| 429 | YOR070C | **GYP1** | 0,0010 | 0,0162 | -10826 | 4 | E |
| 430 | YLR177W | **YLR177W** | 0,0020 | 0,0235 | -10824,7 | 4 | E |
| 431 | YFL025C | **BST1** | 0,0016 | 0,0205 | -10787,4 | 4 | E |
| 432 | YJR096W | **YJR096W** | 0,0046 | 0,0401 | -10764,3 | 4 | E |
| 433 | YEL013W | **VAC8** | 0,0000 | 0,0026 | -10757,1 | 4 | E |
| 434 | YER088C | **DOT6** | 0,0049 | 0,0410 | -10749 | 4 | E |
| 435 | YIL029C | **YIL029C** | 0,0030 | 0,0305 | -10746,2 | 4 | E |
| 436 | YGR166W | **TRS65** | 0,0003 | 0,0076 | -10731,7 | 4 | E |
| 437 | YNL167C | **SKO1** | 0,0034 | 0,0327 | -10714,8 | 4 | E |
| 438 | YOR197W | **MCA1** | 0,0020 | 0,0235 | -10671,5 | 4 | E |
| 439 | YLR334C | **YLR334C** | 0,0064 | 0,0482 | -10655,8 | 4 | E |
| 440 | YLR433C | **CNA1** | 0,0030 | 0,0306 | -10637,4 | 4 | E |
| 441 | YLR257W | **YLR257W** | 0,0046 | 0,0401 | -10619 | 4 | E |
| 442 | YCR010C | **ADY2** | 0,0050 | 0,0413 | -10611,9 | 4 | E |
| 443 | YJL138C | **TIF2** | 0,0017 | 0,0211 | -10607,9 | 4 | E |
| 444 | YCR076C | **FUB1** | 0,0055 | 0,0441 | -10527 | 4 | E |
| 445 | YCR102W-A | **YCR102W-A** | 0,0003 | 0,0072 | -10495,9 | 4 | E |
| 446 | YKL033W-A | **YKL033W-A** | 0,0012 | 0,0171 | -10462,1 | 4 | E |
| 447 | YNR049C | **MSO1** | 0,0003 | 0,0085 | -10419,2 | 4 | E |
| 448 | YCR011C | **ADP1** | 0,0003 | 0,0076 | -10411,7 | 4 | E |
| 449 | YOR121C | **YOR121C** | 0,0013 | 0,0179 | -10397,9 | 4 | E |
| 450 | YOR371C | **GPB1** | 0,0061 | 0,0469 | -10328 | 4 | E |
| 451 | YPR030W | **CSR2** | 0,0056 | 0,0443 | -10327,4 | 4 | E |
| 452 | YBR288C | **APM3** | 0,0030 | 0,0304 | -10321,5 | 4 | E |
| 453 | YFR025C | **HIS2** | 0,0032 | 0,0319 | -10317,8 | 4 | E |
| 454 | YOL004W | **SIN3** | 0,0011 | 0,0165 | -10294,1 | 4 | E |
| 455 | YJR007W | **SUI2** | 0,0017 | 0,0214 | -10288,3 | 4 | E |
| 456 | YKR027W | **BCH2** | 0,0002 | 0,0071 | -10278,9 | 4 | E |
| 457 | YLR168C | **UPS2** | 0,0033 | 0,0321 | -10258,6 | 4 | E |
| 458 | YBR171W | **SEC66** | 0,0040 | 0,0362 | -10253,1 | 4 | E |
| 459 | YCL032W | **STE50** | 0,0003 | 0,0086 | -10186,7 | 4 | E |
| 460 | YKL063C | **YKL063C** | 0,0015 | 0,0196 | -10177,2 | 4 | E |
| 461 | YOR161C | **PNS1** | 0,0035 | 0,0335 | -10146,8 | 4 | E |
| 462 | YCR020C-A | **MAK31** | 0,0006 | 0,0123 | -10142,5 | 4 | E |
| 463 | YOR280C | **FSH3** | 0,0038 | 0,0350 | -10124,7 | 4 | E |
| 464 | YDL085W | **NDE2** | 0,0038 | 0,0352 | -10117,2 | 4 | E |
| 465 | YBR151W | **APD1** | 0,0064 | 0,0480 | -10103 | 4 | E |
| 466 | YKR016W | **MIC60** | 0,0018 | 0,0220 | -10095,1 | 4 | E |
| 467 | YBR122C | **MRPL36** | 0,0004 | 0,0094 | -10088 | 4 | E |
| 468 | YEL004W | **YEA4** | 0,0058 | 0,0457 | -10072 | 4 | E |
| 469 | YBR033W | **EDS1** | 0,0054 | 0,0438 | -10053,9 | 4 | E |
| 470 | YFL003C | **MSH4** | 0,0004 | 0,0094 | -10040,7 | 4 | E |
| 471 | YLL019C | **KNS1** | 0,0011 | 0,0164 | -10011,8 | 28 | E |
| 472 | YKL007W | **CAP1** | 0,0049 | 0,0410 | -9911,44 | 4 | E |
| 473 | YDR474C | **YDR474C** | 0,0008 | 0,0142 | -9887,49 | 4 | E |

| | | | | | | | |
|---|---|---|---|---|---|---|---|
| 474 | YKR001C | **VPS1** | 0,0049 | 0,0410 | -9878,54 | 4 | E |
| 475 | YMR165C | **PAH1** | 0,0002 | 0,0068 | -9874,8 | 4 | E |
| 476 | YBR158W | **AMN1** | 0,0050 | 0,0417 | -9812,17 | 4 | E |
| 477 | YLR191W | **PEX13** | 0,0003 | 0,0080 | -9787,08 | 4 | E |
| 478 | YLR104W | **LCL2** | 0,0006 | 0,0119 | -9762,65 | 4 | E |
| 479 | YOR325W | **YOR325W** | 0,0020 | 0,0236 | -9710,5 | 4 | E |
| 480 | YLR144C | **ACF2** | 0,0002 | 0,0068 | -9688,99 | 4 | E |
| 481 | YER120W | **SCS2** | 0,0012 | 0,0171 | -9685,18 | 4 | E |
| 482 | YLR233C | **EST1** | 0,0013 | 0,0183 | -9684,65 | 28 | E |
| 483 | YLR064W | **PER33** | 0,0025 | 0,0268 | -9658,05 | 4 | E |
| 484 | YAL008W | **FUN14** | 0,0041 | 0,0363 | -9637,18 | 4 | E |
| 485 | YLR050C | **YLR050C** | 0,0063 | 0,0476 | -9606,63 | 4 | E |
| 486 | YDR139C | **RUB1** | 0,0060 | 0,0466 | -9599,14 | 4 | E |
| 487 | YBL101C | **ECM21** | 0,0004 | 0,0098 | -9574,11 | 4 | E |
| 488 | YJR126C | **VPS70** | 0,0031 | 0,0310 | -9398,97 | 4 | E |
| 489 | YGL151W | **NUT1** | 0,0063 | 0,0476 | -9357,33 | 4 | E |
| 490 | YBR052C | **RFS1** | 0,0018 | 0,0218 | -9347,17 | 4 | E |
| 491 | YLR319C | **BUD6** | 0,0060 | 0,0467 | -9318,47 | 4 | E |
| 492 | YKR097W | **PCK1** | 0,0007 | 0,0126 | -9259,88 | 4 | E |
| 493 | YNL094W | **APP1** | 0,0041 | 0,0369 | -9200,8 | 4 | E |
| 494 | YOR173W | **DCS2** | 0,0041 | 0,0364 | -9173,56 | 4 | E |
| 495 | YJR050W | **ISY1** | 0,0023 | 0,0259 | -9164,34 | 4 | E |
| 496 | YIR003W | **AIM21** | 0,0008 | 0,0133 | -9141,96 | 4 | E |
| 497 | YER155C | **BEM2** | 0,0056 | 0,0446 | -9124,76 | 4 | E |
| 498 | YOR233W | **KIN4** | 0,0064 | 0,0479 | -8991,63 | 4 | E |
| 499 | YLR390W | **ECM19** | 0,0033 | 0,0319 | -8974,08 | 4 | E |
| 500 | YGR264C | **MES1** | 0,0031 | 0,0309 | -8945,8 | 4 | E |
| 501 | YIL017C | **VID28** | 0,0065 | 0,0485 | -8942,37 | 4 | E |
| 502 | YJL196C | **ELO1** | 0,0032 | 0,0318 | -8941,64 | 4 | E |
| 503 | YKR026C | **GCN3** | 0,0013 | 0,0180 | -8887,04 | 4 | E |
| 504 | YIL115C | **NUP159** | 0,0006 | 0,0123 | -8835,01 | 4 | E |
| 505 | YKL094W | **YJU3** | 0,0018 | 0,0219 | -8763,87 | 4 | E |
| 506 | YBR072W | **HSP26** | 0,0052 | 0,0424 | -8745,14 | 4 | E |
| 507 | YDL066W | **IDP1** | 0,0061 | 0,0471 | -8732,41 | 4 | E |
| 508 | YKR092C | **SRP40** | 0,0005 | 0,0113 | -8709,84 | 4 | E |
| 509 | YDR051C | **DET1** | 0,0002 | 0,0068 | -8651,73 | 4 | E |
| 510 | YLR385C | **SWC7** | 0,0007 | 0,0129 | -8613,93 | 4 | E |
| 511 | YOR155C | **ISN1** | 0,0007 | 0,0132 | -8582,93 | 4 | E |
| 512 | YBR181C | **RPS6B** | 0,0045 | 0,0394 | -8575,6 | 4 | E |
| 513 | YJL190C | **RPS22A** | 0,0040 | 0,0362 | -8567,24 | 4 | E |
| 514 | YDL142C | **CRD1** | 0,0031 | 0,0310 | -8492,56 | 4 | E |
| 515 | YJL094C | **KHA1** | 0,0022 | 0,0254 | -8446,74 | 28 | E |
| 516 | YER093C-A | **AIM11** | 0,0029 | 0,0302 | -8427,38 | 4 | E |
| 517 | YKL184W | **SPE1** | 0,0029 | 0,0301 | -8401,73 | 4 | E |
| 518 | YER101C | **AST2** | 0,0007 | 0,0130 | -8330,73 | 4 | E |
| 519 | YAL068C | **PAU8** | 0,0037 | 0,0347 | -8251,85 | 4 | E |

| | | | | | | | |
|---|---|---|---|---|---|---|---|
| 520 | YOR284W | **HUA2** | 0,0061 | 0,0471 | -8250,32 | 4 | E |
| 521 | YBR148W | **YSW1** | 0,0045 | 0,0398 | -8243,94 | 4 | E |
| 522 | YLR137W | **RKM5** | 0,0047 | 0,0404 | -8225,45 | 4 | E |
| 523 | YDL110C | **TMA17** | 0,0038 | 0,0350 | -8167,97 | 4 | E |
| 524 | YDL137W | **ARF2** | 0,0032 | 0,0316 | -8080,55 | 4 | E |
| 525 | YER175C | **TMT1** | 0,0054 | 0,0438 | -8077,39 | 4 | E |
| 526 | YBR164C | **ARL1** | 0,0006 | 0,0116 | -8066,31 | 4 | E |
| 527 | YKR095W | **MLP1** | 0,0012 | 0,0171 | -8055,56 | 4 | E |
| 528 | YMR275C | **BUL1** | 0,0047 | 0,0404 | -7962,52 | 4 | E |
| 529 | YIL161W | **YIL161W** | 0,0057 | 0,0451 | -7857,74 | 4 | E |
| 530 | YFL036W | **RPO41** | 0,0060 | 0,0466 | -7815,2 | 4 | E |
| 531 | YKL115C | **YKL115C** | 0,0005 | 0,0103 | -7781,98 | 4 | E |
| 532 | YLL012W | **YEH1** | 0,0010 | 0,0162 | -7673,96 | 4 | E |
| 533 | YBR230C | **OM14** | 0,0046 | 0,0401 | -7527,38 | 4 | E |
| 534 | YKL068W | **NUP100** | 0,0016 | 0,0207 | -7508,49 | 4 | E |
| 535 | YDR496C | **PUF6** | 0,0009 | 0,0156 | -7431,5 | 28 | E |
| 536 | YGR210C | **YGR210C** | 0,0005 | 0,0111 | -7286,42 | 4 | E |
| 537 | YJL153C | **INO1** | 0,0020 | 0,0235 | -7216,46 | 4 | E |
| 538 | YKL198C | **PTK1** | 0,0020 | 0,0235 | -7157,79 | 28 | E |
| 539 | YCL062W | **YCL062W** | 0,0034 | 0,0325 | -7123,9 | 4 | E |
| 540 | YDR528W | **HLR1** | 0,0016 | 0,0201 | -7052,36 | 4 | E |
| 541 | YDR126W | **SWF1** | 0,0026 | 0,0280 | -7047,88 | 4 | E |
| 542 | YKL217W | **JEN1** | 0,0022 | 0,0254 | -7024,08 | 4 | E |
| 543 | YDR515W | **SLF1** | 0,0065 | 0,0485 | -7009,67 | 4 | E |
| 544 | YBR189W | **RPS9B** | 0,0002 | 0,0072 | -6999,74 | 4 | E |
| 545 | YKL221W | **MCH2** | 0,0058 | 0,0453 | -6987,76 | 4 | E |
| 546 | YDL018C | **ERP3** | 0,0046 | 0,0401 | -6924,16 | 4 | E |
| 547 | YDR058C | **TGL2** | 0,0066 | 0,0487 | -6849,99 | 4 | E |
| 548 | YDR289C | **RTT103** | 0,0010 | 0,0162 | -6669,64 | 4 | E |
| 549 | YJR110W | **YMR1** | 0,0038 | 0,0352 | -6557,43 | 4 | E |
| 550 | YGL127C | **SOH1** | 0,0058 | 0,0453 | -6459,66 | 4 | E |
| 551 | YDR286C | **YDR286C** | 0,0025 | 0,0272 | -6405,56 | 4 | E |
| 552 | YKL206C | **ADD66** | 0,0009 | 0,0150 | -6376,7 | 4 | E |
| 553 | YEL001C | **IRC22** | 0,0061 | 0,0471 | -6274,65 | 4 | E |
| 554 | YHR124W | **NDT80** | 0,0065 | 0,0485 | -6127,33 | 4 | E |
| 555 | YNL011C | **YNL011C** | 0,0032 | 0,0316 | -5847,59 | 28 | E |
| 556 | YHR016C | **YSC84** | 0,0026 | 0,0274 | -5791,06 | 4 | E |
| 557 | YIR013C | **GAT4** | 0,0037 | 0,0343 | -5746,89 | 4 | E |
| 558 | YJR119C | **JHD2** | 0,0010 | 0,0162 | -5745,99 | 4 | E |
| 559 | YNL329C | **PEX6** | 0,0051 | 0,0420 | -5662,33 | 4 | E |
| 560 | YCL029C | **BIK1** | 0,0068 | 0,0498 | -5654,88 | 4 | E |
| 561 | YGR085C | **RPL11B** | 0,0016 | 0,0207 | -5555,76 | 4 | E |
| 562 | YJR083C | **ACF4** | 0,0060 | 0,0466 | -5101,03 | 4 | E |
| 563 | YNL097C | **PHO23** | 0,0046 | 0,0399 | -4641,69 | 4 | E |
| 564 | YDR029W | **YDR029W** | 0,0047 | 0,0404 | -4590,47 | 4 | E |
| 565 | YLL007C | **YLL007C** | 0,0052 | 0,0425 | -4524,7 | 4 | E |

| | | | | | | | |
|---|---|---|---|---|---|---|---|
| 566 | YKL129C | **MYO3** | 0,0031 | 0,0310 | -4317,22 | 4 | E |
| 567 | YJR015W | **YJR015W** | 0,0056 | 0,0444 | -4299,9 | 4 | E |
| 568 | YDR164C | **SEC1** | 0,0002 | 0,0052 | -4059,14 | 4 | E |
| 569 | YPL218W | **SAR1** | 0,0063 | 0,0477 | -2797,04 | 4 | E |
| 570 | YPR133C | **SPN1** | 0,0004 | 0,0102 | -2527,57 | 4 | E |
| 571 | YIL011W | **TIR3** | 0,0001 | 0,0047 | -1700,69 | 4 | E |
| 572 | YFR005C | **SAD1** | 0,0023 | 0,0259 | -895,093 | 4 | E |
| 573 | YDR415C | **YDR415C** | 0,0012 | 0,0176 | 6367,65 | 4 | S |
| 574 | YBR139W | **YBR139W** | 0,0026 | 0,0274 | 6630,17 | 4 | S |
| 575 | YML030W | **RCF1** | 0,0016 | 0,0201 | 6849,7 | 28 | S |
| 576 | YPL068C | **YPL068C** | 0,0063 | 0,0477 | 7254,92 | 4 | S |
| 577 | YJR010C-A | **SPC1** | 0,0003 | 0,0072 | 7494,05 | 4 | S |
| 578 | YBR221C | **PDB1** | 0,0038 | 0,0352 | 7570,24 | 4 | S |
| 579 | YKL109W | **HAP4** | 0,0027 | 0,0286 | 7692,03 | 28 | S |
| 580 | YKR005C | **YKR005C** | 0,0033 | 0,0319 | 7754,77 | 4 | S |
| 581 | YNL125C | **ESBP6** | 0,0006 | 0,0115 | 8214,77 | 28 | S |
| 582 | YDL136W | **RPL35B** | 0,0021 | 0,0238 | 8237,35 | 4 | S |
| 583 | YLR021W | **IRC25** | 0,0019 | 0,0226 | 8354,62 | 4 | S |
| 584 | YDL134C-A | **YDL134C-A** | 0,0029 | 0,0302 | 8712,18 | 4 | S |
| 585 | YDL091C | **UBX3** | 0,0026 | 0,0278 | 8924,26 | 4 | S |
| 586 | YGL152C | **YGL152C** | 0,0024 | 0,0264 | 9366,9 | 4 | S |
| 587 | YPL100W | **ATG21** | 0,0011 | 0,0168 | 9430,67 | 4 | S |
| 588 | YKL083W | **YKL083W** | 0,0040 | 0,0360 | 9604,11 | 4 | S |
| 589 | YPR191W | **QCR2** | 0,0014 | 0,0191 | 9613,22 | 4 | S |
| 590 | YBL097W | **BRN1** | 0,0036 | 0,0339 | 9892,78 | 4 | S |
| 591 | YBR258C | **SHG1** | 0,0011 | 0,0165 | 10290,6 | 4 | S |
| 592 | YNL166C | **BNI5** | 0,0050 | 0,0417 | 10858,7 | 4 | S |
| 593 | YER140W | **EMP65** | 0,0005 | 0,0102 | 10879,6 | 4 | S |
| 594 | YKR047W | **YKR047W** | 0,0041 | 0,0364 | 10901 | 4 | S |
| 595 | YJL214W | **HXT8** | 0,0013 | 0,0181 | 10910,1 | 4 | S |
| 596 | YBR103W | **SIF2** | 0,0066 | 0,0487 | 11348,4 | 4 | S |
| 597 | YLR143W | **DPH6** | 0,0046 | 0,0401 | 11511,5 | 4 | S |
| 598 | YNL052W | **COX5A** | 0,0067 | 0,0491 | 11531,7 | 4 | S |
| 599 | YKR028W | **SAP190** | 0,0063 | 0,0477 | 11864 | 4 | S |
| 600 | YOR186W | **YOR186W** | 0,0015 | 0,0193 | 12116,2 | 4 | S |
| 601 | YIL156W | **UBP7** | 0,0013 | 0,0179 | 12121 | 4 | S |
| 602 | YNL233W | **BNI4** | 0,0011 | 0,0165 | 12368,2 | 4 | S |
| 603 | YDL217C | **TIM22** | 0,0004 | 0,0095 | 12391,5 | 4 | S |
| 604 | YLR316C | **TAD3** | 0,0062 | 0,0473 | 12513,5 | 4 | S |
| 605 | YGR178C | **PBP1** | 0,0003 | 0,0076 | 12592,9 | 4 | S |
| 606 | YPR074C | **TKL1** | 0,0012 | 0,0176 | 12757 | 4 | S |
| 607 | YPL001W | **HAT1** | 0,0001 | 0,0031 | 13000,1 | 28 | S |
| 608 | YKL031W | **YKL031W** | 0,0054 | 0,0435 | 13121,3 | 4 | S |
| 609 | YNL253W | **TEX1** | 0,0047 | 0,0401 | 13284,6 | 4 | S |
| 610 | YKL191W | **DPH2** | 0,0008 | 0,0141 | 13721,3 | 4 | S |
| 611 | YGR192C | **TDH3** | 0,0060 | 0,0463 | 14770,8 | 4 | S |

| | | | | | | | |
|---|---|---|---|---|---|---|---|
| 612 | YKR099W | **BAS1** | 0,0001 | 0,0039 | 14887,4 | 4 | S |
| 613 | YFL022C | **FRS2** | 0,0007 | 0,0131 | 15148,4 | 4 | S |
| 614 | YIL103W | **DPH1** | 0,0001 | 0,0034 | 15413,3 | 4 | S |
| 615 | YLR422W | **YLR422W** | 0,0033 | 0,0320 | 15561,9 | 4 | S |
| 616 | YPL139C | **UME1** | 0,0059 | 0,0457 | 15634,4 | 4 | S |
| 617 | YAR002W | **NUP60** | 0,0011 | 0,0168 | 16492,5 | 4 | S |
| 618 | YOR384W | **FRE5** | 0,0063 | 0,0476 | 17481,6 | 4 | S |
| 619 | YDR378C | **LSM6** | 0,0007 | 0,0129 | 17701,8 | 4 | S |
| 620 | YHR017W | **YSC83** | 0,0052 | 0,0424 | 17794,6 | 4 | S |
| 621 | YOR027W | **STI1** | 0,0000 | 0,0005 | 17818,2 | 4 | S |
| 622 | YOL067C | **RTG1** | 0,0005 | 0,0103 | 18261,9 | 4 | S |
| 623 | YDR520C | **URC2** | 0,0022 | 0,0249 | 18285,3 | 4 | S |
| 624 | YLR136C | **TIS11** | 0,0056 | 0,0446 | 18575,3 | 4 | S |
| 625 | YFL002C | **SPB4** | 0,0001 | 0,0034 | 18641,5 | 4 | S |
| 626 | YFL006W | **YFL006W** | 0,0037 | 0,0347 | 18853 | 4 | S |
| 627 | YKL205W | **LOS1** | 0,0015 | 0,0200 | 19112,5 | 4 | S |
| 628 | YOR249C | **APC5** | 0,0010 | 0,0163 | 19134,9 | 4 | S |
| 629 | YGL011C | **SCL1** | 0,0049 | 0,0410 | 19531,5 | 4 | S |
| 630 | YNL140C | **YNL140C** | 0,0003 | 0,0078 | 19600,3 | 4 | S |
| 631 | YNL016W | **PUB1** | 0,0000 | 0,0019 | 19987,3 | 4 | S |
| 632 | YJR097W | **JJJ3** | 0,0003 | 0,0077 | 20012,5 | 4 | S |
| 633 | YGL094C | **PAN2** | 0,0004 | 0,0095 | 20042,3 | 4 | S |
| 634 | YJR043C | **POL32** | 0,0000 | 0,0022 | 20457,1 | 4 | S |
| 635 | YIL097W | **FYV10** | 0,0059 | 0,0457 | 20530 | 4 | S |
| 636 | YDR431W | **YDR431W** | 0,0039 | 0,0352 | 20921 | 4 | S |
| 637 | YBR273C | **UBX7** | 0,0005 | 0,0111 | 22777,8 | 4 | S |
| 638 | YML095C | **RAD10** | 0,0039 | 0,0356 | 22885,4 | 4 | S |
| 639 | YGR027C | **RPS25A** | 0,0001 | 0,0036 | 23314,7 | 4 | S |
| 640 | YDR315C | **IPK1** | 0,0004 | 0,0091 | 25070,4 | 4 | S |
| 641 | YJL157C | **FAR1** | 0,0013 | 0,0184 | 25202,5 | 4 | S |
| 642 | YNL292W | **PUS4** | 0,0007 | 0,0124 | 25454,5 | 4 | S |
| 643 | YLR055C | **SPT8** | 0,0030 | 0,0304 | 25576,4 | 4 | S |
| 644 | YOR344C | **TYE7** | 0,0000 | 0,0026 | 25628,8 | 4 | S |
| 645 | YLR262C-A | **TMA7** | 0,0048 | 0,0404 | 26635,5 | 4 | S |
| 646 | YDL165W | **CDC36** | 0,0031 | 0,0311 | 27476,3 | 4 | S |
| 647 | YLR436C | **ECM30** | 0,0016 | 0,0207 | 27501,9 | 4 | S |
| 648 | YMR316W | **DIA1** | 0,0024 | 0,0264 | 28196,9 | 4 | S |
| 649 | YLR338W | **OPI9** | 0,0067 | 0,0495 | 29466,9 | 4 | S |
| 650 | YDR257C | **RKM4** | 0,0023 | 0,0258 | 29839,8 | 4 | S |
| 651 | YML018C | **YML018C** | 0,0040 | 0,0359 | 30046,2 | 4 | S |
| 652 | YOR315W | **SFG1** | 0,0052 | 0,0424 | 30540,7 | 4 | S |
| 653 | YCR062W | **YCR062W** | 0,0017 | 0,0208 | 31638 | 4 | S |
| 654 | YGL036W | **YGL036W** | 0,0007 | 0,0129 | 32628,6 | 4 | S |
| 655 | YKL032C | **IXR1** | 0,0006 | 0,0123 | 33298,7 | 4 | S |
| 656 | YPL194W | **DDC1** | 0,0001 | 0,0043 | 33936 | 4 | S |
| 657 | YLR289W | **GUF1** | 0,0007 | 0,0131 | 34576,7 | 4 | S |

| | | | | | | | |
|---|---|---|---|---|---|---|---|
| 658 | YPL182C | **YPL182C** | 0,0009 | 0,0158 | 34747,6 | 4 | S |
| 659 | YMR207C | **HFA1** | 0,0009 | 0,0159 | 34829,6 | 4 | S |
| 660 | YMR111C | **YMR111C** | 0,0034 | 0,0327 | 34858,6 | 4 | S |
| 661 | YBR274W | **CHK1** | 0,0000 | 0,0000 | 34864,9 | 28 | S |
| 662 | YER173W | **RAD24** | 0,0000 | 0,0000 | 34980,9 | 28 | S |
| 663 | YOR026W | **BUB3** | 0,0000 | 0,0001 | 35694,1 | 4 | S |
| 664 | YOR368W | **RAD17** | 0,0000 | 0,0000 | 37278,2 | 28 | S |
| 665 | YBL079W | **NUP170** | 0,0030 | 0,0304 | 38597,3 | 4 | S |
| 666 | YJR011C | **YJR011C** | 0,0002 | 0,0052 | 39025,2 | 4 | S |
| 667 | YPL181W | **CTI6** | 0,0009 | 0,0155 | 39849,1 | 4 | S |
| 668 | YNL064C | **YDJ1** | 0,0002 | 0,0052 | 40151,8 | 4 | S |
| 669 | YDR376W | **ARH1** | 0,0006 | 0,0122 | 40898,8 | 4 | S |
| 670 | YDR006C | **SOK1** | 0,0000 | 0,0003 | 40980,4 | 4 | S |
| 671 | YBR206W | **YBR206W** | 0,0048 | 0,0404 | 41217,3 | 4 | S |
| 672 | YOR193W | **PEX27** | 0,0024 | 0,0264 | 42548,6 | 4 | S |
| 673 | YLR381W | **CTF3** | 0,0000 | 0,0010 | 43732,4 | 4 | S |
| 674 | YDR217C | **RAD9** | 0,0000 | 0,0000 | 44615,3 | 28 | S |
| 675 | YIR002C | **MPH1** | 0,0000 | 0,0008 | 45750,3 | 4 | S |
| 676 | YCR079W | **PTC6** | 0,0000 | 0,0003 | 48276,8 | 4 | S |
| 677 | YCR077C | **PAT1** | 0,0000 | 0,0010 | 49618,9 | 4 | S |
| 678 | YNL198C | **YNL198C** | 0,0005 | 0,0109 | 50443,3 | 4 | S |
| 679 | YDR209C | **YDR209C** | 0,0000 | 0,0015 | 52231,3 | 4 | S |
| 680 | YDR335W | **MSN5** | 0,0000 | 0,0011 | 53585,6 | 4 | S |
| 681 | YJL124C | **LSM1** | 0,0005 | 0,0102 | 60245,1 | 4 | S |
| 682 | YNL199C | **GCR2** | 0,0000 | 0,0003 | 61902,4 | 4 | S |
| 683 | YOR327C | **SNC2** | 0,0000 | 0,0009 | 64015,5 | 4 | S |
| 684 | YHR151C | **MTC6** | 0,0003 | 0,0072 | 65480,3 | 4 | S |
| 685 | YML016C | **PPZ1** | 0,0003 | 0,0089 | 68308,4 | 4 | S |
| 686 | YLL002W | **RTT109** | 0,0015 | 0,0196 | 74522,7 | 4 | S |
| 687 | YER112W | **LSM4** | 0,0016 | 0,0205 | 81127,5 | 4 | S |
| 688 | YHR178W | **STB5** | 0,0033 | 0,0319 | 82917,4 | 4 | S |
| 689 | YBR267W | **REI1** | 0,0006 | 0,0119 | 85739,8 | 4 | S |
| 690 | YER008C | **SEC3** | 0,0015 | 0,0193 | 93128,4 | 4 | S |
| 691 | YKR024C | **DBP7** | 0,0020 | 0,0235 | 96306,8 | 4 | S |
| 692 | YKL121W | **DGR2** | 0,0011 | 0,0169 | 97550,9 | 4 | S |
| 693 | YAR019C | **CDC15** | 0,0006 | 0,0123 | 100082 | 4 | S |
| 694 | YLR407W | **YLR407W** | 0,0000 | 0,0003 | 105421 | 4 | S |
| 695 | YAL033W | **POP5** | 0,0005 | 0,0103 | 117003 | 4 | S |
| 696 | YKL006W | **RPL14A** | 0,0001 | 0,0033 | 123711 | 4 | S |
| 697 | YIL040W | **APQ12** | 0,0000 | 0,0026 | 129214 | 4 | S |
| 698 | YHR005C-A | **TIM10** | 0,0000 | 0,0011 | 132653 | 4 | S |
| 699 | YKL069W | **YKL069W** | 0,0004 | 0,0091 | 152024 | 4 | S |
| 700 | YJR145C | **RPS4A** | 0,0001 | 0,0035 | 162701 | 4 | S |
| 701 | YHL015W | **RPS20** | 0,0000 | 0,0010 | 167119 | 4 | S |
| 702 | YGR092W | **DBF2** | 0,0000 | 0,0005 | 254871 | 4 | S |

# Appendix G. 308 genes selected for W303 SGA

Light grey cells – genes identified in S288C SGA as "enhancers" of *dna2*Δ (E).
Dark grey cells – genes identified in S288C SGA as "suppressors" of *dna2*Δ (S).
No-color cells – not identified as "suppressor" or "enhancer" of *dna2*Δ in S288C SGA.
In the group of 308 were some DAmP alleles; W303 library did not contain the DAmP collection and these genes could not be tested. Therefore in the end of this table are 28 genes chosen for further testing (no DAmP alleles). 308 genes were chosen based on: i) the fact that gene deletion was a strong enhancer/suppressor in *dna2*Δ *pCAN1-URA3-DNA2* S288C SGA, ii) the gene belongs to the lab list of interesting genes, so called "Golden List", iii) the gene was studied/mentioned in one of chosen publications. Each gene affiliation to any of indicated groups is marked as "X" in a table below.

| No. | ORF | Gene | Tested or to be tested /Interesting | Eva's Golden list | Median normalised | Telomere related genes (gr.1) | Nuclear telomere cap. cplx (gr.4) | Strong. Enhancers of cdc13-1 (gr.15) | Strong. Suppress. of cdc13-1 (gr.16) | DAmP Long telomeres (gr.21) | Long telomeres Kupiec (gr.22) | DAmP short telomeres (gr.26) | Accelerated senescence (gr.5) | Normal senescence (gr.7) | (Budd et al., 2005) | (Poli et al., 2016) | (Hustedt et al., 2015) | (Hoffman et al., 2015) | (Eriksson et al., 2012) | (Saka et al., 2016) |
|---|---|---|---|---|---|---|---|---|---|---|---|---|---|---|---|---|---|---|---|---|
| 1 | YML102W | **CAC2** | | | | | | | | | | | | | | | | | | X |
| 2 | YMR027W | **YMR027W** | | | | | | | | | | | | | | | | | | X |
| 3 | YGL243W | **TAD1** | | | | | | | | | | | | | | | | | | X |
| 4 | YNL021W | **HDA1** | X | | | | | | | | | | | | | | | | | X |
| 5 | YNL099C | **OCA1** | | | | | | | | | | | | | | | X | | | X |
| 6 | YLR446W | **YLR446W** | | | | | | | | | | | | | | | | | | X |
| 7 | YML121W | **GTR1** | | X | | | | | X | | | | | | | | | | | |
| 8 | YBR088C | **POL30** | X | | | | | | | | X | | | | | | | | | |
| 9 | YOR191W | **RIS1** | X | X | | | | | | | | | | | | | | | | |
| 10 | YML007W | **YAP1** | | | | | | X | | | | | | | | | | | | |
| 11 | YFL013C | **IES1** | X | | | | | | | | | | | | | | X | | | |
| 12 | YER092W | **IES5** | X | | | | | | | | | | | | | X | X | | | X |
| 13 | YMR216C | **SKY1** | | X | | | | | | | | | | | | | | | | |
| 14 | YLR119W | **SRN2** | | X | | | | | X | | | | | | | | | | | |
| 15 | YMR073C | **IRC21** | X | X | | | | X | | | | | | | | | X | | | |
| 16 | YLR234W | **TOP3** | X | | | | | | | | | | | | X | | | | | |
| 17 | YNL206C | **RTT106** | X | | | | | | | | | | | | | | | | X | X |
| 18 | YDL002C | **NHP10** | X | X | | | | | | | | | | | | X | X | | | X |
| 19 | YOR039W | **CKB2** | | X | | | | | X | | | | | | | | | | | X |
| 20 | YFR010W | **UBP6** | | | | | | | X | | | | | | | | | | | |
| 21 | YBR057C | **MUM2** | | X | | | | | X | | | | | | | | | | | |
| 22 | YER164W | **CHD1** | X | | | | | | | | | | | | | | X | | | |
| 23 | YGL212W | **VAM7** | | X | | | | | X | | | | | | | | | | | X |
| 24 | YDR007W | **TRP1** | | | | | | | | | | | | | | | | | | X |
| 25 | YCL010C | **SGF29** | | | | | | | | | | | | | | | X | | | X |
| 26 | YJL047C | **RTT101** | X | | | | | | | | | | X | | | | X | | | X |

| | | | | | | | | | | | | | | | | | | | |
|---|---|---|---|---|---|---|---|---|---|---|---|---|---|---|---|---|---|---|---|
| 27 | YPL213W | **LEA1** | | | | | | | | | X | | X | | | | | | |
| 28 | YNR005C | **YNR005C** | | | | | | | X | | | | | | | | | | |
| 29 | YBR036C | **CSG2** | | X | | | | | | | | | | | | | | | |
| 30 | YLR337C | **VRP1** | | | | | | | | | X | | | | | | | | X |
| 31 | YLR384C | **IKI3** | | X | | | | X | | | | | | | | | | | |
| 32 | YJL092W | **SRS2** | | X | | | | X | | | | | | | X | X | | | X |
| 33 | YDR260C | **SWM1** | | | | | | X | | | | | | | | X | X | | X |
| 34 | YGL042C | **YGL042C** | | | | | | X | | | | | | | | | | | |
| 35 | YER116C | **SLX8** | X | | | | | | | | | | X | | X | | X | | X |
| 36 | YLR102C | **APC9** | | | | | | X | | | | | | | | | | | |
| 37 | YMR078C | **CTF18** | | X | | | | X | | | | | X | | X | | | | X |
| 38 | YBR082C | **UBC4** | | X | | | | | X | | | | | | X | | | | X |
| 39 | YML028W | **TSA1** | X | | X | | | | | | | | X | | | | | | X |
| 40 | YOR033C | **EXO1** | X | X | X | X | | | X | | | | | X | X | | X | | |
| 41 | YKL213C | **DOA1** | | X | | | | | X | | | | | | | X | X | | X |
| 42 | YNL250W | **RAD50** | X | X | X | X | | | | | | X | | | X | | | | X |
| 43 | YDR510W | **SMT3** | | | | | | | | X | | | | | | | | | |
| 44 | YAL002W | **VPS8** | | | | | | | X | | | | | | | | | | |
| 45 | YBL088C | **TEL1** | X | X | | X | | | | | | X | X | | | X | | | X |
| 46 | YOL012C | **HTZ1** | X | | | | | | | | | | | | | X | X | | X | |
| 47 | YJR109C | **CPA2** | | | X | | | | | | | | | | | | | | |
| 48 | YDR075W | **PPH3** | | X | | | | X | | | | | | | | | X | | |
| 49 | YDR174W | **HMO1** | | | | | | | | | X | | X | | | | X | | | X |
| 50 | YFL023W | **BUD27** | | | | | | | X | | | | | | | X | X | | |
| 51 | YGL244W | **RTF1** | | | | | | X | | | | | X | | X | X | X | | | X |
| 52 | YMR038C | **CCS1** | | X | | | | | | | | | | | | | | | | X |
| 53 | YKL110C | **KTI12** | | X | | | | X | | | | | | | | | X | | | |
| 54 | YDR121W | **DPB4** | | | | | | X | | | | | | | | | | | | X |
| 55 | YPL101W | **ELP4** | | | | | | X | | | | | | | | | X | | | |
| 56 | YDR244W | **PEX5** | | X | | | | | | | | | | | | | | | | |
| 57 | YDL074C | **BRE1** | | | X | | | | | | | | | | X | X | X | | | X |
| 58 | YPR108W | **RPN7** | | | | | | | | | | X | | | | | | | | |
| 59 | YLR372W | **SUR4** | | X | | | | | X | | | | | | | | X | | | |
| 60 | YMR224C | **MRE11** | X | X | X | X | | | | | | X | X | | X | | X | | | |
| 61 | YML103C | **NUP188** | | | | | | | | | | | | | | X | X | | | |
| 62 | YLR317W | **YLR317W** | | | | | | | | X | | | | | | | | | | |
| 63 | YLR061W | **RPL22A** | | | | | | | X | | | | | | | | | | | |
| 64 | YKR059W | **TIF1** | | | | | | | | | X | | | | | | | | | |
| 65 | YBR275C | **RIF1** | X | X | | X | X | X | | | | | | | | | | | | X |
| 66 | YGR200C | **ELP2** | | X | | | | X | | | | | | | | | | | | X |
| 67 | YER095W | **RAD51** | | X | | | | X | | | | | | | | | | | | |
| 68 | YKR020W | **VPS51** | | | | | | | X | | | | | | | | | | | |
| 69 | YEL033W | **MTC7** | | | | | | | | | | X | | | | X | X | | | |
| 70 | YPR040W | **TIP41** | | X | | | | X | | | | | | | | | | | | |
| 71 | YPL157W | **TGS1** | | | | | | | | | X | | | | | | | | | |
| 72 | YDR173C | **ARG82** | | | | | | | | | X | | | | | | | | | X |
| 73 | YPL102C | **YPL102C** | | | | | | X | | | | | | | | | | | | |
| 74 | YDL163W | **YDL163W** | | | | | | | | X | | | | | | | | | | |
| 75 | YDR076W | **RAD55** | | X | | | | | | | | | X | | | | | | | |
| 76 | YAL013W | **DEP1** | | | | | | X | | | | | | | | | | | | |
| 77 | YLL039C | **UBI4** | X | | | | | | | | | | | | | | X | | | X |
| 78 | YDR034C | **LYS14** | | | | | | | | | | | | | | | | | | |
| 79 | YML032C | **RAD52** | | X | X | | | | | | | | X | | X | | X | | | X |
| 80 | YKL114C | **APN1** | | X | | | | | | | X | | | | | | | | | X |
| 81 | YCL060C | **:::MRC1** | | X | | | | X | | | | | | | X | | X | | | X |
| 82 | YDR128W | **MTC5** | | X | | | | | X | | | | | | | | | | | |
| 83 | YJL095W | **BCK1** | | X | | | | X | | | | | | | | | | | | |
| 84 | YLR039C | **RIC1** | X | | | | | | X | | | | | | | | | | | X |
| 85 | YPR044C | **OPI11** | | | | | | | X | | | | | | | | | | | X |
| 86 | YPR051W | **MAK3** | | X | | | | X | | | X | | | X | | | | | | X |
| 87 | YOR080W | **DIA2** | | X | | | | | | | | | | | | | X | | | X |
| 88 | YPL008W | **CHL1** | | X | | | | X | | | | | | | | | | | | X |
| 89 | YDR083W | **RRP8** | | | | | | | | | X | | X | | | | | | | |
| 90 | YDR269C | **YDR269C** | | | | | | | | | | | | | | | | | | |
| 91 | YKR074W | **AIM29** | | | | | | X | | | | | | | | | | | | |
| 92 | YOR382W | **FIT2** | | | X | | | | | | | | | | | | | | | |

| | | | | | | | | | | | | | | | | | | | | |
|---|---|---|---|---|---|---|---|---|---|---|---|---|---|---|---|---|---|---|---|---|
| 93 | YPR050C | **YPR050C** | | | | | | X | | | | | | | | | | | | |
| 94 | YER177W | **BMH1** | | X | | | | | X | | | | | X | | X | | | | |
| 95 | YPR119W | **CLB2** | | X | X | | | X | | | | | | | | | | | X | |
| 96 | YFL025C | **BST1** | | X | | | | | X | | | | | | | | | | | X |
| 97 | YJL138C | **TIF2** | | | | | | | | | X | | | | | | | | | |
| 98 | YCR020C-A | **MAK31** | | | | | | X | | | X | | | | | | | | | |
| 99 | YLL019C | **KNS1** | | | X | | | | | | | | | | | | | | | |
| 100 | YMR165C | **PAH1** | | | | | | | X | | | | | | | | | | | |
| 101 | YER120W | **SCS2** | | X | | | | | X | | | | | | | | | | | |
| 102 | YLR233C | **EST1** | | X | | X | | X | | | | X | | | | | | | | |
| 103 | YER155C | **BEM2** | | | | | | X | | | | | | | | | | | | X |
| 104 | YIL017C | **VID28** | | | | | | | X | | | | | | | | | | | |
| 105 | YBR072W | **HSP26** | | | | | | X | | | | | | | | | | | | |
| 106 | YFL036W | **RPO41** | | X | | | | | X | | | | | | | | | | | |
| 107 | YDR496C | **PUF6** | | | X | | | | | | | | | | | X | | | | |
| 108 | YDR289C | **RTT103** | X | | | | | X | | | | | | | X | | | | | X |
| 109 | YGR085C | **RPL11B** | | | | | | | X | | | | | | | | | | | X |
| 110 | YNL097C | **PHO23** | | X | | | | | | | | | | | X | | | | | |
| 111 | YPR133C | **SPN1** | | | | | | | | X | | | | | | | | | | |
| 112 | YFR005C | **SAD1** | | | | | | | | X | | | | | | | | | | |
| 113 | YML030W | **RCF1** | | | X | | | | | | | | | | | | | | | |
| 114 | YJR010C-A | **SPC1** | X | | | | | | | | | | | | | | | | | |
| 115 | YNL125C | **ESBP6** | | | X | | | | | | | | | | | | | | | |
| 116 | YDL136W | **RPL35B** | X | | | | | | | | | | | | | | | | | |
| 117 | YNL166C | **BNI5** | | | | | | | | | | | | | | | | | | X |
| 118 | YBR103W | **SIF2** | | | | | | | | | | | | | | | | | | X |
| 119 | YLR143W | **DPH6** | | | | | | X | | | | | | | | | | | | |
| 120 | YNL052W | **COX5A** | X | | | | | | | | | | | | | | | | | |
| 121 | YKR028W | **SAP190** | | | | | | | | | | | | | | X | X | | | |
| 122 | YNL233W | **BNI4** | | | | | | | | | | | | | | | | | | X |
| 123 | YGR178C | **PBP1** | | | | | | | | | | | | | | X | X | | | |
| 124 | YPR074C | **TKL1** | | X | | | | | X | | | | | | | | | | | |
| 125 | YPL001W | **HAT1** | | | X | | | X | | | | | | | | | | | | |
| 126 | YKL191W | **DPH2** | | | | | | X | | | | | | | | | | | | X |
| 127 | YKR099W | **BAS1** | | X | | | | | X | | | | | | | | | | | |
| 128 | YIL103W | **DPH1** | | X | | | | X | | | | | | | | | | | | |
| 129 | YPL139C | **UME1** | | | | | | X | | | | | | | | | | | | |
| 130 | YAR002W | **NUP60** | | | | | | | | | | | | | | X | X | | | |
| 131 | YDR378C | **LSM6** | X | | | | | | | | | | | | | X | X | | | |
| 132 | YOR027W | **STI1** | | X | | | | X | | | | | | | | | | | | |
| 133 | YOR249C | **APC5** | X | | | | | | | | | | | | | | | | | |
| 134 | YGL011C | **SCL1** | X | | | | | | | | | | | | | | | | | |
| 135 | YNL016W | **PUB1** | | | | | | | | | X | | | | | | | | | |
| 136 | YJR097W | **JJJ3** | | | | | | X | | | | | | | | | | | | |
| 137 | YGL094C | **PAN2** | | X | | | | X | | | | | | | | | | | | X |
| 138 | YJR043C | **POL32** | X | X | | | | X | | | | | X | | | | | | | |
| 139 | YIL097W | **FYV10** | | | | | | | X | | | | | | | | | | | X |
| 140 | YBR273C | **UBX7** | | | | | | | X | | | | | | | | | | | |
| 141 | YML095C | **RAD10** | X | | | | | | | | | | | | | | | | | X |
| 142 | YGR027C | **RPS25A** | X | | | | | | | | | | | | | | | | | |
| 143 | YDR315C | **IPK1** | | | | | | | X | | | | | | | | | | | |
| 144 | YLR055C | **SPT8** | | | | | | | | | | | | | | | X | | | |
| 145 | YOR344C | **TYE7** | | X | | | | | | | | | | | | | | | | |
| 146 | YLR262C-A | **TMA7** | X | | | | | | | | | | | | | | | | | |
| 147 | YDL165W | **CDC36** | | | | | | | | X | | | | | | X | X | | | |
| 148 | YMR316W | **DIA1** | X | | | | | | | | | | | | | | | | | |
| 149 | YDR257C | **RKM4** | X | | | | | | | | | | | | | | | | | |
| 150 | YML018C | **YML018C** | X | | | | | | | | | | | | | | | | | |
| 151 | YKL032C | **IXR1** | X | | | | | | | | | | | | | | | | | |
| 152 | YPL194W | **DDC1** | X | X | | X | | | X | | | | | X | | | X | | | |
| 153 | YLR289W | **GUF1** | X | | | | | | | | | | | | | | | | | |
| 154 | YPL182C | **YPL182C** | X | | | | | | | | | | | | | | | | | |
| 155 | YMR207C | **HFA1** | X | | | | | | | | | | | | | | | | | |
| 156 | YMR111C | **YMR111C** | X | | | | | | | | | | | | | | | | | |
| 157 | YBR274W | **CHK1** | X | X | X | X | | | X | | | | | X | | | | | | |
| 158 | YER173W | **RAD24** | X | X | X | X | | | X | | | | | X | | | | | | X |

| | | | | | | | | | | | | | | | | | | | | |
|---|---|---|---|---|---|---|---|---|---|---|---|---|---|---|---|---|---|---|---|---|
| 159 | YOR026W | **BUB3** | X | | X | | | | | | | | | | | X | X | | | X |
| 160 | YOR368W | **RAD17** | X | X | X | X | | | X | | | | | X | | | | | | |
| 161 | YBL079W | **NUP170** | | | | | | | | | | | | | | X | X | | | |
| 162 | YPL181W | **CTI6** | X | | | | | | | | | | | | | | | | | |
| 163 | YNL064C | **YDJ1** | | | | | | X | | | | | | | | X | X | | | X |
| 164 | YDR376W | **ARH1** | X | | | | | | | | | | | | | | | | | |
| 165 | YDR006C | **SOK1** | | | | | | | X | | | | | | | | | | | |
| 166 | YBR206W | **YBR206W** | X | | | | | | | | | | | | | | | | | |
| 167 | YLR381W | **CTF3** | X | | | | | | | | | | | | | | | | | |
| 168 | YDR217C | **RAD9** | X | X | X | X | | | X | | | | | X | | X | X | | | |
| 169 | YIR002C | **MPH1** | X | X | | | | | X | | | | | | | X | X | | | |
| 170 | YCR079W | **PTC6** | X | | | | | | | | | | | | | | | | | |
| 171 | YCR077C | **PAT1** | | | | | | X | | | | | | | | | | | | |
| 172 | YNL198C | **YNL198C** | | | | | | | | | | | | | | | | | | X |
| 173 | YDR209C | **YDR209C** | X | | | | | | | | | | | | | | | | | |
| 174 | YDR335W | **MSN5** | | | | | | X | | | | | | | | X | X | | | X |
| 175 | YJL124C | **LSM1** | X | | | | | X | | | | | | | | X | X | | | X |
| 176 | YNL199C | **GCR2** | | | | | | | | | | | | | | | | | | X |
| 177 | YHR151C | **MTC6** | X | | | | | | | | | | | | | | | | | X |
| 178 | YLL002W | **RTT109** | X | | | | | | | | | | X | | | | X | | X | X |
| 179 | YER112W | **LSM4** | X | | | | | | | | | | | | | | | | | |
| 180 | YHR178W | **STB5** | X | | | | | | | | | | | | | | | | | |
| 181 | YBR267W | **REI1** | X | | | | | | X | | | | | | | | | | | X |
| 182 | YER008C | **SEC3** | X | | | | | | | | | | | | | | | | | |
| 183 | YKR024C | **DBP7** | X | | | | | | | | | | | | | | | | | X |
| 184 | YKL121W | **DGR2** | X | | | | | | | | | | | | | | | | | X |
| 185 | YAR019C | **CDC15** | X | | | | | | | | | | | | | | | | | |
| 186 | YLR407W | **YLR407W** | X | | | | | | | | | | | | | | | | | |
| 187 | YAL033W | **POP5** | X | | | | | | | | | | | | | | | | | |
| 188 | YKL006W | **RPL14A** | X | | | | | | | | | | | | | | | | | |
| 189 | YIL040W | **APQ12** | X | | | | | | | | | | | | | X | | | | |
| 190 | YHR005C-A | **TIM10** | X | | | | | | | | | | | | | | | | | |
| 191 | YKL069W | **YKL069W** | X | | | | | | | | | | | | | | | | | |
| 192 | YJR145C | **RPS4A** | X | | | | | | | | X | | | | | | | | | |
| 193 | YHL015W | **RPS20** | X | | | | | | | | | | | | | | | | | |
| 194 | YGR092W | **DBF2** | X | | | | | | | | | | | | | | | | | |
| 195 | **YBL007C** | **SLA1** | | X | | | | | X | | | | X | | | | | | | |
| 196 | **YBR034C** | **HMT1** | | X | | | | X | | | | | | | | | | | | |
| 197 | **YCR073W-A** | **SOL2** | | X | | | | | | | X | | | | | | | | | |
| 198 | **YCR095C** | **OCA4** | | X | | | | | | | | | | | | | | | | |
| 199 | **YDL056W** | **MBP1** | | X | | | | | | | | | | | | | X | | X | |
| 200 | **YDL130W** | **RPP1B** | | X | | | | | | | | | | | | | | | | |
| 201 | **YDL236W** | **PHO13** | | X | | | | X | | | | | | | | | | | | |
| 202 | **YDR004W** | **RAD57** | | X | | | | | | | | | X | | | | | | | X |
| 203 | **YDR080W** | **VPS41** | | X | | | | | X | | | | | | | | | | | |
| 204 | **YDR099W** | **BMH2** | | X | | | | | | | | | | X | | | | | | |
| 205 | **YDR143C** | **SAN1** | | X | | | | | X | | | | | | | | | | | X |
| 206 | **YDR206W** | **EBS1** | | X | | X | | | X | | | | | X | | | | | | |
| 207 | **YDR310C** | **SUM1** | | X | | | | | | | | | X | | | | | | | |
| 208 | **YDR369C** | **XRS2** | | X | | X | | X | | | | X | X | | | X | X | | | X |
| 209 | **YGL078C** | **DBP3** | | X | | | | | X | | | | | | | | | | | |
| 210 | **YGL163C** | **RAD54** | | X | | | | X | | | | | X | | | | | | | |
| 211 | **YGL167C** | **PMR1** | | X | | | | | | | | | | | | | X | | | |
| 212 | **YGL173C** | **XRN1** | | X | | | | | X | | | | X | | | | | | | X |
| 213 | **YGL213C** | **SKI8** | | X | | | | | X | | | | | | | | X | | | |
| 214 | **YGR072W** | **UPF3** | X | X | | X | | | X | | | | X | | | | X | | | |
| 215 | **YGR123C** | **PPT1** | | X | | | | X | | | | | | | | | X | | | |
| 216 | **YGR187C** | **HGH1** | | X | | | | X | | | | | | | | | | | | |
| 217 | **YHR077C** | **NMD2** | X | X | | X | | | X | | | | X | | | | X | | | X |
| 218 | **YHR111W** | **UBA4** | | X | | | | X | | | | | | | | | X | | | |
| 219 | **YHR154W** | **RTT107** | | X | | | | | | | | | X | | | | X | | | X |
| 220 | **YHR162W** | **MPC2** | | X | | | | | | | | | | | | | | | | X |
| 221 | **YIL131C** | **FKH1** | | X | | | | X | | | | | | | | | | | | X |
| 222 | **YIL149C** | **MLP2** | | X | | | | | | | X | | | | | | X | | | |
| 223 | **YIL160C** | **POT1** | X | X | | | | | X | | | | | | | | | | | |

| | | | | | | | | | | | | | | | | | | | |
|---|---|---|---|---|---|---|---|---|---|---|---|---|---|---|---|---|---|---|---|
| 224 | YJL121C | RPE1 | | X | | | | | | | | | | | | | | | |
| 225 | YJL197W | UBP12 | | X | | | | | | | | | | | | | | X | |
| 226 | YJL208C | NUC1 | | X | | | | | | | | | | | | | | | |
| 227 | YJR001W | AVT1 | | X | | | | | | | | | | | | | | | |
| 228 | YJR014W | TMA22 | | X | | | | | X | | | | | | | | | | |
| 229 | YJR025C | BNA1 | | X | | | | | | | | | | | | | | | X |
| 230 | YJR074W | MOG1 | | X | | | | | | | | | | | | | | | X |
| 231 | YKL176C | LST4 | | X | | | | | X | | | | | | | | | | X |
| 232 | YLL026W | HSP104 | | X | | | | X | | | | | | | | | | | |
| 233 | YLR172C | DPH5 | | X | | | | X | | | | | | | | | | | |
| 234 | YLR262C | YPT6 | | X | | | | | X | | | | | | | | | | |
| 235 | YLR376C | PSY3 | | X | | | | | | | | | | | | X | | | |
| 236 | YLR398C | SKI2 | | X | | | | | | | | | | | | X | | | |
| 237 | YLR410W | VIP1 | | X | | | | | X | | | | | | | | | | X |
| 238 | YLR418C | CDC73 | X | X | | | | X | | | | | X | | | X | X | | X |
| 239 | YLR453C | RIF2 | X | X | | X | X | | X | | | | | | | | | | X |
| 240 | YML061C | PIF1 | X | X | | | | | | | | | | | | | | | |
| 241 | YMR039C | SUB1 | | X | | | | | X | | | | | | | | | | |
| 242 | YMR048W | CSM3 | | X | | | | X | | | | | | X | | | | | X |
| 243 | YMR055C | BUB2 | X | X | | | | X | | | | | | | X | | X | | |
| 244 | YMR080C | NAM7 | X | X | | X | | | X | | | X | X | | | | X | | |
| 245 | YMR106C | YKU80 | X | X | | X | | X | | | | X | | | | | | | |
| 246 | YMR190C | SGS1 | X | X | | | | | | | | | X | | | | X | | X |
| 247 | YMR219W | ESC1 | | X | | | | | | | | | | | X | | | | |
| 248 | YMR263W | SAP30 | | X | | | | | | | | | | | | | X | | X |
| 249 | YMR284W | YKU70 | X | X | | X | | X | | | | X | | | | | X | | |
| 250 | YNL068C | FKH2 | X | X | | | | X | | | | | | | | | | | X |
| 251 | YNL106C | INP52 | | X | | | | X | | | | | | | | | | | |
| 252 | YNL241C | ZWF1 | | X | | | | | | | | | | | | | | | |
| 253 | YOR123C | LEO1 | | X | | | | X | | | | | | | X | | X | | |
| 254 | YOR144C | ELG1 | X | X | | | | X | | | X | | X | | | X | X | | X |
| 255 | YOR202W | HIS3 | | X | | | | | | | | | | X | X | | | | |
| 256 | YOR279C | RFM1 | | X | | | | | | | | | X | | | | | X | X |
| 257 | YPL086C | ELP3 | | X | | | | X | | | | | | | | | | | |
| 258 | YPL127C | HHO1 | | X | | | | | | | | | | | | | | X | |
| 259 | YPL172C | COX10 | | X | | | | | | | | | | | | | | | X |
| 260 | YPR069C | SPE3 | | X | | | | | | | | | | | | | | | X |
| 261 | YPR120C | CLB5 | | X | | | | X | | | | | | | X | | | | X |
| 262 | YPR135W | CTF4 | | X | | | | X | | | | | | | | | | | X |
| 263 | YDR080W | VPS41 | | X | | | | | X | | | | | | X | | | | |
| 264 | YBL047C | EDE1 | | X | | | | | X | | | | X | | | | | | X |
| 265 | YCL016C | DCC1 | | X | | | | X | | | | | X | | | | X | | X |
| 266 | YDL101C | DUN1 | X | X | | | | | | | | | | | | | | | X |
| 267 | YDR372C | VPS74 | | X | | | | | | | | | | | | | | | |
| 268 | YER020W | GPA2 | | X | | | | | X | | | | | | | | | | |
| 269 | YGL058W | RAD6 | | X | | | | | | | | | | | X | | | | X |
| 270 | YGL086W | MAD1 | | X | | | | | | | | | | | X | | X | | |
| 271 | YIL008W | URM1 | | X | | | | X | | | | | | | | X | X | | |
| 272 | YIL009C-A | EST3 | X | X | | X | | X | | | | X | | | | | | | X |
| 273 | YIL153W | RRD1 | | X | | | | X | | | | | | | | | X | | |
| 274 | YJR040W | GEF1 | | X | | | | | | | | | | | | | | | X |
| 275 | YKL113C | RAD27 | X | X | | | | | | | | | X | | | | X | | X |
| 276 | YKL139W | CTK1 | | X | | | | | | | | | | | X | | X | | |
| 277 | YKR070W | YKR070W | | X | | | | | | | | | | | | | | | |
| 278 | YLR085C | ARP6 | | X | | | | | | | | | | | | | | X | |
| 279 | YNL153C | GIM3 | | X | | | | X | | | | | | | | | | | X |
| 280 | YPL178W | CBC2 | | X | | | | | | | | | | | | | | | X |
| 281 | YJL115W | ASF1 | | | | | | | | | | | X | | X | | X | | X | X |
| 282 | YLR113W | HOG1 | X | | | | | | | | | | | | X | | | | | |
| 283 | YHR031C | RRM3 | | | | X | | | | | | | | | X | | | | | X |
| 284 | YLR320W | MMS22 | | | | | | | | | | | X | | X | | | | | X |
| 285 | YDL013W | SLX5 | | | | | | | | | | | | | X | | X | | | X |
| 286 | YNL102W | POL1 | X | | | | | | | | X | | | | X | | | | | |
| 287 | YIR008C | PRI1 | X | | | | | | | X | | | | | X | | | | | |
| 288 | YDL102W | POL3 | X | | | | | | | | X | | | | X | | | | | |
| 289 | YAR007C | RPA1 | X | | | | | | | | | | | | X | | | | | |

| | | | | | | | | | | | | | | | | | | | |
|---|---|---|---|---|---|---|---|---|---|---|---|---|---|---|---|---|---|---|---|
| 290 | **YGL175C** | **SAE2** | | | | | | | | | | | | | X | | X | | |
| 291 | **YDL164C** | **CDC9** | | | | | | | | | | | | | X | | | | |
| 292 | **YPL153C** | **RAD53** | X | | | | | | | | | | | | X | | | | |
| 293 | **YBR279W** | **PAF1** | | | | | | | | | | | | | X | | | | X |
| 294 | **YMR075W** | **RCO1** | X | | | | | | | | | | | | | X | X | | |
| 295 | **YNL215W** | **IES2** | X | | | | | | | | | | | | | X | X | | X |
| 296 | **YLR015W** | **BRE2** | | | | | | | | | | | | | | X | X | | X |
| 297 | **YMR179W** | **SPT21** | | | | | | | | | | X | | | | X | X | | X |
| 298 | **YPL055C** | **LGE1** | | | | | | | | | | | | | | X | X | | X |
| 299 | **YOL006C** | **TOP1** | | | | | | | | | | | | | | X | X | | X |
| 300 | **YLR318W** | **EST2** | | | | X | | | | | | X | | | | X | | | |
| 301 | **YDL042C** | **SIR2** | | | | | X | | | | | | | | | | | | X |
| 302 | **YLR442C** | **SIR3** | | | | | X | | | | | | | | | | | | |
| 303 | **YDR227W** | **SIR4** | | | | | X | | | | | | | | | | | | |
| 304 | **YLR010C** | **TEN1** | | | | | X | | | | X | | | | | | | | |
| 305 | **YNL216W** | **RAP1** | | | | | X | | | | X | | | | | | | | |
| 306 | **YDL220C** | **CDC13** | | | | | X | | | X | | | | | | | | | |
| 307 | **YDR082W** | **STN1** | | | | | X | | | X | | | | | | | | | |
| 308 | **YGR099W** | **TEL2** | | | | | X | | | | | | | | | | | | |
| 1 | YKL109W | **HAP4** | | | | | | | | | | | | | | | | | |
| 2 | YLR021W | **IRC25** | | | | | | | | | | | | | | | | | |
| 3 | YDL091C | **UBX3** | | | | | | | | | | | | | | | | | |
| 4 | YPL100W | **ATG21** | | | | | | | | | | | | | | | | | |
| 5 | YPR191W | **QCR2** | | | | | | | | | | | | | | | | | |
| 6 | YBR258C | **SHG1** | | | | | | | | | | | | | | | | | |
| 7 | YJL214W | **HXT8** | | | | | | | | | | | | | | | | | |
| 8 | YIL156W | **UBP7** | | | | | | | | | | | | | | | | | |
| 9 | YNL253W | **TEX1** | | | | | | | | | | | | | | | | | |
| 10 | YGR192C | **TDH3** | | | | | | | | | | | | | | | | | |
| 11 | YOR384W | **FRE5** | | | | | | | | | | | | | | | | | |
| 12 | YOL067C | **RTG1** | | | | | | | | | | | | | | | | | |
| 13 | YDR520C | **URC2** | | | | | | | | | | | | | | | | | |
| 14 | YLR136C | **TIS11** | | | | | | | | | | | | | | | | | |
| 15 | YKL205W | **LOS1** | | | | | | | | | | | | | | | | | |
| 16 | YJL157C | **FAR1** | | | | | | | | | | | | | | | | | |
| 17 | YNL292W | **PUS4** | | | | | | | | | | | | | | | | | |
| 18 | YOR344C | **TYE7** | | | | | | | | | | | | | | | | | |
| 19 | YLR436C | **ECM30** | | | | | | | | | | | | | | | | | |
| 20 | YLR338W | **OPI9** | | | | | | | | | | | | | | | | | |
| 21 | YOR315W | **SFG1** | | | | | | | | | | | | | | | | | |
| 22 | YOR193W | **PEX27** | | | | | | | | | | | | | | | | | |
| 23 | YOR327C | **SNC2** | | | | | | | | | | | | | | | | | |
| 24 | YML016C | **PPZ1** | | | | | | | | | | | | | | | | | |
| 25 | YOR140W | **SFL1** | | | | | | | | | | | | | | | | | |
| 26 | YNR006W | **VPS27** | | | | | | | | | | | | | | | | | |
| 27 | YDR293C | **SSD1** | | | | | | | | | | | | | | | | | |
| 28 | YLR176C | **RFX1** | | | | | | | | | | | | | | | | | |

# References


ABBOTT, A. 2015. Researchers pin down risks of low-dose radiation. *Nature,* 523**,** 17-8.

ADDINALL, S. G., DOWNEY, M., YU, M., ZUBKO, M. K., DEWAR, J., LEAKE, A., HALLINAN, J., SHAW, O., JAMES, K., WILKINSON, D. J., WIPAT, A., DUROCHER, D. & LYDALL, D. 2008. A genomewide suppressor and enhancer analysis of cdc13-1 reveals varied cellular processes influencing telomere capping in Saccharomyces cerevisiae. *Genetics,* 180**,** 2251-66.

ADDINALL, S. G., HOLSTEIN, E. M., LAWLESS, C., YU, M., CHAPMAN, K., BANKS, A. P., NGO, H. P., MARINGELE, L., TASCHUK, M., YOUNG, A., CIESIOLKA, A., LISTER, A. L., WIPAT, A., WILKINSON, D. J. & LYDALL, D. 2011. Quantitative fitness analysis shows that NMD proteins and many other protein complexes suppress or enhance distinct telomere cap defects. *PLoS Genet,* 7**,** e1001362.

AHMAD, M. & BUSSEY, H. 1986. Yeast arginine permease: nucleotide sequence of the CAN1 gene. *Curr Genet,* 10**,** 587-92.

ALLSOPP, R. C., CHANG, E., KASHEFI-AAZAM, M., ROGAEV, E. I., PIATYSZEK, M. A., SHAY, J. W. & HARLEY, C. B. 1995. Telomere shortening is associated with cell division in vitro and in vivo. *Exp Cell Res,* 220**,** 194-200.

ALVARO, D., LISBY, M. & ROTHSTEIN, R. 2007. Genome-wide analysis of Rad52 foci reveals diverse mechanisms impacting recombination. *PLoS Genet,* 3**,** e228.

ANBALAGAN, S., BONETTI, D., LUCCHINI, G. & LONGHESE, M. P. 2011. Rif1 supports the function of the CST complex in yeast telomere capping. *PLoS Genet,* 7**,** e1002024.

ASKREE, S. H., YEHUDA, T., SMOLIKOV, S., GUREVICH, R., HAWK, J., COKER, C., KRAUSKOPF, A., KUPIEC, M. & MCEACHERN, M. J. 2004. A genome-wide screen for Saccharomyces cerevisiae deletion mutants that affect telomere length. *Proc Natl Acad Sci U S A,* 101**,** 8658-63.

AYYAGARI, R., GOMES, X. V., GORDENIN, D. A. & BURGERS, P. M. 2003. Okazaki fragment maturation in yeast. I. Distribution of functions between FEN1 AND DNA2. *J Biol Chem,* 278**,** 1618-25.

BAE, K. H., KIM, H. S., BAE, S. H., KANG, H. Y., BRILL, S. & SEO, Y. S. 2003. Bimodal interaction between replication-protein A and Dna2 is critical for Dna2 function both in vivo and in vitro. *Nucleic Acids Res,* 31**,** 3006-15.

BAE, S. H., BAE, K. H., KIM, J. A. & SEO, Y. S. 2001a. RPA governs endonuclease switching during processing of Okazaki fragments in eukaryotes. *Nature,* 412**,** 456-61.

BAE, S. H., KIM, J. A., CHOI, E., LEE, K. H., KANG, H. Y., KIM, H. D., KIM, J. H., BAE, K. H., CHO, Y., PARK, C. & SEO, Y. S. 2001b. Tripartite structure of

Saccharomyces cerevisiae Dna2 helicase/endonuclease. *Nucleic Acids Res,* 29**,** 3069-79.

BAE, S. H. & SEO, Y. S. 2000. Characterization of the enzymatic properties of the yeast dna2 Helicase/endonuclease suggests a new model for Okazaki fragment processing. *J Biol Chem,* 275**,** 38022-31.

BALESTRINI, A., RISTIC, D., DIONNE, I., LIU, X. Z., WYMAN, C., WELLINGER, R. J. & PETRINI, J. H. 2013. The Ku heterodimer and the metabolism of single-ended DNA double-strand breaks. *Cell Rep,* 3**,** 2033-45.

BAMBARA, R. A., MURANTE, R. S. & HENRICKSEN, L. A. 1997. Enzymes and reactions at the eukaryotic DNA replication fork. *J Biol Chem,* 272**,** 4647-50.

BANDARIA, J. N., QIN, P., BERK, V., CHU, S. & YILDIZ, A. 2016. Shelterin Protects Chromosome Ends by Compacting Telomeric Chromatin. *Cell,* 164**,** 735-46.

BARDIN, A. J., BOSELLI, M. G. & AMON, A. 2003. Mitotic exit regulation through distinct domains within the protein kinase Cdc15. *Mol Cell Biol,* 23**,** 5018-30.

BELL, S. P. & LABIB, K. 2016. Chromosome Duplication in Saccharomyces cerevisiae. *Genetics,* 203**,** 1027-67.

BENNETT, R. J., FORCHE, A. & BERMAN, J. 2014. Rapid mechanisms for generating genome diversity: whole ploidy shifts, aneuploidy, and loss of heterozygosity. *Cold Spring Harb Perspect Med,* 4.

BERRY, D. B. & GASCH, A. P. 2008. Stress-activated genomic expression changes serve a preparative role for impending stress in yeast. *Mol Biol Cell,* 19**,** 4580-7.

BERRY, D. B., GUAN, Q., HOSE, J., HAROON, S., GEBBIA, M., HEISLER, L. E., NISLOW, C., GIAEVER, G. & GASCH, A. P. 2011. Multiple means to the same end: the genetic basis of acquired stress resistance in yeast. *PLoS Genet,* 7**,** e1002353.

BHATIA-DEY, N., KANHERKAR, R. R., STAIR, S. E., MAKAREV, E. O. & CSOKA, A. B. 2016. Cellular Senescence as the Causal Nexus of Aging. *Front Genet,* 7**,** 13.

BIANCHI, A. & SHORE, D. 2008. How telomerase reaches its end: mechanism of telomerase regulation by the telomeric complex. *Mol Cell,* 31**,** 153-65.

BINZ, S. K., SHEEHAN, A. M. & WOLD, M. S. 2004. Replication protein A phosphorylation and the cellular response to DNA damage. *DNA Repair (Amst),* 3**,** 1015-24.

BLASCO, M. A. 2007. The epigenetic regulation of mammalian telomeres. *Nat Rev Genet,* 8**,** 299-309.

BLASTYAK, A., PINTER, L., UNK, I., PRAKASH, L., PRAKASH, S. & HARACSKA, L. 2007. Yeast Rad5 protein required for postreplication repair has a DNA helicase activity specific for replication fork regression. *Mol Cell,* 28**,** 167-75.

BLOW, J. J. & LASKEY, R. A. 1988. A role for the nuclear envelope in controlling DNA replication within the cell cycle. *Nature,* 332**,** 546-8.

BOITEUX, S. & JINKS-ROBERTSON, S. 2013. DNA repair mechanisms and the bypass of DNA damage in Saccharomyces cerevisiae. *Genetics,* 193**,** 1025-64.

BOOS, D., SANCHEZ-PULIDO, L., RAPPAS, M., PEARL, L. H., OLIVER, A. W., PONTING, C. P. & DIFFLEY, J. F. 2011. Regulation of DNA replication through Sld3-Dpb11 interaction is conserved from yeast to humans. *Curr Biol,* 21**,** 1152-7.

BOTSTEIN, D. & FINK, G. R. 2011. Yeast: an experimental organism for 21st Century biology. *Genetics,* 189**,** 695-704.

BOULTON, S. J. & JACKSON, S. P. 1996. Identification of a Saccharomyces cerevisiae Ku80 homologue: roles in DNA double strand break rejoining and in telomeric maintenance. *Nucleic Acids Res,* 24**,** 4639-48.

BRODERICK, R., NIEMINUSZCZY, J., BLACKFORD, A. N., WINCZURA, A. & NIEDZWIEDZ, W. 2015. TOPBP1 recruits TOP2A to ultra-fine anaphase bridges to aid in their resolution. *Nat Commun,* 6**,** 6572.

BROOKS, M. & DUMAS, L. B. 1989. DNA primase isolated from the yeast DNA primase-DNA polymerase complex. Immunoaffinity purification and analysis of RNA primer synthesis. *J Biol Chem,* 264**,** 3602-10.

BUDD, M. E., ANTOSHECHKIN, I. A., REIS, C., WOLD, B. J. & CAMPBELL, J. L. 2011. Inviability of a DNA2 deletion mutant is due to the DNA damage checkpoint. *Cell Cycle,* 10**,** 1690-8.

BUDD, M. E. & CAMPBELL, J. L. 2000. The pattern of sensitivity of yeast dna2 mutants to DNA damaging agents suggests a role in DSB and postreplication repair pathways. *Mutat Res,* 459**,** 173-86.

BUDD, M. E., CHOE, W. C. & CAMPBELL, J. L. 1995. DNA2 encodes a DNA helicase essential for replication of eukaryotic chromosomes. *J Biol Chem,* 270**,** 26766-9.

BUDD, M. E., REIS, C. C., SMITH, S., MYUNG, K. & CAMPBELL, J. L. 2006. Evidence suggesting that Pif1 helicase functions in DNA replication with the Dna2 helicase/nuclease and DNA polymerase delta. *Mol Cell Biol,* 26**,** 2490-500.

BUDD, M. E., TONG, A. H., POLACZEK, P., PENG, X., BOONE, C. & CAMPBELL, J. L. 2005. A network of multi-tasking proteins at the DNA replication fork preserves genome stability. *PLoS Genet,* 1**,** e61.

BUFFENSTEIN, R., EDREY, Y. H., YANG, T. & MELE, J. 2008. The oxidative stress theory of aging: embattled or invincible? Insights from non-traditional model organisms. *Age (Dordr),* 30**,** 99-109.

BURGERS, P. M. 2009. Polymerase dynamics at the eukaryotic DNA replication fork. *J Biol Chem,* 284**,** 4041-5.

CAL-BAKOWSKA, M., LITWIN, I., BOCER, T., WYSOCKI, R. & DZIADKOWIEC, D. 2011. The Swi2-Snf2-like protein Uls1 is involved in replication stress response. *Nucleic Acids Res,* 39**,** 8765-77.

CALABRESE, E. 2010. Hormesis: Once Marginalized, Evidence Now Supports Hormesis as the Most Fundamental Dose Response. *In:* MATTSON, M. P., CALABRESE, E. J. (ed.) *Hormesis: A Revolution in Biology, Toxicology and Medicine.* New York: Humana Press.

CALABRESE, E. J. 2004. Hormesis: a revolution in toxicology, risk assessment and medicine. *EMBO Rep,* 5 Spec No**,** S37-40.

CALABRESE, E. J., BACHMANN, K. A., BAILER, A. J., BOLGER, P. M., BORAK, J., CAI, L., CEDERGREEN, N., CHERIAN, M. G., CHIUEH, C. C., CLARKSON, T. W., COOK, R. R., DIAMOND, D. M., DOOLITTLE, D. J., DORATO, M. A., DUKE, S. O., FEINENDEGEN, L., GARDNER, D. E., HART, R. W., HASTINGS, K. L., HAYES, A. W., HOFFMANN, G. R., IVES, J. A., JAWOROWSKI, Z., JOHNSON, T. E., JONAS, W. B., KAMINSKI, N. E., KELLER, J. G., KLAUNIG, J. E., KNUDSEN, T. B., KOZUMBO, W. J., LETTIERI, T., LIU, S. Z., MAISSEU, A., MAYNARD, K. I., MASORO, E. J., MCCLELLAN, R. O., MEHENDALE, H. M., MOTHERSILL, C., NEWLIN, D. B., NIGG, H. N., OEHME, F. W., PHALEN, R. F., PHILBERT, M. A., RATTAN, S. I., RIVIERE, J. E., RODRICKS, J., SAPOLSKY, R. M., SCOTT, B. R., SEYMOUR, C., SINCLAIR, D. A., SMITH-SONNEBORN, J., SNOW, E. T., SPEAR, L., STEVENSON, D. E., THOMAS, Y., TUBIANA, M., WILLIAMS, G. M. & MATTSON, M. P. 2007. Biological stress response terminology: Integrating the concepts of adaptive response and preconditioning stress within a hormetic dose-response framework. *Toxicol Appl Pharmacol,* 222**,** 122-8.

CALABRESE, E. J. & BALDWIN, L. A. 2003. Hormesis: the dose-response revolution. *Annu Rev Pharmacol Toxicol,* 43**,** 175-97.

CALABRESE, E. J., SHAMOUN, D. Y. & HANEKAMP, J. C. 2015. Cancer risk assessment: Optimizing human health through linear dose-response models. *Food Chem Toxicol,* 81**,** 137-40.

CANNAVO, E. & CEJKA, P. 2014. Sae2 promotes dsDNA endonuclease activity within Mre11-Rad50-Xrs2 to resect DNA breaks. *Nature,* 514**,** 122-5.

CARLILE, C. M., PICKART, C. M., MATUNIS, M. J. & COHEN, R. E. 2009. Synthesis of free and proliferating cell nuclear antigen-bound polyubiquitin chains by the RING E3 ubiquitin ligase Rad5. *J Biol Chem,* 284**,** 29326-34.

CARNEIRO, M. C., HENRIQUES, C. M., NABAIS, J., FERREIRA, T., CARVALHO, T. & FERREIRA, M. G. 2016. Short Telomeres in Key Tissues Initiate Local and Systemic Aging in Zebrafish. *PLoS Genet,* 12**,** e1005798.

CESARE, A. J. & REDDEL, R. R. 2010. Alternative lengthening of telomeres: models, mechanisms and implications. *Nat Rev Genet,* 11**,** 319-30.

CHAI, W., ZHENG, L. & SHEN, B. 2013. DNA2, a new player in telomere maintenance and tumor suppression. *Cell Cycle,* 12**,** 1985-6.

CHANDRA, A., HUGHES, T. R., NUGENT, C. I. & LUNDBLAD, V. 2001. Cdc13 both positively and negatively regulates telomere replication. *Genes Dev,* 15**,** 404-14.

CHANG, D. J. & CIMPRICH, K. A. 2009. DNA damage tolerance: when it's OK to make mistakes. *Nat Chem Biol,* 5**,** 82-90.

CHASMAN, D., HO, Y. H., BERRY, D. B., NEMEC, C. M., MACGILVRAY, M. E., HOSE, J., MERRILL, A. E., LEE, M. V., WILL, J. L., COON, J. J., ANSARI, A. Z., CRAVEN, M. & GASCH, A. P. 2014. Pathway connectivity and signaling coordination in the yeast stress-activated signaling network. *Mol Syst Biol,* 10**,** 759.

CHEN, L. Y. & LINGNER, J. 2013. CST for the grand finale of telomere replication. *Nucleus,* 4**,** 277-82.

CHENG, X., DUNAWAY, S. & IVESSA, A. S. 2007. The role of Pif1p, a DNA helicase in Saccharomyces cerevisiae, in maintaining mitochondrial DNA. *Mitochondrion,* 7**,** 211-22.

CHI, P., KWON, Y., VISNAPUU, M. L., LAM, I., SANTA MARIA, S. R., ZHENG, X., EPSHTEIN, A., GREENE, E. C., SUNG, P. & KLEIN, H. L. 2011. Analyses of the yeast Rad51 recombinase A265V mutant reveal different in vivo roles of Swi2-like factors. *Nucleic Acids Res,* 39**,** 6511-22.

CHOE, W., BUDD, M., IMAMURA, O., HOOPES, L. & CAMPBELL, J. L. 2002. Dynamic localization of an Okazaki fragment processing protein suggests a novel role in telomere replication. *Mol Cell Biol,* 22**,** 4202-17.

CHOI, K. M., KWON, Y. Y. & LEE, C. K. 2013. Characterization of global gene expression during assurance of lifespan extension by caloric restriction in budding yeast. *Exp Gerontol,* 48**,** 1455-68.

CHRISTMANN, M. & KAINA, B. 2013. Transcriptional regulation of human DNA repair genes following genotoxic stress: trigger mechanisms, inducible responses and genotoxic adaptation. *Nucleic Acids Res,* 41**,** 8403-20.

CHURIKOV, D., CORDA, Y., LUCIANO, P. & GELI, V. 2013. Cdc13 at a crossroads of telomerase action. *Front Oncol,* 3**,** 39.

CLERICI, M., MANTIERO, D., GUERINI, I., LUCCHINI, G. & LONGHESE, M. P. 2008. The Yku70-Yku80 complex contributes to regulate double-strand break processing and checkpoint activation during the cell cycle. *EMBO Rep,* 9**,** 810-8.

CONCONI, A., PAQUETTE, M., FAHY, D., BESPALOV, V. A. & SMERDON, M. J. 2005. Repair-independent chromatin assembly onto active ribosomal genes in yeast after UV irradiation. *Mol Cell Biol,* 25**,** 9773-83.

COPE, C. L., GILLEY, R., BALMANNO, K., SALE, M. J., HOWARTH, K. D., HAMPSON, M., SMITH, P. D., GUICHARD, S. M. & COOK, S. J. 2014. Adaptation to mTOR kinase inhibitors by amplification of eIF4E to maintain cap-dependent translation. *J Cell Sci,* 127**,** 788-800.

COPPE, J. P., DESPREZ, P. Y., KRTOLICA, A. & CAMPISI, J. 2010. The senescence-associated secretory phenotype: the dark side of tumor suppression. *Annu Rev Pathol,* 5**,** 99-118.

COSGROVE, A. J., NIEDUSZYNSKI, C. A. & DONALDSON, A. D. 2002. Ku complex controls the replication time of DNA in telomere regions. *Genes Dev,* 16**,** 2485-90.

COSTANTINI, D., METCALFE, N. B. & MONAGHAN, P. 2010. Ecological processes in a hormetic framework. *Ecol Lett,* 13**,** 1435-47.

COSTANTINI, D., MONAGHAN, P. & METCALFE, N. B. 2014. Prior hormetic priming is costly under environmental mismatch. *Biol Lett,* 10**,** 20131010.

D'ADDA DI FAGAGNA, F., REAPER, P. M., CLAY-FARRACE, L., FIEGLER, H., CARR, P., VON ZGLINICKI, T., SARETZKI, G., CARTER, N. P. & JACKSON, S. P. 2003. A DNA damage checkpoint response in telomere-initiated senescence. *Nature,* 426**,** 194-8.

D'AMOURS, D. & JACKSON, S. P. 2002. The Mre11 complex: at the crossroads of dna repair and checkpoint signalling. *Nat Rev Mol Cell Biol,* 3**,** 317-27.

DALEY, J. M., PALMBOS, P. L., WU, D. & WILSON, T. E. 2005. Nonhomologous end joining in yeast. *Annu Rev Genet,* 39**,** 431-51.

DAVIES, A. A., NEISS, A. & ULRICH, H. D. 2010. Ubiquitylation of the 9-1-1 checkpoint clamp is independent of rad6-rad18 and DNA damage. *Cell,* 141**,** 1080-7.

DE LANGE, T. 2009. How telomeres solve the end-protection problem. *Science,* 326**,** 948-52.

DE MAGALHAES, J. P. 2004. From cells to ageing: a review of models and mechanisms of cellular senescence and their impact on human ageing. *Exp Cell Res,* 300**,** 1-10.

DE NADAL, E., AMMERER, G. & POSAS, F. 2011. Controlling gene expression in response to stress. *Nat Rev Genet,* 12**,** 833-45.

DEWAR, J. M. & LYDALL, D. 2010a. Pif1- and Exo1-dependent nucleases coordinate checkpoint activation following telomere uncapping. *EMBO J,* 29**,** 4020-34.

DEWAR, J. M. & LYDALL, D. 2010b. Pif1- and Exo1-dependent nucleases coordinate checkpoint activation following telomere uncapping. *Embo Journal,* 29**,** 4020-4034.

DEWAR, J. M. & LYDALL, D. 2012a. Similarities and differences between "uncapped" telomeres and DNA double-strand breaks. *Chromosoma,* 121**,** 117-30.

DEWAR, J. M. & LYDALL, D. 2012b. Simple, non-radioactive measurement of single-stranded DNA at telomeric, sub-telomeric, and genomic loci in budding yeast. *Methods Mol Biol,* 920**,** 341-8.

DI DOMENICO, E. G., AURICHE, C., VISCARDI, V., LONGHESE, M. P., GILSON, E. & ASCENZIONI, F. 2009. The Mec1p and Tel1p checkpoint kinases allow humanized yeast to tolerate chronic telomere dysfunctions by suppressing telomere fusions. *DNA Repair (Amst),* 8**,** 209-18.

DOUGLAS, H. 2008. Science, hormesis and regulation. *Hum Exp Toxicol,* 27**,** 603-7.

DUBARRY, M., LAWLESS, C., BANKS, A. P., COCKELL, S. & LYDALL, D. 2015. Genetic Networks Required to Coordinate Chromosome Replication by DNA Polymerases alpha, delta, and epsilon in Saccharomyces cerevisiae. *G3 (Bethesda),* 5**,** 2187-97.

DURAN, A. L., POTTER, P., WELLS, S., KIRKWOOD, T., VON ZGLINICKI, T., MCARDLE, A., SCUDAMORE, C., MENG, Q. J., DE HAAN, G., CORCORAN, A. & BELLANTUONO, I. 2013. Shared Ageing Research Models (ShARM): a new facility to support ageing research. *Biogerontology,* 14**,** 789-94.

DUXIN, J. P., DAO, B., MARTINSSON, P., RAJALA, N., GUITTAT, L., CAMPBELL, J. L., SPELBRINK, J. N. & STEWART, S. A. 2009. Human Dna2 is a nuclear and mitochondrial DNA maintenance protein. *Mol Cell Biol, 2*9**,** 4274-82.

ECKERT-BOULET, N. & LISBY, M. 2010. Regulation of homologous recombination at telomeres in budding yeast. *FEBS Lett,* 584**,** 3696-702.

ELFVING, N., CHEREJI, R. V., BHARATULA, V., BJORKLUND, S., MOROZOV, A. V. & BROACH, J. R. 2014. A dynamic interplay of nucleosome and Msn2 binding regulates kinetics of gene activation and repression following stress. *Nucleic Acids Res,* 42**,** 5468-82.

ELLISON, V. & STILLMAN, B. 2003. Biochemical characterization of DNA damage checkpoint complexes: clamp loader and clamp complexes with specificity for 5' recessed DNA. *PLoS Biol,* 1**,** E33.

ERIKSSON, P. R., GANGULI, D., NAGARAJAVEL, V. & CLARK, D. J. 2012. Regulation of histone gene expression in budding yeast. *Genetics,* 191**,** 7-20.

ERMOLAEVA, M. A., SEGREF, A., DAKHOVNIK, A., OU, H. L., SCHNEIDER, J. I., UTERMOHLEN, O., HOPPE, T. & SCHUMACHER, B. 2013. DNA damage in germ cells induces an innate immune response that triggers systemic stress resistance. *Nature,* 501**,** 416-20.

FALCK, J., COATES, J. & JACKSON, S. P. 2005. Conserved modes of recruitment of ATM, ATR and DNA-PKcs to sites of DNA damage. *Nature,* 434**,** 605-11.

FELDMANN, H. & WINNACKER, E. L. 1993. A putative homologue of the human autoantigen Ku from Saccharomyces cerevisiae. *J Biol Chem,* 268**,** 12895-900.

FELL, V. L. & SCHILD-POULTER, C. 2015. The Ku heterodimer: function in DNA repair and beyond. *Mutat Res Rev Mutat Res,* 763**,** 15-29.

FINN, K., LOWNDES, N. F. & GRENON, M. 2012. Eukaryotic DNA damage checkpoint activation in response to double-strand breaks. *Cell Mol Life Sci,* 69**,** 1447-73.

FOIANI, M., LUCCHINI, G. & PLEVANI, P. 1997. The DNA polymerase alpha-primase complex couples DNA replication, cell-cycle progression and DNA-damage response. *Trends Biochem Sci,* 22**,** 424-7.

FOSTER, S. S., ZUBKO, M. K., GUILLARD, S. & LYDALL, D. 2006. MRX protects telomeric DNA at uncapped telomeres of budding yeast cdc13-1 mutants. *DNA Repair (Amst),* 5**,** 840-51.

FOURY, F. & LAHAYE, A. 1987. Cloning and sequencing of the PIF gene involved in repair and recombination of yeast mitochondrial DNA. *EMBO J,* 6**,** 1441-9.

FUKUNAGA, K., KWON, Y., SUNG, P. & SUGIMOTO, K. 2011. Activation of protein kinase Tel1 through recognition of protein-bound DNA ends. *Mol Cell Biol,* 31**,** 1959-71.

FULDA, S., GORMAN, A. M., HORI, O. & SAMALI, A. 2010. Cellular stress responses: cell survival and cell death. *Int J Cell Biol,* 2010**,** 214074.

FUMAGALLI, M., ROSSIELLO, F., CLERICI, M., BAROZZI, S., CITTARO, D., KAPLUNOV, J. M., BUCCI, G., DOBREVA, M., MATTI, V., BEAUSEJOUR, C. M., HERBIG, U., LONGHESE, M. P. & D'ADDA DI FAGAGNA, F. 2012. Telomeric DNA damage is irreparable and causes persistent DNA-damage-response activation. *Nat Cell Biol,* 14**,** 355-65.

GALANTY, Y., BELOTSERKOVSKAYA, R., COATES, J. & JACKSON, S. P. 2012. RNF4, a SUMO-targeted ubiquitin E3 ligase, promotes DNA double-strand break repair. *Genes Dev,* 26**,** 1179-95.

GARDNER, R., PUTNAM, C. W. & WEINERT, T. 1999. RAD53, DUN1 and PDS1 define two parallel G2/M checkpoint pathways in budding yeast. *EMBO J,* 18**,** 3173-85.

GARDNER, R. G., NELSON, Z. W. & GOTTSCHLING, D. E. 2005. Degradation-mediated protein quality control in the nucleus. *Cell,* 120**,** 803-15.

GARG, M., GURUNG, R. L., MANSOUBI, S., AHMED, J. O., DAVE, A., WATTS, F. Z. & BIANCHI, A. 2014. Tpz1TPP1 SUMOylation reveals evolutionary conservation of SUMO-dependent Stn1 telomere association. *EMBO Rep,* 15**,** 871-7.

GARVIK, B., CARSON, M. & HARTWELL, L. 1995. Single-stranded DNA arising at telomeres in cdc13 mutants may constitute a specific signal for the RAD9 checkpoint. *Mol Cell Biol,* 15**,** 6128-38.

GASCH, A. P. 2002. The Environmental Stress Response: a common yeast response to environmental stresses. *In:* HOHMANN, S. & MAGER, P. (eds.) *Yeast Stress Responses.* Topics in Current Genetics, Springer-Verlag Heidelberg.

GASCH, A. P. 2007. Comparative genomics of the environmental stress response in ascomycete fungi. *Yeast,* 24**,** 961-76.

GASCH, A. P., SPELLMAN, P. T., KAO, C. M., CARMEL-HAREL, O., EISEN, M. B., STORZ, G., BOTSTEIN, D. & BROWN, P. O. 2000. Genomic expression

programs in the response of yeast cells to environmental changes. *Mol Biol Cell,* 11**,** 4241-57.

GATBONTON, T., IMBESI, M., NELSON, M., AKEY, J. M., RUDERFER, D. M., KRUGLYAK, L., SIMON, J. A. & BEDALOV, A. 2006. Telomere length as a quantitative trait: genome-wide survey and genetic mapping of telomere length-control genes in yeast. *PLoS Genet,* 2**,** e35.

GEORGESCU, R. E., LANGSTON, L., YAO, N. Y., YURIEVA, O., ZHANG, D., FINKELSTEIN, J., AGARWAL, T. & O'DONNELL, M. E. 2014. Mechanism of asymmetric polymerase assembly at the eukaryotic replication fork. *Nat Struct Mol Biol,* 21**,** 664-70.

GHOSAL, G. & MUNIYAPPA, K. 2005. Saccharomyces cerevisiae Mre11 is a high-affinity G4 DNA-binding protein and a G-rich DNA-specific endonuclease: implications for replication of telomeric DNA. *Nucleic Acids Res,* 33**,** 4692-703.

GIBSON, D. G., YOUNG, L., CHUANG, R. Y., VENTER, J. C., HUTCHISON, C. A., 3RD & SMITH, H. O. 2009. Enzymatic assembly of DNA molecules up to several hundred kilobases. *Nat Methods,* 6**,** 343-5.

GILBERT, C. S., GREEN, C. M. & LOWNDES, N. F. 2001. Budding yeast Rad9 is an ATP-dependent Rad53 activating machine. *Mol Cell,* 8**,** 129-36.

GILSON, E., ROBERGE, M., GIRALDO, R., RHODES, D. & GASSER, S. M. 1993. Distortion of the DNA double helix by RAP1 at silencers and multiple telomeric binding sites. *J Mol Biol,* 231**,** 293-310.

GOFFEAU, A., BARRELL, B. G., BUSSEY, H., DAVIS, R. W., DUJON, B., FELDMANN, H., GALIBERT, F., HOHEISEL, J. D., JACQ, C., JOHNSTON, M., LOUIS, E. J., MEWES, H. W., MURAKAMI, Y., PHILIPPSEN, P., TETTELIN, H. & OLIVER, S. G. 1996. Life with 6000 genes. *Science,* 274**,** 546, 563-7.

GRANDIN, N., DAMON, C. & CHARBONNEAU, M. 2001. Ten1 functions in telomere end protection and length regulation in association with Stn1 and Cdc13. *EMBO J,* 20**,** 1173-83.

GRANDIN, N., REED, S. I. & CHARBONNEAU, M. 1997. Stn1, a new Saccharomyces cerevisiae protein, is implicated in telomere size regulation in association with Cdc13. *Genes Dev,* 11**,** 512-27.

GREEN, C. M., ERDJUMENT-BROMAGE, H., TEMPST, P. & LOWNDES, N. F. 2000. A novel Rad24 checkpoint protein complex closely related to replication factor C. *Curr Biol,* 10**,** 39-42.

GREENALL, A., LEI, G., SWAN, D. C., JAMES, K., WANG, L., PETERS, H., WIPAT, A., WILKINSON, D. J. & LYDALL, D. 2008. A genome wide analysis of the response to uncapped telomeres in budding yeast reveals a novel role for the NAD+ biosynthetic gene BNA2 in chromosome end protection. *Genome Biol,* 9**,** R146.

GREIDER, C. W. 1996. Telomere length regulation. *Annu Rev Biochem,* 65**,** 337-65.

GREIDER, C. W. & BLACKBURN, E. H. 1985. Identification of a specific telomere terminal transferase activity in Tetrahymena extracts. *Cell,* 43**,** 405-13.

GUAN, Q., HAROON, S., BRAVO, D. G., WILL, J. L. & GASCH, A. P. 2012. Cellular memory of acquired stress resistance in Saccharomyces cerevisiae. *Genetics,* 192**,** 495-505.

GUIROUILH-BARBAT, J., LAMBERT, S., BERTRAND, P. & LOPEZ, B. S. 2014. Is homologous recombination really an error-free process? *Front Genet,* 5**,** 175.

HAENDELER, J., TISCHLER, V., HOFFMANN, J., ZEIHER, A. M. & DIMMELER, S. 2004. Low doses of reactive oxygen species protect endothelial cells from apoptosis by increasing thioredoxin-1 expression. *FEBS Lett,* 577**,** 427-33.

HAHN, A., KILIAN, J., MOHRHOLZ, A., LADWIG, F., PESCHKE, F., DAUTEL, R., HARTER, K., BERENDZEN, K. W. & WANKE, D. 2013. Plant core environmental stress response genes are systemically coordinated during abiotic stresses. *Int J Mol Sci,* 14**,** 7617-41.

HAN, J., ZHOU, H., HORAZDOVSKY, B., ZHANG, K., XU, R. M. & ZHANG, Z. 2007. Rtt109 acetylates histone H3 lysine 56 and functions in DNA replication. *Science,* 315**,** 653-5.

HANG, L. E., LIU, X., CHEUNG, I., YANG, Y. & ZHAO, X. 2011. SUMOylation regulates telomere length homeostasis by targeting Cdc13. *Nat Struct Mol Biol,* 18**,** 920-6.

HARLEY, C. B., FUTCHER, A. B. & GREIDER, C. W. 1990. Telomeres shorten during ageing of human fibroblasts. *Nature,* 345**,** 458-60.

HARPER, J. W. & ELLEDGE, S. J. 2007. The DNA damage response: ten years after. *Mol Cell,* 28**,** 739-45.

HARRINGTON, J. J. & LIEBER, M. R. 1995. DNA structural elements required for FEN-1 binding. *J Biol Chem,* 270**,** 4503-8.

HARTWELL, L. H. 2002. Nobel Lecture. Yeast and cancer. *Biosci Rep,* 22**,** 373-94.

HARTWELL, L. H., MORTIMER, R. K., CULOTTI, J. & CULOTTI, M. 1973. Genetic Control of the Cell Division Cycle in Yeast: V. Genetic Analysis of cdc Mutants. *Genetics,* 74**,** 267-86.

HASS, E. P. & ZAPPULLA, D. C. 2015. The Ku subunit of telomerase binds Sir4 to recruit telomerase to lengthen telomeres in S. cerevisiae. *Elife,* 4.

HAYFLICK, L. 1998. The clock of ages: Why we age, how we age, winding back the clock. *Gerontologist,* 38**,** 504-508.

HIRAGA, S., ALVINO, G. M., CHANG, F., LIAN, H. Y., SRIDHAR, A., KUBOTA, T., BREWER, B. J., WEINREICH, M., RAGHURAMAN, M. K. & DONALDSON, A. D. 2014. Rif1 controls DNA replication by directing Protein Phosphatase 1 to reverse Cdc7-mediated phosphorylation of the MCM complex. *Genes Dev,* 28**,** 372-83.

HOFFMAN, E. A., MCCULLEY, A., HAARER, B., ARNAK, R. & FENG, W. 2015. Break-seq reveals hydroxyurea-induced chromosome fragility as a result of unscheduled conflict between DNA replication and transcription. *Genome Res,* 25**,** 402-12.

HOLSTEIN, E. M., CLARK, K. R. & LYDALL, D. 2014. Interplay between nonsense-mediated mRNA decay and DNA damage response pathways reveals that Stn1 and Ten1 are the key CST telomere-cap components. *Cell Rep,* 7**,** 1259-69.

HONG, E. J. & ROEDER, G. S. 2002. A role for Ddc1 in signaling meiotic double-strand breaks at the pachytene checkpoint. *Genes Dev,* 16**,** 363-76.

HU, J., SUN, L., SHEN, F., CHEN, Y., HUA, Y., LIU, Y., ZHANG, M., HU, Y., WANG, Q., XU, W., SUN, F., JI, J., MURRAY, J. M., CARR, A. M. & KONG, D. 2012. The intra-S phase checkpoint targets Dna2 to prevent stalled replication forks from reversing. *Cell,* 149**,** 1221-32.

HUGHES, T. R., WEILBAECHER, R. G., WALTERSCHEID, M. & LUNDBLAD, V. 2000. Identification of the single-strand telomeric DNA binding domain of the Saccharomyces cerevisiae Cdc13 protein. *Proc Natl Acad Sci U S A,* 97**,** 6457-62.

HUSTEDT, N., SEEBER, A., SACK, R., TSAI-PFLUGFELDER, M., BHULLAR, B., VLAMING, H., VAN LEEUWEN, F., GUENOLE, A., VAN ATTIKUM, H., SRIVAS, R., IDEKER, T., SHIMADA, K. & GASSER, S. M. 2015. Yeast PP4 interacts with ATR homolog Ddc2-Mec1 and regulates checkpoint signaling. *Mol Cell,* 57**,** 273-89.

IDE, S., SAKA, K. & KOBAYASHI, T. 2013. Rtt109 prevents hyper-amplification of ribosomal RNA genes through histone modification in budding yeast. *PLoS Genet,* 9**,** e1003410.

ILVES, I., PETOJEVIC, T., PESAVENTO, J. J. & BOTCHAN, M. R. 2010. Activation of the MCM2-7 helicase by association with Cdc45 and GINS proteins. *Mol Cell,* 37**,** 247-58.

IVANOV, E. L. & HABER, J. E. 1995. RAD1 and RAD10, but not other excision repair genes, are required for double-strand break-induced recombination in Saccharomyces cerevisiae. *Mol Cell Biol,* 15**,** 2245-51.

JASPERSEN, S. L. & MORGAN, D. O. 2000. Cdc14 activates cdc15 to promote mitotic exit in budding yeast. *Curr Biol,* 10**,** 615-8.

JENKINS, N. L., MCCOLL, G. & LITHGOW, G. J. 2004. Fitness cost of extended lifespan in Caenorhabditis elegans. *Proc Biol Sci,* 271**,** 2523-6.

JIA, X., WEINERT, T. & LYDALL, D. 2004. Mec1 and Rad53 inhibit formation of single-stranded DNA at telomeres of Saccharomyces cerevisiae cdc13-1 mutants. *Genetics,* 166**,** 753-64.

JIANG, H., JU, Z. & RUDOLPH, K. L. 2007. Telomere shortening and ageing. *Z Gerontol Geriatr,* 40**,** 314-24.

JIN, Y. H., AYYAGARI, R., RESNICK, M. A., GORDENIN, D. A. & BURGERS, P. M. 2003. Okazaki fragment maturation in yeast. II. Cooperation between the polymerase and 3'-5'-exonuclease activities of Pol delta in the creation of a ligatable nick. *J Biol Chem,* 278**,** 1626-33.

JOHANSSON, E., GARG, P. & BURGERS, P. M. 2004. The Pol32 subunit of DNA polymerase delta contains separable domains for processive replication and proliferating cell nuclear antigen (PCNA) binding. *J Biol Chem,* 279**,** 1907-15.

KADYK, L. C. & HARTWELL, L. H. 1992. Sister chromatids are preferred over homologs as substrates for recombinational repair in Saccharomyces cerevisiae. *Genetics,* 132**,** 387-402.

KAEBERLEIN, M., MCVEY, M. & GUARENTE, L. 1999. The SIR2/3/4 complex and SIR2 alone promote longevity in Saccharomyces cerevisiae by two different mechanisms. *Genes Dev,* 13**,** 2570-80.

KALIFA, L., QUINTANA, D. F., SCHIRALDI, L. K., PHADNIS, N., COLES, G. L., SIA, R. A. & SIA, E. A. 2012. Mitochondrial genome maintenance: roles for nuclear nonhomologous end-joining proteins in Saccharomyces cerevisiae. *Genetics,* 190**,** 951-64.

KANEMAKI, M. & LABIB, K. 2006. Distinct roles for Sld3 and GINS during establishment and progression of eukaryotic DNA replication forks. *EMBO J,* 25**,** 1753-63.

KANG, Y. H., KANG, M. J., KIM, J. H., LEE, C. H., CHO, I. T., HURWITZ, J. & SEO, Y. S. 2009. The MPH1 gene of Saccharomyces cerevisiae functions in Okazaki fragment processing. *J Biol Chem,* 284**,** 10376-86.

KELLY, T. & OWUSU-APENTEN, R. K. 2015. Effect of methotrexate and tea polyphenols on the viability and oxidative stress in MDA-MB-231 breast cancer cells. *Journal of Applied Life Sciences International,* 2**,** 152-159.

KIPLING, D. 1997. Telomere structure and telomerase expression during mouse development and tumorigenesis. *Eur J Cancer,* 33**,** 792-800.

KIRKPATRICK, D. T. & PETES, T. D. 1997. Repair of DNA loops involves DNA-mismatch and nucleotide-excision repair proteins. *Nature,* 387**,** 929-31.

KIRKWOOD, T. B. 2005. Understanding the odd science of aging. *Cell,* 120**,** 437-47.

KOBAYASHI, T. 2011. How does genome instability affect lifespan?: roles of rDNA and telomeres. *Genes Cells,* 16**,** 617-24.

KOSOY, A., CALONGE, T. M., OUTWIN, E. A. & O'CONNELL, M. J. 2007. Fission yeast Rnf4 homologs are required for DNA repair. *J Biol Chem,* 282**,** 20388-94.

KOZAK, M. 1989. Context effects and inefficient initiation at non-AUG codons in eucaryotic cell-free translation systems. *Mol Cell Biol,* 9**,** 5073-80.

KRAMARZ, K., LITWIN, I., CAL-BAKOWSKA, M., SZAKAL, B., BRANZEI, D., WYSOCKI, R. & DZIADKOWIEC, D. 2014. Swi2/Snf2-like protein Uls1

functions in the Sgs1-dependent pathway of maintenance of rDNA stability and alleviation of replication stress. *DNA Repair (Amst),* 21**,** 24-35.

KUBOTA, T., NISHIMURA, K., KANEMAKI, M. T. & DONALDSON, A. D. 2013. The Elg1 replication factor C-like complex functions in PCNA unloading during DNA replication. *Mol Cell,* 50**,** 273-80.

KULTZ, D. 2005. Molecular and evolutionary basis of the cellular stress response. *Annu Rev Physiol,* 67**,** 225-57.

KUMAR, S. & BURGERS, P. M. 2013. Lagging strand maturation factor Dna2 is a component of the replication checkpoint initiation machinery. *Genes Dev,* 27**,** 313-21.

LADEROUTE, K. R. & WEBSTER, K. A. 1997. Hypoxia/reoxygenation stimulates Jun kinase activity through redox signaling in cardiac myocytes. *Circ Res,* 80**,** 336-44.

LANDER, E. S., LINTON, L. M., BIRREN, B., NUSBAUM, C., ZODY, M. C., BALDWIN, J., DEVON, K., DEWAR, K., DOYLE, M., FITZHUGH, W., FUNKE, R., GAGE, D., HARRIS, K., HEAFORD, A., HOWLAND, J., KANN, L., LEHOCZKY, J., LEVINE, R., MCEWAN, P., MCKERNAN, K., MELDRIM, J., MESIROV, J. P., MIRANDA, C., MORRIS, W., NAYLOR, J., RAYMOND, C., ROSETTI, M., SANTOS, R., SHERIDAN, A., SOUGNEZ, C., STANGE-THOMANN, N., STOJANOVIC, N., SUBRAMANIAN, A., WYMAN, D., ROGERS, J., SULSTON, J., AINSCOUGH, R., BECK, S., BENTLEY, D., BURTON, J., CLEE, C., CARTER, N., COULSON, A., DEADMAN, R., DELOUKAS, P., DUNHAM, A., DUNHAM, I., DURBIN, R., FRENCH, L., GRAFHAM, D., GREGORY, S., HUBBARD, T., HUMPHRAY, S., HUNT, A., JONES, M., LLOYD, C., MCMURRAY, A., MATTHEWS, L., MERCER, S., MILNE, S., MULLIKIN, J. C., MUNGALL, A., PLUMB, R., ROSS, M., SHOWNKEEN, R., SIMS, S., WATERSTON, R. H., WILSON, R. K., HILLIER, L. W., MCPHERSON, J. D., MARRA, M. A., MARDIS, E. R., FULTON, L. A., CHINWALLA, A. T., PEPIN, K. H., GISH, W. R., CHISSOE, S. L., WENDL, M. C., DELEHAUNTY, K. D., MINER, T. L., DELEHAUNTY, A., KRAMER, J. B., COOK, L. L., FULTON, R. S., JOHNSON, D. L., MINX, P. J., CLIFTON, S. W., HAWKINS, T., BRANSCOMB, E., PREDKI, P., RICHARDSON, P., WENNING, S., SLEZAK, T., DOGGETT, N., CHENG, J. F., OLSEN, A., LUCAS, S., ELKIN, C., UBERBACHER, E., FRAZIER, M., et al. 2001. Initial sequencing and analysis of the human genome. *Nature,* 409**,** 860-921.

LARRIVEE, M. & WELLINGER, R. J. 2006. Telomerase- and capping-independent yeast survivors with alternate telomere states. *Nat Cell Biol,* 8**,** 741-7.

LAZZARO, F., SAPOUNTZI, V., GRANATA, M., PELLICIOLI, A., VAZE, M., HABER, J. E., PLEVANI, P., LYDALL, D. & MUZI-FALCONI, M. 2008. Histone methyltransferase Dot1 and Rad9 inhibit single-stranded DNA accumulation at DSBs and uncapped telomeres. *EMBO J,* 27**,** 1502-12.

LE BOURG, E. 2015. Fasting and other mild stresses with hormetic effects in Drosophila melanogaster can additively increase resistance to cold. *Biogerontology,* 16**,** 517-27.

LEE, B. I. & WILSON, D. M., 3RD 1999. The RAD2 domain of human exonuclease 1 exhibits 5' to 3' exonuclease and flap structure-specific endonuclease activities. *J Biol Chem,* 274**,** 37763-9.

LEE, C. H., LEE, M., KANG, H. J., KIM, D. H., KANG, Y. H., BAE, S. H. & SEO, Y. S. 2013. The N-terminal 45-kDa domain of Dna2 endonuclease/helicase targets the enzyme to secondary structure DNA. *J Biol Chem,* 288**,** 9468-81.

LENDVAY, T. S., MORRIS, D. K., SAH, J., BALASUBRAMANIAN, B. & LUNDBLAD, V. 1996. Senescence mutants of Saccharomyces cerevisiae with a defect in telomere replication identify three additional EST genes. *Genetics,* 144**,** 1399-412.

LEONELLI, S. & ANKENY, R. A. 2013. What makes a model organism? *Endeavour,* 37**,** 209-12.

LESCASSE, R., POBIEGA, S., CALLEBAUT, I. & MARCAND, S. 2013. End-joining inhibition at telomeres requires the translocase and polySUMO-dependent ubiquitin ligase Uls1. *EMBO J,* 32**,** 805-15.

LEURAUD, K., RICHARDSON, D. B., CARDIS, E., DANIELS, R. D., GILLIES, M., O'HAGAN, J. A., HAMRA, G. B., HAYLOCK, R., LAURIER, D., MOISSONNIER, M., SCHUBAUER-BERIGAN, M. K., THIERRY-CHEF, I. & KESMINIENE, A. 2015. Ionising radiation and risk of death from leukaemia and lymphoma in radiation-monitored workers (INWORKS): an international cohort study. *Lancet Haematol,* 2**,** e276-e281.

LEVIKOVA, M. & CEJKA, P. 2015. The Saccharomyces cerevisiae Dna2 can function as a sole nuclease in the processing of Okazaki fragments in DNA replication. *Nucleic Acids Res,* 43**,** 7888-97.

LEWIS, J. G., LEARMONTH, R. P. & WATSON, K. 1995. Induction of heat, freezing and salt tolerance by heat and salt shock in Saccharomyces cerevisiae. *Microbiology,* 141 ( Pt 3)**,** 687-94.

LEWIS, L. K., STORICI, F., VAN KOMEN, S., CALERO, S., SUNG, P. & RESNICK, M. A. 2004. Role of the nuclease activity of Saccharomyces cerevisiae Mre11 in repair of DNA double-strand breaks in mitotic cells. *Genetics,* 166**,** 1701-13.

LIN, J. J. & ZAKIAN, V. A. 1996. The Saccharomyces CDC13 protein is a single-strand TG1-3 telomeric DNA-binding protein in vitro that affects telomere behavior in vivo. *Proc Natl Acad Sci U S A,* 93**,** 13760-5.

LIN, W., SAMPATHI, S., DAI, H., LIU, C., ZHOU, M., HU, J., HUANG, Q., CAMPBELL, J., SHIN-YA, K., ZHENG, L., CHAI, W. & SHEN, B. 2013. Mammalian DNA2 helicase/nuclease cleaves G-quadruplex DNA and is required for telomere integrity. *EMBO J,* 32**,** 1425-39.

LINGNER, J. & CECH, T. R. 1996. Purification of telomerase from Euplotes aediculatus: requirement of a primer 3' overhang. *Proc Natl Acad Sci U S A,* 93**,** 10712-7.

LITI, G. 2015. The fascinating and secret wild life of the budding yeast S. cerevisiae. *Elife,* 4.

LONG, Y., YAN, J., SONG, G., LI, X., LI, X., LI, Q. & CUI, Z. 2015. Transcriptional events co-regulated by hypoxia and cold stresses in Zebrafish larvae. *BMC Genomics,* 16**,** 385.

LONGHESE, M. P., BONETTI, D., MANFRINI, N. & CLERICI, M. 2010. Mechanisms and regulation of DNA end resection. *EMBO J,* 29**,** 2864-74.

LONGHESE, M. P., PACIOTTI, V., FRASCHINI, R., ZACCARINI, R., PLEVANI, P. & LUCCHINI, G. 1997. The novel DNA damage checkpoint protein ddc1p is phosphorylated periodically during the cell cycle and in response to DNA damage in budding yeast. *EMBO J,* 16**,** 5216-26.

LONGTINE, M. S., MCKENZIE, A., 3RD, DEMARINI, D. J., SHAH, N. G., WACH, A., BRACHAT, A., PHILIPPSEN, P. & PRINGLE, J. R. 1998a. Additional modules for versatile and economical PCR-based gene deletion and modification in Saccharomyces cerevisiae. *Yeast,* 14**,** 953-61.

LONGTINE, M. S., MCKENZIE, A., DEMARINI, D. J., SHAH, N. G., WACH, A., BRACHAT, A., PHILIPPSEN, P. & PRINGLE, J. R. 1998b. Additional modules for versatile and economical PCR-based gene deletion and modification in Saccharomyces cerevisiae. *Yeast,* 14**,** 953-961.

LOPEZ-MAURY, L., MARGUERAT, S. & BAHLER, J. 2008. Tuning gene expression to changing environments: from rapid responses to evolutionary adaptation. *Nat Rev Genet,* 9**,** 583-93.

LOVETT, S. T. 2007. Polymerase switching in DNA replication. *Mol Cell,* 27**,** 523-6.

LU, W., ZHANG, Y., LIU, D., SONGYANG, Z. & WAN, M. 2013. Telomeres-structure, function, and regulation. *Exp Cell Res,* 319**,** 133-41.

LUNDBLAD, V. & BLACKBURN, E. H. 1993. An alternative pathway for yeast telomere maintenance rescues est1- senescence. *Cell,* 73**,** 347-60.

LUNDBLAD, V. & SZOSTAK, J. W. 1989. A mutant with a defect in telomere elongation leads to senescence in yeast. *Cell,* 57**,** 633-43.

LYDALL, D. 2003. Hiding at the ends of yeast chromosomes: telomeres, nucleases and checkpoint pathways. *J Cell Sci,* 116**,** 4057-65.

LYDALL, D. 2009. Taming the tiger by the tail: modulation of DNA damage responses by telomeres. *EMBO J,* 28**,** 2174-87.

LYDALL, D., NIKOLSKY, Y., BISHOP, D. K. & WEINERT, T. 1996. A meiotic recombination checkpoint controlled by mitotic checkpoint genes. *Nature,* 383**,** 840-3.

LYDALL, D. & WEINERT, T. 1995. Yeast checkpoint genes in DNA damage processing: implications for repair and arrest. *Science,* 270**,** 1488-91.

MAGA, G., VILLANI, G., TILLEMENT, V., STUCKI, M., LOCATELLI, G. A., FROUIN, I., SPADARI, S. & HUBSCHER, U. 2001. Okazaki fragment processing: modulation of the strand displacement activity of DNA polymerase delta by the concerted action of replication protein A, proliferating cell nuclear antigen, and flap endonuclease-1. *Proc Natl Acad Sci U S A,* 98**,** 14298-303.

MAI, B. & BREEDEN, L. 1997. Xbp1, a stress-induced transcriptional repressor of the Saccharomyces cerevisiae Swi4/Mbp1 family. *Mol Cell Biol,* 17**,** 6491-501.

MAILLET, L., GADEN, F., BREVET, V., FOUREL, G., MARTIN, S. G., DUBRANA, K., GASSER, S. M. & GILSON, E. 2001. Ku-deficient yeast strains exhibit alternative states of silencing competence. *EMBO Rep,* 2**,** 203-10.

MAJKA, J., BINZ, S. K., WOLD, M. S. & BURGERS, P. M. 2006. Replication protein A directs loading of the DNA damage checkpoint clamp to 5'-DNA junctions. *J Biol Chem,* 281**,** 27855-61.

MAJKA, J. & BURGERS, P. M. 2003. Yeast Rad17/Mec3/Ddc1: a sliding clamp for the DNA damage checkpoint. *Proc Natl Acad Sci U S A,* 100**,** 2249-54.

MAOZ, N., GABAY, O., WALDMAN BEN-ASHER, H. & COHEN, H. Y. 2015. The yeast forkhead HCM1 controls life span independent of calorie restriction. *J Gerontol A Biol Sci Med Sci,* 70**,** 444-53.

MARINGELE, L. & LYDALL, D. 2002. EXO1-dependent single-stranded DNA at telomeres activates subsets of DNA damage and spindle checkpoint pathways in budding yeast yku70Delta mutants. *Genes Dev,* 16**,** 1919-33.

MARINGELE, L. & LYDALL, D. 2004. EXO1 plays a role in generating type I and type II survivors in budding yeast. *Genetics,* 166**,** 1641-9.

MARKIEWICZ-POTOCZNY, M. & LYDALL, D. 2016. Costs, benefits and redundant mechanisms of adaption to chronic low-dose stress in yeast. *Cell Cycle***,** 1-10.

MARTIN, S. G., LAROCHE, T., SUKA, N., GRUNSTEIN, M. & GASSER, S. M. 1999. Relocalization of telomeric Ku and SIR proteins in response to DNA strand breaks in yeast. *Cell,* 97**,** 621-33.

MARTINA, M., BONETTI, D., VILLA, M., LUCCHINI, G. & LONGHESE, M. P. 2014. Saccharomyces cerevisiae Rif1 cooperates with MRX-Sae2 in promoting DNA-end resection. *EMBO Rep,* 15**,** 695-704.

MARTINEZ-PASTOR, M. T., MARCHLER, G., SCHULLER, C., MARCHLER-BAUER, A., RUIS, H. & ESTRUCH, F. 1996. The Saccharomyces cerevisiae zinc finger proteins Msn2p and Msn4p are required for transcriptional induction through the stress response element (STRE). *EMBO J,* 15**,** 2227-35.

MASUDA-SASA, T., IMAMURA, O. & CAMPBELL, J. L. 2006. Biochemical analysis of human Dna2. *Nucleic Acids Res,* 34**,** 1865-75.

MATTSON, M. P. 2008. Hormesis defined. *Ageing Res Rev,* 7**,** 1-7.

MCCARROLL, S. A., MURPHY, C. T., ZOU, S., PLETCHER, S. D., CHIN, C. S., JAN, Y. N., KENYON, C., BARGMANN, C. I. & LI, H. 2004. Comparing

genomic expression patterns across species identifies shared transcriptional profile in aging. *Nat Genet,* 36**,** 197-204.

MCISAAC, R. S., LEWIS, K. N., GIBNEY, P. A. & BUFFENSTEIN, R. 2016. From yeast to human: exploring the comparative biology of methionine restriction in extending eukaryotic life span. *Ann N Y Acad Sci,* 1363**,** 155-70.

MILES, S., LI, L., DAVISON, J. & BREEDEN, L. L. 2013. Xbp1 directs global repression of budding yeast transcription during the transition to quiescence and is important for the longevity and reversibility of the quiescent state. *PLoS Genet,* 9**,** e1003854.

MILISAV, I., POLJSAK, B. & SUPUT, D. 2012. Adaptive response, evidence of cross-resistance and its potential clinical use. *Int J Mol Sci,* 13**,** 10771-806.

MIMITOU, E. P. & SYMINGTON, L. S. 2008. Sae2, Exo1 and Sgs1 collaborate in DNA double-strand break processing. *Nature,* 455**,** 770-4.

MIMITOU, E. P. & SYMINGTON, L. S. 2009. Nucleases and helicases take center stage in homologous recombination. *Trends Biochem Sci,* 34**,** 264-72.

MIYABE, I., KUNKEL, T. A. & CARR, A. M. 2011. The major roles of DNA polymerases epsilon and delta at the eukaryotic replication fork are evolutionarily conserved. *PLoS Genet,* 7**,** e1002407.

MIYAGAWA, K., LOW, R. S., SANTOSA, V., TSUJI, H., MOSER, B. A., FUJISAWA, S., HARLAND, J. L., RAGUIMOVA, O. N., GO, A., UENO, M., MATSUYAMA, A., YOSHIDA, M., NAKAMURA, T. M. & TANAKA, K. 2014. SUMOylation regulates telomere length by targeting the shelterin subunit Tpz1(Tpp1) to modulate shelterin-Stn1 interaction in fission yeast. *Proc Natl Acad Sci U S A,* 111**,** 5950-5.

MIYAKE, Y., NAKAMURA, M., NABETANI, A., SHIMAMURA, S., TAMURA, M., YONEHARA, S., SAITO, M. & ISHIKAWA, F. 2009. RPA-like mammalian Ctc1-Stn1-Ten1 complex binds to single-stranded DNA and protects telomeres independently of the Pot1 pathway. *Mol Cell,* 36**,** 193-206.

MIYOSHI, T., KANOH, J., SAITO, M. & ISHIKAWA, F. 2008. Fission yeast Pot1-Tpp1 protects telomeres and regulates telomere length. *Science,* 320**,** 1341-4.

MYUNG, K., CHEN, C. & KOLODNER, R. D. 2001. Multiple pathways cooperate in the suppression of genome instability in Saccharomyces cerevisiae. *Nature,* 411**,** 1073-6.

NAUTIYAL, S., DERISI, J. L. & BLACKBURN, E. H. 2002. The genome-wide expression response to telomerase deletion in Saccharomyces cerevisiae. *Proc Natl Acad Sci U S A,* 99**,** 9316-21.

NAVADGI-PATIL, V. M. & BURGERS, P. M. 2009a. A tale of two tails: activation of DNA damage checkpoint kinase Mec1/ATR by the 9-1-1 clamp and by Dpb11/TopBP1. *DNA Repair (Amst),* 8**,** 996-1003.

NAVADGI-PATIL, V. M. & BURGERS, P. M. 2009b. The unstructured C-terminal tail of the 9-1-1 clamp subunit Ddc1 activates Mec1/ATR via two distinct mechanisms. *Mol Cell,* 36**,** 743-53.

NAVADGI-PATIL, V. M. & BURGERS, P. M. 2011. Cell-cycle-specific activators of the Mec1/ATR checkpoint kinase. *Biochem Soc Trans,* 39**,** 600-5.

NAVADGI-PATIL, V. M., KUMAR, S. & BURGERS, P. M. 2011. The unstructured C-terminal tail of yeast Dpb11 (human TopBP1) protein is dispensable for DNA replication and the S phase checkpoint but required for the G2/M checkpoint. *J Biol Chem,* 286**,** 40999-1007.

NEGRINI, S., GORGOULIS, V. G. & HALAZONETIS, T. D. 2010. Genomic instability--an evolving hallmark of cancer. *Nat Rev Mol Cell Biol,* 11**,** 220-8.

NGO, G. H., BALAKRISHNAN, L., DUBARRY, M., CAMPBELL, J. L. & LYDALL, D. 2014. The 9-1-1 checkpoint clamp stimulates DNA resection by Dna2-Sgs1 and Exo1. *Nucleic Acids Res,* 42**,** 10516-28.

NGO, G. H. & LYDALL, D. 2015. The 9-1-1 checkpoint clamp coordinates resection at DNA double strand breaks. *Nucleic Acids Res,* 43**,** 5017-32.

NGO, H. P. & LYDALL, D. 2010. Survival and growth of yeast without telomere capping by Cdc13 in the absence of Sgs1, Exo1, and Rad9. *PLoS Genet,* 6**,** e1001072.

NUGENT, C. I., HUGHES, T. R., LUE, N. F. & LUNDBLAD, V. 1996. Cdc13p: a single-strand telomeric DNA-binding protein with a dual role in yeast telomere maintenance. *Science,* 274**,** 249-52.

OKAZAKI, R., OKAZAKI, T., SAKABE, K., SUGIMOTO, K. & SUGINO, A. 1968. Mechanism of DNA chain growth. I. Possible discontinuity and unusual secondary structure of newly synthesized chains. *Proc Natl Acad Sci U S A,* 59**,** 598-605.

OLOVNIKOV, A. M. 1973. A theory of marginotomy. The incomplete copying of template margin in enzymic synthesis of polynucleotides and biological significance of the phenomenon. *J Theor Biol,* 41**,** 181-90.

PACIOTTI, V., CLERICI, M., LUCCHINI, G. & LONGHESE, M. P. 2000. The checkpoint protein Ddc2, functionally related to S. pombe Rad26, interacts with Mec1 and is regulated by Mec1-dependent phosphorylation in budding yeast. *Genes Dev,* 14**,** 2046-59.

PALM, W. & DE LANGE, T. 2008. How shelterin protects mammalian telomeres. *Annu Rev Genet,* 42**,** 301-34.

PANOWSKI, S. H., WOLFF, S., AGUILANIU, H., DURIEUX, J. & DILLIN, A. 2007. PHA-4/Foxa mediates diet-restriction-induced longevity of C. elegans. *Nature,* 447**,** 550-5.

PARDO, B. & MARCAND, S. 2005. Rap1 prevents telomere fusions by nonhomologous end joining. *EMBO J,* 24**,** 3117-27.

PARENTEAU, J. & WELLINGER, R. J. 1999. Accumulation of single-stranded DNA and destabilization of telomeric repeats in yeast mutant strains carrying a deletion of RAD27. *Mol Cell Biol,* 19**,** 4143-52.

PASSOS, J. F., SARETZKI, G., AHMED, S., NELSON, G., RICHTER, T., PETERS, H., WAPPLER, I., BIRKET, M. J., HAROLD, G., SCHAEUBLE, K., BIRCH-MACHIN, M. A., KIRKWOOD, T. B. & VON ZGLINICKI, T. 2007. Mitochondrial dysfunction accounts for the stochastic heterogeneity in telomere-dependent senescence. *PLoS Biol,* 5**,** e110.

PEAKE, J. M., MARKWORTH, J. F., NOSAKA, K., RAASTAD, T., WADLEY, G. D. & COFFEY, V. G. 2015. Modulating exercise-induced hormesis: Does less equal more? *J Appl Physiol (1985),* 119**,** 172-89.

PENNOCK, E., BUCKLEY, K. & LUNDBLAD, V. 2001. Cdc13 delivers separate complexes to the telomere for end protection and replication. *Cell,* 104**,** 387-96.

PERRY, M. C., DUFOUR, C. R., EICHNER, L. J., TSANG, D. W., DEBLOIS, G., MULLER, W. J. & GIGUERE, V. 2014. ERBB2 deficiency alters an E2F-1-dependent adaptive stress response and leads to cardiac dysfunction. *Mol Cell Biol,* 34**,** 4232-43.

PETREACA, R. C., CHIU, H. C. & NUGENT, C. I. 2007. The role of Stn1p in Saccharomyces cerevisiae telomere capping can be separated from its interaction with Cdc13p. *Genetics,* 177**,** 1459-74.

PFANDER, B. & DIFFLEY, J. F. 2011. Dpb11 coordinates Mec1 kinase activation with cell cycle-regulated Rad9 recruitment. *EMBO J,* 30**,** 4897-907.

PFEIFFER, P., GOEDECKE, W. & OBE, G. 2000. Mechanisms of DNA double-strand break repair and their potential to induce chromosomal aberrations. *Mutagenesis,* 15**,** 289-302.

PHILLIPS, J. A., CHAN, A., PAESCHKE, K. & ZAKIAN, V. A. 2015. The pif1 helicase, a negative regulator of telomerase, acts preferentially at long telomeres. *PLoS Genet,* 11**,** e1005186.

PHIPPS, S. M., BERLETCH, J. B., ANDREWS, L. G. & TOLLEFSBOL, T. O. 2007. Aging cell culture: methods and observations. *Methods Mol Biol,* 371**,** 9-19.

PIKE, J. E., BURGERS, P. M., CAMPBELL, J. L. & BAMBARA, R. A. 2009. Pif1 helicase lengthens some Okazaki fragment flaps necessitating Dna2 nuclease/helicase action in the two-nuclease processing pathway. *J Biol Chem,* 284**,** 25170-80.

POKHAREL, S. & CAMPBELL, J. L. 2012. Cross talk between the nuclease and helicase activities of Dna2: role of an essential iron-sulfur cluster domain. *Nucleic Acids Res,* 40**,** 7821-30.

POLI, J., GERHOLD, C. B., TOSI, A., HUSTEDT, N., SEEBER, A., SACK, R., HERZOG, F., PASERO, P., SHIMADA, K., HOPFNER, K. P. & GASSER, S. M. 2016. Mec1, INO80, and the PAF1 complex cooperate to limit transcription

replication conflicts through RNAPII removal during replication stress. *Genes Dev,* 30**,** 337-54.

POLO, S. E. & JACKSON, S. P. 2011. Dynamics of DNA damage response proteins at DNA breaks: a focus on protein modifications. *Genes Dev,* 25**,** 409-33.

POLOTNIANKA, R. M., LI, J. & LUSTIG, A. J. 1998. The yeast Ku heterodimer is essential for protection of the telomere against nucleolytic and recombinational activities. *Curr Biol,* 8**,** 831-4.

PORTER, S. E., GREENWELL, P. W., RITCHIE, K. B. & PETES, T. D. 1996. The DNA-binding protein Hdf1p (a putative Ku homologue) is required for maintaining normal telomere length in Saccharomyces cerevisiae. *Nucleic Acids Res,* 24**,** 582-5.

PRAMILA, T., WU, W., MILES, S., NOBLE, W. S. & BREEDEN, L. L. 2006. The Forkhead transcription factor Hcm1 regulates chromosome segregation genes and fills the S-phase gap in the transcriptional circuitry of the cell cycle. *Genes Dev,* 20**,** 2266-78.

PUDDU, F., GRANATA, M., DI NOLA, L., BALESTRINI, A., PIERGIOVANNI, G., LAZZARO, F., GIANNATTASIO, M., PLEVANI, P. & MUZI-FALCONI, M. 2008. Phosphorylation of the budding yeast 9-1-1 complex is required for Dpb11 function in the full activation of the UV-induced DNA damage checkpoint. *Mol Cell Biol,* 28**,** 4782-93.

PUDDU, F., PIERGIOVANNI, G., PLEVANI, P. & MUZI-FALCONI, M. 2011. Sensing of replication stress and Mec1 activation act through two independent pathways involving the 9-1-1 complex and DNA polymerase epsilon. *PLoS Genet,* 7**,** e1002022.

PUGLISI, A., BIANCHI, A., LEMMENS, L., DAMAY, P. & SHORE, D. 2008. Distinct roles for yeast Stn1 in telomere capping and telomerase inhibition. *EMBO J,* 27**,** 2328-39.

PURSELL, Z. F., ISOZ, I., LUNDSTROM, E. B., JOHANSSON, E. & KUNKEL, T. A. 2007. Yeast DNA polymerase epsilon participates in leading-strand DNA replication. *Science,* 317**,** 127-30.

RALSER, M., WAMELINK, M. M., STRUYS, E. A., JOPPICH, C., KROBITSCH, S., JAKOBS, C. & LEHRACH, H. 2008. A catabolic block does not sufficiently explain how 2-deoxy-D-glucose inhibits cell growth. *Proc Natl Acad Sci U S A,* 105**,** 17807-11.

RAY, A. & RUNGE, K. W. 1999. The yeast telomere length counting machinery is sensitive to sequences at the telomere-nontelomere junction. *Mol Cell Biol,* 19**,** 31-45.

REAGAN, M. S., PITTENGER, C., SIEDE, W. & FRIEDBERG, E. C. 1995. Characterization of a mutant strain of Saccharomyces cerevisiae with a deletion of the RAD27 gene, a structural homolog of the RAD2 nucleotide excision repair gene. *J Bacteriol,* 177**,** 364-71.

RITCHIE, K. B., MALLORY, J. C. & PETES, T. D. 1999. Interactions of TLC1 (which encodes the RNA subunit of telomerase), TEL1, and MEC1 in regulating telomere length in the yeast Saccharomyces cerevisiae. *Mol Cell Biol,* 19**,** 6065-75.

RODRIGUEZ-COLMAN, M. J., SOROLLA, M. A., VALL-LLAURA, N., TAMARIT, J., ROS, J. & CABISCOL, E. 2013. The FOX transcription factor Hcm1 regulates oxidative metabolism in response to early nutrient limitation in yeast. Role of Snf1 and Tor1/Sch9 kinases. *Biochim Biophys Acta,* 1833**,** 2004-15.

RONCHI, D., DI FONZO, A., LIN, W., BORDONI, A., LIU, C., FASSONE, E., PAGLIARANI, S., RIZZUTI, M., ZHENG, L., FILOSTO, M., FERRO, M. T., RANIERI, M., MAGRI, F., PEVERELLI, L., LI, H., YUAN, Y. C., CORTI, S., SCIACCO, M., MOGGIO, M., BRESOLIN, N., SHEN, B. & COMI, G. P. 2013. Mutations in DNA2 link progressive myopathy to mitochondrial DNA instability. *Am J Hum Genet,* 92**,** 293-300.

ROSSI, M. L. & BAMBARA, R. A. 2006. Reconstituted Okazaki fragment processing indicates two pathways of primer removal. *J Biol Chem,* 281**,** 26051-61.

ROSSI, M. L., PIKE, J. E., WANG, W., BURGERS, P. M., CAMPBELL, J. L. & BAMBARA, R. A. 2008. Pif1 helicase directs eukaryotic Okazaki fragments toward the two-nuclease cleavage pathway for primer removal. *J Biol Chem,* 283**,** 27483-93.

ROY, R., MEIER, B., MCAINSH, A. D., FELDMANN, H. M. & JACKSON, S. P. 2004. Separation-of-function mutants of yeast Ku80 reveal a Yku80p-Sir4p interaction involved in telomeric silencing. *J Biol Chem,* 279**,** 86-94.

RUPEC, R. A. & BAEUERLE, P. A. 1995. The genomic response of tumor cells to hypoxia and reoxygenation. Differential activation of transcription factors AP-1 and NF-kappa B. *Eur J Biochem,* 234**,** 632-40.

SADEH, A., MOVSHOVICH, N., VOLOKH, M., GHEBER, L. & AHARONI, A. 2011. Fine-tuning of the Msn2/4-mediated yeast stress responses as revealed by systematic deletion of Msn2/4 partners. *Mol Biol Cell,* 22**,** 3127-38.

SAKA, K., IDE, S., GANLEY, A. R. & KOBAYASHI, T. 2013. Cellular senescence in yeast is regulated by rDNA noncoding transcription. *Curr Biol,* 23**,** 1794-8.

SAKA, K., TAKAHASHI, A., SASAKI, M. & KOBAYASHI, T. 2016. More than 10% of yeast genes are related to genome stability and influence cellular senescence via rDNA maintenance. *Nucleic Acids Res,* 44**,** 4211-21.

SANCHEZ, Y., BACHANT, J., WANG, H., HU, F., LIU, D., TETZLAFF, M. & ELLEDGE, S. J. 1999. Control of the DNA damage checkpoint by chk1 and rad53 protein kinases through distinct mechanisms. *Science,* 286**,** 1166-71.

SARTO-JACKSON, I. & TOMASKA, L. 2016. How to bake a brain: yeast as a model neuron. *Curr Genet,* 62**,** 347-70.

SCHIESTL, R. H. & PRAKASH, S. 1990. RAD10, an excision repair gene of Saccharomyces cerevisiae, is involved in the RAD1 pathway of mitotic recombination. *Mol Cell Biol,* 10**,** 2485-91.

SCHULTE, P. M. 2014. What is environmental stress? Insights from fish living in a variable environment. *J Exp Biol,* 217**,** 23-34.

SCHULZ, H. 1888. Ueber Hefegifte. *Pflügers Archiv - European Journal of Physiology* 42**,** 517-541.

SCHUMACHER, B. 2009. Transcription-blocking DNA damage in aging: a mechanism for hormesis. *Bioessays,* 31**,** 1347-56.

SCHWEITZER, B. & PHILIPPSEN, P. 1991. CDC15, an essential cell cycle gene in Saccharomyces cerevisiae, encodes a protein kinase domain. *Yeast,* 7**,** 265-73.

SCHWERER, M. J., HEMMER, J., KRAFT, K., MAIER, H., MOLLER, P. & BARTH, T. F. 2003. Endoreduplication in conjunction with tumor progression in an aneuploid laryngeal squamous cell carcinoma. *Virchows Arch,* 443**,** 98-103.

SEKO, Y., TAKAHASHI, N., TOBE, K., KADOWAKI, T. & YAZAKI, Y. 1997. Hypoxia and hypoxia/reoxygenation activate p65PAK, p38 mitogen-activated protein kinase (MAPK), and stress-activated protein kinase (SAPK) in cultured rat cardiac myocytes. *Biochem Biophys Res Commun,* 239**,** 840-4.

SHAH, P. P., ZHENG, X., EPSHTEIN, A., CAREY, J. N., BISHOP, D. K. & KLEIN, H. L. 2010. Swi2/Snf2-related translocases prevent accumulation of toxic Rad51 complexes during mitotic growth. *Mol Cell,* 39**,** 862-72.

SHEAFFER, K. L., UPDIKE, D. L. & MANGO, S. E. 2008. The Target of Rapamycin pathway antagonizes pha-4/FoxA to control development and aging. *Curr Biol,* 18**,** 1355-64.

SHEN, B., SINGH, P., LIU, R., QIU, J., ZHENG, L., FINGER, L. D. & ALAS, S. 2005. Multiple but dissectible functions of FEN-1 nucleases in nucleic acid processing, genome stability and diseases. *Bioessays,* 27**,** 717-29.

SHI, T., BUNKER, R. D., MATTAROCCI, S., RIBEYRE, C., FATY, M., GUT, H., SCRIMA, A., RASS, U., RUBIN, S. M., SHORE, D. & THOMA, N. H. 2013. Rif1 and Rif2 shape telomere function and architecture through multivalent Rap1 interactions. *Cell,* 153**,** 1340-53.

SHIRATORI, A., SHIBATA, T., ARISAWA, M., HANAOKA, F., MURAKAMI, Y. & EKI, T. 1999. Systematic identification, classification, and characterization of the open reading frames which encode novel helicase-related proteins in Saccharomyces cerevisiae by gene disruption and Northern analysis. *Yeast,* 15**,** 219-53.

SIJBERS, A. M., DE LAAT, W. L., ARIZA, R. R., BIGGERSTAFF, M., WEI, Y. F., MOGGS, J. G., CARTER, K. C., SHELL, B. K., EVANS, E., DE JONG, M. C., RADEMAKERS, S., DE ROOIJ, J., JASPERS, N. G., HOEIJMAKERS, J. H. &

WOOD, R. D. 1996. Xeroderma pigmentosum group F caused by a defect in a structure-specific DNA repair endonuclease. *Cell,* 86**,** 811-22.

SINGH, F., CHARLES, A. L., SCHLAGOWSKI, A. I., BOUITBIR, J., BONIFACIO, A., PIQUARD, F., KRAHENBUHL, S., GENY, B. & ZOLL, J. 2015. Reductive stress impairs myoblasts mitochondrial function and triggers mitochondrial hormesis. *Biochim Biophys Acta,* 1853**,** 1574-85.

SINGH, P., ZHENG, L., CHAVEZ, V., QIU, J. & SHEN, B. 2007. Concerted action of exonuclease and Gap-dependent endonuclease activities of FEN-1 contributes to the resolution of triplet repeat sequences (CTG)n- and (GAA)n-derived secondary structures formed during maturation of Okazaki fragments. *J Biol Chem,* 282**,** 3465-77.

SMITH, S., BANERJEE, S., RILO, R. & MYUNG, K. 2008. Dynamic regulation of single-stranded telomeres in Saccharomyces cerevisiae. *Genetics,* 178**,** 693-701.

SRIRAMACHANDRAN, A. M. & DOHMEN, R. J. 2014. SUMO-targeted ubiquitin ligases. *Biochim Biophys Acta,* 1843**,** 75-85.

STEARNS, T., MA, H. & BOTSTEIN, D. 1990. Manipulating yeast genome using plasmid vectors. *Methods Enzymol,* 185**,** 280-97.

STELLWAGEN, A. E., HAIMBERGER, Z. W., VEATCH, J. R. & GOTTSCHLING, D. E. 2003. Ku interacts with telomerase RNA to promote telomere addition at native and broken chromosome ends. *Genes Dev,* 17**,** 2384-95.

STEWART, J. A., MILLER, A. S., CAMPBELL, J. L. & BAMBARA, R. A. 2008. Dynamic removal of replication protein A by Dna2 facilitates primer cleavage during Okazaki fragment processing in Saccharomyces cerevisiae. *J Biol Chem,* 283**,** 31356-65.

STRANAHAN, A. M. & MATTSON, M. P. 2012. Recruiting adaptive cellular stress responses for successful brain ageing. *Nat Rev Neurosci,* 13**,** 209-16.

STRAUSS, C., KORNOWSKI, M., BENVENISTY, A., SHAHAR, A., MASURY, H., BEN-PORATH, I., RAVID, T., ARBEL-EDEN, A. & GOLDBERG, M. 2014. The DNA2 nuclease/helicase is an estrogen-dependent gene mutated in breast and ovarian cancers. *Oncotarget,* 5**,** 9396-409.

SUN, J., PAN, H., LEI, C., YUAN, B., NAIR, S. J., APRIL, C., PARAMESWARAN, B., KLOTZLE, B., FAN, J. B., RUAN, J. & LI, R. 2011a. Genetic and genomic analyses of RNA polymerase II-pausing factor in regulation of mammalian transcription and cell growth. *J Biol Chem,* 286**,** 36248-57.

SUN, J., YANG, Y., WAN, K., MAO, N., YU, T. Y., LIN, Y. C., DEZWAAN, D. C., FREEMAN, B. C., LIN, J. J., LUE, N. F. & LEI, M. 2011b. Structural bases of dimerization of yeast telomere protein Cdc13 and its interaction with the catalytic subunit of DNA polymerase alpha. *Cell Res,* 21**,** 258-74.

SUROVTSEVA, Y. V., CHURIKOV, D., BOLTZ, K. A., SONG, X., LAMB, J. C., WARRINGTON, R., LEEHY, K., HEACOCK, M., PRICE, C. M. & SHIPPEN, D.

E. 2009. Conserved telomere maintenance component 1 interacts with STN1 and maintains chromosome ends in higher eukaryotes. *Mol Cell,* 36**,** 207-18.

SWEENEY, F. D., YANG, F., CHI, A., SHABANOWITZ, J., HUNT, D. F. & DUROCHER, D. 2005. Saccharomyces cerevisiae Rad9 acts as a Mec1 adaptor to allow Rad53 activation. *Curr Biol,* 15**,** 1364-75.

SYMINGTON, L. S. 2002. Role of RAD52 epistasis group genes in homologous recombination and double-strand break repair. *Microbiol Mol Biol Rev,* 66**,** 630-70, table of contents.

SYMINGTON, L. S. & GAUTIER, J. 2011. Double-strand break end resection and repair pathway choice. *Annu Rev Genet,* 45**,** 247-71.

TAGGART, A. K., TENG, S. C. & ZAKIAN, V. A. 2002. Est1p as a cell cycle-regulated activator of telomere-bound telomerase. *Science,* 297**,** 1023-6.

TANAKA, S., KOMEDA, Y., UMEMORI, T., KUBOTA, Y., TAKISAWA, H. & ARAKI, H. 2013. Efficient initiation of DNA replication in eukaryotes requires Dpb11/TopBP1-GINS interaction. *Mol Cell Biol,* 33**,** 2614-22.

TANAKA, S., UMEMORI, T., HIRAI, K., MURAMATSU, S., KAMIMURA, Y. & ARAKI, H. 2007. CDK-dependent phosphorylation of Sld2 and Sld3 initiates DNA replication in budding yeast. *Nature,* 445**,** 328-32.

TAO, R., CHEN, H., GAO, C., XUE, P., YANG, F., HAN, J. D., ZHOU, B. & CHEN, Y. G. 2011. Xbp1-mediated histone H4 deacetylation contributes to DNA double-strand break repair in yeast. *Cell Res,* 21**,** 1619-33.

TAUFFENBERGER, A. & PARKER, J. A. 2014. Heritable transmission of stress resistance by high dietary glucose in Caenorhabditis elegans. *PLoS Genet,* 10**,** e1004346.

TEIXEIRA, M. T., ARNERIC, M., SPERISEN, P. & LINGNER, J. 2004. Telomere length homeostasis is achieved via a switch between telomerase- extendible and -nonextendible states. *Cell,* 117**,** 323-35.

TISHKOFF, D. X., FILOSI, N., GAIDA, G. M. & KOLODNER, R. D. 1997. A novel mutation avoidance mechanism dependent on S. cerevisiae RAD27 is distinct from DNA mismatch repair. *Cell,* 88**,** 253-63.

TOMKINSON, A. E., BARDWELL, A. J., BARDWELL, L., TAPPE, N. J. & FRIEDBERG, E. C. 1993. Yeast DNA repair and recombination proteins Rad1 and Rad10 constitute a single-stranded-DNA endonuclease. *Nature,* 362**,** 860-2.

TORRES-RAMOS, C. A., PRAKASH, S. & PRAKASH, L. 2002. Requirement of RAD5 and MMS2 for postreplication repair of UV-damaged DNA in Saccharomyces cerevisiae. *Mol Cell Biol,* 22**,** 2419-26.

TSUBOUCHI, H. & OGAWA, H. 2000. Exo1 roles for repair of DNA double-strand breaks and meiotic crossing over in Saccharomyces cerevisiae. *Mol Biol Cell,* 11**,** 2221-33.

USUI, T., OGAWA, H. & PETRINI, J. H. 2001. A DNA damage response pathway controlled by Tel1 and the Mre11 complex. *Mol Cell,* 7**,** 1255-66.

UZUNOVA, K., GOTTSCHE, K., MITEVA, M., WEISSHAAR, S. R., GLANEMANN, C., SCHNELLHARDT, M., NIESSEN, M., SCHEEL, H., HOFMANN, K., JOHNSON, E. S., PRAEFCKE, G. J. & DOHMEN, R. J. 2007. Ubiquitin-dependent proteolytic control of SUMO conjugates. *J Biol Chem,* 282**,** 34167-75.

VAISERMAN, A. M. 2010. Hormesis, adaptive epigenetic reorganization, and implications for human health and longevity. *Dose Response,* 8**,** 16-21.

VAN ATTIKUM, H. & GASSER, S. M. 2005. The histone code at DNA breaks: a guide to repair? *Nat Rev Mol Cell Biol,* 6**,** 757-65.

VAN DYCK, E., FOURY, F., STILLMAN, B. & BRILL, S. J. 1992. A single-stranded DNA binding protein required for mitochondrial DNA replication in S. cerevisiae is homologous to E. coli SSB. *EMBO J,* 11**,** 3421-30.

VEGA, L. R., MATEYAK, M. K. & ZAKIAN, V. A. 2003. Getting to the end: telomerase access in yeast and humans. *Nat Rev Mol Cell Biol,* 4**,** 948-59.

VEGA, L. R., PHILLIPS, J. A., THORNTON, B. R., BENANTI, J. A., ONIGBANJO, M. T., TOCZYSKI, D. P. & ZAKIAN, V. A. 2007. Sensitivity of yeast strains with long G-tails to levels of telomere-bound telomerase. *PLoS Genet,* 3**,** e105.

VENCLOVAS, C. & THELEN, M. P. 2000. Structure-based predictions of Rad1, Rad9, Hus1 and Rad17 participation in sliding clamp and clamp-loading complexes. *Nucleic Acids Res,* 28**,** 2481-93.

VON EYSS, B., MAASKOLA, J., MEMCZAK, S., MOLLMANN, K., SCHUETZ, A., LODDENKEMPER, C., TANH, M. D., OTTO, A., MUEGGE, K., HEINEMANN, U., RAJEWSKY, N. & ZIEBOLD, U. 2012. The SNF2-like helicase HELLS mediates E2F3-dependent transcription and cellular transformation. *EMBO J,* 31**,** 972-85.

WALKER, D. W., MCCOLL, G., JENKINS, N. L., HARRIS, J. & LITHGOW, G. J. 2000. Evolution of lifespan in C. elegans. *Nature,* 405**,** 296-7.

WALKER, J. R., CORPINA, R. A. & GOLDBERG, J. 2001. Structure of the Ku heterodimer bound to DNA and its implications for double-strand break repair. *Nature,* 412**,** 607-14.

WANG, F., STEWART, J. A., KASBEK, C., ZHAO, Y., WRIGHT, W. E. & PRICE, C. M. 2012. Human CST has independent functions during telomere duplex replication and C-strand fill-in. *Cell Rep,* 2**,** 1096-103.

WANG, H. & BLACKBURN, E. H. 1997. De novo telomere addition by Tetrahymena telomerase in vitro. *EMBO J,* 16**,** 866-79.

WANROOIJ, P. H. & BURGERS, P. M. 2015. Yet another job for Dna2: Checkpoint activation. *DNA Repair (Amst),* 32**,** 17-23.

WATSON, A., MATA, J., BAHLER, J., CARR, A. & HUMPHREY, T. 2004. Global gene expression responses of fission yeast to ionizing radiation. *Mol Biol Cell,* 15**,** 851-60.

WATSON, J. D. 1972. Origin of concatemeric T7 DNA. *Nat New Biol,* 239**,** 197-201.

WEAVER, B. A. & CLEVELAND, D. W. 2006. Does aneuploidy cause cancer? *Curr Opin Cell Biol,* 18**,** 658-67.

WEINERT, T. A. 1992. Dual cell cycle checkpoints sensitive to chromosome replication and DNA damage in the budding yeast Saccharomyces cerevisiae. *Radiat Res,* 132**,** 141-3.

WEINERT, T. A. & HARTWELL, L. H. 1988. The RAD9 gene controls the cell cycle response to DNA damage in Saccharomyces cerevisiae. *Science,* 241**,** 317-22.

WEINERT, T. A. & HARTWELL, L. H. 1993. Cell cycle arrest of cdc mutants and specificity of the RAD9 checkpoint. *Genetics,* 134**,** 63-80.

WEINERT, T. A., KISER, G. L. & HARTWELL, L. H. 1994. Mitotic checkpoint genes in budding yeast and the dependence of mitosis on DNA replication and repair. *Genes Dev,* 8**,** 652-65.

WELLINGER, R. J., WOLF, A. J. & ZAKIAN, V. A. 1993. Saccharomyces telomeres acquire single-strand TG1-3 tails late in S phase. *Cell,* 72**,** 51-60.

WHELAN, W. L., GOCKE, E. & MANNEY, T. R. 1979. The CAN1 locus of Saccharomyces cerevisiae: fine-structure analysis and forward mutation rates. *Genetics,* 91**,** 35-51.

WIEGANT, F. A., DE POOT, S. A., BOERS-TRILLES, V. E. & SCHREIJ, A. M. 2012. Hormesis and Cellular Quality Control: A Possible Explanation for the Molecular Mechanisms that Underlie the Benefits of Mild Stress. *Dose Response,* 11**,** 413-30.

WOLD, M. S. 1997. Replication protein A: a heterotrimeric, single-stranded DNA-binding protein required for eukaryotic DNA metabolism. *Annu Rev Biochem,* 66**,** 61-92.

WOTTON, D. & SHORE, D. 1997. A novel Rap1p-interacting factor, Rif2p, cooperates with Rif1p to regulate telomere length in Saccharomyces cerevisiae. *Genes Dev,* 11**,** 748-60.

XIE, Y., LIU, Y., ARGUESO, J. L., HENRICKSEN, L. A., KAO, H. I., BAMBARA, R. A. & ALANI, E. 2001. Identification of rad27 mutations that confer differential defects in mutation avoidance, repeat tract instability, and flap cleavage. *Mol Cell Biol,* 21**,** 4889-99.

XU, L., PETREACA, R. C., GASPARYAN, H. J., VU, S. & NUGENT, C. I. 2009. TEN1 is essential for CDC13-mediated telomere capping. *Genetics,* 183**,** 793-810.

YAN, Z., DELANNOY, M., LING, C., DAEE, D., OSMAN, F., MUNIANDY, P. A., SHEN, X., OOSTRA, A. B., DU, H., STELTENPOOL, J., LIN, T., SCHUSTER, B., DECAILLET, C., STASIAK, A., STASIAK, A. Z., STONE, S., HOATLIN, M. E., SCHINDLER, D., WOODCOCK, C. L., JOENJE, H., SEN, R., DE WINTER, J. P., LI, L., SEIDMAN, M. M., WHITBY, M. C., MYUNG, K., CONSTANTINOU, A. & WANG, W. 2010. A histone-fold complex and FANCM form a conserved DNA-remodeling complex to maintain genome stability. *Mol Cell,* 37**,** 865-78.

YEELES, J. T., DEEGAN, T. D., JANSKA, A., EARLY, A. & DIFFLEY, J. F. 2015. Regulated eukaryotic DNA replication origin firing with purified proteins. *Nature,* 519**,** 431-5.

YEOMAN, M., SCUTT, G. & FARAGHER, R. 2012. Insights into CNS ageing from animal models of senescence. *Nat Rev Neurosci,* 13**,** 435-45.

YOUNG, J. W., LOCKE, J. C. & ELOWITZ, M. B. 2013. Rate of environmental change determines stress response specificity. *Proc Natl Acad Sci U S A,* 110**,** 4140-5.

YUZHAKOV, A., KELMAN, Z., HURWITZ, J. & O'DONNELL, M. 1999. Multiple competition reactions for RPA order the assembly of the DNA polymerase delta holoenzyme. *EMBO J,* 18**,** 6189-99.

ZEGERMAN, P. & DIFFLEY, J. F. 2007. Phosphorylation of Sld2 and Sld3 by cyclin-dependent kinases promotes DNA replication in budding yeast. *Nature,* 445**,** 281-5.

ZEMAN, M. K. & CIMPRICH, K. A. 2013. Causes and consequences of replication stress. *Nat Cell Biol,* 16**,** 2-9.

ZHANG, Z., MOO-YOUNG, M. & CHISTI, Y. 1996. Plasmid stability in recombinant Saccharomyces cerevisiae. *Biotechnol Adv,* 14**,** 401-35.

ZHAO, X., MULLER, E. G. & ROTHSTEIN, R. 1998. A suppressor of two essential checkpoint genes identifies a novel protein that negatively affects dNTP pools. *Mol Cell,* 2**,** 329-40.

ZHENG, L., DAI, H., QIU, J., HUANG, Q. & SHEN, B. 2007. Disruption of the FEN-1/PCNA interaction results in DNA replication defects, pulmonary hypoplasia, pancytopenia, and newborn lethality in mice. *Mol Cell Biol,* 27**,** 3176-86.

ZHONG, M., NIU, W., LU, Z. J., SAROV, M., MURRAY, J. I., JANETTE, J., RAHA, D., SHEAFFER, K. L., LAM, H. Y., PRESTON, E., SLIGHTHAM, C., HILLIER, L. W., BROCK, T., AGARWAL, A., AUERBACH, R., HYMAN, A. A., GERSTEIN, M., MANGO, S. E., KIM, S. K., WATERSTON, R. H., REINKE, V. & SNYDER, M. 2010. Genome-wide identification of binding sites defines distinct functions for Caenorhabditis elegans PHA-4/FOXA in development and environmental response. *PLoS Genet,* 6**,** e1000848.

ZHOU, J., MONSON, E. K., TENG, S. C., SCHULZ, V. P. & ZAKIAN, V. A. 2000. Pif1p helicase, a catalytic inhibitor of telomerase in yeast. *Science,* 289**,** 771-4.

ZHOU, W., ZHU, P., WANG, J., PASCUAL, G., OHGI, K. A., LOZACH, J., GLASS, C. K. & ROSENFELD, M. G. 2008. Histone H2A monoubiquitination represses transcription by inhibiting RNA polymerase II transcriptional elongation. *Mol Cell,* 29**,** 69-80.

ZHOU, Y., CARON, P., LEGUBE, G. & PAULL, T. T. 2014. Quantitation of DNA double-strand break resection intermediates in human cells. *Nucleic Acids Res,* 42**,** e19.

ZHOU, Z. W., LIU, C., LI, T. L., BRUHN, C., KRUEGER, A., MIN, W., WANG, Z. Q. & CARR, A. M. 2013. An essential function for the ATR-activation-domain (AAD) of TopBP1 in mouse development and cellular senescence. *PLoS Genet,* 9**,** e1003702.

ZHU, X. D., NIEDERNHOFER, L., KUSTER, B., MANN, M., HOEIJMAKERS, J. H. & DE LANGE, T. 2003. ERCC1/XPF removes the 3' overhang from uncapped telomeres and represses formation of telomeric DNA-containing double minute chromosomes. *Mol Cell,* 12**,** 1489-98.

ZHU, Z., CHUNG, W. H., SHIM, E. Y., LEE, S. E. & IRA, G. 2008. Sgs1 helicase and two nucleases Dna2 and Exo1 resect DNA double-strand break ends. *Cell,* 134**,** 981-94.

ZOU, L. & ELLEDGE, S. J. 2003. Sensing DNA damage through ATRIP recognition of RPA-ssDNA complexes. *Science,* 300**,** 1542-8.

ZUBKO, M. K., GUILLARD, S. & LYDALL, D. 2004. Exo1 and Rad24 differentially regulate generation of ssDNA at telomeres of Saccharomyces cerevisiae cdc13-1 mutants. *Genetics,* 168**,** 103-15.

ZUBKO, M. K. & LYDALL, D. 2006. Linear chromosome maintenance in the absence of essential telomere-capping proteins. *Nat Cell Biol,* 8**,** 734-40.